GEORGIA INSTITUTE OF TECHNOLOGY OFFICE OF CONTRACT ADMINISTRATION

PROJECT ADMINISTRATION DATA SHEET

[X] ORIGINAL [ ] REVISION NO. ______

Project No. E-16-~~380~~ 612 (R-5694-3A0) GTRC/~~XXXX~~ DATE 10/15/85

Project Director: W. Strahle/J. Jogoda School/~~Lab~~ Aerospace Engineering

Sponsor: AFOSR -

Bolling AFB, D. C. 20332-6448

Type Agreement: Grant: 83-0356 Amendment F

Award Period: From 09/30/85 To 09/30/87 (Performance) 11/29/86 (Reports)

Sponsor Amount:

	This Change	Total to Date
Estimated:	$	$
Funded:	$ 195,466	$ 195,466

Cost Sharing Amount: $ 19,725 Cost Sharing No: E-16-380 (R-5694-3A0)

Title: Heterogeneous Diffusion Flame Stabilization

ADMINISTRATIVE DATA

OCA Contact Ralph Grede x 4820

1) Sponsor Technical Contact:

Mr. Leonard H. Caveny
AFOSR/NA
Building 410
Bolling AFB, D. C. 20332-6448
(202) 767-4987

2) Sponsor Admin/Contractual Matters:

Mr. Wanda G. Littles
AFOSR/PKD
Building 410
Bolling AFB, D.C. 20332-6448
(202) 767-5007

Defense Priority Rating: N/A

Military Security Classification: Unclassified

(or) Company/Industrial Proprietary: N/A

RESTRICTIONS

See Attached N/A Supplemental Information Sheet for Additional Requirements.

Travel: Foreign travel must have prior approval — Contact OCA in each case. Domestic travel requires sponsor approval where total will exceed greater of $500 or 125% of approved proposal budget category.

Equipment: Title vests with GIT.

COMMENTS:

This is a continuation of E-16-658

COPIES TO:

SPONSOR'S I. D. NO. 02.104.001.85.014

Project Director
Research Administrative Network
Research Property Management
Accounting

Procurement/GTRI Supply Services
Research Security Services
~~Reports Coordinator (OCA)~~
Research Communications (2)

GTRC
Library
Project File
Other A. Jones

GEORGIA INSTITUTE OF TECHNOLOGY

OFFICE OF CONTRACT ADMINISTRATION

SPONSORED PROJECT TERMINATION/CLOSEOUT SHEET

Date 12/30/87

Project No. E-16-612

School/Lab AE

Includes Subproject No.(s) N/A

Project Director(s) W. Strahle/J. Jogoda

GTRC / GIT

Sponsor AROSR- Bolling AFB, D.C. 20332-6448

Title Heterogeneous Diffusion Flame Stabilization

Effective Completion Date: 9/30/87 (Performance) 11/30/87 (Reports)

Grant/Contract Closeout Actions Remaining:

- [ ] None
- [x] Final Invoice or Final Fiscal Report
- [ ] Closing Documents
- [x] Final Report of Inventions Questionnaire sent to P.I.
- [x] Govt. Property Inventory & Related Certificate
- [ ] Classified Material Certificate
- [ ] Other

Continues Project No. E-16-658

Continued by Project No.

COPIES TO:

Project Director
Research Administrative Network
Research Property Management
Accounting
Procurement/GTRI Supply Services
Research Security Services
Reports Coordinator (OCA)
Legal Services

Library
GTRC
Research Communications (2)
Project File
Other Duane Hutchison
Angela DuBose
Russ Embry

FORM OCA 69.285

E-16-612

GEORGIA INSTITUTE OF TECHNOLOGY

ATLANTA, GEORGIA 30332

SCHOOL OF
AEROSPACE ENGINEERING

404-894-3000

DANIEL GUGGENHEIM SCHOOL
OF AERONAUTICS

April 26, 1986

Dr. Robert Vondra
AFOSR/NA
Bldg. 410
Bolling Air Force Base DC 20332

Subject: Research Summary and Forecast Report for AFOSR 83-0356(F)

Dear Dr. Vondra:

Request: This is a Research Summary and Forecast Report for our work on AFOSR 83-0356(F). Our request is for funding for the option year of the contract, commencing on October 1, 1986.

Research Summary: The program has been concerned with non-reacting and reacting flow behind a backward facing step, with provision for blowing of reactants and inerts from the wall behind the step. This wind tunnel situation models the flowfield in the flame stabilization of a solid fueled ramjet. The program consists of an analytical portion, designed to predict the turbulent flowfield, and an experimental portion, relying heavily on advanced laser-based diagnostics.

In the first one-half year of the current amendment progress has been made in a.) computer program development to treat the fully reacting case, b.) measurements of species concentrations and concentration-velocity covariance in the cold flow case, c.) development of the Raman spectroscopy system and d.) facility modification for the reacting case. The computer work, utilizing a two-equation model of turbulence, has now been developed to the point where it will treat the fast reaction limit case, but without modeling of the effect of turbulent fluctuations on the density determination. This model, which overpredicts temperatures to be expected, has been invaluable in the experiment development in order to warn of regions in the apparatus where over-temperature problems can be expected. Current calculations which have been made include those for methane and hydrogen injection from the bottom wall.

Measurements have been made with pure Rayleigh scattering and combined LDV and Rayleigh scattering for the case of CO_2 injection from the bottom wall. Mean carbon dioxide concentrations have been measured which compare favorably with analytical predictions. Trouble has been encountered, however, with measurement of the concentration-velocity covariance because of excessive noise to signal ratio. Methods for improving signal quality are under investigation.

Continued development is underway on the Raman spectroscopy system for temperature and concentration determination in the hot flow case. A traversing table which permits the Raman measurement location to be kept coincident with that of the LDV has been designed and constructed. The optical set-up for the incident Raman laser and the collection optics has been designed and assembled. A data acquisition system including amplifiers, gated integrators and sample and holds has been selected and assembled. A data reduction scheme, which permits the matching of simultaneously obtained velocity and Raman Stokes and Antistokes values has been developed and the necessary software written and tested.

Conversion of the facility to a hot flow facility has been underway for some time. It has proved to be a far more demanding process for machinists and engineers than originally anticipated. However, the hardware manufacture is within two weeks of completion as of this writing, and system final assembly and checkout procedures are shortly forthcoming. Some of the delay was incurred due to original plan modification as a result of the computer work. Some instrumentation has been added to monitor possible over-temperature problems.

Research Forecast: At the end of the first year of the subject amendment it is anticipated that a.) the facility will have been thoroughly checked out for the hot flow case and will be ready for "production" experiments, b.) the Raman system will be ready for mean and fluctuating temperature measurements as well as for temperature-velocity covariance measurements, c.) the Raman system will be ready to be used for pure Rayleigh scattering measurements in the case the current Rayleigh system noise problems cannot be overcome, d.) another set of experiments will have been completed to attempt extraction of the velocity-concentration covariance by the current LDV-Rayleigh system, e.) the computer model will have incorporated the necessary modifications to treat the effect of turbulent fluctuations on density, but still in the fast reaction limit, and f.) convergence time of the computer model (run time) will have been improved.

For the proposed option year the hot flow work, both analytical and experimental, will proceed with vigor. Finite rate kinetics will be investigated, both experimentally and analytically, to deduce the blowoff characteristics of this flame type. The effects of turbulence on the flame transport mechanisms will be thoroughly explored experimentally and will be incorporated into the computer model as appropriate.

Sincerely,

Warren C. Strahle
Regents' Professor

cc J.I. Jagoda

E-16-612

AFOSR TR-85 0880

EVALUATION OF DATA ON SIMPLE TURBULENT REACTING FLOWS

Edited by

Warren C. Strahle
Spyridon G. Lekoudis

School of Aerospace Engineering
Georgia Institute of Technology
Atlanta, Georgia

Sponsored by:

Air Force Office of Scientific Research
Grant No. 83-0356

September 1985

Unclassified

SECURITY CLASSIFICATION OF THIS PAGE (When Data Entered)

REPORT DOCUMENTATION PAGE

READ INSTRUCTIONS BEFORE COMPLETING FORM

1. REPORT NUMBER AFOSR-TR-85-0880	2. GOVT ACCESSION NO.
3. RECIPIENT'S CATALOG NUMBER	
4. TITLE (and Subtitle) Evaluation of Data on Simple Turbulent Reacting Flows	5. TYPE OF REPORT & PERIOD COVERED Interim Scientific Report 1 Oct. 1984 - 30 Sept. 1985
	6. PERFORMING ORG. REPORT NUMBER
7. AUTHOR(s) Edited by Warren C. Strahle, Spyridon G. Lekoudis	8. CONTRACT OR GRANT NUMBER(s) AFOSR-83-0356
9. PERFORMING ORGANIZATION NAME AND ADDRESS School of Aerospace Engineering, Georgia Institute of Technology, Atlanta, GA 30332	10. PROGRAM ELEMENT, PROJECT, TASK AREA & WORK UNIT NUMBERS
11. CONTROLLING OFFICE NAME AND ADDRESS AFOSR/NA, Bldg. 410, Bolling AFB, DC 20332	12. REPORT DATE September, 1985
	13. NUMBER OF PAGES 476
14. MONITORING AGENCY NAME & ADDRESS(if different from Controlling Office)	15. SECURITY CLASS. (of this report) Unclassified
	15a. DECLASSIFICATION/DOWNGRADING SCHEDULE

16. DISTRIBUTION STATEMENT (of this Report)

Approved for public release; distribution unlimited

17. DISTRIBUTION STATEMENT (of the abstract entered in Block 20, if different from Report)

Approved for public release; distribution unlimited

18. SUPPLEMENTARY NOTES

19. KEY WORDS (Continue on reverse side if necessary and identify by block number)

Turbulence, Reacting Flows, Combustion, Jets, Boundary Layers, Shear Layers

20. ABSTRACT (Continue on reverse side if necessary and identify by block number)

A large number of data sets on simple turbulent reacting and non-reacting flows are reveiwed with a view toward judgement as to their suitability for computational test. Both premixed and nonpremixed flows are considered, but the review is limited to simple geometries and flows which could be analytically treated as an initial value (parabolic) problem. Nine flows are identified as being sufficiently well documented and understood to serve as bases for testing of computational methods and models. The data for these flows are tabulated or graphically displayed in this report.

DD FORM 1 JAN 73 1473 EDITION OF 1 NOV 65 IS OBSOLETE

Unclassified

SECURITY CLASSIFICATION OF THIS PAGE (When Data Entered)

AFOSR TR-85 0880

EVALUATION OF DATA ON SIMPLE TURBULENT REACTING FLOWS

Edited by
Warren C. Strahle
Spyridon G. Lekoudis

School of Aerospace Engineering
Georgia Institute of Technology
Atlanta, Georgia

Sponsored by:

Air Force Office of Scientific Research
Grant No. 83-0356

September, 1985

ACKNOWLEDGEMENT

This effort was supported by the Air Force Office of Scientific Research. Dr. Leonard H. Caveny was the Program Monitor and offered intense encouragement during several trying periods for the editors and authors. The Air Force is to be congratulated for their support of this work, which is expected to be a useful reference work in the field of turbulent reacting flows for years to come.

TABLE OF CONTENTS

CHAPTER 1
INTRODUCTION AND HISTORY

Warren C. Strahle

During the past decade and one-half there has been a largely expanded base of knowledge developed in turbulent reacting flows. This has come about through development of advanced experimental methods and increased computational power. The area has always been an important one since virtually all combustion driven-power extraction devices operate with a turbulent working fluid. In discussions between the author and many members of the technical community during the summer of 1983, it became evident there was concern about a feeling of chaos in the relationship between theory and experiment. Experiments appeared to be diverse in purpose, and several analytical models of different types had been developed with little comparison between methods. Citing the prior efforts at computation/experiment consolidation by NASA(1972), Kline, Morkovin and Moffet (1969) and Kline, Cantwell and Lilley (1981), the author approached the Air Force Office of Scientific Research with an offer to conduct a program similar to that run at Stanford in 1968, but on turbulent reacting flows as opposed to turbulent boundary layers. The Air Force, with Dr. Leonard H. Caveny as program monitor, agreed to the concept and this report is the culmination of the effort that ensued.

Because of their experience in the type of effort envisaged, the author met with Professors S. J. Kline and B. J. Cantwell of Stanford University late in the summer of 1983. At this meeting the author was briefed in the successes, troubles and procedures of the Stanford Conferences. This meeting was valuable and is gratefully acknowledged. The result was a plan for two major Georgia Tech/AFOSR Conferences on Turbulent Reacting Flows. The first would be a data base analysis meeting whereby certain well documented flows would be chosen for data encoding. The second would be a meeting at which computors would test their methods against the documented flows. For reasons below only the first meeting was scheduled and this document is basically a report of that meeting.

An Advisory Committee was first set up to advise the author on personnel and procedures required to actually conduct the effort. The Advisory Committee consisted of

Professor Craig T. Bowman, Stanford University
Professor Howard W. Emmons, Harvard University
Dr. Dan L. Hartley, Sandia National Laboratories
Professor Stanford S. Penner, University of California at La Jolla

From their suggestions an Organization Committee was set-up to conduct the work. The Organization Committee consisted of

Dr. Michael C. Drake, General Electric
Professor Gerard M. Faeth, University of Michigan Professor Frederick C. Gouldin, Cornell University
Dr. Sheridan C. Johnston, Sandia National Laboratories
Professor Wolfgang Kollmann, University of California at Davis
Professor Spyridon G. Lekoudis, Georgia Institute of Technology
Professor Paul A. Libby, University of California at La Jolla
Dr. Geoffrey J. Sturgess, United Technologies Corporation
Professor G. S. Samuelson, University of California at Irvine
Professor J. H. Whitelaw, Imperial College of Science and Technology

As time progressed Dr. Sturgess found that he could no longer serve and he was replaced by Dr. Edward J. Mularz of NASA Lewis Research Center.

The Organization Committee had three meetings. They were at

Reno, Nevada - January 12, 1984
Ann Arbor, Michigan - August 17, 1984
Atlanta, Georgia - December 10-11, 1984

The first meeting was held to determine the scope of the effort and to assign people to be data base analysers. Just as the initial Stanford Conference was highly restricted in the number of flows considered, the committee decided to limit the categories of turbulent reacting flows to be considered. First of all, the decision was made to limit consideration to only those flows that could be analytically treated by parabolic methods. Elliptic flows were eliminated from consideration. Then the following four data classes were identified:

Variable density nonreacting flows
Fast reaction non-premixed flows
Slow reaction non-premixed flows
Premixed flows that could be parabolically treated

The data base analysers chosen for these four categories were Gouldin and Johnston, Faeth and Samuelson, Kollmann and Drake, and Libby and Whitelaw, respectively. As the program progressed and it became evident that a large task was at hand, other workers were drawn in, and their names appear as authors in the Chapters to follow. The charge to the analysers was to a) seek flows in their categories that were suitable for computational test, b) identify, if possible, the accuracy of the data and c) identify gaps in the data.

The second meeting was held primarily as a progress report event, after seven months of effort. At that time, it was becoming evident that there are several problems with the available data bases in turbulent reacting flows. Ideally, the following items would be desireable in a data base which is to be used for computational test:

1. Measurement of a vector, scalar and some turbulence quantity
2. Measurement at many streamwise and cross stream stations
3. Sufficiently high Reyolds number to guarantee turbulence
4. Measurement of some macroscopic variables such as flame length
5. Interpretability of measurement in terms of a Favre or conventional quantity
6. High measurement accuracy or at least an accuracy estimate
7. Large density differences in the case of variable density non-reacting flows
8. Confidence in the parabolic treatment
9. Measurement of initial conditions and adequate mean pressure gradient specification
10. Minimal intrusiveness of measurement
11. Fully turbulent flow everywhere in the computational domain

It was concluded, however, that no available data bases would meet these criteria. Some were sufficiently close to warrant further scrutiny. However, because of the pessimisim at that time, it was decided to delay any efforts at creating a computer-based data encoding process until after the next meeting; it was becoming clear that a computational effort may be premature.

At the final meeting in Atlanta several flows had been identified which could be used for computational test, to varying degrees of completeness and certainty. The Committee had to reach, however, to some data bases that were not yet complete in their documentation in the published literature. Moreover, the evaluation of the data was in two cases carried out partially by workers who were closely allied to the original data taking process. There were, however, sufficient independent checks by non-allied workers that this is not believed to be a problem.

The primary decision at the final meeting was to recommend that a computational effort <u>not</u> be initiated at this time. This decision was unanimous but not applauded. There were several reasons for this opinion, and some of them were independent of the data bases' quality and were linked to an opinion of what the computors could do. Most theories or models of turbulent reacting flows are application-specific and cannot be readily used for flows of different character or chemistry from those for which they were developed. This precludes asking the computor community to calculate several mandatory flows which may cross technical lines (e.g., a premixed flow and a diffusion flame). Indeed, for many flows, even though of relative simplicity, the calculation require a research effort of considerable magnitude. Acknowledging, however, that a computational effort for individual flows might be of use, the decision to abort a large community-wide computational effort finally laid at the quality of the data bases. Here there are some problems with some of the flows in a) completeness, b) low Reynolds number, c) specification of the initial and boundary conditions, d) containment of a laminar-turbulence transition e) uncertainty as to the accuracy of measurement and f) uncertainty in the type of weighting (averaging) of the measurement. Moreover, there is some uncertainty in some of the flows whether or not a parabolic treatment would be adequate, and it is certain in some of the flows that buoyancy would have to be considered. In short, the Committee's opinion was that the computation of each flow is a subject of research, not routine computation, and that calculation of these flows is best handled on an individual basis where the uncertainties can be systmatically explored.

This is not an indictment of the turbulent reacting flows experimental community. Most of the work reviewed was never intended to act as a data base to test models and computation accuracy; they were often intended to test specific physical hypotheses or provide exploratory information. Indeed, the generation of such data bases is a relatively new activity for the community. The Committee, however, was looking for a breadth of information on each flow which was often absent because the data were generated for purposes other than computational test. The fact that some flows were rejected from consideration for the purpose at hand is therefore not intended as a judgement concerning the quality of the work.

Some may question if it is appropriate of the Committee to emphasize relatively simple turbulent flows involving chemical reaction without the complication of complex geometries, radiative transfer and multiple phases. These complications enter significantly in practical applications, and the Committee was well aware that a parallel effort of application of models to these situations is being carried out by industrial and government organizations.It is important to recall that in a simpler but related field, namely in the phenomenology of turbulent flows with constant fluid properties, there is currently much discussion and controversy concerning the new sophisticated methods applicable to such flows. There are some who believe that such methods should develop in an evolutionary manner, through simple toward complex flows, so that ultimately the flows of more practical interest can be treated with soundly based approaches. Others are impatient with this view and consider that use of the new methods is justified by their ability to attack practical problems even though many details of the analysis are uncertain. Moreover, when applied to entirely new situations in the absence of experimental data the results are suspect. In the view of this Committee, the added complexities of turbulent combustion, in particular the presence of significant variation in density, leading to the possibility of new transport and turbulence production mechanisms, suggest that the conservative perspective of the first group should be adopted. It is hoped that in due course the evolving predictive methods assessed and improved on the basis of the experimental data emphasized here, and expected to be forthcoming in the near future, will lead to soundly based methods of direct use to the designer.

The following four chapters contain the results of data base analysis in each of the four chosen areas. For a quick preview of the results the reader may turn directly to the section RECOMMENDED CASES in each of the chapters. Detailed tabulation of the data results are located in the appendices. References for each data area are given at the end of each chapter rather than being all lumped together at the end of the report. There is some overlap of material between the chapters in discussion of experimental methods. It was decided to give the authors their own latitude here, rather than construct a separate section.

REFERENCES

Anon. 1972 Free Turbulent Shear Flows NASA SP-321.

Kline, S. J., Morkovin, M. J. and Moffat 1969 Computation of Turbulent Boundary Layers - 1968 AFOSR-IFP-Stanford Conference.

Kline, S. J., Cantwell, B. J. and Lilley, G. M. 1981 The 1980-81 AFOSR-HTTM-STANFORD Conference on Complex Turbulent Flows: Comparison of Computation and Experiment.

CHAPTER 2

NONREACTING MIXING FLOWS

F. C. Gouldin, S. C. Johnston, W. Kollmann and R. W. Schefer

LITERATURE SEARCH

Introduction

The literature on free shear flows is quite extensive, and there are several reviews available on the subject (see for example Townsend (1976), Hinze (1975), Rajaratnam (1976), Abramovich (1963), Fischer, et al(1979) and List (1982)). Not all of the literature on free shears flows is entirely relevant to combustion problems. Time and space constraints place a practical limit on the types of flows that can be considered in this review. Thus at the outset several conditions and restrictions are made to help define and limit the type of flows reviewed. As noted the overall objective of this work is to review data available on various classes of turbulent flows for their suitability as test flows for the evaluation of turbulence models applicable to reacting flow problems. For this purpose it is required that the flows be stationary and parabolic and have clean, well defined boundary conditions. Furthermore it is appropriate to restrict attention to free shear flows since these flows (as opposed to boundary layer flows) are found in most combustion devices and are typical of the laboratory flames for which model validation data are most likely to be available. In this review attention is limited primarily to studies where both scalar and velocity data are obtained. This focus is quite restrictive but is justified on the grounds that both types of data are necessary for satisfactory evaluation of model performance.

Wake flows will not be considered for several reasons. One, emphasis in the constant density mixing flows part of this review is placed on taking advantage of similarity, and many wake flows are not similar (see below). Two, since the flow immediately behind a bluff body is elliptic, parabolic flow calculations must be initiated downstream of this elliptic flow region where the specification of necessary initial conditions is difficult. Three, since little reactive flow data are available for wake flows, it seems appropriate to concentrate effort on jets and mixing layers, flows for which reacting flow data are available.

Scalar mixing measurements require the introduction of a scalar uniformity either in temperature or composition which generally causes a density nonuniformity. Thus it is necessary to establish a criterion to distinguish those experiments where the density variations are significant from those where they are not. With the exception of two-dimensional mixing layers, very large initial density differences are required for density fluctuations to be significant beyond the initial mixing region. Consequently, surprisingly large initial density differences are acceptable in constant density mixing studies. Exactly how large initial differences may be is not clear. For present purposes we arbitrarily classify those flows with an initial density ratio of high over low density equal to or greater than 1.5 as variable density flows. Flows having a value for this ratio of less than 1.5 are considered constant density mixing flows. Also all mixing layer flows with any but the smallest density difference are considered to be variable density flows.

Data needs for model evaluation

The capability of modern experimental technique is such that copious amounts of very detailed data can now be collected and analyzed (especially for room temperature, constant density flows). Experiments are undertaken for various reasons and no two experiments are likely to generate the same data. Thus a brief discussion of the type of the data required for model evaluation is appropriate.

First and foremost, first moments of axial velocity and scalar quantities are needed at sufficient axial and lateral locations to fully characterize the evolution of the mean velocity and scalar fields. Of equal importance is the specification of necessary inlet and boundary conditions. Of nearly equal importance are data for second-order correlations, eg. Reynolds stresses since these correlations are the quantities predicted by most turbulence models. Most work reports data for other quantities such as spectra, intermittency, dissipation, higher moments, etc. Of this type of information intermittency and data which allow for a comparision of the important terms in equations for turbulence quantities such as a turbulence kinetic energy budget seem exceptionally useful. Also pdf data are extremely valuable to researchers developing model evolution equations for pdf's describing turbulent flows and to those using pdf's in the modeling of nonpremixed flames.

For flows exhibiting similarity the specification of the mean velocity and mean scalar fields is straight forward and requires relatively few data. (However many measurements are usually necessary to establish the existence of similarity.) In similar jet and wake flows (Townsend, 1976)

$$U = U_1 + u_0 f(\frac{z}{l_0})$$

$$\overline{uw} = q_0^2 g_{i,j} f(\frac{z}{l_0}) \tag{1}$$

$$\overline{q^2} = q_0^2 g \ (\frac{z}{l_0})$$

$$\overline{u^2} = q_0^2 g_i \ (\frac{z}{l_0}), etc.$$

The parameters u_0, q_0, and l_0, which are functions of x alone, describe the spreading rate of the mean velocity and turbulence fields, while the functions f, g_{ij}, g_i and g describe the lateral variation of flow field properties. When similarity does not obtain, a large number of measurements at different axial and lateral stations are required to determine the mean field properties. The exact amount of data required depends on the character of the flow and, hence, cannot be predetermined.

For boundary conditions, the axial pressure gradient and conditions at large lateral distance should be investigated. It is easy to underestimate the significance of the boundary conditions. For example, flow entrainment can induce large scale recirculating flows in free jet experiments performed in rooms (Bradshaw 1977). (This flow was induced apparently by jet entrainment.) It is clear that the investigator must exercise great care in avoiding outside and unnoticed interferences. In confined flows it is essential that axial pressure gradients and coflowing stream velocity be carefully measured. Finally, the assumption is frequently made that the flow is non-turbulent away from the jet. This assumption should also be verified.

The determination of appropriate initial conditions is a tricky business with several unresolved problems. First, different modeling approaches, eg., k-ϵ versus a pdf approach, may have widely different requirements for initial conditions, while similar approaches may still have different needs. Second, since most turbulence models do not attempt to model the transition from laminar to turbulent flow it would seem desirable for the inlet flow to be turbulent or have turbulent regions, eg., a turbulent boundary layer. Third, new turbulence models, not yet developed, are likely to require information on the inlet flow not considered at present to be important. Fourth and most significantly there is confusion regarding the influence of initial conditions on the developed, self-preserving, turbulent flow far downstream of the nozzle forming the jet.

Experimental data on jets exhibit considerable variation in spreading rate and in the centerline variation of mean velocity and of its variance (see Table 1). These variations may be manifestations of sensitivity to inlet conditions. (NB: Current turbulence models are unsatisfactory in their ability to predict spreading rate and centerline variations in mean and variance.) There is some experimental evidence (Hill et al. 1976) for free round and plane jets that, when the flow is initially laminar, jet spreading rates, centerline mean velocity decay and centerline turbulence characteristics are functions of the initial velocity and the experimental system. Hill et al. (1976) attribute the observed sensitivity to large scale structures seen by spark schlieren in the laminar but not in the turbulent flow cases. It should be noted that the measurements of Hill et al. (1976) as reported were not carried to large axial distance where one might reasonably expect initial conditions to have little influence on jet properties. According to Wygnanski and Fielder's data (1969), the round jet does not become self-preserving in turbulence quantities until $x/D > 60$, while for a plane jet an $x/D > 40$ is required according to the data of Gutmark and Wygnanski (1976). In view of the large axial distance required to obtain good flow similarity it is reasonable to suspect that the sensitivity to initial conditions reported by Hill et al. (1976) is the result of not obtaining self preserving flow. On the other hand Bradshaw (1966, 1977) attributes variations in jet spread and centerline evolution to different initial conditions and to conditions in the fluid into which the jet is flowing. Clearly there is a significant uncertainty associated with the establishment of appropriate inlet conditions.

One appropriate response, for now, to the problem of choosing and measuring inlet conditions is to design an experiment with well defined and easily determined inlet conditions. Laminar flow with thin laminar boundary layers for which displacement and momentum thicknesses are measured is one example. In this case the inlet flow is well known, but transition to turbulence occurs in the calculation domain.

An alternate strategy for handling initial conditions is to start with a turbulent flow or turbulent boundary layers thus avoiding having transition in the calculation domain and perhaps avoiding large scale structures. The problem with an initially turbulent flow is that careful and extensive measurements are required to specify the turbulent flow and it is likely, given our current imperfect understanding of turbulent flows, that not all quantities needed for future tests would be recognized as important and therefore measured. To guard against this possibility careful and thorough experimentation is recommended, and the raw data should be stored on magnetic tape against future needs to analyze the data for new turbulence properties.

Clearly more research on the sensitivity of turbulent flows to inlet conditions and to conditions in the ambient fluid is needed. At the present time the reviewers believe that for model evaluation purposes it is best to have the initial flow turbulent, whether or not large structures are avoided thereby, since with this initial state transition does not occur in the calculation domain. For the round jet, fully developed turbulent pipe flow seems to be a good choice, while in other cases a turbulent boundary layer can be induced by tripping. (For plane jets the turbulent boundary layer approach is debatable because of the growth of side wall boundary layers in the jet nozzle and possible secondary flows.) For initially turbulent flow, means, variance and important correlation terms should be measured at the nozzle exit as well as the turbulence dissipation rate if at all possible. The measurement of other properties as appropriate should be considered. It should be the obligation of the researcher to know his flow and what should be measured for inlet specification.

Constant density mixing flows

As noted above, the development of a similar flow can be described by relatively few functions and parameters, and this simplification should be utilized whenever possible. Unfortunately the conditions for similarity are quite restrictive, and even when similarity is allowed theoretically, it may not develop or be very late (far downstream) in developing practically. For example the free jet data of Wygnanski and Fielder (1969) show that while first moments appear to have similar profiles after 20 x/D the second moments do not achieve similarity until over 60 x/D at which point the axial decay rate of the centerline mean axial velocity changes.

Townsend (1976) discusses conditions necessary for similarity in two-dimensional free shear flows. As noted above the conditions are very restrictive and as a consequence only a limited subset of free shear flows are truly similar or self-preserving. The similarity constraints are determined by substituting the functional forms presented in Eq. 1 into the appropriate conservation equations and multiplying terms in order to gather the scales, U_1, u_0, etc., into groups. For similarity these groups must be either zero or independent of x, a condition which in turn determines how the scales vary with x. In general the constraint conditions cannot be met. Examples of flows satisfying similarity include the two-dimensional (plane) shear layer, the two-dimensional and axisymmetric jet with no coflow and the axisymmetric jet in a coflowing stream where $u_0 \propto U_1(x - x_0)^a$ and a is a constant. The two-dimensional wake does not satisfy similarity except in the limit $u_0/U_1 \approx 1$.

Townsend also considers the case of passive scalar mixing in free shear flows.

$$\Theta = \theta_0 f_\theta\left(\frac{z}{l_0}\right)$$

$$\overline{\theta^2} = \theta_0{}^2 g_\theta\left(\frac{z}{l_0}\right) \tag{2}$$

$$\overline{\theta w} = \theta_0 u_0 g_{\theta,3}\left(\frac{z}{l_0}\right), etc.$$

In Eq. 2 the scale for scalar fluctuations has been set equal to θ_0 as required for similarity, which means that at large x/D, $\overline{\theta^2}/\theta_0$ approaches a constant on the centerline or plane of symmetry of the flow. It can then be shown that similarity requires for the scalar field that $U_1 dT_1/dx = 0$ (or $U_1 dC_1/dx$) and, for u_0/U_1 constant or $u_0/U_1 \ll 1$, $\theta_0 \propto u_0$. For example, the plane jet data of Browne et al. (1984) show $(U_j/u_0)^2 = 0.143(x/D + 5)$ and $(\theta_j/\theta_0)^2 = 0.18(x/D + 8)$ in good agreement with the foregoing. (NB. In earlier reports of this research a different variation of centerline mean temperature is reported with an unlikely virtual origin of 110.)

For variable density flows a similarity analysis might also be carried out. The Favre-averaged equations, which have the same general form as the Reynolds-averaged equations in constant density flows, could be considered. Then let

$$\overline{\rho} = \rho_1 + \rho_0 k\left(\frac{z}{l_0}\right) \tag{3}$$

and two new scales enter the problem, ρ_1 and ρ_0, as well as the function k. The axial variations of these scales for similarity are related to the variation of the other scales entering the problem, thus greatly restricting the variable density flows which satisfy similarity. For example if one considers a plane jet flow into still air he finds that similarity cannot be achieved. In early work both Keagy and Weller (1950) and Corrsin and Uberoi (1950), for variable density flow, perform similarity analyses. Both analyses are based on unjustified assumptions regarding either axial variations of the important scales in the problem or the functional forms describing radial variations of the jet properties.

In summary, similarity is found to hold for a limited class of constant density free shear flows. For this class of flows it is an extremely useful concept and should be used to check the quality of experimental data and to help report data in a compact form. Unfortunately similarity is not expected for variable density flows.

In the literature there are many reports of data where velocity and scalar quantities were not measured simultaneously. While these measurements are not reviewed in any detail here for reasons stated above, the data are useful for model validation, since they can be used to find the parameters and functions appearing in the similarity expressions. Here we summarize some of these data by presenting in similarity form data for mean and variance. These data are presented in Table 1.

For comparison the data are fit to similarity forms as noted below (see Townsend 1976).

Mixing layer:

$$u_0 = U_1 = \theta_0 = constant$$

$$l_0 = L_u(x - x_0) \tag{4}$$

$$l_\theta = L_\theta(x - x_0)$$

Table 1a. Plane Jet Data.

REFERENCE	Initial Conditions			Velocity						Scalar					COMMENTS
	AR	Re $\times 10^{-3}$	R	C_u	x_o/h	L_u	x_o/h	$\frac{\langle u^2\rangle^{1/2}}{u_o}$	C_u/L_u	C_θ	x_o/h	L_θ	x_o/h	$\frac{\langle \theta^2\rangle^{1/2}}{\theta_o}$	
Robins (Everitt & Robins,1978)	128	16	1	0.18-.21	-	0.10	-	0.23	1.8-2.1						
	64	30	1	0.17-.19	-	.10-.11	-	0.22							
	32	30	1	0.14-.18	-	0.11	-	0.22							
	21	75	1	0.19-.22	-	0.09	-	0.25							
Heskestad (1965)	120	34	1	0.16	6	0.11	6	0.26	1.45	-	-	-	-	-	measures to x/d = 160.
Gutmark and Wygnanski (1976)	38	30	1	0.17	2	0.10	2	0.27	1.7	-	-	-	-	-	
Antonia & coworkers (Table IV)	19.7	7.62	1.087	0.143	9	0.104	5	0.192	1.38	0.18	8	0.128	5	0.170	
Davies, et al. (1975)	6.0	51.8	1.049	0.146	1.17	0.109	1.17	0.19	1.34	0.252	1.17	0.125	1.17	0.165	
Jenkins and Goldschmidt (1973)	23.9	14.3	1.037	0.160	4.0	0.088	-4.5	-	1.82	0.0132*	-7.5*	0.123	-4.8	-	$(\theta_o/\theta_j)^{-1/2} = C_\theta(x/h-x_o/h)$.
			1.070	0.160	4.0	0.091	-3.0	-	-	0.0132*	-7.5*	0.128	-3.6	-	
			1.117	0.160	4.0	0.096	-2.5	-	-	0.0132*	-7.5*	0.137	-3.2	-	
Bashir and Uberoi (1975)	40	2.77	1.201	0.22	2.42	0.088	2.42	0.25	-	0.29	2.42	0.183	2.42	0.22	
	20	-	1.2	0.206	1.94	-	-	0.26	-	0.276	1.94	-	-	0.273	
	144	-	1.2	0.240	4.6	0.104	4.5	0.247	2.31	0.258	4.6	-	-	0.256	
Fischer, et al. (1979)	-	-	-	0.172	-	0.096	-	-	1.79	0.176	-	0.261	-	-	recommended values
van der Hegge Zijnen (1958)**	20	-	1.36	0.161	-0.6	0.096	-	-	-	-	-	0.141	-	-	**Reported by Rajaratnam (1976)
	25	-	1	0.206	-1.2	-	-	-	-	-	-	-	-	-	and by Samaraweera (1978)
Albertson, et al. (1950)	-	-	-	0.190	-	-	-	-	-	-	-	-	-	-	
Abramovich (1963)	-	-	-	0.140	-	0.096	-	-	1.46						

Table 1b. Round Jet Data.

REFERENCE	Initial Conditions: Re $\times 10^{-3}$	Initial Conditions: R	Velocity: C_u	Velocity: x_o/d	Velocity: L_u	Velocity: x_o/d	Velocity: $\frac{\langle u^2\rangle^{1/2}}{u_o}$	Velocity: C_u/L_u	Scalar: C_θ	Scalar: x_o/d	Scalar: L_θ	Scalar: x_o/d	Scalar: $\frac{\langle\theta^2\rangle^{1/2}}{\theta_o}$	COMMENTS
Corrsin (1946)	19.1	1.05	0.18	-	0.17	-	0.25	1.06	0.22	-	0.22	-	-	$U_j/u_o = C_u(x/d)^{1.1}, \theta_j/\theta_o = C_\theta(x/d)^{0.92}$.
Wygnanski & Fiedler (1969)	~100	1	0.179-.203	3-7	0.168	-	0.29	1.07-1.21						
Hinze & van der Hegge Zijen (1949)	-	1	0.17	0.5	0.16	0.5	-	1.06	0.228	2.6	0.172	0		reported in Hinze (1975)
Corrsin and Uberoi (1950)	~55	1.05	0.193	2.6	0.139	5	0.23	1.39	0.28	2.9	0.165	5	-	
	~55	2.00	0.225	2.3	0.231	3	-	-	0.32	2.16	0.286	3	-	
	~55	1.570	0.175	1.01	-	-	0.225	-	0.238	0.87	-	-	0.145	
Kiser (1963)	~30	1	0.164	1.2	0.163	1.2	-	1.01	0.2	1.2	0.208	1.2	-	concentration
Keagy and Weller (1950)	54.7	0.63	0.096	0.8	0.166	-	-	-	0.173	5.7	0.181		-	concentration
	27.7	1.04	0.120	1.1	0.178	-	-	0.67	0.108	3.2	0.209		-	concentration
	3.6	7.25	0.281	8.5	0.221	-	-	-	0.050	16.7	0.312		-	concentration
Wilson and Danckwerts (1964)	20-40	1.07-1.67	$0.155\sqrt{R}$	-	0.2	-	-	0.78	$0.175\sqrt{R}$	-	0.26	3.0	0.18	
Fischer, et al. (1979)**	-	-	0.161	-	0.178	-	-	0.90	0.202	-	0.211	-	-	**recommended values
Lockwood and Moneib (1980)	50.4	1.86							0.278	3.7	0.264	2	0.21	
Dyer (1979)	9.79	0.66							0.228	2.6	0.172	0	0.15	$U_i/U_j = 0.033$
Pitts and Kasawagi (1984)	3.76	1.82							0.166	-3.8	0.216	0	0.29	$U_i/U_j = 0.026$
Birch, et al. (1978)		1.82							0.180	1.8	0.194†	0	0.222	†mass fraction
Becker, et al. (1967)		1							0.186	2.4	0.212	2.4	0.29	marker nephlometry
van der Hegge Zijnen (1958)		1	0.156	-0.6	0.188	-	-	0.83						reported in Rajaratnam (1976)
Albertson, et al. (1950)		1	0.161	-	0.193	-	-	0.83						

Free plane jet

$$U_1 = 0$$

$$(\frac{U_j}{u_0})^2 = C_u(\frac{x}{h} - \frac{x_0}{h})$$

$$\frac{\overline{(u^2)}^{1/2}}{u_0} = constant$$

$$\frac{y_u}{h} = L_u(\frac{x}{h} - \frac{x_0}{h}) \tag{5}$$

$$(\frac{\Theta_j}{\theta_0})^2 = C_\theta(\frac{x}{h} - \frac{x_0}{h})$$

$$\frac{(\overline{\theta^2})^{1/2}}{\theta_0} = constant$$

$$\frac{y_\theta}{h} = L_\theta(\frac{x}{h} - \frac{x_0}{h})$$

Free round jet:

$$U_1 = 0$$

$$(\frac{U_j}{u_0}) = C_u(\frac{x}{D} - \frac{x_0}{D})$$

$$\frac{(\overline{u^2})^{1/2}}{u_0} = constant$$

$$\frac{r_u}{r_j} = L_u(\frac{x}{D} - \frac{x_0}{D}) \tag{6}$$

$$(\frac{\Theta_j}{\theta_0}) = C_\theta(\frac{x}{D} - \frac{x_0}{D})$$

$$\frac{(\overline{\theta^2})^{1/2}}{\theta_0} = constant$$

$$\frac{r_\theta}{D} = L_\theta(\frac{x}{D} - \frac{x_0}{D})$$

9

Here θ refers to any scalar quantity. r_u and r_θ are measures of the round jet diameter defined as the radial point where U/u_0 and Θ/θ_0 are 0.5. y_u and y_θ are corresponding values for the plane jet.

From a review of the literature values for the parameters in Eqs. 5 and 6 were estimated and the results are presented in Table 1 for plane and round jets. Time limitations precluded a similar review for mixing layers.

With regard to Table 1 several comments can be made. Considerable data are available describing the axial and lateral variations in mean quantities. But there is relatively little data on turbulence quantities in part because of the difficulty of obtaining such data. The power law dependency on x predicted from similarity is observed to good accuracy for both spreading rate and velocity and scalar quantities. There is however some scatter in the measured constants of proportionality. While the scatter is not so large as to preclude the use of the data for model development and validation, it is certainly a source of concern. Some of the scatter is most likely the result of experimental problems. For example Wilson and Danckwerts (1964) cite specific experimental problems in Corrsin and Uberoi (1950) (problems relating to the sensor performance). The Keagy and Weller (1952) concentration data also appear questionable perhaps due to bias in sampling from variable density flows. Also some departure from similarity in the Keagy and Weller data is expected since measurements were made only to 24 x/d. The scalar data of Jenkins and Goldschmidt (1973) are suspect since they are reported in an inappropriate similarity form

$$\left(\frac{\Theta_j}{\theta_0}\right)^{1/2} = C_\theta\left(\frac{x}{h} - \frac{x_0}{h}\right)$$

Random error may also be a contributory factor to the scatter in the parameters presented in Table 1. However, axial and lateral profile data do not exhibit sufficient scatter to support this possibility.

Another likely source of problem is that in the regions of most measurements the flow is not fully developed in that the turbulence properties are not fully developed. As noted Wygnanski and Fielder (1969) found that the second moments and correlations do not obtain similarity until $x/D > 60$ and that C_u varied from .179 to .203 when far downstream data are considered in finding its value. Given such a large change in C_u this explanation for scatter in the data seems quite reasonable.

Some of the scatter in the C_u data is attributable to variations from one flow apparatus to another in the initial, mean, axial velocity profile. By definition U_j is a momentum flux weighted velocity; $\rho_j U_j^2 \pi D^2/4 = 2\pi\int \rho_j U^2 r dr$. However jet velocities are frequently obtained from volume flow rate measurements, and in such cases the ratio between U_j and the measured, volume flow rate based U depends on the initial velocity profile. Thus when a volume flow rate weighted velocity is used for U_j, the resulting value for C_u will depend on the initial velocity profile thereby introducing apparent scatter into data for C_u obtained from different experimental apparatuses with differing initial velocity profiles.

For plane jets the question of attainment of similarity is confused by the ultimate transition of the flow from two dimensional to axisymmetric far downstream of the jet nozzle. The region of this transition depends on the aspect ratio of the jet nozzle. The greater the aspect ratio the further downstream the transition occurs, and therefore the greater is the region in which the plane jet can become fully developed. If the jet nozzle aspect ratio is too small, the plane jet will never attain similarity. For higher aspect ratio jets care must be taken to distinguish the plane jet region with similarity from the transition region further downstream. The problems of attaining similarity and differentiating the similar region from the transition region may be the explanation of some of the observed scatter in Table 1b (eg. the data of Heskestad is obtained quite far downstream) and of the variations in C_u and L_u with AR. Other explanations such as dependency on initial conditions and on conditions in the surrounding fluid have been offered as noted above. Such sensitivity may imply that the flow is not fully developed.

Further jet experiments at large x/D are recommended to help determine the cause of the observed variations and to obtain good values for the constants appearing in the similarity relations. These measurements will be quite difficult since the quantities to be measured will be far below their initial values, and there may be subtle room interference effects which will be difficult to detect. Similarity is an important and useful concept, and additional research to answer these questions is fully justified. In the present context for constant density mixing flows, similarity allows data only for velocity and data only for scalar quantities obtained in different experiments or at different times in the same apparatus to be used together for model evaluation purposes.

There is considerable scatter in the data for x_0. Since x_0 depends on the initial conditions and on the development of the initial mixing layers in the potential core region of the jet, this scatter should not be surprising. As most turbulence models are not intended to model both the initial region of mixing and the downstream region, comparison of x_0 from model with experimental data does not seem worthwhile. On the other hand, it should be noted that strict similarity requires that x_0 for velocity and scalar fields be the same, and variations in x_0 between velocity and scalar may be an indication of both lack of similarity and of experimental problems.

With assumptions, the most significant being the introduction of a constant eddy viscosity, expressions for the lateral variation of U/u_0 can be obtained (see Eq. 1). For free jets these expressions are (Townsend, 1976):

Plane jet:

$$f(\varsigma) = sech^2(0.88\varsigma) \tag{7}$$

Round jet:

$$f(\varsigma) = (1 + 0.414\varsigma)^{-2} \tag{8}$$

where ζ equals y/y_u or r/r_u as appropriate.

Experience has shown that for free jets initial density differences between the jet fluid and surrounding fluid are quickly reduced to relatively low levels. Therefore in regions where the flow has become similar, in many cases it may also be considered to be a constant density flow even when there is an initial density difference. For these flow cases, Thring and Newby (1952) using momentum conservation have shown that the influence of the initial density difference on the flow in the similar region may be accounted for replacing D(or r) by

$$D_e = D(\frac{\rho_j}{\rho_1})^{1/2} \tag{9}$$

in the constant density scaling expressions given above. To show this result consider a free round jet. After neglecting contributions to the total momentum flux from normal turbulent stresses and assuming a uniform pressure, one can show for the total momentum flux that

$$2\pi \int_0^\infty r dr \rho_1 \overline{U}^2 = \frac{\pi}{4} D^2 \rho_j U_j^2 = \frac{\pi}{4} D_e^2 \rho_1 U_j^2 \tag{10}$$

It is assumed that $\rho = \rho_1$ at the point of interest. Clearly for this to be true D_e must be defined as above and thence $\overline{U}$ will scale as in the constant density case. Several investigators (eg. Wilson and Danckwerts, 1964) have tested this scaling and found it to be satisfactory. However the alternate length scale, d_e, is used only in the expression for U_j/u_0 and not in the other expressions in Eq. 6 which is not logical. Instead it would be more logical to introduce an alternate velocity scale, U_e, to reflect variations in momentum flux with variations in ρ_j.

$$U_e = U_j(\frac{\rho_j}{\rho_1})^{1/2} \tag{9a}$$

and thus

$$C_u = C_u^e(\frac{\rho_j}{\rho_1})^{1/2}$$

Here C_u is the measured C_u using U_j as the velocity scale, while C_u^e is a constant (independent of ρ_1/ρ_j) velocity scale parameter which one would obtain using U_e as the scale. Similar reasoning for scalar quantities leads to

$$\Theta_e = \Theta_j(\frac{\rho_j}{\rho_1})^{1/2}$$

and $\qquad$ (11)

$$C_\theta = C_\theta^e(\frac{\rho_j}{\rho_1})^{1/2}$$

In the above the scalar could be either temperature or species mass fraction. No correction to Θ is needed when mole fraction units are used for species mixing in a constant temperature, constant pressure jet since in that case ρ does not appear in the species conservation expression. Finally it is noted that for a free plane jet the same correction factors apply.

The data in Tables 1a and 1b are analyzed according to the correction given in Eqs. 9a and 11 with the results presented in Table 2. It is seen that in general the correction gives the right trend, but the quantitative results are not as good as those reported by Wilson and Danckwerts (1964), Table 1a.

By substitution of the similarity relations into the momentum-flux relationship, Eq. 10, an expression relating the constants in the centerline velocity scaling and the scaling for l_0(y_u or r_u) is obtained in terms of f. For a free round jet one obtains

$$\frac{C_u}{L_u} = \left(2\int f^2 \varsigma d\varsigma\right)^{1/2} = 0.897 \tag{12}$$

where f is given above. For free plane jet

$$\frac{C_u}{L_u} = \left(2\int f^2 \varsigma d\varsigma\right) = 1.515 \tag{13}$$

Comparison with experimental results, Table 1, shows satisfactory agreement. But the agreement is not good enough to use either Eq. 12 or Eq. 13 to find one constant from the other. The observed differences may be attributed to at least two causes, other than experimental error: a) the neglect of normal stresses in Eq. 10 and b) an unstaisfactory expression for f. If the f are wrong, and it is likely that they are not absolutely correct, doubt is easily cast on the assumption of constant eddy viscosity.

The data presented in Table 1 are useful in the evaluation of turbulence models, but the results of comparison should be interpreted with discretion. There are enough outstanding questions regarding these data as noted above to make it inappropriate to recommend at this time a particular set of values. This task is for the time being left to the modeler.

Data for free shear flows obtained from experiments where both velocity and scalar were measured are summarized in Table 3. A review of

Table 2.

Reference	R	C_u	C_u^e	C_θ	C_θ^e
Plane jets:					
Antonia and coworkers (1983-84)	1.087	0.143	0.137	0.18	0.173
Davies, et al. (1974)	1.049	0.146	0.142	0.252	0.246
Jenkins and Goldschmidt (1973)	1.037	0.160	0.157		
	1.07	0.160	0.155		
	1.117	0.160	0.151		
Bashir and Uberoi (1975)	1.2	0.22	0.201	0.29	0.265
	1.2	0.206	0.188	0.276	0.252
	1.2	0.24	0.219	0.258	0.235
Round jets:					
Corrsin and Uberoi (1950)	1.05	0.193	0.188	0.28	0.273
	2.00	0.225	0.159	0.32	0.226
	1.57	0.175	0.140	0.238	0.190
Keagy and Weller (1950)	0.63	0.096	0.121	0.173	
	1.04	0.120	0.118	0.108	
	7.25	0.281	0.1044	0.050	
Lockwood and Moneib (1980)	1.86		0.278	0.278	0.204
Wilson and Danckwerts (1964)	range		0.155		0.175

Table 3. Free Shear Flows.

Reference	Flow	Measurements Reported: Velocity	Measurements Reported: Temperature	Measurements Reported: Other	Probe Characteristics	Comments
Antonia and Bilger (1976)	round jet in wind tunnel. d=15.9mm; 305×305mm; θ_j=170C; U_j=45.7m/s; U_j/U_1=16.8, 5.6 & 3.0; R=1.571; Re=26100, 22800, 18500	radial profiles of $\langle U\rangle$, $\langle u^2\rangle^{1/2}$, $\langle u\theta\rangle$ at several x/d. Axial profiles of $\langle u^2\rangle^{1/2}$ to x/d=70.	$\langle\theta\rangle$, $\langle\theta^2\rangle^{1/2}$ radial profiles at several x/d and along centerline to x/d=80.		constant temperature hot-wire for velocity, compensated (to 20 kHz) cold-wire for temperature	$\langle uv\rangle$ and $\langle\theta v\rangle$ inferred from data by calculation
Antonia, Prabhu and Stephenson (1975)	round jet in wind tunnel. d=20.3mm; 305×305mm. θ_j=34C; U_j=32m/s; T_1=15C; U_j/U_i= 6.6, 2.9 & 1.9; Re=41500, 32000, 23200	$\langle U\rangle$, $\langle U\rangle^{(1)}$, $\langle u^2\rangle^{(1)}$, $\langle v^2\rangle^{(1)}$, $\langle uv\rangle^{(1)}$, $\langle uv\rangle$, $\langle v^2\rangle$, S_u, K_u, $S_u^{(1)}$, $K_u^{(1)}$, and S_v, K_v, $S_v^{(1)}$, $K_v^{(1)}$	γ_θ, f_γ, $\langle\theta\rangle$, $\langle\theta\rangle^{(1)}$, $\langle\theta^2\rangle$, $\langle\theta^2\rangle^{(1)}$, $\langle u\theta\rangle$, $\langle u\theta\rangle^{(1)}$, $\langle v\theta\rangle$, $\langle v\theta\rangle^{(1)}$, S_θ, K_θ, $S_\theta^{(1)}$, $K_\theta^{(1)}$	budgets	constant temperature X hot-wire, compensated cold-wire.	Temperature used to obtain I. First moments are similar; higher moments are not. Data only at one axial station, x/d=59.
Bashir and Uberoi (1975)	Plane jet, slot size = 3.175×127mm. θ_j=60C; U_j=15.24m/s; Re=2770.	$\langle U\rangle$, $\langle u^2\rangle^{1/2}$, $\langle v^2\rangle^{1/2}$, $\langle w^2\rangle^{1/2}$ on centerline to x/h=56. f_u x/d=40. $\langle U\rangle$, $\langle u^2\rangle^{1/2}$, $\langle v^2\rangle^{1/2}$, $\langle w^2\rangle^{1/2}$ along centerline for AR=20 & 144.	$\langle\theta\rangle$, $\langle\theta^2\rangle^{1/2}$ at many axial stations to x/h=56. γ_T, $\langle v\theta\rangle$, $\langle v\theta^2\rangle$, $\langle\partial\theta/\partial^2 t\rangle$, f_θ at x/h=40; $\langle\theta\rangle$, $\langle\theta^2\rangle^{1/2}$ along centerline for AR=20 & 144.		Constant temperature hot-wire for velocity and cold-wire for temperature. Temperature checked with thermocouple.	There is significant variation in centerline decay with AR. May be the result of 3-dimensional effects.
Batt (1977)	Plane mixing layer. u_0=23 & 50 ft/s; $\langle u^2\rangle^{1/2}/u_0$ < 0.4%; θ_0=4.5, 35.8, 53.6 C.	$\langle U\rangle$, $\langle u^2\rangle$, f_u, δ, $P(U)$, $\langle vu\rangle$, $R_{uu}(x,\tau)$	$\langle\theta\rangle$, $\langle\theta^2\rangle$, γ_θ, δ, S_θ, K_θ, $P(\theta)$, f_θ, $\langle v\theta\rangle$	$\langle C_{NO_2}\rangle$, $\langle c^2_{NO_2}\rangle^{1/2}$, δ, $P(C_{NO_2})$, f_{NO_2}	Constant temperature hot-wire for velocity, 5 kHz response; cold-wire for temperature, 1 kHz response. NO_2 by fiber-optic probe, vol.=0.1×0.1×0.039ins, flow visualization.	$N_2+N_2O_4 \rightarrow 2NO_2+N_2$ reaction studied. NO_2 probe is large and has poor spatial resolution.
Catalano, Morton and Humphries (1977)	round jet in wind tunnel. U_1=3.20m/s; U_j/U_1=5.1; d=2.14cm; Re=22,600	$\langle U\rangle$, $\langle u^2\rangle^{1/2}$ profiles at x/d=2,4,6,8. $\langle u^2\rangle^{1/2}$ at 0. Also $R_{uu}(\tau)$, f_u.	$\langle u,\theta\rangle$ x/d=2,4,8. γ_θ at x/d=0,2,4,6,8.		LDV and marker nephelometry.	dp/dx not given. Jet marked with dioctyl-phthalate.

Table 3. (Cont.)

Chevray and Tutu (1978)	free jet. θ_j=20C; U_j=25m/s; d=22.5cm, Re=423600.	$\langle U\rangle$, $\langle u^2\rangle$, $\langle v^2\rangle$, $\langle uv\rangle$, $\langle u\theta\rangle$, $\langle v\theta\rangle$	$\langle\theta\rangle$, $\langle\theta^2\rangle$		Constant temperature hot-wire for velocity. Cold-wire for temperature.	Conditional and unconditional measurements at one x/d, x/d = 15.
Davies, Keffer and Baines (1975)	Plane jet. Slot size = 51×305mm. θ_j=14.6C; U_j=13.5m/s; Re=51800	γ_u, $\langle u^2\rangle^{(1)1/2}$ at x/h=20. $\langle U\rangle$, $\langle U\rangle^{(1)}$, $\langle u^2\rangle^{1/2}$ at x/h: 10, 12.5, 15, 17.5, 20, 22.5, 25. y_u, U_j^2/u_o^2 vs. x/h.	$\langle\theta\rangle^{(1)}$, γ_θ, $\langle\theta^2\rangle^{(1)1/2}$ profiles at x/h=10. $\langle\theta\rangle$, $\langle\theta^2\rangle^{1/2}$, $\langle\theta\rangle^{(1)}$ at 10, 12.5, ..., 25. y_θ, y_γ along centerline.		Single constant temperature hot-wire and cold-wire for velocity and temperature, 2 kHz frequency response.	
Fielder (1974)	axisymmetric mixing layer u_o=8m/s; θ_o=26C	$\langle U\rangle$, $\langle V\rangle$, γ_u	$\langle\theta\rangle$, $\langle\theta^2\rangle$, S_θ, K_θ, f_θ, $R_{\theta\theta}(\tau)$, $\langle\theta\rangle^{(1)}$, $\langle\theta^2\rangle^{(1)}$		Parallel constant temperature hot-wire for velocity and cold-wire compensated to 2 kHz for temperature.	Initial mixing layer of free, axisymmetric jet. Self-preserving first moments for x/d > 5/3.
Fielder, et al. (1977)	Axisymmetric mixing layer. u_o=10 m/s; θ_o=26C		$\langle\theta\rangle$, $\langle\theta v\rangle$, $\langle v\theta^2\rangle$, $\langle\theta^2\rangle$			Acoustic excitation of mixing layer studied.
Jenkins and Goldschmidt (1973)	Plane jet. Slot size = 1.27×30.4 cm.	$\langle U\rangle$ on centerline and y_u to x/h=70. $\langle U\rangle$ profiles at x/d=25,35, 45,55.	$\langle\theta\rangle$ on centerline and y_θ to x/h=70. $\langle\theta\rangle$ profiles at x/d=25,35, 45,55.		Pitot-probe and constant temperature hot-wire for velocity. Cold-wire for temperature.	No influence of varying θ_j observed. Reported axial variation of θ_o does not follow similarity. See Table Ia.
Keagy and Weller (1950)	Free jets of He, N_2 and CO_2 (R=7.25, 1.04, 0.63); d=0.128 in, U_j=400 ft/s; Re=3600, 27700, 54700.	$\langle U\rangle$ on centerline, radial profiles at x/d= 8, 16, 24.		$\langle C\rangle$ on centerline and at x/d= 8, 16, 24.	Pitot and gas sampling probes.	Sensitivity of $\langle C\rangle$ to sampling rate found negligible.

Table 3. (Cont.)

Sreenivasan, et al. (1977)	Axisymmetric mixing layer (initial region of large free jet, d=48mm). Θ_j=13C; U_j=15.1 and 4.8 m/s; $\langle\theta^2\rangle_j^{1/2}/\Theta_j < 1\%$.	$\langle U\rangle$. For P(u), $\langle u^2\rangle^{1/2}$, S_u, K_u and $\langle\theta u\rangle$ both conditioned and unconditioned results reported.	$\langle\Theta\rangle$, P(θ). For $\langle\theta^2\rangle^{1/2}$, S_θ and K_θ both conditioned and unconditioned results reported.		Pitot probe and constant temperature hot-wire for velocity. Cold-wire for temperature, 6 kHz frequence response.	Transition to turbulence occurred at x/d=0.25.
Venkataramani et al.(1975)	Round jet. d=22.5cm Re=3×10^5	P(U), P(V) P(U,V), P(V,θ) at x/d=15, r/d=0, 1.0, 1.89. P(U,θ) at r/d=0.	P(Θ), γ_θ at same locations.		Constant temperature hot-wire and cold-wire used.	Limited spatial information. Moments of pdf's reported.
Wilson and Danckwerts (1964)	Round jet. Θ_j=200,181,144,123,99, 79,52,21,12C. $U_j = \leq$ 100m/s d=0.5 in Re=20,000-40,000.	$\langle U\rangle$ on centerline and radial profiles. r_u and u_o reported also.	$\langle\Theta\rangle$ and $\langle\theta^2\rangle^{1/2}$ center-line and radial profiles. r_θ and Θ_o also reported.		Pitot probe for velocity and cold-wire for temperature.	Θ_o and u_o correlated by form of $C^e\sqrt{R}(x/d-x_o/d)$.

this table shows that there are several problems in using the data for model evaluation. In some cases data were obtained at only one or a few axial stations usually at small x/D - eg., Keagy and Weller (1950), Chevray and Tutu (1978), Catalano et al. (1976), Venkatanamie (1975). Also there are cases where only a few or no turbulence properties were measured - eg., Fielder (1974) does not measure $\overline{u\theta}$ or $\overline{uv}$, the only turbulence property measured by Wilson and Danckwerts (1964) is θ^2, and Sreenivasan et al. (1977) do not give data for uv.

With regard to the plane jet data it is noted that Bashir and Uberoi (1975) report data on y_u and U_j/u_0 for three different aspect ratio jets (20, 40 and 144). They find different centerline variations in all three cases. This may be the result of three dimensional effects arising in the downstream portion of the jet. Krothapalli et al. (1981) have studied the effect of nozzle aspect ratio on the development of plane jets. The plane jet is divided into three regions - an initial mixing region, a two-dimensional region, and finally, far downstream, a three-dimensional region in which the plane jet evolves into an axisymmetric jet. As noted above if the nozzle aspect ratio is too small, the two-dimensional region may not be large enough for a similar flow to develop in that region. Even if a similar, two-dimensional flow obtains, care must be taken to distinguish the similar region from ajoining regions both upstream and downstream. The exact cause of the variations observed by Bashir and Uberoi is not clear. Unfortunately data for the 20 and 144 aspect ratio cases are too sparse to detect different regions of jet growth by changes in the centerline variations of u_0 and θ_0. Everitt and Robbins (1978) also report aspect ratio effects in data for the spread of plane jets (see Table 1a).

Of the data in Table 3 those of Batt (1977) and Antonia and Bilger (1976) seem the most useful. However Batt's optical probe is quite large raising concern about spatial resolution and possible flow distortion. In addition the boundary conditions in the experiment are not well defined. The shear flow is obtained by essentially removing one wall of a wind tunnel and entraining ambient air. This type of flow is not as cleanly defined as is a two-dimensional shear flow generated by a splitter plate. Antonia and Bilger (1976) present data obtained in coflowing streams with varying U_j/U_1 over a good range of x/D. As the data verify, these flows do not achieve similarity, and thus they cannot be checked against the data in Table 1. On the other hand in coflowing streams, accurate velocity measurements can be made to large x/D and r/D without encountering error associated with low mean velocities and high turbulent intensity, eg. instantaneous flow reversal, an advantage for measurements in coflowing streams. Antonia and Bilger (1976) present a somewhat limited set of turbulence data, $\overline{u^2}$, $\overline{u\theta}$ and $\overline{\theta^2}$ while uv is inferred from the mean flow data. It should be noted that there are other coflowing stream data from Antonia, Bilger, and coworkers (Antonia and Bilger, 1973, and Antonia et al, 1975) obtained in the same wind tunnel facility. However the data are for different initial jet diameters (D) and therefore while they complement the data of Antonia and Bilger (1976), they do not supplement it.

Recently, Antonia and co-workers have presented a series of papers containing extensive data for a free, plane jet which because of their breadth and depth appear to be well suited for model development and evaluation (Browne et al. 1984, Browne and Antonia, 1983, Antonia and Browne, 1983, Antonia et al., 1983a, Antonia et al., 1983b, Browne et al. 1983, Antonia et al., 1984). The extent of these data is summarized later in Table 6.

Inlet and boundary conditions are well characterized, and a broad range of turbulence data are available as well as profiles of mean velocity and temperature. The initial flow is laminar with laminar boundary layers (0.23 mm momentum thickness). $\overline{u^2}^{1/2}/U_j$ and $\overline{\theta^2}^{1/2}/\Theta_j$ values measured at x/h = 0 vary slightly from paper to paper but are less than 0.002 in all cases. Turbulence data presented in the various papers include lateral profiles of $\overline{q^2}$, $\overline{\theta^2}$, $\overline{uv}$, $\overline{u\theta}$ at as many as 8 axial locations to x/h = 40. Similarity is found to obtain for x/h > 20. The lateral profiles are carried to $y/y_u = 1.4$; beyond this point high turbulence intensity precludes accurate measurements. $P(\theta)$, S_θ, K_θ, f_θ, and correlation data are also presented for many locations in the flow. Antonia and Browne (1983) present data on the dissipation of $1/2\overline{\theta^2}$ which include terms such as $v\theta_z{}^2$. Data for centerline properties are presented to x/h = 40, while several lateral profiles are reported up to x/h = 40. Additional lateral profiles at larger x/h would be desirable especially to see if the evolution of the turbulence properties to similarity is complete.

With a laminar initial flow, transition to turbulence occurs in the calculation domain. For models which do not calculate transition, as is generally the case, some manipulation of the initial conditions is required but certainly is not desirable. Another problem with these data in regards to model validation and evaluation, is the presence of large scale fluctuations at the end of the potential core region and beyond. Several investigators have reported such fluctuations in free plane jets, and Antonia et al. (1983a) present considerable information on the nature of the fluctuations in their jet. (NB: Fluctuations have also now been observed in two-dimensional wake flows up to very high Reynolds number (Tritton, 1977) where previously they were thought not to exist. One wonders how long it will be before they are found regularly in round free jets.) Relative to other plane jet experiments, the aspect ratio of the Antonia and coworker's jet (19.7) is rather small (see Table 1a) as is the initial Reynolds number (7620) based on h. Also the flow constants, C_u and C_θ, are low relative to other results. At this point one cannot say for sure that the data of Antonia and coworkers are free of three-dimensional effects stemming from a low aspect ratio. In spite of these drawbacks these data appear, because of their breadth, to be the most useful data for model development and evaluation available at the present time.

Although perhaps unnecessary, it should be noted that the comments made in this review do not constitute a general evaluation of the quality and value of the experimental data reviewed. Model evaluation is only one of many applications for experimental data and a rather new application. In most of the reviewed research model evaluation was not a consideration or was only one of several considerations in the design and the conduct of the experiment.

Variable density mixing flows

An extensive body of literature exists on turbulent variable density flows. Experimental measurements have been made using numerous experimental techniques under widely varying flow conditions and geometries. A summary of those studies most relevant to the present report is presented in Tables 4 and 5. The two major categories of variable density nonpremixed flows to be considered in the following discussion are axisymmetric and planar jets (Table 4) and two-dimensional shear layers (Table 5). Turbulent jets are a classic turbulent mixing problem that have been studied extensively in the literature. They provide a simplified flow geometry that is well suited to modeling calculations. Unfortunately, large density variations are limited to regions several diameters downstream of the jet exit and rapidly decrease with increasing axial distance. Two-dimensional shear layers have recently received greater attention and provide a mixing region in which density differences can be maintained farther downstream than with jet flows. Recent measurements have identified the possible role of large-scale structures in the mixing process. These structures may cause difficulties in the application of current modeling calculations to flows of this type where large-scale structures play an important role in the mixing process. At the beginning of each table the corresponding geometric configuration is shown. Individual studies are listed in the tables, together with relevant dimensions and flow conditions of the experiment, the diagnostics applied, and the experimental quantities measured.

The experiments presented in Table 4 correspond to jets of one density flowing into either a quiescent or a coflowing gas of different density. This class of flows is further subdivided on the basis of geometry into axisymmetric round jets (Table 4a) and two-dimensional planar jets (Table 4b). It should be noted that the term "two-dimensional" strictly applies to the test section geometry since the three dimensionality of turbulent flowfields is well known. The range of density ratios studied varies from the helium jets of Keagy and Weller (1949) and Aihara et al. (1975) flowing into air (with a density ratio ρ_j/ρ_a of 0.14) to the studies of Dyer (1979) and Schefer et al. (1985a) in which a propane jet into coflowing air was used ($\rho_j/\rho_a = 1.6$). All flows considered in Table 4 are parabolic except for perhaps in the region immediately downstream of the jet exit rim where, depending on the rim thickness, parabolic flow assumptions may be invalid due to flow disturbances and small recirculation zones caused by the jet rim.

Table 4a. Round Jets.

		Measurements Reported				
Reference	Flow	Velocity	Temperature	Other	Probe Characteristics	Comments
Keagy & Weller (1949)	Free round helium & CO_2 jet U_j=122 m/s; D=3.25 mm	$\overline{U}$: one centerline + 3 transverse profiles.		Concentration ($\overline{C}$): one centerline + 3 transverse profiles.	Pitot tube, Sampling probe, .762-mm bore	Low Reynolds number
Aihara, Koyama & Mortshita (1975)	Free round helium jet with and without an air co-flow Re = 2.95×10^3, D=1mm [Air] / [He] = 7	$\overline{U}$, $\overline{u'v'}$, $\overline{u'v'}$: 3 transverse profiles		Concentration ($\overline{C}$,$\overline{c'}$,$\overline{u'c'}$,$\overline{v'c'}$): 3 transverse profiles.	Hot wire for velocity and concentration. Sampling probe for mean concentration, 0.3-mm bore.	Low Reynolds number
Chigier & Strokin (1974)	CH_4 – diffusion flame D = 0.005m, R_e = 6600 U_j = 20.5 m/s, U_e=0.6 m/s	$\overline{U}$, u': one centerline and 2 transverse profiles		Dynamic pressure (ρu^2): one centerline prof. Concentration ($\overline{C}$): one centerline + 4 transverse profiles.	0.12mm coated thermocouple. Probe, 0.2-mm bore.	Flame + cold flow
Birch, Brown, Dodson & Thomas (1978)	Free round CH_4-jet in air R_e = 16000, D = 0.01265m U_e = ? $[CH_4]/[Air]$ = 0.55	u': one centerline profile		Concentration ($\overline{C}$,c') higher moments, integral time scales: one centerline + 3 transverse profiles; autocorrelation, power spectra, pdfs: one transverse profile	Raman spectroscopy probe volume 0.2mm x 2 mm.	Some velocity measurements, density can be inferred from concentration measurement. Axial velocity, mean, and RMS. No direct density measurements.

ROUND JET

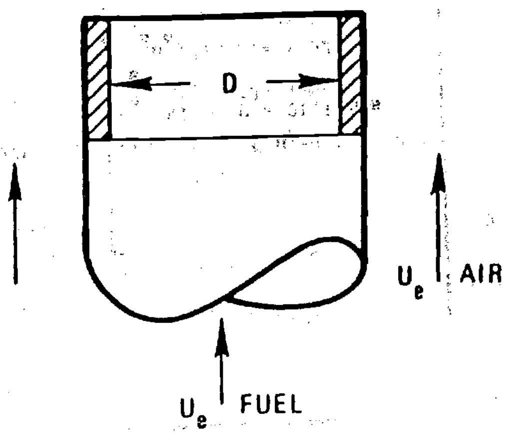

Table 4a. (Cont.)

		Measurements Reported				
Reference	Flow	Velocity	Temperature	Other	Probe Characteristics	Comments
Dyer (1979)	Free round C_3H_8-jet in air R_e = 9790, U_j = 21.1 m/s U_e = 0.7 m/x (air) $[C_3H_8]/[Air]$ = 1.52			Mole fraction ($\overline{X}_{C_3H_8}$): 3 transverse profiles (X/D = 15,20,30); rms: one transverse profile (X/D = 20).	Rayleigh scattering, probe volume 0.2mm x 1mm	No velocity or density measurements.
Lockwood & Moneib (1980)	Heated round jet R_e=5000, D = 19.3mm T_j = 225°C		$\overline{T}$, T', higher moments: one centerline + 8 transverse profiles; pdfs of T: 4 transverse profiles; power spectra.		12.7μm bare-wire thermocouple	Classical experiment. No density measurement. Density fluctuations small. Lots of data. No velocity.
Long, Chu & Chang (1981)	Free round jet R_e = 3240, 4160 [Air]/[Air] = 1.0			Jet Fluid Concentration ($\overline{C}$,c'): contours X/D = 3 to 8; two-point covariance.	Lorentz/Mie scattering (seed) Technique demonstration	Constant density mixing. No velocity Limited spatial regime.
Pitts & Kashiwagi (1984)	Round CH_4-jet in air R_e = U_j = 1.02 m/s, U_e = 0.34 m/s, $[CH_4]/[Air]$ = 0.55			Mass and mole fraction ($\overline{C}$,c'), higher moments, conditional moments, intermittency power spectra: one centerline + 1 transverse profile (X/D = 35).	Rayleigh scattering, time-resolved concentration probe, probe volume 0.035mm x 0.27mm.	No velocity or density measurements. Small density variation. Time resolution 5000 hz, 200μs. Confined, no pressure gradient.

Table 4a. (Cont.)

		Measurements Reported				
Reference	Flow	Velocity	Temperature	Other	Probe Characteristics	Comments
Schefer, Dibble and Hartmann (1985a, 1985b)	Round C_3H_8-jet in air Re=68168, D=5 mm U_j = 53 m/s; U_e=9.5 m/s, T_o - ambient, $\frac{[C_3H_8]}{[Air]} = 1.6$	$\bar{U}$, $\bar{V}$, u', v' u'v' and pdfs: one centerline + 3 transverse profiles.		C_3H_8 mixture fraction, density ($\bar{C}$, $\bar{P}$, C', P'), higher moments, pdfs, power spectra: one centerline + 3 transverse profiles.	2-color LDV, Rayleigh scattering, probe volume 0.2 mm x 1 mm.	Small density variation. Publication in preparation.
Dibble, Hartmann and Schefer (1985c)				C_3H_8, O_2, N_2 concentration ($\bar{C}$,c',u'c',v'c'), joint pdfs: 4 locations.	Simultaneous LDV – laser Raman spectroscopy.	
Dibble, Kollmann and Schefer (1985a)				Instantaneous radial profiles of mixture fraction:	One-dimensional Rayleigh imaging.	

Table 4b. Planar Jets.

		Measurements Reported				
Reference	Flow	Velocity	Temperature	Other	Probe Characteristics	Comments
Anderson, LaRue & Libby (1979)	Two-dimensional jet of helium discharging into moving airstream U_j = 120 m/s, U_e = 4/6 m/s	$\overline{U}$, u': several streamwise locations		Concentration ($\overline{C}$, c'): several streamwise locations	Hot wire for velocity and concentration	
LaRue & Libby (1977)	Boundary layer with He - injection U_j = 5 m/s, U_e = 2 m/s	$\overline{U}$, u', v', u'v': 6 transverse profiles		Concentration ($\overline{C}$, c', c'v'):	Hot wire for velocity and concentration	Geometry difficult. Helium injected into boundary layer.

PLANAR JETS

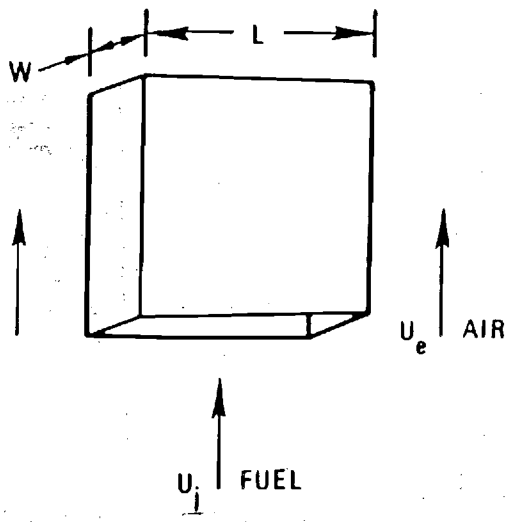

ANDERSON, LARUE & LIBBY (1979)

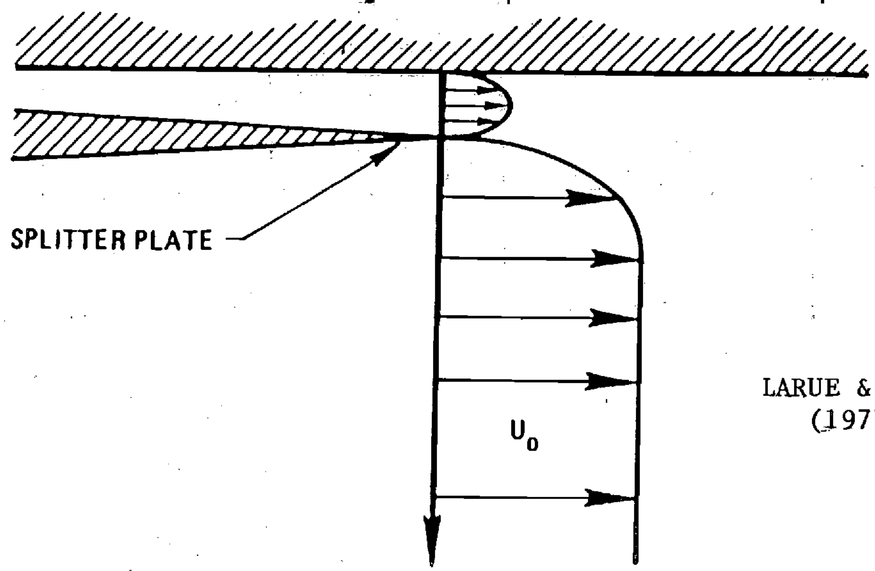

LARUE & LIBBY (1977)

Table 5. Plane Mixing Layer.

		Measurements Reported				
Reference	Flow	Velocity	Temperature	Other	Probe Characteristics	Comments
Rebollo (1973)	Plane mixing layer N_2-H_e at p = 4 atm	$\overline{U}$, u': transverse profiles		Density ($\overline{\rho}, \rho'$): transverse profiles	Pitot probe for velocity, Brown-Roshko probe for density.	
Brown & Roshko (1974)	Plane mixing layer, N_2-H_e $[N_2]/[He] = 7$ P = 7 atm $U_{He} = 5$ m/s; $U_{N_2} = 1.9$ m/s	$\overline{U}$: transverse profiles		Density ($\overline{\rho}$): transverse profiles	Probe, visualization Pitot probe for velocity. Brown-Roshko probe for density.	Low R_e Mean Values
Konrad (1976)	Plane mixing layer + wakes, $N_2 - H_e$, $N_e - H_e + Ar$			Concentration pdfs:	Probe	
Keller & Daily (1983)	Plane mixing layer $U_1 = 15$ m/x, $U_2 - 5$ m/s $T_2/T_1 = 6$	U,V,u',v' u'v', moments: transverse profiles.			2-color LDV forward scatter, probe volume 0.13 mm x 1.8 mm	Not clear that flow was parabolic (maybe elliptic). No scalar measurements.

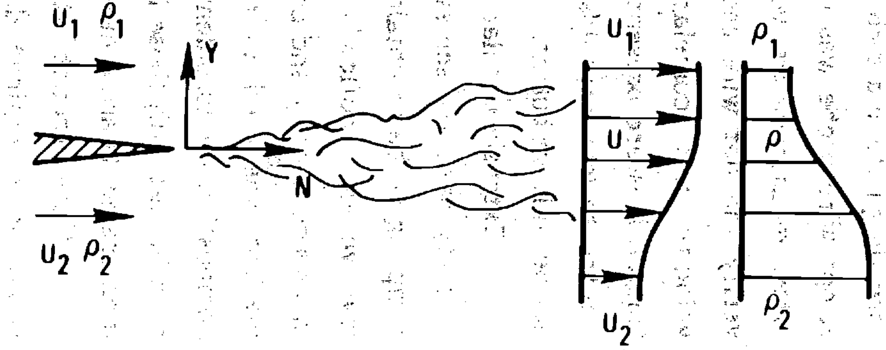

It is likely that these disturbances rapidly disappear downstream where the majority of mixing occurs. In either case modeling assumptions can be made for this region and its influence on downstream mixing can be qualified. Only four of the experiments in Table 4a for axisymmetric jets report measurements of both a scalar and velocity, while both experiments in a planar jet (Table 4b) report scalar and velocity data.

Keagy and Weller (1949) report measurements in 3.25 mm diameter helium and CO_2 jets into still air with a jet velocity of 122 m/s. Concentration and velocity profiles were taken along the centerline, and radial profiles were obtained at three axial locations. The measurements were obtained with a pitot tube for velocity and a sampling probe for concentration and are therefore limited to mean values.

Aihara et al. (1975) studied the effects of coflowing air on the spreading rate and turbulent transport rates in a 1-mm diameter helium jet. A hot wire probe was used to measure velocity and concentration and the latter measurements were compared with sampling probe measurements to verify the hot wire results. Detailed radial profiles of concentration and velocity and correlations between the velocity and concentration fluctuations are presented at several downstream locations. The results are limited to low Reynolds number conditions ($Re = 2950$) where the flow may not be fully turbulent.

Extensive scalar measurements have been made in methane jets but velocity data are somewhat limited. Chigier and Strokin (1974) used a gas sampling probe to obtain concentration measurements in a methane jet with low velocity coflowing air. Mean velocity was determined from the measured density and concentration and the dynamic pressure. A gas tracer method was used to calculate the turbulence intensity. The effects of combustion on turbulent diffusion were studied by comparing results in a reacting jet with those in a cold flow case. Mean concentration and velocity measurements are limited to centerline profiles for the cold flow case.

More recent studies of methane jets have been made using nonintrusive optical diagnostic techniques. Pitts and Kashiwagi (1984) demonstrated the usefulness of Rayleigh scattering for concentration measurements (methane on a mass and mole fraction basis) in turbulent flows and presented comparisons with constant and variable density jets. One radial profile and an axial profile along the centerline were obtained but no velocity data were presented and the jet exit Reynolds number was somewhat low (Re = 4130) for fully turbulent flow. Birch et al. (1978) obtained detailed radial profiles and an axial profile of the mean methane concentration and higher moments (up to the fourth moment). Velocity measurements were limited to axial velocity fluctuations along the centerline and comparisons were made with the centerline concentration fluctuations. This data could provide a suitable data set for modeling calculations in methane jets.

The temperature distribution throughout the flowfield of a heated air jet (T_j = 225 C) was measured by Lockwood and Moneib (1980) using a 12.7-μm thermocouple but no velocity measurements were made. Extensive data were obtained on the means and higher moments, pdf's and spectral density distributions, and comparisons were made with results in the literature.

Recent data has been obtained by Schefer and co-workers in an axisymmetric propane jet with coflowing air (Schefer et al. 1985a and 1985b, Dibble et al. 1985). The data are extensive and are well suited for model evaluation. Axial and radial velocities were measured using two-color laser velocimetry (LV). Velocity statistics conditioned on fluid originating from the jet and air streams were obtained by alternately seeding only the jet originating from the jet and air streams were obtained by alternately seeding only the jet and the coflowing air with LV seed particles. The results thus represent the extremes of biasing errors commonly encountered due to unequal seeding of the jet and air streams flows. Unconditional velocity statistics can be calculated from the intermittency profiles measured using Rayleigh scattering (density and propane mixture fraction) and laser Raman scattering (density, mixture fraction, and concentrations of O_2 and N_2). Time histories, power spectra, and mixing length information were obtained from the Rayleigh scattering measurements, and joint pdf's of individual species concentrations were obtained from the Raman scattering measurements. In addition, the Raman and LV systems were combined to measure simultaneously two velocity components and the scalars.

The flows listed in Table 4b consist of planar two-dimensional jets issuing into coflowing air. They are similar to the studies shown in the previous table in that two initially separated streams of different densities and velocities form a mixing layer downstream of the inlet section. Most apparent is the limited data that is available on plane mixing layers. Only two studies were found with sufficient data to make comparisons with modeling calculations. Anderson et al. (1979) used a three sensor hot wire probe to measure mean and fluctuating velocity and concentration in a helium jet discharging into a coflowing air stream. Spatial resolution of the probe was on the order of three times the estimated Kolmogoroff length scale (approximately 0.5 mm). Mean and fluctuating streamwise velocities and the mean and fluctuating concentration were presented at several streamwise locations. Range-conditioned point statistics were determined to provide the distribution of velocity and concentration statistics in the turbulent fluid elements at several locations.

LaRue and Libby (1977) used a similar hot wire probe to obtain velocity and concentration measurements in a turbulent wall boundary layer of air with helium injection through a slot adjacent to the outer wall. Measurements were reported of the streamwise and transverse velocity components, helium concentration, and density and their higher order correlations. Comparisons were also made between conventionally averaged and Favre averaged statistics. The boundary conditions are more complex than those for conventional axisymmetric and planar jets but the extensive data available make this a suitable case for the evaluation of computational models.

The flows of Table 5 correspond to two-dimensional shear layers in which two initially separated streams of different density and velocity form a mixing region downstream of a splitter plate. As mentioned previously, a major advantage of this flow configuration is that density differences are maintained farther downstream from the inlet than with axisymmetric or planar jets. These flows may, however, be subject to organized large-scale structures which may complicate comparisons with current modeling approaches. They would provide excellent test cases for emerging modeling approaches (e.g., vortex dynamics or hybrid schemes involving both vortex dynamics and large-eddy simulation) which attempt to calculate such large-scale structures.

Rebollo (1973) obtained measurements in a plane mixing layer of nitrogen and helium at a pressure of 4 atm. A pitot probe and a fast-response density probe were used to measure mean streamwise velocity and mean and fluctuating density, respectively. Transverse profiles at several streamwise locations were measured. Similar measurements were made by Brown and Roshko (1974) in a nitrogen and helium mixing layer at a pressure of 7 atmospheres, although only mean transverse velocity and concentration measurements are presented. Flow visualization studies were made showing the existence of large coherent structures which control the mixing layer development in this type of flow. These measurements were extended by Konrad (1976) who mixed argon with the helium flow to study the effects of density ratio.

The velocity measurements of Keller and Daily (1983) were obtained in a mixing layer of high-temperature combustion products and air (T_2/T_1 = 6). A two-color LV system was used to obtain pdf's of the streamwise and transverse components of velocity. From these pdf's transverse profiles of the means and higher moments (up to the fourth moment) and the Reynolds shear stress were determined at several streamwise locations. No scalar measurements are reported and it is not certain that the flow is truly parabolic.

RECOMMENDED CASES

Constant density flow

For reasons given in the LITERATURE SEARCH the recommended case for constant density flows is the plane jet case of Antonia and coworkers (1983-1984). This is done with some reservations concerning the transition to turbulence, large structure and three-dimensional effects mentioned above. Table 6 gives a summary of the flow, and data for comparison with model predictions should be taken from the literature.

Constant temperature hot-wires were used by Antonia and coworkers to obtain velocity data. Three different configurations were used: single wire, X-wires, and two parallel wires for gradient measurements. A constant current, cold-wire was used for temperature measurements. The spatial resolution of these measurements appears to be less than 1 mm. Browne et al. (1984) present accuracy estimates for their measurements; these are reproduced here:

$$\overline{U} = \pm 1.5\% \qquad \overline{\Theta} = \pm 3\%.$$
$$\sqrt{\overline{u^2}} = \pm 3\% \qquad \sqrt{\overline{v^2}}, \sqrt{\overline{w^2}} = \pm 4\% \qquad \sqrt{\overline{\theta^2}} = \pm 4\%.$$
$$\overline{uv} = \pm 7\% \qquad \overline{v\theta} = \pm 12\%.$$
$$Pr_t = \pm 14\%.$$

Variable density flow

The recommended case for variable density flows is the coflowing round jet with a nonreacting propane jet into coflowing air (Schefer et al. 1985a and 1985b; Dibble et al. 1984; Dibble et al. 1985a and 1985b). The description of the experimental facility and diagnostics will be limited since detailed descriptions are available elsewhere. Typical experimental data will be presented and compared with data for constant density and variable density jets found in the literature. Selected data from the present study are tabulated in the Appendix A to facilitate possible future comparisons with modeling calculations. The tabulated results include measurements of mean and fluctuating quantities, higher moments, and probability density distributions at selected locations in the flowfield (see Table 7). A more complete listing can be found in Schefer et al. (1985c) and tabulated data

Table 6

DATA SUMMARY

Flow Free Plane Jet

Data Evaluators Gouldin and Johnston

Case Antonia and Coworkers

Geometry

Re: 7,620
Aspect ratio 19.7
h = 12.7 mm
Mean dp/dx : practically zero

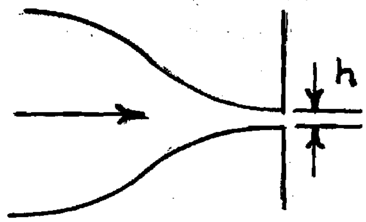

Mean quantities measured

$\bar{U}$ and $\bar{\theta}$ on centerline up to x/h = 40. Lateral profiles at x/h = 5, 7, 8, 9, 15, 20 and 40.

Turbulence quantities measured

$\overline{u'^2}$, $\overline{v'^2}$, $\overline{w'^2}$, $\overline{u'v'}$, $\overline{\theta'^2}$, $\overline{v'\theta'}$ on centerline up to x/h = 40 and lateral profiles at

x/h = 5, 7, 8, 9, 15, 20 and 40.

$p(\theta)$ and S_θ, K_θ on centerline up to x/h = 20.

Budget for $\frac{1}{2}\ \overline{\theta'^2}$ and data for $\overline{u'\frac{\partial\theta'^2}{\partial x}}$ and $\overline{v'\frac{\partial\theta'^2}{\partial x}}$ at x/h = 40

Initial conditions

Measured

Notes

Table 7

DATA SUMMARY

<u>Flow</u> Propane jet (round)

<u>Data Evaluators</u> Schefer and Johnston

<u>Case</u> Schefer, Dibble and Hartmann

<u>Geometry</u>

Re: 68,000
Mean dp/dx: 6 pa/m

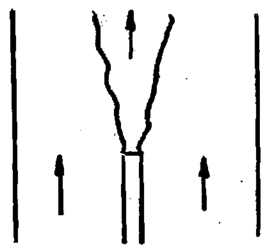

<u>Mean quantities measured</u>

$\bar{u}$ and $\bar{f}$ on centerline up to x/D = 80. Radial profiles at x/D = 15, 30, 50.

<u>Turbulence quantities measured</u>

$\overline{u'^2}$, $\overline{v'^2}$, $\overline{u'v'}$. $\overline{f'^2}$, $\overline{f'^3}$, $\overline{f'^4}$, p (u, v), p(f) on

centerline up to x/D = 80.

Radial profiles at x/D = 15, 30, 50. Also p (u, v, f) at x/D = 30, 50 on r/D = 0, 2.

<u>Initial conditions</u>

$\bar{U}_{air} = 9.2$ m/s, $\overline{u'^2} / \bar{u} = 0.02$, $\bar{u}_{jet} = 53$ m/s and $\bar{u}$, u', $\bar{f}$, f' at x/D = 4.

<u>Notes</u>

No flow visualization

Vertical tunnel

Density obtainable from mixture fraction are currently available on magnetic tape through Sandia National Laboratories Livermore.

Experiment

All measurements were performed in the Sandia Turbulent Diffusion Flame Facility. A complete description of the facility is given in Dibble et al. (1984). The experimental diagnostics used in the study and the corresponding quantities measured are summarized in Table 8. The experimental methodology followed in the investigation is illustrated by the order in which the diagnostic techniques and measurements are listed in the table. Test section dimensions and the inlet conditions are summarized in Table 9. Measurements at the test section inlet using hot-wire anemometry and laser velocimetry showed the velocity profile at the jet exit to be fully-developed turbulent pipe flow. A thin boundary layer was also measured along the outer edge of the jet pipe with a thickness of approximately 0.3 jet diameters at the exit plane of the jet. This facility is similar to that used in previous studies with the exception that the axis of the test section has been oriented vertically instead of horizontally to eliminate flame asymmetry (for combustion measurements) due to buoyancy effects.

Rayleigh scattering was used for single-point density and propane mixture fraction measurements. A complete description of the Rayleigh scattering system is given in Schefer et al. (1985d). Since in the measurements a cw argon ion laser was used, data rates of 16 kHz were possible and spectral information on the time histories of the flow properties at a point could be obtained. The laser beam was focussed with a 35 cm focal length lens to a 200-μm waist diameter. The measurement volume defined by the entrance slit to the photomultiplier tube (3 mm wide, 2 mm high) and the laser beam diameter was 1 mm in length by 0.2 mm in diameter. At each spatial location 64000 measurements were taken at a sample rate of 16000 samples per second. This sample rate resulted in frequency components up to 8 kHz contributing to the mean and fluctuating Rayleigh signal.

TABLE 8. EXPERIMENTAL DIAGNOSTICS

Diagnostic	Quantity Measured
CW Rayleigh Scattering	Single-point density and mixture fraction
Laser Doppler Velocimetry	Simultaneous single-point axial and radial velocities
Raman Scattering	Simultaneous single-point species concentrations (C_3H_8, O_2, N_2)
Combined LDV-Raman Scattering	Simultaneous single-point species concentrations and two-velocity components
One-dimensional Rayleigh Imaging	Instantaneous radial profiles of density and mixture fraction

TABLE 9. TEST SECTION DIMENSIONS AND INLET CONDITIONS

Test Section	30 cm x 30 cm
Jet Tube Exit	0.52 cm (I.D.)
	0.90 cm (O.D.)
Length of Jet Straight section prior to exit	2 m
Jet Velocity (Bulk)	53 m/s
Coflow Air Velocity	9.2 m/s
Reynolds Number (based on jet exit dia.)	68000
Coflow Air Turbulence	0.4%
Axial Pressure Gradient	6 Pa/m

In addition, the single-point Rayleigh scattering measurements were extended to one-dimensional using an optical multichannel analyzer (OMA) to obtain information on instantaneous gradients in the flowfield. This data has been published elsewhere (Dibble et al 1985a) and will not be discussed further.

Velocity measurements were made using a two-color laser velocimeter. The LV system (see Schefer et al. 1985b) includes a two-color, dual-beam, real-fringe system which had a measurement volume, as defined by the image of the pinhole on the beam crossing, 0.3 long by 0.20 mm in diameter. Coincidence of the radial and axial velocity measurements was verified with a multichannel interface with a variable time window set at 10 μs to assure that the velocity measurement in each direction was from the same seed particle.

In the analysis of the velocity data, it is assumed that the seed particles follow the motion of the fluid and that the difference between the diffusivity of the particle and the fluid is negligible. These assumptions are asymptotically valid in the limit of large Reynolds number. With these assumptions, the motion of a seed particle is identical to the motion of a fluid element and fluid originating from the jet can be distinguished from fluid originating from the coflowing air. Thus by alternately seeding only the jet and the coflowing air streams, velocity statistics conditional on the jet fluid and on the coflowing air fluid can be obtained.

The data are presented as mean and fluctuating velocity components (axial and radial velocities) conditional on fluid originating from the jet and air streams, and simultaneous measurements of both velocity components.

Raman measurements of gas species concentrations were made using a high-power pulsed dye laser (1 J/pulse, 2-μs pulsewidth, λ = 514.5 nm, $\Delta\lambda$ = 0.4 nm). Further details of the Raman scattering system can be found in Dibble et al. 1984. The beam was focussed to a 500-μm waist diameter which was aligned to overlap the LV measurement volume. The width of the spectrometer entrance slit determined the length of the Raman probe volume (1 mm), while the height of the probe volume was determined by the laser beam diameter. The vibrational Raman scattered light from C_3H_8 was separated from the collected light with a 3/4 m grating spectrometer and measured on a photomultiplier tube at the exit plane of the spectrometer. At each spatial location a minimum of 2500 simultaneous pairs of axial and radial velocity and mixture fraction were measured.

The data were extended to include simultaneous measurements of two velocity components and species concentrations by combining the Raman scattering system with the two-color LV system (Dibble et al. (1985b). Information on the important turbulent transport terms used in modeling equations was obtained from this data.

Error analysis

Rayleigh scattering has been used to measure concentration, temperature, and density (Johnston et al. (1985)). In addition, recent studies have demonstrated its applicability to both nonreacting and reacting turbulent flows (Pitts and Kashiwagi (1984), Schefer and Dibble (1985d)). In a two-component, isothermal flow such as the nonreacting propane jet reviewed here, the Rayleigh signal intensity is directly related to the propane mole fraction. The primary sources of error in the Rayleigh scattering measurements are background scattering and shot noise. The major source of background scattering was laser light scattered from the test section windows. Background scattered light was measured by moving the collection optics off the laser beam (thus eliminating the Rayleigh scattered light contribution to the total signal). Using this technique the background signal was found to be approximately 4 percent of the Rayleigh signal measured from pure air. At each measurement location the contribution of background scattering was eliminated by subtracting its value from the measured signal. Particle Mie scattering was effectively eliminated as a source of background scattered light by filtering particles from the coflow air upstream of the test section inlet. Detailed discussions of shot noise and its affect on the measurement of turbulent quantities can be found elsewhere (Pitts and Kashiwagi (1984)). An estimate of the shot noise contribution was made for the present experimental configuration from Rayleigh scattering measurements in air and found to be 3 percent.

Conditional statistics were obtained for the mean and fluctuating velocities and the correlation between the axial and radial velocity $\overline{u'v'}$. At each measurement location approximately 3,000 velocity measurements were obtained. This was estimated to be sufficient for the first two moments of the velocity. The correlation $\overline{u'v'}$ calculated from 3,000 measurements was found to agree within 2 percent of the value calculated from up to 10,000 measurements. In the present flow the primary source of error that must be considered is bias due to the proportionality of particle flux through the measurement volume to the instantaneous velocity. This may give rise to a statistical bias toward higher velocities when number-weighted averages are used to calculate stationary statistics. Razdan (1985) has shown in a comparable flow that for velocity fluctuations up to 10 percent the errors are negligible. As the fluctuations increase the velocity bias toward higher velocities also increases. At the maximum fluctuation levels measured in the present flow a maximum bias error of 3 percent would be expected.

Additional sources of error have also been estimated. The error due to velocity-gradient broadening was estimated to be less than 0.3 percent. Errors in time measurement with a counter processor having 0.5-ns resolution are less than 0.2 percent at the highest burst frequencies measured, and the effects of variation in refractive index on movement of the measurement volume are negligible.

Since the velocity of a particle is actually measured with laser velocimetry, particle-velocity lag must also be considered. Using the estimates of Durst et al. (1976), a 0.85-micron particle can follow the flow up to a frequency of 8 kHz with a slip velocity of 1 percent. Based on previous measurements in the current flow this frequency response is sufficient.

The primary sources of error in the Raman scattering measurements are calibration of the light collection system, shot noise, and background flourescence (from the windows where the laser beam enters and exits the test section). Calibration of the Raman system was done in mixtures of

C_3H_8 and N_2. As a measure of the overall efficiency of the collection system 6,000 photoelectrons per Joule of laser light were collected from N_2 in room air. The background flourescence contribution to the Raman signal was measured by scanning the spectrometer away from the Raman line and determined to be less than 0.5%.

Several checks on the data were performed to assess the accuracy of the measurements. Conservation of propane (on a mass basis) was verified by integrating the velocity and the propane mass fraction measurements across the flowfield. The integrations were carried out at three axial locations (x/D = 15, 30 and 50) and the total propane mass flux was compared with the calibrated value based on the mass flowmeter reading. The total propane mass flux at the jet exit was 2.3 gm/sec and the mass flux calculated at each axial location agreed with this value within 5 percent. In addition to the conservation of propane, momentum must also be conserved across the flowfield. Integration of the total momentum at the above three axial locations was found to agree within 3 percent of the inlet value. The long-term repeatability of the measurements was established by repeating most of the measurements one year after the initial data set was obtained. Data reproducibility was found to be within a few percent. Finally, the data have been compared to other published measurements wherever possible.

DISCUSSION OF THE DATA

An expanded discussion of selected data is given in the following sections because at the time of publication of this document, many of the data are not yet available in the literature; publications fully describing these data are in preparation.

Mixture fraction measurements

The centerline variation in the mean and fluctuating component of the mixture fraction are shown in Fig. 1. Axial distance x is normalized by the jet exit diameter D. The rms of the mixture fraction fluctuations f'_{rms} is normalized by the mixture fraction at the centerline $\overline{f_{cl}}$. The mean mixture fraction $\overline{f}$ remains nearly constant over the potential core region, which extends approximately 4 jet diameters downstream of the jet exit before decreasing rapidly as coflowing air is entrained by the high velocity jet and mixes with the propane. After the initial core region, the fluctuations continue to increase but at a slower rate.

Centerline variations in mixture fraction for nonreacting jets can be correlated with distance from the virtual origin $x_{0,1}$ (Pitts and Kashiwagi 1984). This correlation can be expressed as

$$\frac{\overline{f_j}}{\overline{f_{cl}}} = \frac{C_1(x - x_{0,1})}{D(\rho_{jet}/\rho_{air})^{1/2}}, \tag{14}$$

where $\overline{f_j}$ is the value of the mixture fraction at the jet exit ($\overline{f_j} = 1$ for pure propane), and C_1 is a constant independent of the jet density ratio as discussed above. The centerline variation in the reciprocal mean mixture fraction is replotted in Fig. 2 as a function of distance from the virtual origin $(x - x_{0.1})$ times the density ratio. The solid line is the result of a least-square-fit to the data for $x/D > 25$. Also shown for comparison are results for the CH_4-air jet of Pitts and Kashiwagi (1984) and the air-air jet of Becker et al. (1967). The present results agree well with results obtained in the air-air jet, but fall below those obtained in the CH_4-air jet, which has a

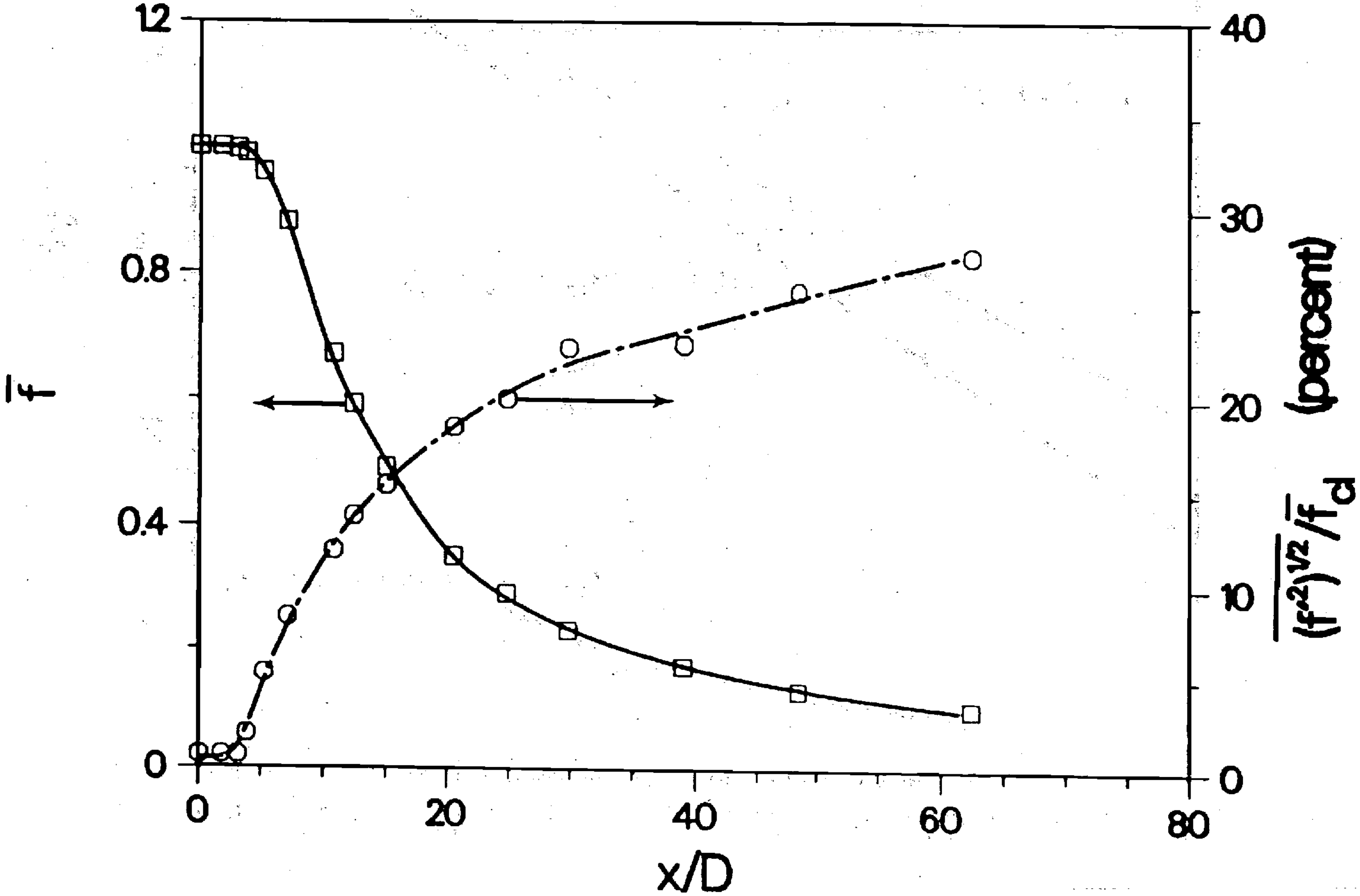

Fig. 1. Mean mixture fraction and mixture fraction fluctuations measured along centerline in turbulent nonreacting propane jet. Bulk jet velocity=53 m/s; coflowing air velocity=9.2 m/s.

Fig. 2. Reciprocal mean mixture fraction along centerline in turbulent nonreacting propane jet. Bulk jet velocity=53 m/s; coflowing air velocity=9.2 m/s.

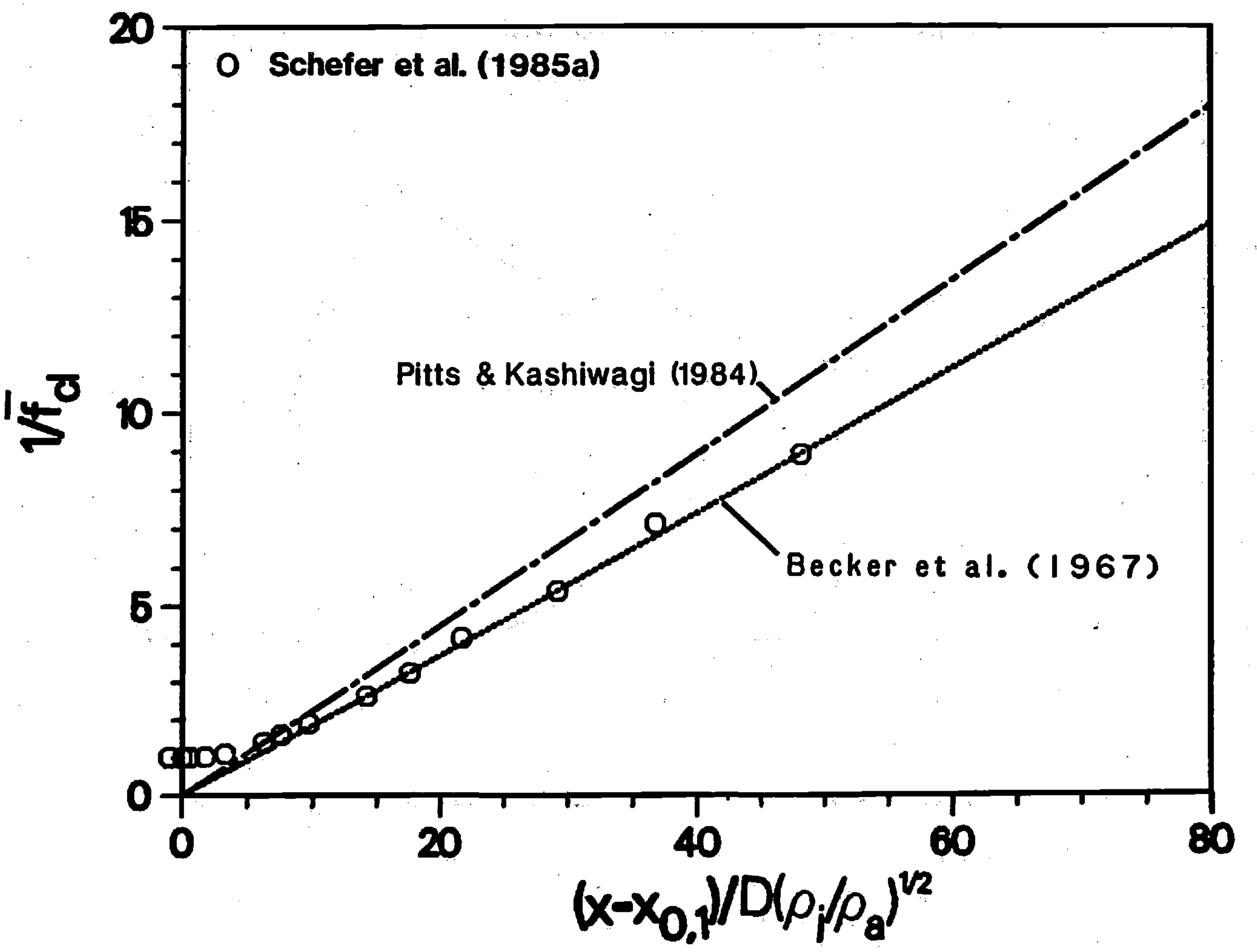

significantly higher centerline decay rate.

Further comparisons of C_1 and $x_{0,1}$ are shown in Table 10. The results of the present investigation give the location of the virtual origin at $x/D = 3.0$ and a value for $C_1 = 0.186$. The values of $x_{0,1}$ listed in the table show considerable scatter. Such variations are not unexpected since the location of the virtual origin is dependent on initial conditions which are likely to vary between experiments. The present values of C_1 compare well with the earlier results of Dyer (1979) for a C_3H_8 jet and, as noted above, with the results of Becker et al. (1967) for an air jet, but are up to 30 percent lower than the values obtained for CH_4 jets. Whether these variations are due to experimental uncertainty or are real density effects which may be unaccounted for by Eq. 14 is uncertain. However, the reasonable agreement between the two data sets for CH_4 jets and the consistency in the values of C_1 for the higher density air and C_3H_8 jets seems to support the conclusion that Eq. 14 does not adequately account for the more rapid centerline decay rate of $\bar{\tilde{f}}$ in the lower density CH_4 jet.

A comparison of the mixture fraction fluctuation intensity $f'_{rms}/\bar{f_j}$ with results for the CH_4-air of Pitts and Kashiwagi (1984) and the air-air jet of Becker et al. (1967) is shown in Fig. 3. The initial increase in fluctuation intensity is considerably more rapid for the CH_4-air and air-air jets. At downstream locations, however, the data for the variable density jets shows good agreement and approaches a considerably higher value than the constant density air-air jet. The present results thus support the conclusions of Pitts and Kashiwagi (1984) and Birch et al. (1978) that centerline scalar fluctuations are higher in variable density jets than in constant density flows.

The jet spreading rate can be determined from the mean mixture fraction profiles and is typically characterized by the mixture-fraction half radius L_f, defined as the radial location at which the mixture fraction is equal to half its value at the centerline. The variation in L_f (normalized by the jet exit diameter) with axial distance is shown in Fig. 4. For distances sufficiently far downstream L_f has been shown to be proportional to the distance from a virtual origin $x_{0,3}$ (Pitts and Kashiwagi (1984)). This

TABLE 10. EXPERIMENTALLY DETERMINED CONSTANTS FOR EQNS. (14 - 15)

Flow	C_1	$X_{0,1}/D$	C_2	$X_{0,2}/D$	Reference
C_3H_8-air	0.185	3.0	0.060	-1.0	Schefer et al. (1985a)
C_3H_8-air	0.180	0.15	-	-	Dyer (1979)
CH_4-air	0.224	-1.0	0.104	0.0	Pitts & Kashiwagi (1984)
CH_4-air	0.250	5.8	0.097	0.0	Birch et al. (1978)
air-air	0.186	2.4	0.106	2.4	Becker et al. (1967)

Fig. 3. Mixture fraction fluctuations along centerline in turbulent nonreacting propane jet. Bulk jet velocity=53 m/s; coflowing air velocity=9.2 m/s.

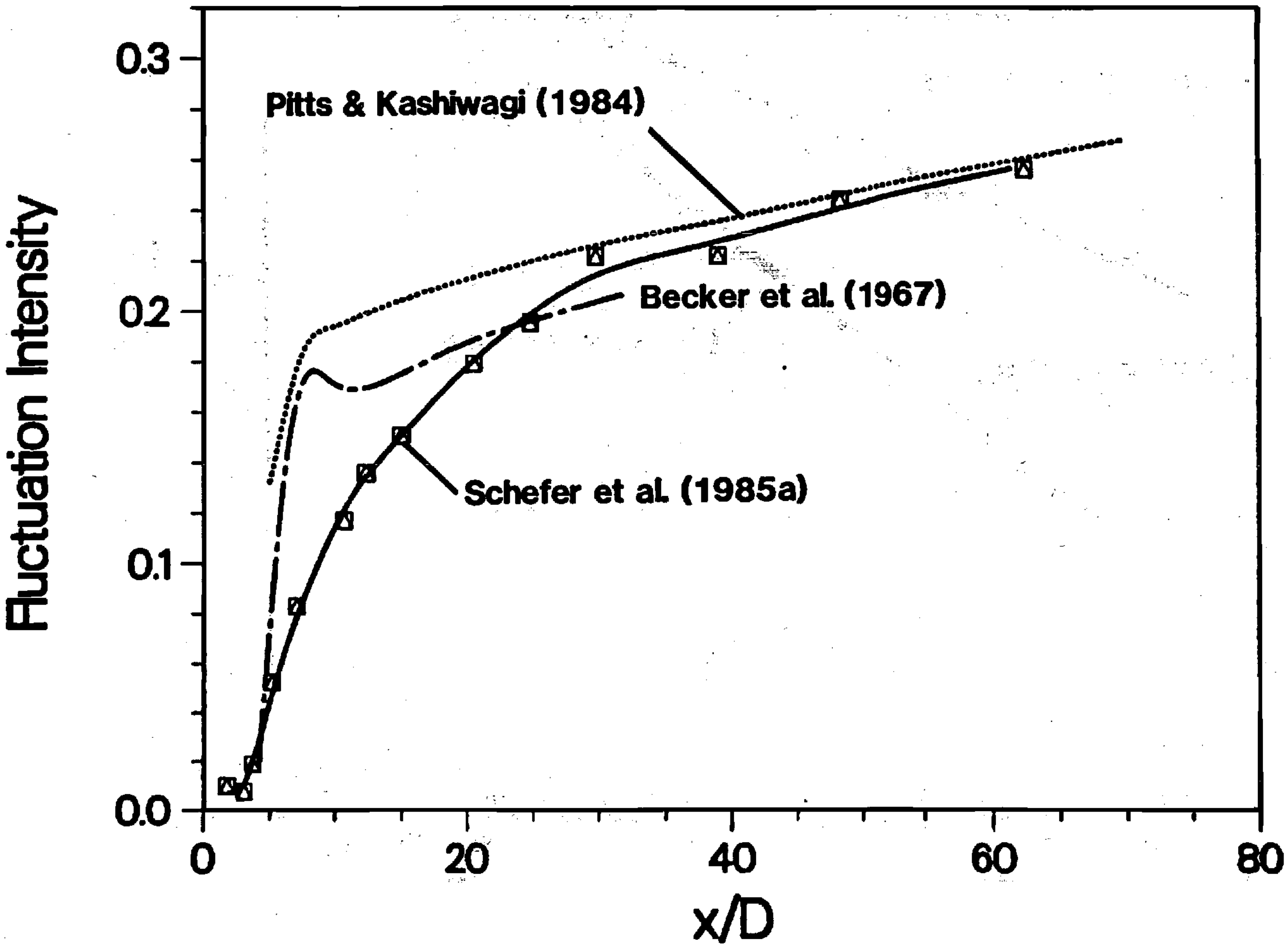

Fig. 4. Variation of mixture fraction half radius with axial distance in turbulent nonreacting propane jet. Bulk jet velocity=53 m/s; coflowing air velocity=9.2 m/s. ○, C_3H_8 jet; ●, CH_4 jet.

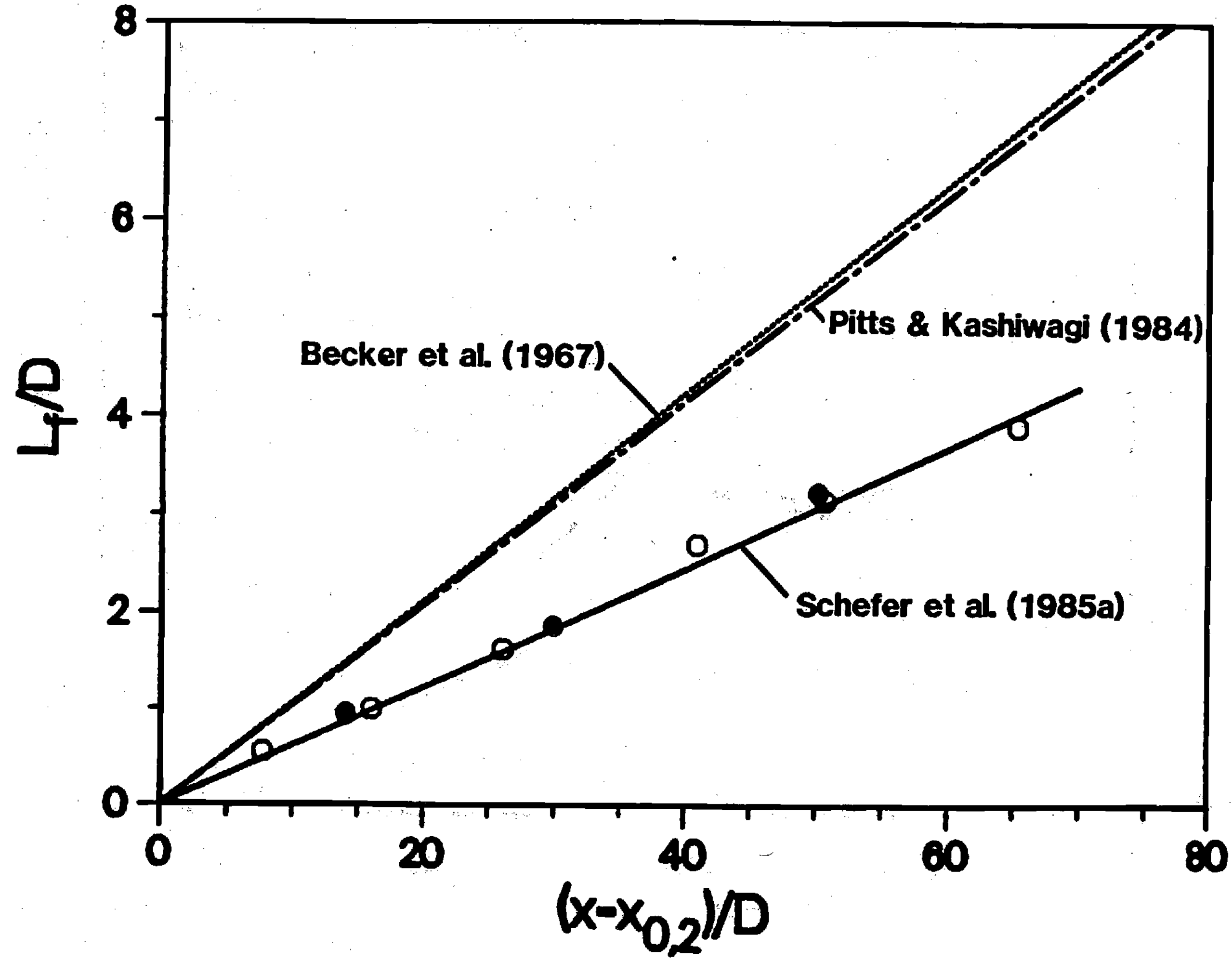

dependence can be written as

$$\frac{L_f}{D} = \frac{C_2(x - x_{0,2})}{D} \tag{15}$$

A fit of the present data in Fig. 4 (solid line) gives a value of $x_{0,2}/D = -1$ and $C_2 = 0.060$. The spreading rate obtained in the present study is considerably less than that measured in a CH_4-air jet (dotted line) or an air-air jet (dashed line). The discrepancy between the present results and the latter studies could be attributed to either the effects of variable density or the effects of coflowing air (both the CH_4-air and air-air jets had coflow air velocities considerably lower than the present study). However, the good agreement between the CH_4-air and air-air jets indicates that the spreading rate is not affected by variable density. Thus, discrepancies between the present propane data and those to which they are compared can be attributed to the effects of co-flow air. Additional measurements using methane instead of propane under identical inlet conditions were obtained to verify this conclusion. These methane data are displayed on Fig. 4 (solid points) and show good agreement with the propane results.

Values of $x_{0,2}$ and C_2 obtained in other jet studies are also listed in Table 10. Although the results of Birch et al. (1978) are based on only one axial location the values for the CH_4-air jets and the air-air jet agree to within 7 percent while the present results are approximately 40 percent lower.

Variations in $\bar{f}$ and f'_{rms} are shown in Fig. 5 as a function of radial distance normalized by L_f. It should be noted that the use of similarity variables such as L_f is not meant to imply that flow similarity exists in variable density jets with high coflow air velocities, but rather to emphasize differences with other jet flows in the literature. The results indicate that the mean mixture fraction approaches similarity over the first 15 diameters downstream of the jet exit (similarity is taken here to mean invariance of the appropriately normalized radial profiles with axial distance). The solid line in Fig. 5(a) is a Gaussian-type function of the form

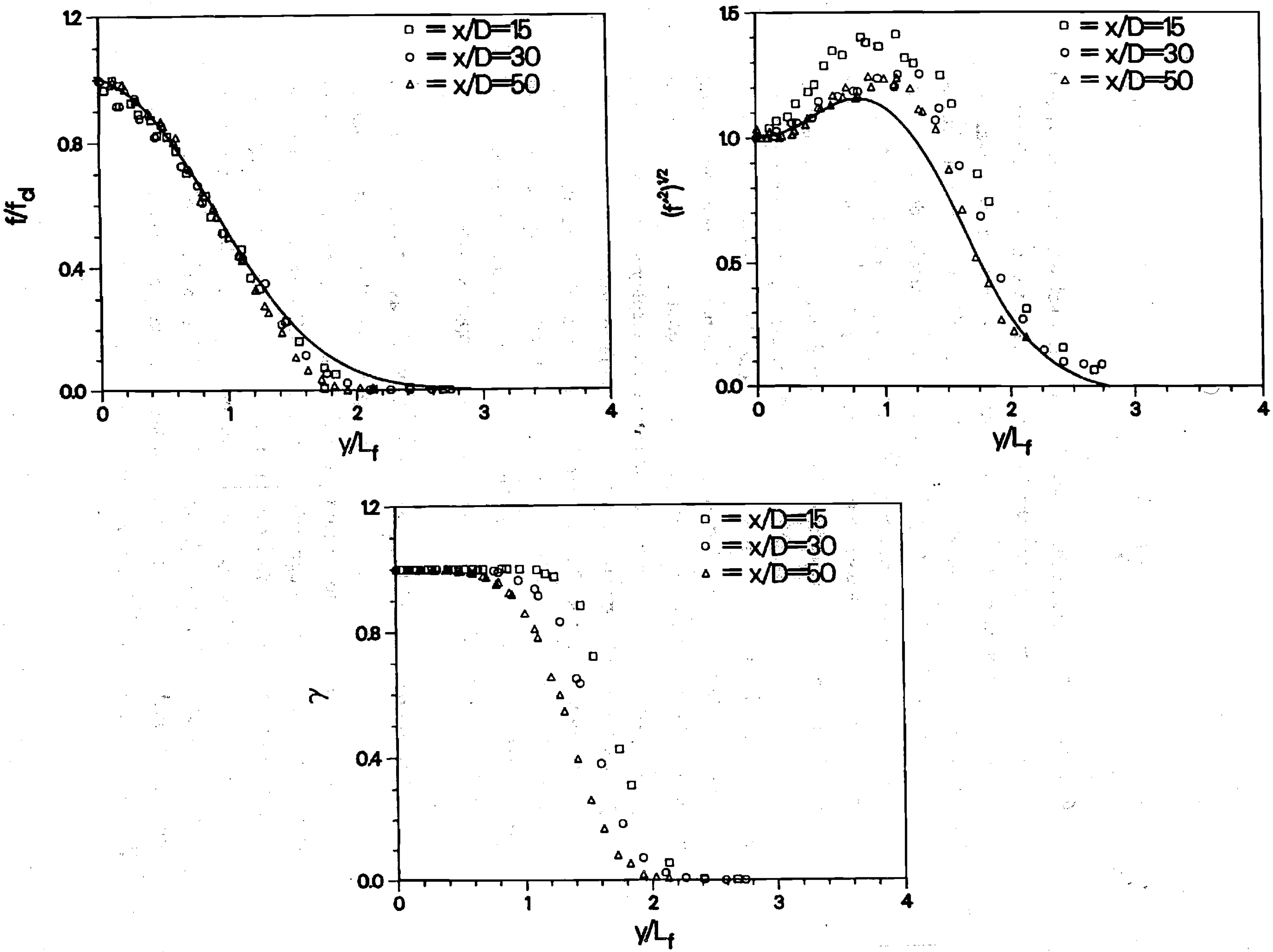

Fig. 5. Normalized radial profiles for a turbulent nonreacting propane jet at axial locations
[illegible] coflowing air velocity=9.2 m/s. (a) Mean

$$\frac{\bar{f}}{\bar{f}_{cl}} = \exp(-0.693(\frac{y}{L_f})^2) \tag{16}$$

This equation has been shown to provide a good fit to data in C H_4-air jets (Pitts and Kashiwagi (1984)) and provides a good fit to the present data for $y/L_f < 1.25$. At larger values of y/L_f the decrease in $\bar{f}$ with radial distance is more rapid than Gaussian as was also observed by Pitts and Kashiwagi (1984) for C H_4-air jets.

The mixture-fraction fluctuations normalized by the centerline value $f'_{rms,cl}$ are shown in Fig. 5(b). The profile at x/D =15 shows consistently higher fluctuations than at the downstream locations for all radial locations. At x/D = 30 and 50 the profiles show good agreement for $y/L_f < 1$ but at larger radial distances the profile at x/D = 50 falls slightly outside the results for x/D = 30. This apparently is due to the effects of the coflowing air stream since radial mean CH_4 concentration profiles at x/D = 20, 30 and 40 in a CH_4-air jet with no coflowing air show good similarity with respect to the normalized radial distance y/L_f (Birch et al. 1978).

Represented as a solid line (Fig. 5(b)) are the results of Pitts and Kashiwagi (1984) and Birch et al. (1978) for CH_4-air jets. The maximum fluctuations for the CH_4-air jets are lower and occur closer to the centerline with respect to L_f. A comparison of the maximum fluctuations $f'_{rms,max}$ and their radial locations is shown in Table 11. While it generally has been concluded that scalar fluctuations are higher in variable density jets (Pitts and Kashiwagi (1984)) (in agreement with the present results), any more specific conclusions on the effect of density variations are difficult to make. The lowest values of $f'_{rms,max}$ occur for constant density air jets in which particles are used as markers for concentration. The maximum fluctuations increase in going from constant density jets to CH_4 and C_3H_8. Fluctuations are also higher in heated jets than in constant density jets. However, it is difficult to explain the significantly higher values of $f'_{rms,max}$ obtained by Lockwood and Moneib (1980) in a heated air jet ($\rho_{jet}/\rho_{air} = 0.54$) than are found in CH_4-air jets ($\rho_{jet}/\rho_{air} = 0.55$) where the

TABLE 11

MAXIMUM MIXTURE FRACTION FLUCTUATION INTENSITIES
and NORMALIZED RADIAL LOCATIONS

Flow	f'_{max}/f	Y_{max}/L_f	Reference
C_3H_8-air	1.24	0.96	Schefer, et al. (1985a)
C_3H_8-air	1.29	0.80	Dyer (1979)
CH_4-air	1.18	0.70	Pitts & Kashiwagi (1984)
CH_4-air	1.20	0.70	Birch, et al. (1978)
air-air	1.15	0.80	Becker, et al. (1976)
air-air	1.14		Shaughnessy & Morton (1977
heated air-air	1.26	0.90	Lockwood & Moneib (1980)

ratios of jet to air density are nearly the same.

Radial variations in the intermittency γ are shown in Fig. 5(c). Here the intermittency is defined as the fraction of time that the mixture fraction is greater than a near-zero threshold (a value of zero corresponding to pure air). Typical probability density distributions in the mixing region consist of an intermittency spike associated with unmixed air and a broader distribution corresponding to mixed air and propane (probability density distributions of f are presented in the following section). The finite width of the intermittency spike often requires the somewhat arbitrary selection of a threshold value to differentiate between unmixed and mixed fluid. Bilger et al. (1976) have shown that the finite width of the intermittency spike can be closely fitted by a Gaussian, and the area under the resulting curve provides a good estimate of $(1-\gamma)$. The threshold value of mixture fraction determined using this method was $f_{th} = 0.015$. Thus for values of f less than f_{th} the flow is considered as unmixed air and for values greater than f_{th} the flow is considered as mixed propane and air. Calculated values of were found to be insensitive to small variations in the threshold level ($\pm$ 0.005).

At all axial locations, a region exists near the centerline for which is unity, indicating that turbulent mixing is insufficient to transport unmixed air into the central region. Only in a relatively well defined mixing region for which γ is between 0 and 1 is the presence of any unmixed air observed. Thus the mixing region can be characterized as consisting of mixed propane and air, and unmixed air which is entrained by the high velocity jet. No unmixed air exists near the centerline at the axial locations shown. These observations are consistent with the view that the center of the jet is relatively well mixed while at increasing radii, engulfment of coflowing air and subsequent mixing occurs.

Radial variations in the third and fourth moments of the mixture fraction (skewness S and kurtosis K, respectively) are shown in Fig. 6(a) and (b). The values of S and K for a Gaussian distribution are 0.0 and 3.0, respectively. At the centerline the skewness has a slightly negative value (S

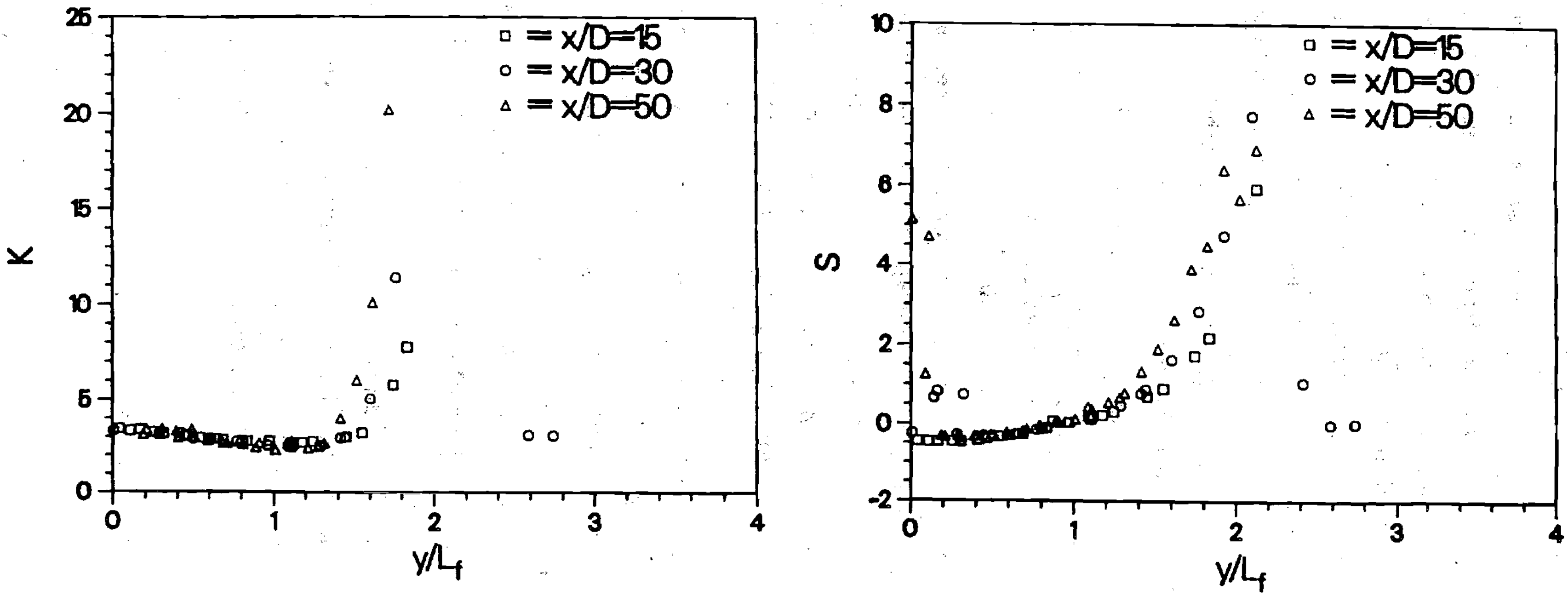

Fig. 6. Normalized radial profiles for a turbulent nonreacting propane jet at axial locations of x/D=15, 30, and 50. Bulk jet velocity=53 m/s; coflowing air velocity=9.2 m/s. (a) Skewness; (b) Kurtosis.

= 0.4) and the kurtosis is 3.5. Outward from the centerline S increases at first slowly, followed by a rapid increase at the outer edge of the mixing layer. The kurtosis initially decreases to a minimum value of 2.8 at a radial location just inside the mixing region before rapidly increasing as the outer iar flow is approached. The rapid increase in S and K in the intermittent mixing region is due to the passage of unmixed air past the measurement volume. This results in periods of time during which the mixture fraction is zero and a sharp cutoff in p(f) at f = 0.

Probability density distributions of the mixture fraction p(f) were calculated from 8000 measurements at each spatial location using 50 bins equally spaced over the 3 sigma limits of the data. Radial variations in p(f) are shown in Fig. 7 for x/D = 30. These distributions are quantitatively similar to conserved scalar distributions observed in nonreacting $C\ H_4$-air jets (Birch et al. 1978) and reacting jets (Drake et al. 1981). Near the centerline the distributions are dominated by a broad Gaussian-like distribution corresponding to a turbulent mixture of propane and entrained air while at outer radial locations a sharp spike corresponding to pure air at f = 0 is observed. In the mixing region the distribution is bimodal and consists of contributions from both the unmixed air and mixed propane and air. At the axial locations shown no pure propane is indicated (f = 1) since sufficient entrainment of coflowing air and mixing has occurred upstream. The smooth transition between the air spike and the broader distribution corresponding to mixed fluid has been attributed to the existence of a viscous superlayer between the unmixed air and the mixed propane and air zones and has led to a proposed composite distribution which includes unmixed air, fully mixed propane and air, and a contribution from the viscous superlayer (Effelsberg and Peters (1983)).

Velocity measurement

The centerline variation in mean axial velocity $\bar{u}$ and the fluctuating components of axial and radial velocity are shown in Fig. 8. The axial and radial velocity fluctuations u'_{rms} and v'_{rms} are normalized by the centerline excess velocity U_{cl} where the centerline excess velocity is defined as the

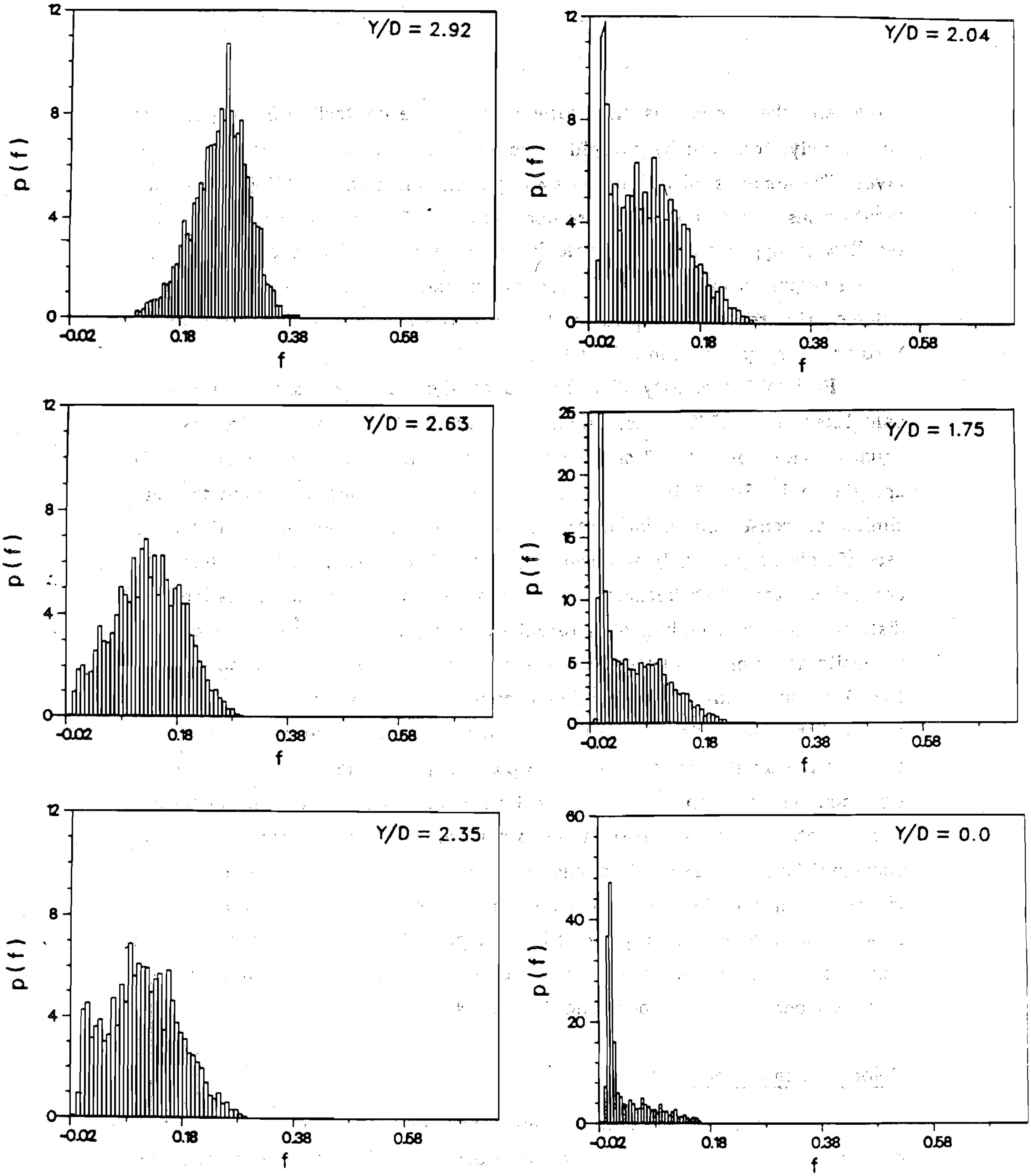

Fig. 7. Probability density distributions of mixture fraction for a turbulent nonreacting propane jet at an axial location of x/D=30. Bulk jet velocity=53 m/s; coflowing air velocity=9.2 m/s. (a) y/D=2.92; (b) y/D=2.63; (c) y/D=2.35; (d) y/D=2.04; (e) y/D=1.75; (f) y/D=0.0.

Fig. 8. Variation of mean axial velocity and normalized axial velocity fluctuations along centerline in turbulent nonreacting propane jet. Bulk jet velocity=53 m/s; coflowing air velocity=9.2 m/s. □, mean axial velocity; ○, axial velocity fluctuations; δ, radial velocity fluctuations.

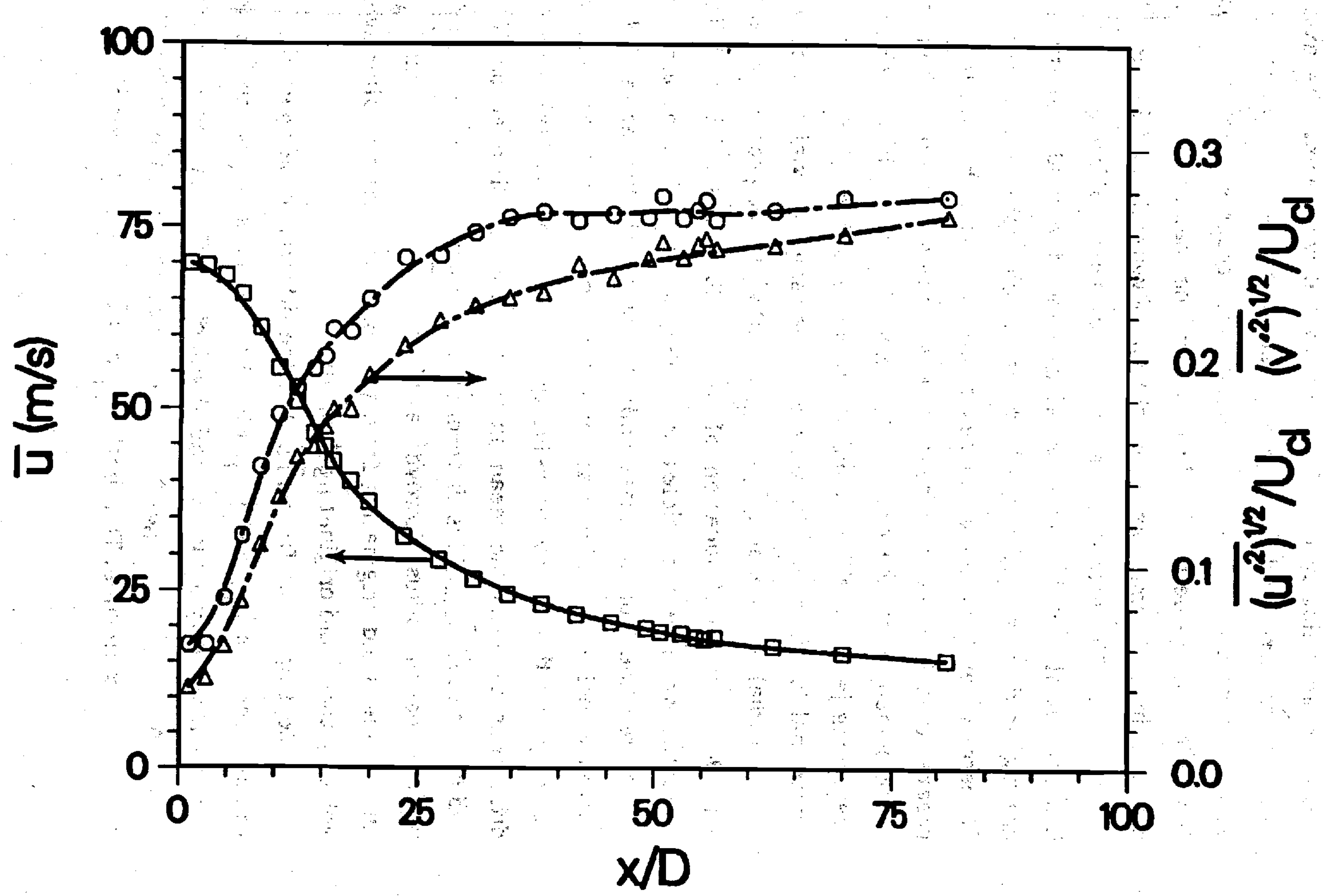

difference between the mean centerline velocity and the coflowing air velocity. The mean axial velocity remains nearly constant over the potential core region, which extends approximately 2 jet diameters downstream of the jet exit, before decreasing rapidly to approach the outer coflowing air velocity of 9.2 m/s farther downstream. The axial velocity fluctuations increase rapidly downstream of the jet exit to a maximum value of approximately 27 percent, and for x/D greater than 40 remain nearly constant. This value is slightly less than the maximum value of 28 percent obtained in isothermal jets into still air (Wygnanski and Fielder (1969)) and the value of 30 percent for a heated jet with coflowing air ($u_j/u_0 = 4.5$) (Antonia et al. (1975)). At all axial locations the axial velocity fluctuations are higher than the radial fluctuations (which approach a maximum value of 26 percent) and the initial increase is more rapid. For axial distances x/D greater than 14 the excess centerline velocity shows a hyporbolic decay rate in agreement with the results of Wygnanski and Fielder (1969) for a self-preserving jet into still air,, and of Antonia and Bilger (1973) for nonreacting isothermal jets into coflowing air over the range of axial distances shown.

Radial profiles of $\bar{u}$, $\bar{v}$, u'_{rms}, and $u'v'$ in the propane jet are shown in Fig. 9 for an axial location of x/D = 30. The solid line indicates data collected when seed particles are added to the coflowing air stream only; the dotted line indicates data collected with only the jet seeded. The mean excess velocity, $\bar{U}$, defined as the difference between the local mean axial velocity and the coflow air velocity, is shown in Fig. 9(a). There is a small difference between the mean axial velocities conditioned on air seed $\bar{U}_{air}$ and on jet seed $\bar{U}_{jet}$. This difference is smallest on centerline and increases with increasing radius. However, at all radii, $\bar{U}_{jet}$ is larger than $\bar{U}_{air}$. Hence, on average, fluid originating from the coflow air has a smaller average axial velocity than fluid originating from the jet.

Most apparent from Fig. 9 is the difference between the conditional radial velocities $\bar{v}_{air}$ and $\bar{v}_{jet}$, Fig. 9(b). In the sign convention adopted for the radial velocity a positive radial velocity indicates flow outward from the centerline, while a negative radial velocity corresponds to flow inward toward the centerline. Thus both $\bar{v}_{air}$ and $\bar{v}_{jet}$ indicate net flux of fluid away

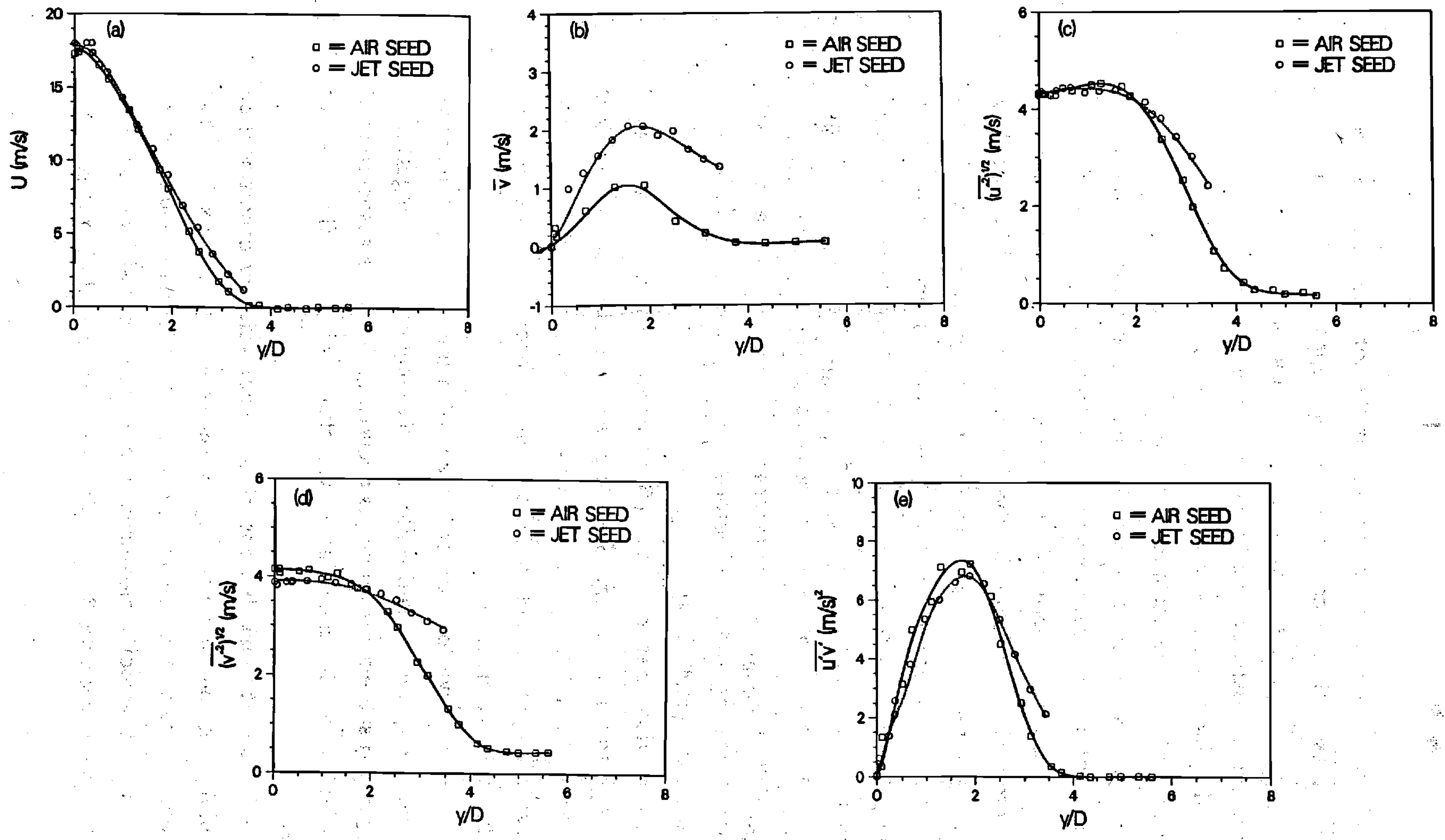

Fig. 9. Radial profiles for a turbulent nonreacting propane jet at an axial location of x/D=30. Bulk jet velocity=53 m/s; coflowing air velocity=9.2 m/s. Solid line indicates data collected with LV seed added to the coflowing air stream only; dashed line indicates data collected with LDV seed added to the propane jet stream only. □, coflowing air seed only; ○, jet seed only. (a) Mean axial velocity; (b) Mean radial velocity; (c) Axial velocity fluctuations; (d) Radial velocity fluctuations; (e) Axial and radial velocity correlation.

away from the centerline; however the flux of the jet fluid, on average, is larger. While these differences are readily apparent, the absolute differences, $\bar{v}_{jet} - \bar{v}_{air}$, are comparable with the absolute differences observed in the conditionally sampled axial velocities.

The axial velocity fluctuations $u'_{rms-jet}$ and $u'_{rms-air}$, Fig. 9(c), are nearly the same at the centerline. Both $u'_{rms-jet}$ and $u'_{rms-air}$ have a maxima in the mixing region between the fuel jet and the coflowing air where the gradient of the mean velocities is largest. At larger radii, $u'_{rms-air}$ tends toward zero more quickly than $u'_{rms-jet}$. The larger value of $u'_{rms-jet}$ at large radii is explained by the fact that jet seeded fluid at these locations has, on average, emerged from the centerline region of the jet and is, therefore, generally more turbulent. When the air is seeded, fluid at large radii, on average, originates from the coflow air which has lower turbulence. The radial velocity fluctuations $v'_{rms-jet}$ and $v'_{rms-air}$, Fig. 9(d) show a trend that is entirely analogous to the radial profiles of $u'_{rms-jet}$ and $u'_{rms-air}$. Both $v'_{rms-jet}$ and $v'_{rms-air}$ are comparable at the centerline and both decrease with increasing radii. As before $v'_{rms-jet}$ does not decrease as quickly with increasing radii as $v_{rms-air}$.

The correlation between the fluctuations in radial and axial velocities, $\overline{u'v'}_{jet}$ and $\overline{u'v'}_{air}$, Fig. 9(e), is directly related to the turbulent transport of momentum. Analogus to the previous results for axial and radial velocity fluctuations the difference is only slight near the centerline and increases at large radial distances.

All of these observations are consistent with the view that the center of the jet is relatively well mixed while at increasing radii, the engulfment of coflowing air and subsequent mixing is occurring. Thus, the association of lower velocities with air and higher velocities with jet fluid is not unreasonable.

Probability density distributions of the axial velocity conditional on the jet fluid $p(u)_{jet}$ and on the air $p(u)_{air}$ are shown in Fig. 10 for x/D = 30 at various distances from the centerline. The distributions shown were calculated from 3000 velocity measurements at each spatial location using 30 bins equally spaced over the 3 sigma limits of the data. As in the previous

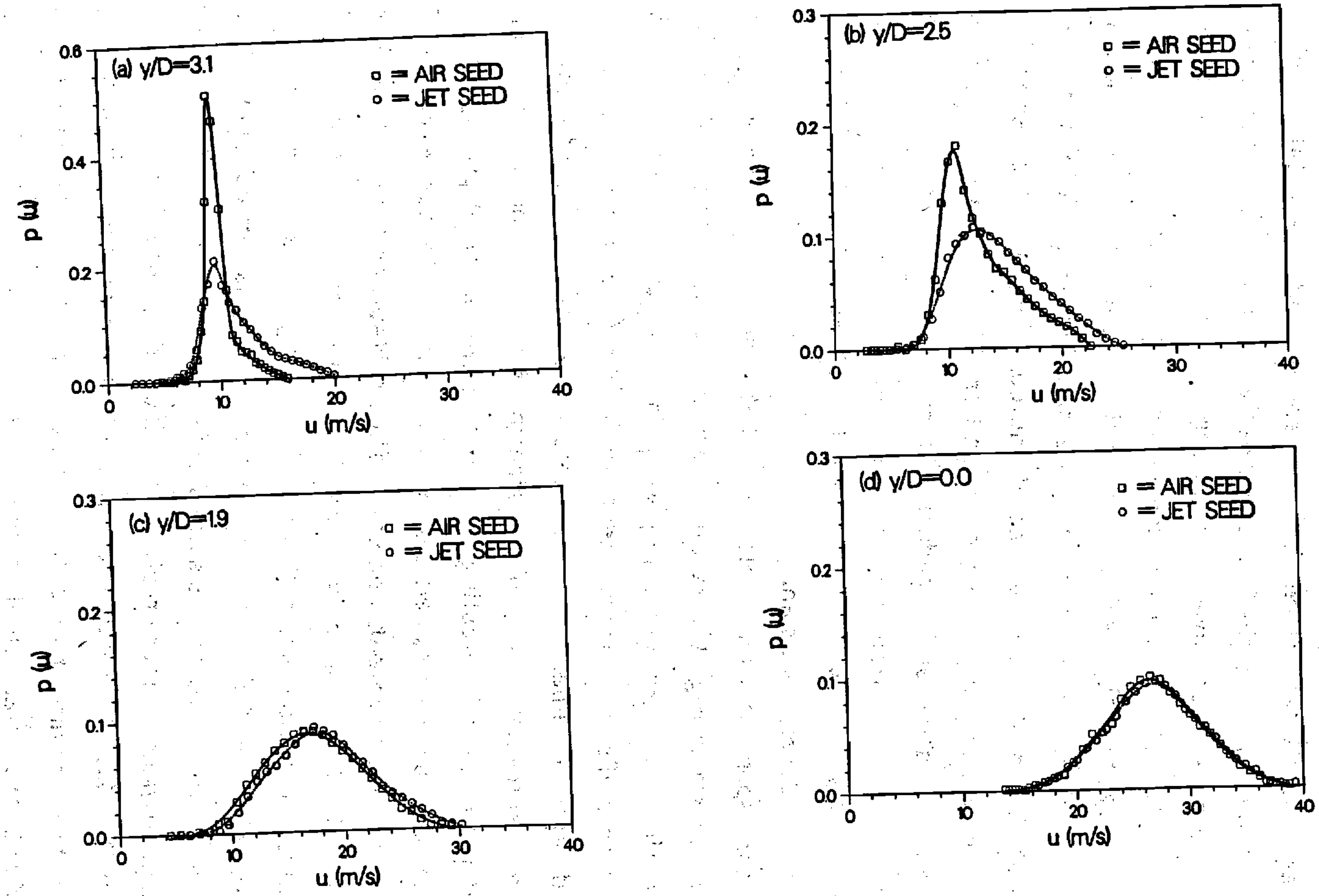

Fig. 10. Conditionally sampled probability density distributions of axial velocity for a turbulent nonreacting propane jet at an axial location of x/D=30. Bulk jet velocity=53 m/s; coflowing air velocity=9.2 m/s. Solid line indicates data collected with LV seed added to the coflowing air stream only; dotted line indicates data with the LDV seed added to the jet stream only. □, coflowing air seed only; ○, jet seed only. (a) y/D=4.4; (b) y/D=2.7; (c) y/D=1.7; (d) y/D=0.0.

section the solid line indicates data conditional on the air and the dotted line indicates data conditional on the jet fluid. The axial velocity distributions are in general characterized by a unimodal distribution which shifts to a higher average velocity as the centerline is approached. The axial velocity distributions conditional on the air are relatively narrow at outer radial locations with a peak value close to that of the coflowing air. Closer to the centerline the distributions become skewed toward higher velocities as fluid is accelerated by the high velocity central jet and approach a nearly Gaussian distribution at the centerline. The distribution conditional on the jet fluid exhibits a peak close to that of the coflowing air at outer radial locations but is skewed toward higher velocities. The peak in $p(u)_{jet}$ shifts toward higher velocities and broadens nearer the centerline due to the higher turbulence associated with the jet fluid. At the centerline the distributions for both cases are nearly identical since sufficient mixing has occurred and are closely Gaussian.

The corresponding radial velocity distributions $p(v)_{air}$ and $p(v)_{jet}$ at $x/D = 30$ are shown in Fig. 11. At the outermost radial location, $y/D = 3.1$, $p(v)_{air}$ is considerably narrower than $p(v)_{jet}$. In both cases the maximums in the radial velocity distributions are centered near zero while the presence of positive and negative radial velocities indicates expansion outward from the centerline and entrainment of fluid originating from both the jet and from the coflowing air. Most interesting are the positive values of $p(v)_{air}$ due to expansion of previously entrained coflowing air, and the negative values of $p(v)_{jet}$ corresponding to re-entrainment of fluid originating from the jet. The positive mean values of radial velocity for both cases (see also Fig. 9(b)) indicate net fluid motion outward from the centerline due to expansion of the high velocity jet fluid. The distribution $p(v)_{jet}$ is considerably more skewed toward positive velocities since fluid originating from the central jet is, on average, expanding more rapidly away from the centerline.

At $y/D = 2.5$ the small peak at negative radial velocity in $p(v)_{air}$ corresponds to entrainment of coflowing air inward toward the centerline. More rapid outward expansion of previously entrained air is also indicated by the increased skewness toward positive velocities. The maximum in the

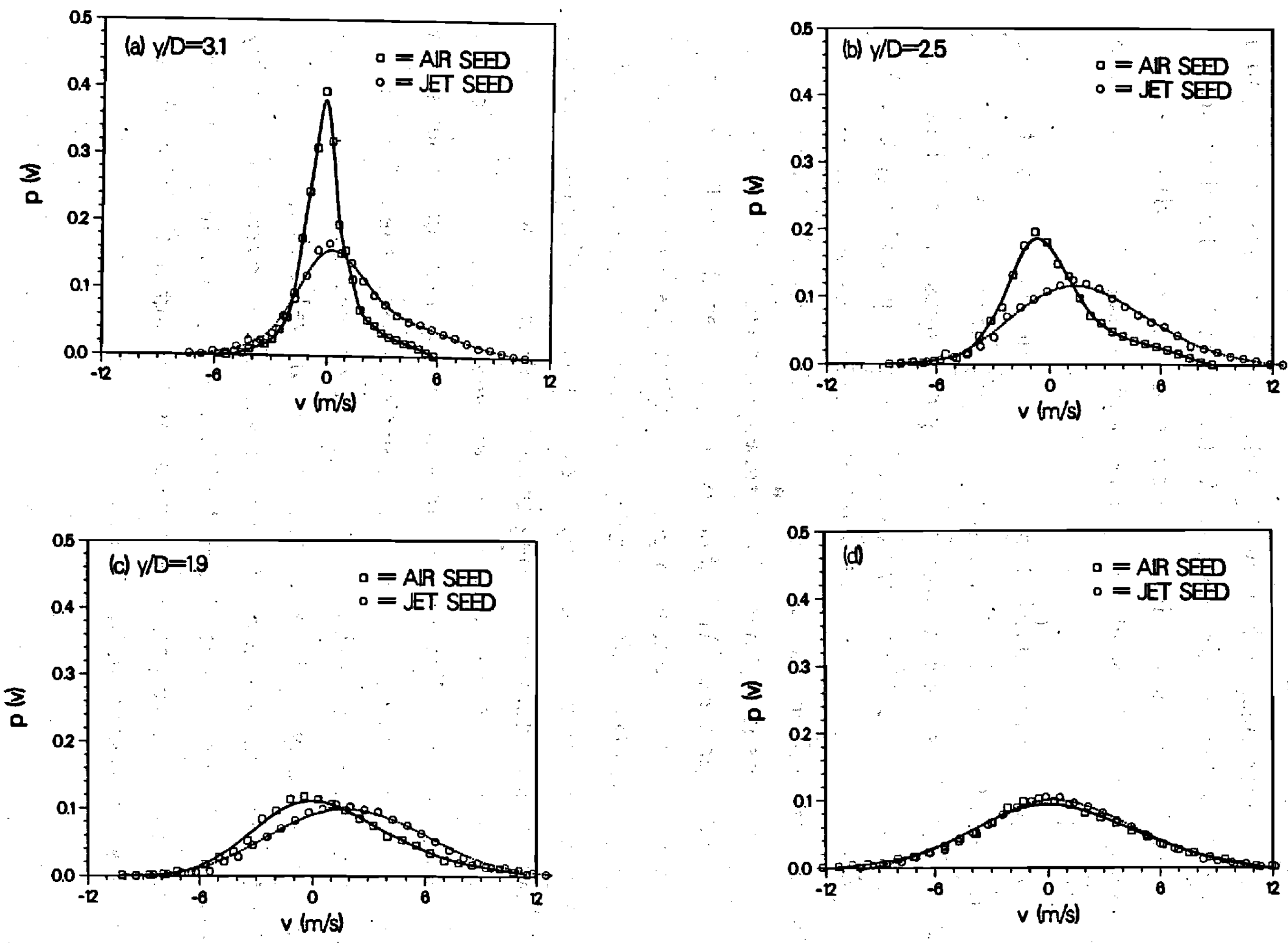

Fig. 11. Conditionally sampled probability density distributions of radial velocity for a turbulent nonreacting propane jet at an axial location of x/D=30. Bulk jet velocity=53 m/s; coflowing air velocity=9.2 m/s. Solid line indicates data collected with LV seed added to the coflowing air stream only; dotted line indicates data with the LDV seed added to the jet stream only. □, coflowing air seed only; ○, jet seed only. (a) y/D=4.4; (b) y/D=2.7; (c) y/D=1.7; (d) y/D=0.0.

$p(v)_{jet}$ is located at positive radial velocities and indicates more rapid outward expansion of jet fluid. At y/D = 1.9 the peak in $p(v)_{air}$ has decreased considerably although entrainment of fluid originating from the airstream is still apparent. The distributions for both cases are nearly identical for positive radial velocities indicating nearly equal expansion of fluid originating from the jet and air streams. At the centerline the distributions are closely Gaussian and nearly identical since, as was seen with the axial velocity distributions, fluid originating from both streams is well mixed in the centerline region.

The joint probability distributions of axial and radial velocity were calculated from 10,000 velocity pairs at each spatial location using 20 axial and radial velocity bins spaced over the 3 sigma limits of the data. The distribution shown in Fig. 12 corresponds to the mixing region (y/D = 2.5) where the difference in conditional velocity statistics is greatest. The distribution conditional on the air $p(u,v)_{air}$ exhibits a peak with the axial velocity distribution centered near the coflowing air velocity and the radial velocity centered near zero. At higher axial velocities the radial velocity distribution is highly skewed toward positive values due to the more rapid expansion of high velocity fluid originating near the centerline. The broader distribution also indicates considerably higher radial velocity fluctuations. It is likely that this is fluid originating from the air stream which has been previously entrained and mixed with higher velocity jet fluid prior to expansion outwards the coflowing air stream. The primary contribution to $p(u,v)_{jet}$ is from fluid moving in the axial direction at near the coflowing air velocity. A maximum again exists in $p(u,v)_{jet}$ at axial velocities close to the coflowing air velocity and, at increased axial velocities, the radial distribution becomes skewed toward negative values. However, considerably more outward radial movement of the fluid is apparent and the fluctuations in both axial and radial velocities are considerably higher (higher velocity fluctuations were also seen in Fig. 9(c)).

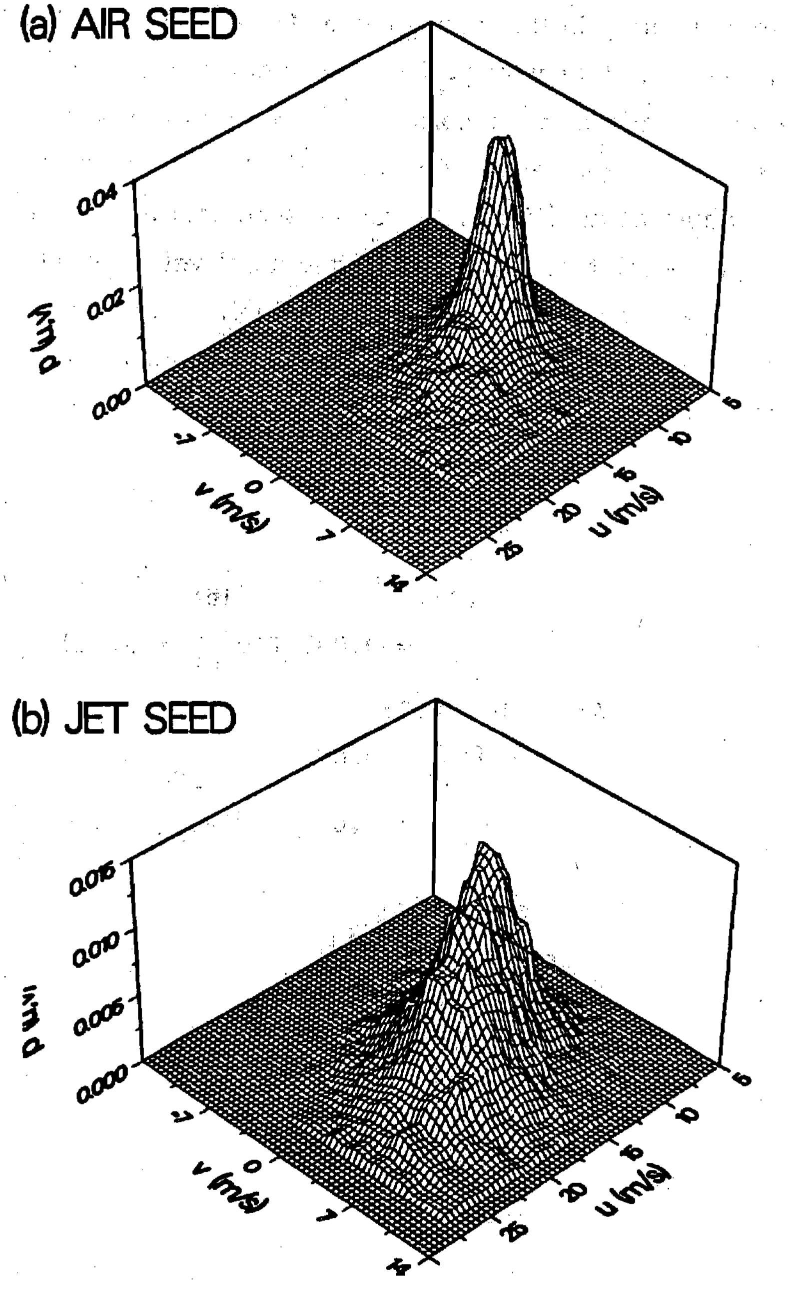

Fig. 12. Joint probability density distributions of axial and radial velocity for a turbulent nonreacting propane jet at an axial location x/D = 30 and a radial location of y/D=2.6. (a) LV seed added to the coflowing air only; (b) LDV seed added to the jet only. Bulk jet velocity=53 m/s; coflowing air velocity=9.2 m/s.

Raman/laser velocimetry results

A scatter plot showing the correlation between mixture fraction and axial and radial velocity in the mixing region (y/D = 2.3) at x/D = 30 is shown in Fig. 13(a) and (b), respectively. These results were obtained for the case where LV seed was added to the coflow air stream only. Biasing errors in the scalar f due to preferential seeding of the jet and air streams are fully discussed in Dibble et al. (1985b). It can be seen that a positive correlation exists between the mixture fraction and the axial velocity, while f and the radial velocity are negatively correlated. Similar measurements at the centerline show that f is uncorrelated with either velocity component. From this data the following values for the correlation coefficients are obtained:

At $y/D = 0.0$:

$$f'u'_{air} = 0.050 \quad f'u'_{jet} = 0.044$$

$$f'v'_{air} = 0.003 \quad f'v'_{jet} = 0.002$$

At $y/D = 2.3$:

$$f'u'_{air} = 0.077 \quad f'u'_{jet} = 0.090$$

$$f'v'_{air} = 0.065 \quad f'v'_{jet} = 0.073$$

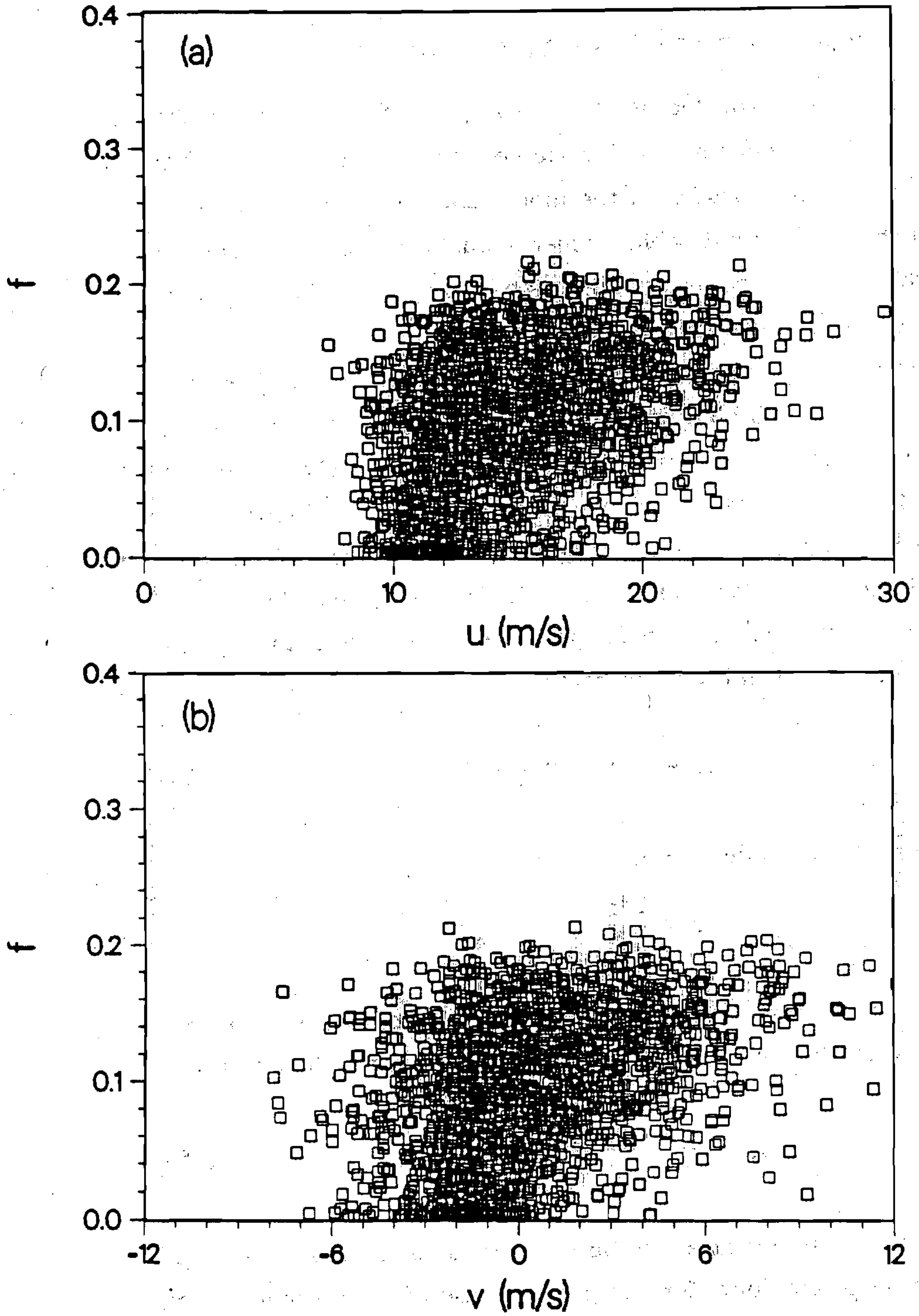

Fig. 13. Scatter plot of correlation between mixture fraction and velocity in a turbulent nonreacting propane jet at an axial locaytion x/D=30 and a radial location y/D=1.9. LV seed is added to the coflowing air only. (a) Mixture fraction and axial velocity; (b) Mixture fraction and radial velocity.

AVAILABLE COMPARISON WITH ANALYSIS

In this section a state-of-the-art modeling approach is used to predict the data chosen for the recommended variable density mixing case. This provides an opportunity to assess both the model and trends in the data and represents a benchmark against which other models can be compared, if desired. Since the model used is not described completely in any single reference, its essential ingredients are discussed below.

The second-order closure model described in Farshchi and Kollmann (1984), Dibble et al. (1985), Dibble et al. (1984), and Rhodes et al. (1974) was used to calculate the isothermal round jet mixing of propane with ambient air. The model consists of transport equations for mean velocity, mean mixture fraction., Reynolds-stress components, variance of mixture fraction, scalar fluxes, kinematic and scalar dissipation rates. The flow is isothermal and, using the ideal gas law for propane and air, we obtain for the density as a local function of mixture fraction f

$$\frac{\rho_1}{\rho(f)} = x + (1 - x) f \tag{17}$$

where x is the ratio of molecular masses

$$x = \frac{M_2}{M_1}$$

and ρ_1 is the density of fluid 1 (i.e, propane). Fluctuations of pressure are neglected in the thermodynamic relations. The normalized mass fraction

$$f = \frac{Y_1 - Y_{1\infty}}{Y_{10} - Y_{1\infty}} \tag{18}$$

of fluid 1 can be taken as mixture fraction (subscript o refers to jet pipe exit and subscript oo to ambient) for the present case of isothermal mixing of two components. The pdf of the mixture fraction P(f) is assumed to be a beta-function which has been found to be a good approximation for isothermal mixing flows (Rhodes et al. 1974). The mean density is then calculated by integration

$$\langle\rho\rangle = \int_0^1 df\,\rho(f)\,P(f) \tag{19}$$

The pdf P(f) is set up using the mean $\widetilde{f}$ and the variance $\widetilde{f''^2}$ which determine the exponents of the beta-function uniquely (Jones 1982).

The turbulence model includes the first order equations for mean velocity

$$\langle\rho\rangle\tilde{D}_t\tilde{f} = -\partial_\alpha\langle p\rangle - \partial_\beta\left(\langle\rho\rangle\widetilde{v''_\alpha v''_\beta}\right) \tag{20}$$

and mean mixture fraction

$$\langle\rho\rangle\tilde{D}_t\hat{f} = -\partial_\alpha\left(\langle\rho\rangle\widetilde{v''_\alpha f''}\right) \tag{21}$$

in exact form. Note that Favre-statistics are applied

$$\tilde{\phi} \equiv \frac{\langle\rho\phi\rangle}{\langle\rho\rangle} \quad , \quad \phi'' = \phi - \tilde{\phi}$$

where appropriate and

$$\tilde{D}_t \equiv \partial_t + \tilde{v}_\alpha\partial_\alpha$$

abbreviates the Stokes derivative for the mean velocity. The closure of the Reynolds-stress equations includes model assumptions for turbulent flux, pressure correlations and dissipation. The following equation emerges (Dibble et al. 1985c)

$$\begin{aligned}\langle\rho\rangle\tilde{D}_t\widetilde{v''_\alpha v''_\beta} = &-\langle\rho\rangle\widetilde{v''_\alpha v''_\gamma}\partial_\gamma\tilde{v}_\beta - \langle\rho\rangle\widetilde{v''_\beta v''_\gamma}\partial_\gamma\tilde{v}_\alpha \\ &+ \partial_\gamma\left(C_s\langle\rho\rangle\,\frac{\tilde{k}}{\tilde{\epsilon}}\,\widetilde{v''_\gamma v''_\delta}\partial_\delta\widetilde{v''_\alpha v''_\beta}\right) \\ &+ \langle\rho\rangle Q_{\alpha\beta} - \langle v''_\alpha\rangle\partial_\beta\langle p\rangle - \langle v''_\beta\rangle\partial_\alpha\langle p\rangle - \frac{2}{3}\,\partial_{\alpha\beta}\langle\rho\rangle\tilde{\epsilon}\end{aligned} \tag{22}$$

where the pressure correlations are modelled by (see Hanjelic and Launder (1972))

$$\begin{aligned} Q_{\alpha\beta} = &-C_1\frac{\tilde{\epsilon}}{\tilde{k}}\left(\widetilde{v''_\alpha v''_\beta} - \frac{2}{3}\,\partial_{\alpha\beta}\tilde{k}\right) \\ &- \frac{C_2+8}{11}\langle\rho\rangle\left(P_{\alpha\beta} - \frac{2}{3}\,\partial_{\alpha\beta}P\right) \\ &- \frac{8C_2-2}{11}\langle\rho\rangle\left(D_{\alpha\beta} - \frac{2}{3}\,\partial_{\alpha\beta}D\right) \\ &+ \frac{30C_2-2}{55}\tilde{k}\left(\partial_\alpha\tilde{v}_\beta + \partial_\beta\tilde{v}_\alpha\right) \end{aligned} \tag{23}$$

and

$$P_{\alpha\beta} = -\widetilde{v''_\alpha v''_\gamma}\partial_\gamma\tilde{v}_\beta - \widetilde{v''_\beta v''_\gamma}\partial_\gamma\tilde{v}_\alpha \quad , \quad P = \frac{1}{2}P_{\alpha\alpha} \tag{24a}$$

$$D_{\alpha\beta} = -\widetilde{v''_\alpha v''_\gamma}\partial_\beta\tilde{v}_\gamma - \widetilde{v''_\beta v''_\gamma}\partial_\alpha\tilde{v}_\gamma \quad , \quad D = \frac{1}{2}D_{\alpha\alpha} \tag{24b}$$

The dissipation rate $\tilde{\epsilon}$ of kinetic energy is determined by solving the equation

$$\begin{aligned} \langle\rho\rangle\tilde{D}_t\tilde{\epsilon} = &\,\partial_\alpha\left(C_\epsilon\langle\rho\rangle\frac{\tilde{k}}{\tilde{\epsilon}}\widetilde{v''_\alpha v''_\beta}\partial_\beta\tilde{\epsilon}\right) - C_{\epsilon 1}\langle\rho\rangle\frac{\tilde{\epsilon}}{\tilde{k}}\widetilde{v''_\alpha v''_\beta}\partial_\beta\tilde{v}_\alpha \\ &- C_{\epsilon 2}\langle\rho\rangle\frac{\tilde{\epsilon}^2}{\tilde{k}} - C_{\epsilon 3}\frac{\tilde{\epsilon}}{\tilde{k}}\frac{\langle\rho' v''_\alpha\rangle}{\langle\rho\rangle}\,\partial_\alpha\langle\rho\rangle \end{aligned} \tag{25}$$

The statistical moments of the scalar field follow from the solutions of (18) and the equations for the variance $\widetilde{f''^2}$, the scalar fluxes $\widetilde{v''_\alpha f''}$ and the scalar dissipation $\tilde{\epsilon}_f$. The variance equation requires only one closure assumption for the turbulent flux of $\widetilde{f''^2}$.

$$\begin{aligned} \langle\rho\rangle\tilde{D}_t\widetilde{f''^2} = &\,\partial_\alpha\left(C_s\langle\rho\rangle\frac{\tilde{k}}{\tilde{\epsilon}}\widetilde{v''_\alpha v''_\beta}\partial_\beta\widetilde{f''^2}\right) \\ &- 2\langle\rho\rangle\widetilde{v''_\alpha f''}\partial_\alpha\tilde{f} - 2\langle\rho\rangle\tilde{\epsilon}_f \end{aligned} \tag{26}$$

The scalar flux equation is given by

$$\begin{aligned}
\langle\rho\rangle\tilde{D}_t\widetilde{v''_\alpha f''} = & -\langle\rho\rangle\widetilde{v''_\alpha v''_\beta}\partial_\beta\tilde{f} - \langle\rho\rangle\widetilde{v''_\beta f''}\partial_\beta\tilde{v}_\alpha \\
& + \partial_\beta\left[C'_s\langle\rho\rangle\frac{\tilde{k}}{\tilde{\epsilon}}\widetilde{v''_\beta v''_\gamma}\partial_\gamma\widetilde{v''_\alpha f''}\right] \\
& - 2C_{f1}\langle\rho\rangle\frac{\tilde{\epsilon}}{\tilde{k}}\widetilde{v''_\alpha f''} - 2C_{f2}\langle\rho\rangle b_{\alpha\beta}\frac{\tilde{\epsilon}}{\tilde{k}}\widetilde{v''_\beta f''} \\
& + 0.8\langle\rho\rangle\widetilde{v''_\beta f''}\partial_\beta\tilde{v}_\alpha - 0.2\langle\rho\rangle\widetilde{v''_\beta f''}\partial_\alpha\tilde{v}_\beta
\end{aligned} \tag{27}$$

where the anisotropy term is defined by

$$b_{\alpha\beta} = \frac{1}{2\tilde{k}}\widetilde{v''_\alpha v''_\beta} - \frac{1}{3}\partial_{\alpha\beta}$$

Finally the scalar dissipation is obtained as a solution of

$$\begin{aligned}
\langle\rho\rangle\tilde{D}_T\tilde{\epsilon}_f = & \partial_\alpha\left(C''_s\langle\rho\rangle\frac{\tilde{k}}{\tilde{\epsilon}}\widetilde{v''_\alpha v''_\beta}\partial_\beta\tilde{\epsilon}_f\right) \\
& - C_{P1}\langle\rho\rangle\tilde{\epsilon}_f\left(\frac{\widetilde{f''v''_\alpha}}{\widetilde{f''^2}}\partial_\alpha\tilde{f} - \frac{C_{D3}}{C_{P1}}\frac{\widetilde{v''_\alpha v''_\beta}}{\tilde{k}}\partial_\beta\tilde{V}_\alpha\right) \\
& - C_{D1}\langle\rho\rangle\frac{\tilde{\epsilon}_f^2}{\widetilde{f''^2}} - C_{D2}\langle\rho\rangle\tilde{\epsilon}_f\frac{\tilde{\epsilon}}{\tilde{k}}
\end{aligned} \tag{28}$$

The constants are summarized in Table 12.

The numerical solution procedure was a finite-difference method solved as marching integration in the jet axis direction. The number of points in the crossflow direction was N = 60 and about two thousand steps were required to reach x/D = 70. Particular care was taken to describe the conditions at the jet pipe exit. The velocity profile was a turbulent pipe flow profile inside the jet pipe, a small coflow velocity for the approximation of the finite thickness of the pipe, and a profile approximating the outer coflowing stresses (Fig. 14).

TABLE 12. MODEL CONSTANTS

C_s	C_1	C_2	C_ϵ	$C_{\epsilon 1}$	$C_{\epsilon 2}$
0.22	1.5	0.4	0.15	1.45	1.9
$C_{\epsilon 3}$	C_s'	C_{f1}	C_{f2}	C_s''	C_{p1}
1.45	0.22	4.7	-4.4	0.18	1.0
C_{D1}	C_{D2}	C_{D3}			
2.0	0.9	2.45			

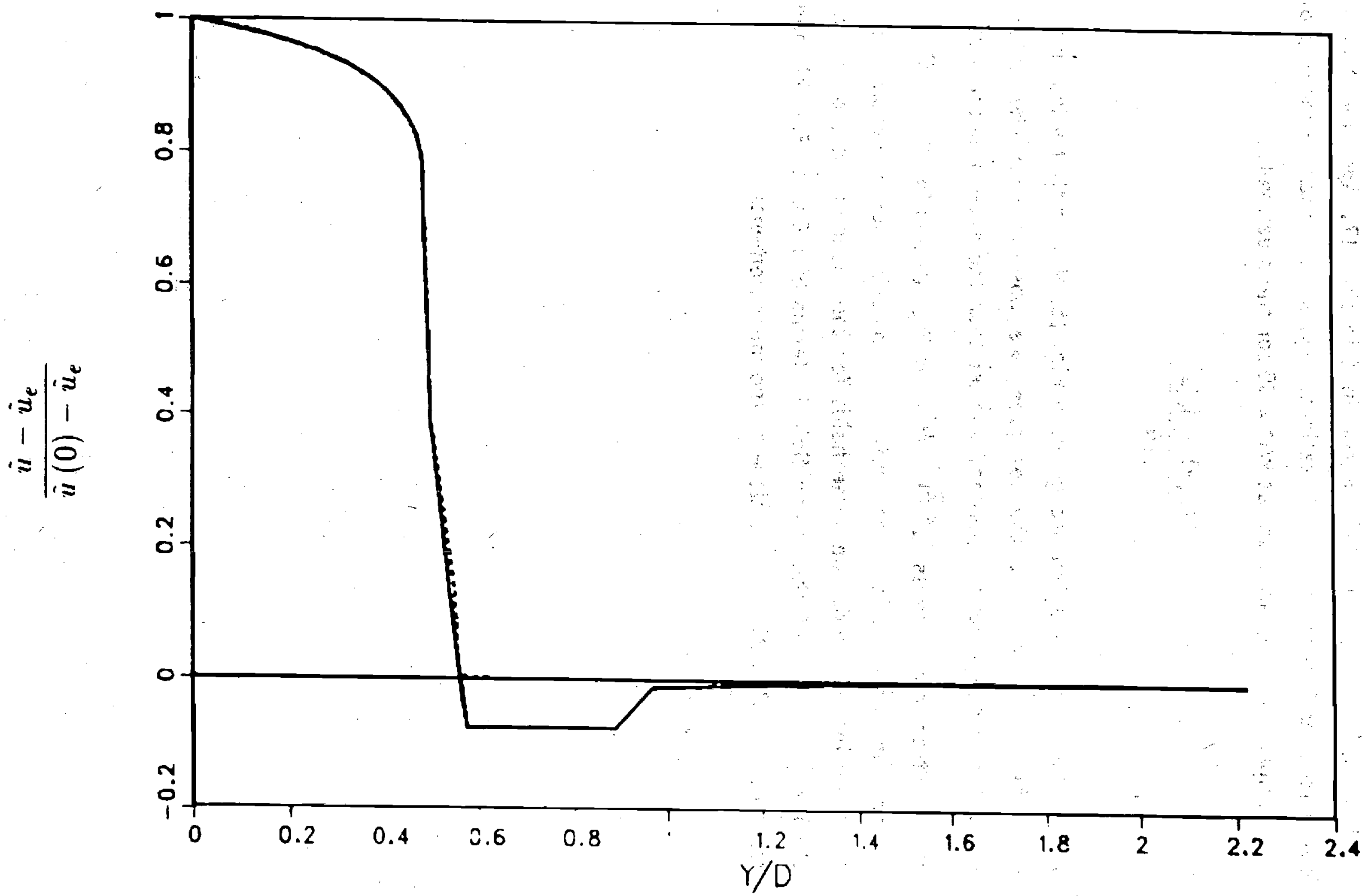

Fig. 14. Inlet velocity profile for model calculation in nonreacting propane jet.

The axial development of the mean velocity is shown in Fig. 15 as well as $(\overline{u''^2})^{1/2}/\Delta\tilde{u}$ in Fig. 16 and ln f in Fig. 17. Agreement between calculation and measurements is satisfactory. Representative radial profiles and comparisons with the data at x/D = 30 for the mean velocity

$$\frac{\tilde{u}(x,r) - \tilde{u}_e(x)}{\Delta\tilde{u}}$$

where $\Delta u = u(x,0) - u_e(x)$, are given in Fig. 18. Noting that y is normalized with the diameter D of the jet pipe, we observe that the calculated spreading rate is about ten percent smaller than the experimental value. The normal stress components $(\overline{u''^2})^{1/2}/\Delta\tilde{u}$ in Fig. 19 and $(\overline{v''^2})^{1/2}/\Delta\tilde{u}$ in Fig. 20 are in good agreement with the measurements considering the uncertainties involved. The same holds for the shear stress profiles in Fig. 21. The prediction of the scalar field in terms of mean $\tilde{f}$ (Fig. 22) and the variance $\overline{f''^2}$ (Fig. 23) is quite close to the measurements.

Fig. 15. Decay of mean excess velocity along centerline in a nonreacting propane-jet. (solid line: prediction, symbols: experiment).

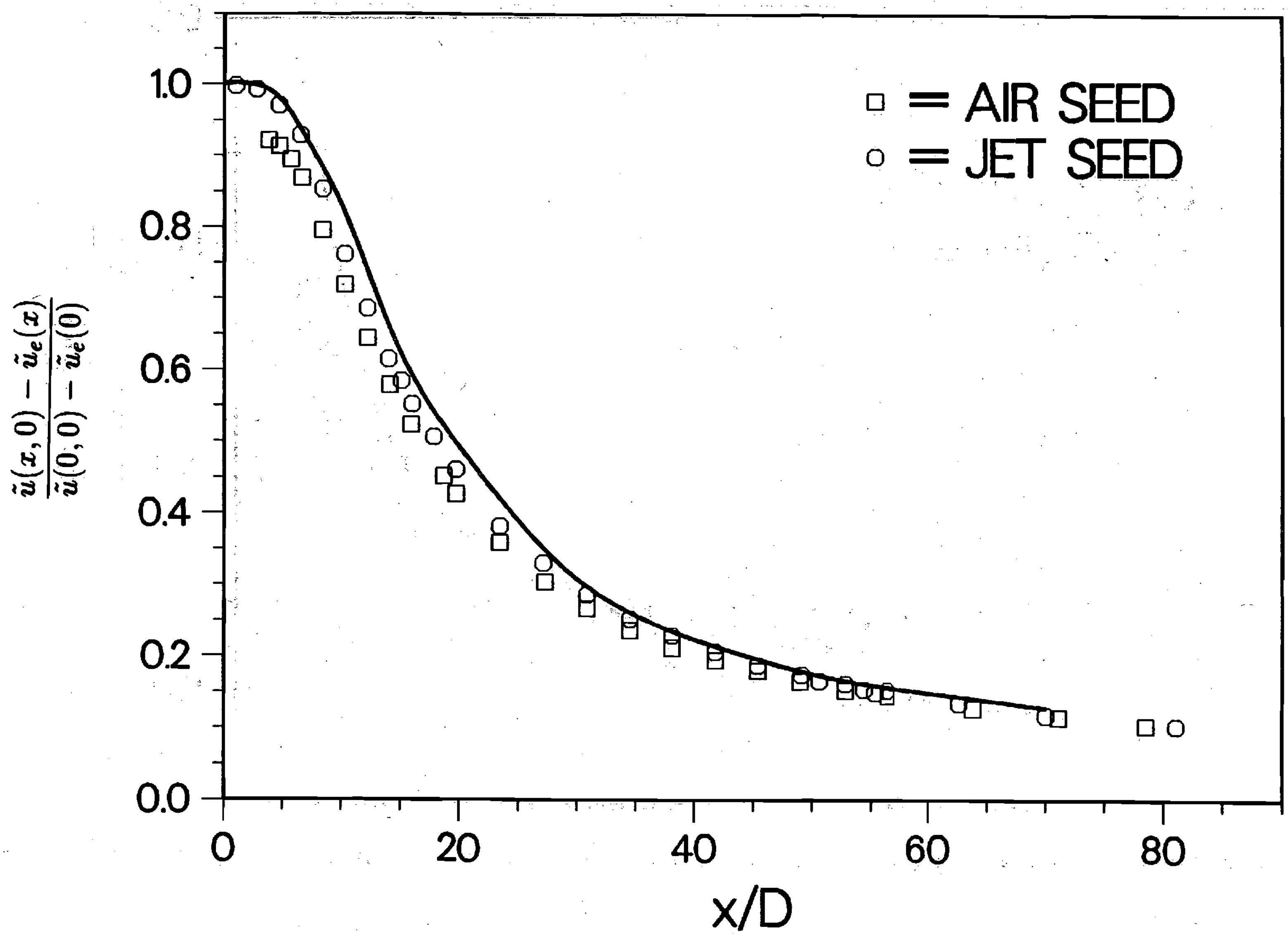

Fig. 16. Centerline variation of axial velocity fluctuations in a nonracting propane jet.

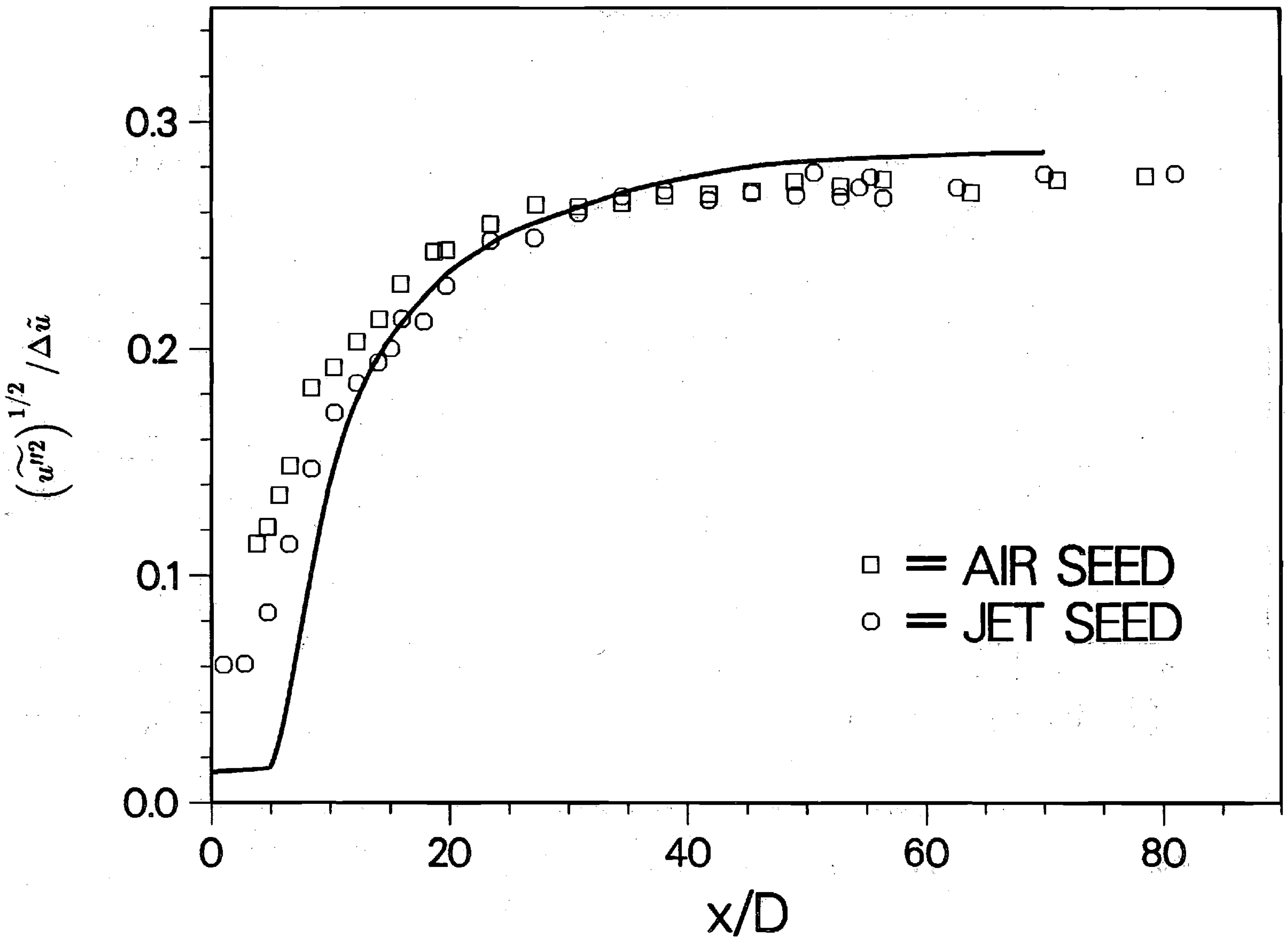

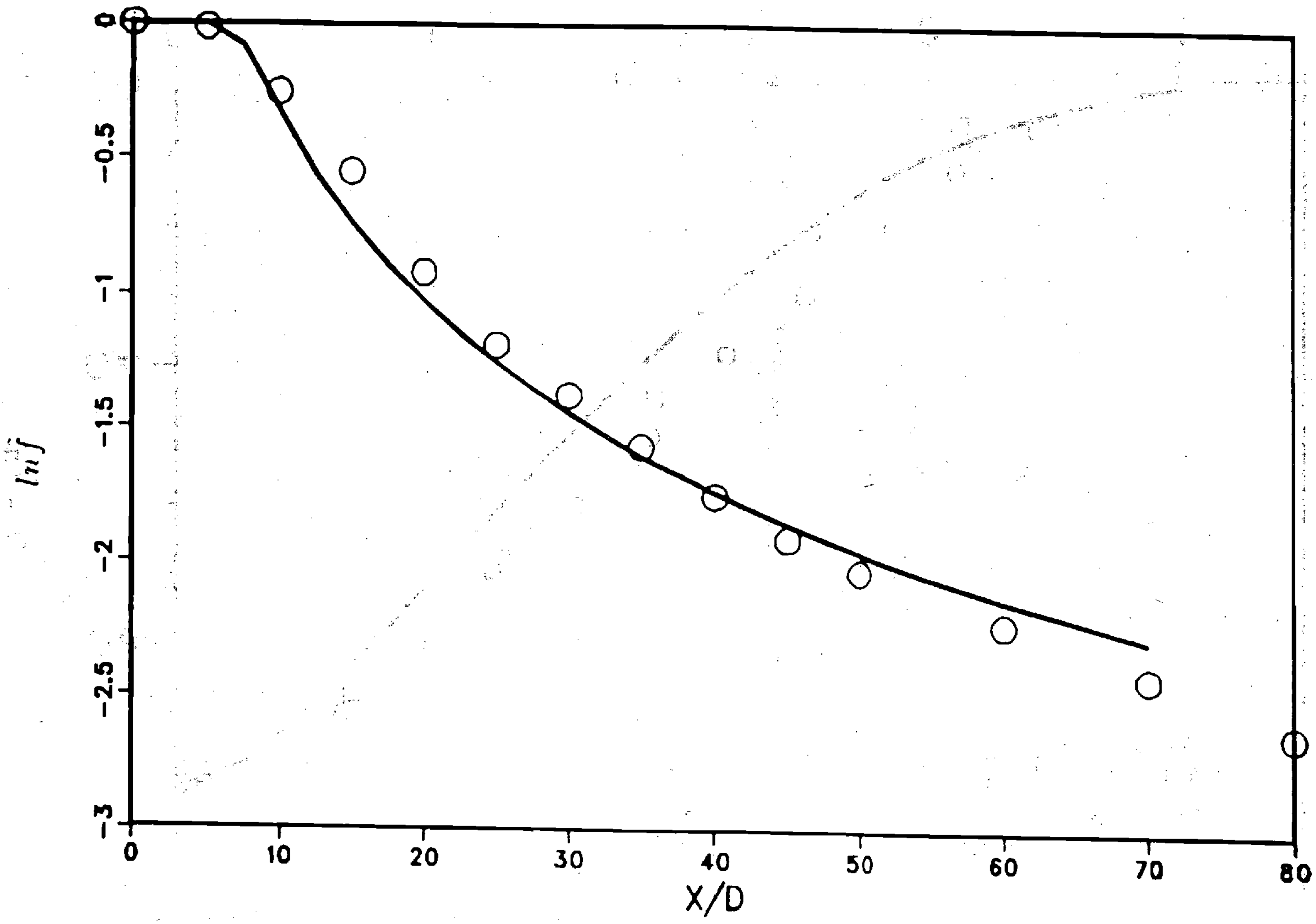

Fig. 17. Centerline variation of mean mixture fraction in a nonreacting propane jet.

Fig. 18. Radial profile of normalized excess axial velocity at x/D=30 in a nonreacting propane jet.

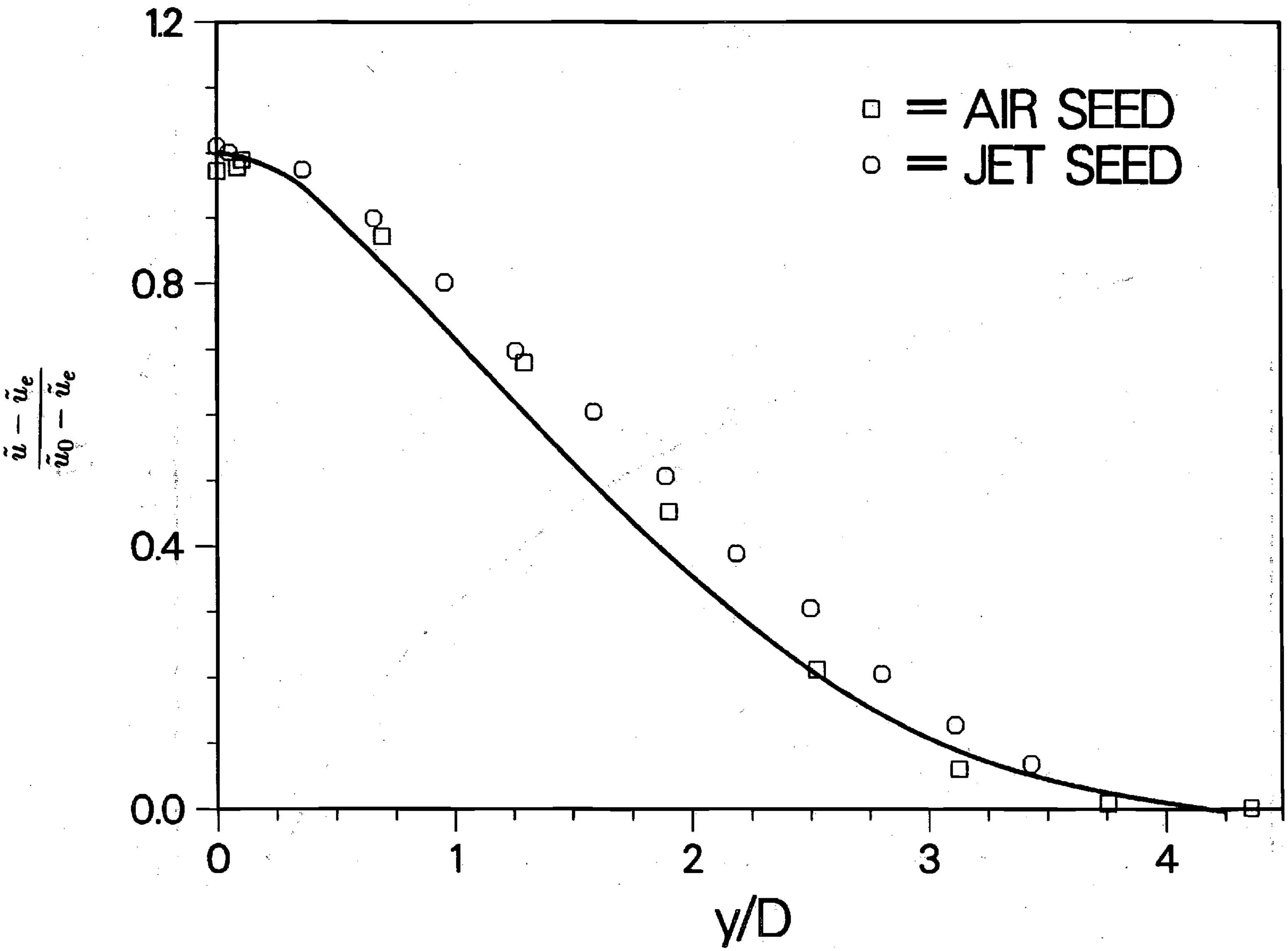

Fig. 19. Radial profile of normal stress (axial) at x/D=30 in a nonreacting propane jet.

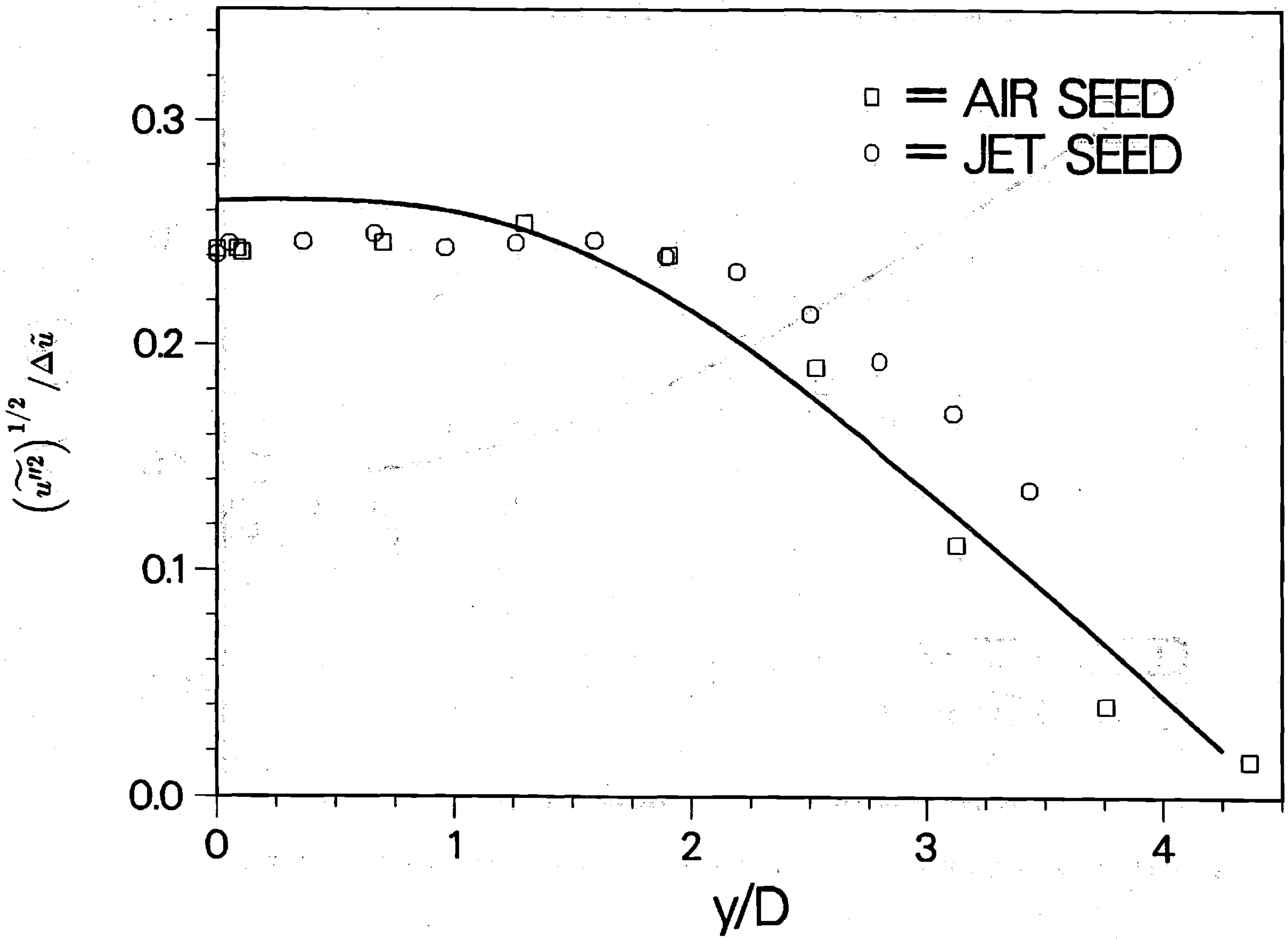

Fig. 20. Radial profile of normal stress (radial) at x/D=30 in a nonreacting propane jet.

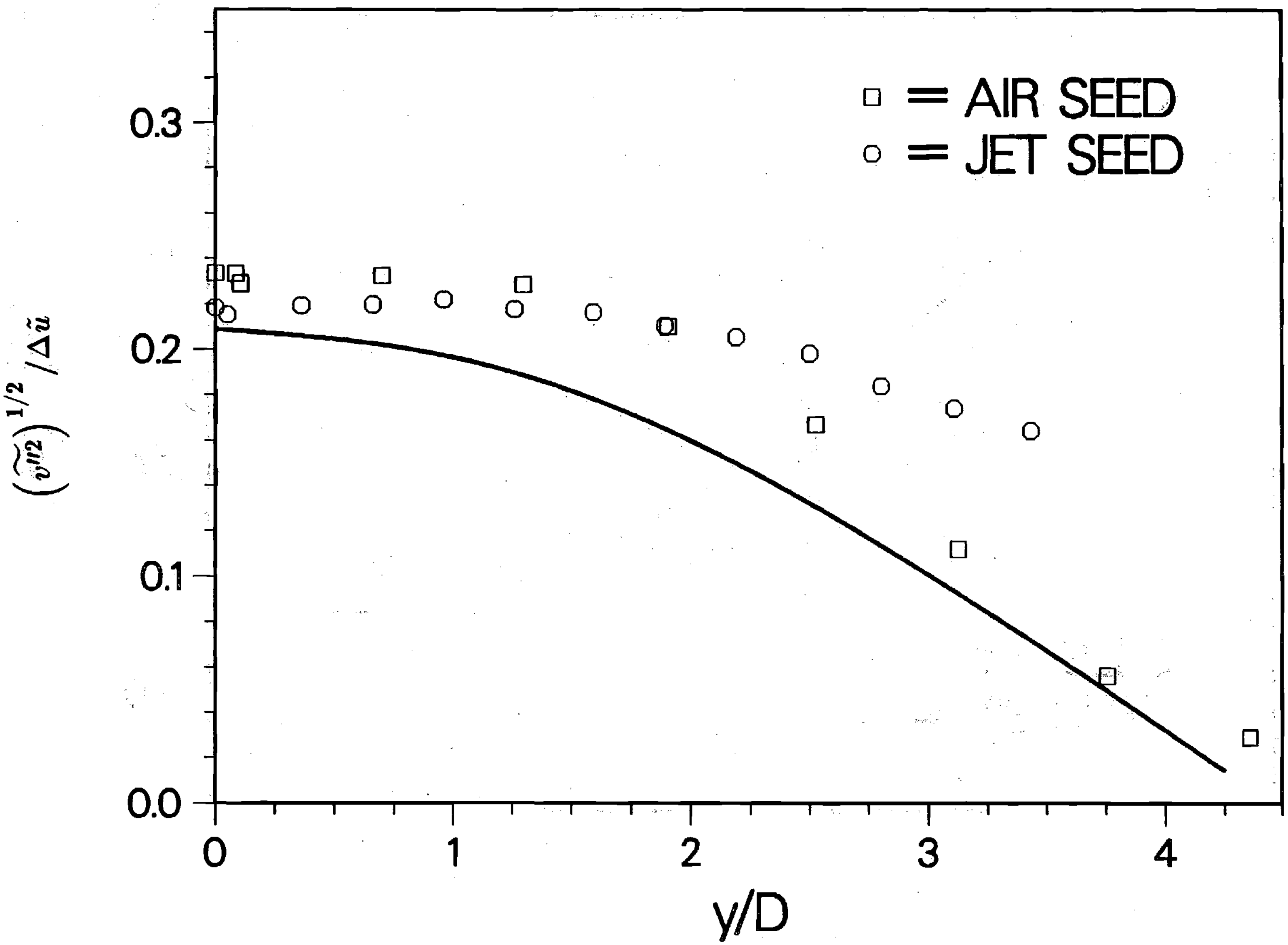

Fig. 21. Radial profile of normalized shear stress at x/D=30 in a nonreacting propane jet.

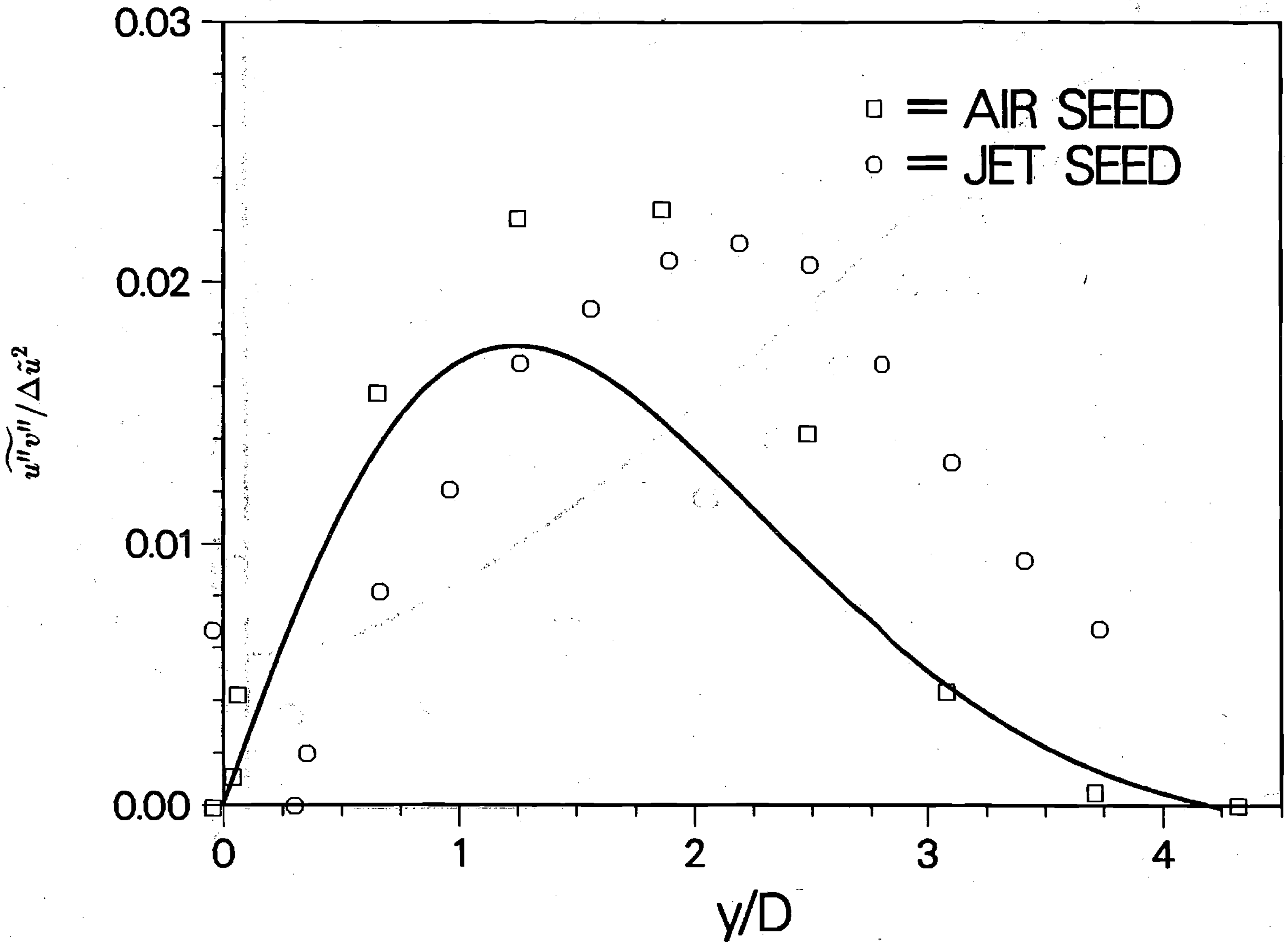

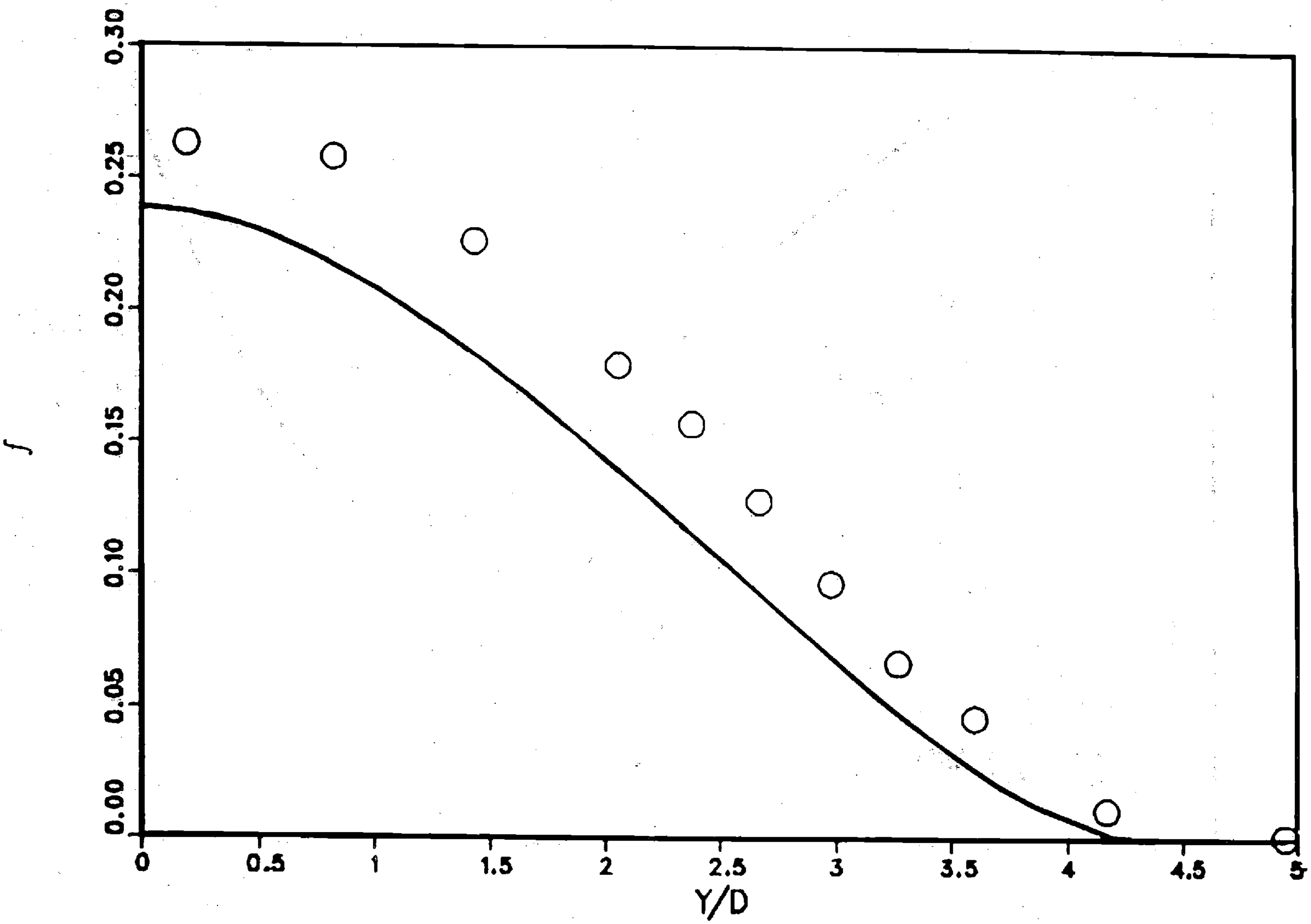

Fig. 22. Radial profile of mean mixture fraction at x/D=30 in a nonreacting propane jet.

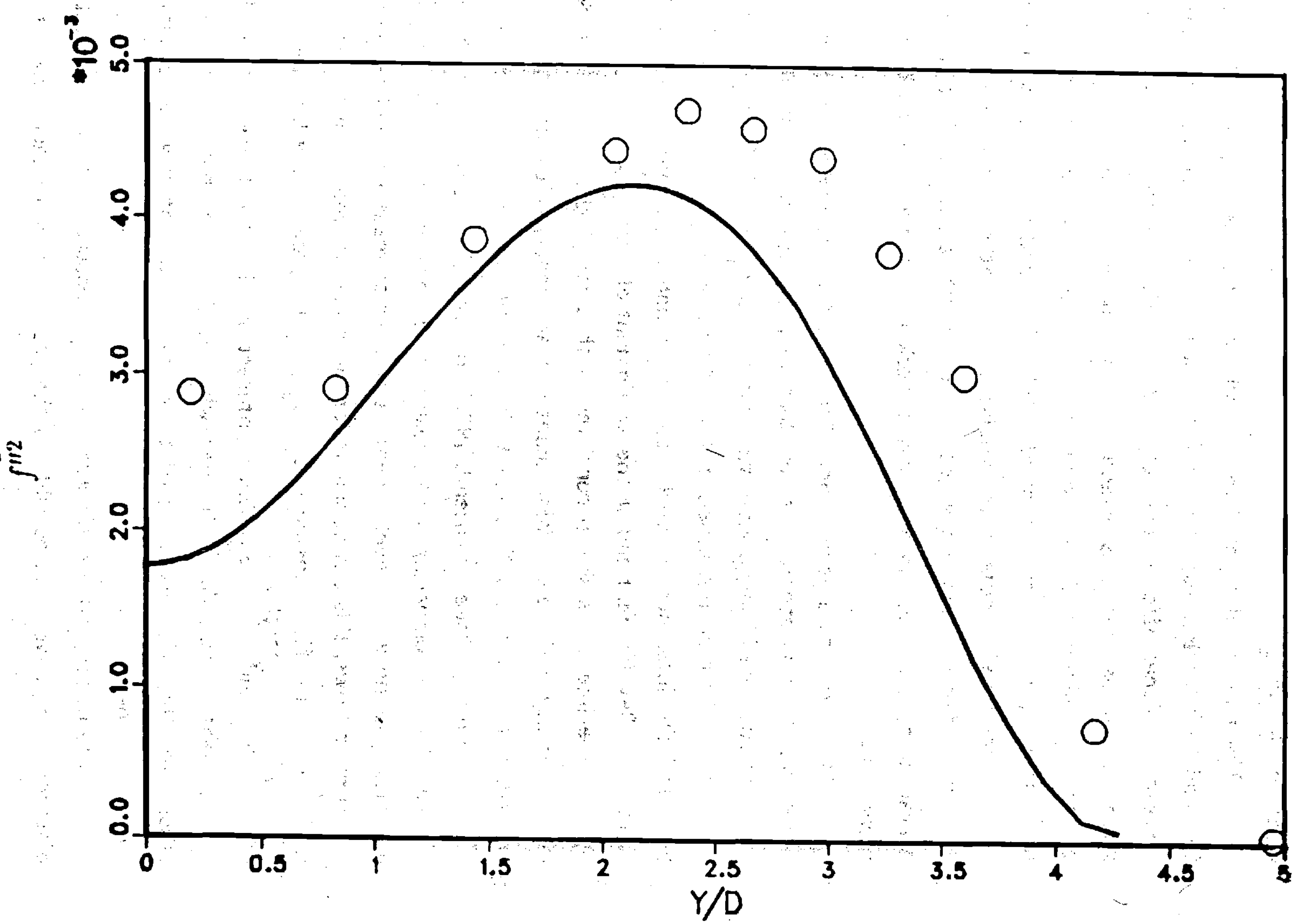

Fig. 23. Radial profile of variance in mixture fraction at x/D=30 in a nonreacting propane jet.

ADDITIONAL DATA NEEDS

Constant density flow

The free jet data of Antonia and coworkers seem quite satisfactory for model evaluation except for the laminar initial flow conditions, possible three-dimensional effects, low Reynolds number and the presence of large scale structures, features which are not explicitly considered in most current turbulence models. It would be helpful if questions concerning large scale structures, the attainment of similar flow and the presence of three-dimensional flow effects were resolved. Also intermittency data for the Antonia and coworkers plane jet would be of value. Data of a similar character to those of Antonia and coworkers are clearly needed for free round jets.

In addition to a general need for more data, especially for round jets, there are several specific issues that require study. Foremost are the presence and role of large scale structures in round as well as plane jets, the attainment of similarity, aspect ratio and three-dimensional effects in plane jets, and the influence of initial conditions and conditions in the ambient fluid on jet development and on the attainment of similarity.

Experiment has shown consistently that radial and lateral profiles of mean velocity and mean scalar quantities are nearly Gaussian when scaled according to similarity. This result is consistent with theory from simple turbulence models (see Townsend, 1976) and from more advanced turbulence models. Thus in comparing model results with experiment, one should focus attention on the axial development of the jet as measured and calculated. For similar flows, this development for mean and second moment quantities is defined by the flow constants, C_u, C_θ , L_u, L_θ , and by the limiting values of $\overline{u^2}^{1/2}/u_0$ and $\overline{\theta^2}^{1/2}/\theta_0$. One's interest in the question of axial flow development is stimulated further when it is noted that to date model results for the axial evolution of turbulent jets do not in general compare well with experiment.

Also of interest are accurate velocity measurements to larger lateral distances than have been possible in the past in order to check the form of the functions f, g and k. Finally it is noted that this review, because of time and space limitations, has essentially excluded two-dimensional shear layers and wakes of all kinds from detailed consideration. Data for these flows need to be reviewed as well.

Variable density flows

A deficiency in the variable density data presented in this section is that the density difference between the jet and the coflowing air is not as large as one would like. Additional measurements in round jets of the type discussed above are needed in flows with increased initial density differences, and in the near-field region downstream of the jet exit where density differences are greatest. For such measurement, care must be exercised in establishing well characterized initial conditions. The measurements should include mean and higher moments of velocity, scalars, and important correlations.

Detailed measurements in planar jets and planar mixing layers would provide useful test cases for model development and evaluation. As mentioned in the introductory comments, both planar jets and planar mixing layers maintain a density difference farther downstream than do axisymmetric jets. Thus, they would provide a more rigorous test of variable density models. Experimental work is needed, however, to establish the possible importance of large scale structures in these flows before the suitability of currently available modelling approaches can be evaluated.

REFERENCES

Abramovich, G. N. (1963) The Theory of Turbulent Jets. MIT Press.

Aihara, Y., Koyama, H. and Morishita, E. (1974) Effects of an air stream on turbulent diffusion of a helium jet from a small nozzle. The Physics of Fluids 17 No. 4, 665-673.

Albertson, M. L., Dai, Y. B., Jensen, R. A. and Rouse, H. (1950) Diffusion of submerged jets. Trans. ASCE 115, 639-697.

Anderson, P., LaRue, J. C. and Libby, P. A. (1979) Prefential entrainment in a two-dimensional turbulent jet in a moving stream. Phys. Fluids, 22, 1857-1861.

Antonia, R. A. and Bilger, R. W. (1973) An experimental investigation of an axisymmetric jet in a coflowing air stream. J. Fluid-Mech., 61, 805-822.

Antonia, R. A., Prabhu, A. and Stephenson, S. E. (1975) Conditionally sampled measurements in a heated turbulent jet. J. Fluid Mech., 72, Pt. 3, 455-480.

Antonia, R. A. and Bilger, R. W. (1976) The heated round jet in a coflowing stream. AIAA J., 14, 1541-1547.

Antonia, R. A., Browne, L. W. B., Chambers, A. J. and Rajagopalan, S. (1983a) Budget of the temperature variance in a turbulent plane jet. Intl. J. Heat Mass Transfer, 26, 41-48.

Antonia, R. A., Browne, L. W. B., Rajagopalan, S. and Chambers, A. J. (1983b) On the organized motion of a turbulent plane jet. J. Fluid Mech., 134, 49-66.

Antonia, R. A., Rajagopalan, S. and Fulachier, L. (1984) Comparison of temperature and velocity spectra in a slightly heated turbulent plane jet. AIAA J., 22, 311-313.

Bashir, J. and Uberoi, M. S. (1975) Experiments on turbulent structure and heat transfer in a two-dimensional jet. Phys. Fluids, 18, 405-410.

Batt, R. G. (1977) Turbulent mixing of passive and chemically reacting species in a low-speed shear layer. J. Fluid Mech., 82, Pt. 1, 53-95.

Becker, H. A., Hottel, H. C. and Williams, G. C. (1967) The nozzle-fluid concentration field of the round, turbulent, free jet. J. Fluid Mech., 30, 285-303.

Bilger, R. W., Antonia, R. A. and Sreevivasan, K. R. (1976) Determination of intermittency from the probability density function of a passive scalar. Phys. Fluids, 19, No. 10, 1471-1474.

Bilger, R. W. (1980) Turbulent flows with nonpremixed reactants. Turbulent Reacting Flows (P. A. Libby and F. A. Williams, Eds.), Springer-Verlag, New York, 65-113.

Birch, A. D., Brown, D. R., Dodson, M. G and Thomas, J. R. (1978) The turbulent concentration field of a methane jet. J. Fluid Mech., 88, 431-449.

Bradshaw, P. (1966) The effect of initial conditions on the development of a free shear layer. J. Fluid Mech., 26, 225-336.

Bradshaw, P. (1977) Effect of external disturbances on the spreading rate of a plane turbulent jet. J. Fluid Mech., 80, 795-797.

Brown, G. L. and Roshko, A. (1974) On density effects and large structure in turbulent mixing layers. J. Fluid Mech., 64, Pt. 4, 775-816.

Browne, L. W. B. and Antonia, R. A. (1983) Measurements of turbulent Prandtl number in a plane jet. Trans. ASME C: J. Heat Transfer, 105, 663-665.

Browne, L. W. B., Antonia, R. A., Rajagopalan, S. and Chambers, A. J. (1983) Interaction region of a two-dimensional turbulent plane jet in still air: Structure of Complex Turbulent Shear Flow (R. Dumas and L. Fulachier, Eds.)

Catalano, G. D., Morton, J. B. and Humphris, R. R. (1976) Experimental investigation of an axisymmetric jet in a coflowing airstream. AIAA J., 14, 1157-1158.

Chevray, R. and Tutu, N. K. (1978) Intermittency and prefential transport of heat in a round jet. J. Fluid Mech., 88, 138-160.

Chigier, N. A. and Strokin, V. (1975) Mixing Processes in a free turbulent diffusion flame. Comb. Sci. and Tech., 9, 111-118.

Corrsin, S. (1946) Investigation of flow in an axially symmetric heated jet of air. NACA Wartime Report 94.

Corrsin, S. and Uberoi, M. S. (1950) Further experiments on the flow and heat transfer in a heated turbulent jet. NACA Report 998.

Davies, A. E., Keffer, J. F. and Baines, D. W. (1975) Spread of a heated plane turbulent jet. Phys. Fluids., 18, 770-775.

Dibble, R. W., Kollmann, W. and Schefer, R. W. (1984) Conserved scalar fluxes measured in a turbulent nonpremixed flame by combined laser doppler velocimetry and laser raman scattering. Combust. Flame, 55, 307-321.

Dibble, R. W., Farshchi, M. and Kollmann, W. (1985c) Second-order closure for turbulent diffusion flows. To be presented at Fifth Symposium on Turbulent Shear Flows, Cornell University.

Dibble, R. W., Kollmann, W. and Schefer, R. W. (1985a) Scalar dissipation in turbulent reacting flows: Measurements and numerical model predictions. Twentieth Symposium (International) on Combustion, The Combustion Institute, Pittsburgh.

Dibble, R. W., Hartmann, V., Schefer, R. W. and Kollmann, W. (1985b) Conditional sampling of velocity and scalars in turbulent flames using simultaneous LDV-Raman scattering. Accepted for publication in Journal of Experiments in Fluids.

Drake, M. C., Lapp, M., Penney, C. M., Warshaw, S. and Gerhold, B. W. (1981) Measurements of temperature and concentration fluctuations in turbulent diffusion flames using pulsed Raman spectroscopy. Eighteenth Symposium (International) on Combustion, The Combustion Institute, 1521-1531.

Drake, M. C., Bilger, R. W. and Starner, S. H. (1983) Raman measurements and conserved scalar modeling in turbulent diffusion flames. Nineteenth Symposium (International) on Combustion, The Combustion Institute, 459-467.

Driscoll, J. F., Schefer, R. W. and Dibble, R. W. (1983) Mass fluxes measured in a turbulent nonpremixed flame. Nineteenth Symposium (International) on Combustion, The Combustion Institute, 477-485.

Durst, F., Melling, A. and Whitelaw, J. A., Principles and practice of laser-Doppler anamometry, Academic Press, London, 1976.

Dyer, T. M. (1979) Rayleigh scattering measurements of time-resolved concentration in a turbulent propane jet. AIAA J. 17, 912-914.

Effelsberg, E. and Peters, N. (1983) A composite model for the conserved scalar PDF. Combust. Flame, 50, 351-360.

Everitt, K. W. and Robbins, A. G. (1978) The development and structure of turbulent plane jets. J. Fluid Mech., 88, 563-583.

Farshchi, M. and Kollmann, W. (1984) Reynolds stress closure for turbulent flows. Presented at ASME-AIChE Conference, Seattle.

Fischer, H. B.. List, E. J., Koh, R. C., Imberger, J. and Brooks, N. H. (1979) Mixing in Inland and Coastal Waters, Academic Press.

Gutmark, E. and Wygnanski, I. (1976) The planar turbulent jet. J. Fluid Mech., 73, 465-495.

van der Hegge Zijnen, B. G. (1958a) Measurements of the distrubution of heat and matter in a plane turbulent jet of air. Appl. Sci. Res., A7, 277-292.

van der Hegge Zijnen, B. G. (1958b) Measurements of the velocity distribution in a plane turbulent jet of air. Appl. Sci. Res., A7, 256-276.

Heskestad, G. (1965) Hot-wire measurements in a plane turbulent jet. Trans. ASME E: J. Appl. Mech., 32, 721-734.

Hill, W. G., Jenkins, R. C. and Gilbert, B. L. (1976) Effects of the initial boundary-layer state on turbulent jet mixing. AIAA J., 14, 1513-1514.

Hinze, J. O. Turbulence 2nd. ed. McGraw-Hill.

Hinze, J. O. and van der Hegge Zijnen, B. G. (1949) Transfer of heat and matter in the turbulent mixing zone of an axially symmetrical jet. Appl. Sci. Res., A1, 435-461.

Honjolie, K. and Launder, B. E. (1972). J. Fluid Mech., 52, 609.

Jenkins, P. E. and Goldschmidt, V. W. (1973) Mean temperature and velocity in a plane turbulent jet. ASME X: J. Fluids Engng., 95, 581-584.

Johnston, S. C., Dibble, R. W., Schefer, R. W., Ashurst, W. T. and Kollmann, W. (1986) Laser measurements and stochastic simulations of turbulent reacting flows. Accepted for publication AIAA J.

Jones, W.P. (1982) Models for turbulent flows with variable density and combustion. Prediction Methods for Turbulent Flows (W. Kollmann, Ed.), Hemisphere Publ.

Keagy, W. R. and Weller, A. E. (1950) A study of freely expanding inhomogeneous jets. Proc. Heat Transfer and Fluid Mech. Inst., 1-3, 89-98.

Keller, J. O. (1982) An experimental study of combustion and the effects of large heat release on a two-dimensional turbulent mixing layer. Ph.D. Dissertation, University of California, Berkeley, CA.

Kiser, K. M. (1963) Material and momentum transport in axisymmetric turbulent jets of water. AIChE J., 9, 386-390.

Krothapalli, A., Baganoff, D. and Karamcheti, K. (1981) On the mixing of a rectangular jet. J. Fluid Mech., 107, 201-220.

LaRue, J. C. and Libby, P. A. (1977) Measurements in the turbulent boundary layer with slot injection of helium. Phys. Fluids, 20, 192-202.

List, E. J. (1982) Turbulent jets and plumes. Ann. Rev. Fluid Mech., 14, 189-212.

Lockwood, F. C. and Moneib, H. A. (1980) Fluctuating temperature measurements in a heated round free jet. Comb. Sci. Tech., 22, 63-81.

Long, M. B., Chu, B. T. and Chang, R. K. (1981) Instantaneous two-dimensional gas concentration measurements by light scattering. AIAA J., 19, 1151-1156.

Moss, J. B. (1980) Simultaneous measurements of concentration and velocity in an open premixed turbulent flame. Comb. Sci. Tech., 22, 119-129.

Pitts, W. M. and Kashiwagi, T. (1984) The application of laser-induced Rayleigh light scattering to the study of turbulent mixing. J. Fluid Mech., 141, 391-429.

Rajaratnam, N. (1976) Turbulent Jets, Elsevier.

Razdan, M. K. and Stevens, J. G., (1985) "CO/air turbulent diffusion flame: measurements and modeling," Combust. Flame, 59, 289.

Rebollo, Ph.D. Thesis, California Institute of Technology, Pasadena, CA.

Rhodes, R. P., Hansha, P. T. and Peters, C. E. (1974) Turbulent kinetic energy analyses of hydrogen-air diffusion flames. Acta Astronautica, 1, 443-470.

Santoro, R. J., Semerjian, H. G., Emmerman, P. J. and Goulard, R. (1981) Optical tomography for flow field diagnostics. Int. J. Heat Mass Transfer, 24, 1139-1150.

Schefer, R. W. and Dibble, R. W. (1985d) Simultaneous measurements of velocity and density in a turbulent nonpremixed flame. AIAA J., 23, 1070-1078.

Schefer, R. W. and Dibble, R. W. (1985a) Mixture fraction measurements in a turbulent nonpremixed propane jet. Submitted for publication.

Schefer, R. W., Hartmann, V. and Dibble, R. W. (1985b) Conditional sampling of velocity in a turbulent nonpremixed propane jet. Submitted for publication.

Schefer, R. W., Dibble, R. W., Johnston, S. C., Gouldin, F. C. and Kollmann, W. (1985c). (Accepted for publication AIAA Journal).

Shaughnessy, E. J. and Morton, J. B. (1977) Laser light-scattering measurements of particle concentration in a turbulent jet. J. Fluid Mech., 80, 129-148.

Sreenivasan, K. R., Antonia, R. A. and Stephenson, S. E. (1977) Conditional Measurements in a heated axisymmetric mixing layer. T. N. - F. M., 5, Dept. Mech. Engr., University of Newcastle.

Thring, M. W. and Newby M. P. (1953) Combustion length of enclosed turbulent jet flames. Fourth Symposium on Combustion, The Combustion Institute, 789-796.

Townsend, A. A. (1976) The Structure of Turbulent Shear Flow, 2nd ed., Cambridge University Press.

Tritton, D. J., (1977) Physical Fluid Dynamics, Van Nostrand Reinhold Company.

Vankataramani, K. S., Tutu, N. K. and Chevray, R. (1975) Probability distributions in a round free jet. Phys. Fluids, 18, 1413-1420.

Warshaw, S., Lapp, M., Penney, C. M. and Drake, M. D. (1980) Temperature-velocity correlation measurements for turbulent diffusion flames from vibrational Raman-scattering diagnostics. Laser Probes for Combustion Chemistry, (D. R. Crosley, Ed.), Paper 19, American Chemical Society Symposium Series, 134, 239-246.

Wilson, R. A. M. and Danckwerts, P. V. (1964) Studies in turbulent mixing-II. Chem. Engng. Sci., 19, 885-895.

Wygnanski, I. and Fielder, H. (1969) Some measurements in the self-preserving jet. J. Fluid Mech., 38, 577-612.

Yanagi, T. and Mimura, Y. (1981) Velocity-temperature correlation in premixed flame. Eighteenth Symposium (International) on Combustion. The Combustion Institute, 1031-1039.

CHAPTER 3

FAST REACTION NON PREMIXED COMBUSTION

G. M. Faeth and G. S. Samuelson

NOMENCLATURE

a	acceleration of gravity
d	jet diameter
D	mass diffusivity, jet diameter
f	mixture fraction
h	slot height
k	turbulence kinetic energy
K_i	kurtosis of random variable i
L	integral length scale
p	pressure
P(i)	probability density function of variable i
r	radial distance
Re	Reynolds number
R_{ij}	correlation coefficient of variables i and j
S_i	skewness of random variable i
T	temperature
u	streamwise velocity
v	crosstream velocity
w_i	reaction rate of species i
x	streamwise direction
x_i	spatial coordinate in direction i
X_i	mole fraction of species i
y	crosstream direction
Y_i	mass fraction of species i
β	streamwise pressure gradient parameter
γ	intermittency
ξ	conserved scalar
ρ	density
φ	generic property
χ	instantaneous scalar dissipation rate

Subscripts

c	centerline
e	free stream
f	flame tip
j	jet or slot exit
max	maximum value
n	nonturbulent fluid
t	turbulent fluid
w	wall exit
o	flow axis or plane of symmetry

Superscripts

$(\bar{\ })$	time-averaged quantity
$(\tilde{\ })$	Favre-averaged quantity
$(\ )'$	fluctuation from time average
$(\ )''$	fluctuation from Favre average
$(\bar{\ })'$	time-averaged fluctuating quantity, $\overline{(\varphi'^2)}^{1/2}$
$(\tilde{\ })''$	Favre-averaged fluctuating quantity, $(\widetilde{\varphi''^2})^{1/2}$
$(\hat{\ })$	averaged quantity indicated by a probe

INTRODUCTION

Burke and Schuman (1928) were among the first to recognize that nonpremixed flames, or other reaction processes, could often be understood without detailed consideration of chemical kinetics. They defined the fast-reacting nonpremixed combustion limit, or classical diffusion flame, where reaction occurs only at a thin flame sheet. At this limit, reaction rates are fast and reactant concentrations are negligible in the flame sheet; therefore, overall rates of reaction and the position of the flame sheet can be found from transport principles alone. Subsequent work has demonstrated the practical utility of this concept, even for complex processes like turbulent flames.

Consideration of flows at the fast-reacting nonpremixed combustion limit is a logical first step in the evaluation of methods proposed for analyzing turbulent reacting flow. At this limit, the reacting flow is only a modest extension of passive turbulent mixing; the main difference being the energy release at the flame sheet and the accompanying changes of scalar properties, e.g., density, temperature, composition, etc. The objective of this chapter is to review past measurements of fast-reacting nonpremixed turbulent reaction processes in order to highlight data bases most suitable for evaluation of theories of turbulent reacting flow. Recommendations are also made concerning measurements that are needed for more definitive evaluation of analysis. Other chapters in this report, by Gouldin and Johnson (1985), Drake and Kollman (1985) and Libby, Sevasegaram and Whitelaw (1985), have similar objectives for passive mixing, slow-reaction nonpremixed combustion and premixed combustion, respectively.

We take a broad definition of fast-reacting nonpremixed turbulent combustion processes. Turbulent reaction processes are considered where chemical transformation is mixing controlled and local thermodynamic equilibrium in maintained (within experimental uncertainties), for major species and temperature. Thus we consider acid/base reactions in liquids, where effects of energy release are small; as well as gaseous diffusion flames, where free radicals and other trace species can be influenced by finite-rate chemistry, even though the major species are often nearly in thermodynamic equilibrium. Reactant combinations in the latter category include hydrogen/air hydrogen/fluorine, carbon monoxide/air, nitric oside/ozone and the dissociation of nitrogen tetroxide in warm air.

Similar to the other chapters in this report (Gouldin and Johnson, 1985: Drake and Kollman, 1985; and Libby et al., 1985), attention has been limited to stationary turbulent flows (flows which are independent of time in the mean) which can be analyzed using a parabolic formulation of the governing equations (flows which satisfy the boundary layer approximations). For convenience, these flows are grouped into three categories, as follows: (1) round free jets, (2) plane free shear layers, and (3) wall boundary layers. Past measurements, however, have largely emphasized the round free jet configuration.

This chapter begins with a general discussion of the properties of experiments involving fast-reacting nonpremixed turbulent combustion. This includes an operational definition of the fast-reaction limit, measurement properties needed to properly define flows for evaluation of analysis, and the characteristics of various measurement techniques. The present discussion of measurement techniques is brief and primarily considers methods having particular interest for nonpremixed flows.

Using principles developed in the section on experimental considerations, the experiments themselves are discussed. The objective here is not to discuss the physics and chemistry disclosed by the experiments, original sources serve best for this purpose. Rather, our intent is to determine available data bases which are most appropriate for evaluation of analysis at the fast-reaction limit. The paper concludes with recommendations concerning existing measurements which are best suited for evaluation of analysis, a format appropriate for data-base documentation, and suggestions for additional measurements.

EXPERIMENTAL CONSIDERATIONS

The general properties of experiments concerning fast-reacting nonpremixed turbulent combustion processes are discussed in this section, prior to describing the measurements themselves in the next. The objective is to point out properties of experiments which make them particularly suitable for evaluation of analysis. In doing this, we do not attempt to anticipate the kind of analysis to be evaluated, aside from the general limitation to stationary parabolic (in the mean) flows. Our view is that any practical analysis should yield information concerning operational properties of the process, i. e., those properties which can be measured in a well-defined manner. Therefore, we concentrate on the operational definition of the fast-reaction limit; the effect of potentially uncontrolled, or unreported, variables on flow properties; and the properties of measurements that have been made during past work.

Fast-reaction criteria

In this section, the present definition of the fast-reaction limit is described. This is followed by an application of this definition to several reactant combinations that have been considered in the past.

The fast-reaction limit of nonpremixed combustion is reached when characteristic transport times of mass diffusion, thermal diffusion, and convection are large in comparison to all characteristic times of reactions in the chemical transformation mechanism. In this case, instantaneous thermodynamic equilibrium is maintained at each point in the flow and scalar properties are fixed by diffusion processes at the molecular level. The simplest realization of this limit occurs when chemical conversion only occurs in a reaction (or flame) sheet which is thin in comparison to other length scales of the process. For flames, this thin-flame limit is generally confined to cases where the activation energies of all relevant reactions are large.

No real nonpremixed reaction or combustion process satisfies the above prescription of the fast-reaction limit for all species in all regions of the flow. Exceptions occur near regions of flame attachment, possibly throughout the flow for free radicals and other trace species (often pollutants), as well as the conventional exception when characteristic diffusion times become comparable to chemical times in a highly turbulent flow. Points of flame attachment fundamentally involve comparable transport and chemical times; therefore, the reaction zone is thick in comparison to local length scales and the full complexity of turbulent reaction processes must be considered. Naturally, all experiments have such a region; however, this zone is assumed to be small and measurements within it are excluded from consideration, for present purposes.

If measurements were excluded due to loss of local equilibrium for free radicals and trace species, there would be very few candidate data bases for the fast-reaction limit. The major problem is that three-body recombination reactions of free radicals are often relatively slow and have low activation energies. This leads to superequilibrium of free radicals and relatively thick zones where their rates of reaction are significant in most flames. Nevertheless, these processes often have only a minor influence on the structure of the flow; therefore, with some lack of rigor, we choose to ignore them in order to preserve the convenience of the fast-reaction limit. Thus, for present purposes, conditions where only major species (reactants and products) approach local equilibrium are accepted as part of the fast-reaction limit.

Given local thermodynamic equilibrium as a criterion for the fast-reaction limit, the next problem is to define an operational method for estimating when this limit is satisfied. Analysis provides one approach. Given information on turbulence scales, estimates of diffusion and convection times can be made. Estimating characteristic chemical times, however, is more difficult. First of all, a complex mechanism is usually involved, and not all reaction steps are well known. Next, nonpremixed combustion processes always involve local variations in the concentrations of elements, yielding a range of reaction conditions which only detailed analysis can resolve.

Activation energy asymptotics, along the lines discussed by Buckmaster and Ludford (1982) and references cited therein, provide one means of treating changes in the local concentrations of elements within the flame sheet formalism, when examining conditions for the fast-reaction limit. However, this is often not appropriate for the processes which are the main issue, e. g., low activation energy reactions of three-body free radical recombination reactions. In such circumstances, perturbation methods (Bilger, 1982) or complete solution of the chemical mechanism offer alternatives. Some examples of the latter will be considered in the following.

Examination of conditions where the fast-reaction limit is appropriate is vastly simplified when condition approximate the requirements of the conserved-scalar formalism (Bilger, 1976). This implies that there are only two reactant streams (fuel-containing and oxidant containing); that flow velocities are low, so that the kinetic energy and viscous dissipation of the mean flow can be ignored; that the exchange between elements of the flow by radiation is negligible; and that instantaneous local thermodynamic equilibrium is maintained. Then, all instantaneous scalar properties are only a function of the degree of mixing of the two streams. The degree of mixing can be represented by a number of parameters, the mixture fraction (the fraction of mass originating from the fuel stream) is a common choice. Relaxation of any of these approximations requires additional parameters to specify the local state of the flow, e. g., three reactant streams would require two mixture fraction parameters to specify the state of mixing.

The type of failure of the conserved scalar formalism of greatest interest here involves loss of local thermodynamic equilibrium. The effect of turbulent mixing on thermodynamic equilibrium can be conveniently examined using an approach described by Bilger (1977) and Liew et al. (1984). First of all, we assume that the mass fraction of species i, Y_i, is solely a function of the conserved scalar, ξ, e.g.

$$Y_i = Y_i(\xi) \tag{1}$$

Then the equation for conservation of i can be written (Bilger, 1977) as follows

$$1/2\, \rho\chi(d^2Y_i/d\xi^2) = -w_i \tag{2}$$

where

$$\chi = 2D(\partial\xi/\partial X_k)^2 \tag{3}$$

In a turbulent flow, χ is the scalar dissipation rate. This parameter reflects effects of flame stretch which lead to locally high values of χ and a tendency to depart from conditions of local thermodynamic equilibrium.

Computations of Liew et al.(1984) directly show the effect of flame stretch on approach to thermodynamic equilibrium. They consider laminar methane/air diffusion flames, using a chemical reaction mechanism involving 38 reactions for 16 species. The laminar flame is progressively stretched, parametrically considering maximum values of the scalar dissipation rate, χ_{max} in the range 0-99 s^{-1}. For low values of χ_{max}, the profiles are nearly universal and the hypothesis that $Y_i = Y_i(\chi)$ is satisfied. As χ_{max} increases, however, it exerts a greater influence on scalar properties, eventually causing the flame to extinguish. A measure of the approach to thermodynamic equilibrium can then be obtained by comparing $Y_i(\xi)$ from the finite-rate analysis with direct computations, using an equilibrium code such as Gordon and McBride (1971), for various values of ξ and the same inlet stream conditions.

Knowledge of mechanisms and rates are often not adequate for an analytical assessment of the fast-reaction limit. More direct methods invloving measurements in laminar and turbulent flames then provide an alternative. Laminar flames generally have a spatial variation of χ; therefore, direct measurement of scalar properties in laminar flames can provide a test of the degree to which local equilibrium is approached for this range of χ. In fact, this is the basis for the laminar flamelet concept of Bilger (1977) and Liew et al. (1981). They observe that plots of scalar properties as a function of ξ frequently are nearly universal functions, even when local thermodynamic equilibrium is not maintained. However, by the

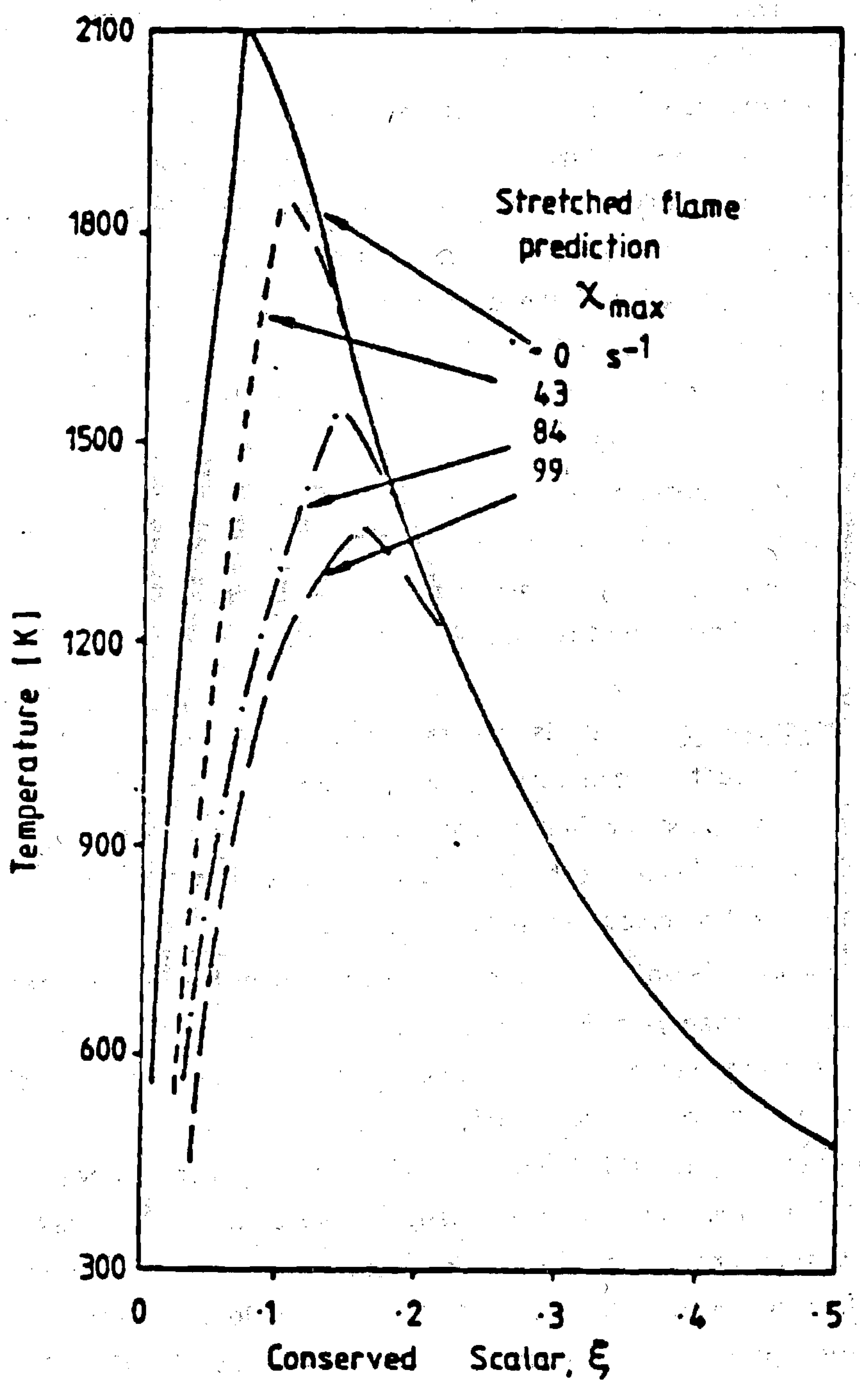

Figure 1. Variation of temperature with the conserved scalar, ξ, for stretched methane/air diffusion flames. From Liew, Bray and Moss (1984).

present criterion for the fast-reaction limit, nonequilibrium situations would not be considered, even if they exhibit universality in ξ coordinates.

A more convincing alternative for establishing conditions at the fast-reaction limit is to directly measure instantaneous scalar properties, sufficient to evaluate ξ, in the turbulent flow. This generally requires advanced experimental techniques, since information on mixing levels requires measurement of the concentrations of several species. Work along these lines, however, is beginning to appear, e. g., Drake and coworkers (1981, 1982, 1984 and 1985) and Dibble and coworkers (1984a, 1984b, 1985a, 1985b, 1985c, and 1985d).

In the following, several combinations will be examined to see if they satisfy the criterion for the fast reaction limit, as follows: hydrogen/air, carbon monoxide/air, hydrocarbon/air, hydrogen/fluorine, nitric oxide/ozone, acid/base, and nitrogen tetroxide dissociation.

Hydrogen/Air It is commonly thought that hydrogen oxidation kinetics are fast in comparison to transport processes in subsonic flows; therefore, hydrogen/air flames are logical candidates for study at the fast-reaction limit. Evidence both supporting this view and suggesting some limitations will be discussed in the following.

Figure 2 is an illustration of species concentrations and temperatures in several hydrogen/air diffusion flames plotted as a function of a conserved scalar (fuel-equivalence ratio). Measurements include results obtained at various points in laminar diffusion flames (Faeth et al., 1985); and Aeschliman et al., 1979) and in turbulent diffusion flames at locations remote from the point of attachment (Drake et al., 1981, 1984).* Two sets of predictions are shown, one considering finite-rate chemistry for Re < 100 by Miller and Kee (1977), the other based on local adiabatic equilibrium using the Gordon and McBride (1977) computer code (CEC 76 Version). The results of Faeth et al. (1985) and Drake et al. (1981, 1985) exhibit close

---

* The effect of position will be quantified later.

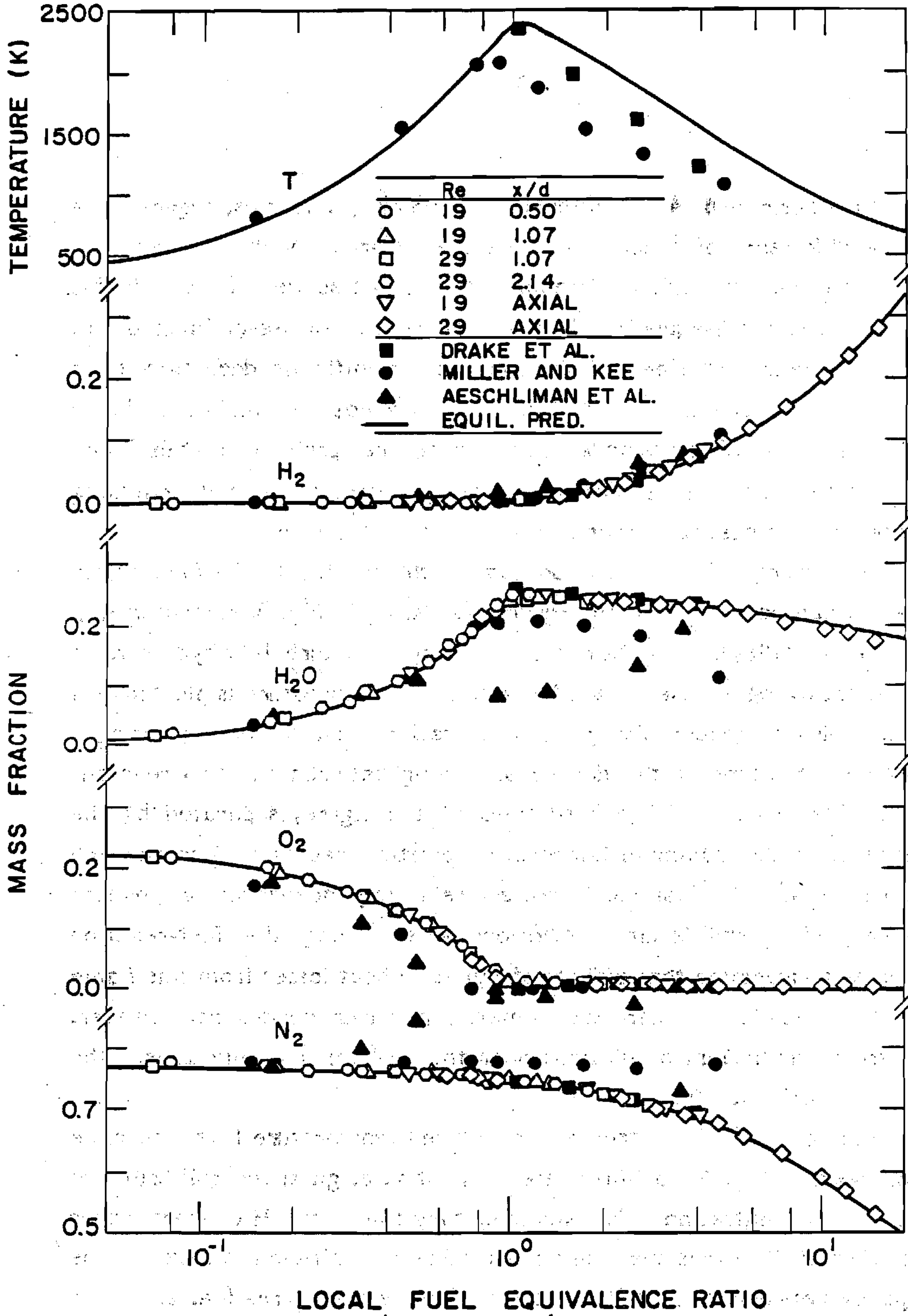

Figure 2. State relationships for hydrogen/air diffusion flames. From Faeth, Jeng and Gore (1985).

approach to thermodynamic equilibrium for major gas species, suggesting a relatively wide range of conditions where the criterion for the fast-reaction limit is satisfied. Equilibrium of temperature is not as well supported; this will be discussed subsequently. The earlier results of Aeschliman et al. (1979) and Miller and Kee (1977) also show significant departure from equilibrium. The reasons for this behavior are not known, but could be caused by differential diffusion which is a particular problem for this flame system due to the low molecular weight of hydrogen, e. g., another mixing parameter may be needed to properly represent all these results.

The effect of position on approach to local thermodynamic equilibrium can be seen from the results appearing in Fig. 3. Measurements of Drake et al. (1984), using Raman spectroscopy, for turbulent hydrogen jet flames in coflowing air are shown. Instantaneous temperature is plotted as a function of instantaneous nitrogen concentration - the latter presenting a single-valued measure of the degree of mixing between the two reactant streams. The upper and lower portions of the figure, separated by the discontinuity at the maximum temperature position, represent lean and rich conditions. Results for lean conditions are relatively independent of position and agree with equilibrium predictions - satisfying the fast-reaction criterion and suggesting that effects of radiative heat losses from this flame are small. Results for near-stoichiometric and rich conditions, however, depart from equilibrium predictions near the injector and only satisfy the fast-reaction criterion for x/d 50.

Drake et al. (1984) attribute the reduced temperature levels near the injector, seen in Fig. 3, to finite-rate chemistry, e. g., superequilibrium of free radical concentrations. For example, they find that OH concentrations on the order of 2.5 times the equilibrium value are sufficient to explain the discrepancy between measured and equilibrium temperatures (ca. 270 K) at x/d = 10. Direct measurements of OH concentrations using laser saturated fluorescence, by Drake et al. (1985), support this view. Figure 4 is an illustration of measured OH concentrations at x/d = 10, along with thermodynamic equilibrium predictions based on the measured mixture fraction. A significant degree of OH superequilibrium is evident. Similar

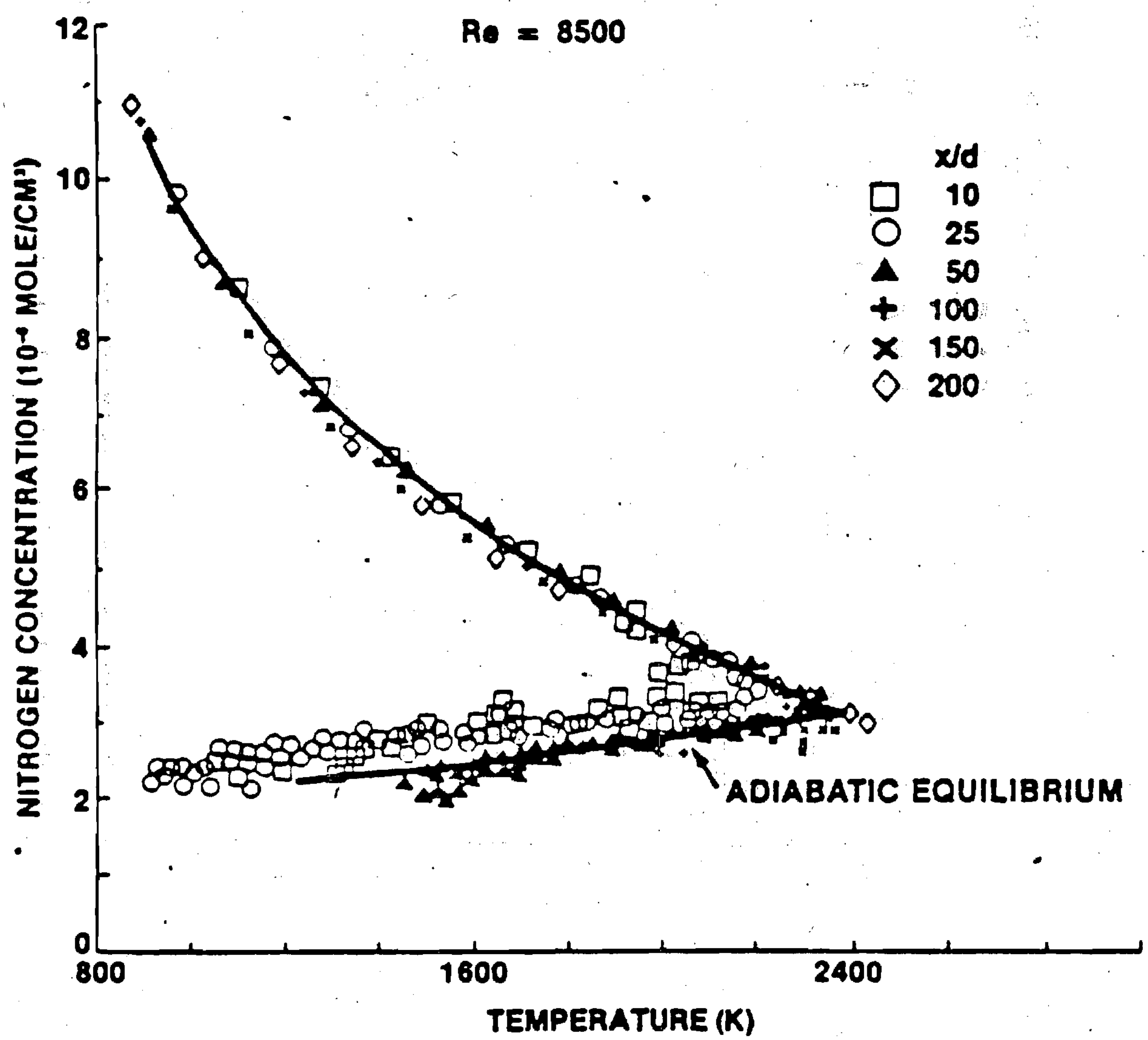

Figure 3. Correlation of average values of nitrogen concentration and temperture at various streamwise positions in a coflowing turbulent hydrogen/air jet diffusion flame ($Re_j = 8500$). From Drake, Pitz and Lapp (1984).

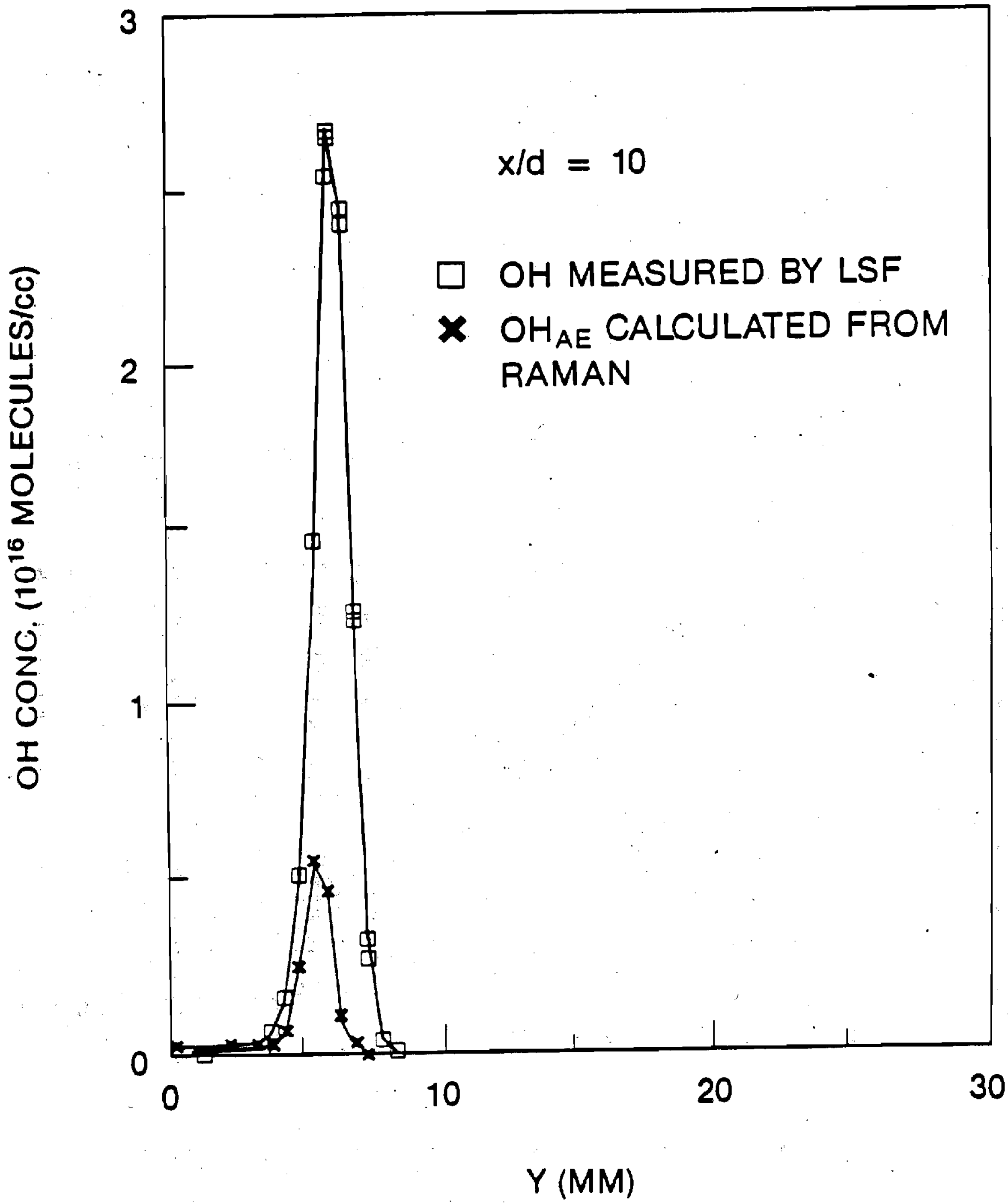

Figure 4. Radial profiles of OH concentrations at x/d = 10 in a coflowing turbulent hydrogen/air jet diffusion flame ($Re_j = 8500$). From Drake, Pitz, Lapp, Fenimore, Lucht, Sweeney and Laurendeau (1985).

results show a progressive decline of OH superequilibrium with increasing distance from the injector. However, superequilibrium levels are still on the order of 20% at x/d = 150. Even though OH concentrations are small in comparison to major species, its presence has a significant effect on temperature due to its high enthalpy of formation. Naturally, these effects are greater for higher Reynolds numbers, using this jet diameter, as well as for the smaller length scales corresponding to smaller burner diameters.

Considering the effect of Reynolds number highlights another problem with hydrogen/air diffusion flames. Some representative measurements, due to Drake et al. (1984), are illustrated in Fig. 5. Instantaneous temperature is plotted as a function of nitrogen concentration, which is taken to be the measure of mixing. The data were obtained at x/d = 50 for jet Reynolds numbers of 1600, 5200 and 8500. Adiabatic equilibrium predictions and the finite-rate chemistry predictions of Miller and Kee (1977), for Re $\leq$ 100. are also shown on the figure. Once again, lean conditions nearly satisfy equilibrium requirements. However, results at rich conditions show a progressive departure from equilibrium predictions toward the low Reynolds number estimates of Miller and Kee (1977) as the jet Reynolds number is reduced. This trend cannot be explained by finite-rate chemistry, since lower Reynolds numbers should provide operation closer to local equilibrium. Instead, effects of differential diffusion, described by Bilger (1982), provide an explanation. At low Reynolds numbers, molecular transport becomes significant in comparison to turbulent transport; therefore, the unusually high molecular mass diffusivity of hydrogen in comparison to other species in the system influences the mixing. It is not known whether local equilibrium is still satisfied for the modified proportions of elements from the initial streams. The results illustrated in Fig. 3 suggest that this might be the case. In any event, proper treatment of differential diffusion, even at the fast-reaction limit, would require consideration of laminar transport effects that are generally ignored when the popular conserved-scalar formalism is used. c. f., Lockwood and Naguib (1975) and Bilger (1982).

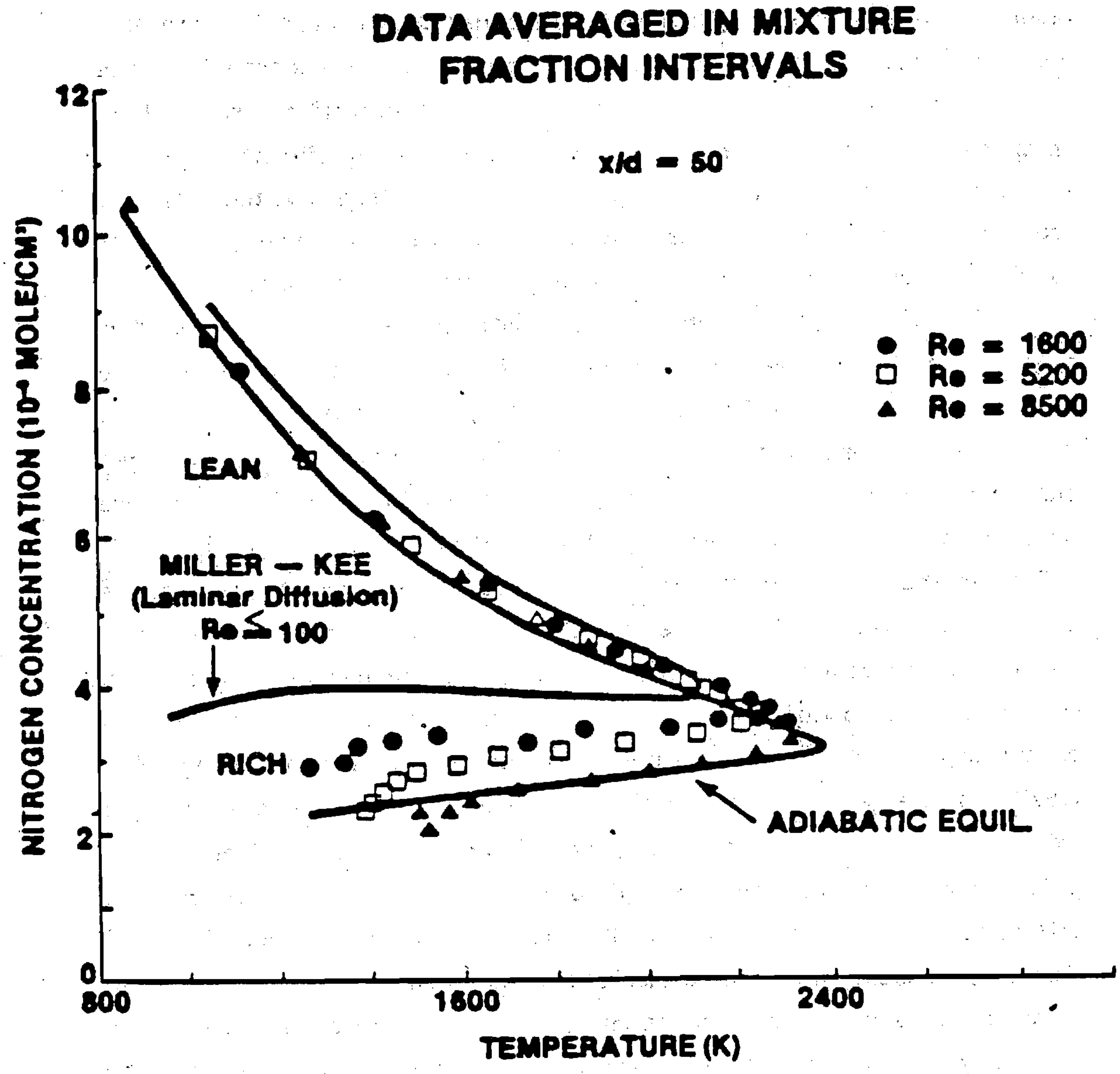

Figure 5. Correlation of average values of nitrogen concentration and temperrature at x/d = 50 for coflowing turbulent hydrogen/air jet diffusion flames. From Drake, Pitz and Lapp (1984).

When assessing measurements, effects of differential diffusion will not be used as a basis for recommendations. Complete analysis at the fast-reaction limit should be able to treat the phenomenon. In most cases, however, the desirability of minimizing effects of laminar/turbulent transition and buoyancy in the flow field precludes most low Reynolds number measurments where differential diffusion is a problem. We conclude that the hydrogen/air diffusion flame results are representative of the fast-reaction limit with respect to major species and temperature, within experimental uncertainties typical of current practive.

Carbon Monoxide/Air. The diffusion coefficients of major gas species are more similar for carbon monoxide/air than for hydrogen/air diffusion flames, reducing difficulties due to differential diffusion. However, carbon monoxide oxidation is not generally thought to be fast in comparision to transport processes in flames. For example, several approximate finite-rate chemistry models for hydrocarbon specifically consider CO oxidation while assuming H_2 oxidation is fast by comparison (Edleman and Fortune, 1969; Westbrook and Dryer, 1981).

Although oxidation of dry carbon monoxide is slow, the presence of trace amounts of hydrogen yields a wet oxidation mechanism which is reasonably fast (Glassman, 1977). Most practical carbon monoxide supplies for turbulent flame experiments contain some hydrogen as a contaminant; therefore, there is evidence that carbon monoxide/air diffusion flames can approach the fast-reaction limit in the laboratory. Measurements of species concentrations and temperatures in laminar carbon monoxide (containing 1.12% hydrogen by volume)/air diffusion flames, by Faeth et al. (1985), are illustrated in Figs. 6 and 7. The degree of mixing is represented by the fuel equivalence ratio (based on measured coarbon and oxygen element concentrations. Predictions from the Gordon and McBride (1971) program (CEC 76 Version) are also shown on the figure. These were obtained assuming adiabatic equilibrium but omitting solid carbon as a potential substance in the system for fuel-rich conditions.

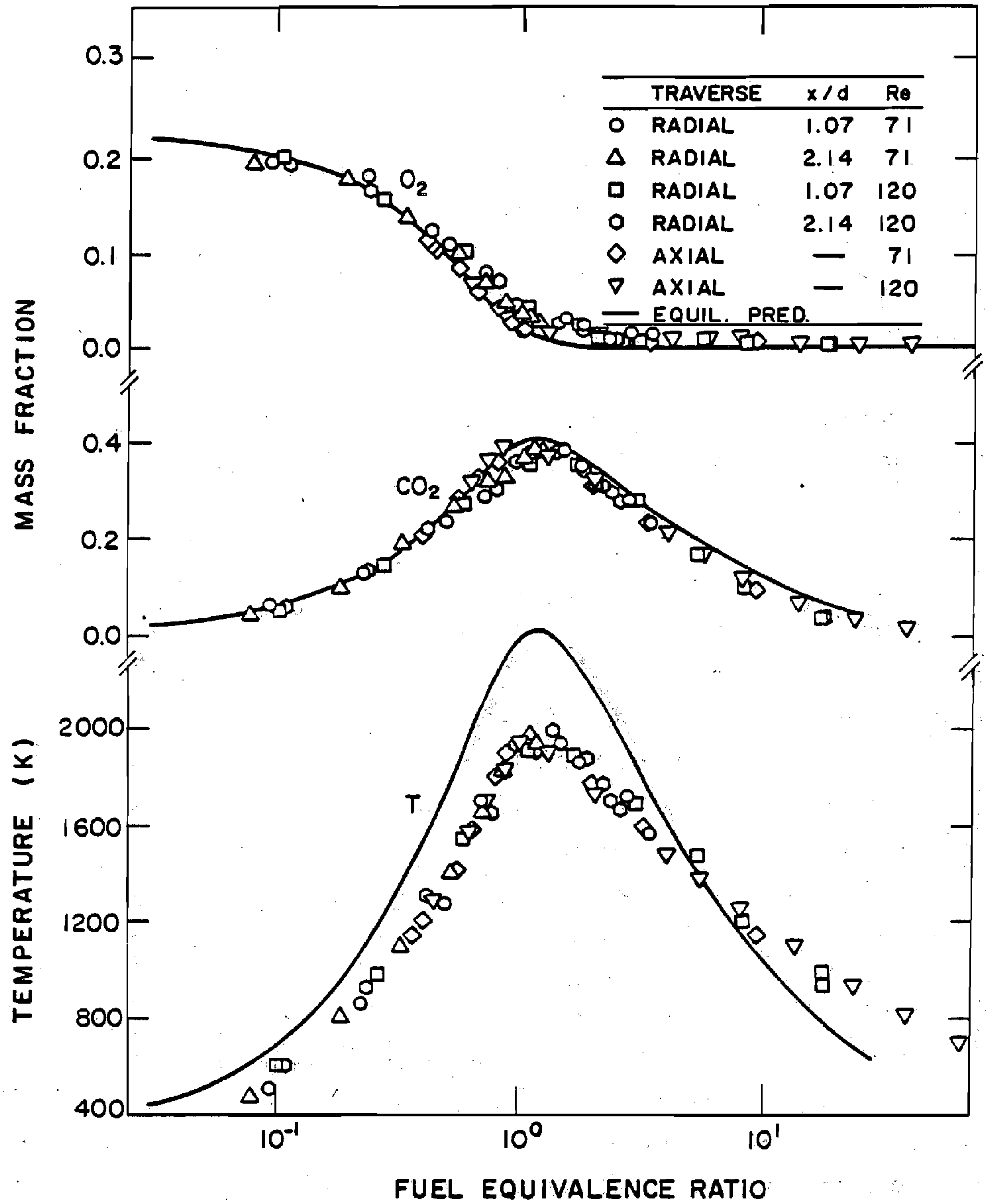

Figure 6. State relationships for carbon monoxide/air diffusion flames. From Jeng, Gore, Chuech and Faeth (1985).

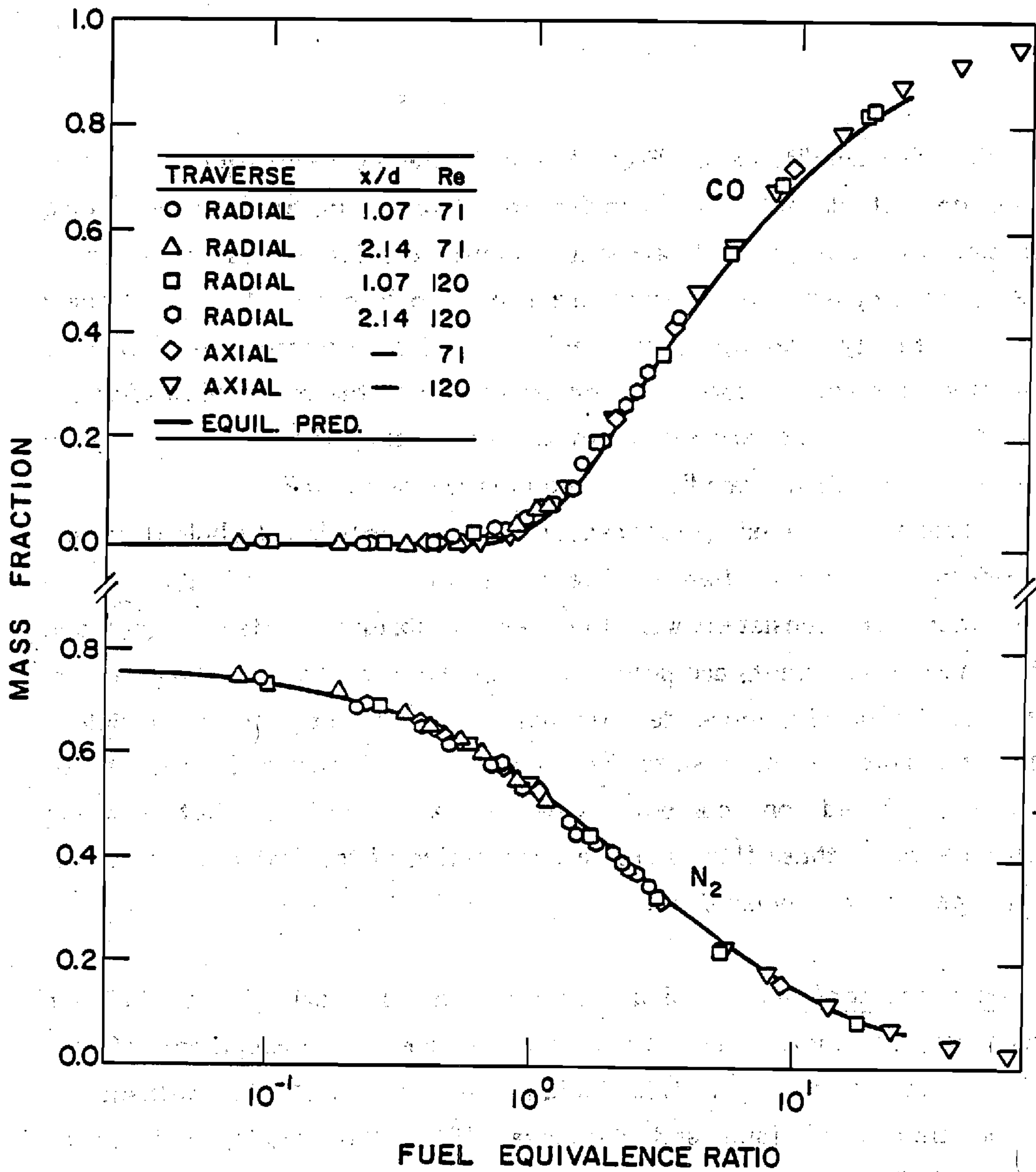

Figure 7. State relationships for carbon monoxide/air diffusion flames (continued). From Jeng, Gore, Chuech and Faeth (1985).

For the conditions of Figs. 5 and 6, the concentrations of major species do not depart very significantly from equilibrium predictions, supporting operation at the fast-reaction limit. Results are less satisfactory for temperature, but these flames are known to lose roughly 20% of their chemical energy release by radiation. Furthermore, temperature measurements were not corrected for errors due to thermocouple radiation. These radiation effects are sufficient to explain the discrepancies between equilibrium temperature predictions and measurements in Fig. 6.

Razdan and Stevens (1985) report measurements in a turbulent carbon monoxide/air diffusion flame. Faeth et al. (1985) find that these measurements are consistent with the near equilibrium results of Figs. 6 and 7; thus the measurements are potentially representative of the fast-reaction limit. Unfortunately, more definite assessment directly in the turbulent flame, analogous to the results for hydrogen/air diffusion flames, is not available. Based on current evidence, we conclude that existing measurements for these flames are representative of the fast-reaction limit, within experimental uncertainty.

Hydrocarbon/Air. Measurements in a variety of laminar hydrocarbon/air flames have been assessed during development of the laminar flamelet concept. This includes measurements in methane/air diffusion flames by Tsuji and Yamaoka (1967, 1969, 1971) and for n-heptane/air diffusion flames by Abdel-Khalek et al. (1975), discussed by Bilger (1977); measurements in propane/air diffusion flames, discussed by Jeng and Faeth (1984a) and Liew et al. (1984); and measurements in ethylene/air diffusion flames, by Faeth et al.(1985).

Hydrocarbon/air diffusion flames yield similar results when considered for the fast-reaction limit. Representative findings for ethylene/air diffusion flames are illustrated in Figs. 8 and 9. Concentrations of major gas species are plotted as a function of local fuel-equivalence ratio for various positions and conditions within laminar diffusion flames. Predictions, assuming local adiabatic equilibrium, are also shown on the

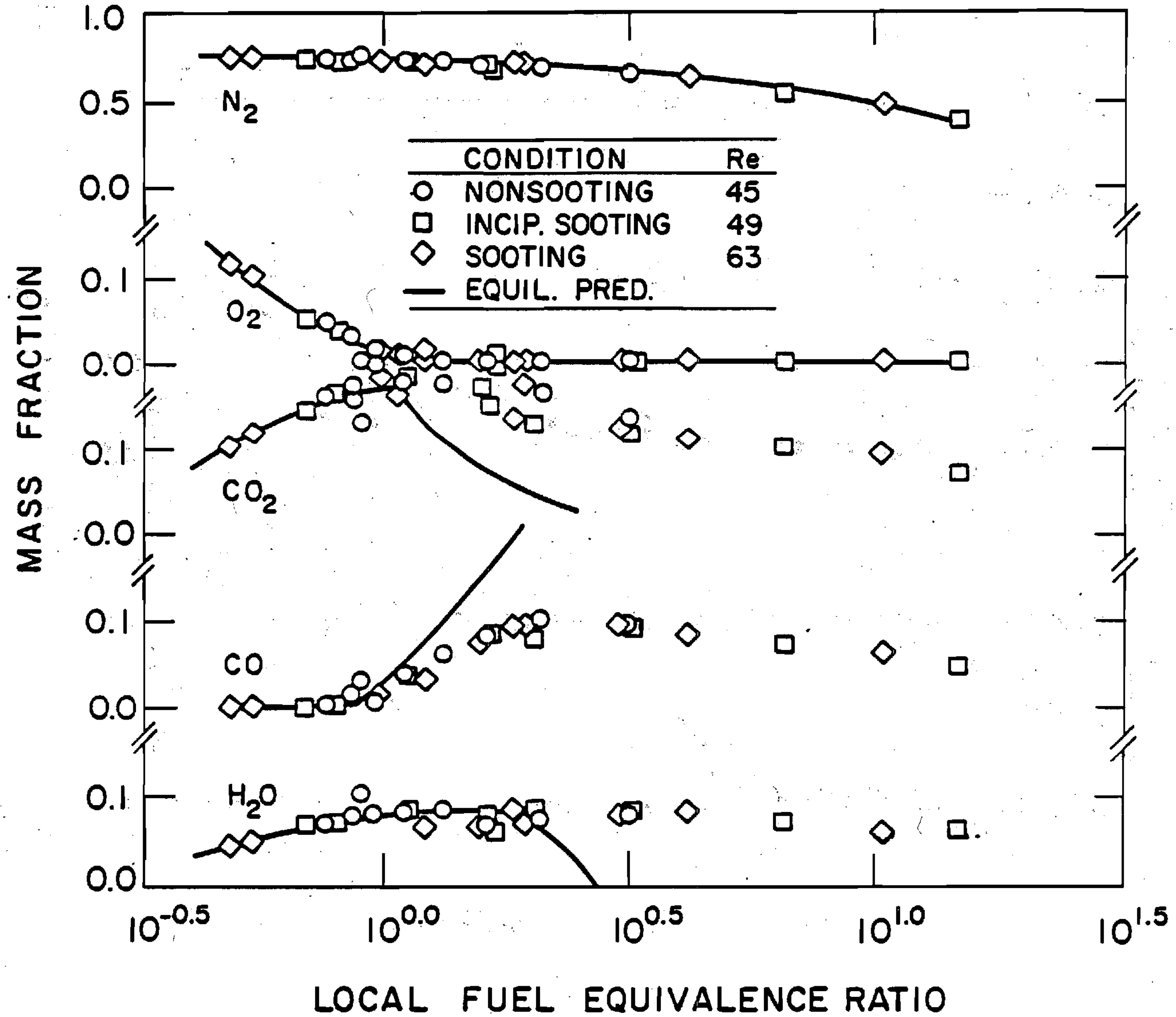

Figure 8. State relationships for ethylene/air diffusion flames. From Faeth, Jeng and Gore (1985).

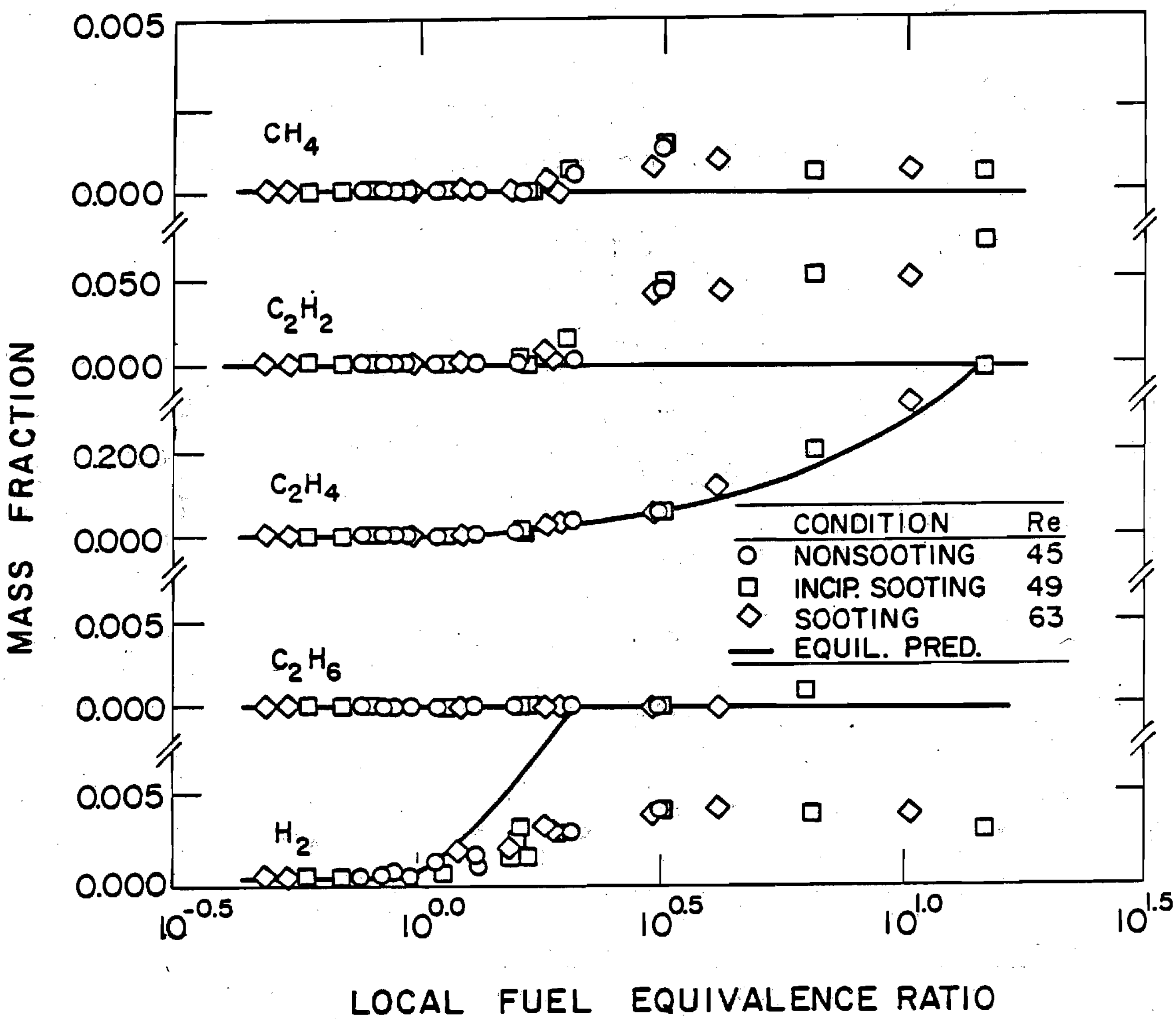

Figure 9. State relationships for ethylene/air diffusion flames (continued). From Faeth, Jeng and Gore (1985).

plots. Similar to the cases considered earlier, properties approach thermodynamic equilibrium for lean conditions. Furthermore, concentrations of O_2, C_2H_4 and nitrogen roughly approximate equilibrium over the full range considered. However, concentrations of major product species, CO_2, CO and H_2O, depart appreciably from equilibrium for fuel-rich conditions. While these major product species roughly follow universal correlations in terms of the conserved scalar, satisfying the laminar flamelet concept for this range of χ, this type of quasi-equilibrium depends on finite-rate chemistry effects. Furthermore, even quasi-equilibrium is less evident for minor species. Thus, hydrocarbon flame systems do not satisfy the present criterion for the fast-reaction limit. Instead, they are considered by Drake and Kollmann (1985) along with other slow-reacting turbulent combustion processes.

<u>Hydrogen/Fluorine</u>. Hydrogen/fluorine diffusion flames, with dilute reactants in inert gases, have been studied in a series of investigations at Cal. Tech. (Mungal, 1983; Mungal et al., 1983; 1984). Reaction rates for this system are generally, fast, but difficulties were still encountered in initiating the reaction at very dilute concentrations. This was resolved by adding trace amounts of nitric oxide to the fluorine-containing stream.

Mungal (1983) estimates the degree to which his test conditions approach the fast-reaction limit, but comparing characteristic large- and small-scale mixing times with the characteristic chemical reaction time. For local fluorine concentrations of 1%, the small-scale mixing time was estimated to be roughly an order of magnitude concentrations of 1%, the small-scale mixing time was estimated to be roughly an order of magnitude larger than characteristic reaction times. However, free-stream fluorine concentrations were only 1-2%, and are necessarily much lower in the reaction zone itself; therefore, these computations are not a very convincing demonstration that the fast-reaction limit was reached.

Nitric Oxide/Ozone. Wallace (1981) considers dilute nitric oxide/ozone diffusion flames with the reactants carried by inert gas flows. In this case, the reactants ignited spontaneously with no additives.

Wallace (1981) estimates large and small scale mixing and chemical reaction times at his measurement location. The chemical and large-scale mixing times were comparable at reactant concentrations having the same order of magnitude. Although the spontaneous reaction suggests a high degree of reactivity for these reactants, this assessment is certainly not convincing evidence that these results approach the fast-reaction limit.

Acid/Base. Koochesfahani (1984) and Dahm (1985) consider the acid/base reaction involving dilute sulfuric acid and sodium hydroxide in water. Characteristic large- and small-scale mixing times are compared with the characteristic chemical time based on the lowest free-stream reactant concentration. For a plane free shear layer configuration, Koochesfahani (1984) finds ratios of small-scale mixing to chemical times on the order of 10^2 in the region of his measurements. For a round free jet configuration, Dahm (1985) finds values of this ratio in the range $10^{3./2}$ - 10^7. These results suggest reasonable prospects for close approach to the fast-reaction limit, even though reaction zone concentrations are lower than free-stream values. These experiments, however, involve negligible effects of scalar property changes due to chemical reaction, since the reaction is primarily an indicator of mixing at the molecular level.

Nitrogen Tetroxide Dissociation. Batt (1977) considers a reacting flow which involves dissociation of nitrogen tetroxide, originally in a cool stream, by higher-temperature air in a second stream. The equilibrium reaction is

$$N_2O_4 \rightleftharpoons 2NO_2$$

In this case, rough estimates suggested that characteristic mixing times were more than an order-of-magnitude larger than characteristic chemical times. Computations employing a detailed mechanism as well as evidence obtained directly from measurements in the turbulent flow also supported the view that these results correspond to the fast-reaction limit (Batt, 1977).

<u>Flow definition</u>

Spalding (1979) has pointed out that turbulent mixing and reaction processes involve both local and history effects. Thus assessment of turbulent reaction analysis requires consideration of the development of the flow, rather than simply properties at a point. This imposes the need for proper initial and boundary conditions for the analysis. In the following, we examine experimental evidence showing the importance of these effects for turbulent reacting flows.

<u>Initial Conditions</u>. Initial conditions must be well-defined for all flow streams involved in the nonpremixed combustion process. Very few experiments are reported without some specification of overall average properties of these flows. Distributions of mean and turbulence quantities, however, are often unavailable. These properties can have effects which extend appreciable distances into the flow field; therefore, lack of such information raises questions concerning the use of such measurements for evaluation of turbulent reaction analysis. Experimental evidence demonstrating these effects will be discussed in the following.

Effects of minor changes in burner exit conditions have been measured by Jeng et al. (1982). The tests considered a methane/air round jet diffusion flame, with methane injected vertically upward in still air from a water-cooled burner (where the cooled burner matched ambient temperatures). Turbulence levels at the burner exit were changed by installing a screen. These changes did not influence the mean properties at the jet exit. Installing a screen, however, caused initial values of turbulence kinetic energy to increase by roughly 10%. Without cooling, the burner surface was 32K above the ambient temperature, which produced a thermal plume visible in shadowgraphs, placing the flame in a slight coflow.

The effect of these changes on mean temperatures and velocities are illustrated in Fig. 10. These results are for an initial jet Reynolds number of 2920, with traverses plotted for x/d = 52.2 to 418. With coflow present, by ending cooling, the flow predictably becomes narrower. Increasing turbulence levels by installing a screen, however, has an opposite effect which is quite significant in view of the relatively small increase in k. These effects were smaller at initial Reynolds numbers of 5,850 and 11,700, but clearly, initial turbulence properties and seemingly minor effects of burner conditions can have a significant effect on flow development.

Costly reactants, problems of flame attachment and approach to the fast-reaction limit, frequently conflict with the desire to provide reasonably high initial Reynolds numbers. In marginal situations, the increased temperature levels in flames causes increases in kinematic viscosities which tend to relaminarize even initially turbulent flows. Takagi et al. (1980, 1981) report measurements in low Reynolds number flames which exhibit relaminarization. The tests involved hydrogen-nitrogen fuel mixtures (2/3 volume ratio) injected vertically upward in still air. Turbulence within the jet tube was promoted; therefore, fully-turbulent conditions were maintained even for tube Reynolds numbers as low as 4,200.

Test results from Takaju et al.(1980) are illustrated in Fig. 11, for a jet Reynolds number of 4200. Mean and fluctuating velocities and mean scalar properties are shown near the jet exit (x/d 2) both with and without a flame present. Even though the mean velocity gradient is somewhat greater when the flame is present, tending to promote production of turbulence, streamwise velocity fluctuations are significantly lower. Furthermore, values of u are clearly reduced in the high temperature region of the flame, strongly suggesting relaminarization due to increased viscosity at increased temperature levels. In spite of this, the flaming condition actually yields a wider flow than the inert flow, e.g., shadowgraphs indicate a somewhat bulbous flow boundary near the jet exit for flaming conditions. This appears to be caused by the presence of the high-temperature region near the edge of the flow, causing diffusion of heat into the relatively slow entrainment flow at low Reynolds numbers. Computing

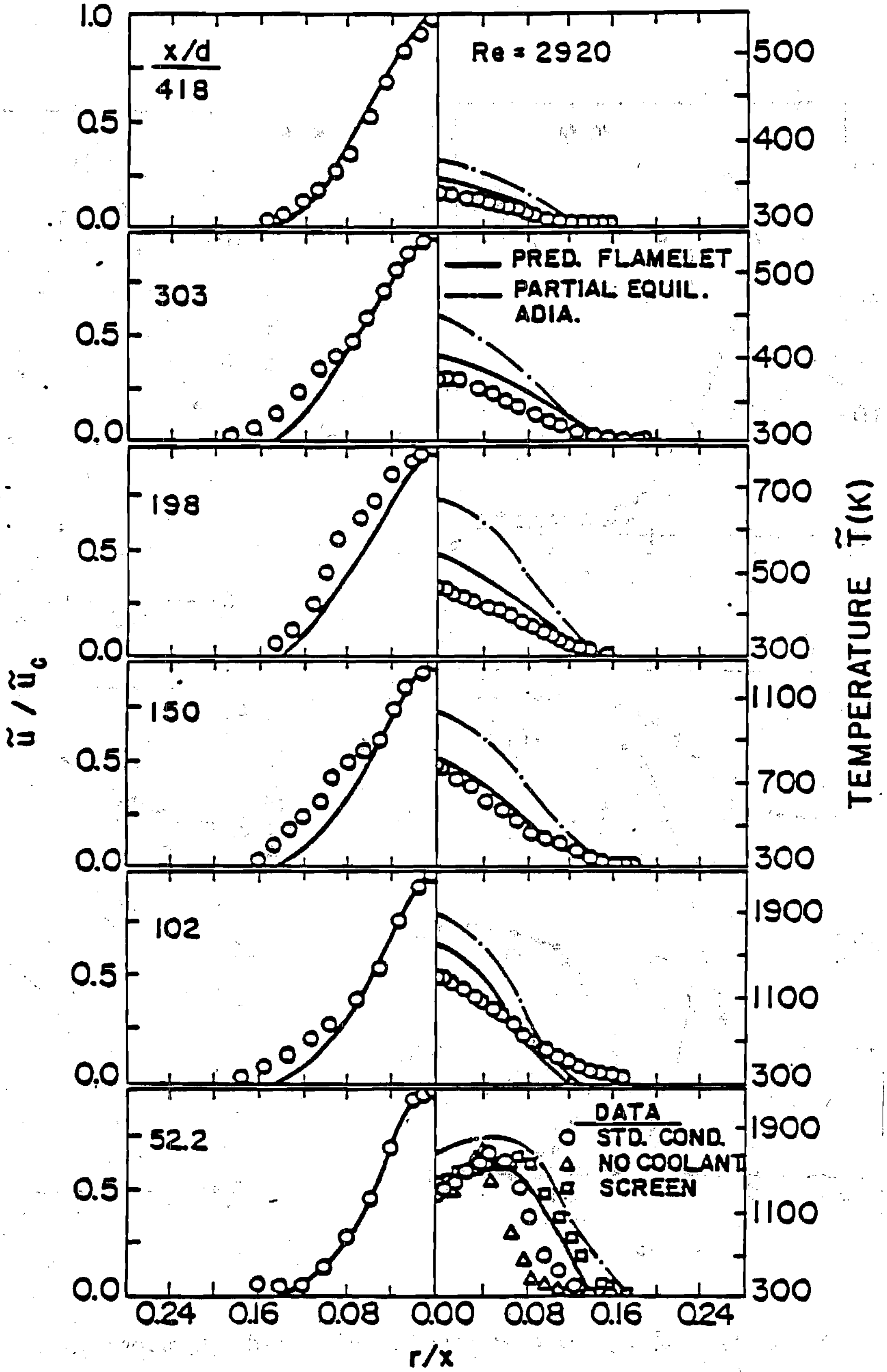

Figure 10. Effect of initial conditions on the structure of a turbulent nonpremixed flame. From Jeng, Chen and Faeth (1982).

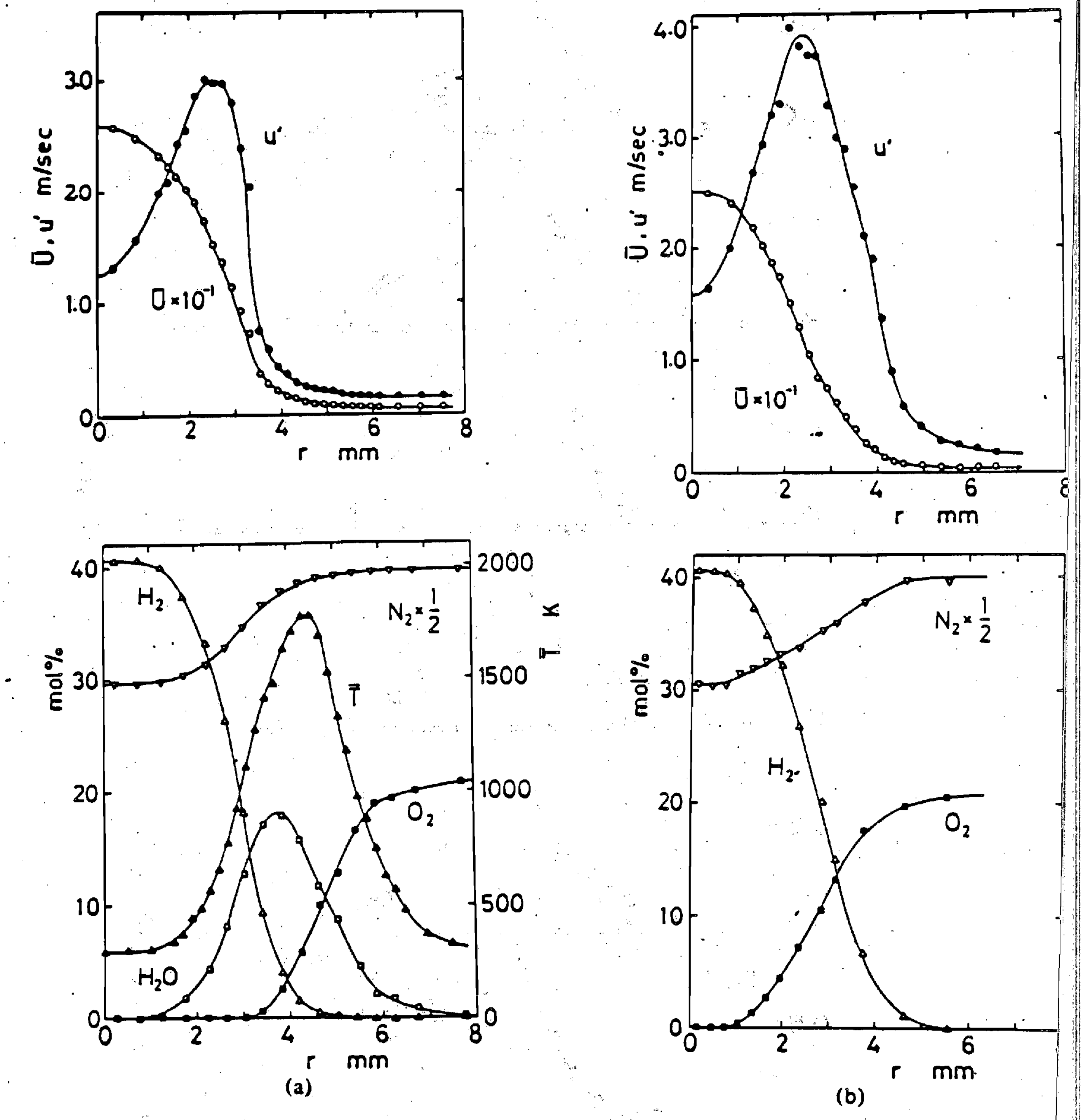

Figure 11. Velocity and scalar properties within a hydrogen/nitrogen jet in co-flowing air ($Re_j = 4200$, $x/d = 2$): (a) with flame, (b) without flame. From Takagi, Shin and Ishio (1980).

these features represents a significant challenge; therefore, even accurate knowledge of initial conditions would probably not make this flow a good candidate for evaluation of turbulent reaction models.

Properties of the air stream have similar importance. Numerous authors have pointed out problems of room disturbances for flames in still air - these effects always acting to increase the apparent rate of spread of the flow. Coflowing jets also exhibit effects of upstream boundary layers, c.f., Kent and Bilger (1973), and Starner and Bilger (1984).

A more subtle effect involves the turbulence levels of the air stream. This has not been examined to a great degree for fast-reacting nonpremixed flames, but is well known from studies of noncombusting turbulent flows. A dramatic example is the plane free shear layer studies of Brown and Roshko (1974) and Chandrasuda et al. (1978). The earlier experiments, involving streams having low turbulence levels, exhibit highly regular turbulent structures in the transitional flow regime, before the mixing transition is reached. In contrast, such structures were not at all evident when the turbulence levels of the streams were increased in the later study of Chandrasuda et al. (1978).

Boundary Conditions. Flows in still environments have readily-defined boundary conditions, aside from difficulties of ambient disturbances noted earlier. Flows in channels, however, introduce effects of streamwise pressure gradients, as well as distortion when the crossectional area of the flow is changed to control static pressure variations. Both effects will be considered in the following.

Starner and Bilger (1980) have reported an extensive study of effects of streamwise pressure gradients on a simple turbulent diffusion flame. The test configuration was a hydrogen jet flame in coflowing air within a rectangular duct. Two sides of the duct could be moved so that the average streamwise pressure gradient could be varied to yield values of -274, -213, -102, -18 and +23 Pa/m. For all these cases, however, there were local variations of $\pm$ 30% of these values, due to the development of the flow in the duct. These conditions gave values of the pressure-gradient parameter

$$\beta = (d/\rho u_j^2)[d\bar{p}/dx] \tag{4}$$

in the range (-1.1 to 0.9) x 10^{-3}.

Mean centerline and free-stream velocities, from Starner and Bilger (1980), are illustrated in Fig. 12. Clearly, these mean velocities are strongly influenced by the streamwise pressure gradient, even for the relatively small values of β which were considered. Positive pressure gradients are particularly problematical. For a pressure gradient of 23 Pa/m, the velocity defect is negative at x/d = 160, since the low-density gas near the axis is rapidly decelerated by the pressure gradient. In fact, evidence for flow separation near the axis was observed farther downstream for this condition.

Effects of mean streamwise pressure gradients on turbulence properties, from Starner and Bilger (1980), are illustrated in Fig. 13. Streamwise velocity fluctuations along the axis, for different mean streamwise pressure gradients, are illustrated as a function of distance from the jet exit. Again, even small values of β cause significant changes in $\bar{u}_o'$, particularly for x/d > 60. For mean pressure gradients of -109 and -274 Pa/m, $\bar{u}_o'$ increases for a time for x/d in the range 40-80. This is probably due to turbulence production by the interaction between the mean pressure gradient and the turbulence (Starner and Bilger, 1980). Similar increases in velocity fluctuations are also observed in vertical buoyant diffusion flames due to hydrostatic pressure variations (Jeng et al., 1982). Such effects clearly indicate the need for specification of streamwise pressure gradients in flames. Cases where this phenomenon is significant are also problematical for analysis at present, since such interactions for variable-density flows are not well understood (Bilger, 1976).

Attempts to control streamwise pressure gradients in ducts generally involve changes in the crossectional area of the duct. This is frequently accomplished by adjusting the position of two opposite sidewalls. The resulting loss of symmetry distorts ambient velocities and causes elliptical, as opposed to axially-symmetric, profiles (Starner and Bilger, 1980). Most

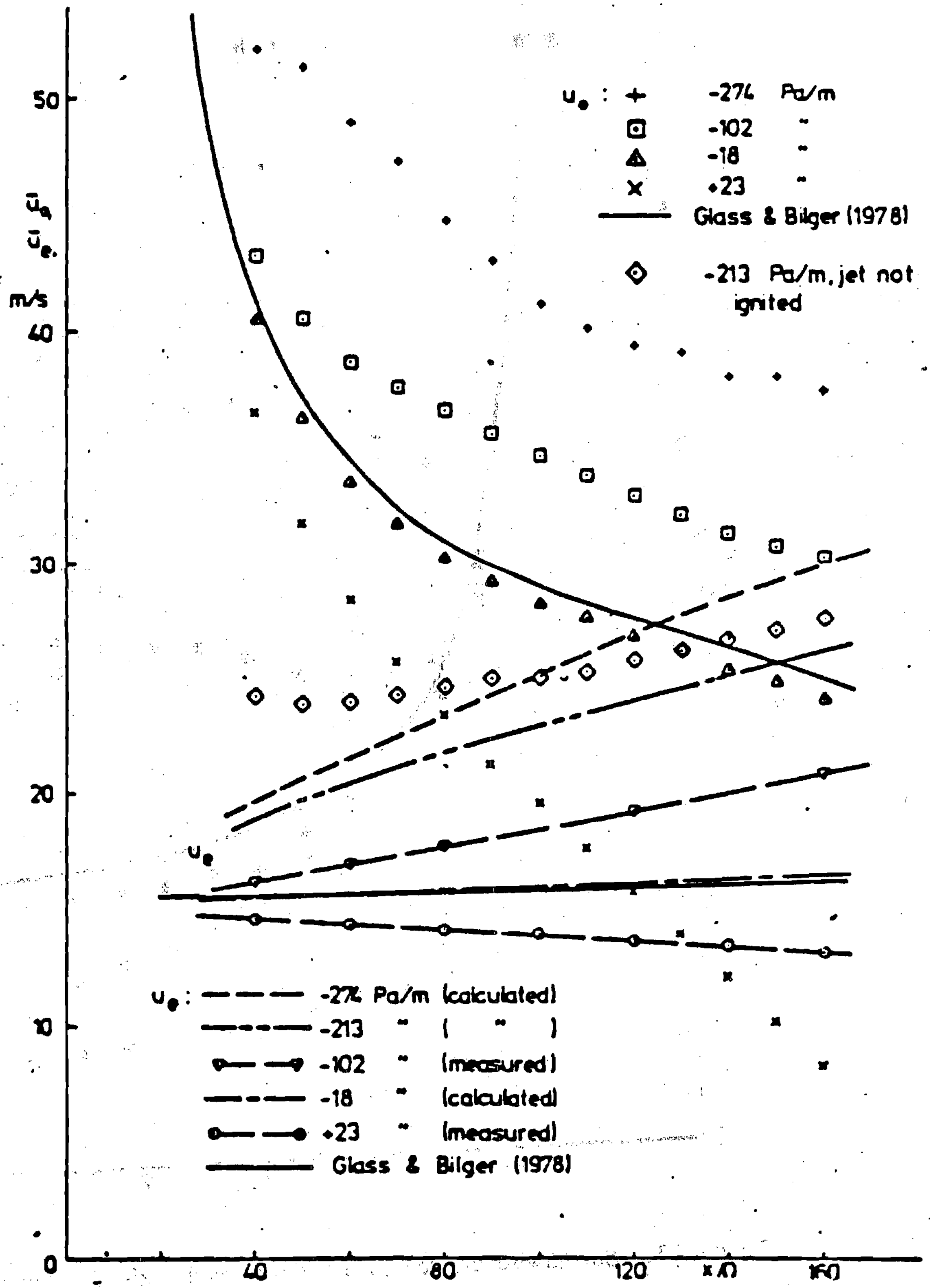

Figure 12. Mean velocities along the axis of coflowing turbulent hydrogen/air jet diffusion flames as a function of streamwise pressure gradient. From Stårner and Bilger (1980). Note, $\bar{u}_o$ on this plot denotes centerline velocity.

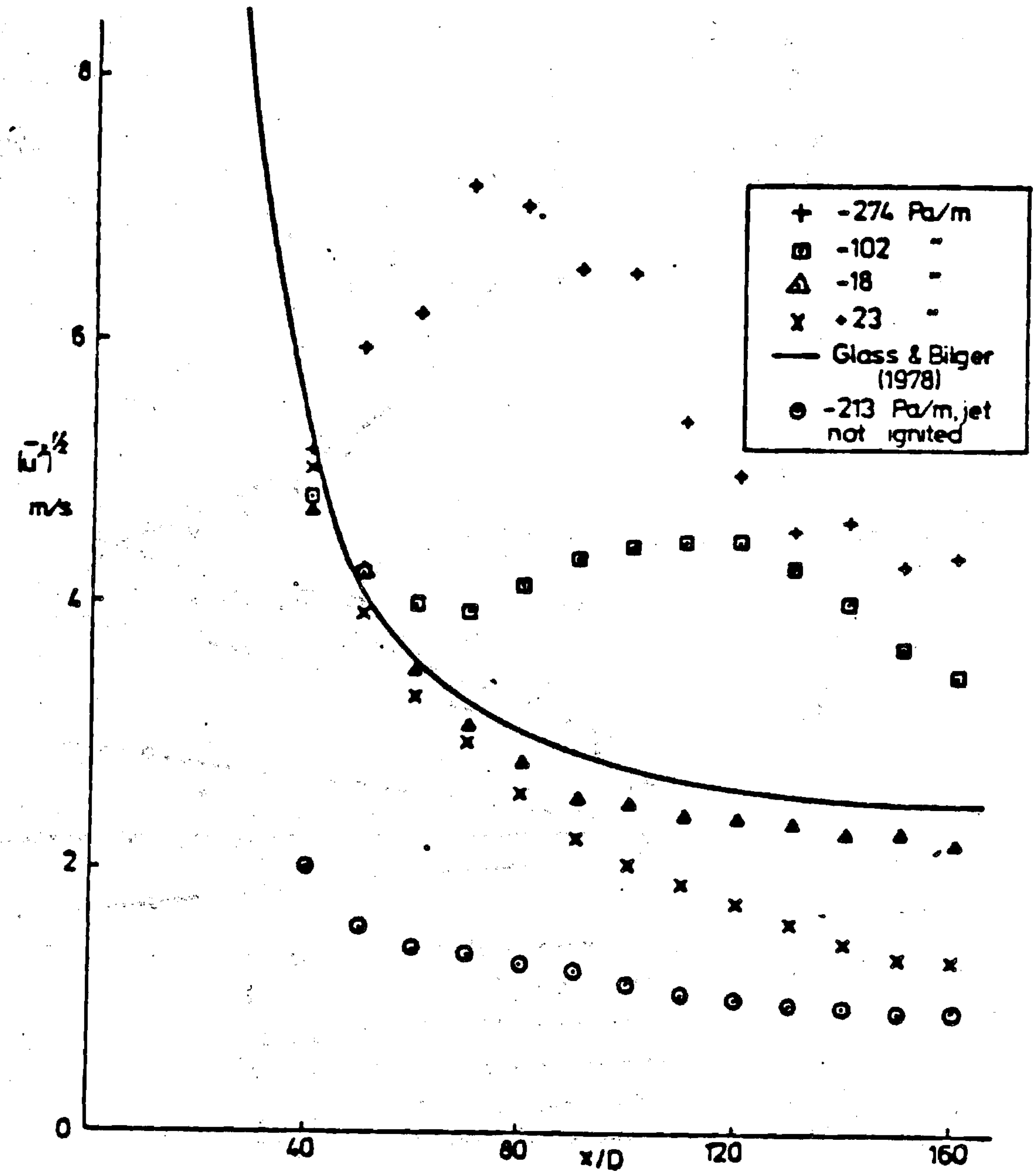

Figure 13. Streamwise turbulence intensities along the axis of coflowing turbulent hydrogen/air jet diffusion flames as a function of streamwise pressure gradient. From Stårner and Bilger (1980).

existing measurements in ducts involve only vertical traverses; therefore, the extent of this problem cannot be evaluated without further study.

Similar effects have not been reported for plane shear layers, but differential boundary layer growth and secondary flows can cause distortion as well. The extent of such effects, however, cannot be evaluated from existing documentation.

Buoyancy. The main issue is to evaluate methods for analyzing turbulent reacting flows; therefore, it is desirable to minimize complications of the turbulence structure. Buoyancy represents such an unwanted effect, since current understanding of buoyancy/turbulence interactions in flows having large density variations is very limited.

Becker and coworkers (1978) have investigated effects of buoyancy on vertical turbulent diffusion flames in still environments. Using integral theory, they develop a simple method for evaluating effects of buoyancy to some extent, particularly near the tip of the flame. The effect is often not detected when considering only mean properties, although turbulence quantities exhibit significant changes as noted earlier. Such changes in the turbulent environment affect processes of turbulent reaction and must be considered when evaluating analysis of reactive flow.

Numerous measurements with jet flames in coflowing air also involve effects of buoyancy which can limit their value for assessing models of turbulent reaction. Authors generally note gross effects, such as the rise of the flame axis above the geometric centerline, and avoid operation at conditions where effects of buoyancy dominate. Nevertheless, there are more subtle effects on turbulence properties which are often overlooked.

Recent measurements by Dibble et al. (1984b) provide insight concerning effects of buoyancy in horizontal flows. The tests involved hydrogen (containing 22% Argon on a molar basis) round jet diffusion flames in coflowing air. Initial jet Reynolds numbers were 24,000 (u_j = 154 m/s, u_e = 8.5 m/s); therefore, effects of buoyancy near the injector might be expected to be small. A combined laser Doppler anemometer (LDA)/Rayleigh scattering (RS) system was used to measure velocities, densities and their corrrelations.

Measurements which highlight effects of buoyancy are illustrated in Figs. 14 and 15 (Dibble et al., 1984b). Vertical traverses of streamwise mean and fluctuating velocities and their correlation, $\overline{\rho' u'}$, are illustrated for x/d = 50. This position is just beyond the flame tip. A Cartesian coordinate system is used for distances, positive and negative values represent positions above and below the axis. Mean velocity profiles have unusually large scatter; however, they roughly indicate a somewhat steeper profile above the axis than below. Velocity fluctuations exhibit greater asymmetry, having maximum values below the axis and trailing off to higher ambient values above the axis. The correlation $\overline{\rho' u'}$ has the greatest asymmetry, having its largest absolute value below the axis and a relatively complex variation over the flow.

The effects seen in Figs. 14 and 15 are primarily attributable to buoyancy. The high-temperature low-density gas near the axis has stable and unstable stratification on its lower and upper surfaces. This has a direct effect on turbulence properties even at x/d = 50. Farther downstream, effects of buoyancy on mean properties are clearly observed. Such three-dimensional effects will clearly complicate analysis of this and other similar flows. Similar experiments in vertical flow (Dibble et al., 1984a, 1985a, 1985b, 1985c) reduces the effect of buoyancy to a symmetric field, providing a more attractive configuration for analysis.

Averages. A complete understanding of turbulent reaction processes would provide a means of calculating moments of velocities and scalar properties using any desired averaging procedure. This is generally not possible at present; therefore, it is necessary to specify the type of averages obtained by both theory and experiment if they are to be properly compared. In cases where they are not the same, estimates of the differences between them must be available.

Two types of averages most commonly appear in current analysis and experiments: (1) conventional unweighted (Reynolds) averages, and (2) density-weighted (Favre) averages. For unweighted averages, the

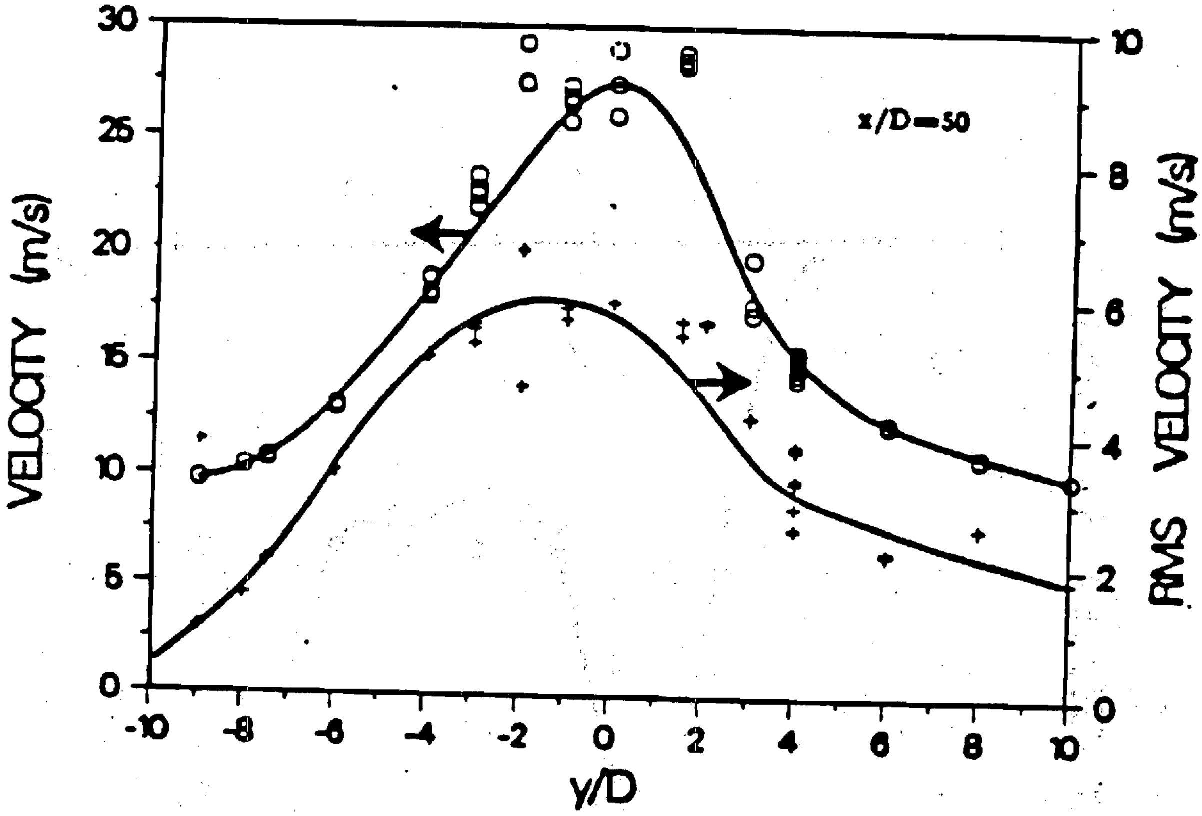

Figure 14. Measured streamwise mean and fluctuating velocities in a turbulent horizontal hydrogen-argon/air jet diffusion flame. Vertical traverse at x/d = 50. From Dibble, Kollmann and Schefer (1984).

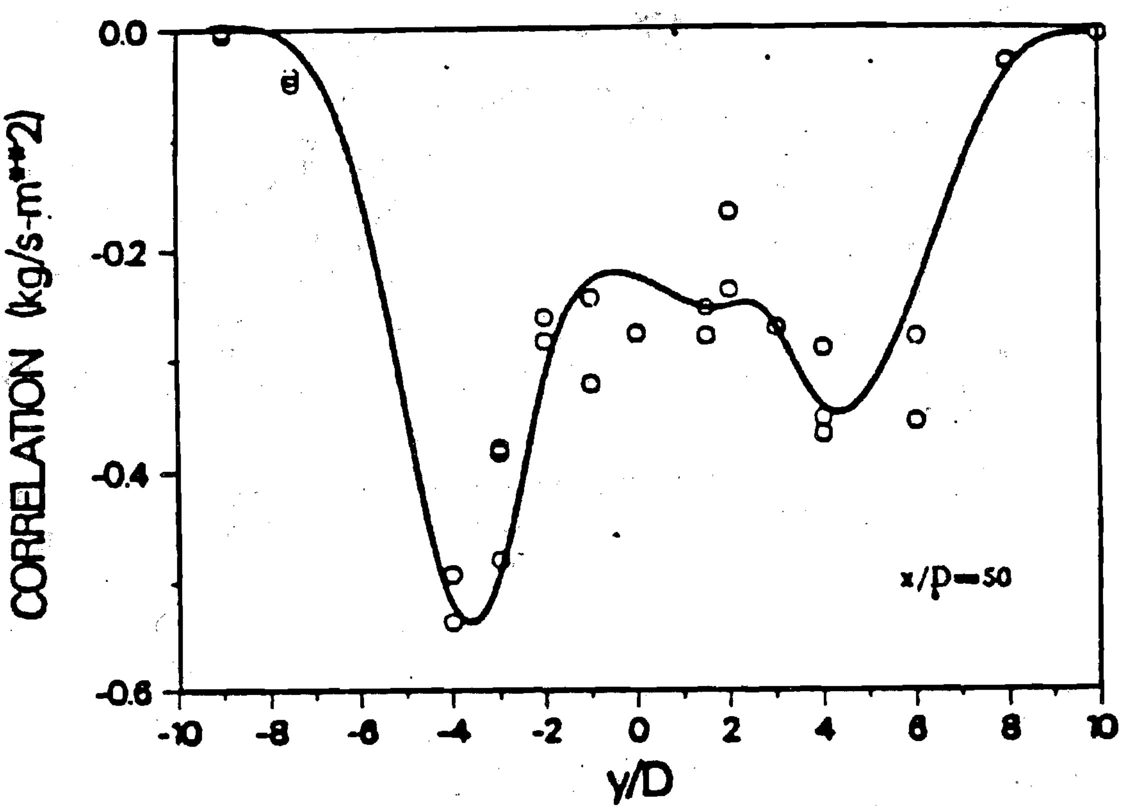

Figure 15. Measured velocity-density correlation $\overline{\rho' u'}$ in a turbulent horizontal hydrogen-argon/air jet diffusion flame. Vertical traverse at x/d = 50. From Dibble, Kollmann and Schefer (1984).

instantaneous value of any generic quantity, Φ , is decomposed into time-averaged and fluctuating components, as follows:

$$\phi = \bar{\phi} + \phi' \tag{5}$$

Clearly, $\overline{\Phi'} = 0$ under this definition. Favre or density-weighted averages have the following definition (Bilger, 1977):

$$\tilde{\phi} = \overline{\rho\phi}/\bar{\rho} \tag{6}$$

The density-weighted mean and fluctuating components become

$$\rho\phi = \bar{\rho}\tilde{\phi} + \rho\phi'' \tag{7}$$

In this case, $\overline{\rho\Phi''} = 0$, but $\overline{\Phi''} \neq 0$ in general. Conventional and Favre averages are identical in constant-density flows, but can be appreciably different in the variable-density flows characteristic of flame environments.

Conditional averages are often reported from experiments, although they play a lesser role in current analysis of fast-reacting turbulent flows. Such averages can be conditioned on turbulent and nonturbulent fluid, in cases when a turbulent stream is mixing with an environment having small turbulence levels; or on mixed and unmixed fluid, in cases where both streams are turbulent. Conditional averages can also be defined in terms of either conventional or Favre averages, yielding a potentially large assortment of properties. In terms of Reynolds averages, we have

$$\bar{\Phi} = \gamma\bar{\Phi}_t + (1-\gamma)\bar{\Phi}_n \tag{8}$$

where $\bar{\Phi}_t$ and $\bar{\Phi}_n$ are conditional averages appropriate to turbulent and nonturbulent fluids, while represents turbulence intermittency, e.g., the fraction of time when turbulent fluid is present at the point in question. An analogous equation can be written using averages conditioned on mixing.

<u>Velocity</u>. Fortunately, conventional- and Favre-averaged mean velocities are not very different in turbulent reacting flows, in view of the experimental uncertainties of typical measurements. From the basic definition of a Favre average, Eq. (6), the difference between these averages

is

$$(\bar{u}-\tilde{u})/\bar{u} = -\overline{\rho' u'}/\bar{\rho}\,\bar{u} \tag{9}$$

Potential differences can be examined by introducing the $\rho' u'$ correlation, $R_{\rho' u'}$, as follows

$$(\bar{u}-\tilde{u})/\bar{u} = -(\bar{\rho}'/\bar{\rho})(\bar{u}'/\bar{u})R_{\rho' u'} \tag{10}$$

In Eq. (10), and in the following, we have adopted the notational convenience that $(\overline{\Phi'^2}/\bar{\Phi}^2)^{1/2} \equiv (\bar{\Phi}'/\bar{\Phi})$; this should not be confused with the fundamental requirement that $\bar{\Phi}' = 0$. The correlation $R_{\rho' u'}$, has been measured by Starner and Bilger (1980, 1981), Scheffer et al. (1982), and Dibble et al. (1984b) for round jet diffusion flames in coflow and Liberdy et al (1979) and Lai and Faeth (1985) for plane buoyant flows. The behavior is similar in both flows with maximum values on the order of -0.5 and values approaching zero near the edge of the flow c.f. Fig. 15. Conservatively estimating $\bar{\rho}'/\bar{\rho} = 1$ and $\bar{u}'/\bar{u} = 0.2$, which are typical of flame environments, yields potential differences between conventional and Favre averages on the order of 10% Starner and Bilger (1981) report direct measurements of $\bar{u}$ and $\tilde{u}$ in the round jet diffusion flames in coflowing yielding differences on the order of 5%, which are well within this limit.

Differences between conventional and Favre averages are larger for velocity fluctuations, and probably for other turbulence quantities as well. Taking streamwise velocity fluctuations as an example, it can be shown that

$$[(\bar{u}'-\tilde{u}'')/(\bar{u}')] = [(\bar{u}')/(\bar{u}'+\tilde{u}'')](\bar{\rho}'/\bar{\rho})[(\bar{\rho}'/\bar{\rho})R_{\rho' u'}{}^2 - R_{\rho' u'^2}] \tag{11}$$

Starner and Bilger (1981) have measured $R_{\rho' u'^2}$ in round jet flames; it is relatively small near the axis and decreases monotonically toward -1 near the edge of the flow. Taking mean values across the flow as follows:

$$\bar{\rho}'/\bar{\rho} = 1, \qquad \bar{u}'/(\bar{u}' + \tilde{u}'') = 0.5, \qquad R_{\rho' u'} = R_{\rho' u'^2} = -0.3,$$

yields differences between $\bar{u}'$ and $\tilde{u}''$ on the order of 20%. This estimate is comparable to direct measurements by Starner and Bilger (1981), although higher values, up to 40%, were observed near the flow edge. These considerations imply that mass weighting has a significant effect on turbulent velocities in flames and strict correspondence with the method of averaging is required for definitive evaluation of analysis.

Velocity measurements are most often made with hot-wire anemometry, Pitot probes and laser Doppler anemometry (LDA). Hot wire anemometry is generally limited to characterization of initial conditions, where the constant density flows present few problems. Pitot probes and LDA, however, are often used to measure flow structure and will be considered in the following.

Becker and Brown (1979) discuss errors and uncertainties associated with the use of Pitot probes. In general, such probes are not very relaible when local turbulence intensities are high, e. g., greater than 20%, due to effects of flow inclination on their reading and the disturbances they introduce. Libby et al. (1985) suggest that Pitot probes indicate a type of density-weighted velocity, e.g.,

$$\hat{u} = (\overline{\rho u^2})^{1/2}/\bar{\rho}^{1/2} \tag{12}$$

which is neither a conventional nor a Favre average. The differences between $\bar{u}$ and $\hat{u}$ can be formulated as follows

$$(\bar{u}-\hat{u})/\bar{u} = (-\bar{u}/(\bar{u}+\hat{u}))(\bar{u}'/\bar{u})^2[1 + R_{\rho'u'}{}^2(\bar{\rho}'/\bar{\rho}) + 2R_{\rho'u'}(\bar{\rho}'/\bar{\rho})(\bar{u}/\bar{u}')] \tag{13}$$

Using the same estimates of mean and fluctuating quantities, and their correlations, as before, yields differences between u and u on the order of 5%.

Errors associated with measurements using LDA are discussed by Libby et al. (1985) and references cited therein. If the instrument is properly frequency-shifted, errors due to directional bias and directional ambiguity can be eliminated; if not, loss of accuracy is comparable to probes and measurements where turbulence intensities exceed 20% have considerable uncertainty. The response of the seeding particles is usually adequate for the characteristic flow lengths and velocities of existing measurements in diffusion flames. However, problems of velocity and concentration bias must be addressed.

If the reactant flow of a premixed flame is uniformly seeded and if the molecular weights of all species are the same, then the concentration of seeding particles is proportional to the density. In this case, if each particle gives only one velocity output upon passing through the measuring volume, a particle-average velocity is equivalent to a Favre-averaged velocity (Libby et al., 1985). Similarly, if the data density is high, implying small time intervals between valid velocity signals in comparison to characteristic flow time, time-averaging the low-pass filtered processor output yields a conventional average. Diffusion flames involve at least two reactant flows, however, and these conveniences are not generally applicable. If both streams are seeded to yield a high data density, then a proper time average is obtained. If high data densities can't be maintained, then the uniform time interval sampling advocated by Stevenson et al. (1982) and Craig et al. (1984) or achiving the time-of-event and subsequent analysis with uniform time intervals as advocated by Brum and Samuelsen (1984) can be used to obtain a reliable tme average as well as a direct estimate of potential bias errors. These approaches, however, have not been used for any of the measurements considered here.

If only one stream is seeded, but seeding densities are high and the signal is conditionally averaged to eliminate periods when only unseeded fluid is present, then a conditional time average is obtained. LDA measurements by Glass and Bilger (1978), Starner and Bilger (1980, 1981) and Starner (1983) were carried out under such conditions. Furthermore, the unseeded flow had a low turbulence level; therefore, these measurements correspond to conditional turbulent fluid averages, which are appreciably different from conventional averages when intermittencies are large. Data of this type, as well as particle-averaged quantities when only one stream is seeded, are not very convenient for evaluation of analysis. Dibble et al. (1984a) establish the limits of the potential bias in the vertical flow of a jet of gaseous fuel into coflowing air. Distributions of velocity and mixture fraction are measured when only the fuel is seeded, when only the air flow is seeded, and when both the fuel jet and coflowing air are seeded. Bias of the data is clearly evident although differences are modest except for the mean and rms radial velocities.

Temperature. Conventional and Favre averages of temperature are appreciably different in flames - up to several hundred degrees Kelvin. Most temperature measuring systems yield values which approach time averages, although optical techniques have the capability to find both types of average. Thermocouple probes and optical methods will be briefly discussed in the following.

Libby et al. (1985) point out that thermocouple probles yield a heat-transfer weighted mean temperature. If the probe is small, this approaches a time-averaged temperature modified by radiation and conduction errors. Whether correcting such readings in the mean is appropriate, due to the nonlinearities associated with radiation and flame structure, has not been assessed to our knowledge; however, this practice is commonly accepted. Errors in such procedures are unlikely to be greater than a fraction of the correction.

Thermocouple probes are generally too large to provide adequate frequency response to measure temperature fluctuations in gaseous flames; therefore several workers have used compensation circuits to improve frequency response. This procedure is only accurate if the appropriate instantaneous time constant of the thermocouple is known. In flame environments, the time constant varies with instantaneous mixture fraction and velocity as well as the state of thermodynamic equilibrium - all of which vary with time; therefore, use of an unvarying time constant in the compensation circuit yields questionable results. Some authors attempt to correct for this by periodically measuring the time constant. Since compensation seeks to increase response, however, such determinations clearly cannot be made rapidly enough to provide reliable compensation for the full range of frequencies in the flow. As a result, we feel that compensated thermocouple measurements provide useful qualitative results concerning temperature fluctuations in reacting gases, but uncertainties in these measurements cannot be specified well enough for their use in definitive assessment of analysis.

Optical techniques for temperature measurements include Rayleigh scattering (for appropriate gas mixtures), spontaneous Raman scattering, and coherent anti-Stokes Raman scattering (CARS). These measurements are normally processed to yield time-averaged mean and fluctuating values. In some cases, sufficient information is available for finding instantaneous density as well and Favre-averaged values are computed as well.

Kent and Bilger (1973) and Drake, Pitz and Lapp (1984) have made measurements in round jet hydrogen/air diffusion flames, for similar conditions, which provide a means of directly comparing results from thermocouple probes and Raman scattering measurements. The results are illustrated in Fig. 16. Differences between the two sets of measurements are similar to experimental uncertainties. The advantage of the Raman measurements, however, is that temperature fluctuations can also be accurately obtained.

<u>Other Scalar Properties</u>. Other scalar properties of interest include mixture fraction, species concentrations and density. Methods most frequently used for these measurements are sampling probes and optical techniques (Mie, Rayleigh and Raman scattering; CARS; and laser-induced fluorescence). Sampling has slow response and has only been used for mean properties in reactive environments. The optical methods can provide temporal, and in some cases Favre, averages of mean and fluctuating quantities.

Sampling is generally thought to provide values which approach Favre averages (Libby et al., 1985). The evidence for this, however, is limited and the difference between conventional and density-weighted averages can be large. The behavior of a particular species or density depends on the state relationships of the reactant systems; therefore, we consider mixture fraction as a representative scalar property to examine the differences

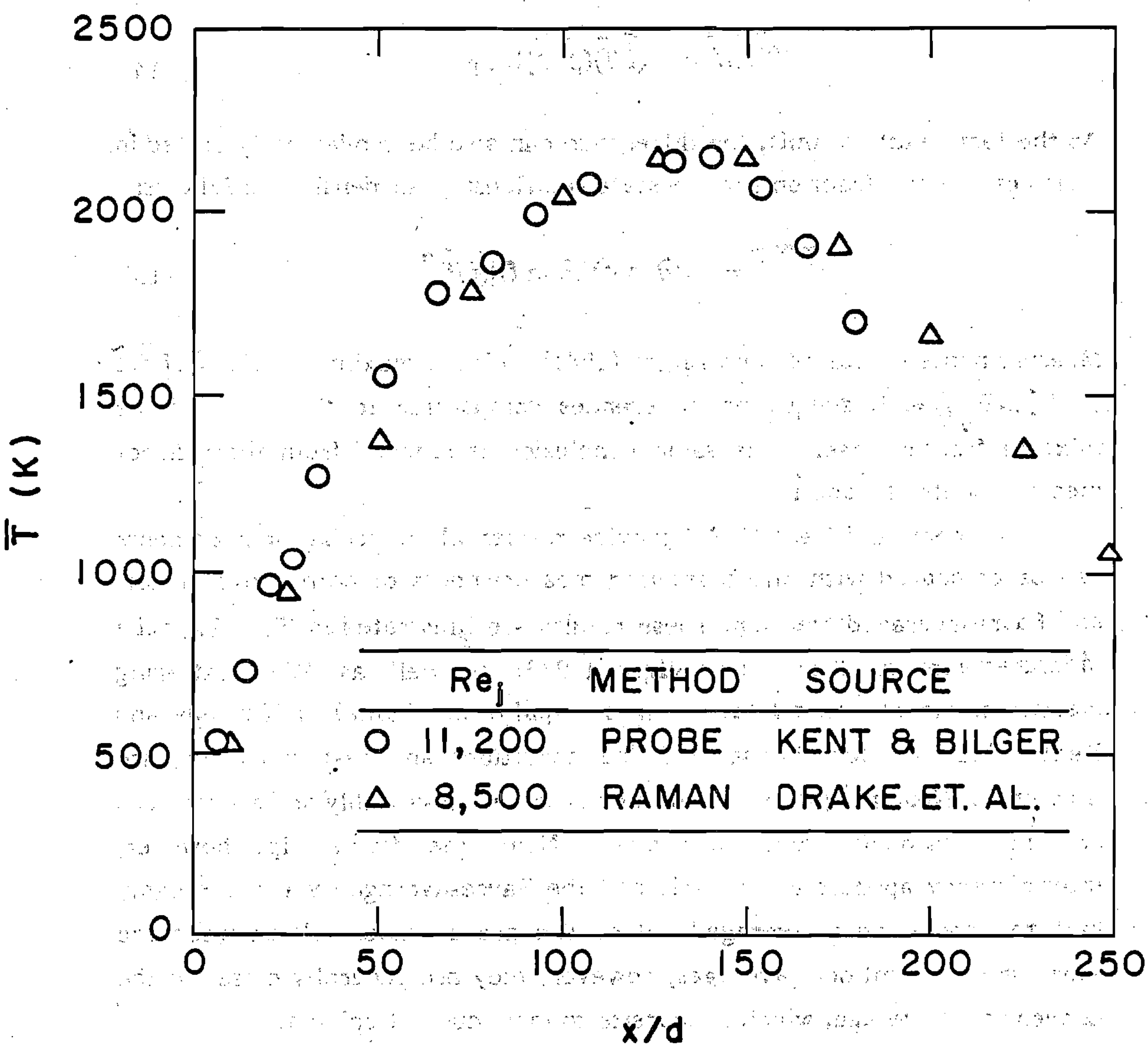

Figure 16. Mean temperatures along the axis of hydrogen/air jet diffusion flames using a thermocouple probe and spontaneous Raman scattering. Data from Kent and Bilger (1973) and Drake, Pitz and Lapp (1984).

between these averages. From the basic definitions

$$(\bar{f}-\tilde{f})/\bar{f} = -(\bar{f}'/\bar{f})(\bar{\rho}'/\bar{\rho})R_{\rho' f'} \tag{14}$$

At the fast-reaction limit, the difference can also be conveniently stated in terms of mixture fraction and the state relationship for density, as follows:

$$(\bar{f}-\tilde{f})/\bar{f} = -[(\partial \ln \rho)/(\partial \ln f)](\bar{f}'/\bar{f})^2 \tag{15}$$

Measurements of Starner and Bilger (1981) indicate maximum values of $\bar{f}'/\bar{f} \approx \bar{\rho}'/\bar{\rho} \approx R_{\rho' f'} \approx 1$, suggesting differences comparable to the value of the mixture fraction itself. The same conclusion is reached from their direct measurements of $\tilde{f}$ and $\bar{f}$.

Kennedy and Kent (1981) provide results where probe measurements can be compared with Mie-scattering measurements of both conventional- and Favre-averaged fraction. These results are illustrated in Fig. 17. Probe measurements of Kent and Bilger (1973) as well as Mie scattering measurements of $\bar{f}$ and $\tilde{f}$ (assuming an equilibrium flame) of Kennedy and Kent (1981), all for the same flame conditions and test apparatus, are illustrated. Near the jet exit, $\bar{f}$ and $\tilde{f}$ don't differ appreciably and all methods are in reasonably good agreement. Near the flame tip, however, intermittency appears at the axis and the Favre-averaged value is roughly half the conventional-averaged value. The probe values fall between the Favre and conventional averages; however, they are generally closer to the conventional average, which is opposite to most current opinion.

Drake, Bilger and Starner (1982) point out that mixture fraction measurements using Mie scattering yield larger differences between conventional- and Favre-averaged values than Raman measurements in hydrogen/air diffusion flames. They suggest effects of differential diffusion as a possible cause for this behavior, e. g. molecular diffusion rates of hydrogen are greater than other permanent gases while particles have negligibly-slow rates of molecular diffusion. In spite of this, however, recent Raman measurements in turbulent hydrogen/air diffusion flames, by Drake,

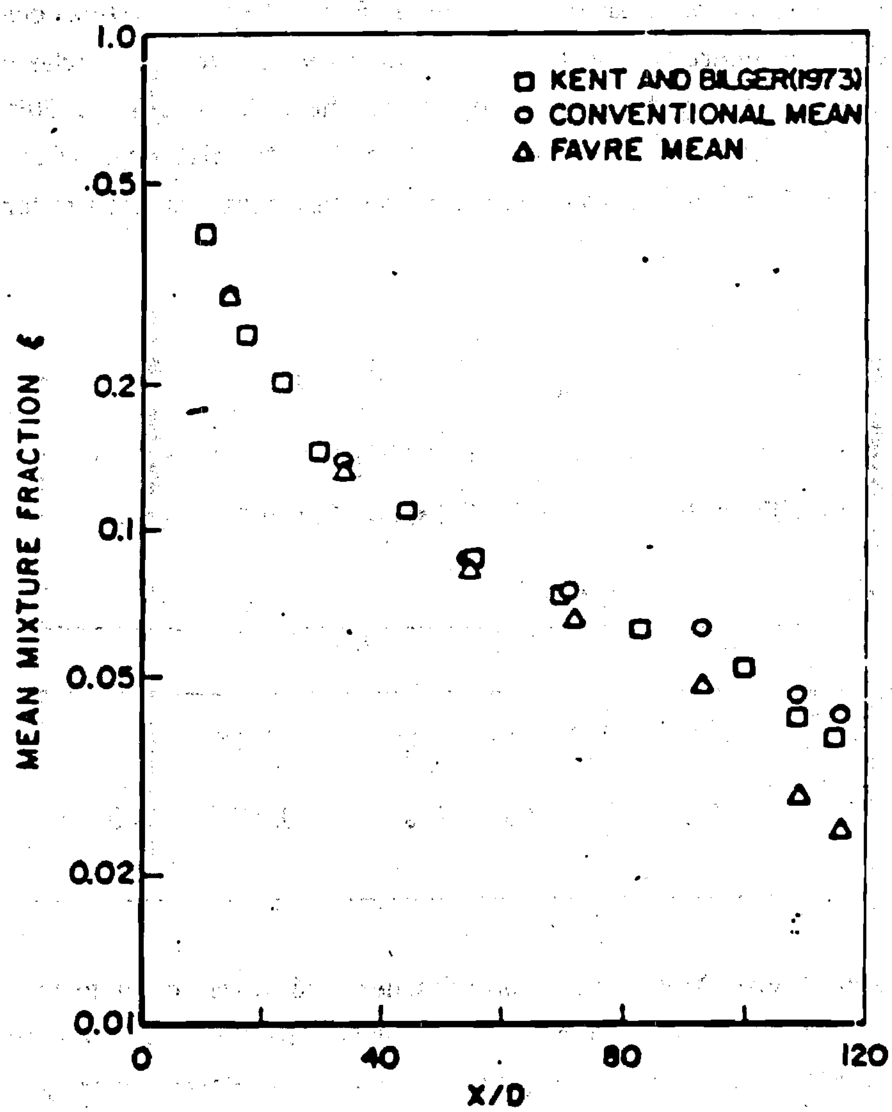

Figure 17. Measurements of mixture fraction along the axis of coflowing turbulent hydrogen/air jet diffusion flames. Comparison of Favre, Reynolds and probe averages. From Kennedy and Kent (1981).

Shyy and Pitz (1985), yield conclusions similar to the Mie-scattering findings. Their mixture fraction measurements, reduced to yield both $\bar{f}$ and $\tilde{f}$ along the flame axis, are summarized in Table 1. For $x/d \leq 150$, differences between $\bar{f}$ and $\tilde{f}$ are generally less than 10%. However, at $x/d = 200$, where intermittency becomes significant on the axis, there is roughly a 50% difference between $\bar{f}$ and $\tilde{f}$. Other areas of high intermittency, which incorporates most of the region where reaction is significant, exhibit similar large differences between $\bar{f}$ and $\tilde{f}$.

Table 1

Conventional- and Favre-Averaged Mixture Fractions

in a Turbulent Round-Jet Diffusion Flame*

x/d	10	25	50	100	150	200
$\bar{f}$	0.463	0.203	0.110	0.0540	0.0315	0.0173
$\tilde{f}$	0.461	0.201	0.109	0.0536	0.0290	0.0126

In agreement with Drake, Bilger and Starner (1982), we conclude that probe measurements yield results having indeterminate levels of density weighting, generally lying between conventional and Favre averages. Furthermore, differences between these averages are large (greater than 30%) in the region where reaction is significant. The reason that probe measurements do not reliably indicate Favre averages is not known at present. More attention to the flow response of specific sampling probes, for

* Along the axis of a hydrogen/air diffusion flame, $Re_j = 8500$. From Drake, Shyy and Pitz (1985).

typical turbulent flame environments, should be pursued to clarify this issue.

Probe measurements of species concentration also appear to have limited accuracy when local turbulence intensities are high (greater than 20%), similar to Pitot probes. Direct evidence of this is presented by Lai et al. (1985), where sampling measurements of mean mixture fraction are compared with LIF and laser absorption measurements in a turbulent wall plume. The optical techniques agreed reasonably well with each other, however, the probe measurements were biased upward near the freestream edge of the flow. Based on the indeterminacy of density weighting and effects of turbulence intensity, it is unlikely that probe measurements can provide a definitive test of turbulent reaction analysis at the fast-reaction limit.

Mie scattering measurements of mixture fraction also exhibit difficulties which limit their usefulness for definitive evaluation of analysis. Use of titanium dioxide particles give high seeding levels, but these particles undergo light-scattering property changes in flames which complicates interpretation of such measurements (Kennedy and Kent, 1979). Use of aluminum oxide particles avoids the property change effect; however, uniform seeding rates at sufficiently high levels to control shot noise are difficult to provide. Effects of differential diffusion and the need to invoke the equilibrium flame assumption to compute other scalar properties also limit the effectiveness of these results - particularly for fluctuating properties. In summary, only carefully-conducted Rayleigh, Raman, LIF and CARS measurements, or other nonintrusive techniques providing a direct measurement of mixture properties, have the potential to provide measurements of scalar properties for definitive evaluation of turbulent reaction analysis.

Visualization. Visualization is a useful and necessary augmentation of the measurements described above. First, "still" photographs complement the experimental schematic by providing a characterization of the physical hardware. Second, still photographs of the flame provide a time-averaged view that is desirable for direct comparison to the spatial distribution of the time-averaged mean measurements. An important corollary to the time-averaged visualization is a documentation of the flame dynamics and scales of turbulent mixing. Although not quantitative, successive frames from a high speed photographic sequence provides a visual indication of the dynamics underlying the time-averaged field and the scales of turbulent mixing, both of which are critical to the interpretation of a modeling data base. Such photographs also provide a means of detecting nonturbulent periodic disturbances that may be present in the flow field.

Conservation checks

The accuracy of structure measurements is frequently evaluated by examining streamwise conservation of mass, momentum and mixture fraction. Reacting flows, however, introduce considerable uncertainties in conservation checks due to effects of density fluctuations and flow acceleration resulting from streamwise pressure gradients and buoyancy. In the following, we examine these uncertainties for fast-reacting turbulent flows.

Starner and Bilger (1981) provide information which is useful for assessing effects of density fluctuations. Conservation of momentum and mixture fraction are taken as examples. Common to most of the current data base, we assume that the following properties are available: time-averaged velocities, time- or Favre-averaged mixture fractions (to cover the limits of probe measurements and time-averaged density.

The principle term to be evaluated for momentum conservation is the momentum flux. In terms of the variables listed above, this can be written (Starner and Bilger, 1981)

$$\overline{\rho u(u-u_e)} = \bar{\rho}\,\bar{u}(\bar{u}-u_e) + (2\bar{u}-u_e)\overline{\rho' u'} + \bar{\rho}\,\overline{u'^2} + \overline{\rho' u'^2} \tag{16}$$

where u_e is included to allow for the presence of a nonzero free-stream velocity. Except in the few cases where density/velocity correlations are available, the conservation check would have to be based on the first term on the RHS of Eq. (16). For their round-jet hydrogen/air diffusion flame, Starner and Bilger (1981) find the use of only the first term yields an overestimation of momentum flux of roughly 30% at a half-width location near the tip of the flame. They indicate that the discrepancy would be even greater near the edge of the flow.

The principle term to be evaluated for conservation of mixture fraction is the mixture fraction flux. In terms of the variables listed earlier, this can be written (Starner and Bilger, 1981) as either

$$\overline{\rho u f} = \bar{\rho}\bar{u}\bar{f} + \bar{\rho}\overline{u'f'} + \bar{u}\overline{\rho'f'} + \bar{f}\overline{\rho'u'} + \overline{\rho'u'f'} \tag{17}$$

in terms of f, or

$$\overline{\rho u f} = \bar{\rho}\,\bar{u}\,\tilde{f} + \bar{\rho}\,\overline{u'f''} + \tilde{f}\,\overline{\rho'u'} + \overline{\rho'u'f''} \tag{18}$$

in terms of $\tilde{f}$. Once again, only the first terms on the RHS of Eqs. (17) and (18) are generally available, while probe measurements yield values which are indeterminate between them. Starner and Bilger (1981) find that use of $\bar{\rho}\ \bar{u}\,\tilde{f}$ gives values within a few percent of the correct mixture fraction flux. However, $\bar{\rho}\ \bar{u}\ \tilde{f}$ is almost four times the correct value at a comparable location. Clearly, the indeterminate nature of the probe measurements, or the unavailability of Favre-averaged measurements, introduces substantial uncertainties in mixture fraction fluxes. The difficulties in momentum conservation checks multiply when streamwise pressure gradients or buoyancy is a factor. Acceleration due to pressure gradients can only be evaluated when static pressure distributions are reported, which is rarely the case. Evaluation of these effects also requires a reasonable number of crossstream traverses in the range of interest. In general few traverses are available, particularly in cases where vital density/velocity correlations are reported. Finally, a momentum conservation check requires good documentation of initial conditions, particularly any wake effects from upstream components. Such information is only occasionally reported.

Examination of existing data indicates that no data set has sufficient information to provide a definitive (within 20-30%) conservation check. Checks made by various authors are reported in the following; however, we did not attempt to apply this normally elementary assessment to any of the data, due to the absence of appropriate information.

LITERATURE SEARCH

The discussion of available experimental data is divided into three main categories: (1) round free jets, (2) plane free shear layers, and (3) wall boundary layers. Within each category the existing studies are organized according to individual laboratories, when several studies were undertaken by a particular research group, or in a general category where single studies are reported.

Round free jets

Table 2 is a summary of studies of turbulent reaction in round free jets at the fast-reaction limit. Most of the work involves round jets in coflow. However, a few studies of round fuel jets in still air are also reported. Much of this work has been carried out by research groups using a particular apparatus for a series of studies, e. g., work at the University of Sydney, General Electric, Sandia, and Osaka University. These studies are grouped according to the organization at the front of the table, while individual studies are at the back.

Studies of round-jet hydrogen/air diffusion flames have been ongoing by Bilger and coworkers at the University of Sydney for more than a decade. The bulk of this work has involved round jets in a horizontal coflow using the same apparatus; however, a few studies considered vertical upflow in nearly stagnant air (Bilger and Beck, 1975; and Kennedy and Kent, 1979). The combined measurements for the coflow configuration, particularly for u_j/u_e = 151.1/15.1 m/s, are very extensive. This includes initial conditions; streamwise pressure variations; mean and fluctuating velocities; mean and fluctuating mixture fraction; mean temperatures and concentrations of major species; density, mixture fraction and velocity cross-correlations; and probability density functions of velocity and mixture fraction. Much of what is currently known concerning this flame system, particularly the hydrodynamic aspects, can be attributed to these experiments.

Nevertheless, the data base measured at the University of Sydney has significant limitations for evaluation of turbulent reaction analysis. The

Table 2. Measurements in Round Free Jets

Reference	Flow	Velocity	Scalars	Other	Instrument Properties	Comments
<u>University of Sydney Studies:</u>						
Kent & Bilger (1973)	Fuel jet in coflow; hydrogen/air; d = 7.62 mm; 305 mm square duct; horizontal; u_j/u_e (m/s) = 48.8/24.4, 107.1/21.4, 147.0/18.4, 151.1/15.1; p(x) known $\bar{u}'_e/\bar{u}_e = 0.1\%$	$\bar{\rho}\bar{u}^2$ and $\bar{v}'$ along axis, $x/d \leq 160$; $\bar{\rho}\bar{u}^2$ traverses at x/d = 40, 80, 120 and 160. $\bar{u}$,$\bar{u}'$ traverses at x=0.	T and mean concentrations of H_2 H_2O and O_2 at x/d = 40, 80 and 160; all for u_j/u_e = 10.		Pitot-static probe; bare-wire thermocouple corrected for radiation; isokinetic sampling with water-cooled probe (1.2 mm inlet); $\bar{v}'$ using NPL static-pressure tube.	
Bilger & Beck (1975)	i) Same as Kent and Bilger (1973); u_j/u_e (m/s) = 151.1/15.1		i) Mean concentrations of H_2, H_2O and O_2 along axis, x/d = 45-190; and traverse, x/d = 80.		Same as Kent and Bilger (1973).	
	ii) Fuel jet in still air; hydrogen/air; d = 1.53 - 6.35 mm; 450 mm round duct; vertical.		ii) Same measurements x/d = 15-110.	ii) Flame length based on stoichiometric mean composition on axis.	Same as Kent and Bilger (1973).	
Glass & Bilger (1978)	Same as Kent and Bilger (1973); u_j/u_e (m/s) = 151.1/15.1	$\bar{u}$,$\bar{u}'$ and $\bar{v}'$ along axis, x/d < 200; $\bar{u}$,$\bar{u}'$,$\bar{v}'$ and $\overline{u'v'}$ traverses at x/d = 40, 80, 120 and 160; $\bar{P}(u)$ traverse at x/d = 80.			Single-channel LDA (0.25 × 1 mm probe volume), no frequency shifting, only hydrogen flow seeded.	Measurements have concentration bias.
Kennedy & Kent (1979)	Fuel jet in still air; hydrogen/air; d = 4.36 mm, u_j = 160 m/s; d = 6.35 mm, u_j = 68 m/s; 1000 mm square screen enclosure.		$\bar{f}$, $\bar{f}'$, $\tilde{f}$ and $\tilde{f}'$ along axis, x/d = 5 - 120, and traverses at x/d 40, 80, and 110; $\bar{P}(f)$ and $\tilde{P}(f)$ along axis and traverses at x/d = 12, 32, 40, 60, 80 and 100.		Mie scattering using titanium dioxide particles (1.4 × 2.5 mm probe volume).	Surface properties of titanium dioxide changed in flame causing experimental uncertainties.

Table 2. Continued.

Reference	Flow	Velocity	Scalars	Other	Instrument Properties	Comments
Stårner & Bilger (1980)	Same as Kent and Bilger (1973); u_j/u_e (m/s) = 151.1/15.1; streamwise pressure gradients from -274 to 23 Pa/m.	$\bar{u}$, $\overline{u'}$, $\bar{v}$, $\overline{v'}$ and $\overline{u'v'}$ along axis, x/d < 160, and traverses at x/d = 40, 60, 80, 120 and 160; K_u, S_u traverse at x/d = 80.		L along axis, x/d < 160, for dp/dx = 23 Pa/m.	Same as Glass and Bilger (1978).	Same as Glass and Bilger (1978).
Kennedy & Kent (1981)	Same as Kent and Bilger (1973); u_j/u_e (m/s) = 151.1/15.1		$\bar{f}$, $\overline{f'}$, $\tilde{f}$ and $\widetilde{f''}$ along axis, x/d < 120; $\bar{f}$ traverses at x/d = 34, 55 and 93; $\overline{f'}$ and $\widetilde{f''}$ traverse at x/d = 55. P(f) and $\tilde{P}$(f) along axis, x/d < 109, and traverse at x/d = 55. Other scalar properties computed from f (equilibrium flame).		Mie scattering using aluminum oxide particles (1.4 × 0.9 mm probe volume). Upper bound for shot noise of 20% for $\bar{f}$ and $\overline{f'}$.	
Stårner & Bilger (1981)	Same as Kent and Bilger (1973); u_j/u_e (m/s) = 151.1/15.1; streamwise pressure gradients from -102 to 23 Pa/m.	$\bar{u}$ and $\overline{u'}$ along axis, x/d < 160, and traverses at x/d = 40, 80 and 120; $\tilde{u}$ and $\widetilde{u'}$ traverse at x/d = 120.	$\bar{f}$, $\tilde{f}$, $\overline{f'}$ and $\widetilde{f''}$ traverse at x/d = 102. $\bar{\rho}$ and $\overline{\rho'}$ traverses at x/d = 40, 80 and 120 computed from f (equilibrium flame).	$\overline{f'u'}$, $\overline{\rho' u'}$ and $\widetilde{u''f''}$ along axis, x/d = 40 - 160; $R_{u'f'}$, $R_{\rho' u'}$, traverses at x/d = 40 and 80.	LDA same as Glass and Bilger (1978); uncertainty in $\bar{u}$ and $\overline{u'}$ of 3 and 5% of centerline values. Mie scattering using aluminum oxide particles (1 × 1.5 mm probe volume 1.4 mm downstream of LDA probe volume); uncertainties in mean and fluctuating scattered light intensities < 15%.	All data tabulated in Stårner (1980). LDA measurements have concentration bias. Scalar properties from equilibrium flame assumption.
Stårner (1983)	Same as Kent and Bilger (1973) u_j/u_e (m/s) = 151.1/15.1; dp/dx = -18 Pa/m.	$\bar{v}$, $\overline{v'}$, S_v, K_v traverse at x/d = 50; $\tilde{v}'$ traverses at x/d = 40, 80, 120 and 160.	$\bar{f}$, $\overline{f'}$, $\tilde{f}$, $\widetilde{f''}$, $\bar{\rho}$ and $\overline{\rho'}$ traverse at x/d = 80.	$\overline{v'f'}$ and $\widetilde{v''f''}$ traverses at x/d = 40, 80, 120 and 160.	Single-channel LDA (0.2 × 1 mm probe volume), frequency shifted, only hydrogen flow seeded, uncertainty of $\overline{v'}$ less than 6% centerline value; Mie scattering using aluminum oxide particles (1.3 × 1.5 mm probe volume) coincident with LDA.	Effects of differential diffusion estimated to increase $\overline{v'f'}$ and $\widetilde{v''f''}$ by 10% (x/d = 40) and 25% (x/d = 160). Scalar properties using equilibrium flame assumption. LDA measurements have concentration bias.
Stårner (1985)	Same as Stårner (1983).	Traverses of ensemble-averaged u and v at x/d = 40, 80 and 120.	Traverses of ensemble-averaged f at x/d = 40, 80 and 120.		LDA same as Stårner (1983), but two-channel system.	Study emphasizes large-scale motions and is not suited for evaluation of moments. Data decomposed into low-frequency, large-scale and small-scale turbulence.

Table 2. Continued.

Reference	Flow	Velocity	Scalars	Other	Instrument Properties	Comments
<u>General Electric Studies</u>						
Drake, Lapp, Penny, Warshaw and Gerhold (1981)	Fuel jet in coflow; hydrogen/air; d = 3.2 mm; 150 mm square duct; horizontal; u_j/u_e (m/s) = 50/10, 75/15; Re_j = 1500 and 2000; p(x) known.		PDF and mean values of temperature and the concentrations of N_2, H_2 and H_2O at x/d = 10 and 100 (Re_j = 1500) and 50 (Re_j = 2200).		Raman scattering (0.3 × 0.7 mm probe volume, 1000 - 2000 ns pulse duration). Standard deviations: T/4% @ 1500 K, > 10% @ 950 K; N_2/3% @ 1500 K; H_2O/6% @ 1550 K; H_2/6% @ 2 × 10^{-6} gmol/cm^3.	
Drake, Bilger & Stårner (1982)	Same as Drake et al. (1981); u_j/u_e (m/s) = 53.6/8.8, 174/13.1 and 285/12.5; corresponding mean streamwise pressure gradients of -10, -32 and -51 Pa/m.		$\bar{f}$, $\tilde{f}$ and $\tilde{f}''$ along axis x/d = 10 - 200 and traverse at x/d = 50 $\tilde{P}(f)$, $\bar{P}(f)$ and $\tilde{P}(T)$ traverse at x/d = 50.	Favre intermittency	Same as Drake et al. (1981). Uncertainties: T/+ 50K, X_i/ ± 1 mole %.	
Drake, Pitz & Lapp (1984)	Same as Drake et al. (1981); u_j/u_e (m/s) = 22/9.3, 53.6/8.8, 174.2/13.3 and 285/12.5; corresponding Re_j = 660, 1600, 5200 and 8500.	$\bar{u}$ and $\bar{u}'$ along axis, x/d = 10 - 220, for Re_j = 1600, 5200 and 8500.	$\tilde{T}$ and $\tilde{T}'$ along axis, x/d = 10 - 250 (Re_j= 1600 and 8500); $\bar{\rho}$, $\bar{T}$,$\bar{T}'$ and mean concentrations of H_2, H_2O, N_2 and O_2 traverses at x/d = 10, 50 and 150 (Re_j = 8500); $\bar{P}(T)$, $\bar{P}_t(T)$, and $\bar{P}_n(T)$ traverse at x/d = 50 (Re_j = 1600 and 8500).	Pulsed laser Schlieren and shadowgraph photographs; planar OH fluorescence images; $\tilde{\gamma}$ traverses for x/d = 50, 100, 150, and 200 (Re_j = 8500).	Same as Drake et al. (1982).	

Table 2 Continued

Reference	Flow	Velocity	Scalars	Other	Instrument Properties	Comments
Sandia-Livermore Studies						
Driscoll, Scheffer & Dibble (1983)	Fuel jet in coflow; hydrogen-argon (22%) /air; d = 5.3 mm; 300 mm square duct; horizontal; u_j/u_e (m/s) = 154/8.5; Re_j = 18000	$\bar{u}, \bar{u}'$ along axis, x/d ≤ 160, and traverses at x/d = 10, 30, 50, 70 and 150.	$\bar{\rho}$ along axis, x/d ≤ 160; $\bar{\rho}, \bar{\rho}'$ traverses at x/d = 10, 30, 50, 70 and 150.	$\overline{\rho'u'}$ along axis, x/d = 30 - 150; $\overline{\rho'u'}$ and $\overline{\rho'v'}$ traverses at x/d = 30 and 50.	Single-channel LDA (0.5 × 2 mm) frequency shifted; cw Rayleigh scattering (8kHz cut off frequency)	Dibble et al. (1984 b) indicate that processing problem limited the
Dibble, Kollman & Scheffer (1984 b)	Same as Driscoll et al. (1983)	$\bar{u}$ and $\bar{u}'$ traverse at x/d = 50. traverse at x/d = 50;	$\bar{\rho}$ along axis, x/d ≤ 180; $\bar{\rho}, \bar{\rho}', \bar{f}$ and $\bar{f}'$ $\bar{T}$ and $\bar{X}_i$ found at these positions assuming equilibrium flame.	$\overline{\rho'u'}, \overline{f'u'}$ and $\overline{T'u'}$ traverse at x/d = 50.	Single-channel LDA (0.5 + 2mm) frequency shifted; Raman scattering 2μs pulse.	Asymmetrical $\overline{\rho'u'}$ suggests effect of buoyancy. $\overline{f'u'}$ correlations within 40% of those of Stårner (1980) who used Mie scattering for f; however, $\overline{\rho'}$ only within a factor of 3.
Scheffer & Dibble (1985)	Same as Driscoll et al. (1983)	$\bar{u}$ and $\bar{u}'$ along axis, x/d ≤ 160, and traverses at x/d = 30, 50, 70, 100 and 150; P(u), $P_t(u)$ and $P_n(u)$ traverse at x/d = 150.	$\bar{\rho}$ and $\bar{\rho}'$ along axis, x/d ≤ 160, and traverses at x/d = 30, 50, 70 and 150; $\bar{\rho}$, $\bar{\rho}_t, \bar{\rho}_n, \bar{\rho}', \bar{\rho}'_t$ and $\bar{\rho}'_n$ traverse at x/d = 50.	$\bar{P}(\rho,u)$ and $\bar{\gamma}$ x/d = 50, y/d = 0.	Same as Driscoll et al. (1983).	Effects of buoyancy on turbulence properties observed at x/d = 50.

Table 2. Continued

Reference	Flow	Velocity	Scalars	Other	Instrument Properties	Comments
Dibble and Schefer (1985d)	Same as Driscoll, et al. (1983)	$\overline{u}$ and $\overline{u'}$ traverses at x/d = 50	$\overline{T}$ and $\overline{T'}$ traverses at x/d = 50	$\overline{\rho' u'}$ at x/d = 50, y/d = 4	Same as Dibble et al. (1984b)	
Dibble, Hartman, Schefer, & Kollmann (1984a)	Fuel Jet in Coflow: hydrogen-argon (22%)/air; d=5.25 mm; 300 mm square duct; vertical; u_j/u_e (m/s) = 7.5/9.2; 150/9.2; 225/9.2 Re_j = 9000	$\overline{u}$, $\overline{v}$, $\overline{u'}$, $\overline{v'}$, $\overline{u'v'}$ traverses at x/d = 30, 50	No scalar for reacting flow		Dual Channel LDA (0.5 x 2.0 mm); Dual Bragg Shift; Coincidence 10 μs ; LDA seed particles added to air only, jet fluid only, and then both.	Investigation of velocity bias due to particle origin; velocity data from both reacting and nonreacting jet.
Dibble, Kollman, Schefer (1985c)	Same as Dibble, et al. (1984a) except Re_j = 18,000	None	$(\frac{\partial\rho}{\partial r})^2$ at x/d = 50		Imaged line segment of pulsed laser beam onto 500 element Optical Multichannel Analyzer.	Instantaneous radial profiles from reacting and nonreacting jet.

Table 2. Continued.

Reference	Flow	Velocity	Scalars	Other	Instrument Properties	Comments
<u>University of Osaka Studies</u>						
Takagi, Ogasawara, Fuji, & Diazo (1975)	Fuel jet in coflow; hydrogen/air; d = 2 mm; 133 mm round duct; vertical; u_j/u_e (m/s) = 108/0.15.	$\bar{u}$ traverse at x/d = 50.	$\bar{T}$ and mean concentrations of H_2, H_2O, O_2 and N_2 traverse at x/d = 50.		Pitot-static probe; bare-wire thermocouple (0.05 and 0.10 mm coated bead) corrected for radiation; isokinetic sampling.	Initial velocity profiles and streamwise pressure gradient are unknown.
Takagi, Shin & Ishio (1980)	Fuel jet in coflow; hydrogen-nitrogen (60%)/air; d = 4.9 mm; vertical; u_j/u_e (m/s) = 20 - 90/0.65; Re_j = 4200 - 1800.	$\bar{u}$ and $\overline{u'}$ traverses at x/d = 2, 10.2 and 27.1	$\bar{T}$ and mean concentrations of H_2, H_2O, O_2 and N_2 traverses at x/d = 2, 10.2 and 27.1	Schlieren photographs at nozzle exit.	Single-channel LDA (0.12 × 1.4 mm probe volume) frequency shifted; bare-wire thermocouple (0.1 mm bead diameter); sampling probe (0.3 mm port) analyzed on dry basis with H_2O computed.	
Takagi, Shin & Ishio (1981)	Same as Takagi et al. (1980); u_j/u_e = 20.4 and 55.7/5.1; Re_j = 4200 and 11000.	$\bar{u}$, $\overline{u'}$ and $\overline{v'}$ along axis, x/d ≤ 51; $\bar{u}$, $\overline{u'}$, $\overline{v'}$, $\overline{w'}$, $\overline{u'v'}$, $\bar{P}(u)$ and $R_{uu}(t)$ traverses at x/d = 18.4 (Re_j = 4200); L_u along axis, x/d ≤ 51, and traverses at x/d = 6.1, 12.2, 18.4 and 32.6; power spectra along axis, x/d ≤ 32.6, and traverse at 18.4.	$\bar{T}$ and mean concentrations of H_2, H_2O, O_2 and N_2 along axis, x/d ≤ 51, and traverses at x/d = 6.1, 12.2, 18.4 and 32.6	Schlieren photographs.	LDA same as Takagi et al. (1980) with macroscales using Taylor's hypothesis; temperature and gas-sampling probes same as Takagi et al. (1981).	
Takagi, Shin & Ishio (1981a)	Same as Takagi et al. (1980); u_j/u_e (m/s) = 20.4/5.1; Re_j = 4200.	$\bar{u}$, $\overline{u'}$ and $\overline{v'}$ traverses at x/d = 18.4 and 32.7	$\bar{T}$, $\overline{T'}$, $\bar{P}(T)$ and mean concentrations of H_2, H_2O, O_2, and N_2 at x/d = 18.4.	$\bar{\gamma}$, $\overline{\gamma'}$, and $\bar{P}(\gamma)$ traverses at x/d = 18.4 and 32.7	LDA and gas sampling same as Takagi et al. (1980); bare-wire thermocouple (0.025 mm bead diameter) with electrical compensation using mean response time. Electrostatic probe for positive ions (0.1 × 1.5 mm probe volume).	Uncertainties in temperature fluctuation measurements due to compensation circuit are difficult to evaluate.

Table 2. Continued.

Reference	Flow	Velocity	Scalars	Other	Instrument Properties	Comments
<u>Other Studies</u>						
Hawthorne, Weddell & Hottel (1949)	Fuel jet in furnace or unconfined; vertical; i) hydrogen/air; $d = 3.2 - 6.4$ mm; $u_j = 49.4 - 152.4$ m/s. ii) carbon monoxide/air; $d = 6.4$ mm, $Re_j = 5095$, lifted frame.		i) $\bar{f}$ along axis, $x/d = 10 - 75$; $\bar{f}$, $\overline{f'}$; and mean concentrations of H_2, O_2 and H_2O at $x/d = 32$, 48 and 66.	Visible flame length.	Sampling and analysis for H_2 and O_2 on a dry basis, computation of H_2O. $\bar{f}$ found from local mean mixture fraction and concentrations assuming Gaussian PDF and flame sheet.	Traverses made for confined configuration which authors felt influenced the results. Only visible flame length for one condition measured for carbon monoxide/air flame.
Takeno & Kotani (1975)	Fuel jet in coflow; hydrogen/air; $d = 1$ mm; vertical; u_j/u_e (m/s) = 157 - 598/5; $Re_j = 1431 - 5439$ $T_e = 300 - 700$ K.			Dark-field and shadowgraph photographs; length to transition.		Primarily a study of transition to turbulent flow.
Becker & Liang (1978)	Fuel jet in still air; hydrogen/air; carbon monoxide/air; $d = 0.69 - 4.57$ mm; vertical; $(\pi a \rho_e / 4\dot{M}_j)^{1/3} x_f = 2.1 - 7.7$ for hydrogen, 1.1 - 4.1 for carbon monoxide.			Visible flame length		See references cited therein for earlier similar work.
Schoenung & Hanson (1982)	Fuel jet in still air; carbon monoxide/air; $d = 15$ mm; vertical; $u_j = 10$ m/s; 1% H_2 in CO, by volume, to stabilize flame.	$\bar{u}$ and $\bar{u}'$ at jet exit.	Mean concentration of CO and CO_2 and concentration fluctuations of CO traverses at $x/d = 2$ and 5; $\bar{P}$(CO) traverses at $x/d = 2$. Power spectral density of CO at $x/d = 5$.		Mean concentrations by sonic probe (0.4 mm inlet, water-cooled); carbon monoxide absorption probe (5 mm path length).	

Table 2. Continued.

Reference	Flow	Velocity	Scalars	Other	Instrument Properties	Comments
Razdan & Stevens (1985)	Fuel jet in coflow; carbon monoxide/air; d = 5 mm; 300 mm round duct; vertical; u_j/u_e (m/s) = 37.5/ 0.13; Re_j = 11400.	$\bar{u}$, k along axis; x/d = 20 - 100, and traverses at x/d = 20, 40, 50 and 60.	$\tilde{f}$, $\bar{T}$ and mean concentrations of CO, CO_2 and O_2 along axis; x/d = 20 - 100, and traverses at x/d = 20, 40, 50 and 60.		Single-channel LDA (0.065 × 0.75 mm probe volume) frequency shifted; bare-wire thermocouple (0.25 mm bead diameter) corrected for radiation; water-cooled sampling probe (1.2 mm inlet). Momentum balance within 30% (ignoring buoyancy). Enthalpy balance within 30%. Element balance within 20%.	
Dahm (1985)	Fuel jet in still environment; dilute acid/base reaction in water; d = 2.54 mm; 850 × 850 × 1590 mm rectangular enclosure; vertical; Re_j = 1000 - 20000.		$\bar{f}$, $\overline{f'}$ and $\bar{P}(f)$ along axis, x/d ≤ 300 (Re_j = 1500 and 3000). Several instantaneous radial concentration profiles at x/d = 300; (Re_j = 5000).	Visible reaction-zone length and its PDF.	LIF (0.6 × 0.5 - 1 mm probe volume) both at a point and along a line.	Flow involves negligible variation of scalar properties and S_c = 600.
Dahm & Dimotakis (1985)	Same as Dahm (1985); Re_j = 1500 - 10000.		$\bar{f}$ and $\overline{f'}$ traverse at x/d = 300 (Re_j = 1500, and and 3000); instantaneous concentration profiles at x/d = 300 (Re_j = 5000).	Visible reaction length and its PDF.	Same as Dahm (1985).	Same as Dahm (1985).

difficulties involve the limited range of conditions tested, relatively low Reynolds numbers, potential effects of buoyancy, and aspects of the instrumentation. Although several operating conditions were considered, only one condition, u_j/u_e = 151.1/15.1 m/s, has a full range of velocity and scalar properties reported. This flow has an initial Reynolds number of 11200, which is lower than desirable due to the tendency toward relaminarization in flaming regions. The authors point out the tendency for the flame tip to rise above the axis of the injector, due to the horizontal configuration, suggesting some influence of buoyancy on mean properties. The findings of Dibble et al. (1984ab) suggest that effects of buoyancy on turbulence properties are probably even more substantial. This loss of symmetry poses increased problems of numerical closure, aside from the obvious difficulties of adequately analysing the turbulence/buoyancy interaction. Except for limited early measurements of mean velocities using a pitot-static probe (Kent and Bilger, 1973), most velocity measurements were made using an LDA. The authors were careful to provide time-averaged velocities, however, only the fuel flow was seeded; therefore, these measurements have concentration bias. This presents significant difficulties for evaluation of most theoretical methods in regions where intermittency is significant. Mixture fractions were measured using Mie scattering. Kennedy and Kent encountered problems of surface property changes with this technique using titanium dioxide particles; therefore, their measurements are questionable. Later use of aluminum oxide particles avoided the property change problem; however, mechanical difficulties of maintaining uniform seeding and avoiding marker shot noise in low mixture fraction regions introduce undesirable uncertainties - particularly for mixture fraction fluctuations. Early probe measurements of mean species concentrations by Kent and Bilger (1973) have indeterminate levels of density weighting which cause significant uncertainties near the flame zone, as noted earlier.

Studies at General Electric, by Drake and coworkers, involved a coflowing jet apparatus, burning hydrogen/air, very similar to that used at the University of Sydney. One difference was that apparatus dimensions were reduced by roughly a factor of two. Limitations in flame attachment resulted in a somewhat lower maximum Reynolds number for the smaller injector diameter, e. g., $Re_{jmax} = 8500$ as opposed to 11200. Instrumentation was improved for these measurements, however, employing Rayleigh and Raman scattering for density and species concentrations along with LDA for velocity measurements. Thus, the scalar property measurements avoid uncertainties due to probes, seeding fluctuations and shot noise; therefore, either Favre or conventional averages can be reported. Both the fuel and air streams were seeded; thus, problems of concentration bias were eliminated as well. Similar to the work at Sydney, initial and boundary conditions are well known, with resolution of pressure ca.Pa/m. The highest Reynolds number used, 8500, yields fewest problems with relaminarization and the most complete measurements are available for this case. As discussed earlier, the higher velocities and smaller injector used in these tests tend to increase problems of reaching the fast-reaction limit. Departure from equilibrium is well documented, however, and the effect of this could be taken into account when assessing analysis at the fast-reaction limit. Effects of buoyancy, similar to Dibble et al. (1984), are probably present in these data due to the horizontal configuration. The smaller injector diameter tends to reduce the effect; however, the investigators still note an appreciable rise, ca 10-15 mm, of the apparent flame axis at the flame tip. LDA measurements of velocity are limited to mean and fluctuating streamwise velocities; therefore, the hydrodynamic properties of these flames are not as well-documented as the University of Sydney work. These difficulties aside, the data set appears to be valuable for development of analysis, if not definitive evaluation.

More recent work at Sandia, by Dibble and coworkers (1984a, 1984b, 1985a, 1985b, 1985c, 1985d) also employs nonintrusive instrumentation for hydrogen/air round jet flames in coflow. The earliest work (Driscoll, Schefer and Dibble, 1983; Dibble, Kollman and Schefer, 1984b; Schefer and Dibble, 1985; Dibble and Schefer, 1985d) employed a jet/duct configuration in horizontal flow having similar dimensions to the apparatus at the University of Sydney. The fuel flow, however, was diluted with argon in order to provide desirable mixture properties for direct measurement of mean and fluctuating density using Rayleigh scattering. Mean and fluctuating velocities were measured using LDA as well as density/velocity fluctuation correlations by combined LDA/Rayleigh scattering measurements. These results are relatively complete and characterization of initial and boundary conditions is available. However, velocity data shows a relatively large degree of scattering and buoyancy clearly influences turbulence properties in this flow - as noted earlier.

The most recent work at Sandia removes the buoyancy difficulties and expands the variables measured (Dibble et al., 1984a, 1985a, 1985b, 1985c). The hydrogen/air jet diffusion flame in coflow was observed for the vertically upward flow configuration. Thus, asymmetries due to buoyancy were eliminated, although effects of buoyancy still influence flow properties near the flame tip. LDA and Rayleigh scattering were used as before; however, Raman scattering measurements were added to provide instantaneous mixture fraction. Data are available for three injector conditions yielding Re_j = 9000, 18000, and 27000. In addition to the impressive list of point measurements obtained in the flow, one-dimensional imaging of the Rayleigh scattering laser beam was also undertaken. This yielded instantaneous radial profiles of density at x/d 50. Radial derivatives were obtained from these data. In our opinion, the measurements of Dibble et al. (1985a), 1985b) can serve for definitive evaluation of analysis at the fast-reaction limit-subject only to some uncertainty concerning the degree to which this limit was approached. It is likely, however, that approach to equilibrium is closer than the conditions considered by Drake and coworkers (1981, 1982, 1984) since injector dimensions are larger and flow velocities are somewhat lower.

Three studies of hydrogen/air diffusion flames have been reported by Takaji and coworkers (1975, 1980, 1981) at the University of Osaka. A vertical orientation with coflow was used. Measurements primarily considered the near-injector region, $x/d < 51$, and included: mean and fluctuating velocities, using a single-channel LDA; mean and fluctuating temperatures, using a compensated thermocouple; and mean concentrations of major species using a sampling probe. Initial conditions and streamwise pressure gradients for these flows are unknown, the sampling measurements have uncertain levels of density weighting, and the temperature fluctuation measurements with compensation are difficult to assess. Thus, use of this data for model evaluation is problematical, even though it is extensive.

Several other studies have been reported as well. The classical work of Hawthorne, Weddell and Hottel (1949) is well known, but uncertainties in these measurements and the definition of operating conditions are large by today's standards. The work of Takeno and Kotani (1975) was limited to flow visualization in a study primarily considering transition to turbulence near the exit of a jet flame. Becker and Liang (1978) measure flame lengths for hydrogen/air and carbon monoxide/air flames; however, it is difficult to associate flame luminousity with parameters computed by typical analysis.

Schoenung and Hanson (1982) and Razdan and Stevens (1985) provide the only structure measurements for carbon monoxide/air flames - both using vertical upflow. The measurements of Razdan and Stevens are most complete, involving mean and fluctuating velocities using LDA, mean temperatures. using a thermocouple and mean concentrations of major species using gas sampling. Initial and boundary conditions for this flow are unknown and there are density weighting uncertainties for the sampling measurements. Clearly, additional work with carbon monoxide/air flames is warranted, particularly since this reactant combination reduces problems of differential diffusion in comparison to hydrogen/air flames.

The last studies in Table 2 involve work carried out at CalTech. (Dahm, 1985 and Dahm and Dimotakis, 1985). These measurements considered dilute acid/base reactions in water; therefore, effects of property variations near the reaction sheet are small. As a result, these results cannot test critical variable property effects on analysis. The measurements provide extensive information on mixture fraction; however, virtually no information is available concerning flow velocities.

Clearly, the round free jet configuration has attracted many investigators. These studies have helped to develop our understanding of turbulent flames at the fast-reaction limit. However, only a few have potential application for definitive evaluation of analysis. The recent study of hydrogen/air flames in vertical upflow, using nonintrusive diagnostics, by Dibble et al. (1985a, 1985b) appears to be adequate for evaluation of analysis, although effects of buoyancy near the flame tip should be considered. Similar measurements by Drake and coworkers (1981, 1982, 1984) are felt to be satisfactory for model development, and perhaps for evaluation as well. However, additional study to determine the extent of asymmetries, due to buoyancy in a horizontal flow, is warranted.

Plane free shear layers

Table 3 is a summary of past studies of turbulent reaction in plane free shear layers, where conditions approach the fast-reaction limit. Most of this work was carried out at the California Institute of Technology. Two independent studies (Batt, 1977 and Wallace, 1981) are also listed. Wallace's investigation was closely associated with the CalTech. studies.

The reacting flow studies at CalTech. were preceded by extensive work concerning passive scalar mixing in shear layers. Gouldin and Johnston (1985) review the passive mixing studies; only the reacting flow studies are discussed here. Two reactant combinations were considered: (1) dilute hydrogen/fluorine mixtures in nitrogen or helium, and (2) acid/base reaction in water.

The hydrogen/fluorine studies are described by Mungal (1983), Mungal, Dimotakis and Broadwell (1983) and Mungal, Dimotakis and Hermanson (1984). The objective of this work was to provide a diffusion flame sturcture with relatively small heat release, e. g., the maximum temperature rise was less than 120 K. This causes difficulties in approach to the fast-reaction limit, as discussed earlier. Well-known hydrogen/fluorine kinetics were also complicated somewhat, since nitric oxide had to be added to the fluorine-containing stream to initiate the reaction. The side walls of the flow channel were adjusted to achieve a zero-streamwise pressure gradient. Static pressures, however, were measured with liquid-filled manometers whose resolution is ca. 100 kPa, at best. Thus effects of pressure gradients at lower levels, seen in Figs. 12 and 13 from Starner and

Table 3. Measurements in Plane Free Shear Layers

Reference	Flow	Velocity	Scalars	Other	Instrument Properties	Comments
<u>Cal. Tech. Studies</u>						
Mungal (1983)	Shear layer in duct; dilute hydrogen/fluorine in nitrogen or helium; 200 × 50 mm and 200 × 100 mm high- and low-speed sides; horizontal; u_j/u_e (m/s) = 23/8.8; $Re_x = 4 \times 10^5$; 120 K maximum temperature rise.	$\bar{u}$ traverses at one station for three cases (one non-combusting).	$\bar{T}$ traverses at one station.	Dark-field photographs	Pitot-tube rake (1.7 mm OD tubes). Resistance wire temperature probe (0.0025 mm dia. × 1.5 mm long)	Side walls adjusted to give zero-static pressure gradient.
Mungal, Dimoakis, and Broadwell (1983)	Same as Mungal (1983).	Same as Mungal (1983).	Same as Mungal (1983).	Same as Mungal (1983).	Same as Mungal (1983).	Same as Mungal (1983).
Mungal, Dimotakis and Hermanson (1984).	Same as Mungal (1983) u_j/u_e (m/s) = 85/13.5.		$\bar{T}$ traverse at one one location.	Schlieren photograph	Same as Mungal (1983).	Same as Mungal (1983).
Koochesfahani (1984)	Shear layer in duct; dilute acid/base (H_2SO_4/NaOH) reaction in water; u_j,u_e (m/s) = 3 - 7; u_j/u_e = 0.38 - 0.45.		$\bar{f}$ and $\bar{P}(f)$ at one location.	Time-resolved LIF visualization along a line crossing the flow.	LIF (0.10 × 0.35 mm probe volume) along a 23 mm line.	Measurements in region of mixing transition.
Koochesfahani and Dimotakis (1984).	Same as Koochesfahani (1984)		Same as Koochesfahani (1984).	Same as Koochesfahani (1984).	Same as Koochesfahani (1984).	Same as Koochesfahani (1984).
<u>Other Studies:</u>						
Batt (1977)	Wall jet in still air; dilute (0.005%) nitrogen tetroxide dissociation; 127 × 610 mm slot; vertical; u_j = 7 m/s.		Time-averaged mean and fluctuating NO_2 concentrations at x = 453 mm.		Fiber-optics probe (1 × 2.5 mm probe volume.	Effects of energy release small for these flows. Extensive measurements available for passive mixing under the same conditions.
Wallace (1981)	Shear layer in duct; dilute nitric oxide/ozone in helium, nitrogen or argon. 100 × 25 mm and 100 × 50 mm low- and high-speed sides; horizontal; u_j/u_e (m/s) = 25/5; $Re_x = 5 \times 10^4$, 200 K maximum temperature rise.	$\bar{u}$ traverse at one station.	$\bar{T}$ traverses at one station.	Blue and uv shadowgraphs.	Pitot probe (0.3 × 3 mm inlet); bare-wire thermocouple (0.013 mm wires).	Side walls adjusted to give zero static pressure gradient.

Bilger (1980), are probably present. Relatively low Reynolds numbers also suggests problems with effects of transition and buoyancy. Initial conditions for these tests were not measured directly, although sufficient information is reported for reasonable estimates. Finally, the data reported are relatively limited, consisting of mean velocity and temperature traverses (the former for noncombusting conditions) at one location.

Work on hydrogen/fluorine flames is continuing at CalTech., but with higher maximum temperatures in the flow. These experiments provide conditions progressively moving towards the variable scalar property effects of flame environments. If more complete measurements can be conducted for these conditions, in spite of the corrosion problems with fluorine at high temperatures, the entire study would be a very useful source of information for reaction in free shear layers.

The investigation of acid/base reactions in water, by Koochesfahani (1984) and Koochesfahani and Dimotakis (1984) involves negligible changes in scalar properties when reaction occurs. Thus, this experiment is more relevant to passive scalar mixing, with the reactants primarily serving as a marker for the extent of mixing. Measurements defining initial and boundary conditions, as well as the flow structure itself, are relatively limited. Thus, even though these results approach the fast-reaction limit, they don't really address the issues of major interest in this review.

Wallace's (1981) study is generally similar to Mungal (1983). Differences involve use of dilute nitric oxide/ozone as reactions and a reduction of apparatus size by roughly a factor of two. Only weak property variations were considered, e. g., maximum temperature changes were less than 200 K. Problems of initial and boundary conditions, low Reynolds numbers and buoyancy, and relatively limited structure data are similar to Mungal (1983).

Batt's (1977) study of nitrogen tetroxide dissociation followed an extensive study of passive scalar mixing in the same apparatus. The reaction experiment involved dissociation of nitrogen tetroxide (in a cool wall jet) to nitrogen dioxide upon mixing with room air. Temperature changes in the flow were small, ca. 50K; therefore, variable property effects are not very representative of flame environments. Vertical downflow in a stagnant environment was considered, simplifying problems of specifying boundary conditions and treating buoyancy. Initial conditions could be inferred from the passive mixing tests, even though they are not specifically reported for the reacting flows. The author also presents a careful evaluation of approach to the fast-reaction limit. Data reported, however, are relatively limited, e.g., mean and fluctuating concentrations of nitrogen dioxide. These results were obtained with a relatively bulky probe, suggesting large measurement uncertainties near the edge of the flow, where turbulence intensities are high in a stagnant environment.

All the plane free shear layer flows have significant limitations for definitive evaluation of turbulent reaction analysis. Clearly, additional systematic experimentation with plane free shear layers is merited - particularly for conditions having greater energy release rates, Reynolds numbers, and preferably in vertical upflow to simplify treating effects of buoyancy. Such experiments will be costly, since plane flows involve relatively large rates of reactant consumption, for adequate aspect ratios, in comparison to round jets. The test arrangemnt used by Kremer (1967) to study hydrocarbon diffusion flames offers advantages for experiments of this type, but curiously has not been used by subsequent workers.

Wall boundary layers

Reasonable turbulence levels and aspect ratios in wall boundary layers cause the greatest problems of reactant consumption; therefore, relatively few studies have been reported for this flow at the fast-reaction limit. This is surprising, in spite of the cost, since this configuration is important for natural fires and solid rocket applications. Table 4 is a summary of the two studies that could be found, both by Ueda and coworkers (1982, 1984). Similar results are also reported by Ueda, Mizomoto and Ikai (1983).

The test arrangement of Ueda and coworkers involvved a hydrogen/nitrogen mixture flowing from a porous plane surface. The porous surface formed the bottom of an air flow channel at some distance from the inlet. The combined studies provide mean and fluctuating streamwise velocities and the Reynolds stress. However, these measurements used an LDA with particle averages; therefore, the results involve uncertain levels of velocity bias. The mean temperatures are reported - the latter for only the first study. The mean temperatures are not corrected for radiation; however, sufficient information is available to make reasonable estimates of this effect. The temperature fluctuation measurements are difficult to assess for uncertainties until more is known concerning the accuracy of this approach in flame environments. The authors did not provide a zero streamwise pressure gradient during their experiments, although they do estimate the pressure gradient. The effect was sufficient to accelerate reaction zone velocities to values greater than the free-stream velocity. This and wall effects present significant challenges for analysis of turbulence in this flow.

The main difficulty with this configuration is that past measurements are too sparse, really only one test condition, to adequately test analysis. Measurement of species concentrations would also be desirable, to assess the approach to the fast-reaction limit and effects of differential diffusion. Frequent crosstream traverses are also needed to properly characterize the flow from the leading edge of the porous plate. More experimentation for this important flow is clearly needed.

Table 4. Measurements in Wall Boundary Layers

Reference	Flow	Velocity	Scalars	Other	Instrument Properties	Comments
Ueda, Mizomoto & Ikai (1982)	Fuel injected from porous wall on floor of a duct; dilute hydrogen (4% by mass in N_2)/air; 96 × 200 mm plate; horizontal-facing upward; 100 × 200 mm duct; $(\rho v)_w/(\rho u)_e = 0.01$; u_e = 10 m/s; $\overline{u'}_e/\overline{u}_e = 0.7\%$; streamwise static pressure gradient - 61 Pa/m (est.)	$\overline{u}$ and $\overline{u'}$ traverses at x = 60, 120 and 180 mm.	$\overline{T}$ and $\overline{T'}$ traverses at x = 60, 120 and 180 mm.	Dark-field photograph	Single-channel LDA using particle-averaged properties; bare-wire thermocouple (0.05 mm bead diameter) uncorrected for radiation with a compensation circuit.	$\overline{u}$ and $\overline{u'}$ measurements are velocity biased. $\overline{T}$ uncertainties largely due to use of compensated thermocouple.
Ueda, Mizomoto, Matsubayashi & Ikai (1984).	Same as Ueda et al. (1982).	$\overline{u}$, $\overline{u'}$ and $\overline{u'v'}$ profiles at x = 150 and 180 mm.	$\overline{T}$ profiles at x = 150 and 180 mm.		Same as Ueda et al. (1982).	Same as Ueda et al. (1982).

RECOMMENDED CASES

Developing data for evaluating analysis of turbulent reacting flow, even at the apparently simple fast-reaction limit, represents a substantial experimental challenge. Measurements of flow structure involve many variables, including hydrodynamic and scalar properties, their correlations, and their spectral properties (to ensure that systematic large-scale perturbations are not mistaken for turbulence, as recommended by Libby et al., 1985). Boundary and initial conditions must be known and controlled over lengthy periods of experimentation. Large Reynolds numbers are desirable to minimize effects of transition and buoyancy which can complicate both analysis and interpretation of measurements. At the same time, requirements for flame attachment, approach to the fast-reaction limit, and the cost of apparatus and reactants impose limitations on the practical range of conditions available for testing. Costly nonintrusive instrumentation is to be preferred over the use of probes, to avoid uncertainties concerning the type of averages measured and to obtain information on fluctuating properties which are the hallmark of turbulent flows. Finally, a sufficient number of operating conditions, and traverses at a given operating condition, are needed to reduce the possibility of fortuitous agreement between predictions and measurements.

It is also essential that this information be available for several flow geometries - even within the relatively limited class of parabolic flows. For example, axisymmetric and plane free shear flows require different empirical constants for many current turbulence models (Pope, 1978). The presence of surfaces also clearly modifies turbulence structure due to low Reynolds number effects. Practical problems involve this range of conditions; therefore, results are needed for round jets, free plane shear layers and wall boundary layers - at a minimum. Thus, all the difficulties for different flow configurations, highlighted by the Stanford conferences for turbulent fluid flow modeling, are present for reacting flows - with the additional complications of evaluating mixing and a host of scalar properties.

Based on this perspective, it is clear that in spite of significant progress in gaining a better understanding of turbulent fast-reacting flows, based on the studies discussed here, we are far from the experimental goal of providing an adequate data base for the evaluation of analysis. Work completed thus far has provided a background to help avoid experimental pitfalls. We have a much better understanding of the types of averages to be defined; effects of systematic biases; the importance of seemingly modest changes in initial and boundary conditions; and the ubiquitous, but complex, effects of buoyancy on even relatively high speed flows.

Clearly, work providing a proper data base will involve careful consideration of both hydrodynamic and chemical effects, which is the nature of practical combustion processes. Skills and interest in these disparate areas are rarely found in one individual; thus we agree with Libby et al. (1985) that teams of workers will be needed to develop this data base. The work should also be coordinated with theoreticians, so that the sensitivity of analysis to various experimental parameters can be determined. Past work also suggests that a series of experiments, using an apparatus over an extended period of time, is needed to fully develop an adequate range of test conditions and measured variables.

At present, only the most recent work, exclusively using nonintrusive diagnostics, comes close to meeting these needs. In particular, measurements by Dibble and coworkers (1984a, 1985a, 1985b, 1985c) at Sandia are recommended at this time for evaluation of analysis at the fast-reaction limit. The test case is summarized in Table 5. Test conditions involve hydrogen/air combustion in a round jet configuration in coflow. Reynolds numbers are reasonably high and vertical upflow is used, minimizing complications due to relaminarization and buoyancy. Initial and boundary conditions are well-defined, a range of test conditions is available, and flow structure is reasonably defined with frequent traverses. Experimental uncertainties are known so that discrepancies between theory and experiment can be rationally evaluated. Clearly, this work has benefitted from the experience of these workers during earlier studies, as well as by past work by other investigators. Data provided by Dibble and coworkers (1985a, 1985b) are summarized in Appendix B-1 for use in evaluation of analysis.

Table 5

DATA SUMMARY

Flow Hydrogen/air diffusion flame

Data evaluators G. M. Faeth G. S. Samuelson

Gases Dibble et al (1984a, b, 1985a b, c)

Geometry Round hydrogen jet in coflowing air. Re = 9,000 18,000, 27,000. Jet velocity 75, 150 225, m/sec, air velocity 9.2 m/sec.

Mean quantities measured

$\bar{u}$, $\bar{v}$, $\bar{\rho}$, equilibrium temperatures, concentration of species.

Turbulence quantities measured

u', v', ρ', intermittency, flatness and skewings

Notes

LDV, Rayleigh and Raman scattering used. Vertical flame, initial conditions measured.

Complementary work by Drake (1984) is also recommended for development of analysis. These tests, summarized in Table 6, also involve a hydrogen/air diffusion flame in the round-jet coflow configuration. However, the measurements involve several difficulties, as follows: Reynolds numbers are relatively low ($Re_j = 8500$); the flow was horizontal, suggesting loss of symmetry of at least turbulence properties due to buoyancy; the scale of the experiments is relatively small (d = 3 mm), so that approach to the fast-reaction limit is marginal over much of the flow field; and velocity measurements and velocity/scalar correlations are relatively incomplete. While recognizing these problems, it is still felt that the measurements provide a useful extension of the range of conditions for which data are available; therefore, these results are summarized in Appendix B-2 for use in development of analysis.

ADDITIONAL DATA NEEDS

Additional work is clearly needed. Experiments using carbon monoxide/air should be considered, since these reactants offer application of nonintrusive diagnostics similar to hydrogen/air, but are less influenced by low Reynolds number and differential diffusion difficulties. While data is still needed for the round jet configuration, greater attention should be given to plane shear layers and wall boundary layers than in the past.

Data obtained using probes involves unacceptable uncertainties for definitive evaluation of analysis, except for routine monitoring applications. Only nonintrusive measurements should be seriously considered for benchmark experiments.

Finally, this effort has demonstrated the need for a format for the documentation of a data base. A format for data base documentation is presented in Appendix B-3. The format reflects the issues presented in the present chapter with respect to the use of a data base for modeling development, verification, and general application. An example of the use of this format is provided in Appendix B-1. The Sandia data (Dibble et al., 1985a, 1985b) were compiled during the period that the format requirements evolved. As a result, Sandia was asked to provide the additional information (and, in some cases, make the additional measurements) necessary to fulfill the requirements of the format.

Table 6

DATA SUMMARY

Flow Hydrogen/air diffusion flame

Data evaluators G. M. Faeth, G. S. Samuelson

Case Drake (1984)

Geometry Round hydrogen jet in coflowing air; Re = 8,500, exit jet diameter 3 mm.

Mean quantities measured

$\bar{u}$, $\bar{\rho}$, $\bar{T}$ and concentration H_2, H_2O, N_2 and O_2

Turbulence quantities measured

u', T', ρ', skewness and flatness of mixture fractions.

Notes

LDV, Raman and saturated fluorescence used. Horizontal flow.

REFERENCES

Abdul-Khalik, S.I., Tamura, T. and El-Wakil, M.M. (1975) A chromatographic and interferometric study of the diffusion flame around a simulated drop. Fifteenth Symposium (International) on Combustion, 389.

Aeschliman, D.P., Cummings, J.C. and Hill, R.S. (1979) Raman spectroscopic study of a laminar hydrogen diffusion flame in air. J. Quant. Spectrosc. Radiat. Trans. 21, 293.

Batt, R.G. (1977) Turbulent mixing of passive and chemically reacting species in a low-speed shear layer. J. Fluid Mech. 82, 53.

Becker, H.A. and Brown, A.P.G. (1974) Response of pitot probes in turbulent streams. J. Fluid Mech. 62, 85.

Becker, H.A. and Liang, D. (1978) Visible length of vertical free turbulent diffusion flames. Comb. Flame 32, 115.

Becker, H.A. and Yamazaki, S. (1978) Entrainment, momentum flux and temperature in vertical free turbulent diffusion flames. Comb. Flame 33, 123.

Bilger, R.W. (1976) Turbulent jet diffusion flames. Prog. Energy Combust. Sci. 1, 87.

Bilger, R.W. (1977) Reaction rates in diffusion flames. Comb. Flame 30, 277.

Bilger, R.W. (1977a) Probe measurements in turbulent combusion. Prog. in Astro. and Aero. 53, 49.

Bilger, R. (1982) Molecular transport effects in turbulent diffusion flames at moderate Reynolds numbers. AIAAJ. 20, 962.

Bilger, R.W. and Beck, R.E. (1975) Further experiments on turbulent jet diffusion flames. Fifteenth Symposium (International) on Combustion, 541.

Bilger, R.W. and Starner, S.H. (1983) A simple model for carbon monoxide in laminar and turbulent hydrocarbon diffusion flames. Comb. Flame 51, 155.

Breidenthal, R.E. (1978) A chemically reacting turbulent shear layer. Ph.D. Thesis, California Institute of Technology.

Breidenthal, R.E. (1981) Structure in turbulent mixing layers and wakes using a chemical reaction. J. Fluid Mech. 109, 1.

Brown, G.L. and Roshko, A. (1974) On density effects and large scale structures in turbulent mixing layers. J. Fluid Mech. 64, 775.

Brum, R.D. and Samuelsen, G.S. (1984) Two-component laser anemometry measurements in nonreacting and reacting complex flows in a swirl-stabilized combustor. Experimental techniques in turbulent reacting and non-reacting Flows (So, R.M.C., Whitelaw, J.H. and Lapp, M., eds.), AMD-Vol. 66, ASME, New York, 275.

Buckmaster, J.D. and Ludford, G.S.S. (1982) Theory of laminar flames, Cambridge University Press, Cambridge.

Burke, S.P. and Schuman, T.E.W. (1928) Diffusion flames. Ind. Eng. Chem. 20, 998.

Chandrasuda, C., Mehta, R.D., Weir, A.D. and Bradshaw, P. (1978) Effect of freestream turbulence on large scale structure in turbulent mixing layers. J. Fluid Mech. 85, 693.

Correa, S.M., Drake, M.C., Pitz, R.W. and Shyy, W. (1985) Prediction and measurement of non-equilibrium turbulent diffusion flame. Twentieth Symposium (International) on Combustion, in press.

Craig, R.R., Nejad, A.S., Hahn, E.Y. and Schwartzkopf, K.E. (1984) A general approach for obtaining unbiased LDV data in highly turbulent non-reacting and reacting flows. AIAA Paper No. 84-0366.

Dahm, W.J.A. (1985) Experiments on entrainment, mixing and chemical reactions in turbulent jets at large Schmidt number. Ph.D. Thesis, California Institute of Technology.

Dahm, W.J.A., Dimotakis, P.E. and Broadwell, J.E. (1984) Non-premixed turbulent jet flames. AIAA Paper No. 84-0369.

Dahm, W.J.A. and Dimotakis, P.E. (1985) Measurements of entrainment and mixing in turbulent jets. AIAA Paper No. 85-0056.

Dibble, R.W., Hartmann, V., Schefer, R.W., and Kollmann, W. (1984a). An investigation of temperature and velocity correlations in turbulent flames. Experimental measurements and techniques in turbulent reacting and nonreacting Flows (So, R.M.C., Whitelaw, J.H. and Lapp, M., Eds.), AMD-Vol. 66, ASME, New York 291. Also, Experiments in Fluids, in press, and Sandia Report SAND84-8860.

Dibble, R.W. and Hollenbach, R.E. (1981) Laser Rayleigh thermometry in turbulent flames. Eighteenth Symposium (International) on Combustion, 1489.

Dibble, R.W., Kollmann, W. and Schefer, R.W. (1984b) Conserved scalar fluxes measured in a turublent nonpremixed flame by combined laser Doppler velocimetry and laser Raman scattering. Comb. Flame 55, 307.

Dibble, R.W., Schefer, R.W., Hartman, V., and Kollman, W. (1985a) Velocity and density measurements in a turbulent nonpremixed flame, Sandia Report SAND85-8233.

Dibble, R.W., Schefer, R.W. and Kollman, W. (1985b) Measurements and predictions of scalar dissipation in turbulent jet flames. Twentieth Symposium (International) on Combustion, in press.

Dibble, R.W., Schefer, R.W., Hartman, V., and Kollman, W. (1985c) Simultaneous velocity and concentration measurements in a turbulent nonpremixed flame, Sandia Report SAND85-8234.

Dibble, R.W. and Schefer, R.W. (1985d) Simultaneous Measurements of velocity and scalars in a turbulent nonpremixed flame by combined-laser doppler velocimetry and laser Raman scattering, in Bradbury, L.J.S., Durst, F., Launder, B.E., Schmidt, F.W. and Whitelaw, J.H. (Eds.), Turbulent Shear Flows 4, Springer-Verlag, pp. 319-327. Also available as Sandia Report SAND83-8772.

Dimotakis, P.E. Broadwell, J.E. and Howard, R.D. (1983) Chemically reacting turbulent jets. AIAA Paper No. 83-0474.

Drake, M.C. (1984a). Personal communication.

Drake, M.C., Bilger, R.W. and Starner, S.H. (1982) Raman measurements and conserved scalar modeling in turbulent flames. Nineteenth Symposium (International) on Combustion, 459.

Drake, M. and Kollmann, W. (1985) Simple turbulent reacting flows: slow reaction nonpremixed combustion. This volume.

Drake, M.C., Lapp, M., Penney, C.M., Warshaw, S. and Gerhold, B.W. (1981a) Measurements of temperature and concentration fluctuations in turbulent diffusion flames using pulsed Raman spectroscopy. Eighteenth Symposium (International) on Combustion, 1521.

Drake, M.C., Lapp, M. , Penney, C.M., Warshaw, S., and Gerhold, B.W. (1981b) Probability density functions and correlations of temperature and molecular concentrations in turbulent diffusion flames. AIAA Paper No. 81-0103.

Drake, M.C. and Pitz, R.W. (1984) Intermittency and conditional averaging in a turbulent nonpremixed flame by Raman scattering. AIAA Paper No. 84-0197.

Drake, M.C., Pitz, R.W. and Lapp, M. (1984) Laser measurements on nonpremixed hydrogen-air flames for assessment of turbulent combustion models. AIAA Paper No. 84-0544.

Drake, M.C., Pitz, R.W., Lapp, M., Fenimore, C.P., Lucht, R.P., Sweeney, D.W. and Laurendeau, N.M. (1985) Measurements of superequilibrium hydrosyl concentrations in turbulent nonpremixed flames using saturated fluorescence. Twentieth Symposium (International) on Combustion, in press.

Drake, M.C., Shyy, W. and Pitz, R.W. (1985) Superlayer contributions to conserved-scalar pdf's in an H_2 turbulent jet diffusion flame. Fifth Symposium on Turbulent Shear Flows.

Driscoll, J.F., Schefer, R.W. and Dibble, R.W. (1983) Mass fluxes $\rho' u'$ and $\rho' v'$ measured in a turbulent nonpremixed flame. Nineteenth Symposium (International) on Combustion, 477.

Durst, F., Melling, A., and Whitelaw, J.H. (1976). Principles and Practice of Laser Doppler Anemometry, Academic Press.

Edelman, R.B. and Fortune, O.F. (1969) A quasi-global chemical kinetic model for the finite rate combustion of hydrocarbon fuels with application to turbulent burning and mixing in hypersonic engines and nozzles. AIAA Paper No. 69-086.

Eickhoff, H. (1982) Turbulent hydrocarbon jet flames. Prog. Energy Combust. Sci. 8, 159.

Faeth, G.M., Jeng, S.-M. and Gore, J. (1985) Radiation from fires. Heat Transfer in Fire and Combustion Systems (Law, C.K., Jaluria, Y., Yuen, W.W. and Miyasaka, K., Eds., HTD-Vol. 45, ASME, New York, 181.

Glass, M.G. and Bilger, R.W. (1978) The turbulent jet diffusion flame in a co-flowing stream - some velocity measurements. Comb. Sci. Tech. 18, 165.

Glassman, I. (1977) Combustion. Academic Press, New York, 34.

Gordon, A.S. and McBride, B.J. (1971) Computer program for calculation of complex chemical equilibrium compositions, rocket performance, incident and reflected shocks and Chapman-Jouguet detonations. NASA SP-273.

Gouldin, F. and Johnston, S. (1985) Simple turbulent reacting flows: variable-density non-reacting flows. This volume.

Hassan, M.M.A., Lockwood, F.C. and Moneib, H.A. (1980) Fluctuating temperature and mean concentration measurements in a vertical turbulent free jet diffusion flame. Imperial College, Mech. Eng. Dept. Report FS/80/21.

Hawthorne, W.R., Weddell, D.S. and Hottel, H.C. (1949) Mixing and combustion in turbulent gas jets. Third Symposium on Combustion, Flame and Explosion Phenomena, 266.

Jeng, S.-M., Chen, L.-D. and Faeth, G.M. (1982) The structure of buoyant methane and propane diffusion flames. Nineteenth Symposium (International) on Combustion, 349.

Jeng, S.-M. and Faeth, G.M. (1984) Species concentrations and turbulence properties in buoyant methane diffusion flames. J. Heat Trans. 106, 721.

Jeng, S.-M. and Faeth, G.M. (1984a) Predictions of mean scalar properties in turbulent propane diffusion flames. J. Heat Trans 106, 891.

Jeng, S.-M., Gore, J., Chuech, S.G. and Faeth, G.M. (1985) An investigation of turbulent fires on vertical and inclined walls: flame radiation. Department of Mechanical Engineering, the Pennsylvania State University.

Johnston, S.C., Dibble, R.W., Schefer, R.W., Ashurst, W.T. and Kollmann, W. (1984) Laser measurements and stochastic simulations of turbulent reacting flows. AIAA Paper No. 84-0543.

Jones, W.P. (1980) Models for turbulent flows with variable density. VKI Lecture Series 1979-2, Prediction Methods in Turbulent Flows (W. Kollmann, Ed.), Hemisphere Publishing Corp., Washington.

Jones, W.P. and Whitelaw, J.H. (1982) Calculation methods for reacting turbulent flows: a review. Comb. and Flame 48, 1.

Kennedy, I.M. and Kent, T.H. (1979) Measurements of a conserved scalar in turbulent jet diffusion flames. Seventeenth Symposium (International) on Combustion, 279.

Kennedy, I.M. and Kent, J.H. (1981) Scalar measurements in a co-flowing turbulent diffusion flame. Comb. Sci. Tech. 25, 109.

Kent, J.K. (1972) Turbulent jet diffusion flames. Ph.D. Thesis, The University of Sydney.

Kent, J.H. and Bilger, R.W. (1973) Turbulent diffusion flames. Fourteenth Symposium (International) on Combustion, 615.

Kent, J.H. and Bilger, R.W. (1977) The prediction of turbulent diffusion flame fields and nitric oxide formation. Sixteenth Symposium (International) on Combustion, 1643.

Koochesfahani, M.M. (1984) Experiments on turbulent mixing and chemical reactions in a liquid mixing layer. Ph.D. Thesis, California Institute of Technology.

Koochesfahani, M.M., Dimotakis, P.E. and Broadwell, J.E. (1983) Chemically reacting shear layers. AIAA Paper No. 83-0475.

Koochesfahani, M.M. and Dimotakis, P.E. (1984) Laser induced fluorescence measurements of concentration in a plane mixing layer. AIAA Paper No. 84-0198.

Kremer, H. (1967) Mixing in a plane free turbulent-jet diffusion flame. Eleventh Symposium (International) on Combustion, 799.

Kychakoff, G., Howe, R.D., Hanson, R.K., Drake, M.C., Pitz, R.W., Lapp, M. and Penney, C.M. (1984) The visualization of turbulent flame fronts using planar laser-induced fluorescence. Science 224, 382.

Lapp, M., Drake, M.C., Penney, C.M., Pitz, R.W. and Correa, S. (1983) Turbulent combustion experiments and modeling. General Electric Report 83SRD049.

Lai, M.-C. and Faeth, G.M. (1985) Scalar fluxes in turbulent wall plumes. To be published.

Lai, M.-C., Jeng, S.-M. and Faeth, G.M. (1985) Structure of adiabatic wall plumes. Fire and Combustion Systems (Law, C.K., Jaluria, Y., Yuen, W.W. and Miyasaka, K., eds.), HTD-Vol. 45, ASME, ew York, 181.

Libby, P.A., Sevasegaram, S. and Whitelaw, J.H. (1985) Simple turbulent reacting flows: premixed combustion. This volume.

Liburdy, J.A., Groff, E.G. and Faeth, G.M. (1979) Structure of a turbulent thermal plume rising along an isothermal wall. J. Heat Transfer 101, 249.

Liew, S.K., Bray, K.N.C. and Moss, J.B. (1981) A flamelet model of turbulent non-premixed combustion. Comb. Sci. Tech. 27, 69.

Liew, S.K., Bray, K.N.C. and Moss, J.B. (1984) A stretched laminar flamelet model of turbulent nonpremixed combustion. Comb. Flame 56, 199.

Lockwood, F.C. and Moneib, H.A. (1982) Fluctuating temperature measurements in turbulent jet diffusion flame. Comb. Flame 47, 291.

Lockwood, F.C. and Naguib, A.S. (1975) The prediction of the fluctuations in the properties of free, round-jet turbulent diffusion flames. Comb. Flame 24, 109.

Lockwood, F.C. and Odidi, A.O. (1975) Measurement of mean and fluctuating temperature and of ion concentration in round free-jet turbulent diffusion and premixed flames. Fifteenth Symposium (International) on Combustion, 561.

Lucht, R.P., Sweeney, D.W., Laurendeau, N.M., Drake, M.C., Lapp, M. and Pitz, R.W. (1984) Single pulse, laser-saturated fluorescence measurements of OH in turbulent nonpremixed flames. Opt. Lett. 9, 90.

Melvin, A., Moss, J.B. and Clarke, J.F. (1971) The structure of a reaction-broadened diffusion flame. Comb. Sci. Tech. 4, 17.

Miller, J.A. and Kee, R.J. (1977) Chemical nonequilibrium effects in hydrogen-air laminar jet diffusion flames. J. Phys. Chem. 81, 2534.

Mitchell, R.E., Sarofim, A.F. and Clomberg, L.A. (1980) Experimental and numerical investigation of confined laminar diffusion flames. Comb. Flame 37, 227.

Moss, J.B. and Roberts, P.T. (1979) A note on the conserved scalar approach to diffusion flame modeling. Comb. Flame 34, 335.

Mungal, M.C. (1983) Experiments on mixing and combustion with low heat release in a turbulent shear flow, Ph.D. Thesis, California Institute of Technology.

Mungal, M.C., Dimotakis, P.E. and Broadwell, J.E. (1984) Turbulent mixing and combustion in a reacting shear layer. AIAA J. 22, 797.

Mungal, M.C., Dimotakis, P.E. and Hermanson, J.C. (1984) Reynolds number effects on mixing and combustion in a reacting shear layer. AIAA Paper No. 84-0371.

Pope, S.G. (1978) An explanation of the turbulent round-jet/plane jet anomaly. AIAA J. 16, 279.

Razdan, M.K. and Stevens, J.G. (1985) CO/air turbulent diffusion flame: measurements and modeling. Comb. Flame 59, 289.

Schefer, R.W. and Dibble, R.W. (1983) Simultaneous measurements of velocity and density in a turbulent nonpremixed flame. Sandia Report SAND82-8810.

Schefer, R. W. and Dibble, R.W. (1985) Simultaneous measurements of velocity and density in a turbulent nonpremixed flame. AIAA J. 23, 1070.

Schoenung, S.M. and Hanson, R.K. (1982) Temporally and spatially resolved measurements of fuel mole fraction in a turbulent CO diffusion flame. Nineteenth Symposium (International) on Combustion, 449.

Shea, J.R. (1976) A chemical reaction in a turbulent jet. Ph.D. Thesis, California Institute of Technology.

Spalding, D.B. (1979) The influence of laminar transport and chemical kinetics on the time-mean reaction rate in a turbulent flame. Seventeenth Symposium (International) on Combustion, 431.

Starner, S.H. (1980) Investigations of turbulent diffusion flames. Ph.D. Thesis, The University of Sydney.

Starner, S.H. (1983) Joint measurements of radial velocity and scalars in a turbulent diffusion flame. Comb. Sci. Tech. 30, 145.

Starner, S.H. (1985) Conditional sampling in a turbulent diffusion flame. Comb. Sci. Tech. 42, 283.

Starner, S.H. and Bilger, R.W. (1980) LDA measurements in a turbulent diffusion flame with axial pressure gradient. Comb. Sci. Tech. 21, 259.

Starner, S.H. and Bilger, R.W. (1981) Measurement of scalar-velocity correlations in a turbulent diffusion flame. Eighteenth Symposium (International) on Combustion, 921.

Stevenson, W.H., Thompson, H.D. and Roesler, T.C. (1982) Direct measurement of laser velocimeter bias errors in a turbulent flow. AIAA J. 20, 1720.

Takagi, T., Ogasawara, M., Fujii, K. and Daizo, M. (1975) A study of nitric oxide formation in turbulent diffusion flames. Fifteenth Symposium (International) on Combustion, 1051.

Takagi, T., Shin, H.-D. and Ishio, A. (1980) Local laminarization in turbulent diffusion flames. Comb. Flame 37, 163.

Takagi, T., Shin, H.-D. and Ishio, A. (1981) Properties of turbulence in turbulent diffusion flames. Comb. Flame 40, 121.

Takagi, T., Shin, H.-D. and Ishio, A. (1981a) A study on the structure of turbulent diffusion flame: properties of fluctuations of velocity, temperature, and ion concentration. Comb. Flame 41, 261.

Takahashi, F. and Ikai, S. (1982) Velocity and temperature fluctuations in a flat plate boundary layer diffusion flame. Comb. Sci. Tech. 27, 133.

Takeno, T. and Kotani, I. (1975) An experimental study on the stability of jet diffusion flames. Acta Astronautica 2, 999.

Tsuji, H. and Yamaoka, I. (1967) The counterflow diffusion flames in the forward stagnation region of a porous cylinder. Eleventh Symposium (International) on Combustion, 970.

Tsuji, H. and Yamaoka, I. (1969) The structure of counterflow diffusion flames in the forward stagnation region of a porous cylinder. Twelfth Symposium (International) on Combustion, 997.

Tsuji, H. and Yamaoka, I. (1971) Structure analysis of counterflow diffusion flames in the forward stagnation region of a porous cylinder. Thirteenth Symposium (International) on Combustion, 723.

Ueda, T., Mizomoto, M. and Ikai, S. (1982) Velocity and temperature fluctuations in a flat plate boundary layer diffusion flame. Comb. Sci. Tech. 27, 133.

Ueda, T., Mizomoto, M. and Ikai, S. (1983) Thermal structure of a flat plate turbulent boundary layer diffusion flame. Bul. JSME 26, 399.

Ueda, T., Mizomoto, M., Matsubayashi, Y., and Ikai, S. (1984) Turbulent properties of a flat-plate boundary layer with a diffusion flame. AIAA J. 22, 664.

Wallace, A.K. (1981) Experimental investigation on the effects of chemical heat release in the reacting plane shear layer. Ph.D. Thesis, University of Adelaide.

Westbrook, C.K. and Dryer, F.L. (1981) Simplified reaction mechanisms for oxidation of hydrocarbon fuels in flames. Comb. Sci. Tech. 27, 31.

CHAPTER 4

SLOW CHEMISTRY NONPREMIXED FLOWS

M. C. Drake and W. Kollmann

LITERATURE SEARCH

Introduction

Turbulent reacting flows that exhibit measurable effects of finite-rate chemistry can be classified in two groups: flows with strongly exothermic reactions (combustion flows) and flows with reactions that show only weak exo- or endothermic effects. The first group is characterized by strong interaction of scalar and velocity fields via the fluctuating density, whereas the second group can be considered as constant density flows unless the participants have large differences in their molecular weight. A second classification within the general class of parabolic turbulent flows can be set up according to the geometrical properties of the mean flow field (i.e., plane mixing layers and axisymmetric jets). The present literature survey will follow this classification.

The survey of the existing literature included articles in journals, conference proceedings, and research reports. The criteria for selection as laid out at the beginning of this report were significantly relaxed for the inclusion in this survey because of the difficulties of measurements in turbulent reacting flows and the relative scarcity of data. The flows considered here are turbulent shear flows with non-premixed chemical reactions such that the chemical reaction rates are not much faster than mixing rates. The chemical reactions are, therefore, considered slow, if one of the mean thermodynamic variables (density and temperature) or one of the mean values of the stable components of the reacting mixture show measurable departure from chemical equilibrium. Since there is, in most cases, no direct experimental evidence of nonequilibrium effects, comparison with equilibrium or nonequilibrium calculations (if available) or estimates for mean reaction rates were used as indicators of slow reactions.

Mixing layers

Mixing layers have played a special role in turbulence research for several reasons. The discovery of persistent large vortical structures and the investigation of their dynamics by Brown and Roshko and their coworkers [Breidenthal (1979), Breidenthal (1981), Brown and Roshko (1974), Konrad (1976), Koochesfahani (1984), Mungal (1983), Rebello (1973)] changed the accepted view of turbulence. A second reason is that mixing layers allow the maintenance of high levels of density fluctuations without heat release due to chemical reactions and, furthermore, the initial region of jets consists of mixing layers. Measurements in mixing layers with chemical reactions are, however, not numerous.

First, mixing layers in liquids are reviewed. The flows reviewed are shown in Table 1. Breidenthal (1978, 1981) used a water tunnel to create a plane mixing layer reaching the Reynolds number Re = 10^4 based on velocity difference and vorticity thickness $\delta = \Delta U/(\partial u/\partial y)_{max}$. One of the streams was diluted with small amounts of phenolphthalein and the other stream with sodium hydroxide. They react in a complex series of steps to form a red product which was used for visualization studies and selected quantitative measurements. The reaction was, under the given conditions, diffusion limited and, therefore, too fast to yield information on finite-rate chemistry. Bousgarbies and Neroult (1983) added ammonium hydroxide to one of the water streams and acetic acid to the other (high speed) stream upstream of the end of the splitter plate. The velocity ratio was 0.5 and 0.75 and the Reynolds number at their last measurement station was about 300 (based on velocity difference and their reported thickness). The turbulence level in the freestreams was high at about 10%. Their results must be considered unsuitable for comparison with computational methods based on high Re-numbers due to the low value for the Re-number. The thesis of Koochesfahani (1984) continues the mixing layer research at Caltech with measurements in a water tunnel using an acid-base reaction between sulfuric acid (H_2SO_4) and sodium hydroxide (NaOH) to produce a fluorescing product suitable for laser induced fluorescence. The reaction is, again, diffusion controlled and not appropriate for the study of the interaction between turbulence and chemical kinetics.

Table 1. Slow Chemistry - Non-Premixed Flows: Mixing Layers

Flow conditions: Fuel	Flow conditions: Set-up	Quantities measured	Techniques	Results	References
Gas $N_2 + N_2O_4 \leftrightarrow 2NO_2 + N_2$	$Re \leq 7 \times 10^5$ $u_1 = 15.25$ m/s $u_2 \approx 0.0$ $T_1/T_2 = 0.82$, 0.88, 0.985 $T_2 = 305$ K	u, T, X_i	Probe	Rad: $\langle u \rangle$, $\langle T \rangle$, $\langle X_{NO_2} \rangle$ + rms + flatness + skewness. Pdf of X_{NX_2}, T, u. Intermittency factor γ, spectra, two-point correlations of u, T.	Alber, Batt (1976) Batt (1977)
Liquid (water) Ammonium hydroxide-acetic acid	Re = 300 $u_1 = 0.06$ m/s $u_2 = 0.02$ m/s	u, concentration	LDV, probe	Rad: $\langle u \rangle$, $\langle u'^2 \rangle$, $\langle c \rangle$, $\langle c'^2 \rangle$, $\langle u'c' \rangle$, $\langle v'c' \rangle$	Bousgarbies, Herault (1983)
Liquid (water) Phenolphthalein-sodium hydroxide	$Re \leq 10^4$ Transitional $u_1 = 3$ m/s	Flow visualization Product thickness P, vorticity thickness σ	Photography	$P/\sigma = f(Re)$	Breidenthal (1979)
Gas $N_2 - H_e + Ar$	$Re \leq 7 \times 10^4$ $u_1 = 6/10.4/10$ m/s $u_2 = 2.26/3.9/3.75$ m/s	u, c, γ, Pdf spectra	Probe, Hot wire	Only for nonreacting mixing layers and wake: $\langle u \rangle$, $\langle c \rangle$, $\langle c'^2 \rangle$ γ, Pdf for c, spectra for c	Konrad (1976)
Liquid (water) Sulfuric acid-sodium hydroxide	$Re \approx 2.3 \times 10^4$ $u_1 = 0.7$ m/s $u_1/u_2 = 0.38$	Concentration c	Laser fluorescence	c, Pdf of c	Koochesfahani (1984)
Gas: N_2 $NO + NO_3 + O_2$	$Re \leq 3000$ $u_1 = 6$ m/s $u_2 = 3$ m/s	u, c	Hot wire, Fiberoptic probe + chemi-luminescent analyzer	$\bar{C}_{O_2}$, rms, $\bar{C}_{NO_2}$ γ, Pdf of C_{O_3}. Spectra $\bar{u}$, rms Initial conditions	Masutani (1985)

Table 1 (Cont'd)

Gas: N_2 $H_2 + F_2 \rightarrow 2HF$	$Re = 30800$ $u_1 = 22$ m/s $u_2 = 8.8$ m/s	u, T	Pitot probes, Cold wires, Photography	$\bar{T}$, conditional mean, Pdf of T, $\bar{u}$	Mungal (1983)
Gas: N_2, air $NO + O_3 \rightarrow NO_2 + O_2$ and $NH_3 + HCl \rightarrow NH_4Cl$	$Re \leq 250,000$ $u_2/u_1 = 0.76$ $u_2/u_1 = 0.3$	Concentration c, Mixture fraction f	Fiberoptic probe Flow visualization LDV	Only visualization results so far	Sherikar (1981)
Gas: He, N_2, Ar $NO + O_3 \rightarrow NO_2 + O_2$	$Re \leq 5 \times 10^4$ $u_1 = 25$ m/s $u_2 = 5$ m/s	u, T	Pitot tube, Thermocouple Ultraviolet absorption meter	$\bar{u}$, $\bar{T}$	Wallace (1981)

The second group of mixing layers contain chemical reactions in the gaseous phase. The air mixing layer investigated by Alber and Batt (1976) and Batt (1977) is seeded at the high speed and low temperature side with N_2O_4 which reacts with the N_2 in air to form NO_2 according to

$$N_2 + N_2O_4 \quad 2\,NO_2 + N_2$$

Measurements of NO_2 (mean and variance of concentration) were performed using a fiber-optics probe. The results indicate the influence of chemical kinetics on the mean profile for $[NO_2]$ at the lowest temperature (T = 252 K) in the seeded high-speed stream. Calculations of Janicka and Kollmann (1978) with a two-equation turbulence model and chemical kinetics in terms of source terms expanded as Taylor series around the mean state confirm a moderate effect of chemical kinetics on the measured concentration profiles. The experimental information for the reacting case is, however, too limited for an extensive comparison with advanced closure schemes. Konrad's (1976) work on a mixing layer was confined to diffusion-controlled reaction and must be eliminated for this reason. Sherikar and Chevray (1981) considered two different reactions in the gaseous phase:

$$NH_3 + HC\ell \quad NH_4C\ell$$

which is fast and its product forms a dense white fume at room temperature suitable for flow visualization studies. The second reaction is

$$NO + O_3 \quad NO_2 + O_2 + h\nu$$

which is also diffusion limited at room temperature. This case is, therefore, not suitable for finite-rate chemistry effects under the conditions suggested by Sherikar and Chevray (1981). Wallace uses the same nitric oxide reaction as Sherikar and Chevray (1981) in a temperature range from room temperature to 200°C in a mixing layer flow with Re-number up to 5×10^4. Their results show also that the reaction is essentially diffusion limited under the conditions considered. Mungal's (1983) mixing layer work is based on the reaction of H_2 with F_2

$$H_2 + F_2 \quad 2HF$$

in highly diluted form in order to keep the adiabatic flame temperature rise below 165 K. The reaction is fast but addition of small amounts of NO (J. Broadwell, private communication 1985) allow slowing of the reactions. No results are available for this case, however. Extensive measurements, including first and second order moments in a plane mixing layer with the nitric oxide-ozone reaction were made by Masutani (1985). The Re-number (based on velocity difference and vorticity thickness) is, however, low (less than 3000) and the reaction is essentially diffusion limited.

Jet flows

The experimental study of turbulent round jet diffusion flames dates from the classic work of Hawthorne et al. (1949). Since then, many other researchers have explored this combustion configuration. Attention in this section is restricted to nonswirling diffusion flames with gaseous fuels which show marked slow chemistry effects. The flows reviewed are shown in Table 2.

Hydrogen flames

Flames fueled with pure hydrogen can be considered diffusion limited in good approximation. For example, temperature and concentration of stable components can be predicted with good accuracy using an infinitely fast global reaction step. Departures from the classical "fast chemistry" or equilibrium assumption in typical laboratory H_2-air turbulent diffusion flames have been predicted using a perturbation analysis [Bilger (1980)] or a two-scalar pdf approach [Janicka and Kollman (1979), (1982)]. Finite rate chemistry effects due to superequilibrium radical formation are predicted by Drake, Bilger and Starner (1982) to lower mean temperatures by only 40K at x/d with 50 in an Re = 8500 H_2 flame. Comparable effects were calculated

Table 2. Slow Chemistry - Non-Premixed Flows: Jets

Flow Conditions: Fuel	Flow Conditions: Set-up	Quantities measured	Techniques	Results	References
CO, H_2, CH_4 etc.	Vertical diffusion	Flame length	Photography	ℓ	Becker et al.(1978)
C_3H_8-air	D = 0.0087 m u_e/u_j = 45,61,75 u_e = 2.54-8.04 m/s Mild swirl S = 0.3	Mole fractions X_i, T	Probes + analyzers (infrared, chemi-luminescent) Thermocouple	$\bar{X}_{CO}$, $\bar{X}_{CO_2}$, $\bar{X}_{C_3H_8}$, $\bar{X}_{H_2O}$, $\bar{X}_{O_2}$, $\bar{X}_{NO_2}$; $\bar{X}_{NO_2}$	Cernansky et al.(1974)
CH_4-air	D = 0.008 m Re = 6600 u_j = 20.5m/s u_ℓ = 0.6 m/s	T, u, c_i	Thermocouple Probes + gas chromatograph	$\bar{u}$, $\bar{T}$, $\bar{c}_i$	Chigier et al.(1974)
$CO/H_2/N_2$-air	Confined coaxial Re = 8500 u_j = 54.6 m/s u_ℓ = 2.4 m/s	T, ρ, X_i, u'	Pulsed Raman LDV Sat. Flouresence Probe	$\bar{X}_{N_2}$, $\bar{X}_{O_2}$, $\bar{X}_{H_2}$, $\bar{X}_{CO}$, $\bar{X}_{CO_2}$, $\bar{X}_{H_2O}$, $\bar{u}$, $\bar{T}$, $\bar{\rho}$, $\overline{u'^2}$, Pdf, γ, $\bar{X}_{OH}$	Correa et al. (1984) Drake et al.(1984) Lapp et al.(1983)
Natural gas-air	Vertical free Re = 37500 D = 0.008 m	Nozzle fluid concentration	Scattering techn. using seed part. LDV	$\bar{c}$, $\overline{c'^2}$, $\overline{u'^2}$	Ebrahimi et al. (1976)
C_3H_8-air	Re = 12000 D = 0.01 m u_j = 40/54 m/s	u, T, mass	LDV, probes	$\bar{T}$, $\tilde{Y}_{CO}$, $\tilde{Y}_{CO_2}$, $\tilde{Y}_{H_2}$, $\overline{u'^2}$	Eickhoff (1982)
Natural (U.K.) gas-air	Free flame Re $\leq 3.10^4$ D = 0.00774 m	u, unburnt hydrocarbons T, X_i	LDV, Thermocouple Quartz microprobe	$\bar{T}$, Pdf(T), rms $\bar{X}_{O_2}$, spectra	El-Banhawy et al. (1983) Lockwood et al. (1974,1982)
C_3H_8-air	Free vertical flame Re $\leq$ 42700 D = 0.006 m	X_i	Probe + gas chromatograph, Infrared analyzer Ionization detector	$\bar{X}_{CO}$; $\bar{X}_{CO_2}$, $\bar{X}_{O_2}$, $\bar{X}_{UHC}$	Godoy (1982)

Table 2 (Cont'd)

Natural gas-air	Vertical stabil. flame Re = 24000 Re = 37000 D = 0.008 m	u, T, f	LDV, Thermocouple	$\bar{T}$, Pdf(T), $\overline{u'^2}$, $\overline{T'^2}$	Gunther et al. (1981) Lenz et al. (1980)
CH_4-air C_3H_8-air	Re = 17200-58300 (C_3H_8-air) Re = 2920-11700 (CH_4-air)	T, u, Radiation	LDV, Thermocouple Probe + gas chromatograph	$\bar{T}$, $\bar{u}$, $\overline{u'^2}$	Jeng et al. (1982a,b,1984)
$NO + O_3 \rightarrow NO +_2 O$	Jet (Re = 1700), Plume in grid-generated turbulence (Re_M = 15000)	U, T, X_i	Probe + chemi-luminescent detector, LDV	$\bar{u}$, $\bar{T}$, $\bar{X}_{NO}$, $\overline{u'v'}$, $\overline{u'T'}$, $\overline{v'T'}$	Kamori et al (1984)
H_2-air NO_x formation	Re = 4500 (four flames)	Mass fractions Y_i	Probe + chemi-luminescence	$\bar{Y}_{O_2}$, $\bar{Y}_{H_2O}$, $\bar{Y}_{H_2}$, $\bar{Y}_{NO}$ NO-production rate	Lavoie et al. (1974)
Natural gas-air	Flame in combustor D = 0.008 m u_j = 21.3 m/s u_a = 34.3 m/s T_a = 598 K	Mole fraction X_i, Mixture fraction f	Probe + gas chromatograph, Thermocouple	$\bar{X}_{O_2}$, $\bar{X}_{H_2}$, $\bar{X}_{CO_2}$, $\bar{X}_{CH_4}$, $\bar{f}$, $\bar{X}_{N_2}$, $\bar{X}_{H_2O}$	Lewis et al. (1981)
C_3H_8-air	Re = 23600 u_j = 88.7 m/s u_a = 0.0	u, T, Y_i	LDV, Thermocouple, Probe + gas	$\bar{u}$, $\bar{T}$, $\overline{u'v'}$ $\bar{Y}_{N_2}$, $\bar{Y}_{O_2}$, $\bar{Y}_{CO}$, $\bar{Y}_{C_3H_8}$ $\bar{Y}_{CO_2}$, $\bar{Y}_{H_2}$, $\bar{Y}_{H_2O}$	Mao et al. (1986)
C_3H_8-air	Re = 14000 u_j = 15.8 m/s u_a = 3.7 m/s D = 0.004 m Furnace flame	u, T, X_i	Pitot tube, Thermocouple, Probe + gas chromatograph	$\bar{u}$, $\bar{T}$, $\bar{X}_{O_2}$, $\bar{X}_{CO}$, $\bar{X}_{CO_2}$, $\bar{X}_{C_3H_8}$, $\bar{X}_{UHC}$	Onuma et al (1974,1977)

Table 2 (Cont'd)

H_2/N_2-air with additives ion chemistry	Re = 10^4 Damköhler: D_I = 0 - 14	Concentration	Electrostatic probe	Autocorrelations ion concentrations	Page et al.(1974)
H_2-air, CH_4-air, Nat. gas-air C_3H_8-air	Vertical flame Re = 2500-7000 Fr = 1000-32500	NO	Probe	NO-formation rate	Peters et al.(1981)
CO + 3% H_2-air	Re = 11400 u_j = 35.7 m/s u_e = 0.13 m/s	T, u X_i	Thermocouple, Probe + infrared analyzer, LDV	$\bar{T}$, $\bar{X}_{O_2}$, $\bar{X}_{CO}$, $\bar{X}_{CO_2}$, $\bar{u}$	Razdan et al.(1983,1985)
CH_4-air	Re = 9200 u_j = 24 m/s D = 0.006 m	T	Thermocouple	$\bar{T}$, $\overline{T'^2}$, Pdf(T)	Roberts et al.(1981)
CO-air	Re = 12000 D = 0.015 m Free flame	X_i	Optical laser absorption Pdf (X_{CO}), Spectra	$\bar{X}_{CO}$, $\bar{X}_{CO_2}$, $\overline{X'^2_{CO}}$	Schoenung et al.(1982)
C_3H_8-air H_2/CO-air N_2, NH_3, NO added Inlet air temp. varied	Confined D = 0.002 m $\bar{u}_j$ = 28.6 m/s	T, X_i, u C_i	Thermocouple, Probe + infrared analyzer, gas chromatograph, Pitot tube	$\bar{T}$, $\bar{X}_{CO_2}$, $\bar{X}_{H_2O}$, $\bar{X}_{O_2}$, $\bar{X}_N$, $\bar{X}_{NO}$, $\bar{X}_{CO}$, $\bar{X}_{H_2}$, $\bar{u}$ $\bar{C}_{HCN}$, $\bar{C}_{NH_3}$, $\bar{C}_{NO}$ NO-formation rates	Takagi et al.(1974,1976)
H_2/N_2-air	Re = 4200-18000 u_j = 20-90 m/s u_e = 0.65 m/s	u, X_i, T	LDV Probe + gas chromatograph, Thermocouple	u, $\overline{u'^2}$, $\overline{v'^2}$, $\overline{w'^2}$, $\overline{u'v'}$ $\bar{T}$, $\bar{X}_{H_2}$, $\bar{X}_{O_2}$, $\bar{X}_{H_2O}$, $\bar{X}_{N_2}$ Pdf(u), Spectra, Macroscales	Takagi et al.(1980,1981a,b)
Natural gas -air	Re = 70-356	u, T, Y_i, f	LDV, Thermocouple, Probe + gas chromatograph	$\bar{u}$, $\bar{T}$, $\bar{f}$, $\bar{Y}_{N_2}$, $\bar{Y}_{O_2}$, $\bar{Y}_{CO_2}$ $\bar{Y}_{H_2O}$, $\bar{Y}_{CO}$, $\bar{Y}_{CH_2}$, $\bar{Y}_{H_2}$ $\overline{u'^2}$, $\overline{u'v'}$	You & Faeth (1982)

by Dibble, Kollmann and Schefer (1984) in an Ar/H_2 jet flame at Re = 24,000. For this reason hydrogen flames are not taken into account as appropriate test cases for turbulent flows with slow chemistry.

However, finite rate chemistry processes are evident in H_2 jet flames when more sensitive indicators of nonequilibrium (i.e., conditionally averaged temperature measurements of concentrations of radical species) are considered. When instantaneous simultaneous measurements of mixture fraction and temperature using pulsed Raman scattering are conditionally averaged in mixture fraction intervals, the maximum measured flame temperatures equal the adiabatic flame temperature far downstream ($x/d >= 100$) in the flame [Drake, Pitz and Lapp (1984a)]. However, closer to the fuel nozzle, the conditionally averaged maximum temperature is much smaller (by as much as 270 K at $x/d = 10$). This trend is qualitatively consistent with the model predictions [Bilger (1980), Janicka and Kollman (1979), (1982), and Dibble, et al (1984)] which suggest that the amount of superequilibrium should be largest close to the nozzle and decrease further downstream. Using a partial equilibrium thermodynamic calculation [Drake et al. (1984c)], a temperature decrement ($T_{\overline{AE}}$ $\overline{T}$) of 270 K corresponds to an average OH concentation for a stoichometric H_2-air mixture which is ≈ 2.5 times its equilibrium value. Such large superequilibrium 0H concentrations have been measured directly in the same H_2 flames using single pulse 0H laser saturated fluorescence [(Drake, et al (1984c)].

Hydrogen flames have also been used as a test bed for investigation of other turbulence-chemical kinetic interactions. For example, many of the experimental studies of turbulent H_2 diffusion flames have focused on N0 formation. Lavoie and Schlader (1974) have measured concentration profiles of H_2, N_2, 0_2 and N0 using probe sampling with gas chromatographic and chemiluminiscent analyses. Peters and Donnerhack (1981) determined and correlated exhaust N0 emissions from jet flames over a range of Reynolds and Froude numbers. Takagi et al. (1974) expanded the range of variables measured to include more species concentrations, temperature by thermocouples, and velocity by pitot tubes and explored the effects on N0 formation of heating the inlet air or adding N_2 to the fuel. Kent and Bilger (1977) and Bilger and Beck (1975) also investigated thermal NO formation in turbulent H_2 jet flames. Many discrepancies exist between these experiments. Two water-cooled stainless steel probes on the same flame by Bilger and Beck (1975) and Kent and Bilger (1977) gave quite different results for unexplained reasons, and both probes unexpectedly indicated peak NO formation in rich flame zones. Lavoie and Schlader (1974), using quartz probes, found peak NO formation near stoichiometric flame zones and reported overall NO levels very different from Bilger and Beck (1975) for similar flames. The results of Peters and Donnerhack (1981) for NO emissions, particularly after normalization for Froude and Reynolds number effects, are in agreement with Lavoie and Schlader (1984) while Bilger's (1975) results are low by a factor of ≈ 2 or 3. Unfortunately, with these discrepancies no definitive conclusions can be drawn from the literature about the effects of turbulence on thermal NO formation even in H_2 flames. However, Lavoie and Schlader (1974) and Takagi et al (1974) suggest that superequilibrium O atom concentrations must be important in thermal NO formation while Peters and Donnerhack (1981) and Broadwell (1982) suggest that large-scale structures and not superequilibrium are dominant influences in thermal NO formation.

In other studies, Page, Roberts and Williams (1974) injected a series of additives into their H_2-N_2 diffusion flame to study slow recombination reactions of ions such as In^+ and H_3O^+. Their measurements cover mainly auto-correlation coefficients in time of additive and ion concentrations. For all experiments described here the finite rate chemistry effects (superequilibrium, thermal NO_x formation, and ion recombination) in H_2 flames do not appreciably change mean densitities or temperatures. For these effects, carbon monoxide or hydrocarbon fuels have been studied.

Carbon monoxide flames

Experiments on turbulent jet flames containing CO are summarized. Many of the studies [Hawthorne et al. (1949), Peters and Donnerhack (1981), and Takagi et al. (1976)] are extensions of studies of turbulent H_2 jet flames described previously with similar quantities measured, techniques used, and results obtained. Becker and Liang (1978) measured flame length and thermal emission from a H_2 stabilized CO free jet flame and Schoenung and Hanson (1982) applied CO absorption of diode lasers to measure pdf's and power spectra very near the nozzle of a CO jet with and without combustion.

Two studies in the literature that provide reasonably complete characterizations of CO-containing jet flames are those of Razdan and Stevens (1983), (1985) and Drake et al. (1984a), Lapp et al. (1983) and Correa et al. (1984). Razdan and Stevens studied a CO jet (with 3% by volume H_2) with an average velocity of 35.7 m/s issuing vertically from a 5 mm diameter nozzle into a coflowing (v = 0.13 m/s) air stream. No pilot flame stabilization was required. Average temperatures were measured by thermocouples and average concentrations of O_2, CO, and CO_2 by probe sampling and conventional gas analysis. Mean and fluctuating axial velocities were determined by LV. The authors claim reasonable agreement with a turbulent combustion calculation with a chemistry model based upon a laminar flamelet calculation and a global CO reaction rate. However, large differences are observed at some locations where the measured average temperature is lower than that predicted by as much as 500 K and the mass fraction of CO_2 is lower and the mass fractions of CO and O_2 higher than predicted. These differences between experiment and model are consistent with finite rate CO kinetics, but could also be caused by the effect of turbulent fluctuations, or by the neglect of buoyancy, radiation loss and intermittency. Conclusions about the influence of turbulence-chemistry interactions involving the finite rate oxidation of CO are still somewhat speculative.

Drake et al (1984a), Lapp et al (1983) and Correa et al (1984) studied a turbulent jet diffusion flame in a coflowing air stream with a simulated medium BTU syngas (39.7% CO, 29.7% N_2, 29.9% H_2 and 0.7% CH_4 by volume) fuel.This data set was chosen as a test case because initial conditions are provided; no pilot flame stabilization was necessary; extensive time-resolved measurements (means, rms values and pdf's) of velocity, mixture fraction, density, temperature and molecular species (CO,

H_2, H_2O, N_2, O_2) concentrations are available using nonperturbing laser-based diagnostic techniques; OH radical concentrations are determined directly by laser saturated fluorescence; and experimental results have been compared with turbulent combustion models. Large effects attributed to finite rate chemistry effects are observed (i.e., mean OH concentrations are several times larger than equilibrium and measured mean temperature are as much as 250 K below equilibrium). However, this is certainly not an ideal case because of uncertainties in molecular compositions since CO_2 was not measured directly, unquantified temperature measurement accuracy, the possibility of preferential diffusion of hydrogen, and the relatively low value of the Reynolds number ($Re_d = 8500$). Data and detailed description of this case are presented in the section on RECOMMENDED CASES.

Hydrocarbon flames

Experiments on turbulent hydrocarbon (methane and propane) flames are summarized. As in H_2 and CO flames, some of the studies are designed to elucidate one specific aspect of turbulent flames and thus involve a rather limited characterization of even average scalar values. For CH_4 flames, this includes work on jet flame structure by [Hawthorne et al. (1949)], on NO emission levels by [Peters and Donnerhack (1981) and Takagi et al. (1974), (1976), (1980), (1981)], on radiation and soot formation by [Becker and Liang (1978)], and on temperature by [Roberts and Moss (1981)] and concentration fluctuations by [Ebrahimi and Kleine (1976)]. Studies designed for comparison with turbulent combustion models include a more complete description of at least average values of important scalars and are summarized briefly.

Chigier and Strokin (1974) obtained mean temperature (thermocouple) and dynamic head (quartz probe) in a CH_4-air diffusion flame for Re = 6600. Gas samples were analyzed in a gas chromatograph and results for unreacted species concentration were reported.

Roberts and Moss (1981) discuss the interpretation of temperature fluctuations in an open CH_4-diffusion flame (Re = 9200) in terms of the wrinkled laminar flame theory. The experimental results reported include temperature measurements (average and rms values and pdf's) at two positions (x/D = 40, 60).

Lewis and Smoot (1981) used thermocouples, and gas chromatographic analysis of probe samples to measure average values of temperature and major species concentrations in a turbulent natural gas flame burning in a cylindrical combustor. Some argon was added to the fuel and its concentration provided direct values of mixture fraction. The concentration of water was obtained from an H atom balance. The variability of initial conditions and the accuracy, reproducibility, and self-consistency of the data were quantitatively analyzed in this careful study. Unfortunately, no velocity data are reported and the geometry of the combustor indicates that non-parabolic flow is likely.

Lockwood and co-workers have investigated a free natural gas jet flame using thermocouples, probe sampling, and laser velocimetry. [El-Banhawy et al. (1983)] report mean velocity and $\overline{u'^2}$ and unburned hydrocarbons for a natural (U.K.) gas flame along the centerline for Re = 15000 - 30000. Since only the initial jet flow was seeded with particles, velocities could be obtained only in fully turbulent regions of the flow [El-Banhawy et al. (1983)]. The measured temperature statistics (pdf's and moments of the distribution) are reported in great detail in Lockwood and Moneib (1982) using fine wire thermocouples.

Gunther and co-workers have investigated a natural gas jet flame into still air (Re = 37000) [Lenz and Gunther (1980 and Gunther (1981)] using probes for average scalar values and fine wire thermocouples for pdf's, power spectra and fluctuation values for temperature. Results are in good agreement with a k-ε turbulence model and a laminar flamelet combustion model [Eickhoff (1982)]. Similar experiments in a confined natural gas jet flame in a coflowing air stream by Gunther and Wittmer (1981) used LDV, thermocouple and ionization probe to measure mean velocity $\overline{u}$, normal stress $\overline{u'^2}$, shear stress $\overline{u'v'}$ and mean tempeature, temperature variance, temperature flux $\overline{u'T'}$ and ionization macroscale. The Re-number was 24000 and axial and radial profiles for x/D = 10, 60 were reported. Measurements were compared with nonreacting flow and length scales interpreted in terms of flat flame sheets oriented parallel to the main flow direction Ahlheim and Gunther (1979) and Gunther (1981).

Extensive experimental measurements on turbulent CH_4 jet flames have been reported by Faeth and co-workers. Only the work of Jeng, Chen and Faeth (1982a), (1982b) and Jeng (1984) on buoyant, axisymmetric, turbulent jet diffusion flames of CH_4 into still air is discussed here since it supersedes earlier work by You and Faeth (1982) due to improvements in initial condition measurements and reduction of room air disturbances and transitional and elliptic flow near the nozzle. The natural gas fuel (95% methane) flowed from a cooled 5 mm diameter nozzle into still air inside a large screened enclosure to minimize disturbances. The flames were stabilized at the burner exit by a small flow of hydrogen from an angular slot and the jet Reynolds number was varied from 2920 to 11,700.

Initial conditions were measured and detailed measurements throughout the flame zone include mean and rms values of axial and radial velocity and Reynolds stress using LV, mean temperatures using radiation-corrected silica-coated fine wire thermocouples, mean major species concentrations using gas chromatographic analysis of isokinetically drawn samples, and radiant heat flux by a heat flux transducer.

This data set was chosen as a test case because of the relative completeness of the velocity and scalar measurements and because of the published comparisons between measurements and equilibrium and nonequilibrium combustion models which suggests the presence of some finite chemistry effects. Details are presented in the RECOMMENDED CASES section.

Cernansky and Sawyer (1974) measured mean temperature and composition (C_3H_8, H_20, 0_2, $C0$, $C0_2$, $N0$, $N0_2$) in a C_3H_8-diffusion flame. The flame had a mild swirl, but no velocity measurements were included. Research on spray combustion frequently includes measurements on propane gas flames as in Onuma and Ogasawara (1974), (1977) and Mao, et al (1980). Results for a propane flame at Re = 23600 are reported by Mao et al covering velocity (mean velocity and shear stress measured with LDV), temperature (mean measured with thermocouple) and composition fields (mass fractions for N_2, 0_2, H_2, H_20, C0, C_3H_8, $C0_2$ measured with gas chromatograph). Takagi et al (1974) and Takagi et al (1976) studied N0-formation in propane and C0+H_2 flames. They added N0 or NH_3 to the fuel and report measurements of N0, HCH, NH_3 concentrations along the axis and at two stations (x/D = 50, 100). Peters and Donnerhack (1981) investigated thermal $N0_x$ formation in propane flames (as well as H_2, CH_4, natural gas and C0/10% H_2 fuels) over a range of Froude and Reynolds numbers.

Jeng, Chen and Faeth (1982a) investigated free propane diffusion flames at Re = 5890, 11780 and 23560 in the same apparatus as described for their CH_4 flames. However, mean species concentration profiles have not been published on the propane flames which makes assessment of chemical kinetic effects difficult.

The data set selected from the propane jet flames studied is that of Godoy (1982) on a vertically burning, pilot flame stabilized flame into still air. It is described in detail in the following section and was chosen because of its extensive composition measurements, its high Reynolds number (Re_d = 42,700), and the demonstrated chemical nonequilibrium detected (i.e., the mole fraction of carbon monoxide was found to be smaller by a factor of three than the corresponding values at chemical equilibrium). Major deficiencies are the lack of velocity data and of fluctuation data for all scalars.

RECOMMENDED CASES

Since none of the reviewed papers contains a test case satisfying all the criteria for selection, a combination of flows is considered as the best available case. Data from three round jet diffusion flames are presented for this purpose.

Syngas/air flame

The first test case is summarized in Table 3 and the data are tabulated in Appendix C. This set of experiments was selected for the following reasons:

- Initial conditions are well documented.
- Velocity and scalar pdf's are measured at many radial locations for three radial positions.
- Concentrations of radical species (0H) and of N0 are available. Non-intrusive diagnostics are used for most of the reported measurements.
- Experimental evidence for substantial chemical nonequilibrium is available through published comparisons with models.

There are some disadvantages, however. The Re-number (Re = 8500) is rather low, and the high initial H_2 concentration may lead to preferential diffusion complications. Only one of the four Reynolds-stress components was measured, and no scalar-fluxes are available. Carbon dioxide concentrations were not determined directly and uncertainties in temperature and molecular composition are difficult to quantify.

Experimental set-up and test conditions

The configuration for this turbulent jet diffusion flame consists of a central jet of fuel surrounded by a co-flowing stream of air. The details of the set-up are given in Fig. 1. The main part of the apparatus is the turbulent jet diffusion flame combustor section. The combustor section is a rectangular tunnel with the round fuel pipe in the center. It has large

Table 3

DATA SUMMARY

<u>Flow</u> Coaxial fuel jet with coflowing air

<u>Data evaluator</u> Kollmann

<u>Case</u> Lapp, Drake, Correa et al (1983, 1984,1984a)

<u>Geometry</u> Round jet diffusion flame

$d\bar{p}/dx \cong 0$

Re $\simeq$ 8,500

<u>Mean quantities measured</u>

$\bar{\rho}$, $\bar{u}$, $\bar{T}$, concentration of radical species at three axial and several radial positions

<u>Turbulence quantities measured</u>

Probability density functions of u, T, Y_i, f, $\tilde{f}$, ρ at three axial and several radial positions.

<u>Notes</u>

Initial conditions measured, Horizontal tunnel

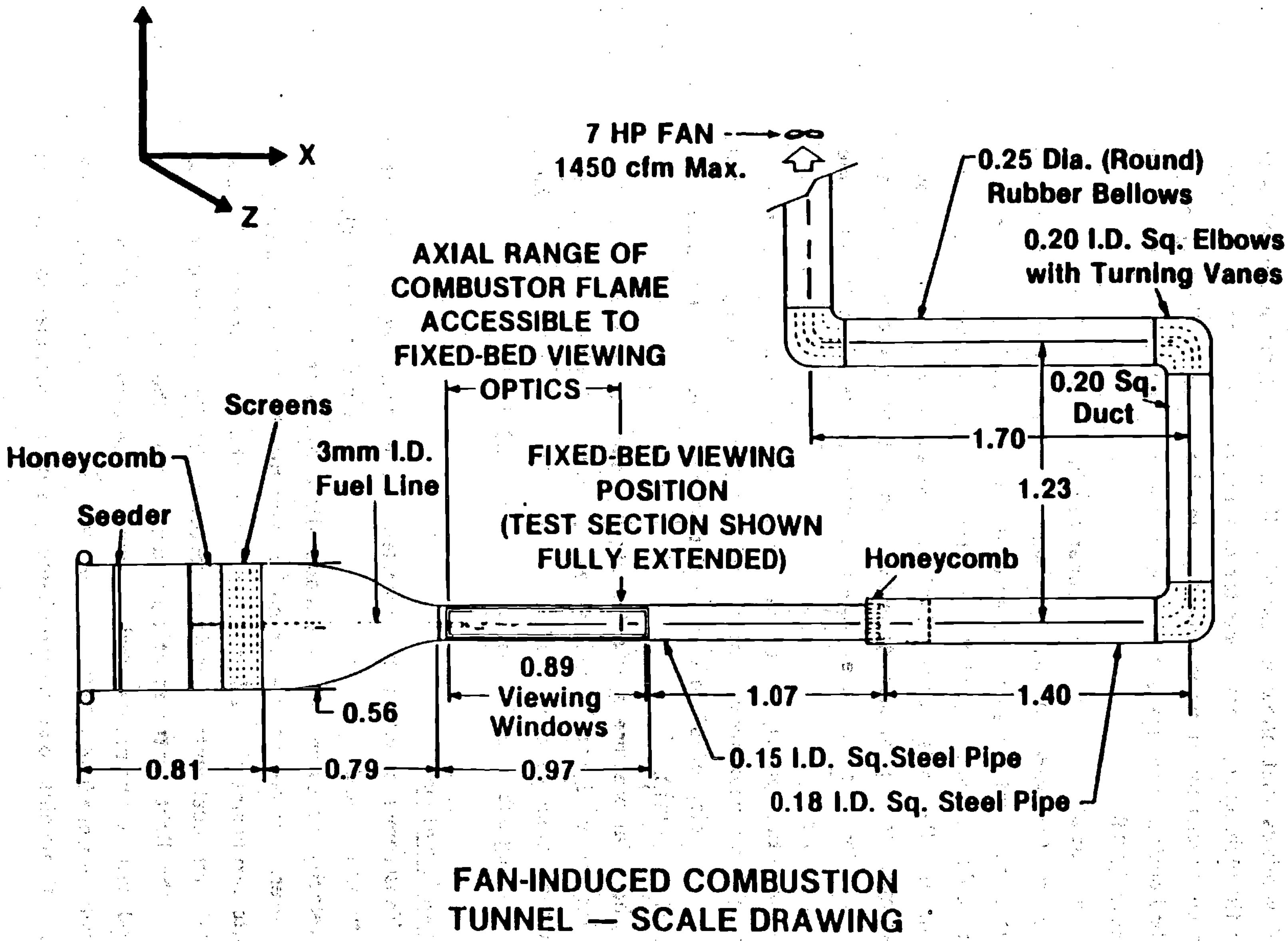

Fig. 1 Experimental schematic, approximately to scale, of fan-induced square-cross-section coaxial jet combustion tunnel.

optical windows that allow access with little optical distortion for laser diagnostic techniques, access ports for measurements requiring solid probes, and three dimensions of translational motion for flame profile studies with fixed bed optics. The relevant features of the combustor are summarized in Lapp et al. (1983).

The initial conditions are summarized in Table 4. The initial mole ratios of the fuel were obtained by flowing each constituent (obtained from industrial grade bottled gas) through calibrated critical flow orifices. The average cold flow velocity of the fuel through the fuel tube was 54.6 m/s resulting in a Reynolds number of 8500. The air velocity, controlled by a servo-control on the exhaust fan, was 2.4 m/s. The Reynolds number and jet-to-air velocity ratio were chosen to match those of an H_2/air flame described earlier.

The initial velocity profile was measured one millimeter from the jet nozzle by laser velocimetry and is shown in Fig. 2. The peak measured centerline velocity of 68 m/s is consistent with the turbulent pipe flow theory ($U_c \cong 1.28\bar{U}_j$).

The axial pressure gradient along the test zone was determined by measuring the axial velocity in the free stream (y = 50 mm). The measured free stream velocity increase is 0.35 m/s per meter of tunnel distance which indicates a negligibly small pressure gradient of -1.0 Pa/m.

Diagnostic methods

Measurements within the turbulent flame zones were made with nonperturbing optical diagnostics with high spatial and temporal resolution. Axial velocity measurements were made with a dual beam, real fringe laser velocimeter. The output of an argon ion laser tuned to the 488 mm line was split into two beams with a 50 mm separation. The two beams were focused by a 250 mm focal length lens and directed vertically into the combustion tunnel. The light scattered at right angles from the incident laser was analyzed with a commerical period counter. The dimensions of the laser probe volume were 0.08 x 0.08 x 0.5 mm. Both the fuel and air streams were seeded with nominal one micron diameter alumina particles to minimize

Table 4.

SYNGAS/AIR FLAME

Fuel Gas Composition: (mole %)	29.9% H_2
	29.7 N_2
	39.7 CO
	0.7 CH_4
Re = 8500	$d = 3.18$
$F_r = \frac{\bar{U}_j^2}{gd} = 9.6 \times 10^4$	$\bar{U}_j = 54.6$ m/s
$\frac{\bar{U}_j}{\bar{U}_e} = 22.8$	$\bar{U}_e = 2.4$ m/s
	$\rho_j = 0.835$ Kg/m^3
$\frac{\rho_j}{\rho_e} = 0.70$	$\rho_a = 1.20$ Kg/m^3

Initial profiles [Papp et al (1983)]

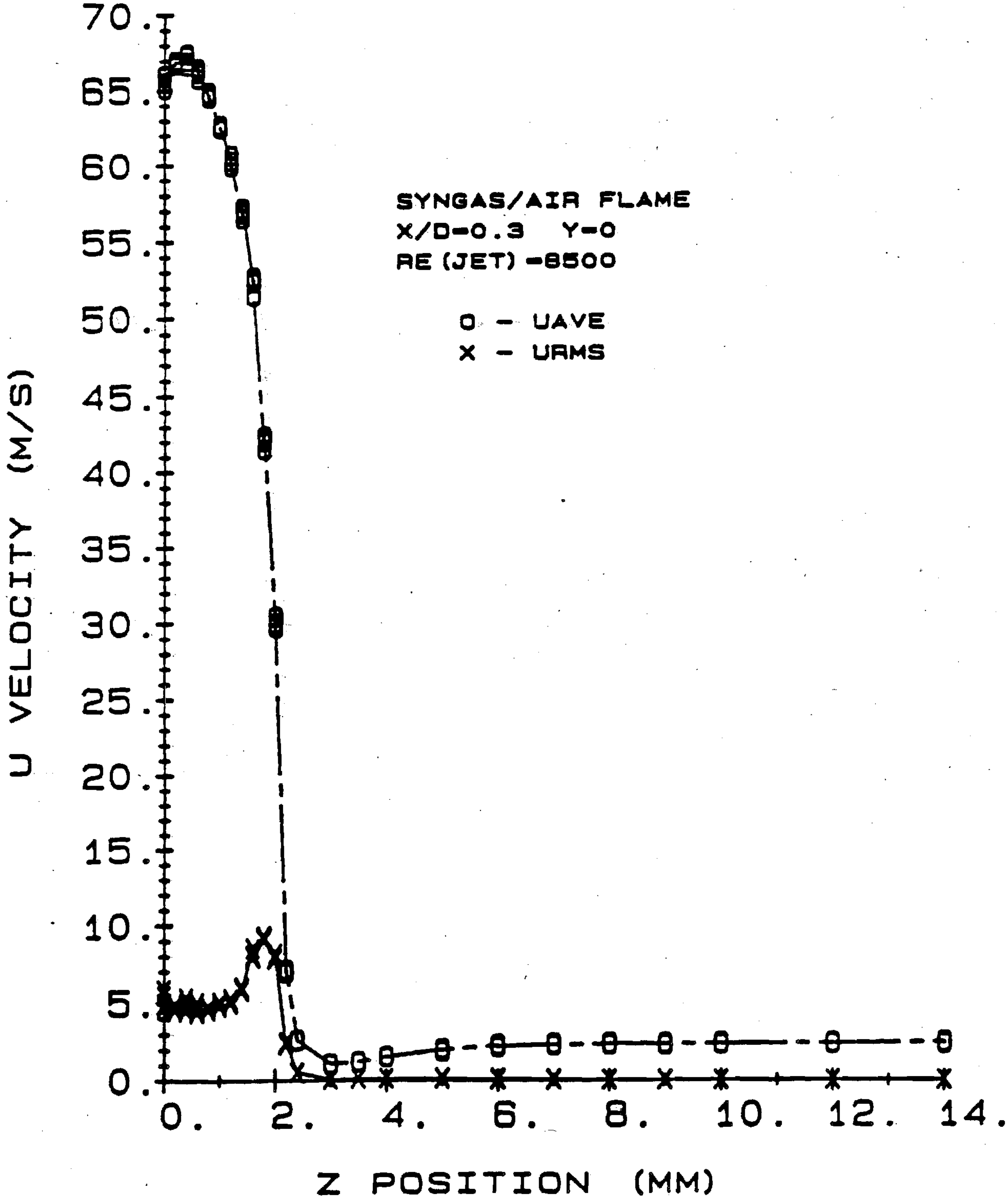

Fig. 2. **Initial velocity profile.**

sampling biases.

Temperature, concentrations of H_2, O_2, N_2, CO and H_2O, density and mixture fraction were simultaneously measured using pulsed Raman scattering. Temperature was determined from the Raman data by two methods (rationing the intensities of Stokes and anti-Stokes vibrational Raman scattering from N_2 molecules and from the sum of all molecular concentrations measured by Stokes Raman intensities assuming the ideal gas law). The concentration of CO_2 was calculated assuming that the atomic ratios of carbon and hydrogen was invariant throughout the flame and equal to the carbon-to-hydrogen ratio in the fuel. The Raman signals were calibrated by measurements of room temperature gases and of laminar H_2/air premixed flames of known composition and temperature.

The Raman system has a temporal resolution of $2 \mu s$ (limited by the laser pulse length), a spatial resolution of 0.3 x 0.3 x 0.7 mm, and a data acquisition rate of 1 pps. Repetitively pulsing the laser at a given flame location permits measurement of means and rms values and probability density functions of each variable measured. Absolute concentrations of OH molecules are reported with a temporal resolution of 2 ns and a spatial resolution of 0.1 mm^3 using single pulse laser saturated fluorescence.

Finally, N0 and $N0_x$ were determined by uncooled quartz probe extraction and chemiluminescent detection. Only measurements far downstream at the flame zone are reported where probe sampling errors are believed to be small [Drake et al. (1984a)].

Accuracy

The accuracy of the Raman scattering measurements was evaluated in H_2-air flames to be $\Delta T \pm 50$ K for temperature and $\Delta X \simeq \pm 1\%$ for mole fractions. For the syngas flame the use of the ratio of anti-Stokes to Stokes N_2 vibrational intensities to determine temperature was complicated by $C0_2$ chemiluminescence so the temperature accuracy is reduced. For example, the two methods of calculating temperature from the Raman data give values in agreement (within 50K) at temperatures less than ~ 1200 K. However, at higher temperatures, the calculated values can differ by as much as 200 K with the Stokes/anti-Stokes method always giving higher temperature values. The determination of CO_2 concentration suffered from an additional difficulty, because the CO_2 vibrational Raman contour is complicated because of Fermi resonance interactions between the vibrational modes. The CO_2 concentration was determined by a relationship that assumes that the atomic ratios of carbon and hydrogen are invarient throughout the flame and are equal to the carbon-to-hydrogen ratio in the fuel. Thus, differential diffusion of H_2 is neglected which is a small effect in H_2 jet diffusion flames at Re = 8500 and is expected to be small in this syngas flame as well. In addition, the vibrational Raman contours of N_2 and CO and CO_2 and O_2 overlap at high temperatures. Although the data analysis procedures accounted for these overlaps, the experimental accuracy could be decreased. Work is continuing to reduce systematic errors in Raman measurements of temperature and CO_2 concentrations.

Published comparisons with model calculations

The data have been compared with model calculations to identify finite-rate chemistry effects [Lapp et al. (1983) and Correa et al. (1984)]. Results from an adiabatic equilibrium calculation for this fuel are shown in Figs. 3 and 4. A scatter plot of simultaneously determined (from single-laser-shot measurements) temperature and N_2 mole fraction are shown in Fig. 5. The measured peak temperatures are considerably below the calculated adiabatic equilibrium temperatures (shown as the solid curve in Fig. 5).

The data have been compared with a k l turbulence model with two different chemistry models (a one-scalar model assuming chemical equilibrium and a two-scalar non-equilibrium model [Correa et al. (1984)]. Experiment/model comparisons of radial profiles of mean temperature [calculated by the Stokes/anti-Stokes method] (Fig. 6) and mean OH concentration (Fig. 7) demonstrate that nonequilibrium (finite rate chemistry) processes lower the mean temperature by more than 250 K and raise the mean OH concentration by a factor of 4 at this flame location.

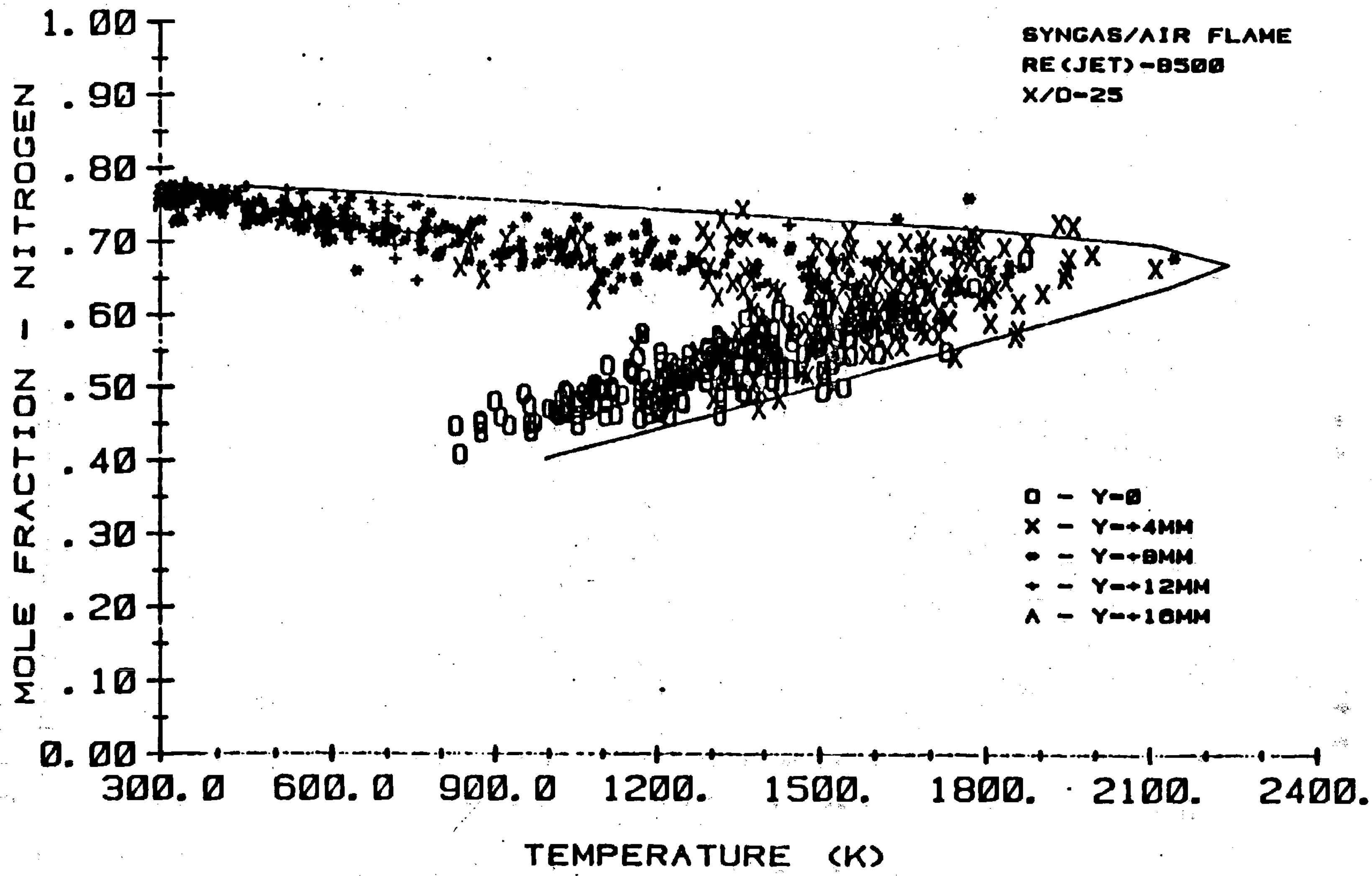

Fig. 3 Comparison of simultaneously acquired nitrogen mole fractions and temperature data obtained from a variety of radial positions (y = 0-6 mm), at an axial location of 25 fuel-tip-diameters, with an adiabatic equilibrium calculation (solid curve).

Thermochemical data (from Ref. [29]

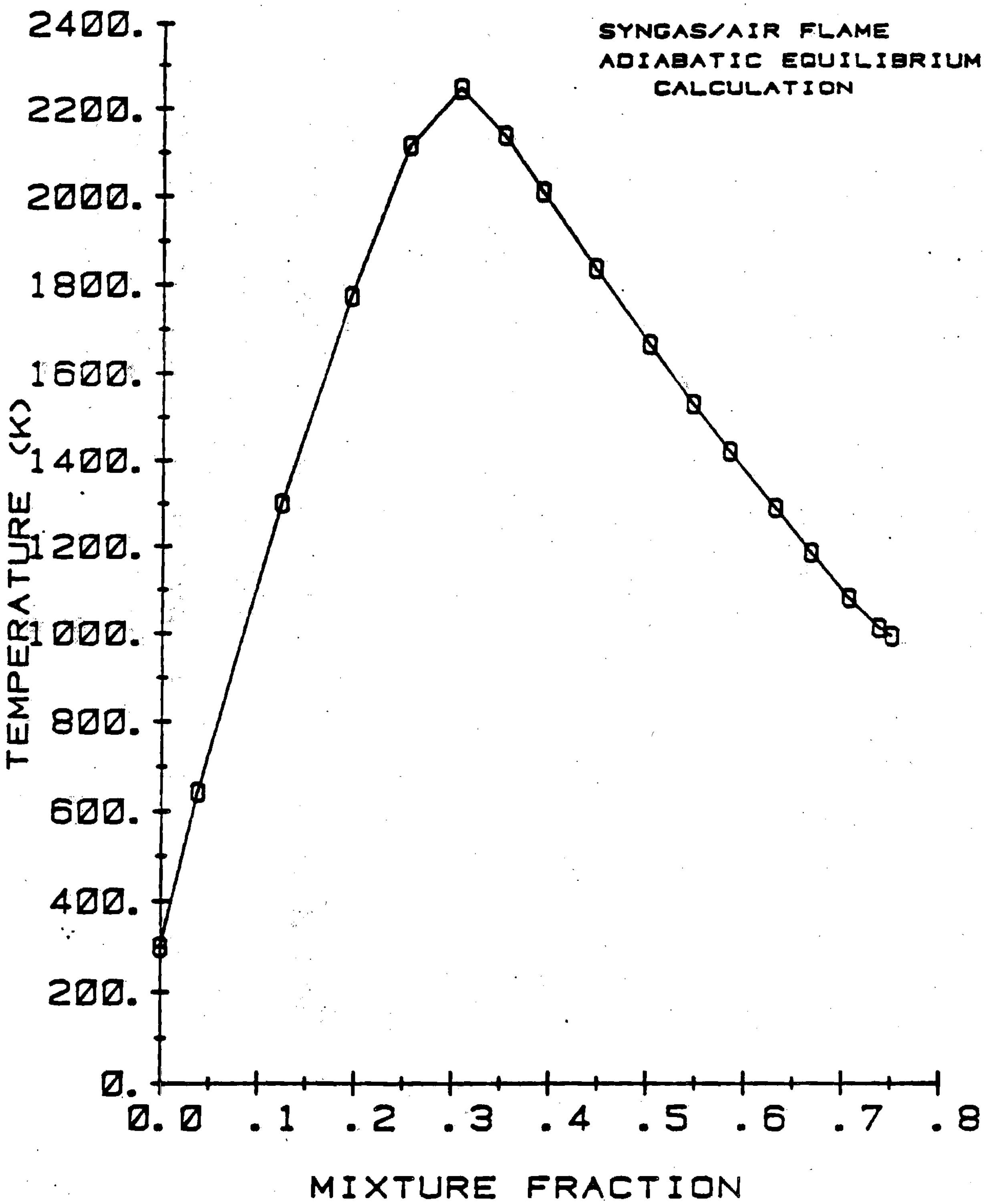

Fig. 4. **Temperature vs mixture fraction for a syngas-air flame calculated using an adiabatic equilibrium computer program.**

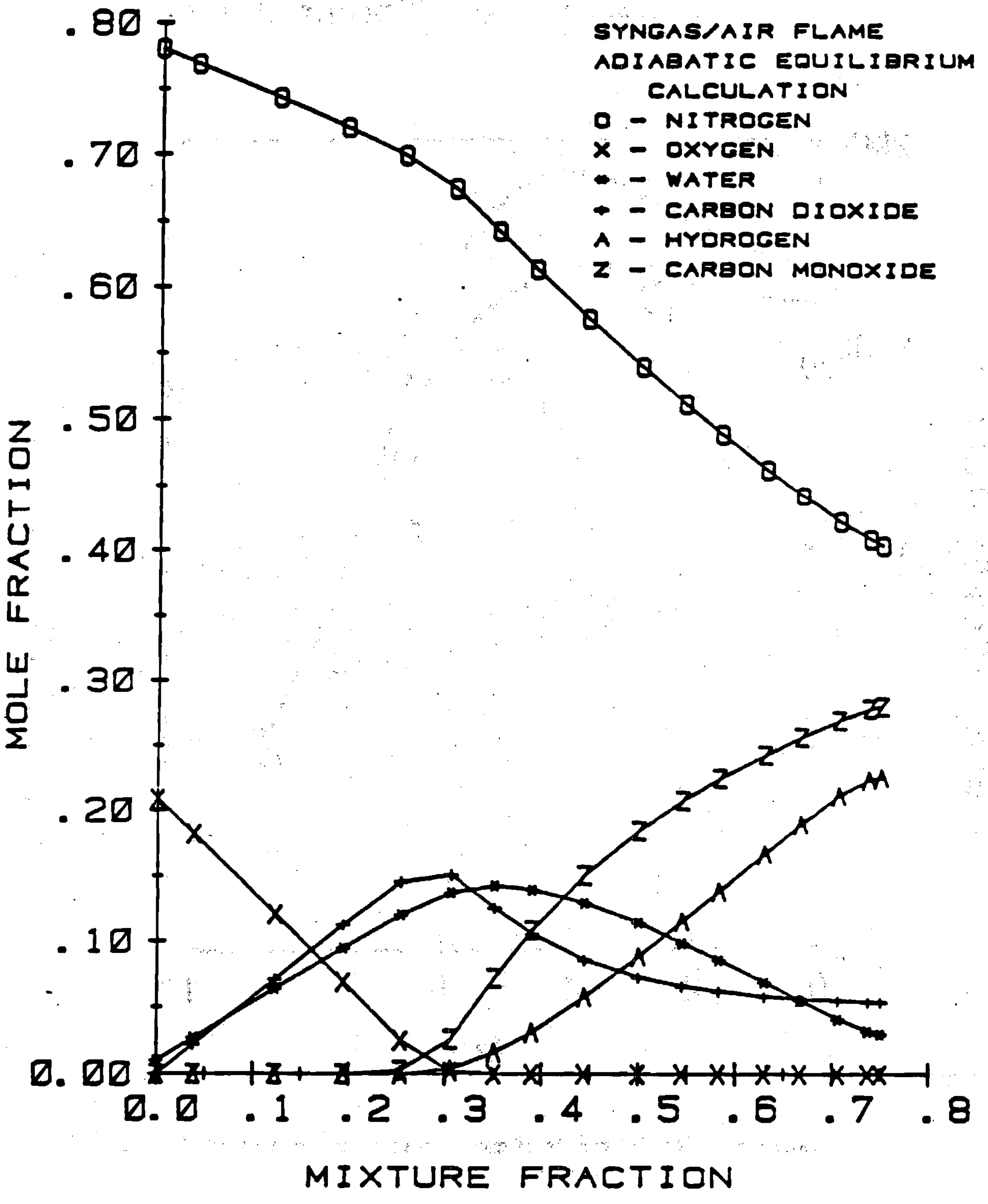

Fig. 5. **Major species mole fractions vs mixture fraction for a syngas-air flame calculated using an adiabatic equilibrium computer program.**

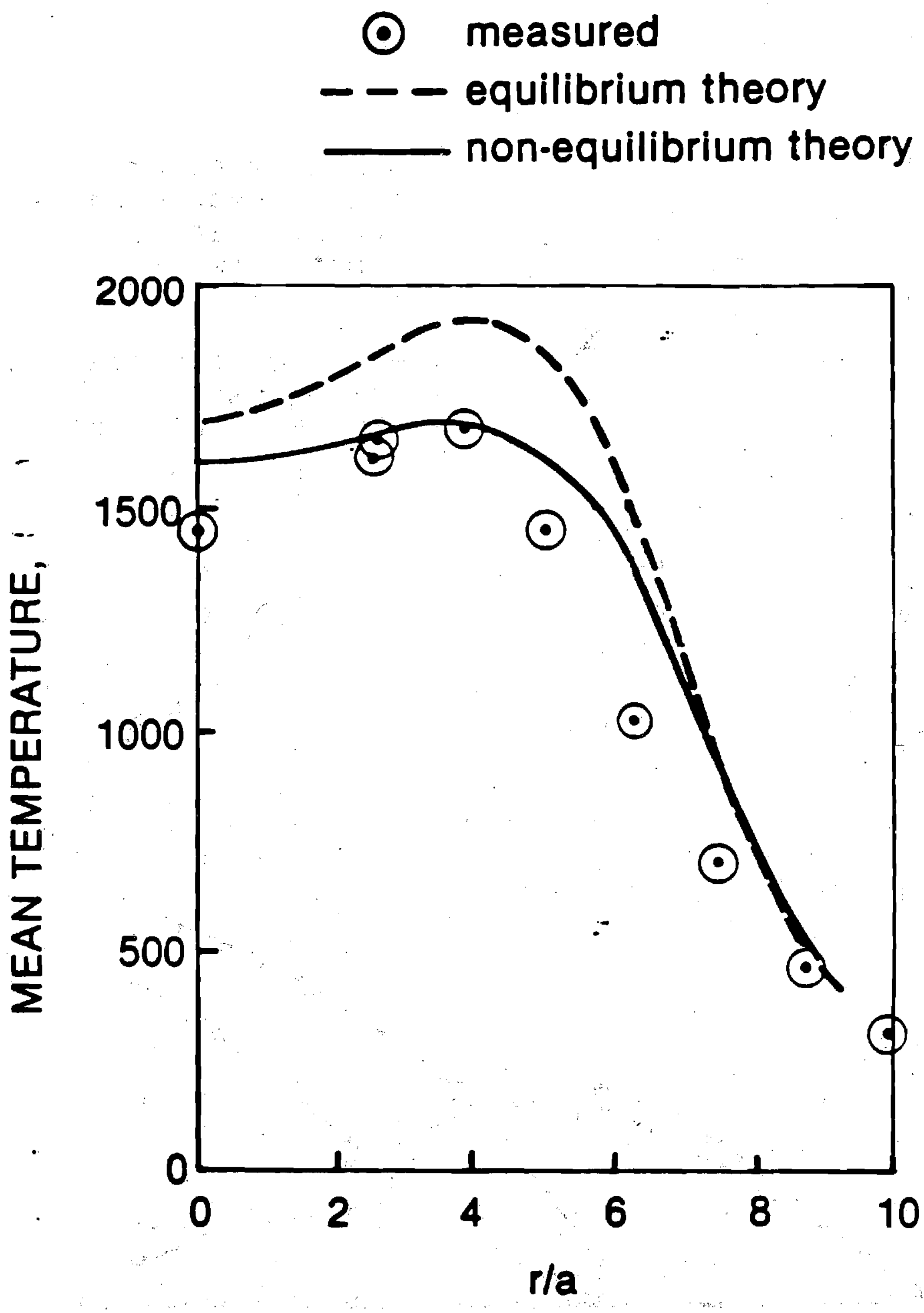

Figure 6. **Radial profile of mean temperature at x/d = 25.**

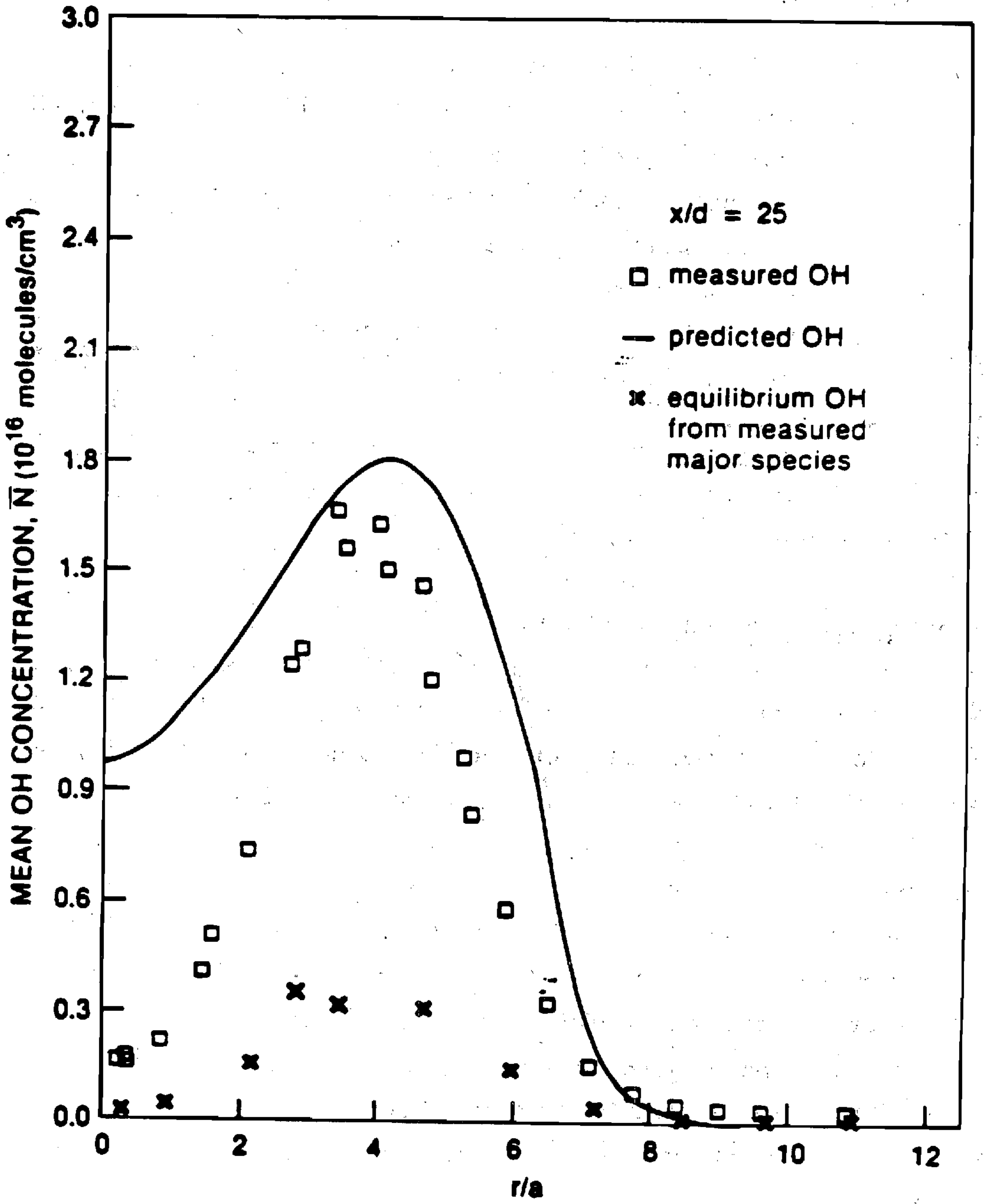

Figure 7. **Radial profile of mean OH concentration at x/d = 25.**

Natural gas/air jet flame

The second test case is summarized in Table 5 and was selected for thefollowing reasons:

- Well documented initial condition
- Extensive measurements of mean and fluctuations of all three velocity components and u'v'
- Extensive mass fraction measurements of all major species by isokinetic probe sampling and GC
- Detailed error analysis
- Comparisons with partial equilibrium or laminar flamelet models indicate substantial finite rate chemistry effects.

The limitations of this data set are the relatively low Reynolds number of the flow and the lack of fluctuation measurement of mixture fraction and species concentrations.

Experimental setup and test conditions

The setup for this free jet of methane into still air is shown in Fig. 8. The burner was directed upward inside a screened 1.1 m x 1.2 m x 2.7 m enclosure to minimize the effects of room disturbances, and both the burner and enclosure were translated during measurements. The brass burner, shown in detail in Fig. 9, was designed to give a uniform velocity profile. Initial conditions and fuel composites are summarized in Table 6. Although three flames were studied, the flame with the highest Reynolds number (11,700) has been chosen as the most appropriate test case. The natural gas velocity measured at the burner exit was 49.8 m/s and the typical composition (94.9% CH_4, 3.8% methane) is given in Jeng (1984). The natural gas flame was stabilized by a small annular H_2 flow (vol. flow rate H_2/vol. flow rate nat. gas = 0.15) and the burner was maintained at room temperature by water cooling.

Table 5

DATA SUMMARY

Flow — Fuel jet into still air

Data evaluation — Drake

Case — Jeng, Chen and Faeth (1982a,b) and Jeng (1984)

Geometry — Round jet diffusion flame (Natural gas, 95% CH_4) screened enclosure 1.1 m x 1.1 m x 2.7 m. Re = 11,700 d = 0.005 m.

Mean quantities measured

$\bar{u}$, $\bar{v}$, $\bar{T}$, mass fraction of all major species is at several axial and radial locations

Turbulence quantities measured

u', v', w' at several axial and radial locations

Notes

LDV, coated thermocouple used. Initial conditions measured.

Vertical flame, screened enclosure, H_2 stabilized

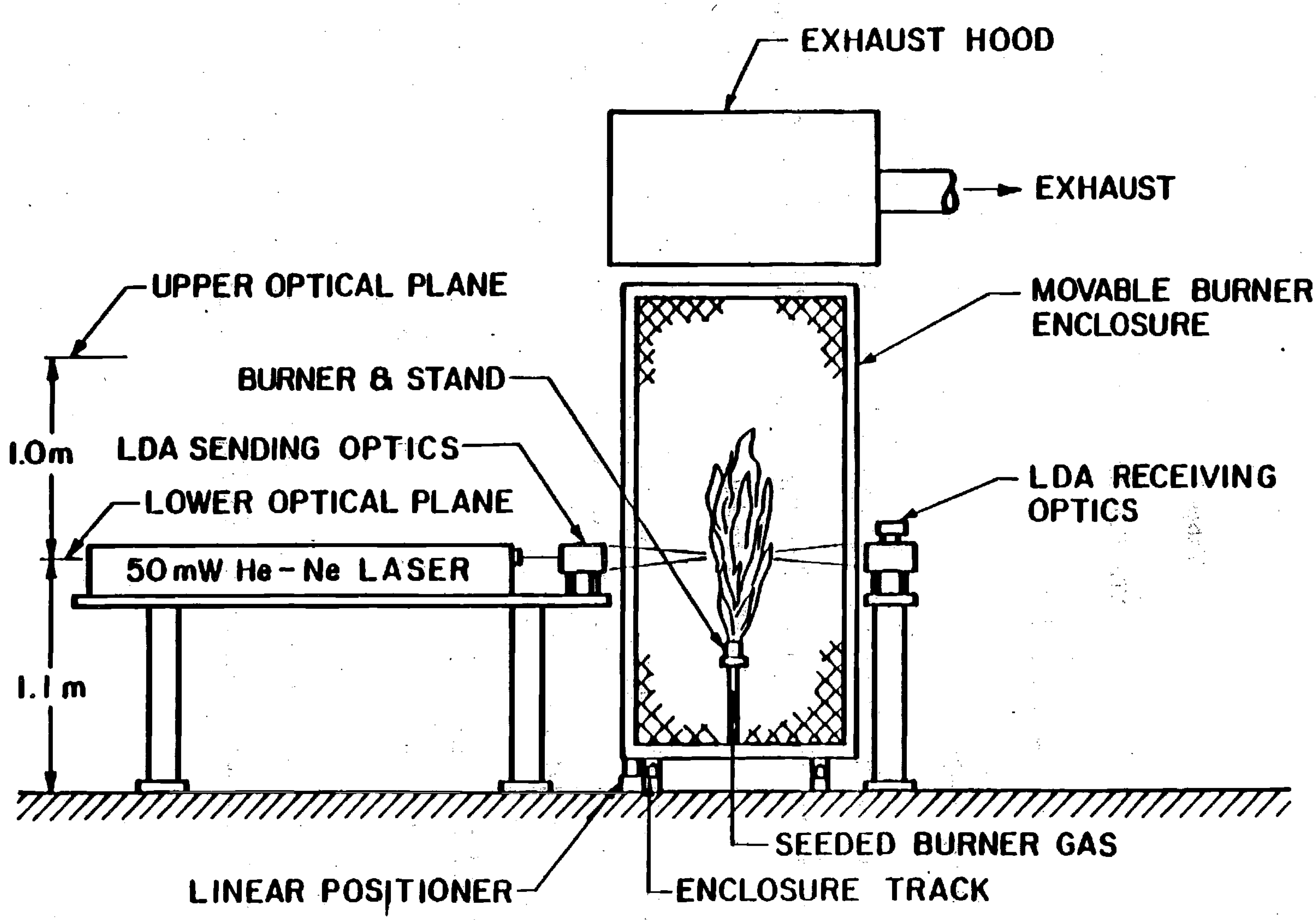

Figure 8. Sketch of the methane flame test apparatus.

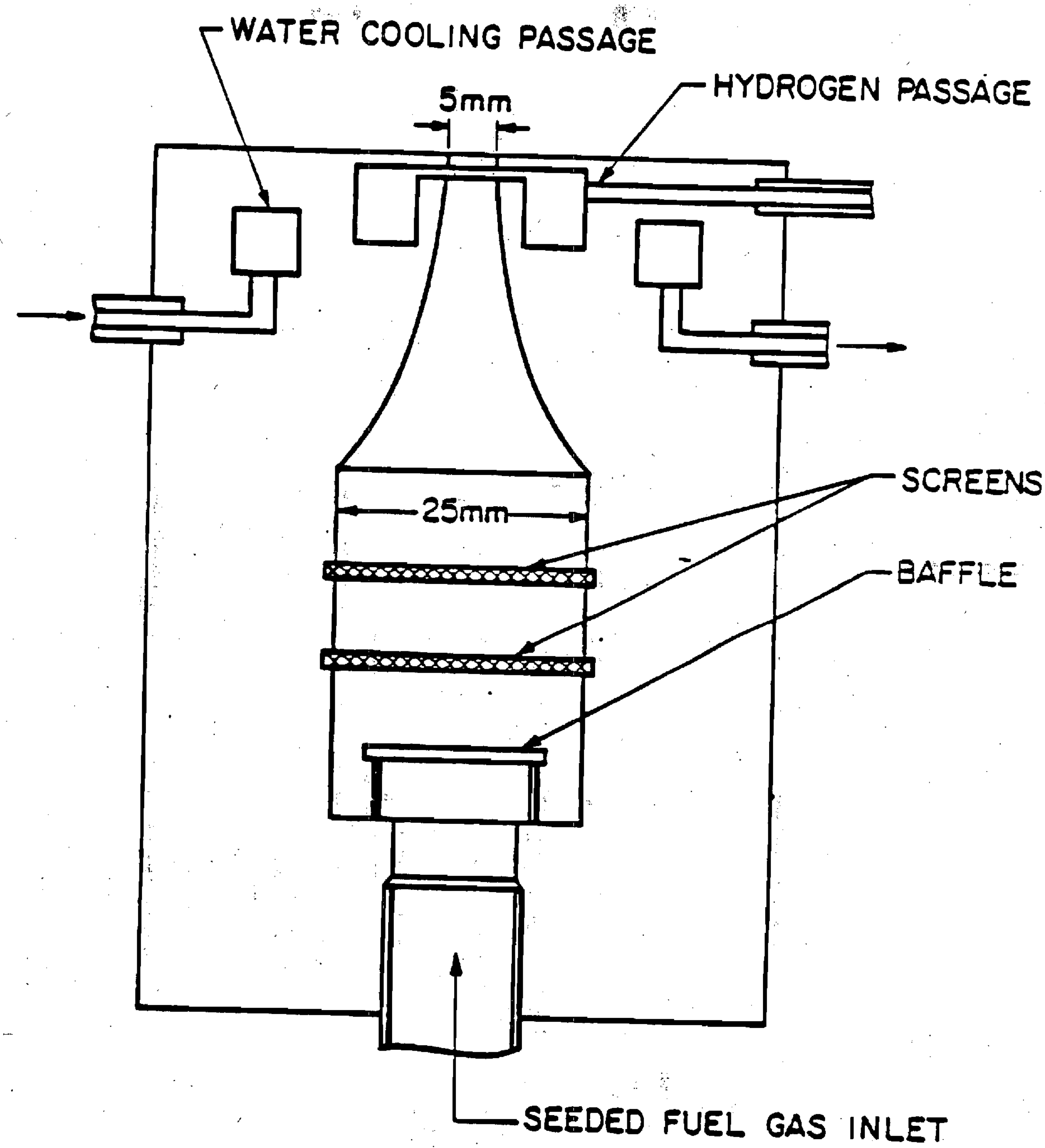

Figure 9. Sketch of the methane burner assembly.

Table 6.

Summary of Test Conditions for Buoyant Flames

Reynolds Number	Richardson Number	d (mm)	$\bar{u}_o$ (m/s)[c] est.	$\bar{u}_o$ (m/s)[c] meas.	$k_o^{1/2}/u_o$ [d]	$\dot{Q}$ (kW)	$\dot{Q}_{rad}/\dot{Q}$ (%)	Flow Rates (mg/s) Fuel	Flow Rates (mg/s) Hydrogen
Methane Flames,[f] Present Study:									
2920	4.53×10^{-4}	5.0	11.8	12.9	0.0346	6.8	14.0	130	2.3
5850	1.13×10^{-4}	5.0	22.9	23.9	0.0346	13.7	18.7	260	3.3
11700	2.80×10^{-5}	5.0	48.2	49.8	0.0164	27.4	18.4	520	10.1

[a] $Re = u_o d/\nu_o$, based on fuel gas properties and estimated velocity at burner exit.

[b] $Ri = gd/u_o^2$, based on estimated velocity at burner exit.

[c] $u_{o\ est} = 4\,\dot{m}_o/\pi d^2\bar{\rho}_o$ based on fuel gas density at burner exit, $u_{o\ meas}$ = average velocity for $r \leq 0.4d$.

[d] Based on $u_{o\ meas}$.

[e] Commercial propane.

[f] Natural gas.

Natural Gas, Columbia Gas Co., Typical Composition:

Methane	94.863
Ethane	3.753
Propane	0.266
iso-Butane	0.039
n-Butane	0.047
iso-Pentane	0.019
mono-Sulfur	0.009
di-Sulfur	0.012
Mercaptans	0.016
n-Pentane	0.016
Hexane	0.084
Nitrogen	0.408
Carbon Dioxide	0.423
neo-Pentane	0.006
Hydrogen Sulfide	0.019
Hydrogen	0.020

Diagnostic measurements

Mean and fluctuating velocities were measured with a frequency-shifted laser velocimeter with a spatial resolution of 0.12 x 0.10 mm close to the nozzle and 0.72 x 0.24 mm at x/d >= 50. Both fuel and air were seeded to minimize sampling bias.

Mean temperatures were measured with Pt/Pt-10% Rh thermocouples (225 m junction), coated to avoid catalytic effects and corrected for radiant heat losses. Both total and spectrally resolved radiant heat fluxes from the flame were measured. Mean concentrations of major flame species were obtained by isokinetic sampling from a water cooled 2 mm internal bore stainless steel probe.

Accuracy

The accuracy of this data set is described in detail in Jeng (1984). In most regions of the flow, the errors in mean velocity and velocity fluctuations are estimated to be of the order of 5% and 10% respectively. Somewhat greater errors due to gradient broadening occur near the end of the potential core.

The accuracy of the temperature measurements is limited by the corrections due to radiation and conduction. The largest radiation correction was 160 K and the uncertainty in this correction was estimated to be no better than 5% of the total correction.

Calibration experiments by You and Faeth (1982) indicate variations in gas sampling rates within 50% of the local mean velocity had little influence on the composition measurements.

The reproducibility of measurements was tested by independent measurements taken over a several month period. Mean velocities, velocity fluctuations and mean temperatures were repeatable to within 5%, 10% and 40 K, respectively. The repeatability of mean composition is expected to be 15%, based upon that found by You and Faeth (1982) using similar techniques.

Published comparisons with model calculations

The natural gas flame data have been compared with a $k_{\varepsilon}g$ turbulence model using two different chemistry submodels [Jeng et al. (1982b) and Jeng (1984)]. A partial equilibrium submodel assumed that chemical equilibrium exists at all equivalence ratios between 0 and some critical fuel/air equivalence ratio $\varphi > \varphi_c$. The value of φ_c was determined to be 1.2 by comparison (as in Fig. 10) of calculated and experimentally measured CO mass fractions in laminar methane diffusion flames. The second chemistry submodel assumes that turbulent flames are a collection of laminar flamelets and that the thermodynamic state relationships are the same as those experimentally measured in laminar methane diffusion flames. Both approaches give similar results for temperature and major species concentration in laminar CH_4 flames (see Fig. 11). Both approaches are in reasonable agreement with the present turbulent natural gas jet diffusion flame data (Figs. 12-14), suggesting their utility in modeling finite rate chemistry processes in turbulent combustion. The experiment/model discrepancies in the H_2 mass fraction are believed to be caused by the H_2 stabilizing flow used [Jeng (1984)].

Propane/air flame

The third set of experiments is summarized in Table 7. It complements the other data sets in the following sense:

- High Re-number
- Extensive composition measurements

This set is, however, incomplete due to the lack of velocity data. Effects of chemical non-equilibrium were detected. The mole fraction of carbon monoxide were found to be smaller (by approximately a factor of three) than the corresponding values for chemical equilibrium.

Experimental set-up and test conditions

The set-up consisted of a burner [see Fig. 15 from Godoy (1982)], which produced a freely burning axisymmetric, stabilized jet diffusion

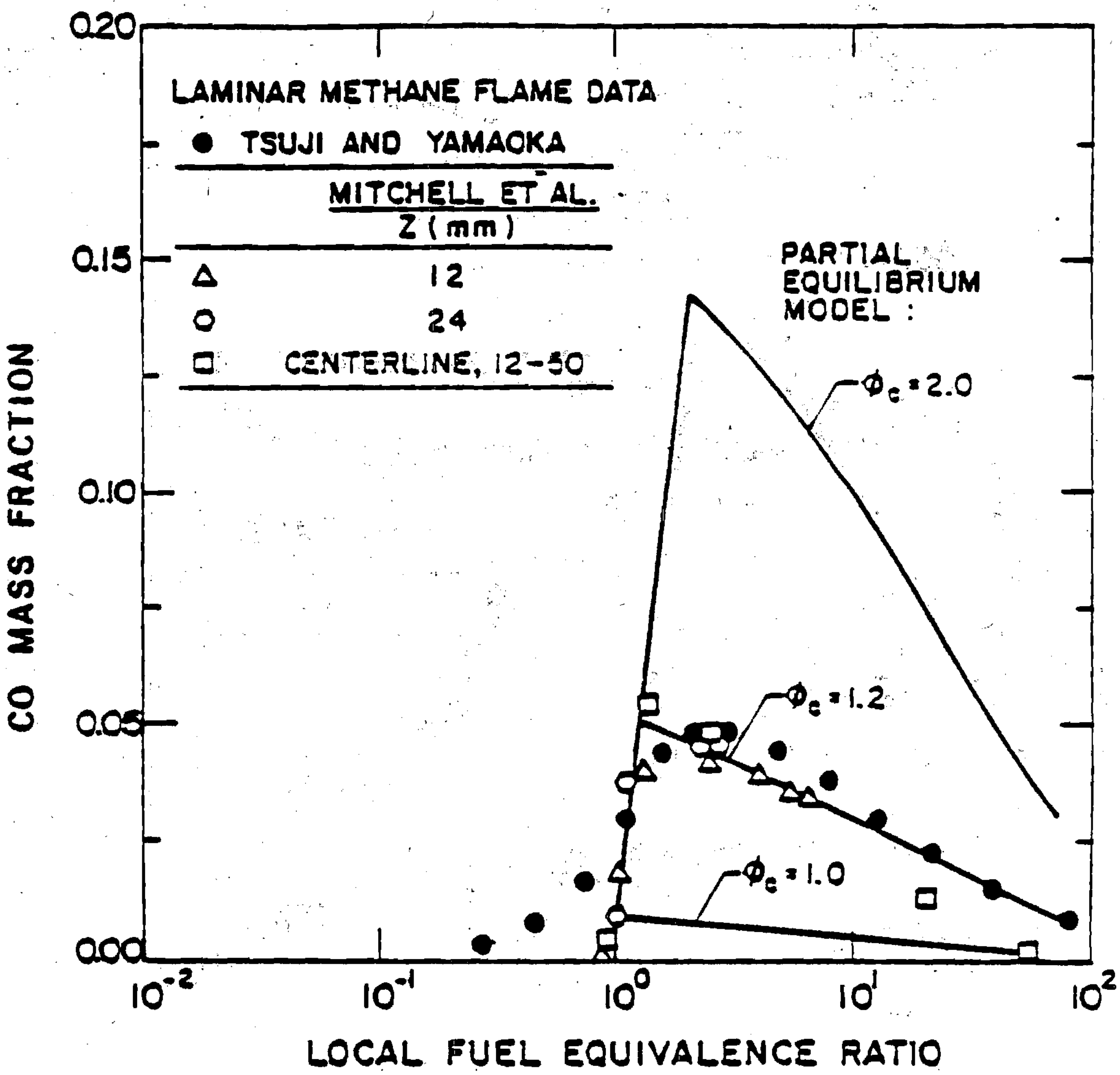

Figure 10. Mass fraction of CO as a function of mixture fraction for laminar methane diffusion flames.

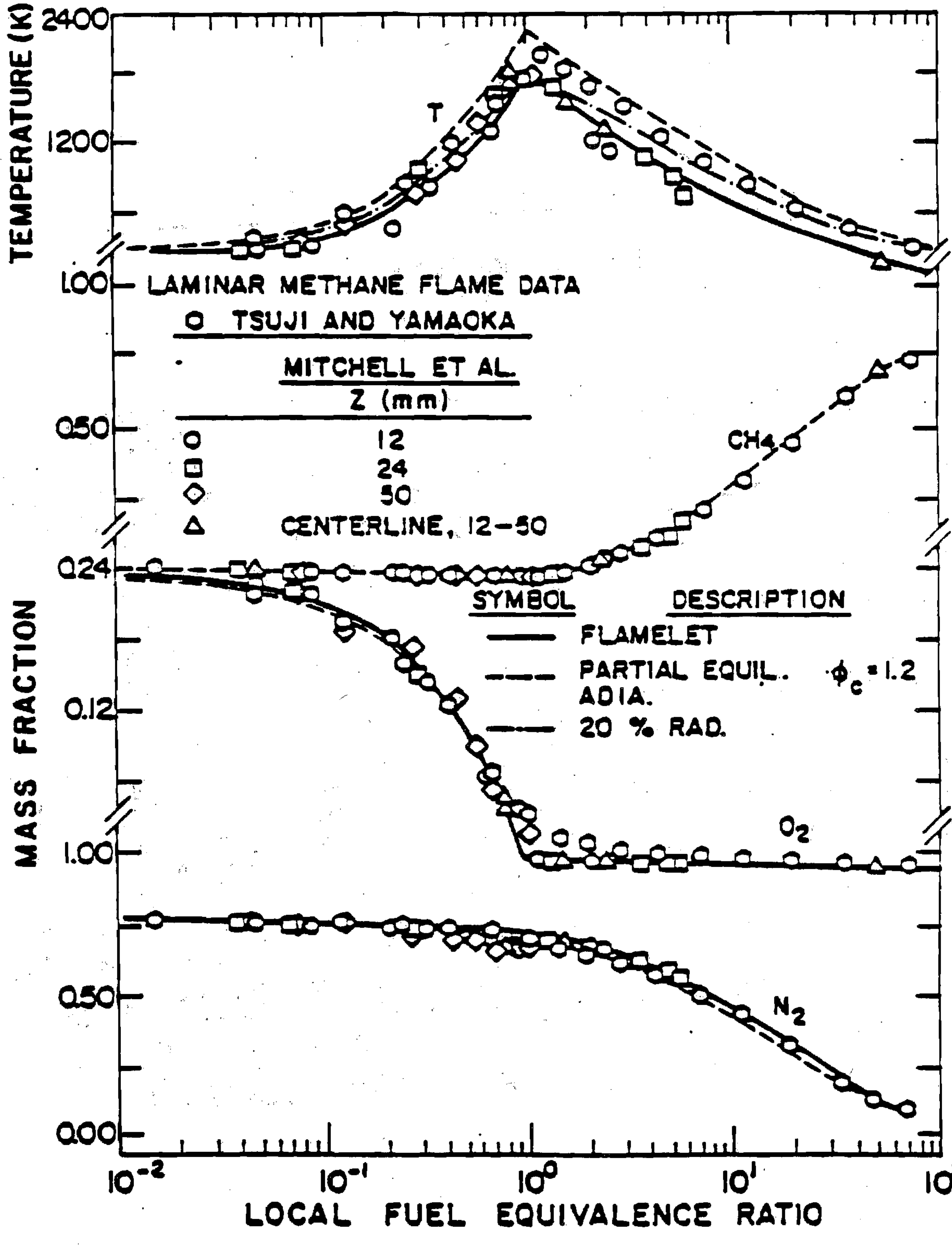

Figure 11. State relationships for methane diffusion flames burning in air.

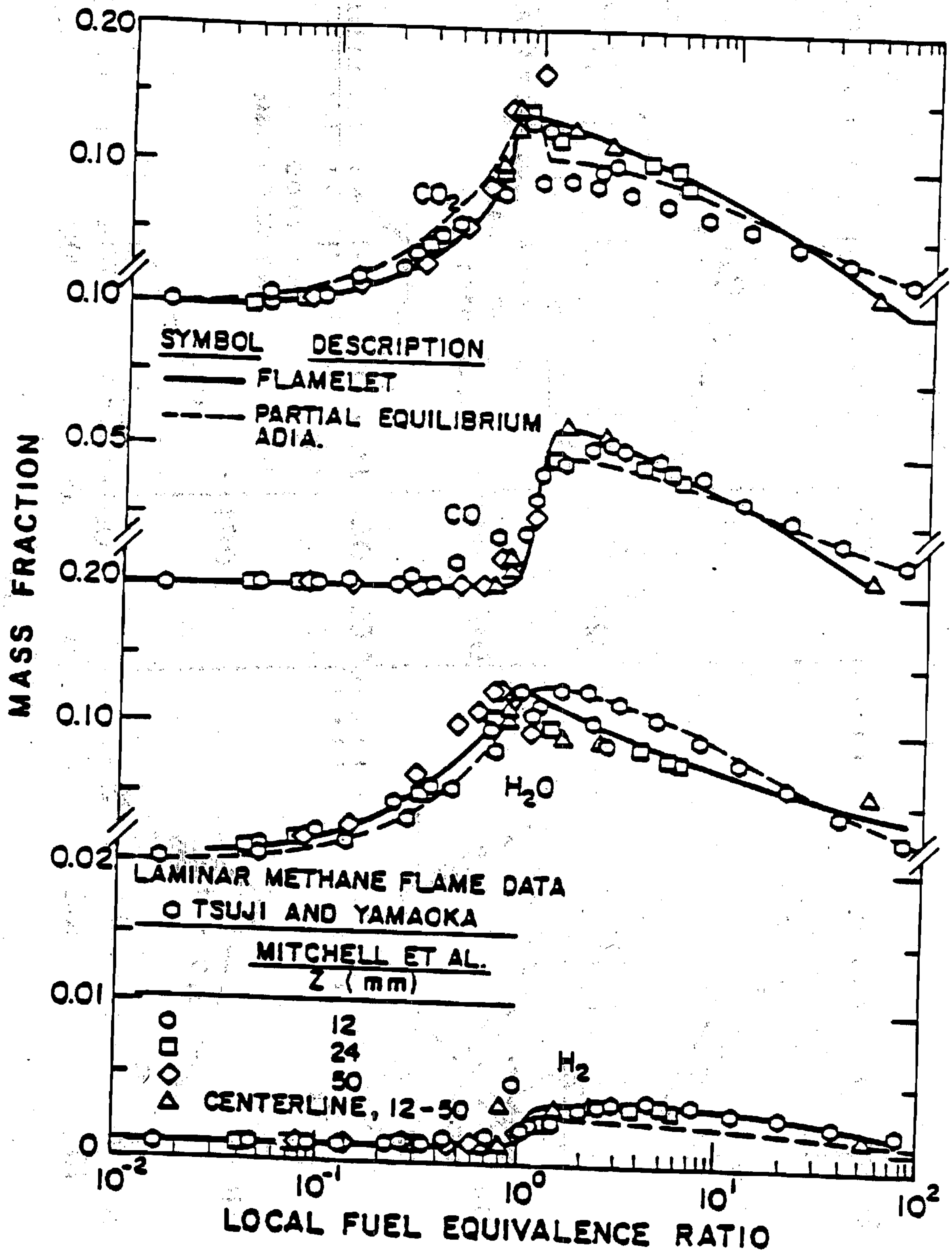

Figure 11. Continued). State relationships of methane diffusion flames burning in air.

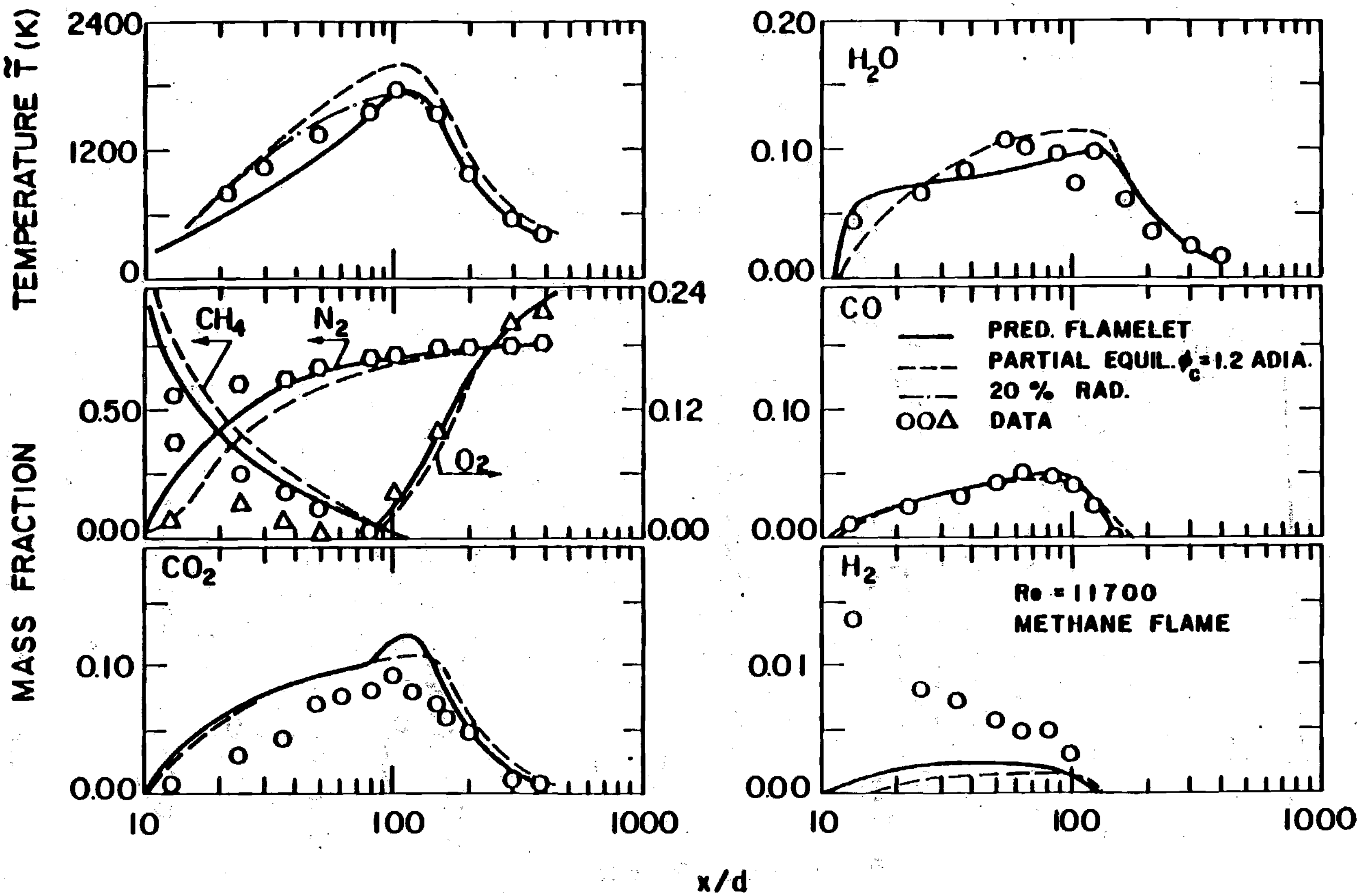

Figure 12. Axial variation of mean temperature and species concentrations: Methane, Re = 11,700.

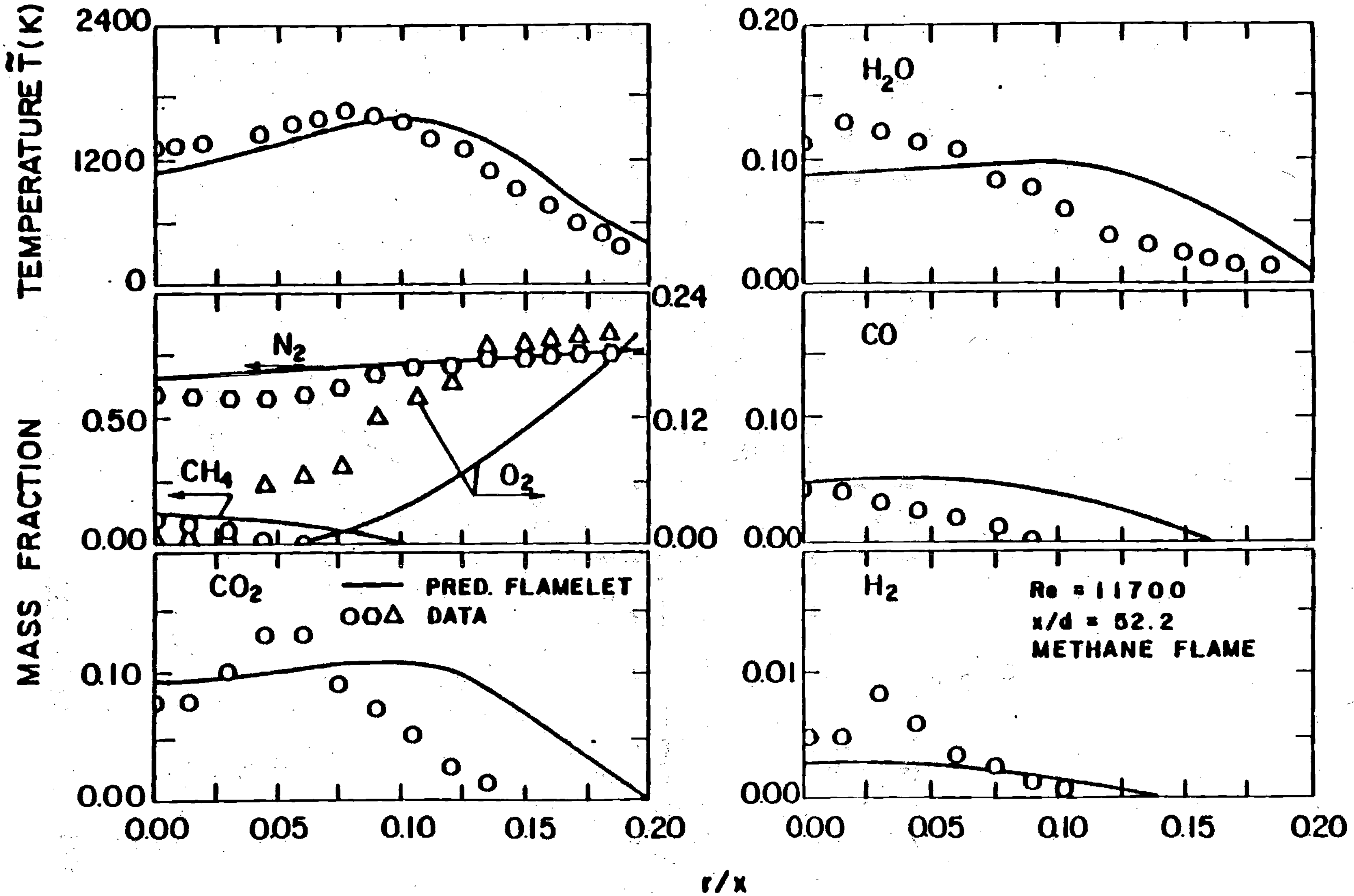

Figure 13. Radial variation of mean temperature and species concentrations: Methane, Re = 11,700, x/d = 52.2.

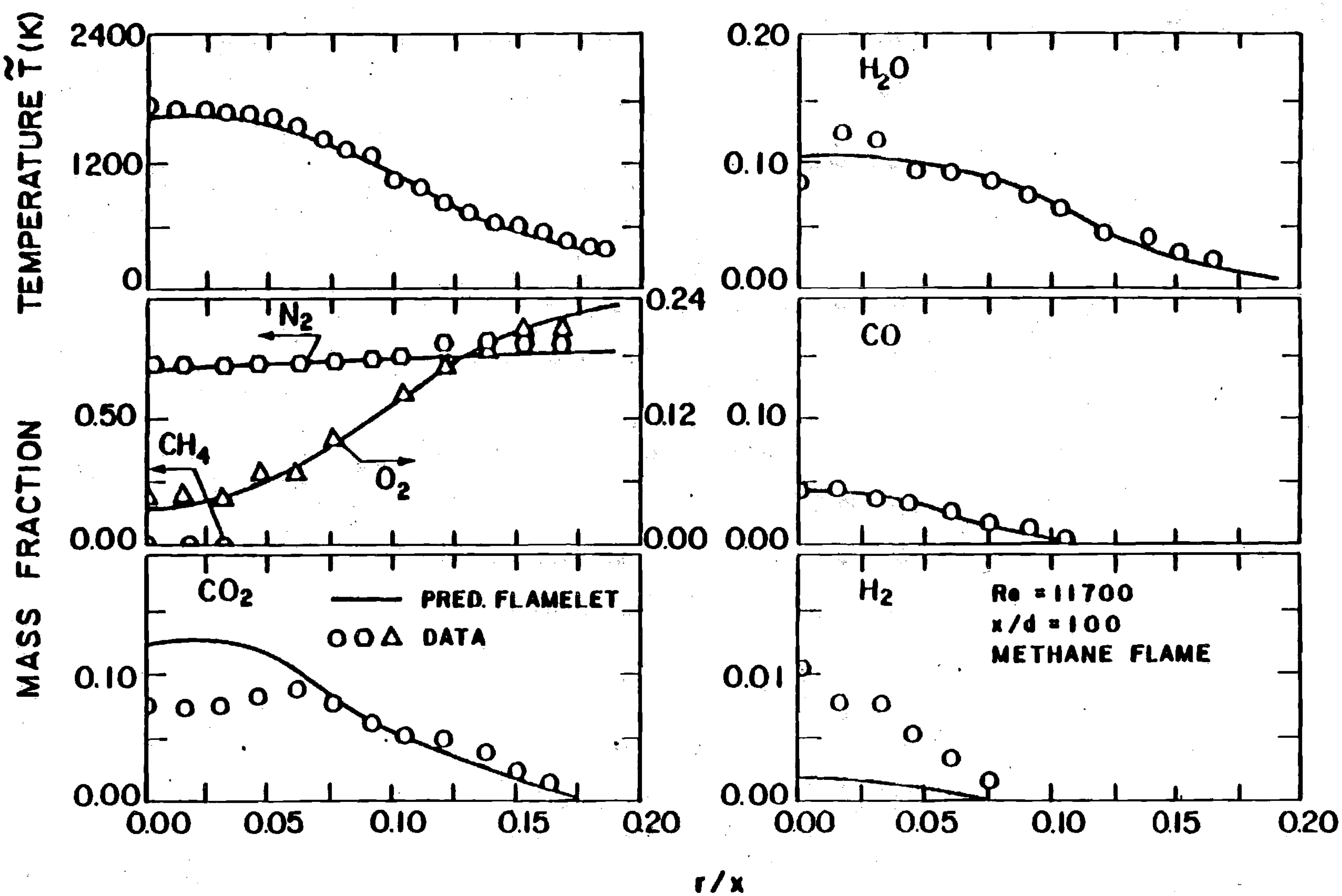

Figure 14. Radial variation of mean temperature and species concentrations: Methane, Re = 11,700, x/d = 100.

Table 7

DATA SUMMARY

Flow	Fuel jet into still air
Data evaluator	Kollman
Case	Godoy, S. (1982)
Geometry	Propane-air axisymmetric jet diffusion stabilized flame. $d\overline{p}/dx$ 0 Re = 24,000, 31,500, 42,700

Mean quantities measured

Mole fractions of CO, CO_2, O_2, unburnt hydrocarbons

Turbulence quantities measured

Notes	Vertical flame, intrusive probe

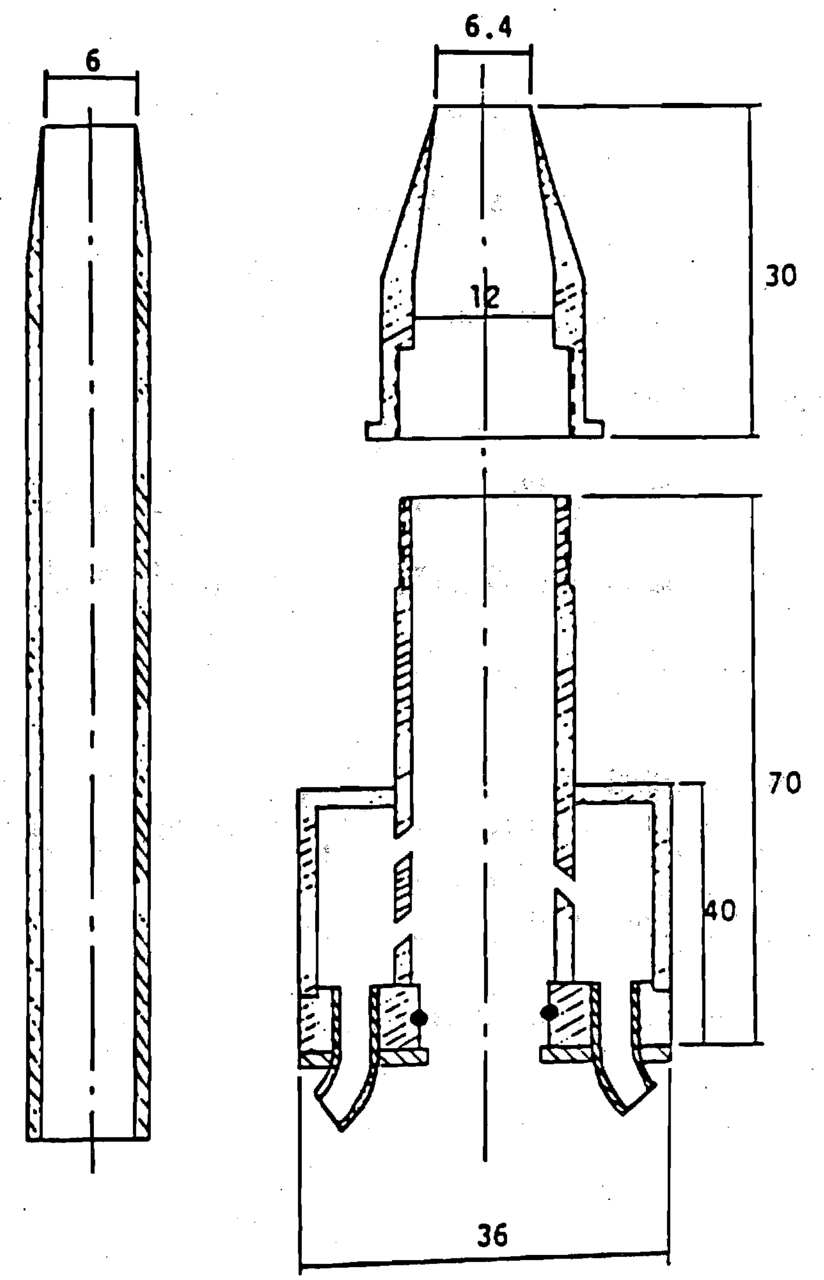

Fig. 15 Burner (all measures in mm)

flame. The flame was directed vertically upward to avoid destruction of symmetry of the mean fields due to buoyancy. An annular pilot hydrogen flame was used for stabilization. The mass flow rate of the pilot flame was kept very low compared to the propane flow rate. Most of the measurements were taken with an intrusive probe for which a traversing mechanism was constructed, allowing measurements up to x/D = 250.

The main data for the tests are given in Table 8. Buoyancy effects became significant for the three flames at distances greater than x/D = 80 (Re = 2.4×10^4) and x/D = 110 (Re = 4.27×10^4).

The conditions at the fuel pipe exit are known as fully developed turbulent pipe flow. The pilot flame reaches only a length of about 1 cm and its influence can be neglected for x/D >= 10. The jet flame issues into still air and the pressure gradient is zero.

Diagnostic methods

Composition was measured by extracting samples from the flow field using probes. The water cooled stainless steel probes had an outer diameter of 7.5 mm and tip diameters of 1 mm and 2 mm. The probe tip was tapered to reduce the disturbance of the flow field. Most of the measurements were taken with the probe with the larger tip diameter to avoid blockage by soot particles. The smaller probe served for accuracy checks. The gas samples were removed from the flow field with sampling velocity of 10.6 m/s (small probe) or 2.65 m/s (large probe). The sampled gas was then dried filtered to remove soot, and fed into infrared analyzer and gas chromatograph. The infrared analyzer yields carbon monoxide and carbon dioxide. Nitrogen and oxygen were measured by gas chromatography. Unburned hydrocarbons were measured with a flame ionization detector.

Accuracy

Since the measurements were done with an intrusive probe, the influence of the probe size and sampling velocity on the results were checked. The change of mole fraction of stable components from the large to the small probe was less than 5% for CO and CO_2. Mass balance checks could not be carried out, because not all components were measured.

Table 8. Test Data

$$Re \equiv U_j D/\nu = 2.4 \times 10^4 , \quad U_j = 17.16 \text{ m/s}$$

$$= 3.15 \times 10^4 , \quad U_j = 23.13 \text{ m/s}$$

$$= 4.27 \times 10^4 , \quad U_j = 31.36 \text{ m/s}$$

RECOMMENDED WORK

From the review of the available experimental data sets, it is apparent that an ideal test case for a turbulent nonpremixed flow showing effects of nonequilibrium chemistry has not yet appeared. However, the three cases selected document that finite rate chemistry effects are observable experimentally in turbulent jet diffusion flames of $CO/H_2/N_2$, CH_4 and C_3H_8 fuels, and published experiment/modeling comparisons demonstrate their utility in testing finite-rate chemistry submodels.

The first recommendation for future work is the establishment of a set of experiments in a CO or hydrocarbon jet flame where the initial conditions are well known and the Reynolds number is high enough to exclude differential diffusion and other low Reynolds number phenomena. Extensive measurements of velocity, temperature, density and all major species concentrations should be obtained to permit mass and elemental balances. The data would preferably be obtained with laser-based methods with high spatial and temporal resolution to permit the direct determination of pdf's, moments, correlations, Favre and conventional averages and conditional measurements.

Although not analyzed to the extent that it could be included in the review of the literature, such data are becoming available from pilot-stabilized CH_4 jet flames (Masri, Dibble and Bilger, private communication, May 1985). Instantaneous pulsed Raman and Rayleigh measurements of major species concentrations and temperature from this flame are correlated in scatter plots as shown in Fig. 16. For a fully attached, stable flame (v_{CH_4} = 41 m/s; v_{air} = 115 m/s, d = 0.0072m), a wide range of temperatures is observed for any given mixture fraction indicating a wide variation in reactedness. The solid lines in the figure correspond to a Burke-Shumann model with reactedness of 0, 0.5 and 1.0 and the dotted line corresponds to a laminar flamelet relationship in a slightly stretched (= 10 sec^{-1}) CH_4 counterflow diffusion flame.

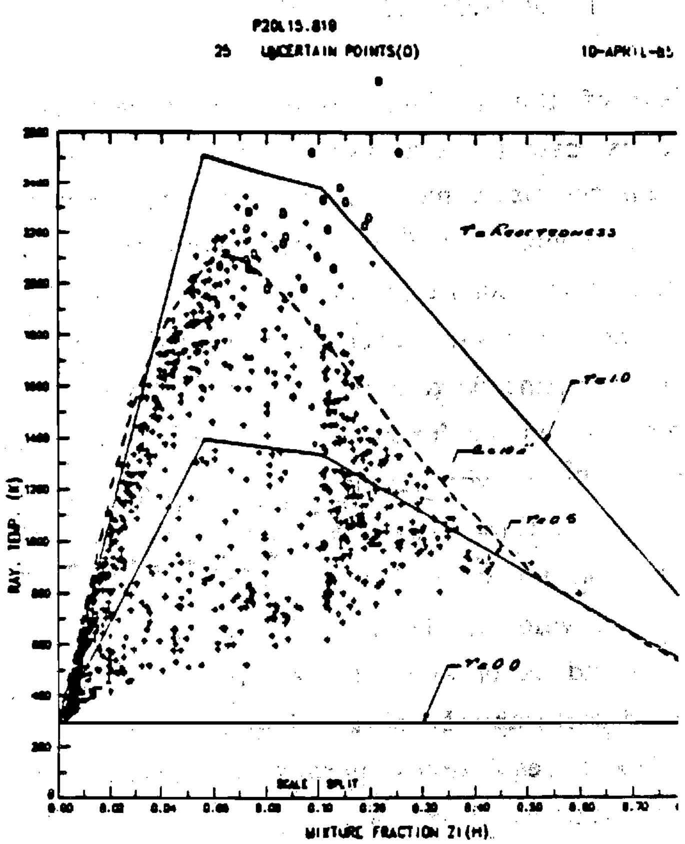

Fig. 16. Comparison of mixture fraction vs. temperature in a pilot flame stabilized CH_4 jet diffusion flame from Masri, Dibble and Bilger (private communication).

Further recommendations for future work include measurements of minor species (CO and H_2 in hydrocarbon flames and radial species in C0 and hydrocarbon flames) which provide more sensitive tests of combustion chemistry submodels. Finally, continuous time-resolved measurements and imaging experiments are needed that allow direct determination of length scales, two point correlations, gradients, and scalar dissipation.

REFERENCES

Ahlheim, M. and Gunther, R. (1979) Ionization measurements in free-jet-diffusion flames. Comb. Flame 36, 117.

Alber, J. E. and Batt, R. G. (1976) Diffusion limited chemical reaction in a turbulent shear layer. AIAA J. 14, 70.

Batt, R. G. (1977) Turbulent mixing of passive and chemically reacting species in a low-speed shear layer. JFM 82, 53.

Becker, H. A. and Liang, D. (1978) Visible length of vertical free turbulent diffusion flames. Comb. Flame 32, 115.

Bilger, R. W. (1980) Perturbation analysis of turbulent nonpremixed combustion. Comb. Sci. Tech. 22, 251.

Bilger, R. W. and Beck, R. W. (1975) Further experiments on turbulent jet diffusion flames. Fifteenth Symposium (Int). Comb., 541.

Bousgarbies, J. L. and Nerault, J. (1983) Concentration and velocity measurements in a turbulent reacting mixing layer. Flames, Lasers, Reactive Systems, (J. R. Bowen et al., eds.), Progr. Astron. & Aeron., 88, 105.

Breidenthal, R. (1978) Chemically reacting turbulent shear layer. AIAA J. 17, 310.

Breidenthal, R. (1981) Structure in turbulent mixing layers and wakes using a chemical reaction. JFM 109, 1.

Broadwell, J. E. (1982) A model of turbulent diffusion flames and nitric oxide generation, Part I. TRW Document No. 38515-6001-UT-00, EER Final Report.

Brown, G. L. and Roshko, A. (1974) On density effects and large structure in turbulent mixing layers. JFM 64, 775.

Cernansky, N. P. and Sawyer, R. F. (1974) NO and NO_2 formation in a turbulent hydrocarbon/air diffusion flame. Fifteenth Symposium (International) on Combustion, 1039.

Chigier, N. A. and Strokin, V. (1974) Mixing process in a free turbulent diffusion flame. Comb. Sci. Tech. 9, 111.

Correa, S. M., Drake, M. C., Pitz, R. W., Shyy, W. (1984) Prediction and measurement of a non-equilibrium turbulent diffusion flame. GE Research Lab Report 84-CRD-171. Twentieth Symposium (International) on Combustion.

Dibble, R. W., Kollmann, W. and Schefer, R. W. (1984) Conserved scalar fluxes measured in a turbulent nonpremixed flame by combined laser doppler velocimetry and laser Raman scattering. Comb. Flame 55, 307.

Drake, M. C., Bilger, R. W. and Starner, S. H. (1982) Raman measurements and conserved scalar modeling in turbulent diffusion flames. Nineteenth Symposium (International) on Combustion, 459.

Drake, M. C., Pitz, R. W., Correa, S. M. and Lapp, M. (1984a) Nitric oxide formation from Thermal and Fuel-bound nitrogen sources in a turbulent nonpremixed syngas flame. GE Research Lab Report 84-CRD-194.

Drake, M. C., Pitz, R. W. and Lapp, M. (1984b) Laser measurements on nonpremixed hydrogen-air flames for assessment of turbulent combustion models. AIAA Paper 84-0544, to be published AIAA J.

Drake, M. C., Pitz, R. W., Lapp, M., Fenimore, C. P., Lucht, R. P., Sweeney, D. W. and Laurendeau, N. M. (1984c) Measurements of super equilibrium hydroxyl concentrations in turbulent nonpremixed flames using saturated fluorescence. Twentieth Symposium (International) on Combustion.

Ebrahimi, I. and Kleine, R. (1976) The nozzle fluid concentration fluctuation field in round turbulent free jets and jet diffusion flames. Sixteenth Symposium (International) on Combustion. 1711.

Eickhoff, H. (1982) Turbulent hydrocarbon jet flames. Progr. Energy Comb. Sci. 8, 159.

El-Banhawy, Y., Hassan, M. A., Lockwood, F. C. and Moneib, H. A. (1983) Velocity and unburned hydrocarbon measurements in a vertical turbulent free jet diffusion flame. Comb. Flame 53, 145.

Godoy, S. (1982) Turbulent diffusion flame. Ph.D. Thesis, University of London.

Gunther, R. and Wittmer, V. (1981) The turbulent reaction field in a concentric diffusion flame. Eighteenth Symposium (International) on Combustion, 961.

Gunther, R. (1981) Flow turbulence and combustion. Ind. Chem. Eng. 21, 595.

Hawthorne, W. R., Weddell, D. S. and Hottel, H. C. (1949) Mixing and combustion in turbulent as jets. Third Symposium (International) on Combustion, 266.

Janicka, J. and Kollmann, W. (1978) Ein Rechenmodell fur reagierende turbulente Scherstromungen in chemischem Nichtgleichgewicht. Warme-Stoffubertragung 11, 157.

Janicka, J. and Kollmann, W. (1979) A two-variable formalism for the treatment of chemical reactions in turbulent H_2-air diffusion flames. Seventeenth Symposium (International) on Combustion, 421.

Janicka, J. and Kollman, W. (1982) The calculation of mean radical concentrations in turbulent diffusion flames. Comb. Flame 44, 319.

Jeng, S. -M., Chen, L. -D., and Faeth, G. M. (1982a) The structure of buoyant methane and propane diffusion flames. Nineteenth Symposium (International) on Combustion, 349.

Jeng, S. -M., Chen, L. -D. and Faeth, G. M. (1982b) Predictions and measurements of turbulence properties of buoyant diffusion flame. Eastern Sect. Comb. Inst., Atlantic City.

Jeng, S. -M. (1984) An investigation of structure and radiation properties of turbulent buoyant diffusion flames. Ph. D. Thesis, The Pennsylvania State University.

Johnston, S. C., Dibble, R. W., Schefer, R. W., Ashurst, W. T. and Kollmann, W. (1984) Laser measurements and stochastic simulations of turbulent reacting flows. AIAA Paper No. 84-0543, to be published in AIAA J.

Kent, J. H. and Bilger, R. W. (1977) The prediction of turbulent diffusion flame fields and nitric oxide formation. Sixteenth Symposium (International) on Combustion, 1643.

Komori, S. and Ueda, H. (1984) Turbulent effects on the chemical reaction for a jet in a nonturbulent stream and for a plume in a grid-generated turbulence. Phys. Fluids 27, 77.

Konrad, J. H. (1976) An experimental investigation of mixing in two-dimensional turbulent shear flows with applications to diffusion-limited chemical reactions. Project SQUID Techn. Rep. CI-8-PU.

Koochesfahani, M. M. (1984) Experiments on turbulent mixing and chemical reactions in a liquid mixing layer. Ph.D. Thesis, Caltech.

Lapp, M., Drake, M. C., Penney, C.M., Pitz, R. W. and Correa, S. (1983) Turbulent combustion experiments and modeling. GE Research Lab Report 83-SRD-049.

Lavoie, G. A., Schlader, A. F. (1974) A scaling study of NO formation in turbulent diffusion flames of hydrogen burning in air. Comb. Sci. Technol. 8, 215.

Lenz, W. and Gunther, R. (1980) Measurements of fluctuating temperature in a free-jet diffusion flame. Comb. Flame 37, 63.

Lewis, M. H. and Smoot, D. (1981) Turbulent gaseous combustion Part I: Local species concentration measurements. Comb. Flame 42, 183.

Lockwood, F. C. and Odidi, A. O. O. (1974) Measurement of mean and fluctuating temperature and of ion concentration in round free jet turbulent diffusion and premixed flames. Fifteenth Symposium (International) on Combustion, 561.

Lockwood, F. C. and Moneib, H. A. (1982) Fluctuating temperature measurements in turbulent jet diffusion flames. Comb. Flame 47, 291.

Mao, C. -P., Szekely, Jr., G. A. and Faeth, G. M. (1980) Evaluation of a locally homogeneous flow model of spray combustion. J. Energy 4, 78.

Masutani, S. M. (1985) An experimental investigation of mixing and chemical reaction in a plane mixing layer. Ph.D. Thesis, Stanford University and HTGL Report T-246

Mungal, M. G. (1983) Experiments on mixing and combustion with low heat release in a turbulent shear flow. Ph.D. Thesis, Caltech.

Onuma, Y. and Ogasawara, M. (1974) Studies on the structure of a spray combustion flame. Fifteenth Symposium (International) Combustion, 453.

Onuma, Y. and Ogasawara, M. (1977) An approach to the theoretical description of turbulent jet diffusion flames - Part I: Combustion model and calculation. Comb. Flame 30, 163.

Page, F. M., Roberts, W. G. and Williams, H. (1974) An experimental study of the interaction of chemical kinetic effects and turbulent flow in flames. Fifteenth Symposium (International) on Combustion, Tokyo, 617.

Peters, N. and Donnerhack, S. (1981) Structure and similarity of nitric oxide production in turbulent diffusion flames. Eighteenth Symposium (International) on Combustion, 33.

Razdan, M. K. and Stevens, J. G. (1983) Analysis of turbulent diffusion flames using unique relationships from laminar flame calculations. AIAA Paper 83-1363, Nineteenth Joint Propulsion Conference, Seattle.

Razdan, M. K. and Stevens, J. G. (9185) CO/Air turbulent diffusion flame: Measurements and modelling. Comb. Flame 59, 289.

Rebollo, M. (1973) Analytical and experimental investigation of a turbulent mixing layer of different gases in a pressure gradient. Ph.D. Thesis, Caltech.

Roberts, P. T. and Moss, J. B. (1981) A wrinkled flame interpretation of the open turbulent diffusion flame. Eighteenth Symposium (International) on Combustion, 941.

Schoenung, S. M. and Hanson, R. K. (1982) Temporally and spatially resolved measurements of fuel mole fraction in a turbulent CO diffusion flame. Nineteenth Symposium (International) on Combustion, 449.

Sherikar, S. V. and Chevray, R. (1981) A chemically reacting plane mixing layer. Third Symposium Turbulent Shear Flows, Davis, 3.7.

Takagi, T., Ogasawara, M., Daizo, M. and Tatsumi, T. (1976) NO_x formation from nitrogen in fuel and air during turbulent diffusion combustion. Sixteenth Symposium (International) on Combustion, 181.

Takagi, T., Ogasawara, M., Fujii, K. and Daizo, M. (1979) A study on nitric oxide formation in turbulent diffusion flames. Fifteenth Symposium (International) on Combustion, 1051.

Takagi, T., Shin, H. -D. and Ishio, A. (1980) Local laminarization in turbulent diffusion flame. Comb. Flame 37, 163.

Takagi, T., Shin, H. -D. and Ishio, A. (1981) A study of the structure of turbulent diffusion flame: Properties of fluctuations of velocity temperature, and Ion concentration. Comb. flame 41, 261.

Wallace, A. K. (1981) Experimental investigation on the effects of chemical heat release in the reacting turbulent plane shear layer. Report AFOSR-TR-84-0650, University of Adelaide, Australia.

You, H. -Z., and Faeth, G. M. (1982) Buoyant axisymmetric turbulent diffusion flames in still air. Comb. Flame 44. 261.

CHAPTER 5

PREMIXED COMBUSTION

P. A. Libby, S. Sivasegaram and J. H. Whitelaw

LITERATURE SEARCH

Many measurements have been made in premixed flames varying in complexity from the visual observation of flammability and stability limits to the detailed consideration of local turbulence characteristics. Such measurements are considered in the following paragraphs which divide them according to the geometrical configuration and summarize the properties measured and the equivalence ratio and Reynolds number ranges of the experiments.

The emphasis in the measurements is on local flow properties including velocity, temperature and species concentrations while important characteristics such as burning velocity, heat release rates and flammability limits tend to be overlooked, perhaps because their dependence upon chemical factors makes them difficult to calculate a priori. With laminar flow the average rate of chemical reaction can be readily deduced from the thickness of a reaction region and the burning velocity. Where turbulence is involved, such measurements are impossible and recourse is made to stirred reactors in which premixed reactants are supposed to mix instantaneously with hot burned gases. The resulting reaction is presumed to be homogeneous and to be chemically controlled. The experiments of Longwell, Frost and Weiss (1953) and Clarke et al (1962) are examples of this type of investigation which, as a whole, reveals a dependence upon the reactor as well as on variables such as pressure and fuel. It is evident, therefore, that apparently simple properties such as reaction rate are not well documented and cannot provide a satisfactory test of calculation methods for chemically-controlled turbulent flames.

It might equally be expected that flammability limits, such as those associated with bluff-body stabilized flames, could provide useful limiting tests of models. Lean and rich extinction limits of fuel-air mixtures of Wright (1959), Filippi and Mazza (1962), Broman and Zukoski (1962), Heitor et al (1984) and others could serve in this way. Unfortunately, as with mean reaction rates, the prediction of chemically-controlled turbulent reaction is still outside the capabilities of present models and future developments of calculation methods must extend from physically-controlled flames towards those involving chemical control. A first step in this direction involves the incorporation of statistical information on the rates of strain to which laminar flamelets are subjected by the turbulence, since we know from the theory of premixed laminar flames (cf. Libby et al 1983) that, if the rate of strain is excessive, no creation of product takes place. A turbulent flame with an "excessive number" of such flamelets presumably cannot exist. It remains to determine the value of that number and its dependence on aerothermochemical parameters.

The two major classes of premixed flows are those which involve reactants issuing from a pipe with the flame stabilized on its rim and those with reactants flowing in a pipe with a bluff-body flame stabilizer. In the former case, the equivalence ratio is constant only in the region away from the outer edge of the jet flame and in the latter the system is premixed only within the length of the pipe. In both cases the flow may exhibit regions of recirculation or may conform to the usual assumptions of boundary-layer flows and, since this can be of importance to the appraisal of calculation methods, experiments considered under these two headings are subdivided according to the nature of the equations which are likely to be required to represent them. This classification is imperfect, particularly since one arrangement can tend to the other and because two-dimensional, plane geometrical configurations have also been investigated; the experiments conducted in plane flows are included in the class to which they appear more closely linked.

A third class of flows comprises configurations where the premixed flame is submerged in an opposing flow involving premixed reactants, products or air.

Some flames with swirling flow have been investigated but are not included in the tables to follow in view of their unsuitability for the present purpose. Syred and Beer (1973), for example, examined the stability of an open premixed swirling jet flame. Also, swirl-stabilized, confined premixed flames in a 460mm diameter furnace of 1.4m length and 225mm diameter furnace of 0.9m length have been examined by Beltagui and Maccallum (1976). Although their study includes profiles of the three velocity components, temperature and CO_2 concentration, it was undertaken mainly to determine the overall behavior of the furnace and the measurements are not suitable for the detailed evaluation of combustion models. Preliminary calculations of these and other furnace flows are reported by Khalil et al (1975) who show that it is comparatively easy to represent the general features of such flows but much more difficult to determine details with an accuracy approaching that of high-quality measurements.

The experiments of Table 1a involve unconfined flows downstream of single or concentric pipes with the particular arrangements shown. In all cases the equivalence ratio of the premixed fuel and air is constant in the central core of the flame while the outer edge is contaminated by transport of air to and from the premixed reactants and products. As a consequence, detailed calculations of the entire flame characteristics require consideration of premixed and diffusion controlled combustion unless the reactants are fuel lean. The fuels are mainly methane and propane with natural gas and L. P. gas in two cases. Although the burner rim thickness is not always specified, the largest ratio of burner rim thickness to pipe inside diameter was 0.125 for the 8mm burner of Yanagi and Mimura (1981) and the 12mm burner of Kilham and Kirmani (1979). In larger burners this ratio reduces to around 0.06. No flame is described as lifted from the burner rim although a hydrogen stabilizing flame is used in several cases. All flows may be represented by boundary-layer equations except perhaps in the vicinity of the burner rim and assumptions can readily be made for this region and their influence quantified. Buoyancy appears to play an important role in this class of flows and should be taken into account in predictions. Nine of the references provide measurements of a vector and a scalar as considered further below.

Table 1a

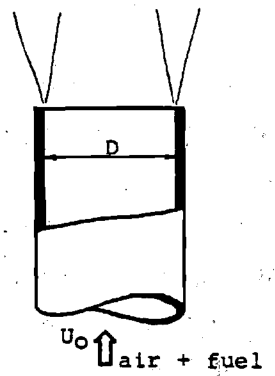

Sommer & Stojannof (1979)
Suzuki, Hirano & Tsuji (1979 a,b)
Moss (1980)
Yule, Ventura & Chigier (1981)
Shepherd & Moss (1982,1983)
Suzuki & Hirano (1983)

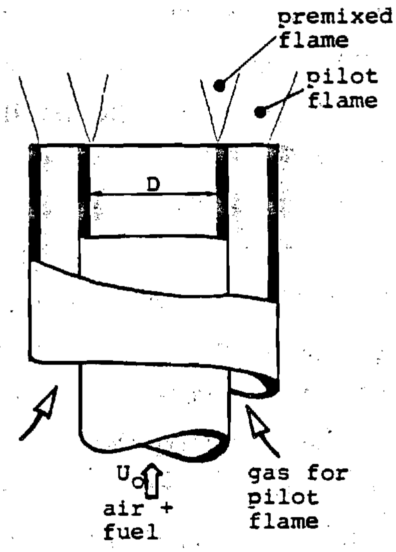

Durst & Kline (1973)
Yoshida & Tsuji (1978,1982)
Kilham & Kirmani (1979)
Yoshida & Gunther (1980,1981)
Yoshida (1981,1983)
Yanagi & Mimura (1981)
Tanaka & Yanagi (1983)

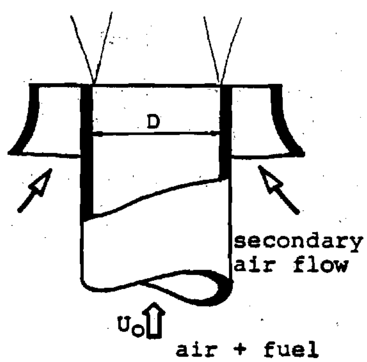

Matsumoto, Nakajima, Kimoto, Noda & Maeda (1982)
Noda, Kimoto, Matsumoto, Nakajima & Kawai (1983)

Table 1a

		Measurements Reported				
Reference	Flow	Velocity	Temperature	Other	Probe characteristics	Comments
Durst & Kline (1973)	30mm jet natural gas-air $\Phi = 1$ $U_o \sim 8$m/s T_o ambient $u_o'/U_o \sim 5\%$ $Re_D \sim 16{,}000$	$\bar{U}, \bar{v}, u', v'$. $\overline{uv}$: one centerline & 6 transverse profiles	-	-	LDV, forward scatter 0.11mm^2 x 1.5mm probe volume	signal rate around 600Hz
Yoshida & Tsuji (1978)	10mm jet C_3H_8 - air $\Phi = 0.724$ $U_o = 9.07$m/s T_o - ambient $u_o'/U_o \sim 2\%$ $Re_D \sim 6000$	$\bar{U}$, u': one centerline & 3 transverse profiles	$\bar{T}, \theta'$, pdfs : one centerline & 3 transverse traverses	-	LDV, forward scatter 50 μm bare wire thermocouple	LDV signal rate low τ_T 40 - 400ms
Kilham & Kirmani (1979)	10mm jet CH_4-air; C_3H_8-air C_2H_4-air; C_3H_8-air $\Phi = 1.0, 0.8$ $U_o \sim 30$ m/s T_o - ambient $Re_D \sim 20{,}000$	$\bar{U}$, u': centerline profiles	-	turbulent flame speeds	LDV, forward scatter probe volume: 0.144mm x 2.5mm	8 flames (involving the use of 3 turbulence generators)

Table 1a

		Measurements Reported				
Reference	Flow	Velocity	Temperature	Other	Probe characteristics	Comments
Sommer & Stojannof (1979)	14mm jet CH_4 - air $\Phi = 1$ $U_o \sim 11.5$ m/s T_o - ambient $Re_D \sim 10{,}800$	$\bar{U}$: one centerline profile & 8 transverse profiles	$\bar{T}$: one centerline profile & 9 transverse profiles	CH_4, CO_2, O_2, H_2O composition: centerline profile	LDV, forward scatter temperature probe with 250 μm spatial resolution somewhat large sampling probe 0.25mm bore	
Suzuki, Hirano & Tsuji (1979a)	54mm jet C_3H_8 - air $\Phi \sim 1$ $U_o \sim 4.5$m/s T_o - ambient $u_o'/U_o \sim 6.3\%$ $Re_D \sim 8000$	-	-	mean ion current $\bar{I}$: contours	pair of 0.1mm Pt wires as ion current sensors	

Table 1a

Reference	Flow	Velocity	Temperature	Other	Probe characteristics	Comments
		Measurements Reported				
Suzuki, Hirano & Tsuji (1979b)	54mm jet C_3H_8 - air Φ = 1.1 U_o = 1.65, 4.5m/s T_o - ambient $u_o'/U_o \sim 2\%, 5.7\%, 6.3\%$ $Re_D \sim$ 6000 - 16,000	-	-	photometric and relative light intensities: centerline profiles & contours	-	one flame at $\bar{U}_o$ = 1.64m/s two flames at $\bar{U}_o$ = 4.5m/s
Moss (1980)	50mm jet LPG (70% C_3H_8 + 30% C_3H_6) - air Φ - not specified $U_o \sim$ 4m/s T_o - ambient $u_o'/U_o \sim$ 5.5% $Re_D \sim$ 13,000	$\bar{U}$,u': traverse parallel to axis, across flame front; conditional pdfs of U	-	scattered light intensity (mean & rms) reaction progress variable - velocity: joint pdfs	LDV, forward scatter probe volume 0.2 x 1.2mm; Mie scatter	

Table 1a

Measurements Reported

Reference	Flow	Velocity	Temperature	Other	Probe characteristics	Comments
Yoshida & Gunther (1980)	40mm jet natural gas-air $\Phi = 0.8, 0.9$ $U_o = 5.44$m/s T_o - ambient $u_o'/U_o \sim$ 4-9% $Re_D \sim$ 14,500	-	$\bar{T}, \bar{\theta}$: 5 transverse profiles; pdf; one transverse traverse; power spectra		50mm bare wire thermocouple	4 flames, temperature measurements in detail for each of 3 flames $\tau_T \sim$ 40-400ms
Yoshida & Gunther (1981)	40mm jet natural gas-air $\Phi = 0.8$ $U_o = 5.44$m/s T_o - ambient $u_o'/U_o \sim$ 6% $Re_D \sim$ 14,500	-	$\bar{T}, \theta'$: one centerline & 3 transverse profiles one transverse pdf traverse	ion current $(\bar{I}, i')$: 3 transverse profiles one transverse pdf traverse	50 μm bare-wire thermocouple 0.6mm Pt bead ion current probe	some temperature measurements reported for $\Phi = 0.85, 0.9$ $\tau_T \sim$ 20ms
Yoshida (1981)	40mm jet natural gas-air $\Phi = 0.8$ $U_o = 5.44$m/s T_o - ambient $u_o'/U_o \sim$ 6% $Re_D \sim$ 14,500	$\bar{U}, \bar{V}, u', v'$ $\overline{uv}$: 4 transverse profiles; velocity vector field plot	$\bar{T}, \theta'$: one centerline & 3 transverse profiles. T contour		LDV, forward scatter 50 μm bare wire thermocouple	$\tau_T \sim$ 20ms

Table 1a

Reference	Flow	Velocity	Temperature	Other	Probe characteristics	Comments
		Measurements Reported				
Yanagi & Minura (1981)	8mm jet natural gas-air $\Phi = 0.6$ $U_o = 6.7$ m/s T_o - ambient $Re_D \sim 3600$	$\bar{U}, u'$: transverse profiles and pdfs of U at one station	$\bar{T}, \theta'$: transverse profiles and pdfs of T at one station	$\overline{u\theta}$ correlation	LDV, forward scatter probe volume 0.2mm x 2mm 50 μm bare-wire thermocouple	LDV signal rate 1000 s^{-1} $\tau_T \sim$ 30-40ms
Yule, Ventura & Chigier (1981)	25.4mm jet C_3H_8 - air $\Phi = 2.2$ to 8.7 $U_o \sim$ 3-9 m/s T_o - ambient $u_o'/U_o \sim 0.1\%$ $Re_D \sim$ 5000-15,000	-	-	ion current ($\bar{I}, i'$): contours, signal spectra at 2 locations	0.35mm Pt wire 1.5mm long and a pair of 0.1mm; Pt wires used as ion current probes	5 flames reported

Table 1a

Reference	Flow	Velocity	Temperature	Other	Probe characteristics	Comments
		Measurements Reported				
Matsumoto, Nakajima, Kimoto, Noda & Maeda (1982)	10mm jet with 100mm secondary air jet C_3H_8 - air $\Phi = 1.1$ $U_o \sim 3$m/s T_o - ambient (secondary air flow at 0, 0.13, 0.25, 0.37 m/s) $u_o'/U_o \sim 2\%$ $Re_D \sim 2000$	$\bar{U}, \bar{V}, u', v'$, pdfs of U: transverse traverses at 10 stations. (one flame)	$\bar{T}$: 10 transverse profiles	shadowgraphs	LDV, forward scatter 73.5 μm bare wire thermocouple	measurement of temperature fluctuation frequencies over wide range of flow conditions $\tau_T \sim 100$ms
Shepherd & Moss (1982)	50mm jet C_3H_8 - air $\Phi = 1.6$ $U_o \sim 2.8$ m/s T_o - ambient $u_o'/U_o \sim 11\%$ $Re_D \sim 9300$	$\bar{U}, u'$: traverse parallel to axis; U, U_r, U_p pdfs: one location	-	reaction progress variable: distribution along velocity traverse	LDV, forward scatter, probe volume 0.2 x 1.2mm; Mie scatter	

Table 1a

Reference	Flow	Velocity	Temperature	Other	Probe characteristics	Comments
			Measurements Reported			
Yoshida & Tsuji (1982)	10mm jet C_3H_8 - air $\Phi = 0.68$ $U_o \sim 4, 8$m/s T_o - ambient $u_o'/U_o \sim 2.-8\%$ $Re_D \sim 2600\text{-}5300$	-	$\bar{T}, \theta'$: 3 transverse profiles; one transverse pdf traverse	schlieren pictures (4 flames) time scale of burnt and unburnt gas	50 μm bare-wire tehrmocouple	4 flames; detailed report of one flame only ($U_o \sim 8$m/s) $u_o'/U_o \sim 2\%$) τ_T 40-400ms
Shepherd & Moss (1983)	50mm jet C_3H_8 - air $\Phi = 1.6$ $U_o = 3.05$m/s T_o - ambient $u_o'/U_o \sim 8.6\%$ $Re_D \sim 10{,}000$	$\bar{U}$: traverse parallel to axis across flame front	-	reaction progress variable: distribution along velocity traverse	LDV, forward scatter probe volume, 0.2mm x 1.2mm Mie scatter: probe volume, 0.2mm x 1.2mm	

Table 1a

		Measurements Reported				
Reference	Flow	Velocity	Temperature	Other	Probe Characteristics	Comments
Noda, Kimoto, Matusmoto, Nakajima & Kawai (1983)	10mm jet with 100mm secondary air jet C_3H_8 - air $\Phi = 1.1$ $U_o \sim 3$m/s $T_o \sim$ ambient (secondary air flow at 0.25 m/s) $Re_D \sim 2000$	$\bar{U},\bar{V},u',v',\overline{uv}$: two transverse traverses	-	shadowgraph, direct photograph of flame	LDV, forward scatter	
Suzuki & Hirano (1983)	54mm jet C_3H_8 - air $\Phi = 1.1$ $U_o \sim 4.5$m/s T_o - ambient $u_o'/U_o \sim 6.3\%$ $Re \sim 16{,}000$	-	-	ion current $\bar{I}, i'$: 4 transverse profiles	pair of ion current probes, 0.1mm Pt wire	

8

Table 1a

Reference	Flow	Measurements Reported			Probe Characteristics	Comments
		Velocity	Temperature	Other		
Tanaka & Yanagi (1983)	10mm jet natural gas-air = 0.6 U_o = 4.89 m/s T_o - ambient u_o/U_o 6% Re 3000	U,u ,V,v : contours	T, : contours	u , v : One centerline & one transverse profile	LDV, forward center 50 m bare-wire thermocouple	simultaneous temperature and velocity measurements T 25ms
Yoshida (1983)	10mm jet; 15mm jet C_3H_8 - air = 0.6-0.72 U_o 3, 4, 8 m/s T_o - ambient u_o/U_o 3-9% Re 2600-5200	-	pdfs one transverse traverse (one flame)	schlieren picture of one flame	50 m bare-wire thermocouple	7 flames studied

The measurements reported by Moss (1980) and Shepherd and Moss (1982, 1983) make use of a 50mm diameter jet with bulk-flow velocities of 2.8, 3.05 and 4 m/s and an equivalence ratio of 1.6. The results are obtained with a combination of laser-Doppler velocimetry and nephelometry and emphasize the region of the turbulent flame. Possible errors associated with the measurement techniques are not explored but it is evident from the results that counter-gradient diffusion of the reaction progress variable exists and should be represented in any combustion model. The data are obtained to study processes within the flame and thus do not extend to the entire flow field.

The early results of Yosjida and Tsuji (1978) are obtained with 10mm diameter jets and extended to a 40mm diameter jet by Yoshida (1981). The results of Yoshida (1981) appear to provide a possible basis for the evaluation of calculation methods in that the development of the flame is represented by measurements at three axial stations. On the other hand, velocities of the order of 3m/s and a 10mm diameter burner tube imply an exit Reynolds number of 2000 and, with the considerable reduction of kinematic viscosity with temperature, the resulting flames are unlikely to be more than weakly turbulent.

Sommer and Stojanoff (1979) provide data on methane-air flames in terms of profiles of mean velocity, temperature and concentrations. The velocities and mass concentrations are likely to be closer to density weighted mean values than to unweighted values and the mean temperatures are subject to some uncertainty since the size of the thermocouple is not given. Although the pipe exit Reynolds number is of the order of 14,000, it is unlikely that this flow can be considered to be controlled by turbulent transport. Matsumoto et al (1982) provide detailed information for one flame obtained with a 10mm diameter jet with a bulk velocity of 3m/s. Tanaka and Yanagi (1983) also report measurements obtained with a 10mm diameter jet but with a velocity of 4.9m/s. They include values of velocity-temperature correlations which suggest counter-gradient diffusion but again the low values of local Reynolds number imply that turbulent fluxes may be comparatively small.

The presence of a large rms value of velocity fluctuations is treated by many authors as evidence of turbulent flow but the upstream Reynolds numbers, based on pipe diameter, are less than around 15,000 in all the flames of Table 1a. Moreover, the rise in temperature downstream of the burner exit implies that the effective Reynolds number falls by a factor of 5 or so to yield flows which are laminar or, at best, transitional. These large velocity fluctuations observed in some flames with low Reynolds numbers may well result from instabilities rather than turbulence. Certainly, turbulent flow cannot be presumed and measurements of energy spectra are to be encouraged.

The flames of Table 1b are similar to those of Table 1a in that the premixed fuel and air emerge from a pipe or nozzle. In this case, however, each flame is stabilized by a small-diameter rod located normal to the axis of the jet and along a diameter. A range of hydrocarbon fuels are investigated, particularly by Dandekar and Gouldin (1982), and the jet diameters are sufficiently large so that a constant value of the equivalence ratio is maintained for a large number of rod diameters downstream. None of the investigations cited in Table 1b include measurements of vector and scalar quantities but those of Smith and Gouldin (1979) and Dandekar and Gouldin (1982, 1984) are obtained in the same flow configurations and, together, provide values of mean temperature and velocity, though the latter are restricted to one axial plane. The mean temperature measurements of Smith and Gouldin are likely to be subject to errors of the order of 100K and the rms temperature is unlikely to be reliable in view of the large size of the temperature probe. As with the flow in the vicinity of a burner rim, that close to the stabilizing rod is difficult to analyze.

The various experiments of Table 1b relate to flows which may involve relatively weak turbulence. In several cases, the pipe-exit velocities are so low as to raise doubts as to the structure of the flow emerging from the pipe and, with the exception of the flow of Smith and Gouldin, the Reynolds numbers based on the rod diameter are less than 500.

The flows of Table 1c are nearly two-dimensional and correspond to a mixing region formed by premixed reactants and hot burned products flowing

Table 1b

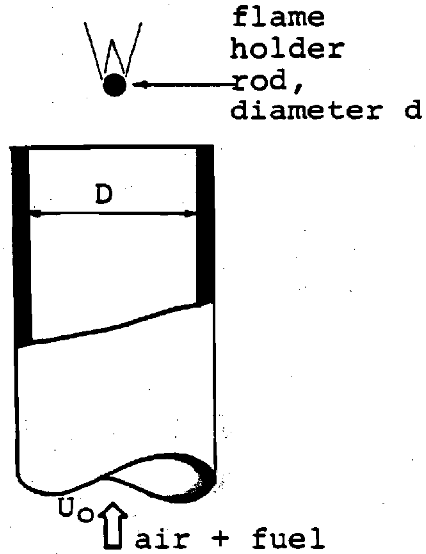

Smith & Gouldin (1977)

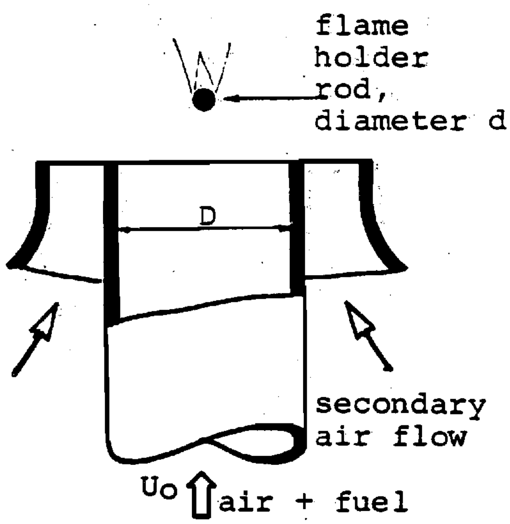

Bill, Namer, Talbot, Cheng & Robben (1981)

Bill, Namer, Talbot & Robben (1982)

Cheng & Ng (1983)

Dandeker & Gouldin (1983)

Cheng (1983)

Cheng, Talbot & Robben (1984)

Namazian, Talbot & Robben (1984)

Gouldin & Dandekar(1984)

Table 1b

Reference	Flow	Measurements Reported			Probe Characteristics	Comments
		Velocity	Temperature	Other		
Smith & Gouldin (1977)	1.25mm rod across 50mm jet CH_4 - air Φ = 0.75, 0.85 U_o = 7.5, 14m/s T_o - ambient $u_o'/U_o \sim$ 2, 3, 5.5% $Re_D \sim$ 25,000 - 46,000 $Re_d \sim$ 600-1150	-	$\bar{T}$, θ: 3 transverse profiles (each of 3 flames)	flame speed data from hot film measurements	125 μm SiO_2 coated thermo- couple for T; 75 μm bare-wire thermocouple for θ'. hot film sensor diameter 25 μm	frequency response of uncompensated thermocouple 3Hz
Bill, Namer, Talbot, Cheng & Robben (1981)	1mm rod across 51mm jet 102mm secondary air jet C_2H_4 - air Φ = 0.55, 0.75 U_o = 2.45-6.8m/s T_o - ambient $u_o'/U_o \sim$ 3.5 - 5% $Re_D \sim$ 8,300 - 23,000 $Re_d \sim$ 160-460	$\bar{U}$, u': up to 4 transverse profiles per flame, one local pdf	-	density ($\bar{\rho}$, ρ'): one transverse profile, one local pdf	LDV, forward scatter 0.15mm probe volume Rayleigh scatter from 40 mm waist	5 flames LDV data rate 5000 - 20000s^{-1} Rayleigh scatter photon count 10^8 s^{-1}

Table 1b

Measurements Reported

Reference	Flow	Velocity	Temperature	Other	Probe characteristics	Comments
Bill, Namer, Talbot & Robben (1982)	1mm rod across 51mm jet, 102 secondary air jet C_2H_4 - air Φ = 0.5 - 0.75 U_o = 2.50 - 6.84m/s T_o - ambient u_o'/U_o 4% $Re_D \sim$ 8,500 - 23,000 $Re_d \sim$ 170-460	-	-	density ($\bar{\rho}$, ρ', pdf): transverse traverse at one station	Rayleigh scatter from 40mm	results reported for Φ = 0.75 only density moments evaluated from Rayleigh signals and not the pdfs
Cheng & Ng (1983)	1mm rod across 51mm jet, 102mm secondary air jet C_2H_4 - air Φ = 0.66 - 0.8 $U_o \sim$ 5-7m/s T_o - ambient $u_o'/U_o \sim$ 4-8.5% $Re_D \sim$ 17,000-24,000 $Re_d \sim$ 330-480	mean velocity vector field (3 flames) $\bar{u}$, v', $\overline{uv}$: some transverse profiles & pdfs of U	-	schlieren pictures (5 flames)	LDV, forward scatter 0.15mm probe volume	6 flames (different flow rates, levels of turbulence & equivalence ratios)

Table 1b

		Measurements Reported				
Reference	Flow	Velocity	Temperature	Other	Probe characteristics	Comments
Dandekar & Gouldin (1983)	1.25mm rod across 50mm jet, 76mm outer jet C_3H_8-air, C_2H_4-air $\Phi = 0.65 - 1.0$ $U_o \sim 7.5$m/s T_o - ambient $Re_D \sim$ 25,000 $Re_d \sim 500$	$\bar{U}, u'$: one transverse profile each (8 flames) $\bar{V}, \bar{W}, v', w'$: one transverse profile each (one flame)	-	-	LDV, forward scatter	8 flames (different fuels, air fuel ratios, and turbulence levels) LDV data rate 400 s^{-1} in cold flow
Cheng (1983)	1mm rod across 50mm jet 100mm secondary air jet C_2H_4 - air $\Phi = 0.7$ $U_o \sim 5.5$ m/s T_o - ambient $u_o'/U_o \sim 5\%$ $Re_D \sim$ 18,500 $Re_d \sim$ 370	$\bar{U}, \bar{V}, u', v', \overline{uv}$: conventional & (unburnt) conditional values: 6 transverse profiles	-	-	2-color LDV forward scatter silicon oil seeding for conditioned data and Al_2O_3 seeding for unconditioned data	signal rate 5 kHz (unconditioned) 0.6 - 2kHz (covalidated data)

Table 1b

Reference	Flow	Velocity	Temperature	Other	Probe characteristics	Comments
		Measurements Reported				
Cheng, Talbot & Robben (1984)	1mm rod across 50mm jet, 100mm secondary air jet C_2H_4-air, CH_4-air $\Phi = 0.7, 0.83$ $U_o \sim 5.5$m/s T_o - ambient $u_o'/U_o \sim 5\%, 7\%$ $Re_D \sim 18{,}500$ $Re_d \sim 370$	k_{max}, its position & associated $\overline{uv}$ and conditioned components of k_{max} & $\overline{uv}$.	-	-	2 color LDV forward scatter; silicon oil seeding for conditional data and Al_2O_3 seeding for unconditional data	4 flames
Gouldin & Dandekar (1984)	1.25mm rod across 50mm jet, 75mm secondary air jet. CH_4 - air $\Phi = 0.8$ $U_o \sim 4$m/s T_o - ambient $Re_D \sim 13{,}500$ $Re_d \sim 270$	$\bar{U}, u', \bar{V}, v'$: two transverse profiles	-	density ($\bar{\rho}, \rho'$, pdfs): two transverse traverses	LDV forward scatter Rayleigh scatter from 0.1mm waist	

Table 1b

		Measurements Reported				
Reference	Flow	Velocity	Temperature	Other	Probe characteristics	Comments
Namazian, Talbot & Robben (1984)	1mm rod across 50mm jet 100mm secondary air jet. C_2H_4 - air $\Phi = 0.6, 0.8$ $U_o \sim 7$m/s $T_o \sim$ ambient $Re_D \sim 23{,}000$ $Re_d \sim 460$	-	-	density (ρ, ρ', pdf)	two-point Rayleigh scatter	3 flames

Table 1c

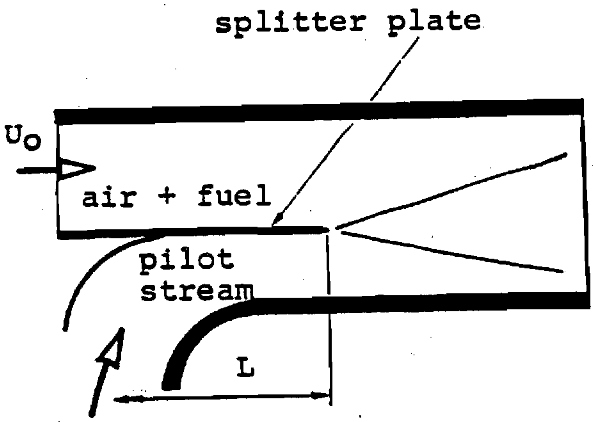

Borghi & Moreau (1977)
Moreau & Boutier (1977)
Moreau & Labbe (1978)
Moreau (1981)
Keller & Daily (1983)
Daily & Lundquist (1984)
Shepherd & Daily (1984)

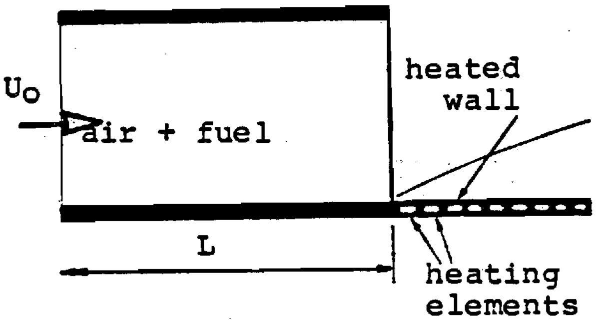

Cheng, Bill & Robben (1981)
Ng, Cheng, Robben & Talbot (1982)

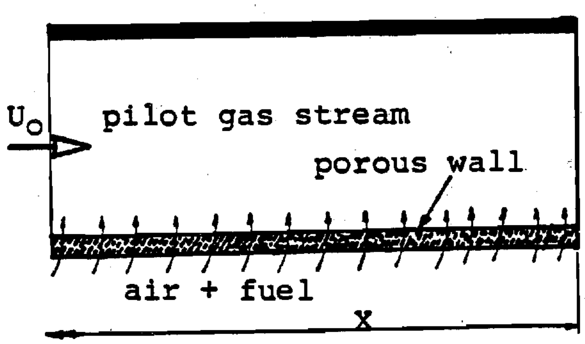

Meunier, Champion & Bellet (1983)

Table 1c

Measurements Reported

Reference	Flow	Velocity	Temperature	Other	Probe Characteristics	Comments
Borghi & Moreau (1977)	100mm square duct, 20mm thick pilot stream. CH_4 - air $\Phi = 0.84$ $U_o \sim 68$m/s $T_o \sim 600$K (pilot stream: 130m/s, 2000K) $Re_L > 1,000,000$	-	$\bar{T}$: contours	O_2, N_2, CH_4, CO, CO_2, H_2 composition: contours	pneumatic, oil-cooled gas sampling probe	splitter plate dimensions not specified
Moreau & Boutier (1977)	100mm square duct, 20mm thick pilot stream. CH_4 - air $\Phi = 0.8$ $U_o \sim 65$m/s $T_o \sim 600$K (pilot stream: 65, 130m/s; 2000K $u_o'/U_o \sim$ 7-10% $Re_L > 1,000,000$	$\bar{U}$, u': 8 transverse profiles per flame; U exit profiles compared for 3 levels of turbulence	-	CH_4 composition: 4 profiles (one flame)	LDV, forward scatter probe volume 0.13mm x 0.5mm pneumatic, oil-cooled gas sampling probe	2 flames (for 2 velocities of pilot stream) See Borghi & Moreau (1977) above.

Table 1c

Reference	Flow	Measurements Reported			Probe Characteristics	Comments
		Velocity	Temperature	Other		
Moreau & Labbe (1978)	100mm square duct, 20mm thick pilot stream. CH_4 - air $\Phi = 0.8$ $U_o \sim 70$ m/s $T_o \sim 600K$ (pilot stream 130 m/s, 2000K) $Re_L > 1,000,000$	$\bar{U}, \bar{V}, u', v'$ pdfs of U: 8 transverse traverses	-	-	LDV forward scatter probe volume 0.13mm x 0.5mm	See Borghi & Moreau (1977) above.
Moreau (1981)	100mm square duct, 20mm thick pilot stream. CH_4 - air $\Phi = 0.8$ $U_o \sim 65$m/s $T_o \sim 600K$ (pilot stream: 65, 135m/s; 2000K) $u_o'/U_o \sim 8\%$ $Re_L > 1,000,000$	$\bar{U}, u'$, pdfs: 3 or more transverse traverses (2 flames)	pdfs	-	LDV, forward scatter temperature measured using emission at CO_2 wave length	temperature measurements for test purposes only. See Borghi & Moreau (1977) above.

Table 1c

		Measurements Reported				
Reference	Flow	Velocity	Temperature	Other	Probe Characteristics	Comments
Cheng, Bill & Robben (1981)	boundary layer on 25mm wide, open heated wall H_2 - air $\Phi = 0.1, 0.2$ $U_o \sim$ 18-22m/s T_o - ambient $T_{wall} \sim$ 1100 to 1300K $u_o'/U_o \sim 0.5\%$ $Re_L \sim 100{,}000$	$\bar{U}, u'$: one transverse profile	-	$\bar{\rho}$, ρ', pdf: one transverse traverse (2 flame)	LDV, forward scatter Rayleigh scatter	LDV signal rate 500-1000 s^{-1}
Ng, Cheng, Robben & Talbot (1982)	boundary layer on 100mm wide, open heated wall C_2H_4 - air $\Phi = 0.35$ $U_o \sim$ 10.7m/s T_o - ambient T_{wall} - 1250K $Re_L \sim 250{,}000$	$\bar{U}, \bar{V}, u', v', \overline{uv}$: 3 transverse profiles; boundary layer integral parameters	-	schlieren pictures; $\bar{\rho}$: 3 transverse profiles	LDV, forward scatter, Rayleigh scatter from 100 μm waist	LDV signal rate 3000 s^{-1}

Table 1c

Reference	Flow	Velocity	Temperature	Other	Probe Characteristics	Comments
		Measurements Reported				
Meunier, Champion & Bellet (1983)	mixture injected along porous wall of 100mm square channel. C_3H_8 - air $\Phi \gtrsim 1$ $U_o \sim$ not specified injection rate 1%, 1.4% $T_o \sim 1370K$ $T_{mixture}$ - 290K $Re_x \sim 50{,}000$	$\bar{U}, u'$: transverse profile at one station	$\bar{T}$: transverse profile at one station	-	LDV, forward scatter	2 flames
Keller & Daily (1983)	57mm high x 122mm wide duct, premixed/pilot streams of equal thickness C_3H_8 - air Φ = 0, 0.2, 0.4, 0.6, 0.8 $U_o \sim$ 15m/s T_o = 293K (pilot stream: $\sim$ 5m/s, 117K $Re_L \sim$ 1,000,000	$\bar{U}, \bar{V}, \overline{uv}$: transverse profiles (4 flames); boundary layer parameters	-	schlieren pictures and direct photographs of flame	2-color LDV forward scatter	strong shear flow; splitter plate boundary layer displacement thickness around 1mm for premix flow and around 0.5mm for pilot flow

Table 1c

Measurements Reported

Reference	Flow	Velocity	Temperature	Other	Probe Characteristics	Comments
Daily & Lundquist (1984)	57mm high x 122mm wide duct. premixed/pilot streams of equal thickness C_3H_8 - air Φ = 0, 0.2, 0.4, 0.6, 0.8 $U_o \sim$ 15m/s T_o = 293K (pilot stream: $\sim$ 5m/s, 1170K $Re_L \sim$ 1,000,000	-	-	schlieren pictures (side and plan view)	-	shows the presence of organized 3-dimensional structures; see Keller & Daily (1983) above.
Shepherd & Daily (1984)	57mm high x 122mm wide duct, premix and pilot streams of equal thickness C_3H_8 - air Φ = 0.6 $U_o \sim$ 15m/s T_o = 293K (pilot stream $\sim$5m/s, 1170K) $Re_L \sim$ 1,000,000	-	-	$\bar{\rho}$, pdfs of ρ : 2 transverse traverses	Rayleigh scatter from 300 μm x 1mm probe volume	see Keller & Daily (1983) above

along a wall. Flames are stabilized on the downstream edge of a splitter plate which has a thickness small in relation to the overall duct height. Moreau (1981) and Moreau and Boutier (1977) provide velocity, temperature and unburned hydrocarbon measurements at three planes and for two flames and this information appears suitable for the evaluation of calculation methods although the flow may be subject to the organized three-dimensional structures observed by Keller and Daily (1983) and Daily and Lundquist (1984). The measurement technique used by Moreau for the temperature pdfs is not well established although comparison is possible with the measurements of mean temperature of Borghi and Moreau although (1977) who do not give particulars about the probe used. The temperature pdfs do, however, tend to be qualitative rather than quantitative.

The temperature and species concentrations of Borghi and Moreau (1977) are obtained in a flame almost identical to one of the two flames of Moreau and Boutier (1977), for which detailed measurements of mean and fluctuating axial velocity and of unburned hydrocarbon are reported. These studies, together with those of Moreau (1981) and Moreau and Labbe (1978), constitute a comprehensive investigation of a high Reynolds number mixing layer. The density measurements of Shepherd and Daily (1984) were obtained by the Rayleigh scatter technique in a flame identical with one whose velocity field is investigated by Keller and Daily (1983). The combined data provide a detailed set of measurements of a vector and a scalar in a high Reynolds number flow but the suitability of the data, of course, is subject to the validity of the interpretation of the Rayleigh scatter information. Similar information has also been provided by Cheng et al (1981) and Ng et al (1982).

Meunier et al (1983) made measurements of mean and fluctuating velocity and of mean temperatures with laser velocimetry and thermocouples respectively. The flow comprised a wall boundary layer of hot products of combustion with transpiration of a near stoichiometric mixture of propane and air through the wall. The measurements encompass the high-Reynolds number region of the flow which can be represented by boundary-layer equations, albeit with provision for mass flow through the wall. The experiment and instrumentation are not described in detail in the paper but presumably the necessary additional information is available in relevant reports. In general, the work appears to provide information useful for the evaluation of calculation methods.

To allow detailed comparison between measured and calculated mean flow properties in a premixed flame, it is desirable to have geometries which allow for most of the reaction to take place at constant equivalence ratios and these are restricted to flames stabilized on thin rods or the downstream edge of a splitter plate. The possibility of organized structures certainly exists in these near two-dimensional flames and deserves careful consideration, particularly in view of the experimental work of Brown and Roshko (1974), but it should be remembered that small amounts of turbulence in the upstream flow can be sufficient to destroy such structures as demonstrated by Chandrasuda et al (1978). It is, of course, desirable for experiments to provide details of the flow boundary conditions including those associated with turbulence properties but these can often be estimated and the uncertainties associated with such estimates evaluated as part of the calculation method.

The premixed flames of Table 2 are also divided into three sections which deal respectively with the two-dimensional flows corresponding to flames stabilized by a rod or a gutter located in a rectangular duct, with sudden expansion flows, and with axisymmetric duct flows involving flames stabilized on a disc. In all cases the presence of a duct and the energy associated with combustion can give rise to severe pressure oscillations and investigations concerned solely with the combustion oscillations are omitted from our review.

Howe et al (1962) report measurements in three flames stabilized on a rod in a duct and include detailed mean velocity data using a Pitot tube and concentration data at one station. Such measurements probably correspond closely to the density weighted mean values. These early measurements do not appear to be subject to discrete frequency oscillations and appear suitable for calculation purposes. The later investigations of Lewis and Moss (1979) and Katsuki (1983) are concerned with the premixed

Table 2a

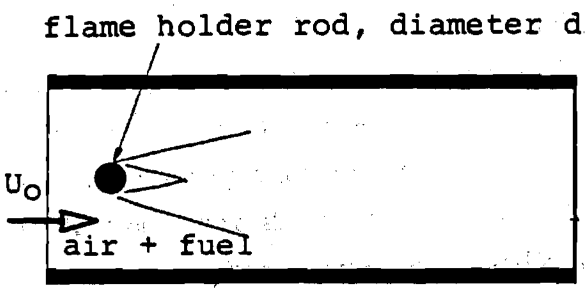

Wright & Zukoski (1962)

Howe, Shipman & Vranos (1962)

Lewis & Moss (1973)

Katsuki, Mizutani, Ohta & Choi (1983)

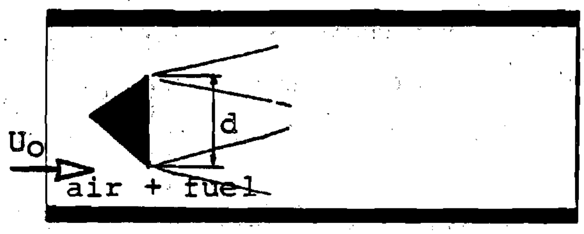

Fujii & Eguchi (1981)

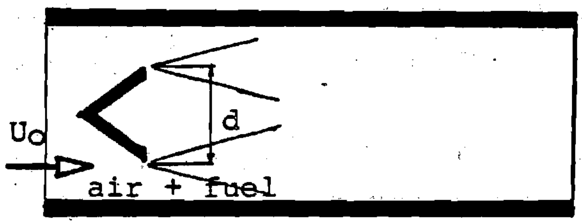

Clare, Durao, Melling & Whitelaw (1976)

Table 2a

Reference	Flow	Velocity	Temperature	Other	Probe Characteristics	Comments
		Measurements Reported				
Wright & Zukoski (1962)	flow past 3,6,12,25 50mm rods in 150mm high x 75mm wide duct gasoline-like hydrocarbon - air Φ = 1.0 $U_o \sim$ 30 - 100m/s $T_o \sim$ 373K $Re_d \sim$ 1200 - 30,000	total pressure: 3 transverse profiles ($U_o \sim$ 90m/s) & one centerline profile ($U_o \sim$ 60m/s)	-	schlieren pictures and direct photographs		dependence of flame width on Φ, U_o, rod diameter axial distance investigated
Howe, Shipman & Vranos (1962)	flow past 2.5, 5.1mm rods in 76mm high x 25mm wide duct C_3H_8 - air Φ = 1.55 $U_o \sim$ 18,30,52m/s T_o - ambient $Re_d \sim$ 5000 - 10,000	$\bar{U}$: transverse profiles, streamlines	-	CO_2, O_2, CH, CO%: one transverse profile	pitot tube 6mm dia. sampling probe 0.5mm bore	3 flames at $U_o \sim$ 30m/s reported in detail

Table 2a

Reference	Flow	Velocity	Temperature	Other	Probe Characteristics	Comments
		Measurements Reported				
Clare, Durao Melling & Whitelaw (1976)	flow past 25.4mm wide, 45^o V-gutter in 102mm sq. duct C_3H_8 - air $\Phi = 0.7$ $U_o = 58.2$m/s T_o - ambient $Re_d \sim 100{,}000$	$\bar{U}$, u': centerline profiles	-	sequence of 4 schlieren pictures at 5ms intervals	LDV, forward scatter probe volume, 0.2mm x 2mm	
Lewis & Moss (1979)	flow past 5mm rod in 26mm wide x 76mm high duct C_3H_8 - air $\Phi = 1.0$ $U_o \sim$ 20,30,45 60m/s T_o - ambient $Re_d \sim 6600 - 20{,}000$	-	$\bar{T}$, θ: 2 transverse profiles (2 flames) pdfs, power spectra	schlieren pictures (4 flames) ion current ($\bar{I}$) power spectra	125 μm bare-wire thermocouple 0.125mm ion current probe	4 flames

Table 2a

Measurements Reported

Reference	Flow	Velocity	Temperature	Other	Probe characteristics	Comments
Fujii & Eguchi (1981)	flow past 25mm sided triangular rod in 50mm sq. duct C_3H_8 - air $\Phi = 0.7$ $U_o \sim 10$m/s T_o - ambient $u_o'/U_o \sim 2\%$ $Re_d \sim 16{,}600$	$\bar{U}, \bar{V}, u', v', \overline{uv}$: one transverse profile; other turbulence parameters: 2 transverse and one centerline profile for $\Phi = 0.6 - 1.4$	-	-	LDV, forward scatter	signal rate $10 - 50\ s^{-1}$
Katsuki, Mizutani, Ohta & Choi (1983)	flow past 20mm rod in 100mm high x 30mm wide duct natural gas-air $\Phi = 0.65$ to 0.8 $U_o \sim 5, 11$m/s T_o - ambient $u_o'/U_o \sim 0.8$ to 1.2% $Re_d \sim 6600 - 14{,}500$	-	$\bar{T}, \theta'$, pdfs: 2 transverse traverses power spectra	schlieren pictures (4 flames) ion current ($\bar{I}$) pdfs: 2 transverse traverses	25 μm bare-wire thermocouple 0.1mm ion current probe	4 flames $\tau_T \sim 7$ms time-resolved simultaneous T, I measurements

flame which exists downstream of the long rod located in the rectangular channel. In both cases, the investigations concentrate on the measurement of temperature and its probability density distribution. The latter investigation provides measurements with a 25 m thermocouple which has adequate frequency resolution for the measurement of temperature fluctuations. The time constant of the thermocouple used by Lewis and Moss is of the order of 100ms and, as a consequence, their temperature-fluctuation results are unlikely to be reliable. The interpretation of ion current measurements of Katsuki tends to be qualitative with correspondingly reduced significance for the evaluation of calculation methods. Of the available data on confined flames stabilized on rods only those of Howe et al (1962) contain vector and scalar field measurements and suggest flames which are clearly turbulent. There is, nevertheless, a problem in interpreting the mean velocity data since they are neither unweighted nor density weighted values.

The backward-facing step measurements of El Banhawy et al (1983) and Shepherd et al (1982, 1983) involve step heights ranging from 10 to 20mm and bulk velocities from 7 to 18.5m/s and provide complementary information. It is evident from the work of Shepherd and his co-workers that the details of the flame-front region require consideration of counter-diffusion and the extensive flow results of El Banhawy et al are sufficient to allow the testing of calculation methods which embody this principle. It should be emphasized, however, that the investigations of Pitz and Daily (1979) and El Banhawy et al were intended to determine the nature of severe combustion driven oscillations and that, although the measurements of El Banhawy et al with the equivalence ratios of 0.77 and 0.95 did not provide evidence of strong oscillations, they may be present.

Stevenson et al (1982) present data on flames stabilized behind a step in an axisymmetric configuration. Experimental detail is not, however, provided and a satisfactory evaluation of the results is impossible. Of the available data on step-stabilized flames it appears that only those of El Banhawy et al (1983) are adequate in content and of acceptable experimental precision; however, the rms temperature measurements are

Table 2b

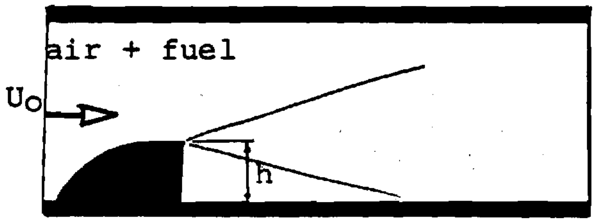

Shepherd, Moss & Bray (1982)

ElBanhawy, Sivasegaram & Whitelaw (1983)

Shepherd & Moss (1983)

Sivasegaram & Whitelaw (1983)

Pitz & Daily (1983)

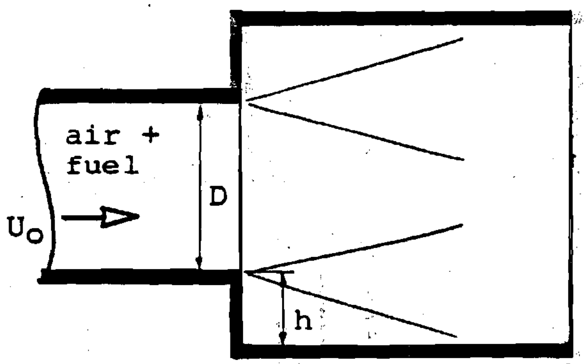

ElBanhawy, Melling & Whitelaw (1978)

Stevenson, Thompson, Gould & Craig (1982)

Table 2b

Measurements Reported

Reference	Flow	Velocity	Temperature	Other	Probe characteristics	Comments
El Banhawy, Melling & Whitelaw (1978)	23.1mm diameter pipe following 6.6mm pipe C_3H_8 - air Φ = 0.965 - 1.077 $U_o \sim$ 45m/s $Re_h \sim$ 26,500 $Re_D \sim$ 20,000	$\bar{U}$, u': centerline profiles				
Stevenson, Thompson, Gould & Craig (1982)	152mm diameter pipe following 76mm pipe C_3H_8 - air Φ = 0.28 $U_o \sim$ 22m/s T_o - ambient $u_o'/U_o \sim$ 4% $Re_h \sim$ 56,000	$\bar{U}$,u': 8 transverse profiles	T: contour across one transverse section	-	LDV, forward scatter	

Table 2b

Reference	Flow	Measurements Reported			Probe characteristics	Comments
		Velocity	Temperature	Other		
Shepherd, Bray & Moss (1982)	76mm high x 25mm wide duct; 12.5mm step C_3H_8 - air Φ = 1.2 $U_o \sim$ 18.5m/s T_o - ambient $Re_h \sim$ 15,500	$\bar{U}$, u', pdfs conditional & continuous values: one centerline & one transverse traverse	-	reaction progress variable	LDV, forward scatter probe volume 0.2mm x 1.2mm Mie scatter probe volume 0.2mm x 2.0mm	
El Banhawy, Sivasegaram & Whitelaw (1983)	40mm high x 150mm wide duct; 10mm, 20mm steps natural gas-air Φ = 0.77, 0.90, 0.95 $U_o \sim$ 7m/s, 10m/s T_o - ambient $Re_h \sim$ 4600 - 13,000	$\bar{U}$, u': contours (one flame)	$\bar{T}$, θ': contours (6 flames) 8 transverse profiles (one flame)	O_2, CO, CO_2%: contours (6 flames) CH %: contours (3 flames)	LDV, forward scatter 15 μm, 40 μm & 80 μm bare-wire thermocouples	six flames $\tau_T \sim$ 2.5ms uncompensated θ' measurements
Sivasegaram & Whitelaw (1983)	40mm high x 150mm wide duct; 20mm step natural gas-air Φ = 0.8 $U_o \sim$ 10,5,2m/s T_o - ambient $Re_h \sim$ 2600 - 13,000	-	$\bar{T}$: contours (3 flames): θ', pdf: 3 transverse traverses (one flame), power spectra	-	15 μm bare-wire thermocouple	three flames $\tau_T \sim$ 2.5ms

Table 2b

Measurements Reported

Reference	Flow	Velocity	Temperature	Other	Probe characteristics	Comments
Shepherd & Moss (1983)	76mm high x 25mm wide duct; 12.5mm step C_3H_8 - air $\Phi = 1.0$ $U_o \sim 18.5$m/s T_o - ambient $Re_h \sim 15{,}500$	$\bar{U}$: traverse parallel to axis, across flame front	-	reaction progress variable traverse as for $\bar{U}$	LDV, forward scatter probe volume 0.2mm x 1.2mm Mie scatter: probe volume 0.2mm x 1.2mm	
Pitz and Daily (1983)	51mm high x 173mm wide duct; 25mm step. C_3H_8 - air $\Phi = 0.57$ $U_o \sim 9, 13, 22$m/s T_o - ambient $u_o'/U_o \sim 4$-7% $Re_h \sim 15{,}000 - 36{,}700$	$\bar{U}, u', v'$: several transverse profiles (one flame)	-	schlieren pictures	LDV, forward scatter	3 flames (three flow rates)

Table 2c

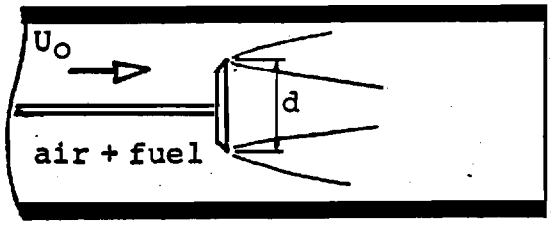

Taylor & Whitelaw (1980)
Taylor (1981)
Heitor (1985)

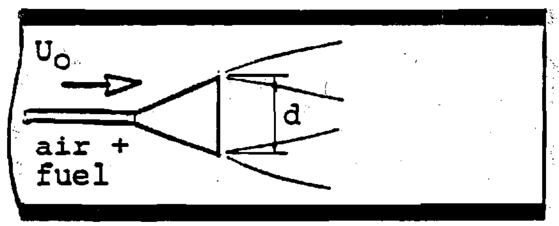

Taylor & Whitelaw (1980)
Taylor (1981)
Heitor (1985)

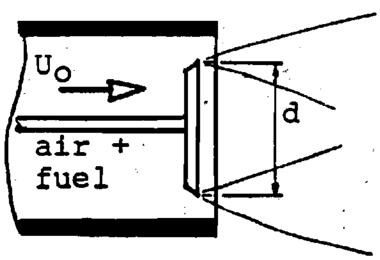

Heitor (1985)
Heitor, Taylor & Whitelaw (1983)

Table 2c

Measurements Reported

Reference	Flow	Velocity	Temperature	Other	Probe characteristics	Comments
Taylor & Whitelaw (1980); Taylor (1981)	flow past 56mm 40mm disks & 40mm cone in 80mm pipe natural gas-air $\Phi = 0.56$ $U_o \sim$ 6.8m/s T_o - ambient $Re_d \sim$ 18,000 - 36,000	$\bar{U}$, u': centerline profile, 3 transverse profiles	$\bar{T}$: centerline profile	-	LDV, forward scatter probe volume 0.2mm x 2mm 80 μm bare-wire thermocouple	LDV signal rate 5000 s^{-1}
Heitor, Taylor & Whitelaw (1983) Heitor (1985)	flow past 56mm, 40mm disks at exit of 80mm pipe natural gas-air $\Phi = 0.8$ $U_o \sim$ 10 - 18m/s T_o - ambient $Re_d \sim$ 33,000-60,000	$\bar{U}$, $\bar{V}$, u', v', $\overline{uv}$ $\tilde{U}$, $\tilde{V}$, u'', v'', $\widetilde{uv}$ continuous & conditional: traverse parallel to axis, across flame front and 7 transverse traverses	$\bar{T}$, θ', pdfs $\tilde{T}$, θ'', pdfs continuous & conditional values: traverses as for velocity	-	LDV, forward scatter probe volume 0.2mm x 5mm 15 μm bare-wire thermocouple	two flames simultaneous velocity and temperature measurements: LDV signal rate 20Hz $\tau_T \sim$ 2 - 3ms compensation with $\tau_T = \tau_T\,(U,T)$

Table 2c

Reference	Flow	Velocity	Measurements Reported: Temperature	Other	Probe characteristics	Comments
Heitor (1985)	flow past 56mm 40mm disks of 40mm cone in 80mm pipe natural gas-air $\Phi = 0.7$ $U_o \sim 6.8$m/s T_o - ambient $Re_d \sim 18{,}000 - 36{,}000$	-	T: contours	CO, CO_2, O_2, CH% contours	40 μm, 80 μm bare-wire thermocouples	

not acceptable as no compensation was made for thermal inertia of the temperature probe.

Axisymmetric configurations may provide a better vehicle for testing calculation methods which make use of time-averaged equations since disc-stabilized flows are known to give rise to insignificant eddy shedding. The isothermal flow results of Calvert (1967), for example, suggest that inclination of a disk is necessary to provide significant eddy shedding and the measurements of Taylor and Whitelaw (1984), with a disk orthogonal to the duct axis, confirm the absence of shedding. Apart from the data discussed in the previous paragraph, the disk stabilized flames of Heitor (1985) obtained with equivalence ratios which do not reveal discrete-frequency oscillations, may be useful for the evaluation of calculation methods. They were obtained at disk Reynolds numbers of 2×10^4 to 3×10^4 and with an equivalence ratio of 0.7 and include details of the axial velocity and normal stress, unweighted temperature and concentrations of CO, CO_2 and UHC. Calculations of these flows can, of course, suffer from the numerical difficulties associated with recirculating regions and the prescription of initial conditions, particularly for the velocity components, introduces uncertainties which may be important. Taylor and Whitelaw (1980) and Taylor (1981) investigated the velocity characteristics of three flames stabilized on axisymmetric bluff bodies in a round duct and Heitor (1985) measured mean temperature and chemical composition for three similar flames with the same burner. The temperature measurements were carried out with an 80 m thermocouple and are likely to be up to 100K lower than the true unweighted averages. The velocity measurements and chemical composition are density weighted.

The disk stabilized flame in an open pipe flow investigated by Heitor et al (1984) and Heitor (1985) provides the most precise and detailed measurement of the fluctuating temperature currently available. The temperature probes were digitally compensated with the time constant specified as a function of the instantaneous temperature and velocity. The data includes unconditioned and conditioned mean values with and without density weighting for both velocity and temperature. The results, which include conditionally sampled velocity values, confirm the need for consideration of non-gradient diffusion and provide quantitative evidence with which related calculation methods can be tested. It is evident, however, that the flow is not adiabatic and that the external mixing layer requires assumptions appropriate to non-premixed flames.

Of the data in Table 3 only those of Yamaguchi et al (1975a, b, 1976) and Ohiwa et al (1975) include vector and scalar property measurements. The flames are not entirely premixed and diffusion effects are strong in the flame zone. The large size of the thermocouple implies large uncertainty in the mean temperature and the interpretation of velocity measurements present problems since details given about the measurement technique seem inadequate.

Temperature and species concentration measurements are reported by Abdella et al (1981, 1982) for their closed conical burner and by McDannel et al (1982) for their flame stabilized by the interaction between a jet in an opposed main flow. The complexity of the geometry of the burner used by Abdella et al may cause problems in prediction and the lack of information of the velocity field represents a serious defect since the accuracy of its calculation cannot be evaluated. McDannel et al present comprehensive information of their flow field with mean temperature and UHC, O_2, NO and NO_x composition measurements. The Reynolds number of the jet and its interaction with the opposing flow suggest turbulent flow and the measurements encompass a useful range of equivalence ratios. The paper provides detailed information for one flame but, like that of Abdella et al, does not include information of the velocity field. It can be supposed, however, that the limited region of the jet can be represented by boundary-layer equations and the relevant boundary conditions can be surmized. Stabilization takes place on a front some way downstream of the jet and the main reaction in the region after the small-diameter jet has turned. As a consequence, the main reacting region must be represented by elliptic equations with consequent numerical difficulties. Velocity information relevant to this flow has been recently reported by Brum and Samuelsen (1983) and helps to provide comparatively complete information.

Table 3

McDannel, Peterson & Samuelsen (1982)

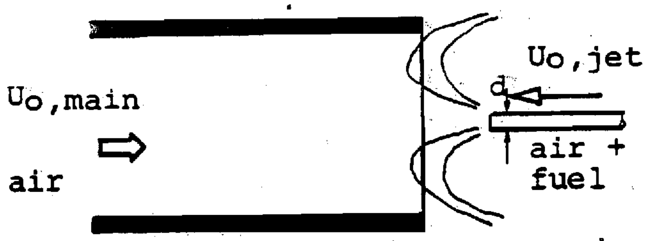

Yamaguchi, Ohiwa & Kinoshita (1975a,b)

Yamaguchi, Ohiwa & Izumi (1976)

Ohiwa, Senda, Yamaguchi & Izumi (1975)

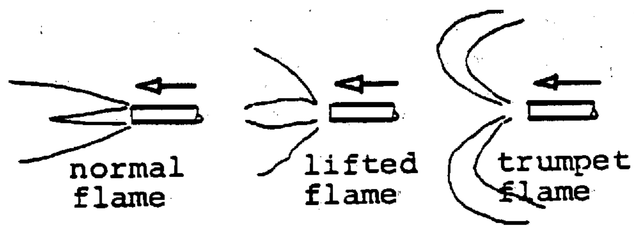

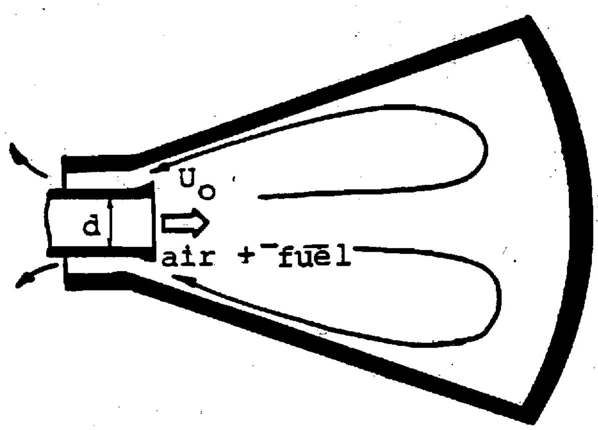

Abdella, Ali, Bradley & Chin (1981)

Abdella, Bradley, Chin & Lam (1982)

Table 3

Measurements Reported

Reference	Flow	Velocity	Temperature	Other	Probe characteristics	Comments
Yamaguchi, Ohiwa & Kinoshita (1975a,b); Yamaguchi, Ohiwa & Izumi (1976); Ohiwa, Senda, Yamaguchi, Kaga & Izumi (1975)	2mm jet inside 80mm tube carrying air C_3H_8 - air Φ = 1.8, 3.8, 6.4 U_o (jet) specified indirectly U_o (main) $\sim$0-30m/s T_o - ambient $Re_d \sim 4000$	flow pattern and streamlines	$\bar{T}$: centerline profile	-	300 μm bare-wire thermocouple 0.3mm bore platinum pitot tube	one trumpet and one standard flame reported
Abdella, Ali, Bradley & Chin (1981)	conical burner, volume 159ml: 9.5mm premix jet CH_4 - air Φ = 0.84 U_o = 130, 250m/s T_o = 295K $Re_c \sim$ 80,000-150,000	-	$\bar{T}$: 2 transverse profiles	CH_4, CO, NO% 2 transverse profiles ion current $(\bar{I})$: 2 transverse profiles	100 μm bare-wire thermocouple; 0.84mm bore gas sampling probe 0.15 μm bead on current probe	three flames, two with stratified mixture stream

Table 3

Measurements Reported

Reference	Flow	Velocity	Temperature	Other	Probe characteristics	Comments
Abdella, Bradley, Chin & Lam (1982)	Conical burner, volume 159ml: 9.5mm premix jet CH_4 - air $\Phi = 0.84$ $U_o = 130, 10m/s$ T_o - ambient $Re_d \sim 4800 - 80{,}000$	-	$\bar{T}$, θ', pdf: one transverse traverse	CH_4, CO% one transverse profile	100 μm SiO_2 coated and 50 μm bare-wire thermocouples: 0.84mm bore gas sampling probe	
McDannel, Peterson & Samuelsen (1982)	1.32mm jet facing 51mm pipe exit C_3H_8 - air $\Phi_{jet} = \Phi_{main} = 1.0$ $U_{o,jet} = 135m/s$ $U_{o,main} = 7.5m/s$ T_o - ambient $Re_d \sim 20{,}000$	-	$\bar{T}$: contours (to show effects of varying Φ and flow velocities)	HC, O_2, CO NO_x & NO%: contours for one flame; profiles for some flames.	wire size not given for thermocouple 1.3mm bore gas sampling tube	additional data at $U_{o,jet} = 70m/s$ $U_{o,main} = 15m/s$ $\Phi_{jet} = 0.8 - 1.6$ $\Phi_{main} = 0.6\text{-}1.2$ (24 flames)

RECOMMENDED CASES

It is evident from the preceeding pages, and from the tables, that considerable efforts have been exerted to provide data relevant to the understanding of premixed combustion. The evaluation of combustion models can presently be carried out in a limited and direct manner, as for example to demonstrate the need to consider non-gradient diffusion of species concentrations, but a more general evaluation of prediction procedures requires consideration of the possible errors which can arise due to shortcomings of the turbulence, heat transfer and combustion models and of the numerical techniques employed.

All of the experiments referred to in the tables of the prior section provide useful information. Equally, all have limitations in terms of their suitability for the evaluation of calculation methods. Indeed, it is proper to view the development and evaluation of calculation methods for premixed combusting flows as a research task of some considerable magnitude.

The flows of Yoshida (1981), Yoshida and Gunther (1980, 1981) and of Keller and Daily (1983), Shepherd and Daily (1984) and Daily and Lundquist (1984) may be represented by boundary-layer equations so that numerical difficulties are reduced. In the case of the pipe flames of the former authors, the Reynolds number is moderate and may not ensure fully turbulent flow; pressure gradients due to buoyancy need to be considered; and the external region of the flame is not premixed. In the mixing region studied by the latter authors, the influence of organized structures may make prediction difficult. The recommended flows are summarized in Tables 4 and 5. Selected results, intended for comparison with computation, have been extracted from the primary references and are located in Appendix D.

The flows of Heitor (1985) and Heitor et al(1983) and of McDannel et al (1982) and Brum and Samuelson (1983) also contain comparatively complete information but require the solution of elliptic equations with consequent numerical difficulties and may also require consideration of heat transfer from the flame to the surroundings and, in the former case, of non-premixed combustion in the outer region. These flows are not included as recommended cases because of the emphasis in this review on the parabolic treatment. In all premixed combustion flows, care must be taken to ensure that the calculations and measurements correspond to the same type of averaging, the differences between unweighted and density-weighted averages can be significant.

Table 4

DATA SUMMARY

Flow Jet from a pipe

Data Evaluators P. A. Libby, S. Sivasegaram and J. H. Whitelaw

Case Yoshida (1981) and Yoshida and Gunther (1980, 1981)

Geometry

Natural gas and air issuing from a pipe. Flame stabilized by a small annular pilot flame of H_2

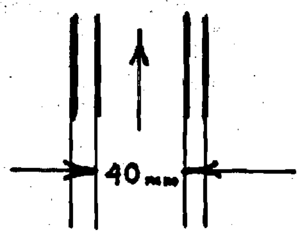

Re = 14,500

Mean Quantities Measured

$\bar{u}$ at 4 axial stations and $\bar{T}$ at 5 axial stations.

Turbulence Quantities Measured

u' at 3 and T' at 5 axial stations. Also ion current $\bar{I}$, I' and p(T) at 3 stations.

Notes

Axisymmetric flow assumed; velocity profile prescribed as uniform at pipe exit, except for a very thin layer near the pipe wall. Upstream turbulence intensity 6%; mixture composition uniform at a uniform temperature of 293°K; effect of pilot flame negligible; outer boundary assumed to be still air at 293°K.

Table 5

DATA SUMMARY

Flow — Flow in duct with splitter plate

Data Evaluator — P. A. Libby, S. Sivasegaram and J. H. Whitelaw

Case — Keller and Daily (1983), Shepherd and Daily (1983), and Daily and Lundquist (1984).

Geometry — C_3H_8 and air flow in rectangular duct, 57mm high and 122mm wide, divided into premixed and pilot streams each 28.5mm thick by a splitter plate. The splitter plates edge is 229mm from the duct exit.

dp/dx measured

$R_L \sim 10^6$

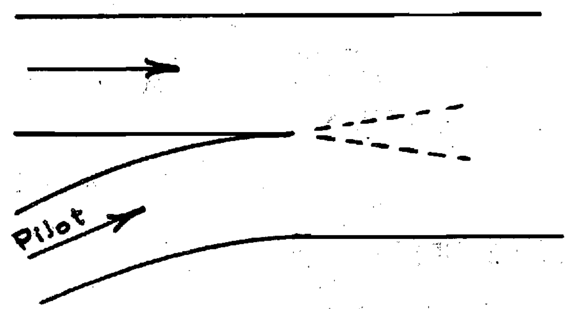

Mean Quantities Measured

$\bar{u}$, $\bar{\rho}$ at 9 axial stations

Turbulence Quantities Measured

$\overline{\mu' v'}$, ρ', $P(\rho)$, at 9 axial stations

Notes

Two-dimensional flow assumed; profiles of $\bar{u}$, $\bar{v}$, u', v' specified at the start of the shear layer; premixed stream of uniform composition and uniform temperature of 293°K; pilot stream comprising products of combustion of C_3H_8 + air mixture of equivalence ratio 0.64, at uniform temperature of 1170°K. All walls assumed adiabatic.

AVAILABLE MODELS AND COMPARISON

Of the available models for premixed flames, that of Bray and Moss (1977) has probably been subjected to the most intensive development. If reaction can be characterized by a single global step and the flow is adiabatic, then the instantaneous thermodynamic state of the mixture can be uniquely determined as a function of a single reaction progress variable, usually taken to be the ratio of the product mass fraction and its fully burned value. In the Bray-Moss model fluctuations in reaction rate are described by the introduction of a probability density function with separate parts to represent reactants, the fully burnt state and the burning mode, the latter being determined from a laminar flamelet assumption. The model has been extended to more complex reaction schemes including, the one-dimensional propane air flame of Champion, Bray and Moss (1978) for which reaction is assumed to involve a delay zone described by the single global fuel breakdown reaction of Edelman and Fortune (1969) and a combustion zone with a complex mechanism which is simplified by equilibrating three chain branching reactions and introducing the 'ad hoc' assumption that the ratio of the oxygen element to hydrogen element mass fractions is constant. This latter assumption is necessary to retain the single scalar specification. No comparisons with experiment are described though plausible results are obtained.

The Bray-Moss model has also been applied to premixed combustion in a turbulent boundary layer developing over a flat plate by Meunier, Champion and Bellet (1983) who use the density weighted $k-\epsilon$ model together with a single global reaction step and reaction progress variable pdf to calculate the premixed combustion arising from the injection of a propane-air mixture through a porous plate past with an external stream of hot gas. For injection rates of up to 1% the calculated mean velocity and temperature profiles are found to be in close agreement with the measurements. For higher injection rates (up to 2%) the agreement is less satisfactory and this is attributed to limitations in the $k-\epsilon$ model associated with transverse pressure gradient-fluctuating density influences and dissipation rate in the presence of heat release.

An interesting and promising extension of the Bray-Moss model is described by Libby and Bray (1980,1981) and Bray, Libby, Masuya and Moss (1981) in which a laminar flamelet description of premixed turbulent flames is combined with the Bray-Moss theory through the introduction of a joint probability density function for the velocity and the reaction progress variable. Thin flame burning is assumed and the reaction progress variable is then used to 'condition' the velocity.

Two of the more important features of the model are that gradient diffusion arguments are avoided throughout and that counter-gradient transport which arises through the preferential influence of mean pressure gradient on high and low density gas 'packets' appears to be accurately described. The model gives excellent results when compared with the measurements of Moss (1980) in an open burner premixed flame and further experimental support provided by the simultaneous velocity and mixture state measurements of Shepherd, Moss and Bray (1982) in a ducted premixed flame. The flames studied exhibit thin flame burning and thus justify the conditioning of velocity. An important notion which arises from both the theoretical and experimental results is that the pdf of the velocity component normal to the flame is far from Gaussian but rather consists of two nearly Gaussian distributions, one for reactants and the other for products. Thus theories based on the assumption of a normal distribution for this velocity component are flawed.

A further extension of the model is given by Bray, Libby and Moss (1985) when the conditioned pdf is used to derive a full second order closure for the density weighted Reynolds stress and scalar flux in which previously formulated constant density models are combined with a laminar flamelet description for the density fluctuations. While the complete model contains all of the effects included in the earlier nongradient one-dimensional theory there are additional terms which may alter the results. Largely for this reason the closure must be regarded as provisional until detailed comparisons with experiment are undertaken.

The present development of the Bray-Moss theory in which the flow is assumed adiabatic and the effects of rates of strain on the characteristics of the laminar flamelets are not taken into account cannot describe important phenomena such as those connected with ignition and extinction. Further research is required to incorporate these effects.

One of the central problems of all theories of turbulent combustion, premixed and nonpremixed, relates to combustion induced pressure fluctuations It should be noted that the several terms involving such fluctuations in the equations for constant density turbulence have received considerable attention and are subject to considerable uncertainty despite their apparent importance in determining turbulence behavior. Thus it should not be surprising that the modelling of combustion induced pressure fluctuations which are due to an entirely different mechanism is in a poor state of development. This problem has been studied by Strahle (1982). A laminar flamelet description is combined with an analysis of the rotational and potential fields in an open premixed flame. For the case of a plane flame the results of the analysis are used to construct a model for the velocity-pressure gradient correlation. This model differs from most previous proposals though it is of similar form to the closure assembled by Jones (1980) for variable density/combusting flows.

Borghi and Dutoya (1979) have investigated the influence of reaction on the turbulent transport of chemical species (scalar flux) in premixed flames. The exact balance equation for the scalar flux contains correlation between the fluctuating velocity and the reaction rate and this is modelled by the introduction of a joint velocity-scalar pdf which is assumed to be joint normal. It is shown that reaction has a large direct effect on turbulent transport in premixed flames where the reaction rate is fast. The effect can be positive or negative depending on the situation and in the context of a gradient diffusion model would imply values of turbulent Schmidt number far from unity and dependent on the ratio of reaction to turbulence time scales. For the case of slow reaction the effect is shown to be negligible.

The solution of a modelled transport equation for the joint pdf of up to N species has been proposed, for example by Dopazo (1976) and Pope (1979) and has the possible advantage that the terms involving reaction appear in closed form. Difficulties in the modelling of other terms in the equation do, however, occur and none of the models so far proposed appear to be entirely satisfactory Jones and Whitelaw[(1982, 1984)]. Pope (1981) makes use of the Monte Carlo technique to solve the equation for the one-dimensional premixed propane/air flame of Robinson (1974) with good results. Pope (1982) has also suggested the use of a joint pdf for velocity and the set of scalars: this approach retains the advantages of the previous formalism and allows the turbulent transport terms to appear in closed form although modeling is still required.

Combinations of models to represent chemical and physical control have also been proposed for the calculation of premixed or partially premixed flames. The eddy break-up assumptions of Spalding (1971) and of Magnusson and Hjertager (1976) represent the averaged source of fuel by the expressions

$$S_{fu} = C_R \bar{\rho} \frac{\epsilon}{k} \left(\overline{m'^2}\right)^{1/2}$$

and

$$S_{fu} = C(\nu\epsilon/k^2)^{0.25} \, (\epsilon/k) \, \bar{m}_{min} \, \bar{F} \, \bar{\rho}$$

respectively. Since chemical control cannot be ruled out, one or the other of these expressions is usually evaluated and compared with the source obtained from an Arrhenius-type expression, for example

$$S_{fu} = A\bar{\rho}\bar{m}_{fu}\bar{m}_{ox}\exp(-E/R\bar{T})$$

This approach has merit in that it will allow solutions to premixed flame problems and it has been used, for example by Lockwood et al (1983) and Attya and Whitelaw (1984) who selected the lower of the physically and chemically controlled sources at any location. It appears to provide suitable solutions within limited ranges of variables but it cannot be regarded as better than a rough guide and it should be recognized that the eddy break-up assumptions, though intuitively correct, do not give rise to unique solutions.

ADDITIONAL DATA NEEDS

The main recommendation of this chapter is that new work on premixed combustion be supported so that predictive procedures can be developed and quantitatively evaluated. Of necessity, this requires that experiments and calculations be performed in close harmony with each other so that each can provide guidance to the other. The work should be carried out by research teams which are known to have the necessary expertise: this may require the formation of teams between individuals or groups who work in different locations so that best use can be made of expertise of the different constituent components of models and of experimental techniques.

The flows to be investigated should include a wall boundary-layer flow similar to that of Cheng et al (1981) and Ng et al (1982), a rod stabilized arrangement similar to that of Gouldin and Dandekar (1984), confined and unconfined axisymmetric duct flows similar to those of Heitor (1985) and Heitor et al (1983) and an opposed jet flame similar to that of McDannel et al (1982). Equivalence ratio and hydrocarbon fuel should be regarded as variables and the Reynolds number should be sufficiently large so that spectral measurements are able to confirm turbulent flow. The measurements should include velocity, temperature, concentrations and, where possible, correlations.

REFERENCES

Abdella, A. Y., Ali, B. B., Bradley, D. and Chin, S. B. (1981) Stratified combustion in recirculating flow. Comb. and Flame 43, 131.

Abdella, A. Y., Bradley, D., Chin, S. B. and Lam, C. (1982) Temperature fluctuations in a jet-stirred reactor and modelling implications. Nineteenth Symposium (International) on Combustion, 495.

Attya, A. M. and Whitelaw, J. H. (1984) Measurements and calculations of preheated and unpreheated confined kerosene spray flames. Comb. and Flame.

Beltagui, S. A. and MacCallum, N. R. L. (1976) Aerodynamics of vane-swirled flames in furnaces. J. Institute of Fuel 49, 193.

Bill, R. G., Namer, I., Talbot, L., Cheng, R. K. and Robben, F. (1981) Flame propagation in grid induced turbulence. Comb. and Flame 43, 229.

Bill, R. G., Namer, I., Talbot, L. and Robben, F. (1982) Density fluctuations of flames in grid induced turbulence. Comb. and Flame 44, 227.

Borghi, R. and Dutoya, D. (1979) On the scales of the fluctuations in turbulent combustion. Seventeenth Symposium (International) on Combustion, 235.

Borghi, R. and Moreau, P. (1977) Turbulent combustion in a premixed flow. Acta Astronautica 4, 321.

Bray, K. N. C., Libby, P. A., Masuya, G. and Moss, J. B. (1981) Turbulence production in premixed flames. Comb. Sci. and Tech. 25, 127.

Bray, K. N. C. and Moss, J. B. (1977) A unified statistical model of the premixed turbulent flame. Acta Astronautica, 4, 291.

Bray, K. N. C., Libby, P. A. and Moss, J. B. (1985) Unified modelling approach for premixed turbulent combustion. Part I, General Formation. Comb. and Flame (to appear).

Broman, G. E. and Zukoski, E. E. (1962) Experimental investigation of flame stabilization in a deflected jet, Eighth Symposium (International) on Combustion, 944.

Brown, G. L. and Roshko, A. (1974). On density effects and large scale structures in turbulent mixing layers. J. Fluid Mech. 64, 775.

Brum, R. D. and Samuelsen, G. S. (1983) Laser anemometry measurements of non-reacting and reacting flows in the opposed jet combustor. University of California, Irvine, Report UCI-ACTR-83-18.

Calvert, J. R. (1967) Experiments on the flow past an inclined disk. J. Fluid Mech. 29, 691.

Chandrasuda, C., Mehta, R. D., Weir, A. D., and Bradshaw, P. (1978) Effect of freestream turbulence on large scale structure in turbulent mixing layers. J. Fluid Mech. 85, 693.

Champion, M., Bray, K. N.C. and Moss, J. B. (1978) The turbulent combustion of a propane-air mixture. Acta Astronautica 5, 1063.

Cheng, R. K. (1983) Conditional sampling of turbulence intensities and Reynolds stresses in a premixed turbulent flame. Submitted for publication.

Cheng, R. K., Bill, R. G. and Robben, F. (1981) Experimental study of combustion in a turbulent boundary layer. Eighteenth Symposium (International) on Combustion, 1021.

Cheng, R. K. and Ng, T. T. (1983) Velocity statistics in premixed turbulent flames. Comb. and Flame 52, 185.

Cheng, R. K., Talbot, L. and Robben, F. (1984) Critical velocity statistics in premixed CH_4-air, C_2H_4-air turbulent flames. Applied Science Division, Lawrence Berkeley Laboratory, University of California, Berkeley.

Clare, H., Durao, D. F. G., Melling, A. and Whitelaw, J. H. (1976) Investigation of a V-gutter stabilized flame by laser anemometry and schlieren photography. AGARD Conference Proc. 193, Applications on Non-Intrusive Instrumentation in Fluid Flow Research.

Clarke, A. E., Odgers, J. and Ryan, P. (1962) Further studies of combustion phenomena in a spherical combustor. Ninth Symposium (International) on Combustion, 878.

Daily, J. W. and Lundquist, W. J. (1984) Three dimensional structure in a turbulent combusting mixing layer. Submitted for publication.

Dandekar, K. V. and Gouldin, F. C. (1982) Temperature and velocity measurements in premixed turbulent flames. AIAA J. 20, 652.

Dopazo, C. (1976) A probabilistic approach to turbulent flame theory. Acta Astronautica, 3, 853.

Durst, F. and Kline, R. (1973) Velocity measurements in turbulent premixed flames by means of laser-Doppler anemometry. Sixth German Flame Conference, Essen.

Edelman, R. B. and Fortune, O. F. (1969) A quasi-global chemical kinetic model for the finite rate combustion of hydrocarbon fuels with application to turbulent burning and mixing in hypersonic engines and nozzles. AIAA Paper No. 69-0086.

El Banhawy, Y., Sivasegaram, S. and Whitelaw, J. H. (1983) Premixed turbulent combustion of a sudden expansion flow. Comb. and Flame 50, 153.

Filippi, F. and Mazza, L. F. (1962) Control of bluff body flame holder stability limits. Eighth Symposium (International) on Combustion, 956.

Fujii, S. and Eguchi, K. (1981) A comparison of cold and reacting flows around a bluff-body flame stabilizer. Trans. ASME, J. Fluids Eng. 103, 328.

Gouldin, F. C. and Dandekar, K. V. (1984) Time-solved density measurements in premixed turbulent flames. AIAA J. 22, 655.

Heitor, M., Taylor, A. M. K. P. and Whitelaw, J. H. (1984) Influence of confinement on combustion instabilities of premixed flames stabilized on axisymmetric baffles. Comb. and Flame 57, 109.

Heitor, M. V., Taylor, A. M. K. P. and Whitelaw, J. H. (1983) Simultaneous velocity and temperature measurements in a disc-stabilized premixed flame. Imperial College, Mech. Eng. Dept. Report FS/83/26.

Heitor, M. V. (1985) Ph.D. Thesis, University of London.

Howe, N. M., Shipman, C. W. and Vranos, A. (1962) Turbulent mass transfer and rates of combustion in confined turbulent flames. Ninth Symposium (International) on Combustion, 36.

Jones, W. P. (1980) Models for turbulent flows with variable density in Prediction methods for turbulent flow, Hemisphere Pub. Corp.

Jones, W. P. and Whitelaw, J. H. (1982) Calculation methods for reacting turbulent flows: a review. Comb. and Flame 48, 1.

Jones, W. P. and Whitelaw, J. H. (1984) Modelling and measurements in turbulent combustion. Twentieth Symposium (International) on Combustion. Invited Lecture.

Katsuki, M., Mizutani, Y., Ohta, A. and Choi, B. R. (1983) Structure of premixed turbulent flames stabilized by a cylindrical flame holder. Thermal Engineering Conference ASME-JSME, 175.

Keller, J. O. and Daily, J. W. (1983) The effect of large heat release on a two-dimensional mixing layer. AIAA Paper 83-0472.

Khalil, E. E., Spalding, D. B. and Whitelaw, J. H. (1975) The calculation of local flow properties in two-dimensional furnaces. Int. J. Heat and Mass Transfer 18, 760.

Kilham, J. K. and Kirmani, N. (1979) The effect of turbulence on premixed flame noise. Seventeenth Symposium (International) on Combustion, 327.

Lewis, K. J. and Moss, J. B. (1979) Time resolved scalar measurements in a confined turbulent premixed flame. Seventeenth Symposium (International) on Combustion, 267.

Libby, P. A. and Bray, K. N. C. (1980) Implications of the laminar flamelet model in premixed turbulent combustion. Comb. and Flame 39, 33.

Libby, P. A. and Bray, K. N. C. (1981) Counter gradient diffusion in premixed turbulent flames. AIAA J 19, 205.

Libby, P. A., Linan, A. and Williams, F. A. (1983) Strained premixed laminar flames with non-unity Lewis number. Comb. Sci. and Tech. 34, 257.

Lockwood, F. C. McGuirk, J. J. and Shah, N. G. (1983) Radiation transfer in gas turbine combustors. AIAA Paper 83-1506.

Longwell, J. P., Frost, E. E. and Weiss, M. A. (1953) Flame stability in bluff body recirculation zones. Industrial Engineering Chemistry 45, 1630.

McDannel, M. D., Peterson, P. R. and Samuelsen, G. S. (1982) Species concentration and temperature measurements in a lean premixed flow stabilized by a reverse jet. Comb. Sci. and Tech. 28, 211.

Magnussen, B. P. and Hjertager, H. (1976) On mathematical modelling of turbulent combustion with special emphasis on soot formation and combustion. Sixteenth Symposium (International) on Combustion, 719.

Matsumoto, R., Nakajima, T., Kimoto, K., Noda, S. and Maeda, S. (1982) An experimental study on low frequency oscillation and flame generated turbulence in premixed and diffusion flames. Comb. Sci. and Tech. 27, 103.

Meunier, S., Champion, M. and Bellet, J. C. (1983). Premixed combustion on a turbulent boundary layer with injection. Comb. Flame 50, 231.

Moreau, P. (1981) Experimental determination of probability density functions within a turbulent high velocity premixed flame. Eighteenth Symposium (International) on Combustion, 993.

Moreau, P. and Boutier, A. (1977) Laser velocimeter measurements in a turbulent flame. Sixteenth Symposium (International) on Combustion, 1747.

Moreau, P. and Labbe, J. (1978) Laser velocimetry in high velocity combusting flow. Third International Workshop on Laser Velocimetry, Purdue, 136.

Moss, J. B. (1980) Simultaneous measurements of concentration and velocity in an open premixed turbulent flame. Comb. Sci. and Tech. 22, 119.

Namazian, M., Talbot, L. and Robben, F. (1984) Density fluctuations in premixed turbulent flames. Submitted for publication.

Ng, T. T., Cheng, R. K., Robben, F. and Talbot, L. (1982) Combustion-turbulence interaction in the turbulent boundary layer over a hot surface. Nineteenth Symposium (International) on Combustion, 359.

Noda, S., Kimoto, K., Matsumoto, R., Nakajima, T. and Kawai, W. (1983) An experimental study of the turbulence structure in a premixed jet flame. ASME-JSME Thermal Engineering Conference 4, 159.

Ohiwa, N., Senda, K., Yamaguchi, S., Kaga, S. and Izumi, R. (1975) A study on opposed gaseous jet flames stabilized in a uniform air stream, 3rd report. Bull, JSME 18, 736.

Pitz, R. W. and Daily, J. W. (1979) Experimental studies of combustion in a two-dimensional free shear layer. Proc. Second Symposium on Turbulent Shear Flows. Imperial College, London, 5.1.

Pitz, R. W. and Daily, J. W. (1983) Combustion in a turbulent mixing layer fixed at a rearward facing step. AIAA J. 21, 1565.

Pope, S. B. (1979) The statistical theory of turbulent flames. Phil. Trans. 291, 529.

Pope, S. B. (1982) Monte Carlo calculations of premixed turbulent flames. Eighteenth Symposium (International) on Combustion, 1001.

Pope, S. B. (1982) An improved turbulent mixing model. Comb. Sci. and Tech, 28, 131. Robinson, G. P. (1974) Pollutant formation in turbulent flames. Ph.D. Thesis, Northwestern University, USA.

Shepherd, I. G. and Daily, J. W. (1984) Rayleigh scattering measurements in a two-stream free mixing layer. University of California, Berkeley College of Engineering, Mech. Eng., Paper 84-45.

Shepherd, I. G. and Moss, J. B. (1982) Measurement of conditioned velocities in a turbulent premixed flame. AIAA J. 20, 566.

Shepherd, I. G. and Moss, J. B. (1983) Characteristic scales for density fluctuations in a turbulent premixed flame. Comb. Sci. and Tech. 33, 231.

Shepherd, I. G., Moss, J. B. and Bray, K. N. C. (1982) Turbulent transport in a confined premixed flame. Nineteenth Symposium (International) on Combustion, 423.

Sivasegaram, S. and Whitelaw, J. H. (1983) Temperature characteristics of turbulent premixed flames. Experiments in Fluids 1, 161.

Smith, K. O. and Gouldin, F. C. (1979) Experimental investigation of flow turbulence effects on premixed methane-air flames. AIAA J. 17, 1243.

Sommer, H. T. and Stojanoff, C. G. (1979) Numerical prediction and experimental investigation of a premixed CH_4-air flame. Second Symposium on Turbulent Shear Flows, 317.

Spalding, D. B. (1971) Mixing and Chemical reaction in steady confined turbulent flames. Thirteenth Symposium (International on Combustion, 649.

Stevenson, W. H., Thompson, H. D., Gould, R. D. and Craig, R. R. (1982) Laser velocimeter measurements in a separated flow with combustion. LDA Symposium, Lisbon, Paper 11.5.

Strahle, W. (1982) Estimation of some correlations in a premixed reactive turbulent flow. Comb. Sci. and Tech. 29, 243.

Suzuki, T., Hirano, T. and Tsuji, H. (1979a) Flame front movements of a turbulent premixed flame. Seventeenth Symposium (International) on Combustion, 289.

Suzuki, T., Oba, M., Hirano, T. and Tsuji, H. (1979b) an experimental study of premixed flames. Bull. JSME 22, 848.

Suzuki, T. and Hirano, T. (1983) Ion current correlations measurements in a turbulent premixed flame. ASME-JSME Thermal Engineering Conference 4, 151.

Syred, N. and Beer, J. M. (1973) Effect of combustion upon precessing vortex cores generated by swirl generators. Fourteenth Symposium (International) on Combustion, 537.

Tanaka, H. and Yanagi, T. (1983) Cross-correlation of velocity and temperature in a premixed turbulent flame. Comb. and Flame 51, 183.

Taylor, A. M. K. P. (1981) Confined isothermal and combusting flows behind axisymmetric baffles. Ph.D. Thesis, University of London.

Taylor, A. M. K. P. and Whitelaw, J. H. (1980) Velocity and temperature measurements in a premixed flame with an axisymmetric combustor. AGARD Conference Proc. 281, Paper 14.

Taylor, A. M. K. P. and Whitelaw, J. H. (1984) Velocity characteristics in the turbulent shear flows of confined axisymmetric bluff bodies. J. Fluid Mech. 139, 391.

Wright, F. H. (1959) Bluff-body flame stabilization: blockage effects. Comb. and Flame 26, 319.

Wright, F. H. and Zukoski, E. E. (1962) Flame spreading from bluff-body flame holders. Eighth Symposium (International) on Combustion, 933.

Yamaguchi, S., Ohiwa, N. and Kinoshita, S. (1975a) A study on opposed gaseous jet flame stabilized in a uniform air stream, 1st report Bull. JSME 18, 722.

Yamaguchi, S., Ohiwa, N. and Kinoshita, S. (1975b) A study on opposed gaseous jet flame stabilized in a uniform air stream, 2nd report. Bull JSME 18, 729.

Yamaguchi, S., Ohiwa, N. and Izumi, R. (1976) A study on opposed gaseous jet flame stabilized in a uniform air stream, 4th report. Bull. JSME 19, 431.

Yanagi, T. and Mimura, Y. (1981) Velocity-temperature correlation in premixed flame. Eighteenth Symposium (International) on Combustion, 1031.

Yoshida, A. (1981) Experimental study of wrinkled laminar flame. Eighteenth Symposium (International) on Combustion, 931.

Yoshida, A. (1983) Effect of mixture turbulence and composition on flame wrinkling in turbulent premixed flames. ASME-JSME Thermal Engineering Conference 4, 167.

Yoshida, A. and Gunther, R. (1980) Experimental investigation of thermal structures of turbulent premixed flames. Comb. and Flame 38, 249.

Yoshida, A. and Gunther, R. (1981) An experimental study of structure and reaction rate in turbulent premixed flames. Comb. Sci. and Tech. 26, 43.

Yoshida, A. and Tsuji, H. (1978) Measurements of fluctuating temperature and velocity in a turbulent premixed flame. Seventeenth Symposium (International) on Combustion, 945.

Yoshida, A. and Tsuji, H. (1982) Characteristic scale of wrinkles in turbulent premixed flames. Nineteenth Symposium (International)on Combustion, 403.

Yule, A. J., Ventura, J. M. P. and Chigier, N. A. (1981) On large scale eddy structures and turbulent mixing in flames. Symposium on Energy, Department of Energy - University of Missouri-Rolla, 73.

CHAPTER 6

CONCLUSION

W. C. Strahle and S. G. Lekoudis

By way of a Committee action, data bases of numerous turbulent reacting and non-reacting flows have been reviewed concerning their adequacy for computational test. The flows reviewed have been categorized as "simple" flows, as outlined in Chapter 1. Nine flows have been chosen as the "best", or most completely documented and understood in the sense of experimental error, and have been put forth in detail in this document. It is recognized that during the review effort several other data base generation processes were taking place, and other flows could have been chosen if the selection process were delayed. However, it was judged timely that the review process be terminated within an originally determined schedule.

Insofar as their suitability for comparison of analytical models, the flows chosen are quite adequate but not completely flawless. Consequently, the reader is cautioned to monitor the discussion of these flows as contained in the individual chapters of this document. In particular, the individual chapters contain recommendations for further work in each area, which would remove many of the limitations of the current data bases. The dominant problems arise from low Reynolds number, completeness of data and satisfactory understanding of data measurement, and recommendations are given to overcome these difficulties. Nevertheless, the cases presented should provide useful standards against which turbulence modellers and computors can test their methods.

It is hoped that this document will provide a good reference source for some time and will be used by members of the turbulent reacting flow community. The authors of Chapters 2-5 are to be congratulated for a valuable service to their profession and they are thanked by the editors of this volume.

APPENDIX A
TABULATED RESULTS
FOR CHAPTER 2

Rayleigh and velocity data for the propane jet corresponding to the results presented in Figures 1-13 of Chapter 2 of this review is tabulated in this appendix. These data have been tabulated for the use of those interested in the details of the measurements and to facilitate comparisons with modeling calculations and the results of other investigators. A complete set of tabulated data at all measurement locations (see Table 7 of Chapter 2) is available from Sandia National Laboratories, Livermore. Copies of the tables have been stored on magnetic tape and are also available.

The Rayleigh data is presented in Tables A1-A8 and the velocity data in Tables A9-A24. The presentation of the Rayleigh data is as follows. In Tables A1-A4 the data corresponding to an axial profile along the centerline and radial profiles at x/D = 15, 30 and 50 are presented. In the format adopted the first two columns give the axial and radial locations x/D and y/D, respectively. The remaining columns give the mean density and propane mixture fraction, the rms of the fluctuations, the intermittency, and the third and fourth moments. Comment lines at the top of each table give descriptive information on the filename the data is stored in on magnetic tape, the flow conditions and the type of profile presented. Tables A5-A8 contain the corresponding probability density distributions of the mixture fraction for x/D = 30 at each radial location. Two columns are given for each location, the mixture fraction f and the probability P(f) corresponding to that mixture fraction. All pdf's were calculated for 50 bins equally spaced over the 3 standard deviation limits of the data at each location.

The velocity data presented in Tables A9-A24 are presented in a similar format. A centerline profile and radial profiles at x/D = 15, 30 and 50 are given in Tables A9-A16. Axial and radial locations are again located in the first two columns. In addition the mean axial and radial velocities U and V, the rms of each velocity component, and the correlation of u and v are given. At each location two sets of data are tabulated, the first corresponding to results with only the coflowing air seeded with LV particles and the second corresponding to LV seed added to the propane jet. The pdf's of axial and radial velocity at x/D = 30 are given in Tables A17-A24. At each location the pdf of the axial velocity p(u) is located in columns 1 and 2 and the pdf of the radial velocity p(v) in columns 3 and 4. Again, two data sets are given at each location corresponding to whether the measurements were made with LV seed added to the coflowing air or the propane jet.

Table A1

C FILENAME: PAX.RAY
C Propane Jet in Coflowing Air Stream
C Axial Profile Measured using Rayleigh
C Radial Position, y/D= 0.0
C Bulk Jet Velocity=53 m/s, Jet Reynolds No.=68168
C Coflowing Air Velocity=9.5 m/s

C x/D	y/D	RHOmean (kg/m*3)	Fmean	RHOsigma (kg/m*3)	Fsigma	I	Skew	Kurt
1.78	0.00	0.206E+01	1.000	0.118E-01	0.966E-02	1.000	-.182E+01	0.569E+01
3.08	0.00	0.200E+01	1.005	0.842E-02	0.749E-02	1.000	-.101E+02	0.133E+03
3.75	0.00	0.200E+01	1.000	0.209E-01	0.188E-01	1.000	-.551E+01	0.449E+02
5.22	0.00	0.195E+01	0.988	0.550E-01	0.517E-01	1.000	-.180E+01	0.659E+01
7.12	0.00	0.187E+01	0.910	0.754E-01	0.755E-01	1.000	-.921E+00	0.395E+01
10.78	0.00	0.168E+01	0.711	0.696E-01	0.832E-01	1.000	-.583E+00	0.357E+01
12.42	0.00	0.161E+01	0.621	0.665E-01	0.843E-01	1.000	-.105E+00	0.466E+01
15.03	0.00	0.153E+01	0.522	0.567E-01	0.786E-01	1.000	-.214E+00	0.472E+01
20.55	0.00	0.143E+01	0.379	0.438E-01	0.679E-01	1.000	-.846E-01	0.588E+01
24.78	0.00	0.139E+01	0.307	0.364E-01	0.600E-01	1.000	-.194E+00	0.458E+01
29.79	0.00	0.135E+01	0.239	0.309E-01	0.530E-01	1.000	0.225E+00	0.948E+01
39.00	0.00	0.132E+01	0.185	0.227E-01	0.411E-01	1.000	-.246E+00	0.370E+01
48.34	0.00	0.129E+01	0.140	0.184E-01	0.342E-01	1.000	0.221E+00	0.113E+02
62.42	0.00	0.128E+01	0.112	0.160E-01	0.287E-01	1.000	0.324E+01	0.105E+03

Table A2

C FILENAME: P15.RAY
C Propane Jet in Coflowing Air Stream
C Radial Profile Measured using Rayleigh
C Axial Position, x/D= 15.020
C Bulk Jet Velocity=53 m/s, Jet Reynolds No.=68168
C Coflowing Air Velocity=9.5 m/s

C x/D	y/D	RHOmean (kg/m*3)	Fmean	RHOrms (kg/m*3)	Frms	I	Skew	Kurt
15.02	-2.73	0.122E+01	0.000	0.228E-02	0.465E-02	0.001	0.494E+01	0.137E+03
15.01	-2.46	0.122E+01	0.004	0.396E-02	0.108E-01	0.005	0.443E+01	0.101E+03
15.01	-2.17	0.122E+01	0.001	0.112E-01	0.220E-01	0.056	0.592E+01	0.460E+02
15.01	-1.87	0.123E+01	0.027	0.268E-01	0.519E-01	0.311	0.218E+01	0.774E+01
15.01	-1.58	0.126E+01	0.083	0.420E-01	0.793E-01	0.722	0.886E+00	0.318E+01
15.00	-1.27	0.131E+01	0.172	0.506E-01	0.907E-01	0.974	0.309E+00	0.270E+01
15.00	-1.13	0.135E+01	0.237	0.575E-01	0.988E-01	0.997	0.120E+00	0.265E+01
15.00	-0.99	0.136E+01	0.264	0.564E-01	0.954E-01	0.998	0.362E-01	0.273E+01
15.00	-0.85	0.140E+01	0.326	0.605E-01	0.980E-01	1.000	-.952E-01	0.274E+01
15.00	-0.70	0.142E+01	0.365	0.588E-01	0.931E-01	1.000	-.263E+00	0.280E+01
15.00	-0.55	0.146E+01	0.425	0.596E-01	0.901E-01	1.000	-.330E+00	0.292E+01
15.00	-0.42	0.148E+01	0.453	0.560E-01	0.829E-01	1.000	-.427E+00	0.314E+01
15.00	-0.26	0.150E+01	0.480	0.524E-01	0.760E-01	1.000	-.459E+00	0.322E+01
15.00	-0.11	0.153E+01	0.517	0.517E-01	0.727E-01	1.000	-.466E+00	0.331E+01
15.00	0.04	0.152E+01	0.501	0.491E-01	0.700E-01	1.000	-.457E+00	0.341E+01
15.00	0.17	0.152E+01	0.509	0.528E-01	0.748E-01	1.000	-.463E+00	0.338E+01
15.00	0.32	0.149E+01	0.462	0.541E-01	0.796E-01	1.000	-.460E+00	0.316E+01
15.00	0.47	0.147E+01	0.427	0.562E-01	0.849E-01	1.000	-.385E+00	0.306E+01
15.00	0.62	0.145E+01	0.401	0.612E-01	0.942E-01	1.000	-.303E+00	0.285E+01
15.00	0.89	0.138E+01	0.291	0.588E-01	0.965E-01	1.000	0.723E-01	0.433E+01
15.00	1.20	0.132E+01	0.190	0.519E-01	0.922E-01	0.984	0.219E+00	0.266E+01
15.00	1.48	0.128E+01	0.117	0.473E-01	0.874E-01	0.883	0.692E+00	0.296E+01
15.00	1.78	0.124E+01	0.038	0.311E-01	0.599E-01	0.427	0.173E+01	0.575E+01
15.00	1.78	0.122E+01	0.004	0.200E-02	0.819E-02	0.000	-.130E+01	0.186E+01
15.00	1.78	0.122E+01	0.003	0.196E-02	0.770E-02	0.000	-.131E+01	0.190E+01

Table A3

C FILENAME: P30.RAY
C Propane Jet in Coflowing Air Stream
C Radial Profile Measured using Rayleigh
C Axial Position, x/D= 30.000
C Bulk Jet Velocity=53 m/s, Jet Reynolds No.=68168
C Coflowing Air Velocity=9.5 m/s

C x/D	y/D	RHOmean (kg/m*3)	Fmean	RHOrms (kg/m*3)	Frms	I	Skew	Kurt
30.00	-5.00	0.122E+01	0.000	0.219E-02	0.450E-02	0.000	0.246E-02	0.303E+01
30.00	-4.72	0.122E+01	0.000	0.223E-02	0.458E-02	0.000	-.223E-01	0.306E+01
30.00	-4.41	0.122E+01	0.000	0.244E-02	0.500E-02	0.002	0.105E+01	0.185E+02
30.00	-4.13	0.122E+01	0.000	0.372E-02	0.742E-02	0.007	0.106E+02	0.227E+03
30.00	-3.83	0.122E+01	0.000	0.698E-02	0.138E-01	0.024	0.772E+01	0.790E+02
30.00	-3.51	0.122E+01	0.006	0.113E-01	0.222E-01	0.073	0.474E+01	0.292E+02
30.00	-3.22	0.123E+01	0.014	0.177E-01	0.347E-01	0.186	0.283E+01	0.114E+02
30.00	-2.92	0.123E+01	0.029	0.230E-01	0.451E-01	0.381	0.161E+01	0.500E+01
30.00	-2.63	0.125E+01	0.057	0.292E-01	0.567E-01	0.635	0.869E+00	0.295E+01
30.00	-2.35	0.127E+01	0.089	0.333E-01	0.636E-01	0.831	0.467E+00	0.248E+01
30.00	-2.04	0.128E+01	0.109	0.336E-01	0.636E-01	0.914	0.194E+00	0.243E+01
30.00	-1.76	0.129E+01	0.130	0.336E-01	0.628E-01	0.963	0.259E-01	0.251E+01
30.00	-1.47	0.130E+01	0.155	0.326E-01	0.602E-01	0.989	-.108E+00	0.267E+01
30.00	-1.18	0.132E+01	0.185	0.327E-01	0.592E-01	0.997	-.263E+00	0.288E+01
30.00	-0.90	0.134E+01	0.218	0.329E-01	0.582E-01	1.000	-.313E+00	0.289E+01
29.99	-0.59	0.134E+01	0.224	0.326E-01	0.539E-01	1.000	0.739E+00	0.300E+02
30.00	-0.30	0.134E+01	0.234	0.313E-01	0.522E-01	1.000	0.823E+00	0.263E+02
30.00	-0.01	0.136E+01	0.254	0.295E-01	0.508E-01	1.000	-.257E+00	0.330E+01
30.00	0.26	0.134E+01	0.234	0.307E-01	0.512E-01	1.000	0.659E+00	0.264E+02
30.00	0.52	0.135E+01	0.240	0.310E-01	0.539E-01	1.000	-.280E+00	0.312E+01
30.00	0.81	0.133E+01	0.209	0.308E-01	0.549E-01	1.000	-.309E+00	0.301E+01
30.00	1.41	0.131E+01	0.169	0.330E-01	0.603E-01	0.994	-.148E+00	0.272E+01
30.00	1.99	0.128E+01	0.111	0.323E-01	0.611E-01	0.936	0.156E+00	0.248E+01
30.00	2.58	0.125E+01	0.055	0.279E-01	0.543E-01	0.851	0.777E+00	0.292E+01

Table A4

C FILENAME: P50.RAY
C Propane Jet in Coflowing Air Stream
C Radial Profile Measured using Rayleigh
C Axial Position, x/D= 50.000
C Bulk Jet Velocity=53 m/s, Jet Reynolds No.=68168
C Coflowing Air Velocity=9.5 m/s

C x/D	y/D	RHOmean (kg/m*3)	Fmean	RHOrms (kg/m*3)	Frms	I	Skew	Kurt
50.00	-6.21	0.122E+01	0.001	0.332E-02	0.671E-02	0.007	0.690E+01	0.946E+02
50.00	-5.92	0.122E+01	0.001	0.360E-02	0.750E-02	0.010	0.567E+01	0.696E+02
50.00	-5.63	0.122E+01	0.000	0.449E-02	0.906E-02	0.019	0.640E+01	0.667E+02
49.99	-5.33	0.122E+01	0.002	0.696E-02	0.140E-01	0.054	0.449E+01	0.264E+02
50.00	-5.04	0.122E+01	0.005	0.875E-02	0.175E-01	0.083	0.390E+01	0.202E+02
50.00	-4.73	0.122E+01	0.009	0.119E-01	0.239E-01	0.169	0.263E+01	0.101E+02
50.00	-4.44	0.123E+01	0.015	0.147E-01	0.293E-01	0.266	0.190E+01	0.599E+01
50.00	-4.14	0.123E+01	0.026	0.175E-01	0.347E-01	0.396	0.134E+01	0.396E+01
50.00	-3.84	0.124E+01	0.035	0.187E-01	0.371E-01	0.546	0.791E+00	0.263E+01
50.00	-3.56	0.124E+01	0.045	0.203E-01	0.402E-01	0.657	0.546E+00	0.235E+01
50.00	-3.25	0.125E+01	0.058	0.212E-01	0.416E-01	0.782	0.357E+00	0.276E+01
50.00	-2.96	0.125E+01	0.068	0.212E-01	0.415E-01	0.859	0.115E+00	0.227E+01
50.00	-2.66	0.126E+01	0.077	0.208E-01	0.404E-01	0.918	0.376E-01	0.263E+01
50.00	-2.36	0.126E+01	0.088	0.202E-01	0.391E-01	0.958	-.120E+00	0.257E+01
50.00	-2.08	0.127E+01	0.098	0.210E-01	0.404E-01	0.974	-.128E+00	0.264E+01
50.00	-1.77	0.128E+01	0.112	0.206E-01	0.393E-01	0.987	-.304E+00	0.286E+01
50.00	-1.49	0.128E+01	0.117	0.198E-01	0.376E-01	0.994	-.296E+00	0.293E+01
50.00	-1.18	0.128E+01	0.122	0.192E-01	0.363E-01	0.997	-.310E+00	0.295E+01
50.00	-0.89	0.129E+01	0.128	0.184E-01	0.346E-01	0.997	-.371E+00	0.343E+01
50.00	-0.61	0.129E+01	0.133	0.181E-01	0.339E-01	0.999	-.330E+00	0.337E+01
50.00	-0.32	0.129E+01	0.136	0.216E-01	0.345E-01	1.000	0.471E+01	0.196E+03
50.00	-0.02	0.129E+01	0.137	0.219E-01	0.348E-01	1.000	0.514E+01	0.208E+03
50.00	0.26	0.129E+01	0.135	0.186E-01	0.336E-01	1.000	0.125E+01	0.455E+02
50.00	0.55	0.129E+01	0.135	0.180E-01	0.337E-01	0.999	-.309E+00	0.312E+01
50.00	0.84	0.129E+01	0.128	0.181E-01	0.341E-01	0.998	-.317E+00	0.313E+01
50.00	1.14	0.128E+01	0.123	0.187E-01	0.354E-01	0.997	-.320E+00	0.328E+01
50.00	1.43	0.128E+01	0.119	0.199E-01	0.377E-01	0.993	-.283E+00	0.340E+01
50.00	1.72	0.128E+01	0.110	0.199E-01	0.380E-01	0.991	-.218E+00	0.278E+01
50.00	2.01	0.127E+01	0.099	0.203E-01	0.391E-01	0.978	-.178E+00	0.264E+01
50.00	2.31	0.126E+01	0.084	0.201E-01	0.389E-01	0.952	-.306E-01	0.279E+01
50.00	2.60	0.126E+01	0.081	0.215E-01	0.418E-01	0.924	0.606E-01	0.240E+01
50.00	3.18	0.125E+01	0.060	0.208E-01	0.407E-01	0.810	0.436E+00	0.629E+01
50.00	3.75	0.124E+01	0.038	0.188E-01	0.374E-01	0.599	0.674E+00	0.246E+01

Table A5

FILENAME: P30F3.PDF
C Propane Jet in Coflowing Air Stream
C PDF of Mixture Fraction Measured using Rayleigh
C Axial Position, x/D= 30.00
C Bulk Jet Velocity=53 m/s, Jet Reynolds No.=68168
C Coflowing Air Velocity=9.5 m/s
C

y/D= -3.22		y/D= -2.92		y/D= -2.63	
f	P(f)	f	P(f)	f	P(f)
0.114E+00	0.555E+00	0.159E+00	0.518E+00	0.221E+00	0.296E+00
0.110E+00	0.924E+00	0.154E+00	0.104E+01	0.214E+00	0.296E+00
0.106E+00	0.863E+00	0.148E+00	0.127E+01	0.207E+00	0.555E+00
0.101E+00	0.129E+01	0.143E+00	0.847E+00	0.200E+00	0.702E+00
0.973E-01	0.863E+00	0.137E+00	0.118E+01	0.193E+00	0.813E+00
0.931E-01	0.216E+01	0.132E+00	0.165E+01	0.186E+00	0.592E+00
0.889E-01	0.986E+00	0.127E+00	0.137E+01	0.180E+00	0.115E+01
0.848E-01	0.142E+01	0.121E+00	0.122E+01	0.173E+00	0.148E+01
0.806E-01	0.117E+01	0.116E+00	0.278E+01	0.166E+00	0.129E+01
0.764E-01	0.924E+00	0.110E+00	0.231E+01	0.159E+00	0.185E+01
0.723E-01	0.136E+01	0.105E+00	0.155E+01	0.153E+00	0.244E+01
0.681E-01	0.117E+01	0.995E-01	0.240E+01	0.146E+00	0.248E+01
0.640E-01	0.185E+01	0.941E-01	0.240E+01	0.139E+00	0.240E+01
0.598E-01	0.117E+01	0.887E-01	0.381E+01	0.132E+00	0.274E+01
0.556E-01	0.259E+01	0.833E-01	0.212E+01	0.125E+00	0.337E+01
0.515E-01	0.111E+01	0.779E-01	0.273E+01	0.118E+00	0.322E+01
0.473E-01	0.154E+01	0.724E-01	0.264E+01	0.112E+00	0.403E+01
0.431E-01	0.240E+01	0.670E-01	0.330E+01	0.105E+00	0.529E+01
0.390E-01	0.160E+01	0.616E-01	0.372E+01	0.980E-01	0.492E+01
0.348E-01	0.117E+01	0.562E-01	0.508E+01	0.912E-01	0.484E+01
0.306E-01	0.284E+01	0.508E-01	0.296E+01	0.844E-01	0.488E+01
0.265E-01	0.179E+01	0.454E-01	0.287E+01	0.776E-01	0.466E+01
0.223E-01	0.290E+01	0.400E-01	0.386E+01	0.708E-01	0.499E+01
0.182E-01	0.203E+01	0.345E-01	0.461E+01	0.640E-01	0.410E+01
0.140E-01	0.364E+01	0.291E-01	0.348E+01	0.572E-01	0.444E+01
0.983E-02	0.102E+02	0.237E-01	0.381E+01	0.504E-01	0.447E+01
0.567E-02	0.337E+02	0.183E-01	0.527E+01	0.436E-01	0.529E+01
0.151E-02	0.585E+02	0.129E-01	0.598E+01	0.368E-01	0.492E+01
-.266E-02	0.624E+02	0.747E-02	0.162E+02	0.300E-01	0.514E+01
-.682E-02	0.324E+02	0.205E-02	0.472E+02	0.232E-01	0.529E+01
-.110E-01	0.253E+01	-.336E-02	0.368E+02	0.164E-01	0.754E+01
-.152E-01	0.616E-01	-.878E-02	0.730E+01	0.961E-02	0.107E+02
-.193E-01	0.000E+00	-.142E-01	0.377E+00	0.281E-02	0.254E+02
-.235E-01	0.000E+00	-.196E-01	0.000E+00	-.399E-02	0.102E+02
-.276E-01	0.000E+00	-.250E-01	0.000E+00	-.108E-01	0.333E+00
-.318E-01	0.000E+00	-.304E-01	0.000E+00	-.176E-01	0.000E+00
-.360E-01	0.000E+00	-.358E-01	0.000E+00	-.244E-01	0.000E+00
-.401E-01	0.000E+00	-.413E-01	0.000E+00	-.312E-01	0.000E+00
-.443E-01	0.000E+00	-.467E-01	0.000E+00	-.380E-01	0.000E+00
-.485E-01	0.000E+00	-.521E-01	0.000E+00	-.448E-01	0.000E+00
-.526E-01	0.000E+00	-.575E-01	0.000E+00	-.516E-01	0.000E+00
-.568E-01	0.000E+00	-.629E-01	0.000E+00	-.584E-01	0.000E+00
-.609E-01	0.000E+00	-.684E-01	0.000E+00	-.652E-01	0.000E+00
-.651E-01	0.000E+00	-.738E-01	0.000E+00	-.720E-01	0.000E+00
-.693E-01	0.000E+00	-.792E-01	0.000E+00	-.788E-01	0.000E+00
-.734E-01	0.000E+00	-.846E-01	0.000E+00	-.856E-01	0.000E+00
-.776E-01	0.000E+00	-.900E-01	0.000E+00	-.924E-01	0.000E+00
-.818E-01	0.000E+00	-.954E-01	0.000E+00	-.992E-01	0.000E+00
-.859E-01	0.000E+00	-.101E+00	0.000E+00	-.106E+00	0.000E+00
-.901E-01	0.000E+00	-.106E+00	0.000E+00	-.113E+00	0.000E+00

Table A6

FILENAME: P30F4.PDF

C Propane Jet in Coflowing Air Stream
C PDF of Mixture Fraction Measured using Rayleigh
C Axial Position, x/D= 30.00
C Bulk Jet Velocity=53 m/s, Jet Reynolds No.=68168
C Coflowing Air Velocity=9.5 m/s
C

y/D= -2.36		y/D= -2.04		y/D= -1.75	
f	P(f)	f	P(f)	f	P(f)
0.272E+00	0.132E+00	0.292E+00	0.656E-01	0.311E+00	0.000E+00
0.264E+00	0.263E+00	0.284E+00	0.164E+00	0.304E+00	0.000E+00
0.257E+00	0.296E+00	0.277E+00	0.328E+00	0.296E+00	0.332E-01
0.249E+00	0.526E+00	0.269E+00	0.328E+00	0.289E+00	0.995E-01
0.241E+00	0.624E+00	0.261E+00	0.623E+00	0.281E+00	0.299E+00
0.234E+00	0.624E+00	0.254E+00	0.558E+00	0.273E+00	0.299E+00
0.226E+00	0.963E+00	0.246E+00	0.984E+00	0.266E+00	0.597E+00
0.218E+00	0.148E+01	0.238E+00	0.754E+00	0.258E+00	0.730E+00
0.211E+00	0.128E+01	0.231E+00	0.886E+00	0.251E+00	0.106E+01
0.203E+00	0.102E+01	0.223E+00	0.141E+01	0.243E+00	0.103E+01
0.195E+00	0.154E+01	0.216E+00	0.197E+01	0.236E+00	0.143E+01
0.188E+00	0.204E+01	0.208E+00	0.220E+01	0.228E+00	0.199E+01
0.180E+00	0.237E+01	0.200E+00	0.249E+01	0.221E+00	0.219E+01
0.172E+00	0.227E+01	0.193E+00	0.256E+01	0.213E+00	0.279E+01
0.165E+00	0.269E+01	0.185E+00	0.312E+01	0.206E+00	0.318E+01
0.157E+00	0.375E+01	0.177E+00	0.338E+01	0.198E+00	0.441E+01
0.150E+00	0.394E+01	0.170E+00	0.377E+01	0.191E+00	0.441E+01
0.142E+00	0.296E+01	0.162E+00	0.463E+01	0.183E+00	0.511E+01
0.134E+00	0.453E+01	0.155E+00	0.584E+01	0.176E+00	0.498E+01
0.127E+00	0.493E+01	0.147E+00	0.348E+01	0.168E+00	0.431E+01
0.119E+00	0.414E+01	0.139E+00	0.571E+01	0.160E+00	0.531E+01
0.111E+00	0.549E+01	0.132E+00	0.548E+01	0.153E+00	0.624E+01
0.104E+00	0.427E+01	0.124E+00	0.495E+01	0.145E+00	0.474E+01
0.962E-01	0.654E+01	0.116E+00	0.594E+01	0.138E+00	0.624E+01
0.885E-01	0.421E+01	0.109E+00	0.597E+01	0.130E+00	0.541E+01
0.809E-01	0.522E+01	0.101E+00	0.610E+01	0.123E+00	0.687E+01
0.733E-01	0.457E+01	0.936E-01	0.561E+01	0.115E+00	0.650E+01
0.656E-01	0.634E+01	0.859E-01	0.689E+01	0.108E+00	0.464E+01
0.580E-01	0.506E+01	0.783E-01	0.456E+01	0.100E+00	0.614E+01
0.504E-01	0.509E+01	0.707E-01	0.525E+01	0.926E-01	0.445E+01
0.427E-01	0.463E+01	0.631E-01	0.364E+01	0.850E-01	0.474E+01
0.351E-01	0.365E+01	0.554E-01	0.472E+01	0.775E-01	0.504E+01
0.275E-01	0.552E+01	0.478E-01	0.328E+01	0.699E-01	0.395E+01
0.198E-01	0.513E+01	0.402E-01	0.302E+01	0.624E-01	0.325E+01
0.122E-01	0.858E+01	0.325E-01	0.387E+01	0.549E-01	0.289E+01
0.455E-02	0.118E+02	0.249E-01	0.361E+01	0.473E-01	0.295E+01
-.308E-02	0.250E+01	0.173E-01	0.315E+01	0.398E-01	0.352E+01
-.107E-01	0.000E+00	0.964E-02	0.453E+01	0.323E-01	0.259E+01
-.183E-01	0.000E+00	0.201E-02	0.426E+01	0.247E-01	0.176E+01
-.260E-01	0.000E+00	-.561E-02	0.951E+00	0.172E-01	0.166E+01
-.336E-01	0.000E+00	-.132E-01	0.656E-01	0.965E-02	0.202E+01
-.413E-01	0.000E+00	-.209E-01	0.000E+00	0.212E-02	0.186E+01
-.489E-01	0.000E+00	-.285E-01	0.000E+00	-.542E-02	0.982E+00
-.565E-01	0.000E+00	-.361E-01	0.000E+00	-.130E-01	0.332E-01
-.641E-01	0.000E+00	-.438E-01	0.000E+00	-.205E-01	0.000E+00
-.718E-01	0.000E+00	-.514E-01	0.000E+00	-.280E-01	0.000E+00
-.794E-01	0.000E+00	-.590E-01	0.000E+00	-.356E-01	0.000E+00
-.871E-01	0.000E+00	-.667E-01	0.000E+00	-.431E-01	0.000E+00
-.947E-01	0.000E+00	-.743E-01	0.000E+00	-.506E-01	0.000E+00
-.102E+00	0.000E+00	-.819E-01	0.000E+00	-.582E-01	0.000E+00

Table A7

FILENAME: P30F5.PDF
C Propane Jet in Coflowing Air Stream
C PDF of Mixture Fraction Measured using Rayleigh
C Axial Position, x/D= 30.00
C Bulk Jet Velocity=53 m/s, Jet Reynolds No.=68168
C Coflowing Air Velocity=9.5 m/s
C

y/D= -1.47		y/D= -1.18		y/D= -0.90	
f	P(f)	f	P(f)	f	P(f)
0.329E+00	0.000E+00	0.355E+00	0.352E-01	0.386E+00	0.358E-01
0.321E+00	0.692E-01	0.348E+00	0.352E-01	0.379E+00	0.000E+00
0.314E+00	0.104E+00	0.341E+00	0.141E+00	0.372E+00	0.108E+00
0.307E+00	0.208E+00	0.334E+00	0.247E+00	0.365E+00	0.358E-01
0.300E+00	0.312E+00	0.327E+00	0.247E+00	0.358E+00	0.108E+00
0.292E+00	0.450E+00	0.320E+00	0.317E+00	0.351E+00	0.359E+00
0.285E+00	0.485E+00	0.313E+00	0.493E+00	0.344E+00	0.538E+00
0.278E+00	0.623E+00	0.305E+00	0.811E+00	0.337E+00	0.681E+00
0.271E+00	0.104E+01	0.298E+00	0.916E+00	0.330E+00	0.825E+00
0.264E+00	0.121E+01	0.291E+00	0.194E+01	0.323E+00	0.118E+01
0.256E+00	0.190E+01	0.284E+00	0.208E+01	0.316E+00	0.165E+01
0.249E+00	0.260E+01	0.277E+00	0.180E+01	0.309E+00	0.212E+01
0.242E+00	0.305E+01	0.270E+00	0.271E+01	0.302E+00	0.282E+01
0.235E+00	0.336E+01	0.263E+00	0.384E+01	0.295E+00	0.319E+01
0.228E+00	0.291E+01	0.256E+00	0.388E+01	0.288E+00	0.466E+01
0.220E+00	0.512E+01	0.249E+00	0.405E+01	0.281E+00	0.498E+01
0.213E+00	0.481E+01	0.242E+00	0.529E+01	0.274E+00	0.488E+01
0.206E+00	0.426E+01	0.234E+00	0.578E+01	0.267E+00	0.638E+01
0.199E+00	0.571E+01	0.227E+00	0.539E+01	0.260E+00	0.574E+01
0.191E+00	0.526E+01	0.220E+00	0.663E+01	0.253E+00	0.495E+01
0.184E+00	0.706E+01	0.213E+00	0.687E+01	0.246E+00	0.706E+01
0.177E+00	0.661E+01	0.206E+00	0.578E+01	0.239E+00	0.706E+01
0.170E+00	0.505E+01	0.199E+00	0.638E+01	0.232E+00	0.516E+01
0.162E+00	0.699E+01	0.192E+00	0.627E+01	0.225E+00	0.739E+01
0.155E+00	0.554E+01	0.185E+00	0.705E+01	0.218E+00	0.581E+01
0.148E+00	0.654E+01	0.178E+00	0.620E+01	0.211E+00	0.652E+01
0.141E+00	0.630E+01	0.170E+00	0.670E+01	0.204E+00	0.530E+01
0.134E+00	0.582E+01	0.163E+00	0.585E+01	0.197E+00	0.678E+01
0.126E+00	0.509E+01	0.156E+00	0.514E+01	0.190E+00	0.502E+01
0.119E+00	0.516E+01	0.149E+00	0.543E+01	0.183E+00	0.595E+01
0.112E+00	0.488E+01	0.142E+00	0.352E+01	0.176E+00	0.437E+01
0.105E+00	0.467E+01	0.135E+00	0.412E+01	0.169E+00	0.419E+01
0.975E-01	0.350E+01	0.128E+00	0.384E+01	0.162E+00	0.459E+01
0.903E-01	0.350E+01	0.121E+00	0.285E+01	0.155E+00	0.283E+01
0.830E-01	0.398E+01	0.114E+00	0.292E+01	0.148E+00	0.258E+01
0.758E-01	0.284E+01	0.106E+00	0.310E+01	0.141E+00	0.369E+01
0.686E-01	0.190E+01	0.994E-01	0.204E+01	0.134E+00	0.212E+01
0.614E-01	0.176E+01	0.923E-01	0.166E+01	0.127E+00	0.219E+01
0.542E-01	0.159E+01	0.852E-01	0.169E+01	0.120E+00	0.179E+01
0.469E-01	0.152E+01	0.781E-01	0.951E+00	0.113E+00	0.186E+01
0.397E-01	0.121E+01	0.710E-01	0.134E+01	0.106E+00	0.151E+01
0.325E-01	0.111E+01	0.639E-01	0.113E+01	0.992E-01	0.122E+01
0.253E-01	0.623E+00	0.568E-01	0.493E+00	0.922E-01	0.645E+00
0.180E-01	0.658E+00	0.497E-01	0.599E+00	0.852E-01	0.538E+00
0.108E-01	0.554E+00	0.426E-01	0.775E+00	0.783E-01	0.609E+00
0.360E-02	0.415E+00	0.355E-01	0.317E+00	0.713E-01	0.538E+00
-.362E-02	0.104E+00	0.284E-01	0.282E+00	0.643E-01	0.251E+00
-.109E-01	0.000E+00	0.213E-01	0.282E+00	0.573E-01	0.359E+00
-.181E-01	0.000E+00	0.142E-01	0.247E+00	0.503E-01	0.143E+00
-.253E-01	0.000E+00	0.709E-02	0.317E+00	0.433E-01	0.717E-01

Table A8

FILENAME: P30F8.PDF
C Propane Jet in Coflowing Air Stream
C PDF of Mixture Fraction Measured using Rayleigh
C Axial Position, x/D= 30.00
C Bulk Jet Velocity=53 m/s, Jet Reynolds No.=68168
C Coflowing Air Velocity=9.5 m/s
C

C y/D=	-0.59	y/D=	-0.30	y/D=	-0.01
C f	P(f)	f	P(f)	f	P(f)
0.380E+00	0.776E-01	0.384E+00	0.000E+00	0.400E+00	0.000E+00
0.373E+00	0.776E-01	0.378E+00	0.000E+00	0.394E+00	0.123E+00
0.367E+00	0.000E+00	0.371E+00	0.000E+00	0.388E+00	0.123E+00
0.360E+00	0.116E+00	0.365E+00	0.120E+00	0.382E+00	0.822E-01
0.354E+00	0.388E-01	0.359E+00	0.280E+00	0.376E+00	0.123E+00
0.347E+00	0.233E+00	0.352E+00	0.320E+00	0.370E+00	0.822E-01
0.341E+00	0.349E+00	0.346E+00	0.200E+00	0.363E+00	0.493E+00
0.334E+00	0.815E+00	0.340E+00	0.481E+00	0.357E+00	0.493E+00
0.328E+00	0.815E+00	0.334E+00	0.921E+00	0.351E+00	0.111E+01
0.321E+00	0.136E+01	0.327E+00	0.801E+00	0.345E+00	0.127E+01
0.315E+00	0.190E+01	0.321E+00	0.180E+01	0.339E+00	0.138E+01
0.308E+00	0.237E+01	0.315E+00	0.236E+01	0.333E+00	0.173E+01
0.302E+00	0.221E+01	0.309E+00	0.228E+01	0.327E+00	0.354E+01
0.296E+00	0.431E+01	0.302E+00	0.449E+01	0.321E+00	0.362E+01
0.289E+00	0.299E+01	0.296E+00	0.404E+01	0.315E+00	0.378E+01
0.283E+00	0.489E+01	0.290E+00	0.416E+01	0.308E+00	0.481E+01
0.276E+00	0.757E+01	0.284E+00	0.569E+01	0.302E+00	0.555E+01
0.270E+00	0.489E+01	0.277E+00	0.553E+01	0.296E+00	0.604E+01
0.263E+00	0.559E+01	0.271E+00	0.597E+01	0.290E+00	0.773E+01
0.257E+00	0.761E+01	0.265E+00	0.629E+01	0.284E+00	0.724E+01
0.250E+00	0.710E+01	0.259E+00	0.757E+01	0.278E+00	0.711E+01
0.244E+00	0.664E+01	0.252E+00	0.102E+02	0.272E+00	0.810E+01
0.237E+00	0.958E+01	0.246E+00	0.753E+01	0.266E+00	0.107E+02
0.231E+00	0.722E+01	0.240E+00	0.697E+01	0.260E+00	0.773E+01
0.224E+00	0.776E+01	0.234E+00	0.845E+01	0.254E+00	0.818E+01
0.218E+00	0.718E+01	0.227E+00	0.785E+01	0.248E+00	0.732E+01
0.211E+00	0.632E+01	0.221E+00	0.717E+01	0.241E+00	0.682E+01
0.205E+00	0.764E+01	0.215E+00	0.649E+01	0.235E+00	0.678E+01
0.199E+00	0.551E+01	0.208E+00	0.665E+01	0.229E+00	0.670E+01
0.192E+00	0.555E+01	0.202E+00	0.593E+01	0.223E+00	0.510E+01
0.186E+00	0.485E+01	0.196E+00	0.557E+01	0.217E+00	0.534E+01
0.179E+00	0.536E+01	0.190E+00	0.484E+01	0.211E+00	0.477E+01
0.173E+00	0.380E+01	0.183E+00	0.501E+01	0.205E+00	0.456E+01
0.166E+00	0.392E+01	0.177E+00	0.348E+01	0.199E+00	0.304E+01
0.160E+00	0.291E+01	0.171E+00	0.340E+01	0.193E+00	0.329E+01
0.153E+00	0.299E+01	0.165E+00	0.280E+01	0.187E+00	0.387E+01
0.147E+00	0.210E+01	0.158E+00	0.196E+01	0.181E+00	0.284E+01
0.140E+00	0.167E+01	0.152E+00	0.252E+01	0.174E+00	0.214E+01
0.134E+00	0.186E+01	0.146E+00	0.208E+01	0.168E+00	0.202E+01
0.127E+00	0.136E+01	0.140E+00	0.116E+01	0.162E+00	0.144E+01
0.121E+00	0.737E+00	0.133E+00	0.136E+01	0.156E+00	0.132E+01
0.114E+00	0.120E+01	0.127E+00	0.124E+01	0.150E+00	0.136E+01
0.108E+00	0.543E+00	0.121E+00	0.881E+00	0.144E+00	0.781E+00
0.101E+00	0.698E+00	0.115E+00	0.921E+00	0.138E+00	0.699E+00
0.950E-01	0.582E+00	0.108E+00	0.320E+00	0.132E+00	0.699E+00
0.886E-01	0.543E+00	0.102E+00	0.320E+00	0.126E+00	0.658E+00
0.821E-01	0.310E+00	0.957E-01	0.360E+00	0.119E+00	0.576E+00
0.756E-01	0.776E-01	0.895E-01	0.320E+00	0.113E+00	0.329E+00
0.692E-01	0.194E+00	0.832E-01	0.400E+00	0.107E+00	0.206E+00
0.627E-01	0.233E+00	0.769E-01	0.200E+00	0.101E+00	0.247E+00

Table A9

C FILENAME: paxv.air
C Propane Jet in Coflowing Air Stream
C Axial Velocity Profile Measured using LDV
C LDV Seed Added to air Stream
C Radial Position, y/D= 0.000
C Bulk Jet Velocity=53 m/s, Jet Reynolds No.=68168

C	x/D	y/D	U mean (m/s)	V mean (m/s)	Urms (m/s)	Vrms (m/s)	UV (m/s)*2
	3.8000	0.0000	65.2396	-0.5639	6.3936	6.2687	8.9503
	4.7000	0.0000	64.7194	-0.7535	6.7425	6.5890	5.7576
	5.7000	0.0000	63.5897	-0.5344	7.3678	6.5470	6.1010
	6.6000	0.0000	62.0262	-0.6116	7.8428	6.8174	7.1495
	8.4000	0.0000	57.5861	-0.5383	8.8367	7.2980	7.6422
	10.3000	0.0000	52.8915	-0.0259	8.3822	7.3914	4.9029
	12.2000	0.0000	48.3937	-0.2179	7.9641	7.1923	7.2959
	14.1000	0.0000	44.4272	-0.8421	7.5089	6.9365	3.7471
	15.9000	0.0000	41.0563	-0.6855	7.2787	6.4547	3.9174
	18.7000	0.0000	36.6680	-0.7007	6.6669	5.8410	4.3533
	19.7000	0.0000	35.1428	-0.6890	6.3167	5.6242	2.5073
	23.4000	0.0100	30.9775	-0.4620	5.5485	4.9818	2.9693
	27.2000	0.0100	27.6461	-0.3941	4.8579	4.4990	1.5442
	30.8000	0.0000	25.3710	-0.2261	4.2429	4.0077	1.7635
	34.5000	0.0000	23.5361	-0.2586	3.7865	3.6499	1.1931
	38.1000	0.0100	22.0471	-0.3162	3.4359	3.3322	0.8741
	41.8000	0.0000	20.9665	-0.2012	3.1557	3.1654	0.4953
	45.4000	0.0000	20.1087	-0.2082	2.9383	2.8961	0.8157
	49.0000	0.0000	19.2475	-0.2205	2.7487	2.6857	0.4827
	52.8000	0.0000	18.4748	-0.2018	2.5170	2.4918	0.5720
	56.4000	0.0000	17.9799	-0.1822	2.4092	2.3645	0.4180
	63.8000	0.0000	16.9347	-0.1296	2.0768	2.0660	0.4079
	71.1000	0.0100	16.1915	-0.1404	1.9158	1.9317	0.1771
	78.5000	0.0100	15.4913	-0.2146	1.7349	1.7266	0.2164

Table A10

C FILENAME: paxv.jet
C Propane Jet in Coflowing Air Stream
C Axial Velocity Profile Measured using LDV
C LDV Seed Added to jet Stream
C Radial Position, y/D= 0.000
C Bulk Jet Velocity=53 m/s, Jet Reynolds No.=68168

C x/D	y/D	U mean (m/s)	V mean (m/s)	Urms (m/s)	Vrms (m/s)	UV (m/s)*2
1.0000	0.0000	69.8761	-0.0786	3.6850	2.4169	1.1256
2.8000	0.0000	69.5874	-0.2318	3.6937	2.6737	1.9098
4.7000	0.0000	68.2228	-0.3877	4.9434	3.5727	4.9724
6.5000	0.0000	65.6946	-0.1103	6.4282	4.6569	8.4324
8.4000	0.0000	61.0932	-0.3367	7.6296	5.7011	9.4519
10.3000	0.0000	55.5319	-0.6288	7.9649	6.1389	9.9100
12.2000	0.0000	50.9027	-0.2858	7.7127	6.3279	6.3905
14.0000	0.0000	46.5681	-0.3502	7.2500	5.8519	6.7454
15.1000	0.0000	44.7755	-0.4745	7.1163	5.9168	6.7669
16.0000	0.0000	42.7374	-0.2853	7.1505	5.8593	5.9880
17.8000	0.0000	40.0048	-0.2676	6.5276	5.3797	3.1394
19.7000	0.0000	37.1893	-0.1676	6.3749	5.3501	3.7087
23.4000	0.0000	32.4000	-0.2293	5.7426	4.7658	2.8385
27.1000	0.0000	29.2220	-0.2854	4.9815	4.3537	2.7748
30.8000	0.0000	26.5396	-0.1210	4.5026	3.8973	1.8360
34.5000	0.0000	24.4917	-0.1135	4.0838	3.4963	0.5695
38.1000	0.0000	23.1257	-0.1022	3.7545	3.2145	1.0355
41.8000	0.0000	21.7031	-0.2230	3.3196	3.0591	0.6570
45.4000	0.0000	20.5845	-0.0618	3.0585	2.7134	0.5853
49.1000	0.0000	19.8040	0.0006	2.8370	2.6271	0.1253
50.6000	0.0100	19.2527	-0.0437	2.7895	2.5701	0.2474
52.8000	0.0100	19.0490	-0.1068	2.6292	2.4450	0.4107
54.4000	0.0100	18.5281	-0.1601	2.5283	2.3772	0.3503
55.3000	0.0000	18.2617	-0.0721	2.4959	2.3322	0.1257
56.4000	0.0000	18.4889	-0.0470	2.4727	2.3458	0.3905
62.6000	0.0000	17.3547	-0.1399	2.2084	2.0726	0.2010
70.0000	0.0100	16.3415	-0.0773	1.9765	1.8528	0.2479
81.0000	0.0000	15.3957	-0.1158	1.7153	1.6089	0.1163

Table A11

C FILENAME: P15V.AIR
C Propane Jet in Coflowing Air Stream
C Radial Velocity Profile Measured using LDV
C LDV Seed Added to AIR Stream
C Axial Position, x/D= 15
C Bulk Jet Velocity=53 m/s, Jet Reynolds No.=68168

C x/D	y/D	U mean (m/s)	V mean (m/s)	Urms (m/s)	Vrms (m/s)	UV (m/s)*2
15.0000	0.1550	42.4248	0.7036	7.3050	6.4240	7.0642
15.0000	0.4550	37.2420	1.1297	7.7935	6.6726	19.9978
15.0000	0.7650	30.0102	1.1623	7.6789	6.3641	22.8278
15.0000	1.0650	23.4409	1.3128	6.9968	5.7734	18.9338
15.0000	1.3650	17.3306	0.8145	5.7541	4.9435	14.1773
15.0000	1.6750	12.1895	0.0100	4.0119	3.4160	6.3022
15.0000	1.9850	9.5587	-0.2285	1.5565	1.8568	0.8466
15.0000	2.2850	9.1358	-0.1834	0.6697	0.9936	0.0074
15.0000	2.6050	9.1639	-0.2006	0.3811	0.5596	-0.0178
15.0000	2.9050	9.1932	-0.1794	0.2668	0.4272	-0.0109
15.0000	3.2050	9.2310	-0.1164	0.2037	0.3783	-0.0085
15.0000	3.5150	9.1977	-0.0088	0.1941	0.3707	-0.0090
15.0000	3.8350	9.2128	0.0616	0.1771	0.3661	-0.0119
15.0000	3.8350	9.2634	-0.0897	0.1803	0.4107	-0.0097
15.0000	4.4350	9.2660	-0.0680	0.1560	0.6243	-0.0040
15.0000	5.0650	9.2684	-0.0057	0.1314	0.5020	-0.0034
15.0000	0.1750	41.8680	0.7693	7.3516	6.5468	9.6179
15.0000	-0.1150	42.6637	0.0097	7.2258	6.4643	-5.9070
15.0000	-0.4150	38.0513	-0.1588	7.8311	6.4767	-19.6830
15.0000	-0.7250	30.5850	-0.0903	7.4299	6.1887	-20.4905
15.0000	-1.0250	24.5866	-0.5314	7.0175	5.7273	-18.8300
15.0000	-1.3350	18.2714	-0.3587	6.0889	5.0277	-14.9174
15.0000	-1.6350	13.2455	0.0396	4.5832	3.8681	-8.5106
15.0000	-1.9450	9.8256	0.3558	2.1933	2.3530	-1.9028
15.0000	-2.2450	9.0347	0.4916	0.8701	1.2310	-0.1939
15.0000	-2.5550	8.9767	0.4358	0.5005	0.7226	-0.0115
15.0000	-3.1550	9.0641	0.3334	0.3264	0.4600	0.0286
15.0000	-3.7650	9.1236	0.2658	0.2700	0.4235	0.0253
15.0000	-4.3650	9.1779	0.2202	0.2294	0.4140	0.0205
15.0000	-4.9750	9.2236	0.1826	0.2033	0.4648	0.0164

Table A12

C FILENAME: P15V.JET
C Propane Jet in Coflowing Air Stream
C Radial Velocity Profile Measured using LDV
C LDV Seed Added to JET Stream
C Axial Position, x/D= 15
C Bulk Jet Velocity=53 m/s, Jet Reynolds No.=68168

C x/D	y/D	U mean (m/s)	V mean (m/s)	Urms (m/s)	Vrms (m/s)	UV (m/s)*2
15.0000	0.0150	44.8958	0.3321	7.1771	5.6900	1.4699
15.0000	-0.2850	41.6917	-0.1982	7.3328	5.7329	-9.8240
15.0000	-0.5850	35.3606	-1.1258	7.5711	5.9357	-19.0254
15.0000	-0.9050	28.3497	-1.7782	7.4667	5.6984	-20.0328
15.0000	-1.2050	22.0488	-1.9225	6.5861	5.4641	-16.7067
15.0000	-1.5050	16.5894	-1.6676	5.2386	4.8063	-11.5806
15.0000	-1.8050	12.7360	-1.6399	4.1187	4.1684	-7.5445
15.0000	-2.1150	10.3997	-1.5682	2.9596	3.7210	-4.4139
15.0000	-0.3050	41.8068	-0.2906	7.2741	5.8350	-10.7525
15.0000	-0.0050	44.4876	0.0066	6.9647	5.7782	2.5069
15.0000	0.2850	41.6054	1.2090	7.4678	6.0126	12.3282
15.0000	0.5850	35.4018	2.3377	7.6559	6.1897	19.2849
15.0000	0.9050	28.3728	2.6458	7.3572	5.9547	19.1863
15.0000	1.2050	21.6987	2.7148	6.6111	5.5152	18.5659
15.0000	1.5150	17.0096	2.4776	5.7376	4.9740	12.8629
15.0000	1.8150	12.8655	1.8684	4.1692	4.1083	6.4024
15.5000	0.0250	45.7245	0.3380	7.3253	6.3931	1.6290

Table A13

C FILENAME: P30V.AIR
C Propane Jet in Coflowing Air Stream
C Radial Velocity Profile Measured using LDV
C LDV Seed Added to AIR Stream
C Axial Position, x/D= 30
C Bulk Jet Velocity=53 m/s, Jet Reynolds No.=68168

C x/D	y/D	U mean (m/s)	V mean (m/s)	Urms (m/s)	Vrms (m/s)	UV (m/s)*2
30.0000	0.0850	26.6076	0.3301	4.3296	4.1529	0.3389
30.0000	0.6950	24.7257	0.6135	4.3814	4.1378	4.9881
30.0000	1.2950	21.3149	1.0115	4.5335	4.0665	7.1148
30.0000	1.9050	17.2592	1.0421	4.2815	3.7390	7.2211
30.0000	2.5250	12.9690	0.4241	3.3891	2.9706	4.5069
30.0000	3.1250	10.2722	0.2146	1.9821	1.9909	1.3742
30.0000	3.7550	9.3543	0.0582	0.7139	0.9986	0.1509
30.0000	4.3650	9.2298	0.0455	0.2829	0.5165	-0.0050
30.0000	4.9850	9.2550	0.0644	0.1875	0.4333	-0.0069
30.0000	5.5950	9.2575	0.0693	0.1553	0.4395	-0.0032
30.0000	0.1050	26.8012	0.1783	4.3014	4.0739	1.3339
30.0000	-0.4950	25.7008	0.0003	4.4365	4.1051	-3.1438
30.0000	-1.1050	22.6270	-0.4823	4.5053	3.9823	-5.9391
30.0000	-1.7250	18.5433	-0.5705	4.4719	3.7639	-6.9460
30.0000	-2.3250	14.3543	-0.3657	3.8990	3.2870	-6.1209
30.0000	-2.9250	10.9527	-0.0192	2.5393	2.2627	-2.5119
30.0000	-3.5450	9.3528	0.1309	1.0688	1.3174	-0.3523
30.0000	-4.1450	9.1333	0.1824	0.4224	0.6137	0.0326
30.0000	-4.7450	9.1447	0.1625	0.2702	0.4579	0.0178
30.0000	-5.3450	9.1838	0.1192	0.2148	0.4360	0.0133
30.0000	-0.4950	25.7008	0.0003	4.4365	4.1051	-3.1438
30.0000	0.0000	26.5076	0.0101	4.3265	4.1563	-0.0389

Table A14

C FILENAME: P30V.JET
C Propane Jet in Coflowing Air Stream
C Radial Velocity Profile Measured using LDV
C LDV Seed Added to JET Stream
C Axial Position, x/D= 30
C Bulk Jet Velocity=53 m/s, Jet Reynolds No.=68168

C x/D	y/D	U mean (m/s)	V mean (m/s)	Urms (m/s)	Vrms (m/s)	UV (m/s)*2
30.0000	-0.3450	27.2156	0.0000	4.2814	3.8927	2.1034
30.0000	-0.2400	27.2156	-0.0403	4.2814	3.8927	0.0024
30.0000	0.0500	27.0278	0.2375	4.3707	3.8306	0.6222
30.0000	0.3600	26.5386	0.9989	4.3840	3.9039	2.5776
30.0000	0.6600	25.2197	1.2639	4.4505	3.9105	3.8157
30.0000	0.9600	23.4739	1.5529	4.3413	3.9492	5.2533
30.0000	1.2600	21.6279	1.8211	4.3746	3.8739	6.0105
30.0000	1.5900	19.9672	2.0547	4.3974	3.8525	6.6033
30.0000	1.8900	18.2087	2.0521	4.2724	3.7468	6.8145
30.0000	2.1900	16.1187	1.8949	4.1540	3.6561	6.5505
30.0000	2.5000	14.6293	1.9700	3.8151	3.5271	5.3436
30.0000	2.8000	12.8444	1.6550	3.4368	3.2732	4.1565
30.0000	3.1100	11.4630	1.4881	3.0249	3.0975	2.9676
30.0000	3.4300	10.4134	1.3571	2.4218	2.9225	2.1307
30.0000	0.0000	27.1907	-0.0020	4.2830	3.8879	-1.3899

Table A15

C FILENAME: P50V.AIR
C Propane Jet in Coflowing Air Stream
C Radial Velocity Profile Measured using LDV
C LDV Seed Added to AIR Stream
C Axial Position, x/D= 50
C Bulk Jet Velocity=53 m/s, Jet Reynolds No.=68168

C x/D	y/D	U mean (m/s)	V mean (m/s)	Urms (m/s)	Vrms (m/s)	UV (m/s)*2
50.0000	-0.1100	18.7849	0.0053	2.7435	2.6224	0.0608
50.0000	0.1900	18.7530	0.4473	2.7480	2.6482	0.6790
50.0000	0.5000	18.4087	0.5961	2.7792	2.6364	1.0864
50.0000	0.8000	18.0630	0.5806	2.8101	2.5771	1.5635
50.0000	1.1100	17.4901	0.6553	2.8713	2.6369	2.1513
50.0000	1.4100	16.7726	0.6615	2.9215	2.6520	2.4448
50.0000	1.7300	16.1502	0.7023	2.8293	2.5575	2.4597
50.0000	2.0300	15.2986	0.7395	2.7990	2.4932	2.9519
50.0000	2.3300	14.5733	0.6266	2.7431	2.5289	2.9431
50.0000	2.9500	13.1313	0.5439	2.4486	2.2577	2.4516
50.0000	3.5700	11.7713	0.5715	2.2131	2.0741	1.9284
50.0000	4.1800	10.5835	0.5817	1.7463	1.7957	1.1288
50.0000	4.8000	9.7917	0.4376	1.2234	1.4879	0.6340
50.0000	5.4300	9.3453	0.2926	0.6810	1.0161	0.1688
50.0000	6.0400	9.2269	0.2184	0.3889	0.8047	0.0294
50.0000	-0.1300	18.6109	0.1291	2.6881	2.6004	-0.0516
50.0000	-0.4300	18.5291	0.1337	2.7752	2.6271	-0.4924
50.0000	-1.0400	17.8554	0.1464	2.8401	2.5591	-1.6071
50.0000	-1.3400	17.1999	0.0893	2.8411	2.6597	-1.9148
50.0000	-1.6400	16.5768	0.0577	2.9007	2.5454	-2.3689
50.0000	-1.9500	15.7972	0.0074	2.8299	2.5086	-2.5002
50.0000	-2.2500	15.1294	-0.0049	2.7524	2.4382	-2.4950
50.0000	-2.8600	13.6983	-0.1072	2.5779	2.3118	-2.3464
50.0000	-3.4700	12.1495	0.0462	2.2314	1.9852	-1.9009
50.0000	-4.0800	10.8638	0.0844	1.8478	1.6999	-1.1813
50.0000	-4.6800	9.8600	0.1042	1.2475	1.2772	-0.4653
50.0000	-5.2800	9.3236	0.0941	0.6848	0.9738	-0.1132
50.0000	0.0000	18.7670	0.0273	2.7451	2.6382	0.0790

Table A16

C FILENAME: P50V.JET
C Propane Jet in Coflowing Air Stream
C Radial Velocity Profile Measured using LDV
C LDV Seed Added to JET Stream
C Axial Position, x/D= 50
C Bulk Jet Velocity=53 m/s, Jet Reynolds No.=68168

C x/D	y/D	U mean (m/s)	V mean (m/s)	Urms (m/s)	Vrms (m/s)	UV (m/s)*2
50.0000	-0.2800	19.5020	0.1147	2.7520	2.6558	-0.5740
50.0000	0.3100	19.4254	0.4463	2.7791	2.5906	0.6016
50.0000	0.9100	18.8203	0.6928	2.8733	2.6149	1.7379
50.0000	1.5400	17.5486	0.9799	2.9078	2.6558	2.1417
50.0000	2.1400	16.1826	1.0816	2.8628	2.5640	2.7022
50.0000	2.7500	14.6541	1.1207	2.6715	2.4298	2.3342
50.0000	3.3800	13.0956	1.0006	2.5880	2.4538	2.5852
50.0000	3.9800	11.7163	0.9465	2.2154	2.2532	1.6313
50.0000	4.6100	10.6926	1.1179	1.9129	2.1780	1.3707
50.0000	5.2300	9.7792	0.9998	1.5184	1.9197	0.6499
50.0000	-0.8800	18.9680	-0.1716	2.8687	2.5824	-1.5015
50.0000	-1.4800	17.8127	-0.4184	2.8871	2.5024	-2.4553
50.0000	-2.0900	16.2354	-0.5340	2.8732	2.4690	-2.1515
50.0000	-2.7000	14.7201	-0.7544	2.6978	2.5087	-2.2700
50.0000	-3.3100	13.4741	-0.7233	2.5164	2.3499	-2.1901
50.0000	-3.9100	11.9933	-0.8051	2.4017	2.1370	-1.7562
50.0000	-4.5200	10.9573	-0.7901	1.8995	2.0654	-1.3796
50.0000	-5.1100	10.1046	-0.6248	1.6842	1.7819	-0.9179
50.0000	-5.7200	9.5009	-0.8493	1.4205	1.6759	-0.6937
50.0000	0.0000	19.4654	0.0463	2.7691	2.6204	0.0316

Table A17

FILENAME: P30A06.PDF
C Propane Jet in Coflowing Air Stream
C PDF of Velocity Measured using LDV
C LDV Seed Added to AIR Stream
C Radial Profile, Axial Position, x/D= 30.00
C Bulk Jet Velocity=53 m/s, Jet Reynolds No.=68168
C Coflowing Air Velocity=9.2 m/s
C
C y/D= 3.13

u	P(u)	v	P(v)
0.158E+02	0.107E-02	0.579E+01	0.158E-02
0.154E+02	0.406E-02	0.539E+01	0.620E-02
0.150E+02	0.868E-02	0.499E+01	0.120E-01
0.146E+02	0.108E-01	0.459E+01	0.180E-01
0.142E+02	0.157E-01	0.420E+01	0.197E-01
0.138E+02	0.201E-01	0.380E+01	0.253E-01
0.134E+02	0.269E-01	0.340E+01	0.287E-01
0.131E+02	0.303E-01	0.300E+01	0.353E-01
0.126E+02	0.442E-01	0.260E+01	0.461E-01
0.123E+02	0.485E-01	0.220E+01	0.541E-01
0.119E+02	0.511E-01	0.181E+01	0.686E-01
0.115E+02	0.685E-01	0.141E+01	0.114E+00
0.111E+02	0.797E-01	0.101E+01	0.157E+00
0.107E+02	0.160E+00	0.613E+00	0.196E+00
0.103E+02	0.306E+00	0.215E+00	0.320E+00
0.988E+01	0.464E+00	-.184E+00	0.394E+00
0.948E+01	0.509E+00	-.582E+00	0.310E+00
0.908E+01	0.320E+00	-.980E+00	0.244E+00
0.869E+01	0.141E+00	-.138E+01	0.175E+00
0.829E+01	0.884E-01	-.178E+01	0.935E-01
0.789E+01	0.381E-01	-.217E+01	0.566E-01
0.750E+01	0.208E-01	-.257E+01	0.386E-01
0.710E+01	0.113E-01	-.297E+01	0.240E-01
0.670E+01	0.260E-02	-.337E+01	0.172E-01
0.631E+01	0.780E-02	-.377E+01	0.180E-01
0.591E+01	0.347E-02	-.416E+01	0.944E-02
0.551E+01	0.000E+00	-.456E+01	0.343E-02
0.512E+01	0.000E+00	-.496E+01	0.429E-02
0.472E+01	0.173E-02	-.536E+01	0.858E-03
0.433E+01	0.000E+00	-.576E+01	0.172E-02

Table A18

```
 FILENAME: P30A05.PDF
C Propane Jet in Coflowing Air Stream
C PDF of Velocity Measured using LDV
C LDV Seed Added to AIR Stream
C Radial Profile, Axial Position, x/D=   30.00
C Bulk Jet Velocity=53 m/s, Jet Reynolds No.=68168
C Coflowing Air Velocity=9.2 m/s
C
C                 y/D=   2.53
C     u           P(u)         v          P(v)
 0.225E+02  0.455E-03  0.874E+01  0.102E-02
 0.218E+02  0.745E-02  0.815E+01  0.439E-02
 0.211E+02  0.139E-01  0.755E+01  0.101E-01
 0.204E+02  0.183E-01  0.696E+01  0.159E-01
 0.198E+02  0.223E-01  0.636E+01  0.216E-01
 0.191E+02  0.258E-01  0.577E+01  0.258E-01
 0.184E+02  0.308E-01  0.518E+01  0.301E-01
 0.177E+02  0.368E-01  0.458E+01  0.341E-01
 0.170E+02  0.432E-01  0.399E+01  0.409E-01
 0.164E+02  0.507E-01  0.339E+01  0.477E-01
 0.157E+02  0.601E-01  0.280E+01  0.603E-01
 0.150E+02  0.675E-01  0.221E+01  0.710E-01
 0.143E+02  0.710E-01  0.161E+01  0.973E-01
 0.136E+02  0.835E-01  0.102E+01  0.130E+00
 0.130E+02  0.102E+00  0.424E+00  0.148E+00
 0.123E+02  0.116E+00  -.170E+00  0.180E+00
 0.116E+02  0.141E+00  -.764E+00  0.196E+00
 0.109E+02  0.181E+00  -.136E+01  0.176E+00
 0.103E+02  0.167E+00  -.195E+01  0.132E+00
 0.958E+01  0.130E+00  -.255E+01  0.835E-01
 0.890E+01  0.616E-01  -.314E+01  0.642E-01
 0.822E+01  0.303E-01  -.373E+01  0.409E-01
 0.755E+01  0.844E-02  -.433E+01  0.170E-01
 0.687E+01  0.397E-02  -.492E+01  0.909E-02
 0.619E+01  0.000E+00  -.552E+01  0.148E-01
 0.551E+01  0.298E-02  -.611E+01  0.454E-02
 0.484E+01  0.000E+00  -.670E+01  0.227E-02
 0.416E+01  0.000E+00  -.730E+01  0.284E-02
 0.348E+01  0.000E+00  -.789E+01  0.170E-02
 0.280E+01  0.000E+00  -.849E+01  0.000E+00
```

Table A19

```
FILENAME. P30A04.PDF
C Propane Jet in Coflowing Air Stream
C PDF of Velocity Measured using LDV
C LDV Seed Added to AIR Stream
C Radial Profile, Axial Position, x/D=   30.00
C Bulk Jet Velocity=53 m/s, Jet Reynolds No.=68168
C Coflowing Air Velocity=9.2 m/s
C
C                y/D=   1.90
C     u          P(u)        v          P(v)
 0.293E+02  0.196E-02  0.115E+02  0.359E-02
 0.284E+02  0.313E-02  0.108E+02  0.673E-02
 0.275E+02  0.353E-02  0.100E+02  0.112E-01
 0.267E+02  0.862E-02  0.927E+01  0.135E-01
 0.258E+02  0.153E-01  0.852E+01  0.170E-01
 0.250E+02  0.184E-01  0.777E+01  0.197E-01
 0.241E+02  0.280E-01  0.702E+01  0.230E-01
 0.233E+02  0.356E-01  0.628E+01  0.336E-01
 0.224E+02  0.458E-01  0.553E+01  0.451E-01
 0.215E+02  0.545E-01  0.478E+01  0.529E-01
 0.207E+02  0.638E-01  0.403E+01  0.583E-01
 0.198E+02  0.705E-01  0.329E+01  0.744E-01
 0.190E+02  0.782E-01  0.254E+01  0.852E-01
 0.181E+02  0.855E-01  0.179E+01  0.976E-01
 0.173E+02  0.887E-01  0.104E+01  0.107E+00
 0.164E+02  0.893E-01  0.294E+00  0.114E+00
 0.156E+02  0.865E-01  -.454E+00  0.118E+00
 0.147E+02  0.792E-01  -.120E+01  0.114E+00
 0.138E+02  0.725E-01  -.195E+01  0.969E-01
 0.130E+02  0.621E-01  -.270E+01  0.843E-01
 0.121E+02  0.528E-01  -.344E+01  0.520E-01
 0.113E+02  0.431E-01  -.419E+01  0.359E-01
 0.104E+02  0.278E-01  -.494E+01  0.282E-01
 0.955E+01  0.110E-01  -.569E+01  0.175E-01
 0.870E+01  0.940E-02  -.644E+01  0.628E-02
 0.784E+01  0.196E-02  -.718E+01  0.717E-02
 0.698E+01  0.235E-02  -.793E+01  0.269E-02
 0.613E+01  0.000E+00  -.868E+01  0.134E-02
 0.527E+01  0.392E-03  -.943E+01  0.448E-03
 0.441E+01  0.000E+00  -.102E+02  0.897E-03
```

Table A20

FILENAME: P30A01.PDF
C Propane Jet in Coflowing Air Stream
C PDF of Velocity Measured using LDV
C LDV Seed Added to AIR Stream
C Radial Profile, Axial Position, x/D= 30.00
C Bulk Jet Velocity=53 m/s, Jet Reynolds No.=68168
C Coflowing Air Velocity=9.2 m/s
C
C y/D= 0.09

C u	P(u)	v	P(v)
0.387E+02	0.154E-02	0.120E+02	0.241E-02
0.379E+02	0.308E-02	0.111E+02	0.282E-02
0.370E+02	0.463E-02	0.103E+02	0.483E-02
0.361E+02	0.908E-02	0.947E+01	0.121E-01
0.353E+02	0.139E-01	0.864E+01	0.157E-01
0.344E+02	0.189E-01	0.780E+01	0.221E-01
0.335E+02	0.285E-01	0.697E+01	0.266E-01
0.327E+02	0.378E-01	0.614E+01	0.342E-01
0.318E+02	0.478E-01	0.531E+01	0.451E-01
0.309E+02	0.543E-01	0.448E+01	0.541E-01
0.301E+02	0.648E-01	0.365E+01	0.662E-01
0.292E+02	0.748E-01	0.282E+01	0.745E-01
0.283E+02	0.851E-01	0.199E+01	0.817E-01
0.275E+02	0.964E-01	0.116E+01	0.936E-01
0.266E+02	0.996E-01	0.330E+00	0.984E-01
0.257E+02	0.960E-01	-.501E+00	0.102E+00
0.249E+02	0.906E-01	-.133E+01	0.986E-01
0.240E+02	0.798E-01	-.216E+01	0.890E-01
0.231E+02	0.582E-01	-.299E+01	0.668E-01
0.223E+02	0.509E-01	-.382E+01	0.503E-01
0.214E+02	0.493E-01	-.465E+01	0.431E-01
0.205E+02	0.358E-01	-.548E+01	0.321E-01
0.197E+02	0.246E-01	-.632E+01	0.229E-01
0.188E+02	0.139E-01	-.714E+01	0.165E-01
0.180E+02	0.113E-01	-.798E+01	0.133E-01
0.171E+02	0.771E-02	-.881E+01	0.725E-02
0.162E+02	0.505E-02	-.964E+01	0.563E-02
0.154E+02	0.771E-03	-.105E+02	0.443E-02
0.145E+02	0.116E-02	-.113E+02	0.161E-02
0.136E+02	0.154E-02	-.121E+02	0.805E-03

Table A21

```
 FILENAME: P30J12.PDF
C Propane Jet in Coflowing Air Stream
C PDF of Velocity Measured using LDV
C LDV Seed Added to JET Stream
C Radial Profile, Axial Position, x/D=   30.00
C Bulk Jet Velocity=53 m/s, Jet Reynolds No.=68168
C Coflowing Air Velocity=9.2 m/s
C
C              y/D=   3.11
C    u          P(u)        v          P(v)
 0.199E+02  0.357E-02  -.732E+01  0.162E-02
 0.193E+02  0.100E-01  -.670E+01  0.108E-02
 0.187E+02  0.132E-01  -.608E+01  0.595E-02
 0.181E+02  0.195E-01  -.546E+01  0.433E-02
 0.175E+02  0.240E-01  -.484E+01  0.130E-01
 0.169E+02  0.292E-01  -.422E+01  0.222E-01
 0.163E+02  0.321E-01  -.360E+01  0.227E-01
 0.157E+02  0.361E-01  -.298E+01  0.330E-01
 0.151E+02  0.396E-01  -.236E+01  0.590E-01
 0.145E+02  0.494E-01  -.174E+01  0.844E-01
 0.139E+02  0.590E-01  -.112E+01  0.119E+00
 0.133E+02  0.746E-01  -.500E+00  0.157E+00
 0.127E+02  0.891E-01  0.119E+00  0.167E+00
 0.121E+02  0.102E+00  0.739E+00  0.153E+00
 0.115E+02  0.124E+00  0.136E+01  0.139E+00
 0.109E+02  0.138E+00  0.198E+01  0.112E+00
 0.103E+02  0.169E+00  0.260E+01  0.910E-01
 0.965E+01  0.213E+00  0.322E+01  0.770E-01
 0.904E+01  0.172E+00  0.384E+01  0.611E-01
 0.844E+01  0.130E+00  0.446E+01  0.514E-01
 0.783E+01  0.557E-01  0.507E+01  0.474E-01
 0.723E+01  0.290E-01  0.570E+01  0.406E-01
 0.662E+01  0.150E-01  0.631E+01  0.340E-01
 0.602E+01  0.835E-02  0.693E+01  0.286E-01
 0.541E+01  0.334E-02  0.755E+01  0.206E-01
 0.481E+01  0.111E-02  0.817E+01  0.135E-01
 0.420E+01  0.000E+00  0.879E+01  0.119E-01
 0.360E+01  0.000E+00  0.941E+01  0.714E-02
 0.299E+01  0.000E+00  0.100E+02  0.271E-02
 0.239E+01  0.000E+00  0.106E+02  0.329E-03
```

Table A22

```
 FILENAME: P30J10.PDF
C Propane Jet in Coflowing Air Stream
C PDF of Velocity Measured using LDV
C LDV Seed Added to JET Stream
C Radial Profile, Axial Position, x/D=   30.00
C Bulk Jet Velocity=53 m/s, Jet Reynolds No.=68168
C Coflowing Air Velocity=9.2 m/s
C
C             y/D=   2.50
C     u        P(u)        v          P(v)
 0.253E+02  0.516E-03  -.791E+01  0.475E-03
 0.245E+02  0.308E-02  -.720E+01  0.332E-02
 0.238E+02  0.659E-02  -.649E+01  0.380E-02
 0.230E+02  0.114E-01  -.579E+01  0.617E-02
 0.223E+02  0.207E-01  -.508E+01  0.109E-01
 0.215E+02  0.255E-01  -.438E+01  0.142E-01
 0.207E+02  0.325E-01  -.367E+01  0.261E-01
 0.200E+02  0.395E-01  -.297E+01  0.394E-01
 0.192E+02  0.448E-01  -.226E+01  0.698E-01
 0.184E+02  0.536E-01  -.156E+01  0.835E-01
 0.177E+02  0.593E-01  -.852E+00  0.959E-01
 0.169E+02  0.693E-01  -.146E+00  0.108E+00
 0.162E+02  0.771E-01  0.559E+00  0.117E+00
 0.154E+02  0.848E-01  0.126E+01  0.124E+00
 0.146E+02  0.945E-01  0.197E+01  0.119E+00
 0.139E+02  0.993E-01  0.267E+01  0.112E+00
 0.131E+02  0.104E+00  0.338E+01  0.970E-01
 0.123E+02  0.108E+00  0.409E+01  0.845E-01
 0.116E+02  0.101E+00  0.479E+01  0.721E-01
 0.108E+02  0.932E-01  0.550E+01  0.617E-01
 0.101E+02  0.809E-01  0.620E+01  0.551E-01
 0.929E+01  0.505E-01  0.691E+01  0.422E-01
 0.852E+01  0.264E-01  0.761E+01  0.270E-01
 0.776E+01  0.105E-01  0.832E+01  0.237E-01
 0.700E+01  0.440E-02  0.902E+01  0.188E-01
 0.624E+01  0.176E-02  0.973E+01  0.124E-01
 0.547E+01  0.439E-03  0.104E+02  0.949E-02
 0.471E+01  0.000E+00  0.111E+02  0.617E-02
 0.395E+01  0.000E+00  0.119E+02  0.190E-02
 0.318E+01  0.000E+00  0.126E+02  0.848E-03
```

Table A23

```
 FILENAME: P30J08.PDF
C Propane Jet in Coflowing Air Stream
C PDF of Velocity Measured using LDV
C LDV Seed Added to JET Stream
C Radial Profile, Axial Position, x/D=   30.00
C Bulk Jet Velocity=53 m/s, Jet Reynolds No.=68168
C Coflowing Air Velocity=9.2 m/s
C
C               y/D=   1.89
C    u            P(u)          v          P(v)
 0.302E+02  0.274E-02  -.844E+01  0.178E-02
 0.293E+02  0.391E-02  -.769E+01  0.268E-02
 0.285E+02  0.547E-02  -.694E+01  0.491E-02
 0.276E+02  0.121E-01  -.619E+01  0.580E-02
 0.268E+02  0.172E-01  -.544E+01  0.714E-02
 0.259E+02  0.227E-01  -.469E+01  0.214E-01
 0.250E+02  0.276E-01  -.394E+01  0.281E-01
 0.242E+02  0.325E-01  -.319E+01  0.455E-01
 0.233E+02  0.387E-01  -.244E+01  0.580E-01
 0.225E+02  0.509E-01  -.170E+01  0.704E-01
 0.216E+02  0.602E-01  -.945E+00  0.825E-01
 0.208E+02  0.649E-01  -.196E+00  0.946E-01
 0.199E+02  0.760E-01  0.553E+00  0.994E-01
 0.191E+02  0.851E-01  0.130E+01  0.106E+00
 0.182E+02  0.889E-01  0.205E+01  0.103E+00
 0.174E+02  0.926E-01  0.280E+01  0.982E-01
 0.165E+02  0.884E-01  0.355E+01  0.950E-01
 0.156E+02  0.778E-01  0.430E+01  0.834E-01
 0.148E+02  0.680E-01  0.505E+01  0.746E-01
 0.139E+02  0.594E-01  0.580E+01  0.627E-01
 0.131E+02  0.541E-01  0.655E+01  0.505E-01
 0.122E+02  0.457E-01  0.730E+01  0.379E-01
 0.114E+02  0.329E-01  0.805E+01  0.268E-01
 0.105E+02  0.188E-01  0.880E+01  0.201E-01
 0.966E+01  0.821E-02  0.955E+01  0.129E-01
 0.881E+01  0.274E-02  0.103E+02  0.129E-01
 0.795E+01  0.313E-02  0.110E+02  0.937E-02
 0.710E+01  0.782E-03  0.118E+02  0.535E-02
 0.625E+01  0.000E+00  0.125E+02  0.312E-02
 0.539E+01  0.000E+00  0.133E+02  0.223E-02
```

Table A24

FILENAME: P30J02.PDF
C Propane Jet in Coflowing Air Stream
C PDF of Velocity Measured using LDV
C LDV Seed Added to JET Stream
C Radial Profile, Axial Position, x/D= 30.00
C Bulk Jet Velocity=53 m/s, Jet Reynolds No.=68168
C Coflowing Air Velocity=9.2 m/s
C
C y/D= 0.05

C u	P(u)	v	P(v)
0.393E+02	0.306E-02	-.101E+02	0.131E-02
0.384E+02	0.153E-02	-.932E+01	0.392E-02
0.375E+02	0.268E-02	-.856E+01	0.672E-02
0.366E+02	0.459E-02	-.779E+01	0.872E-02
0.358E+02	0.149E-01	-.702E+01	0.161E-01
0.349E+02	0.195E-01	-.626E+01	0.220E-01
0.340E+02	0.249E-01	-.549E+01	0.266E-01
0.332E+02	0.321E-01	-.472E+01	0.386E-01
0.323E+02	0.439E-01	-.396E+01	0.510E-01
0.314E+02	0.538E-01	-.319E+01	0.638E-01
0.305E+02	0.609E-01	-.243E+01	0.785E-01
0.296E+02	0.692E-01	-.166E+01	0.893E-01
0.288E+02	0.822E-01	-.895E+00	0.982E-01
0.279E+02	0.910E-01	-.129E+00	0.104E+00
0.270E+02	0.960E-01	0.637E+00	0.104E+00
0.261E+02	0.932E-01	0.140E+01	0.967E-01
0.253E+02	0.861E-01	0.217E+01	0.901E-01
0.244E+02	0.776E-01	0.294E+01	0.800E-01
0.235E+02	0.647E-01	0.370E+01	0.691E-01
0.227E+02	0.532E-01	0.447E+01	0.597E-01
0.218E+02	0.437E-01	0.523E+01	0.480E-01
0.209E+02	0.371E-01	0.600E+01	0.349E-01
0.200E+02	0.268E-01	0.677E+01	0.285E-01
0.192E+02	0.208E-01	0.753E+01	0.214E-01
0.183E+02	0.127E-01	0.830E+01	0.122E-01
0.174E+02	0.865E-02	0.906E+01	0.100E-01
0.165E+02	0.495E-02	0.983E+01	0.829E-02
0.157E+02	0.306E-02	0.106E+02	0.567E-02
0.148E+02	0.153E-02	0.114E+02	0.174E-02
0.139E+02	0.115E-02	0.121E+02	0.218E-02

APPENDIX B-1

SUMMARY OF SANDIA-LIVERMORE DATA

Experimental Facility

These data were obtained in the Turbulent Combustion Tunnel Facility which is located at the Combustion Research Facility of Sandia National Laboratories, Livermore, California. The data base is formally documented in Dibble et al. (1985a) and Dibble et al. (1985b), both of which are availabel from NTIS. Papers presented and published as a result of this work are listed in Table 3 under "Sandia-Livermore Studies (vertical tunnel)."

Experimental Configuration

The measurements were made in a forced draft vertical wind tunnel with an axisymmetric fuel jet located at the upstream end of a test section (Figure B.1). The fully windowed test section is 200 cm long, with a 300 mm-square cross section. The test section empties into an exhaust hood which draws air from the room in addition to flow from the test section. The fuel nozzle consists of two concentric tubes with an inside diameter d of 5.2 mm and an outside diameter of 9.5 mm; the tube walls are 0.7 mm thick. The annular void region has no gas flow. The fuel tube is straight for more than 500 diameters. The coflow air originates from the building air-conditioning and is therefore at a consistent temperature and humidity ($T = 20 \pm 2^{\circ}C$, $RH = 31 \pm 9\%$).

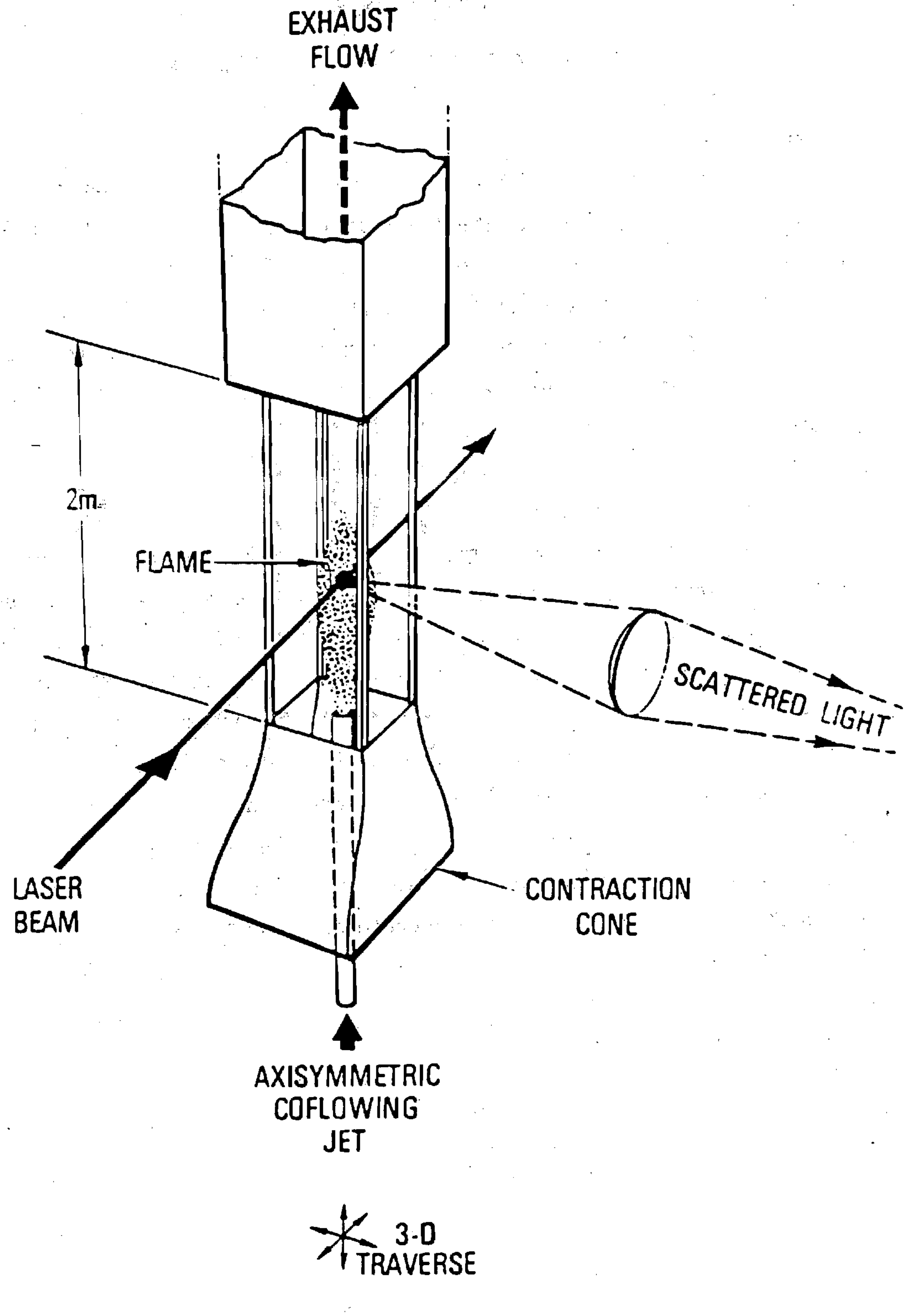

Figure B.1. Sketch of the Sandia turbulent combustion tunnel facility (Dibble et al., 1985a)

Test Conditions

Data are provided for the three cases presented in Table B-1. The

Table B.1
Test Cases

Case	Jet Reynolds Number	Jet Velocity (m/s)	Coflow Air Velocity (m/s)
A	9,000	75	9.2
B	18,000	150	9.2
C	27,000	225	9.2

fuel mixture injected through the jet is 22 mole percent argon-in-hydrogen. The fuel has a density of 0.421 kg/m^3 and viscosity of 186 micro-Poise (180 10^{-7} kg/m/s) at 300 K and one atmosphere. The jet Reynolds number tabulated above is based on the pipe inside diameter, the bulk fuel velocity, and the above referenced density and viscosity. A listing of the equilibrium temperature, concentrations, and physical properties of this fuel mixed with air is given in Table B.2. The tunnel is operated at atmospheric pressure.

Inlet and Boundary Conditions

The radial profile of coflow air velocity at the nozzle plane (x/d = 0) was measured with a hot-wire anemometer (Data FILENAME "INPUT."). A 6 mm and 8 mm boundary layer resides on the test section walls and on the outer wall of the fuel tube respectively.

The length of the straight fuel tube (500 diameters) allows the assumption of a developed velocity profile in the fuel tube. The axial pressure gradient dp/dx in the wind tunnel is 6 Pascals/meter. This gradient is determined by measuring, with a capacitance manometer (Validyne Model DP103-18), the pressure drop between a pressure tap at thenozzle plane (x/d = 0), and at the exit of the test section, which is located two meters from

Table B.2
Equilibrium Temperatures, Concentrations, and Fuel Properties of 22%, by mole, Argon-in-Hydrogen

Fmass	ZIatomic	RHO	RHO/RHOo	KELVINS	CGS VISCOSITY	FUEL/AIR
0.0000	0.0000	1.1720	1.0000	300.	1.867E-04	0.000E+00
0.0043	0.0107	0.9279	0.7920	378.	2.200E-04	1.215E-02
0.0088	0.0214	0.7673	0.6549	456.	2.505E-04	2.459E-02
0.0132	0.0322	0.6539	0.5581	533.	2.789E-04	3.734E-02
0.0178	0.0430	0.5698	0.4863	610.	3.055E-04	5.042E-02
0.0224	0.0538	0.5049	0.4309	686.	3.307E-04	6.383E-02
0.0271	0.0646	0.4534	0.3870	761.	3.546E-04	7.759E-02
0.0319	0.0755	0.4115	0.3512	836.	3.775E-04	9.170E-02
0.0367	0.0864	0.3767	0.3216	910.	3.995E-04	1.062E-01
0.0417	0.0973	0.3474	0.2965	984.	4.208E-04	1.211E-01
0.0467	0.1082	0.3222	0.2750	1057.	4.414E-04	1.364E-01
0.0518	0.1192	0.3004	0.2564	1130.	4.615E-04	1.521E-01
0.0570	0.1302	0.2813	0.2401	1202.	4.812E-04	1.682E-01
0.0622	0.1413	0.2644	0.2257	1274.	5.004E-04	1.848E-01
0.0676	0.1523	0.2494	0.2128	1346.	5.193E-04	2.019E-01
0.0731	0.1634	0.2359	0.2013	1418.	5.379E-04	2.195E-01
0.0786	0.1746	0.2237	0.1910	1490.	5.561E-04	2.376E-01
0.0843	0.1857	0.2127	0.1816	1561.	5.741E-04	2.563E-01
0.0900	0.1969	0.2027	0.1730	1632.	5.919E-04	2.755E-01
0.0959	0.2081	0.1936	0.1652	1702.	6.094E-04	2.953E-01
0.1019	0.2194	0.1852	0.1581	1772.	6.266E-04	3.158E-01
0.1079	0.2307	0.1775	0.1515	1842.	6.436E-04	3.369E-01
0.1141	0.2420	0.1704	0.1455	1910.	6.603E-04	3.587E-01
0.1204	0.2533	0.1639	0.1399	1977.	6.766E-04	3.812E-01
0.1268	0.2647	0.1579	0.1348	2044.	6.926E-04	4.045E-01
0.1334	0.2761	0.1524	0.1301	2108.	7.081E-04	4.286E-01
0.1491	0.3028	0.1413	0.1206	2246.	7.413E-04	4.881E-01
0.1656	0.3298	0.1338	0.1142	2332.	7.624E-04	5.528E-01
0.1829	0.3568	0.1320	0.1127	2301.	7.561E-04	6.234E-01
0.2010	0.3841	0.1320	0.1126	2234.	7.416E-04	7.007E-01
0.2201	0.4115	0.1323	0.1129	2161.	7.256E-04	7.857E-01
0.2401	0.4391	0.1328	0.1134	2085.	7.087E-04	8.797E-01
0.2611	0.4669	0.1337	0.1141	2006.	6.909E-04	9.841E-01
0.2833	0.4949	0.1347	0.1150	1926.	6.723E-04	1.101E+00
0.3068	0.5230	0.1361	0.1161	1843.	6.529E-04	1.232E+00
0.3315	0.5514	0.1377	0.1176	1759.	6.327E-04	1.381E+00
0.3577	0.5799	0.1398	0.1193	1673.	6.117E-04	1.551E+00
0.3856	0.6086	0.1423	0.1214	1585.	5.898E-04	1.747E+00
0.4151	0.6375	0.1453	0.1240	1496.	5.670E-04	1.976E+00
0.4466	0.6666	0.1489	0.1271	1405.	5.433E-04	2.247E+00
0.4801	0.6959	0.1534	0.1309	1312.	5.185E-04	2.571E+00
0.5160	0.7254	0.1588	0.1355	1217.	4.927E-04	2.968E+00
0.5544	0.7551	0.1655	0.1412	1121.	4.655E-04	3.464E+00
0.5957	0.7850	0.1738	0.1484	1023.	4.370E-04	4.102E+00
0.6401	0.8151	0.1844	0.1574	923.	4.071E-04	4.952E+00
0.6881	0.8454	0.1981	0.1691	821.	3.754E-04	6.143E+00
0.7401	0.8759	0.2162	0.1845	718.	3.420E-04	7.929E+00
0.7966	0.9066	0.2408	0.2056	614.	3.066E-04	1.090E+01
0.8582	0.9375	0.2759	0.2355	509.	2.690E-04	1.686E+01
0.9257	0.9686	0.3294	0.2812	405.	2.285E-04	3.471E+01
1.0000	1.0000	0.4208	0.3591	300.	1.840E-04	1.000E+04

Table B.2 (continued)

Fmass	KELVINS	N2	O2	H2	H2O	ARGON
0.0000	300.	7.900E-01	2.100E-01	0.000E+00	0.000E+00	0.000E+00
0.0043	378.	6.229E-01	1.619E-01	0.000E+00	7.470E-03	2.107E-03
0.0088	456.	5.128E-01	1.301E-01	0.000E+00	1.245E-02	3.512E-03
0.0132	533.	4.351E-01	1.076E-01	1.768E-23	1.604E-02	4.525E-03
0.0178	610.	3.774E-01	9.094E-02	2.196E-20	1.878E-02	5.298E-03
0.0224	686.	3.328E-01	7.799E-02	5.383E-18	2.097E-02	5.917E-03
0.0271	761.	2.974E-01	6.766E-02	4.262E-16	2.278E-02	6.427E-03
0.0319	836.	2.686E-01	5.924E-02	1.510E-14	2.432E-02	6.862E-03
0.0367	910.	2.447E-01	5.221E-02	2.941E-13	2.566E-02	7.236E-03
0.0417	984.	2.245E-01	4.626E-02	3.637E-12	2.683E-02	7.567E-03
0.0467	1057.	2.071E-01	4.111E-02	3.160E-11	2.788E-02	7.864E-03
0.0518	1130.	1.920E-01	3.662E-02	2.074E-10	2.881E-02	8.132E-03
0.0570	1202.	1.789E-01	3.271E-02	1.086E-09	2.971E-02	8.379E-03
0.0622	1274.	1.672E-01	2.919E-02	4.714E-09	3.053E-02	8.607E-03
0.0676	1346.	1.568E-01	2.606E-02	1.753E-08	3.126E-02	8.818E-03
0.0731	1418.	1.474E-01	2.322E-02	5.721E-08	3.196E-02	9.014E-03
0.0786	1490.	1.390E-01	2.064E-02	1.672E-07	3.259E-02	9.196E-03
0.0843	1561.	1.313E-01	1.829E-02	4.447E-07	3.322E-02	9.374E-03
0.0900	1632.	1.244E-01	1.613E-02	1.090E-06	3.380E-02	9.542E-03
0.0959	1702.	1.180E-01	1.415E-02	2.493E-06	3.438E-02	9.707E-03
0.1019	1772.	1.122E-01	1.230E-02	5.360E-06	3.490E-02	9.863E-03
0.1079	1842.	1.067E-01	1.058E-02	1.092E-05	3.542E-02	1.001E-02
0.1141	1910.	1.018E-01	8.984E-03	2.127E-05	3.592E-02	1.017E-02
0.1204	1977.	9.723E-02	7.485E-03	3.983E-05	3.640E-02	1.032E-02
0.1268	2044.	9.294E-02	6.075E-03	7.224E-05	3.685E-02	1.047E-02
0.1334	2108.	8.902E-02	4.758E-03	1.277E-04	3.730E-02	1.062E-02
0.1491	2246.	8.105E-02	2.060E-03	4.658E-04	3.821E-02	1.102E-02
0.1656	2332.	7.527E-02	3.189E-04	1.950E-03	3.875E-02	1.159E-02
0.1829	2301.	7.272E-02	2.224E-05	6.149E-03	3.834E-02	1.263E-02
0.2010	2234.	7.109E-02	2.953E-06	1.133E-02	3.765E-02	1.388E-02
0.2201	2161.	6.956E-02	5.255E-07	1.690E-02	3.691E-02	1.522E-02
0.2401	2085.	6.805E-02	1.024E-07	2.286E-02	3.616E-02	1.667E-02
0.2611	2006.	6.659E-02	2.002E-08	2.925E-02	3.538E-02	1.825E-02
0.2833	1926.	6.508E-02	3.702E-09	3.610E-02	3.459E-02	1.996E-02
0.3068	1843.	6.360E-02	6.232E-10	4.354E-02	3.382E-02	2.182E-02
0.3315	1759.	6.208E-02	9.191E-11	5.163E-02	3.300E-02	2.387E-02
0.3577	1673.	6.052E-02	1.145E-11	6.050E-02	3.218E-02	2.615E-02
0.3856	1585.	5.896E-02	1.153E-12	7.036E-02	3.134E-02	2.868E-02
0.4151	1496.	5.729E-02	8.913E-14	8.132E-02	3.045E-02	3.153E-02
0.4466	1405.	5.556E-02	4.958E-15	9.373E-02	2.954E-02	3.477E-02
0.4801	1312.	5.375E-02	1.822E-16	1.079E-01	2.857E-02	3.850E-02
0.5160	1217.	5.183E-02	3.948E-18	1.244E-01	2.757E-02	4.286E-02
0.5544	1121.	4.971E-02	4.313E-20	1.436E-01	2.643E-02	4.795E-02
0.5957	1023.	4.738E-02	1.902E-22	1.667E-01	2.518E-02	5.412E-02
0.6401	923.	4.476E-02	2.472E-25	1.950E-01	2.379E-02	6.170E-02
0.6881	821.	4.168E-02	0.000E+00	2.305E-01	2.215E-02	7.126E-02
0.7401	718.	3.789E-02	0.000E+00	2.765E-01	2.014E-02	8.367E-02
0.7966	614.	3.303E-02	0.000E+00	3.380E-01	1.756E-02	1.003E-01
0.8582	509.	2.638E-02	0.000E+00	4.249E-01	1.402E-02	1.238E-01
0.9257	405.	1.650E-02	0.000E+00	5.566E-01	8.770E-03	1.595E-01
1.0000	300.	0.000E+00	0.000E+00	7.800E-01	0.000E+00	2.200E-01

Table B.2 (concluded)

Fmass	KELVINS	O	H	OH	RAY*	RHO/RAY
0.0000	300.	0.000E+00	0.000E+00	0.000E+00	1.003E+00	9.966E-01
0.0043	378.	0.000E+00	0.000E+00	3.148E-22	1.002E+00	9.956E-01
0.0088	456.	9.276E-27	0.000E+00	2.324E-18	9.994E-01	9.946E-01
0.0132	533.	1.149E-22	0.000E+00	1.183E-15	9.975E-01	9.933E-01
0.0178	610.	1.235E-19	9.542E-27	1.183E-13	9.955E-01	9.921E-01
0.0224	686.	2.657E-17	1.754E-23	4.082E-12	9.935E-01	9.910E-01
0.0271	761.	1.860E-15	6.841E-21	6.719E-11	9.914E-01	9.900E-01
0.0319	836.	5.838E-14	8.829E-19	6.520E-10	9.893E-01	9.887E-01
0.0367	910.	1.011E-12	5.010E-17	4.278E-09	9.872E-01	9.877E-01
0.0417	984.	1.112E-11	1.522E-15	2.083E-08	9.852E-01	9.863E-01
0.0467	1057.	8.603E-11	2.845E-14	8.049E-08	9.830E-01	9.853E-01
0.0518	1130.	5.033E-10	3.614E-13	2.587E-07	9.808E-01	9.844E-01
0.0570	1202.	2.347E-09	3.366E-12	7.170E-07	9.788E-01	9.826E-01
0.0622	1274.	9.076E-09	2.422E-11	1.757E-06	9.765E-01	9.812E-01
0.0676	1346.	3.003E-08	1.406E-10	3.886E-06	9.744E-01	9.796E-01
0.0731	1418.	8.700E-08	6.821E-10	7.879E-06	9.721E-01	9.785E-01
0.0786	1490.	2.252E-07	2.838E-09	1.484E-05	9.698E-01	9.778E-01
0.0843	1561.	5.283E-07	1.036E-08	2.622E-05	9.675E-01	9.763E-01
0.0900	1632.	1.137E-06	3.371E-08	4.378E-05	9.651E-01	9.748E-01
0.0959	1702.	2.268E-06	9.932E-08	6.958E-05	9.627E-01	9.732E-01
0.1019	1772.	4.219E-06	2.679E-07	1.057E-04	9.603E-01	9.722E-01
0.1079	1842.	7.361E-06	6.685E-07	1.541E-04	9.577E-01	9.709E-01
0.1141	1910.	1.210E-05	1.556E-06	2.164E-04	9.551E-01	9.695E-01
0.1204	1977.	1.878E-05	3.405E-06	2.930E-04	9.524E-01	9.677E-01
0.1268	2044.	2.750E-05	7.049E-06	3.825E-04	9.496E-01	9.669E-01
0.1334	2108.	3.787E-05	1.386E-05	4.812E-04	9.465E-01	9.656E-01
0.1491	2246.	5.910E-05	5.689E-05	6.889E-04	9.381E-01	9.621E-01
0.1656	2332.	3.803E-05	1.800E-04	5.969E-04	9.250E-01	9.594E-01
0.1829	2301.	8.436E-06	2.739E-04	2.727E-04	9.012E-01	9.589E-01
0.2010	2234.	2.088E-06	2.638E-04	1.273E-04	8.747E-01	9.583E-01
0.2201	2161.	5.620E-07	2.165E-04	6.128E-05	8.480E-01	9.587E-01
0.2401	2085.	1.501E-07	1.615E-04	2.918E-05	8.215E-01	9.591E-01
0.2611	2006.	3.804E-08	1.116E-04	1.341E-05	7.952E-01	9.591E-01
0.2833	1926.	8.805E-09	7.163E-05	5.832E-06	7.693E-01	9.594E-01
0.3068	1843.	1.811E-09	4.269E-05	2.366E-06	7.436E-01	9.589E-01
0.3315	1759.	3.206E-10	2.346E-05	8.793E-07	7.181E-01	9.598E-01
0.3577	1673.	4.736E-11	1.178E-05	2.942E-07	6.930E-01	9.597E-01
0.3856	1585.	5.610E-12	5.322E-06	8.655E-08	6.683E-01	9.595E-01
0.4151	1496.	5.069E-13	2.124E-06	2.177E-08	6.438E-01	9.602E-01
0.4466	1405.	3.281E-14	7.301E-07	4.518E-09	6.195E-01	9.605E-01
0.4801	1312.	1.401E-15	2.087E-07	7.368E-10	5.956E-01	9.609E-01
0.5160	1217.	3.521E-17	4.735E-08	8.853E-11	5.721E-01	9.605E-01
0.5544	1121.	4.457E-19	7.964E-09	7.158E-12	5.487E-01	9.613E-01
0.5957	1023.	2.284E-21	9.044E-10	3.432E-13	5.257E-01	9.622E-01
0.6401	923.	3.451E-24	6.060E-11	8.135E-15	5.030E-01	9.621E-01
0.6881	821.	9.543E-28	1.945E-12	7.225E-17	4.805E-01	9.626E-01
0.7401	718.	0.000E+00	2.184E-14	1.578E-19	4.583E-01	9.628E-01
0.7966	614.	0.000E+00	5.036E-17	4.139E-23	4.363E-01	9.638E-01
0.8582	509.	0.000E+00	9.149E-21	0.000E+00	4.147E-01	9.639E-01
0.9257	405.	0.000E+00	1.872E-26	0.000E+00	3.932E-01	9.646E-01
1.0000	300.	0.000E+00	0.000E+00	0.000E+00	3.721E-01	9.651E-01

* RAY is the mole fraction weighted sum of Rayleigh cross sections.

the nozzle plane. The pressure gradient of 6 Pascals/meter does not change for the different flame cases, and increases to 6.5 Pascals/meter when the fuel flow is zero.

Quantities Measured

The quantities measured, tabulated, and archived are presented in Table B.3.

Diagnostics

Laser Doppler Anemometer. The axial and radial components of velocity are measured with a two component laser Doppler anemometer (Figure B.2). Two beams (488 and 514.5 mm) from a 4-watt laser are split and focused in an optical volume having a diameter of 0.5 mm and a length of 2.0 mm. Dual Bragg cells, used for the radial velocity component, are driven by 30 MHz and 40 MHz; the 10 MHz difference allows unambiguous velocity determinations to 30 m/s in the radial component.

Rayleigh Scattering. The density is determined from the intensity of Rayleigh scattering from a laser beam. The laser Rayleigh scattering system (Figure B.3) utilizes light from a 5-watt laser beam (488 mm) collected by an F/2 lens (focal length = 30 cm) and relayed, at a magnification of 1.5, to slits in front of a cooled photomultiplier tube (RCA 8575). With this magnification, a slit opening of 3 mm along the axis of the laser beam allows a 2 mm line segment of the laser beam to pass through to the photomultiplier tube.

The slit opening orthogonal to the laser beam is 4 mm which is larger than the laser beam diameter of 300 microns. The excessive opening ensures that a segment of the laser beam passes through the slit in spite of fluctuations in the position of the laser beam caused by density fluctuations in the turbulent flame. Between the slits and the photomultiplier tube, a 1 mm bandpass interference filter (488 nm) and a polarizing filter are used to reduce background from flame luminescence. With the laser off, a signal change is undiscernable whether the flame is on or off. Current from the

Table B.3
Quantities Measured

Quantity Measured	Quantity Tabulated	Quantity Archived[a]	Case	Locations: Axial (x/d)	Locations: Radial (number points)	Diagnostic
inlet u,v	$\overline{u}$, $\overline{u'}$ coflow air only	+		0 (B)[b]	half[c]	hot-wire
u,v	$\overline{u}$, $\overline{v}$, $\overline{u'}$, $\overline{v'}$, $\overline{u'v'}$	+	A	5, 10, 20, 30, 40, 50, 60, 70, 80, 90 (B)	℄	two-component LDA
				15, 30, 50, 70, (B, J, A)	full	
			B	3.5, 4, 10, 15, 20, 25, 30, 40, 45, 50, 60, 70, 80 (J)	℄	
				3, 70 (B)	full	
				30, 50 70 (J, A)	full	
ρ	$\overline{\rho}$, $\overline{\rho'}$, % turb	+	A	5, 7, 9, 11, 13, 15, 17, 19, 20, 25, 30, 35, 40, 45, 50, 60, 70	℄	Rayleigh Scattering
	$\overline{\rho}$, $\overline{\rho'}$, % turb, skew, flat, Int[d]	+		15, 30, 50	full	

	ρ, ρ', % turb	+	B	5, 6, 7, 8, 9, 10, 11, 12, 13, 14, 15, 20, 25, 30, 35, 40, 45, 50, 55, 60, 70 85, 104, 150	℄	
	$\overline{\rho}$, $\overline{\rho'}$, % turb, skew, flat, Int	+		15, 30, 50	half^{+}	
	$\overline{\rho}$, $\overline{\rho'}$, % turb		C	5, 6, 7, 8, 9, 10, 11, 12, 13, 14, 15, 16, 17, 18, 19, 20, 25, 30, 35, 40, 45, 50, 60, 70, 80	℄	
	$\overline{\rho}$, $\overline{\rho'}$, % turb skew, flat, Int	+		15, 30, 50	half^{+}	
u, v, f	$\overline{u}$, $\overline{v}$, $\overline{u'}$, $\overline{v'}$, $\overline{u'f'}$, $\overline{v'f'}$	u,v,f	A	30, 50	three points (middle and edge of shear layer)	Simultaneous Raman/LDA
light emission	mean, rms		A	1, 5, 9, 14, 19, 24, 28, 35, 40, 44, 49, 50, 55, 60, 65, 70, 74, 79, 84, 89	℄	Line-of-sight emission
				15, 30, 50, 70	full	

a. Format of data archived on magnetic tape and floppy disk (+ indicates data archived as presented in column "Quantity Tabulated").

b. (B), (J), and (A) refer to LDA seed in Both streams, the fuel Jet stream only, and the coflow Air stream only.

c. half: radial traverse from stream layer on one edge to centerline
half^{+}: radial traverse from shear layer on one edge to a few points beyond the centerline, toward the opposite edge.
full: traverse from shear layer on one edge, to shear layer on opposite edge
℄ : axial traverse at the geometric centerline

d. % Turb: rms mean   flat: flatness
skew: skewness   Int: Intermittency

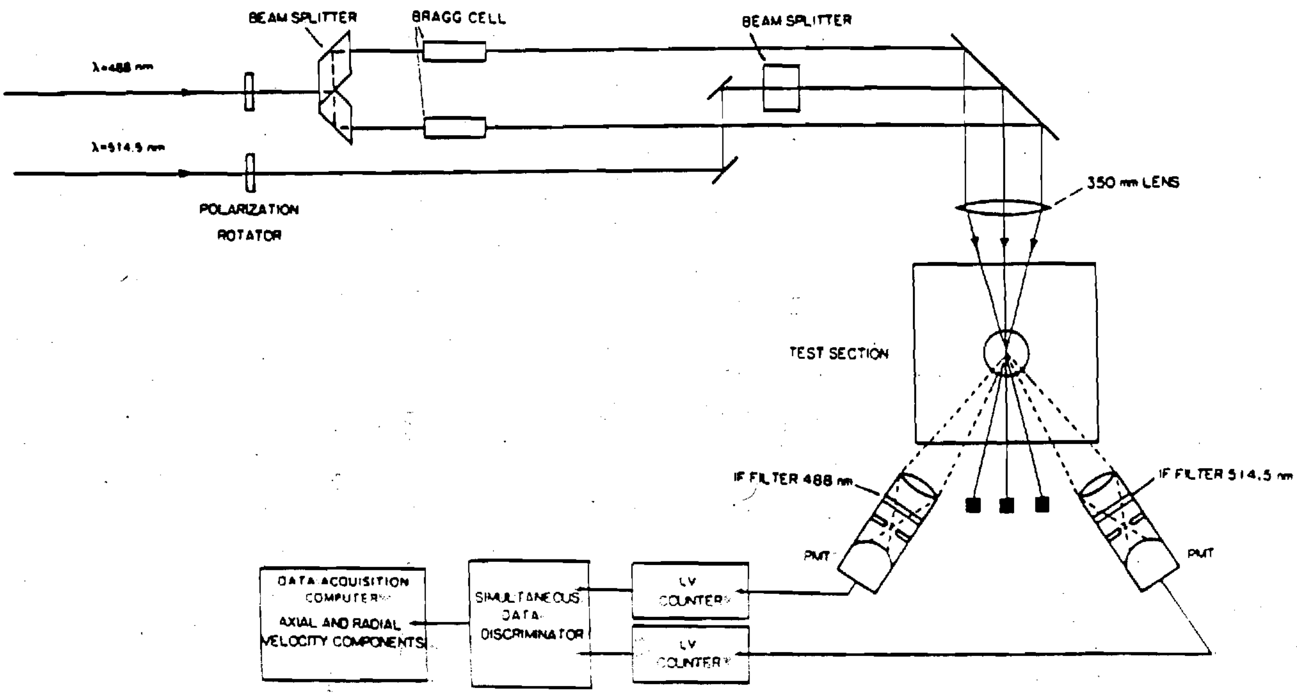

Figure B.2. Sketch of the two-component laser Doppler anemometer arrangement (Dibble et al., 1985a).

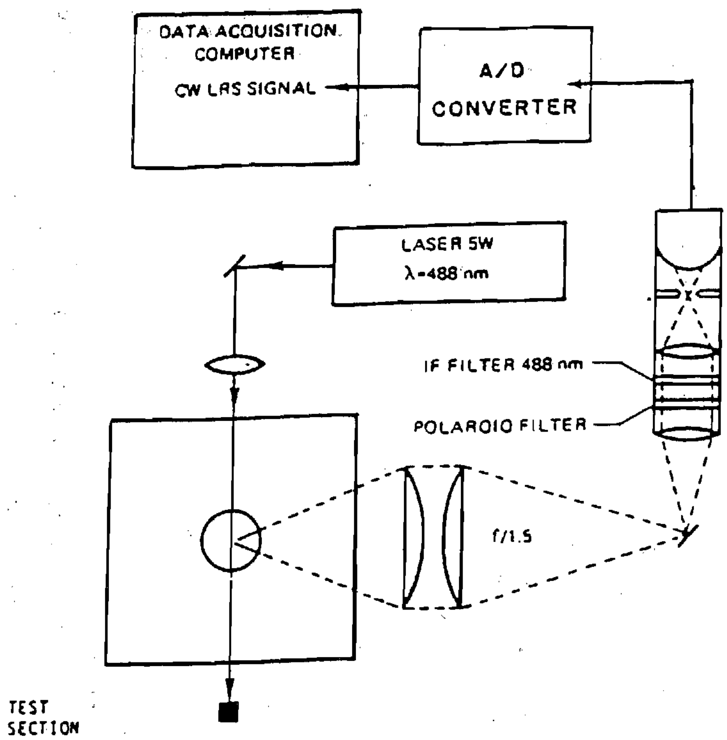

Figure B.3. Sketch of laser Rayleigh scattering system (Dibble et al., 1985a) photomultiplier tube is integrated by an RC filter with a cutoff frequency of 8 kHz. A time series of the Rayleigh intensity, and hence gas density, is obtained by digitization, at 16 kHz, of the filtered signal.

Simultaneous LDA-Laser Raman Scattering. Raman measurements of gas species concentrations are made using a high-power pulsed dye laser (1 J/pulse, 2- s pulsewidth, λ = 514.5 mm, $\Delta\lambda$ = 0.4 nm). The beam is focused to a 500- m waist diameter which is aligned to overlap the LDA measurement volume. The width of the spectrometer entrance slit determines the length of the Raman probe volume (1 nm), while the height of the probe volume is determined by the laser beam diameter. The vibrational Raman scattered light from the major species ($[N_2]$, $[O_2]$, $[H_2O]$, and $[H_2]$) and the antistokes of $[N_2]$ is separated from the collected light with a 3/4 m grating spectrometer and measured on photomultiplier tubes at the exit plane of the spectrometer. As a measure of the overall efficiency of the collection system, 6000 photoelectrons per joule of laser light are collected from nitrogen in room air. From the combined Raman measurements, the fuel mixture fraction f can be determined for each signal laser pulse.

Simultaneous measurements of two velocity components and species concentrations are made by combining the Raman scattering system with the two-color LDA system.The Raman laser is triggered by a pulse from the LDA electronics which indicates a valid radial and axial velocity event. The time between the LDA event and the Raman laser pulse is typically 40 sec. At each spatial location, a minimum of 2500 simultaneous triplets of axial velocity, radial velocity, and mixture fraction are measured. These simultaneous measurements are made for the Case A flame at three radial locations at two axial locations (x/d = 30 and x/d = 50).

Line-of-Sight Emission. Line-of-sight emission is measured with the laser Rayleigh scattering collection system.The laser line interference filter is removed so that all of the emission collected by the F/2 optics is relayed to the photomultiplier tube (RCA 8575).

Photography. The framing speed of the high-speed photography is limited by the total amount of light emission from the flame. The hydrogen flame has little light emission relative to hydrocarbon flames of comparable conditions. For the high-speed films, the luminosity of the flame is increased by replacing the argon diluent with dichloro-difluro-methane (freon-12). The flow conditions are those of Case A with one exception. The replacement of the argon in the fuel with freon-12, which has a higher molecular weight, doubles the pipe Reynolds number. For this condition, 200 frames/second are possible with ASA 500 film using a Redlake LOCAM framing camera. At 4 x 5 format Calumet camera is used for the time-averaged picture.

Unusual Measurement Methods

No special or unusual measurement methods, in addition to those described above, were employed.

Experimental Protocol

The laser Rayleigh, laser Doppler anemometry, and simultaneous laser Doppler anemometry and laser Raman experiments described in this report span a period from September 1983 to August 1985. Other experiments, not reported here, were performed in the Combustion Tunnel Facility during this period. The laser Rayleigh data were collected, in the Fall of 1983, prior to the laser Doppler anemometry experiments which were collected in the Spring of 1984. In this manner, the laser Rayleigh experiments, which demand a minimal presence of particles in the flow, were completed before the wind tunnel was contaminated with particles needed for the laser Doppler anemometryexperiments. (It has since been determined that the particle contamination due to residual laser Doppler velocimetry seed particle is not severe. A day of operation without LDA seed is sufficient to reduce the residual particles to a level acceptable for laser Rayleigh scattering.) The laser Raman system was combined with the laser Doppler velocimeter and used for the simultaneous measurements in the Summer of 1984. Axial profiles of density were remeasured in the Spring of 1985.

Quality Control

Mass Balance. Mass balances on the total throughput were attempted using the laser Doppler anemometry (LDA) data. The results established that mass was conserved. However, because the mass balance is dominated by the mass flux in the outer region of the tunnel, such a mass balance was not a critical test of mass balance in the core of the flow. A mass balance on hydrogen, the critical test of interest, could not be conducted due to the few radial measurements made of mixture fraction.

Reproducibility and Repeatability. No checks for reproducibility were conducted. A few repeatability checks, described under Error Analysis below, were completed.

LDA Seeding. Both the fuel jet and coflowing air were seeded. However, the concentration of seed in the two flows are not controlled. Hence, an evaluation of concentration bias was conducted. No attempt was made to remove velocity bias by equal time interval sampling. The errors associated with LDA seeding are delinated below.

Control of Test Conditions. Test conditions were established by settings on the metering devices employed for the coflowing air and fuel. No additional checks were made for establishing flow test to test whether the conditions were repeated.

Tests of Sensitivity to Boundary Conditions. The principal boundary conditions with a potential influence on the present experiment is exhaust suction. To establish the extent of influence, the exhaust hood flow rate was varied while monitoring the velocity and density at one point in the flow.

Error Analysis

Velocity. In the present flow, the primary potential for error in velocity is 'velocity bias' which is due to the proportionality of particle flux, through the measurement volume, to the instantaneous velocity. Razdan and Stevens (1985) have shown in a comparable flow that for velocity fluctuations up to 10 percent, this bias is negligible. As velocity fluctuations increase, the velocity statistics are increasingly biased toward higher velocities. At the maximum fluctuation levels measured in the present flow a maximum bias error of 3 percent in the mean is estimated. The velocity data presented here are not modified for the effects of velocity bias.

Other potential sources of velocity error have also been estimated. The error due to velocity-gradient broadening is estimated to be less than 0.3 percent. Errors in time measurement with a counter processor having 0.5-ns resolution are less than 0.2 percent at the highest burst frequencies measured, and the effects of variation in refractive index on movement of the measurement volume are negligible.

Since the velocity of a particle is actually measured with laser anemometry, particle-velocity lag is considered. Using the estimates of Durst et. al. (1976), a 0.85-micron particle can follow the flow up to a frequency of 8 kHz with a slip velocity of 1 percent. Based on previous measurements in the current flow, this frequency response is sufficient.

In mixing flows, such as the nonpremixed flame herein described, the measured velocity depends on the density of LDA seed particles added to each of the inlet streams. In this study, the velocity bias resulting from the origin of LDA seed particles is bounded by measurements of velocity when seed particles are added to the fuel only, followed by measurements when seed particles are added to the coflow air only. Table B.4 shows the results of some of these measurements. In all cases, the seeding of the fuel (*.JET) consistently produces slightly higher mean velocities than the seeding of the air (*.AIR). The true velocity lies between these two cases. The difference between these two cases, which is typically three percent of the mean axial velocity, is considered to be the largest source of uncertainty in the velocity data.

<u>Density via Laser Rayleigh Scattering</u>. It is often the case in Rayleigh scattering experiments that a fraction of the light collected by the Rayleigh scattering system is not due to Rayleigh scattering from molecules in the probe volume. This non-Rayleigh signal is most commonly due to minute amounts of scattering of laser light from optical or diffuse surfaces throughout the laboratory. This background scattering can be measured in a variety of ways.

Table B.4
Velocity Data: Effect of Seed Concentration Bias[a]

Case	Axial Location x/d	Velocity (m/s)			
		AAX.BOT[b]	AXX.AIR	AXX.BOT	AXX.JET
A	15	74.6	70.2	72.6	73.5
	30	51.4	47.7	48.8	50.9
	50	35.1	32.0	33.5	33.4
	70	24.0	21.8	23.3	23.8
		BAX.BOT[b]	BOX.AIR	BOX.JET	BXX.BOT
B	30	91.6	85.6	87.99	
	50	54.3	53.7	55.3	
	70	36.9	37.0	37.8	36.8

a Repeatability of velocity data by comparison of velocity (m/s) at same spatial location and different seeding conditions.

b FILENAME

In most of these experiments, the background is inferred by moving the collection system above and below the horizontal laser beam. Once the laser beam is not imaged onto the slits, the remaining signal is only weakly sensitive to further movement of the collection system; this remaining signal is considered the background. Another method to determine the background scattering takes advantage of the fact that the Rayleigh scattering intensity, from the fuel-rich side of the laminar argon-in-hydrogen flame, is nearly constant and independent of position. Measurements made in room air and then in the fuel-rich zone of the flame are used to determine the background contribution. When these two methods are compared, the former method produces a background that is 10 percent lower than the latter; in either case, the background is typically 4 percent of the Rayleigh signal from room air.

A comparison of measurements of density from three different experiments conducted on different days is presented in Table B.5. The three experiments include data from axial and radial density profiles and, in addition, from measurements using the improved background measurement technique. Because of this improvement, the latter data are weighted twice in generation of statistics. The Table shows 90 percent confidence intervals which have been enlarged by t-value estimates associated with four observations. These confidence interval estimates, less than 15 percent of the mean, are considered satisfactory. These estimates are conservative since they do not take into account the lower limit of density (relative to air) which is 0.112.

The inference of density from the Rayleigh scattering intensity assumes that the ratio the gas density to the sum of the mole fraction weighted Rayleigh scattering cross sections is a constant. As the right column in Table B.5 shows, this assumption systematically underpredicts the density by 4 percent on the fuel rich side of the flame.

Raman Scattering. The primary potential sources for error in the Raman scattering measurements are calibration of the light collection system and background fluorescence (from the windows where the laser beam enters and exits the test section). The Raman system is calibrated in the post-flame gases above flat-flame of hydrogen burning with air. Calibrations of the gases at various temperatures is conducted by operating the burner fuel-lean and then fuel-rich. When the burner is fuel-lean, the laser thermometry is calibrated to a radiation-corrected thermocouple. The laser thermometry is used when the flame is fuel-rich since thermocouple measurements are questionable under these conditions. The concentrations of the post-flame gases are determined from the mass flow meters and the assumption of chemical equilibrium in the combustion products. Through these calibrations, the relationship between Raman intensity and concentration is established. The shot noise associated with the 6000 photoelectrons is 1.2 percent. However, in the flame zone, the concentrations of the major species are about an order of magnitude less than the concentration of nitrogen in room air; accordingly, the shot noise increases to 4 percent. Since the mixture fraction f is derived from various combinations of the major species concentrations, f will have an associated shot noise of less than 6 percent. The background fluorescence contribution

Table B.5
Density Data: Repeatability[a]

Case	Axial Location x/d	---[b]	Density[c] AAX.DEN[d]	AXX.DEN	Statistics MEAN	SIG	90%[e]
A	15	0.194	0.190	0.188	0.1915	0.00259	0.0060
	30	0.122	0.123	0.141	0.127	0.0081	0.019
	50	0.118	0.121	0.131	0.122	0.0053	0.012
	70	0.144	0.153				
	85	0.20					
	104	0.25					
	150	0.40					
			BAX.DEN[d]	BXX.DEN			
B	15	0.2316	0.188	0.199	0.2125	0.0194	0.044
	30	0.112	0.134	0.131	0.122	0.0103	0.023
	50	0.120	0.117	0.116	0.118	0.00178	0.0041
	70	0.144	0.138				
	85	0.201					
	104	0.228					
	150	0.375					

a Repeatability of data by comparison of density at same spatial location measured on different days.

b The data in this column were collected several months after the other density and velocity data; these data are weighted twice in the calculation of the MEAN in column six.

c Density values are normalized to the inlet air density.

d FILENAME

e The 90% confidence interval is generated from the standard deviation, column seven, and student t-value (2.35) for four observations.

to the Raman signal is measured by scanning the spectrometer away from the Raman line and was determined to be less than 0.5%.

Pressure drop across a venturi is related to the air velocity in the wind tunnel. The relationship between the pressure drop and the coflow air velocity is determined with the laser Doppler anemometer. In the course of an experiment, the pressure drop may change slightly and therefore require manual readjustment of the rotational speed of the air supply fan. These excursions in the coflow air velocity of 9.2 m/s amount to a standard deviation of 0.12 m/s.

Other. Changes in the exhaust hood flow rate by +/- 25 percent have no effect on the velocity in the test section, or on the density, measured at x/d = 30 and a radial position where the gradient is large and hence most sensitive to small changes in the flow field.

Availability of Data

The data base is formally documented in Dibble, et al. (1985a) and Dibble et al. (1985b). Velocity (LDA) and density (laser Rayleigh scattering) are provided in the former, and simultaneous LDA/Raman data are provided in the latter. Both reports are available from the National Technical Information Service (NTIS), 5285 Port Royal Road, Springfield, VA 22161. The data files may be obtained on either magnetic tape or floppy disk from the Combustion Research Facility, Sandia National Laboratories, Livermore, California, 94550.

References

Dibble, R. W., Schefer, R, W., Hartman, V. and Kollman, W. (1985a). Velocity and Density Measurements in a Turbulent Nonpremixed Flame, Sandia Report SAND 85-8233; available from NTIS.

Dibble, R. W., Schefer, R. W., Hartman, V., and Kollman, W. (1985b). Simultaneous Velocity and Concentration Measurements in a Turbulent Nonpremixed Flame, Sandia Report SAND 85-8234; available from NTIS.

Durst, F., Melling, A., and Whitelaw, J. H. (1976). Principles and Practice of Laser Doppler Anemometry, Academic Press.

Razdan, M. K., and Stevens, J. G. (1985). CO/air Turbulent Diffusion Flame: Measurements and Modeling, Combustion and Flame, 59, 289.

Data

Static Photograph. Light emission from the flame for Case A photographed in a time averaged mode, is presented in Figure B.4. In addition, radial and axial profile data of the line-of-sight emission (mean and standard deviation) are reported below for this case.

Time-Resolved Photographs. A sequence of 10 black and white photographs is presented in Figure B.5. This framing speed is sufficient to capture large scale structures of the flame; however, with this framing speed, the evolution of these structures from one frame to the next is difficult to follow.

Tabulated Data. Data files are presented on the following pages. (To place the tabulated data into perspecitve, select data files are plotted in Figures B.6 through B.7).

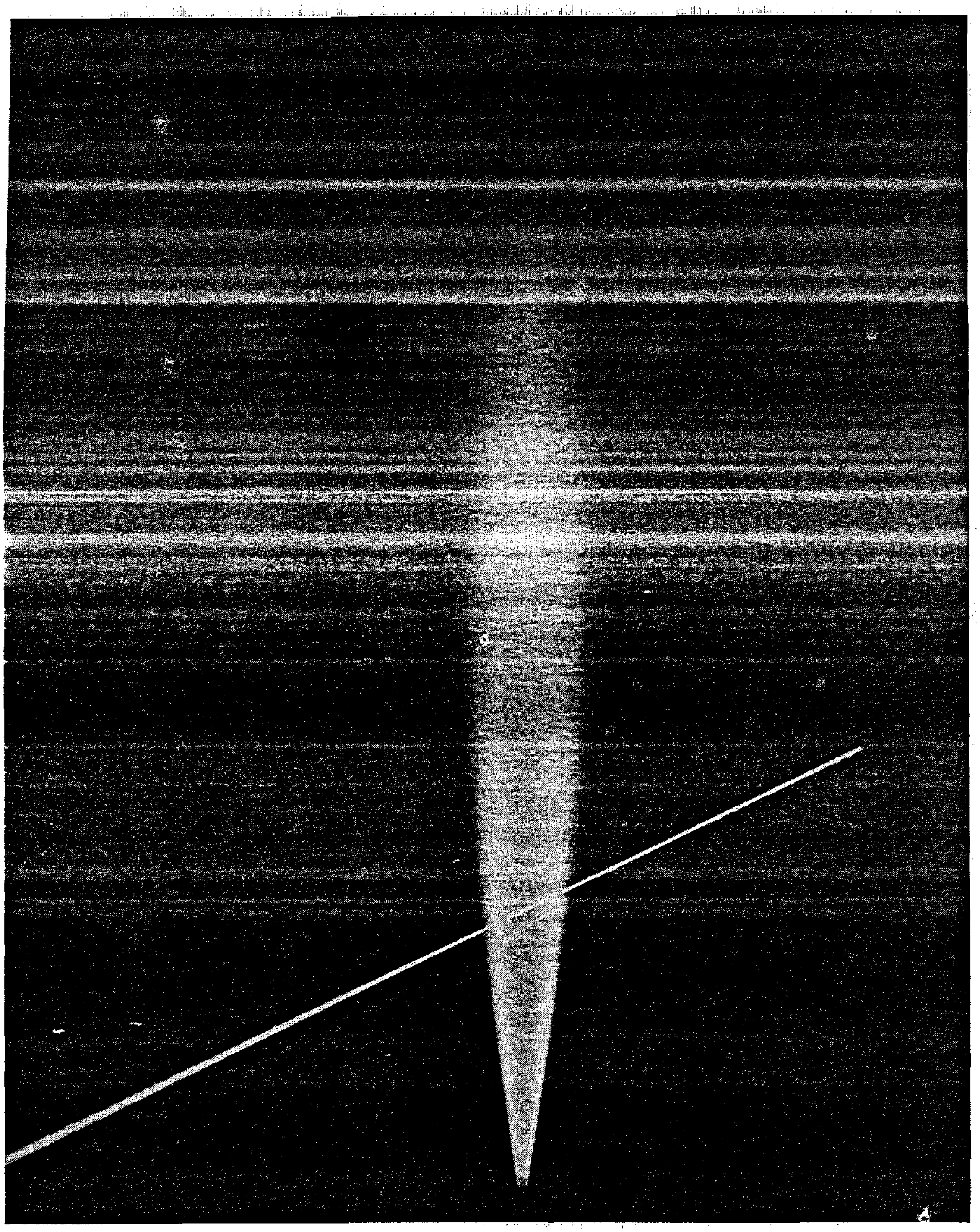

Figure B.4. Time-averaged photograph of light emission (Case A) (Dibble et al., 1985a)

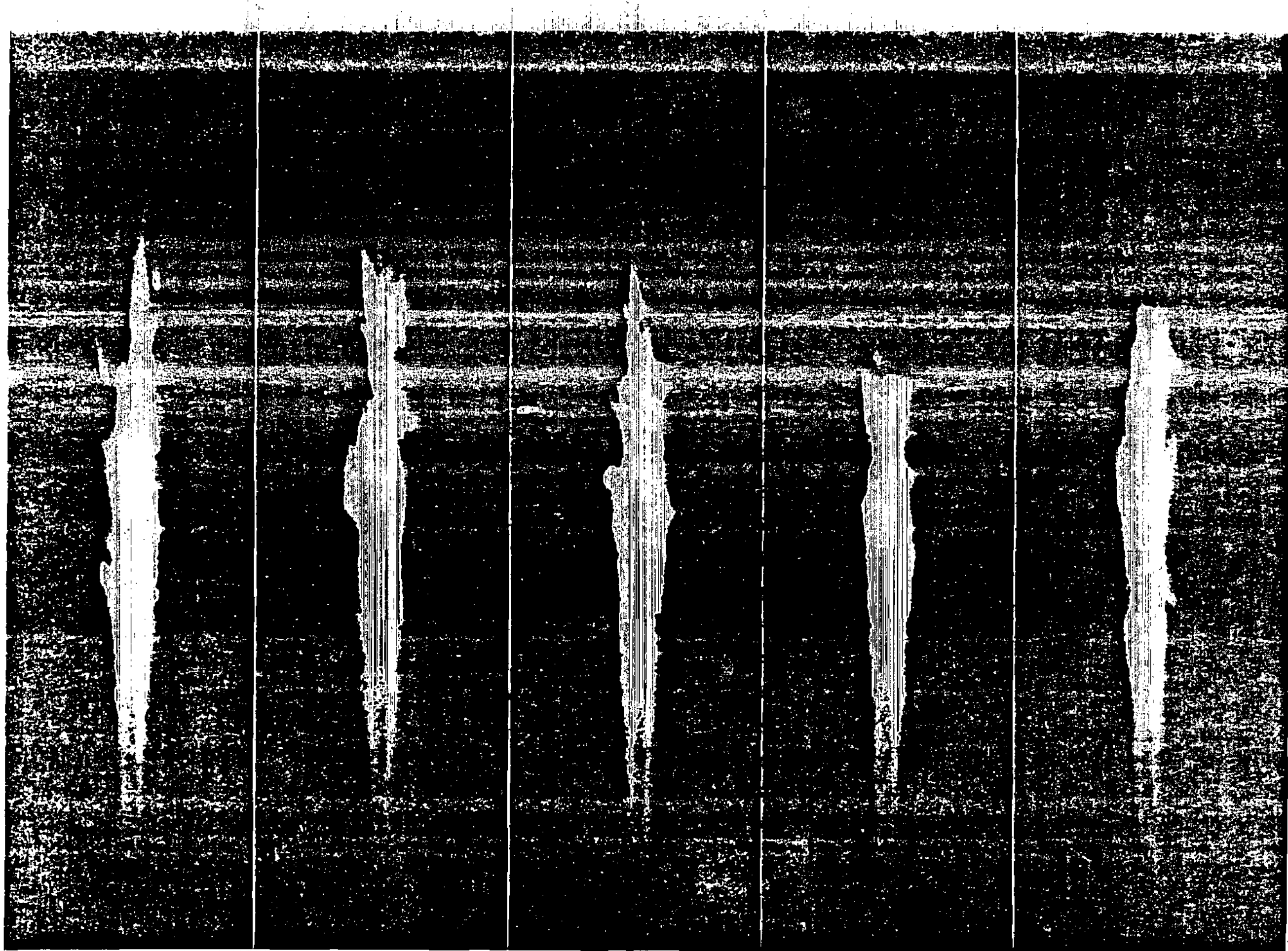

Figure B.5. High-speed (200 frames/sec) photograph sequence of light emission (Case A) (time increases from left to right) (Dibble et al., 1985a)

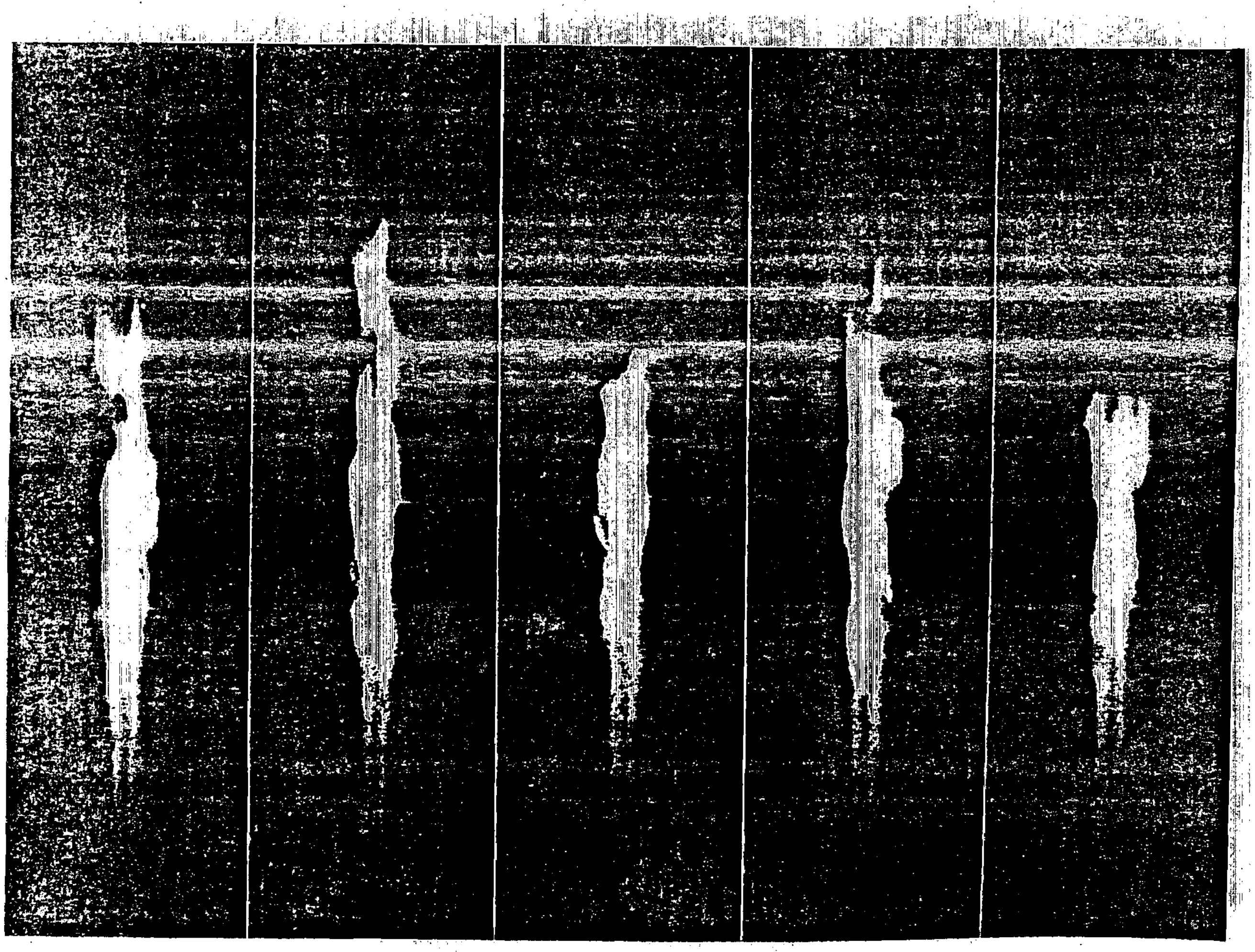

Figure B.5. (concluded)

File Format

Each table is headed with a FILENAME. The FILENAMEs have the following format for the velocity and density data: AXX.YYY.

If A=A, 75. m/s is the average velocity at nozzle exit.
=B, 150. m/s.
=C, 225. m/s.

In all cases (A, B, and C), the coflow air velocity is 9.2 m/s.

If XX= a number, the file is a radial profile at axial position XX.
= AX, the file is an axial profile along the jet centerline.
If YYY=DEN, the file is a density profile.
=JET, the file is a velocity profile with LDA particles added to nozzle fuel only.
=AIR, the file is a velocity profile with LDA particles added to the coflow air only.
=BOT, the file is a velocity profile with LDA particles added to both coflow air and nozzle fluid.

For the simultaneous LDA-laser Raman, the FILENAMEs have the following format: AXXNYY.UVF

If N=J, the file contains data with LDA particles added to the nozzle fuel only.
N=A, the file contains data with LDA particles added to the coflow air only.
N=N, the file contains only scalar data, with no LDA particles added (laser Raman system triggered independent of LDA).
and YY= radial position.

For the line-of-sight emission data, the FILENAMEs have the following format: ALITXX.DAT

Units for velocity data are m/s; the density data are normalized to the density of air at the inlet; the units for the light emission data are arbitrary.

Data Files Available

Inlet profiles are provided in INPUT.

For Case A (bulk fuel velocity at nozzle exit of 75. m/s, Re = 9000), the following data files are provided:

AAX.BOT				
	A15.BOT	A30.BOT	A50.BOT	A70.BOT
	A15.JET	A30.JET	A50.JET	A70.JET
	A15.AIR	A30.AIR	A50.AIR	A70.AIR
AAX.DEN				
	A15.DEN	A30.DEN	A50.DEN	
ALITAX.DAT				
	ALIT15.DAT	ALIT30.DAT	ALIT50.DAT	ALIT70.DAT

For Case B (bulk fuel velocity at nozzle exit of 150. m/s, Re = 18,000), the following data files are provided:

BAX.JET				
B03.BOT				B70.BOT
		B30.JET	B50.JET	B70.JET
		B30.AIR	B50.AIR	B70.AIR
BAX.DEN	B15.DEN	B30.DEN	B50.DEN	

For Case C (bulk fuel velocity at nozzle exit of 225. m/s, Re = 27,000), the following data files are provided:

CAX.DEN			
	C15.DEN	C30.DEN	C50.DEN

Due to the volumious data associated with the simultaneous LDA-laser Raman, data are not tabulated in the present summary. Full data sets are available in Dibble, et al. (1985b).

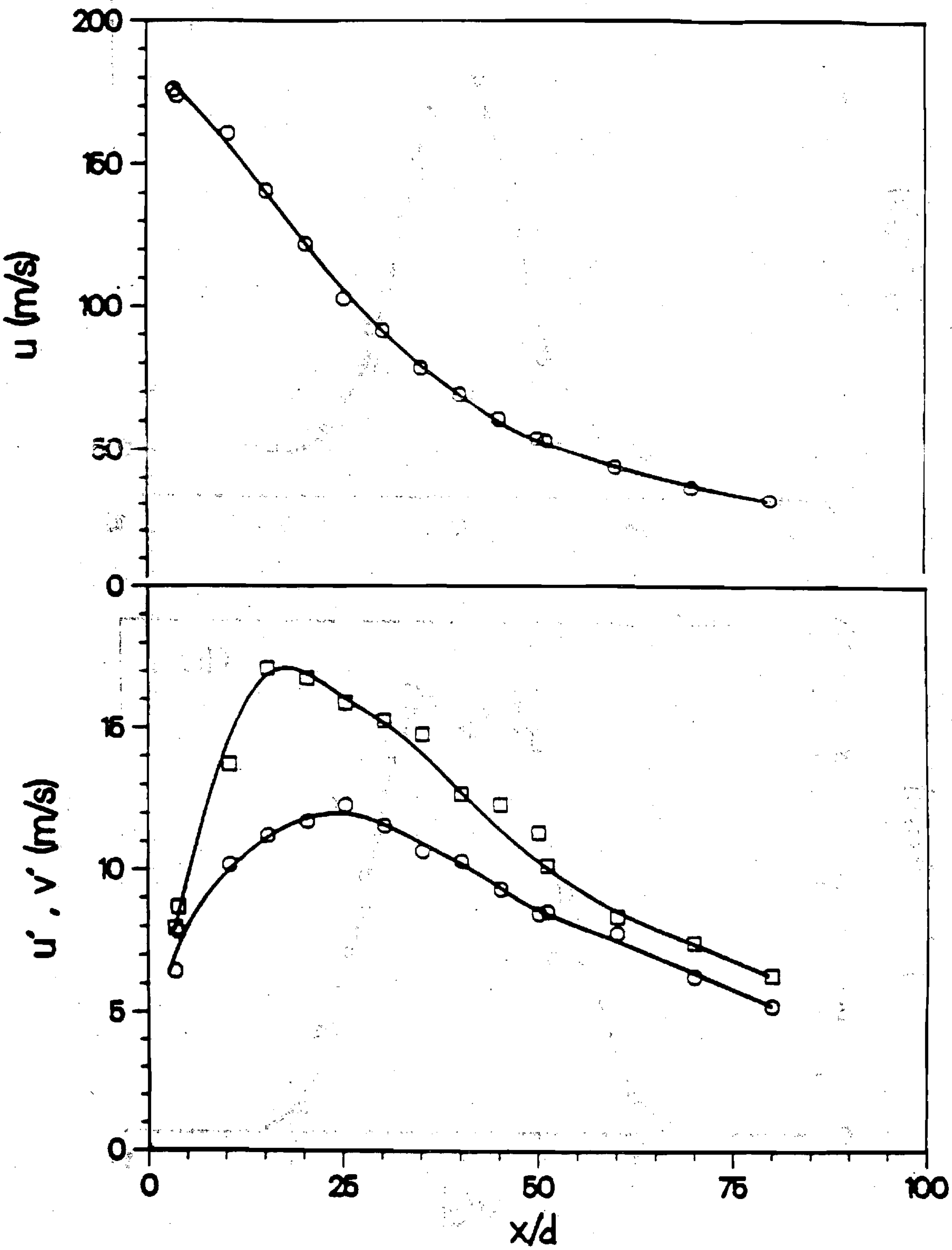

Figure B.6. Axial centerline profiles of velocity (Case B)
FILENAME: BAX.JET (Dibble et al., 1985a)

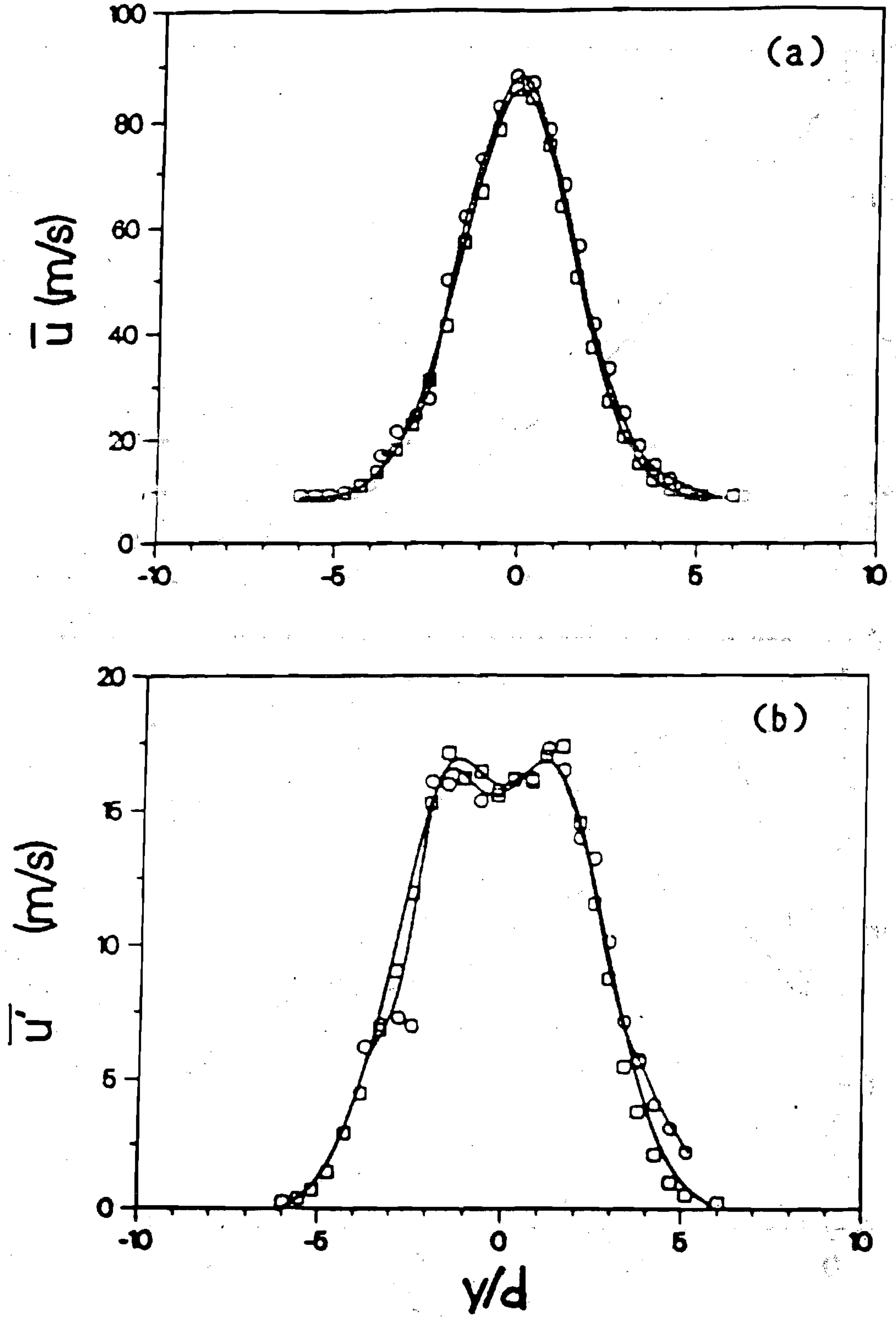

Figure B.7. Radial profiles of velocity at x/d = 30 (Case B)
FILENAMES: B30.JET(○); B30.AIR(□)
(Dibble et al., 1985a)

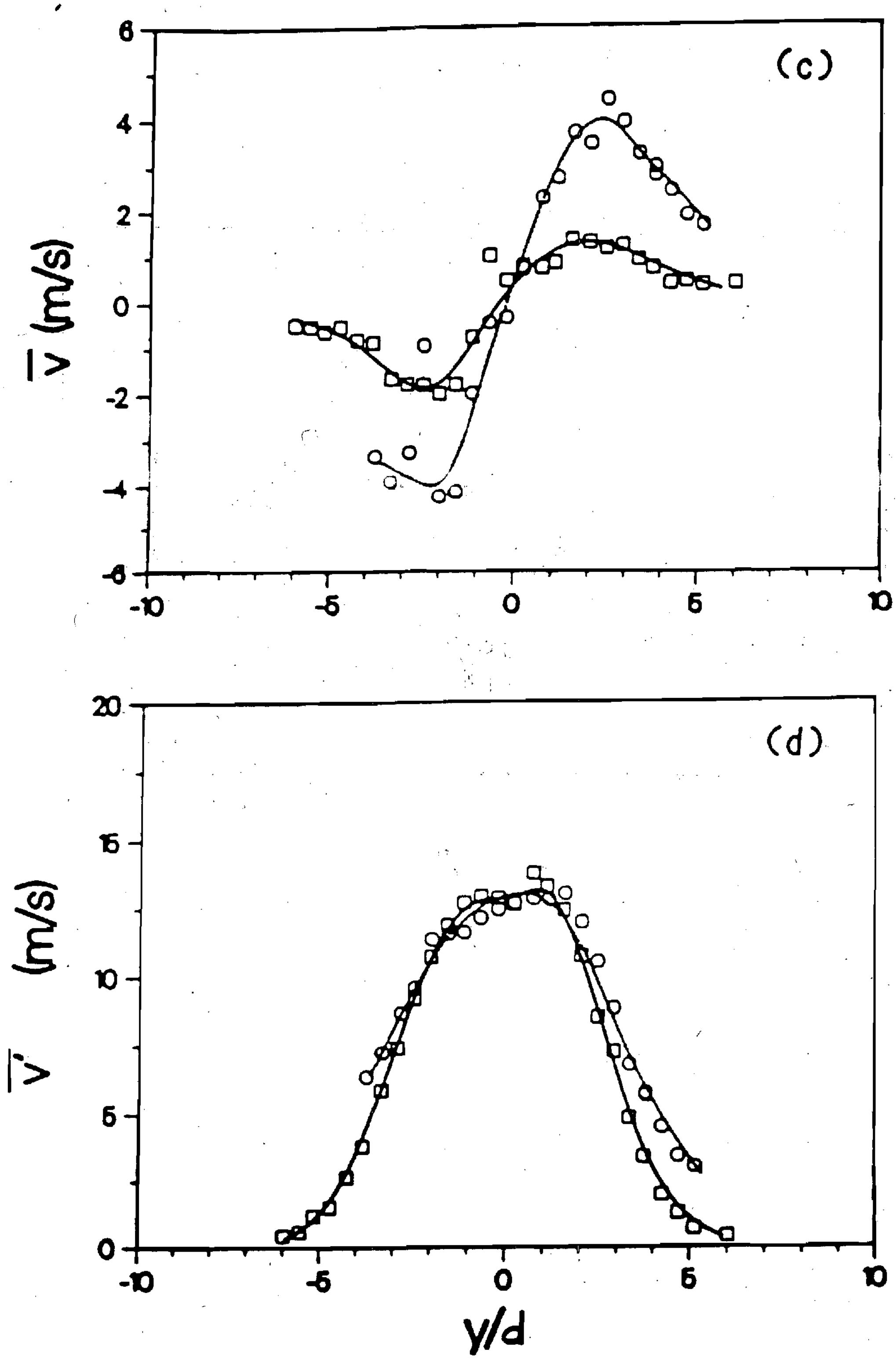

Figure B.7. (continued)

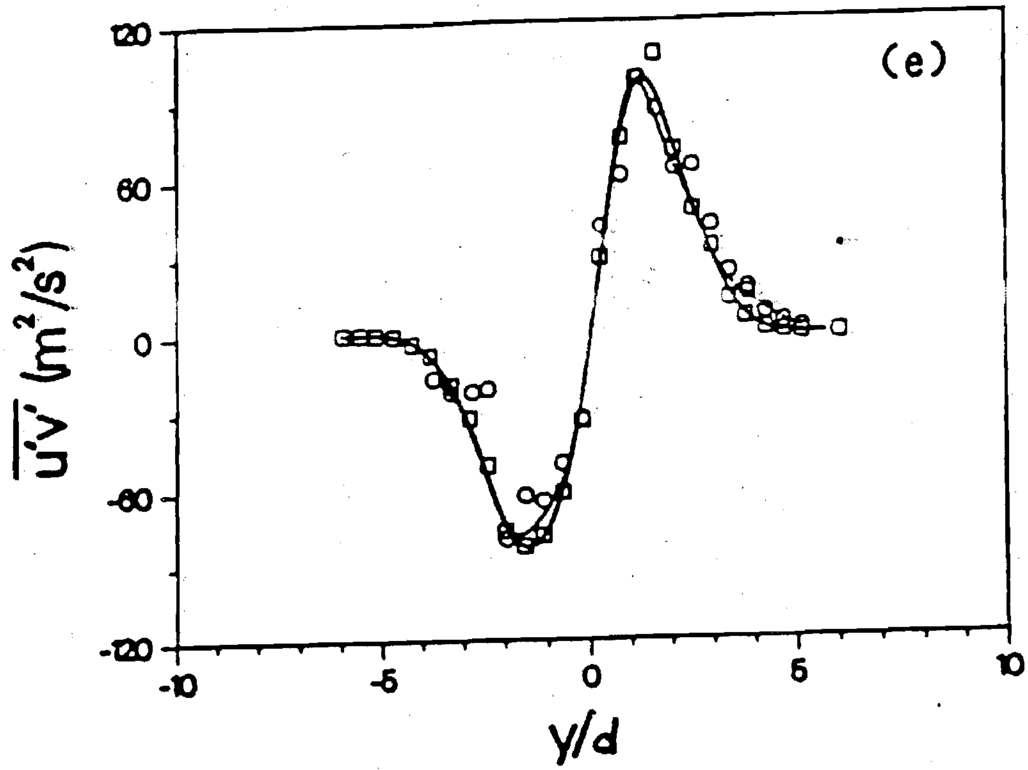

Figure B.7. (concluded)

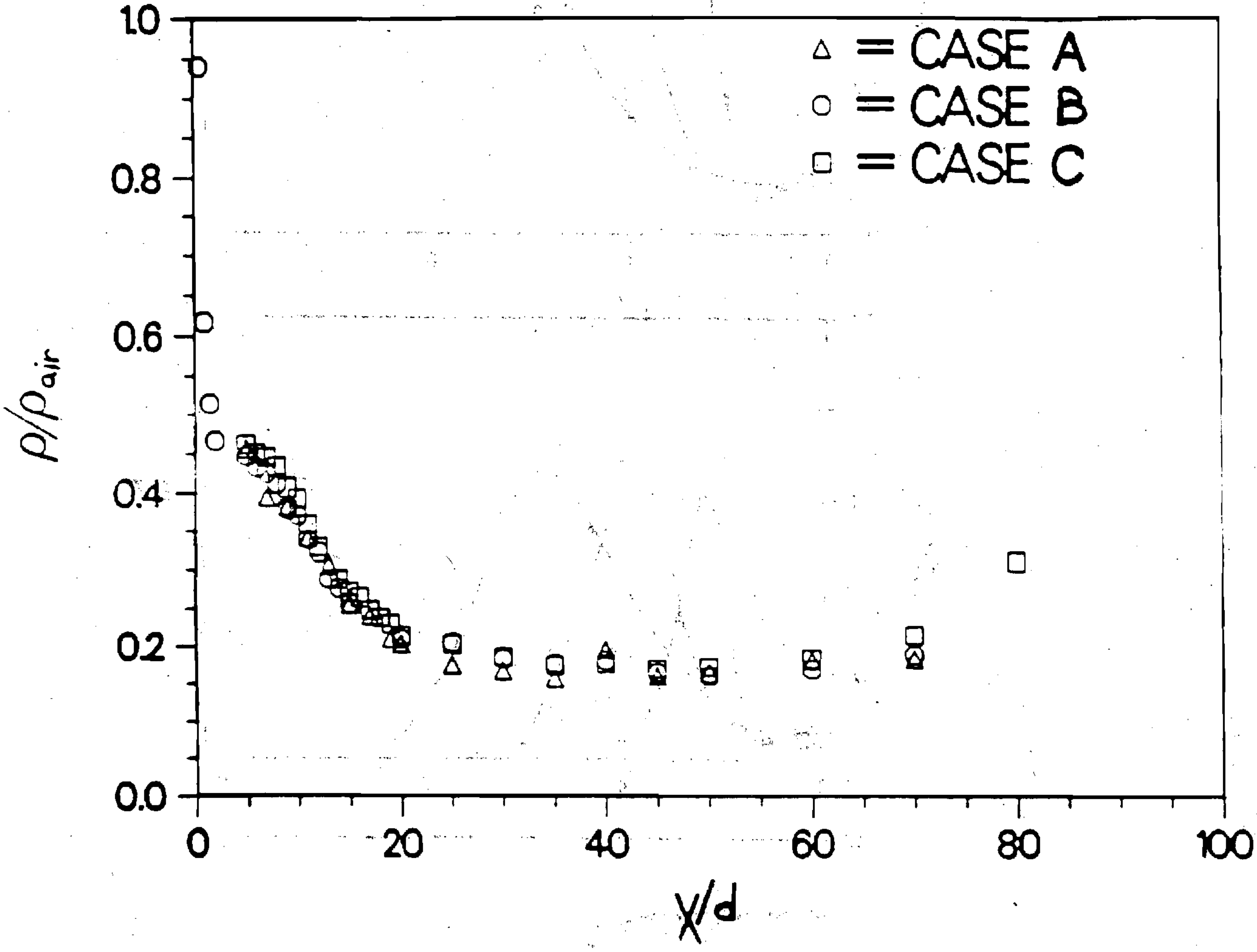

Figure B.8. Axial centerline profiles of density
FILENAMES: AAX.DEN(△); BAX.DEN(○); CAX.DEN(□)
(Dibble et al., 1985a)

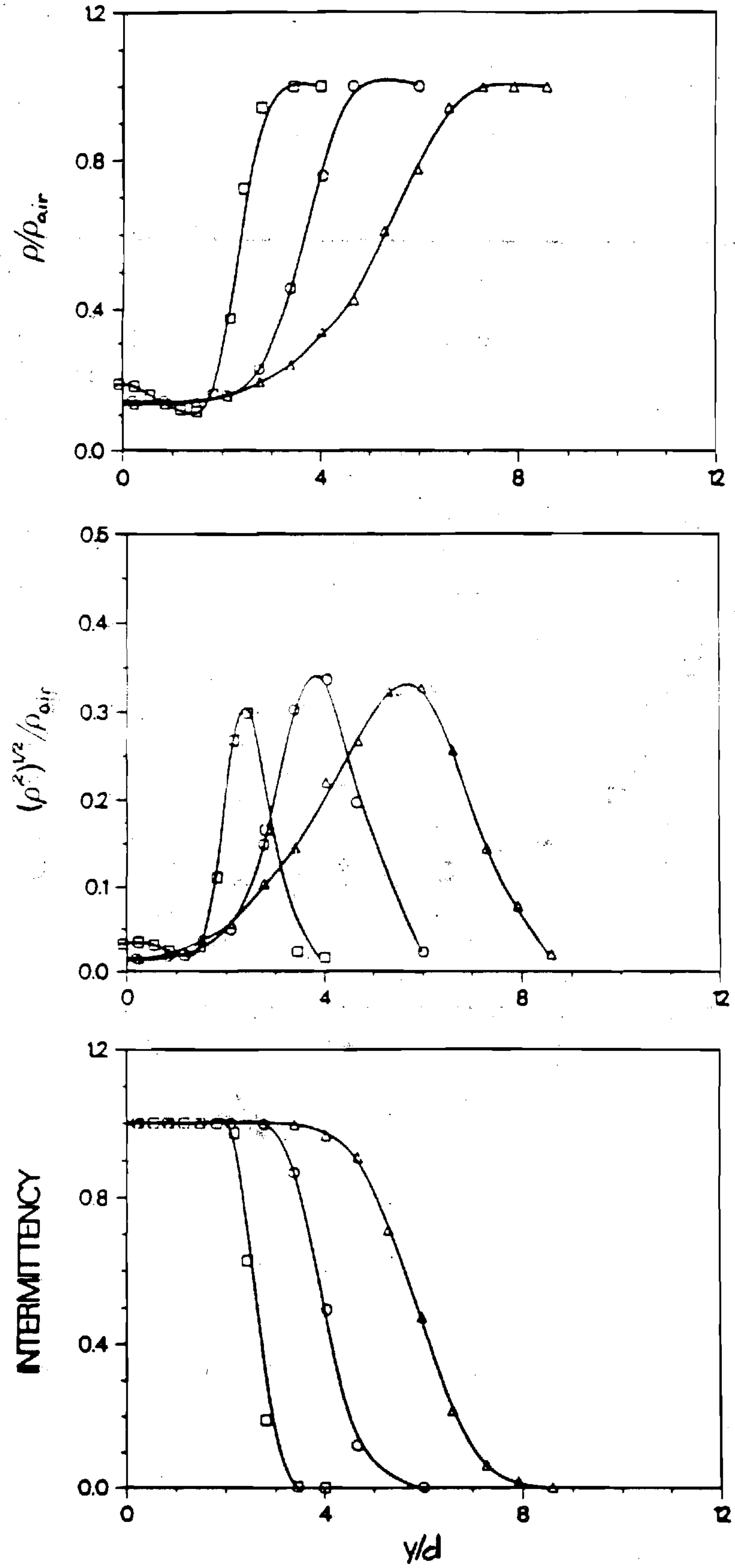

Figure B.9.a. Radial profiles of density (Case A)
FILENAMES: A15.DEN(□); A30.DEN(○); A50.DEN(△)
(Dibble et al., 1985a)

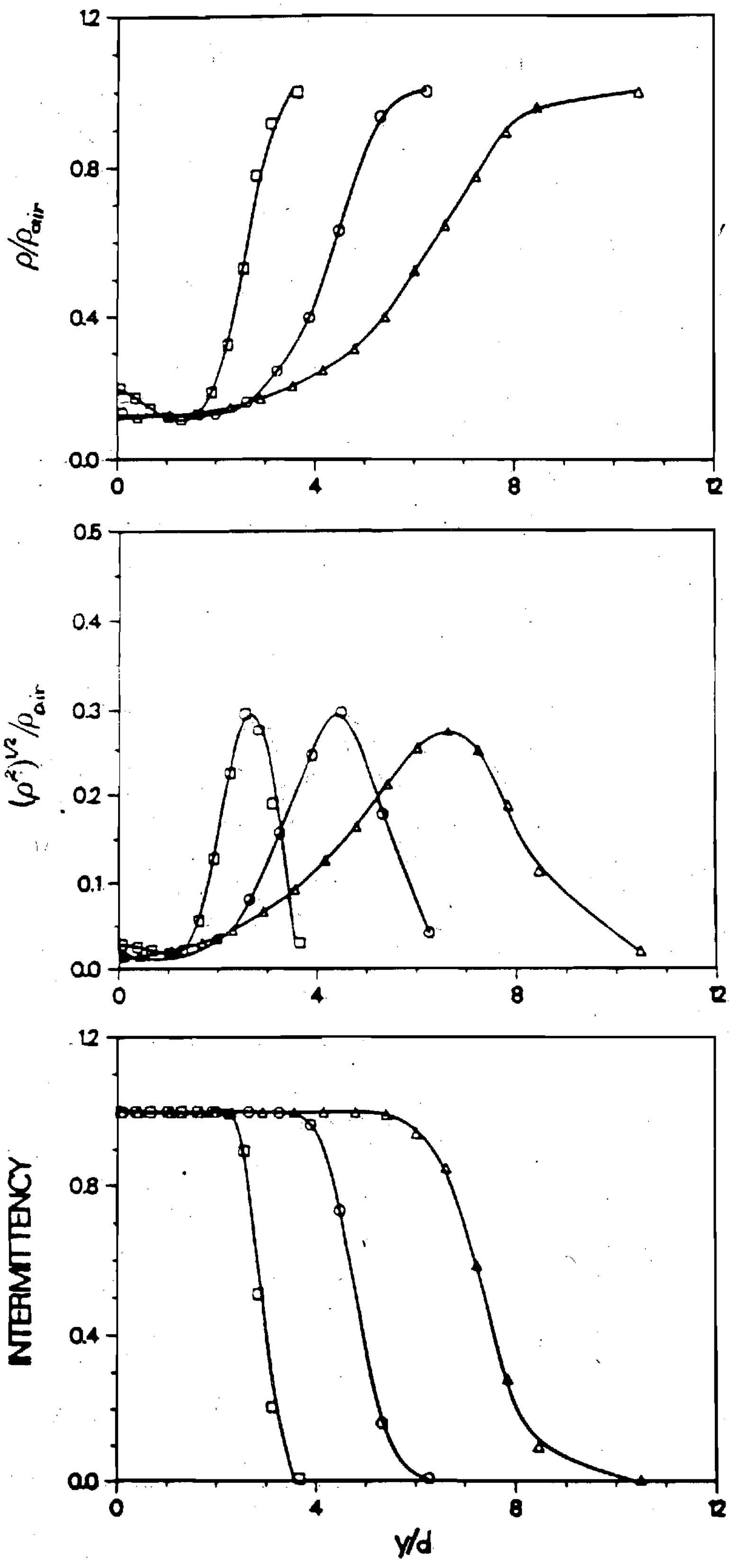

Figure B.9.b. Radial profiles of density (Case B)
FILENAMES: B15.DEN(□); B30.DEN(○); B50.DEN(△)
(Dibble et al., 1985a)

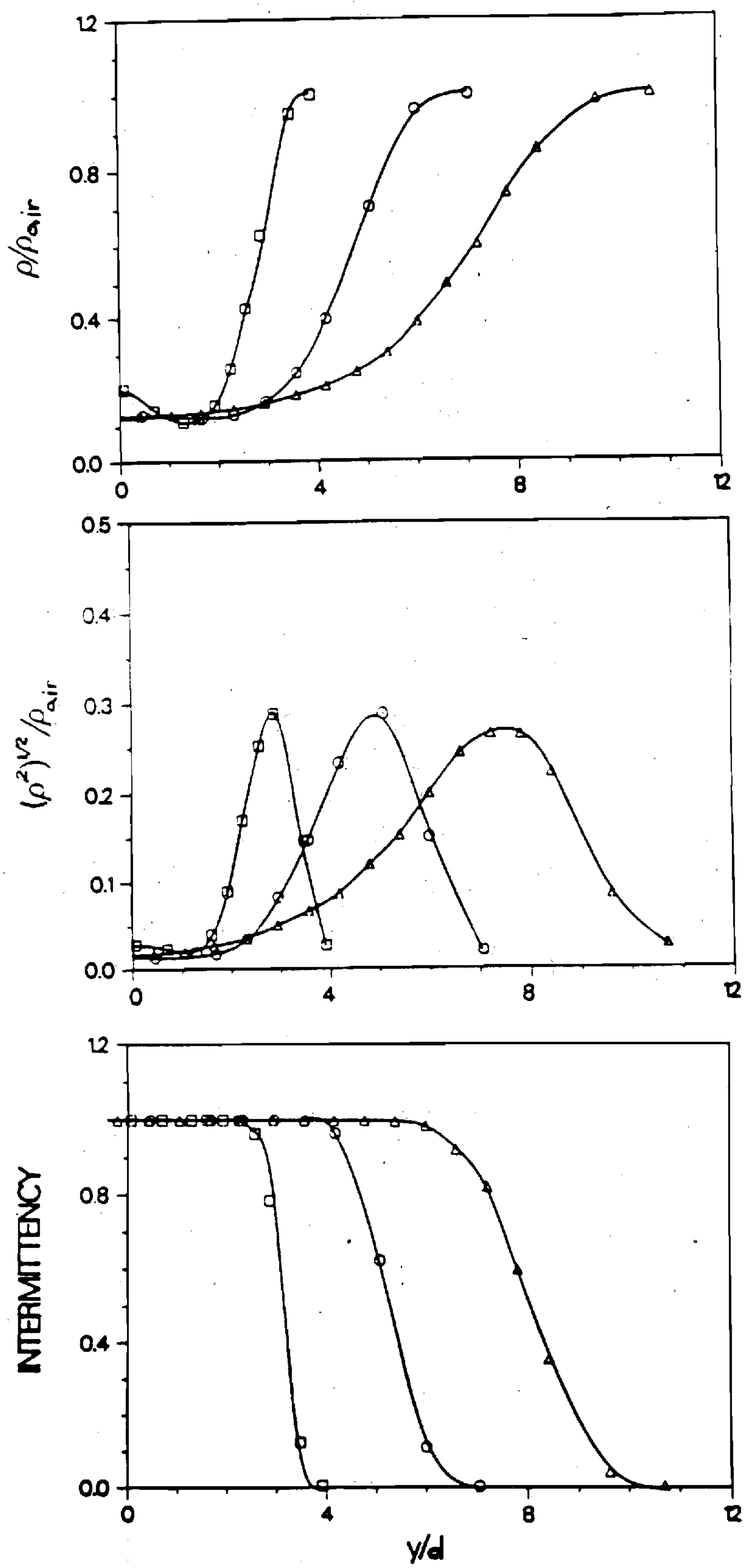

Figure B.9.c. Radial profiles of density (Case C)
FILENAMES: C15.DEN(□); C30.DEN(○); C50.DEN(△)
(Dibble et al., 1985a)

```
CC FILENAME: INLET.
CC
CC Inlet Axial Velocity Profile, measured with Hot Wire
CC Axial Position, x/d=0  d=5.207 mm
CC Inside Nozzle Diameter d=5.207 mm,    (y/d=0.500)
CC Outside Nozzle Diameter=9.525 mm,     (y/d=0.914)
CC Air Flow in the Nozzle is u =55 m/s
CC      this radial profile is not sensitive to Uavg
CC Wind Tunnel Walls are at y/d=+/-29.2,
CC Wind tunnel wall boundry layer is less than 6mm thick.
CC
CC  y/d           u (m/s)             u' (m/s)
 1.16             8.16                0.038
 1.38             8.41                0.044
 1.59             8.65                0.046
 1.73             8.81                0.048
 2.42             9.25                0.060
 3.10             9.38                0.031
 4.47             9.45                0.038
 5.81             9.44                0.040
 7.12             9.41                0.053
```

```
C  FILENAME=  AAX.BOT
C
C  FOR THIS AXIAL VELOCITY PROFILE, BOTH AIR AND JET ARE SEEDED
C                 T912
C
C x/d      y/d        u      v           u'     v'     u'v'
5.00     0.100E-03  93.7   -0.424       4.27   3.42   -1.24
10.0     0.100E-03  86.1   -0.246       6.58   5.86   -2.24
20.0     0.100E-03  66.7    0.231       9.06   7.20   -5.15
30.0     0.100E-03  51.4   -0.294       6.71   6.13   0.198
39.9     0.100E-03  42.4   -0.616       6.11   5.04   0.247
39.9     0.100E-03  42.6    0.214       5.69   5.30    1.42
49.8     0.100E-03  35.1   -0.268       5.48   4.07   -1.63
59.8     0.100E-03  28.6   -0.176       4.64   3.71   0.265
67.3     0.100E-03  24.0   -0.528E-01   3.92   3.30    1.01
79.8     0.100E-03  20.8   -0.402       3.40   2.73   0.563E-01
86.3     0.100E-03  20.0   -0.188       2.86   2.46   0.229
```

```
C  FILENAME=  A15.BOT
C
C     LDV SEED PARTICLES ADDED TO BOTH AIR AND JET.
C     T900
C
C x/d      y/d         u        v          u'         v'          u'v'
15.2      -4.35       9.14    -0.438     0.166      0.234      0.990E-02
15.2      -3.99       9.12    -0.456     0.191      0.243      0.128E-01
15.3      -3.54       9.05    -0.473     0.306      0.280      0.258E-01
15.2      -3.10       8.90    -0.510     0.414      0.321      0.374E-01
15.2      -2.66       8.79    -0.520     0.593      0.540     -0.116E-01
15.2      -2.22       9.43    -0.576      2.20       1.67      -1.88
15.2      -1.78       17.5     -1.25      6.67       4.25      -12.7
15.2      -1.34       34.9     -2.65      10.4       6.96      -39.8
15.2     -0.820       51.2     -2.35      11.6       7.71      -37.7
15.2     -0.460       67.3     -2.26      8.83       7.28      -17.6
15.2      0.600E-01   72.6     0.716      7.30       6.84      0.129
15.2      0.500       63.5      2.05      9.75       7.84       26.5
15.2      0.930       47.0      3.27      11.9       8.28       46.1
15.3       1.37       29.5      2.25      9.80       6.94       34.4
15.2       1.89       13.5     0.979      5.53       3.60       11.0
15.2       2.33       8.87     0.339      1.04      0.972      0.340
15.2       2.70       8.88     0.320     0.440      0.401      0.000E+00
15.2       3.14       9.02     0.313     0.275      0.292      0.000E+00
15.2       3.65       9.11     0.282     0.167      0.217      0.000E+00
15.2       4.09       9.15     0.261     0.137      0.191      0.000E+00
```

```
C    FILENAME=    A30.BOT
C
C   LDV SEED PARTICLES TO BOTH JET AND AIR.
C   T850
C
C x/d      y/d          u        v             u'        v'         u'v'
30.2      -5.95        9.25     -0.486        0.171     0.267      0.650E-02
30.2      -5.80        9.22     -0.495        0.188     0.278      0.990E-02
30.2      -5.36        9.23     -0.524        0.224     0.302      0.153E-01
30.2      -4.92        9.24     -0.534        0.287     0.422      0.440E-02
30.2      -4.48        9.24     -0.558        0.420     0.553     -0.127E-01
30.2      -4.04        9.25     -0.559        0.848     0.773     -0.925E-01
30.2      -3.59        10.1     -0.488         1.75      1.43     -1.23
30.2      -3.15        12.2     -0.702         3.54      2.68     -5.11
30.2      -2.64        15.3     -0.734         5.00      3.50     -8.49
30.2      -2.27        20.1     -0.599         6.43      4.50     -13.5
30.2      -1.76        28.2      -1.11         9.07      5.55     -27.4
30.2      -1.31        38.7      -2.13         8.31      6.17     -24.4
30.2      -0.870       44.0      -1.59         7.10      6.55     -17.3
30.2      -0.430       47.4     -0.664         6.30      6.31     -9.83
30.2      0.100E-01    48.8     -0.483E-01     6.45      6.04      1.91
30.2      0.450        47.0      0.443         6.37      6.12      7.47
30.2      0.880        42.9       1.73         7.22      6.32      16.2
30.2       1.76        29.5       2.60         9.09      6.54      25.8
30.2       2.28        20.2       1.62         7.24      4.95      19.2
30.2       2.65        15.2       1.38         5.39      3.77      11.9
30.2       3.09        11.3      0.663         3.07      2.43      3.82
30.2       3.53        9.83      0.534         1.70      1.52      1.12
30.2       3.97        9.26      0.392        0.657     0.656      0.169E-01
30.2       4.41        9.23      0.352        0.342     0.445      0.000E+00
30.2       4.85        9.28      0.302        0.239     0.379      0.000E+00
30.2       5.29        9.27      0.288        0.246     0.330      0.000E+00
30.2       5.74        9.25      0.259        0.248     0.273      0.000E+00
30.2       6.18        9.24      0.258        0.220     0.253      0.000E+00
30.2       6.62        9.24      0.234        0.207     0.222      0.000E+00
30.2       7.06        9.23      0.224        0.154     0.202      0.000E+00
30.2       7.50        9.22      0.195        0.157     0.238      0.000E+00
30.2       7.65        9.25      0.186        0.151     0.237      0.000E+00
```

```
C    FILENAME=  A50.BOT
C
C     LDV SEED PARTICLES ADDED TO BOTH JET AND AIR FLOW.
C           T1000
C
C x/d       y/d          u        v         u'        v'        u'v'
50.0      -6.16        9.71    -1.08      1.59      1.73     -0.675
50.0      -5.28       10.8     -1.12      2.19      2.08     -1.82
50.0      -4.44       13.1     -1.25      3.12      2.55     -3.92
50.0      -3.52       16.9     -1.77      4.53      3.66     -8.43
50.0      -2.67       21.3     -1.80      5.62      4.04     -10.1
50.0      -1.75       26.8     -1.67      5.86      4.41     -9.82
50.0     -0.870       31.6     -1.13      5.79      4.43     -6.08
50.0      0.900E-01   33.5     -0.489     5.51      4.33      0.949
50.0      0.200       33.4     -0.341     5.70      4.15      1.76
50.0      0.930       30.9      0.377     5.98      4.37      6.92
50.0       1.84       26.3      0.869     6.17      4.35      11.5
50.0       2.65       20.6      1.30      5.34      3.96      9.12
50.0       3.53       15.9      1.14      4.31      3.22      7.06
50.0       4.45       12.5      0.766     2.94      2.53      3.36
50.0       5.30       10.6      0.711     2.08      1.97      1.99
50.0       6.22        9.38     0.511     0.950     1.25      0.295
50.0       2.61       22.1      1.69      5.13      4.17      8.10
50.0       2.72       22.5      1.74      5.05      3.88      7.71
50.0       2.61       19.4      1.25      4.61      3.88      7.31
50.1       2.72       18.9      1.08      4.02      3.76      5.21
50.0      0.270       25.8     -0.826     4.60      4.79      2.24
50.0      0.310       25.7     -0.987     4.55      4.81      1.85
```

```
C     FILENAME=  A70.BOT
C
C     LDV SEED PARTICLES ADDED TO BOTH FUEL AND AIR.
C     T950
C
C x/d      y/d        u        v         u'        v'       u'v'
70.0     -8.72      9.46    -0.338     0.256     0.394    -0.124E-01
70.0     -7.91      9.49    -0.246     0.407     0.469    -0.425E-01
69.9     -7.02      9.75    -0.254     0.807     0.813    -0.265
69.9     -6.14      10.5    -0.324     1.45      1.32     -0.846
69.9     -5.26      12.0    -0.436     2.25      1.89     -2.27
69.9     -4.38      13.7    -0.813     2.84      2.38     -3.53
69.9     -3.42      15.8    -0.724     3.50      2.79     -4.52
69.9     -2.54      18.2    -0.696     3.79      2.99     -4.51
69.9     -1.66      20.3    -0.686     3.94      3.01     -4.15
69.9     -1.66      20.6    -0.736     4.06      3.22     -4.42
69.9     -0.770     22.6    -0.449     3.83      3.20     -1.92
69.9      0.180     23.3    -0.318     3.81      3.16      0.432
69.9      0.980     22.2     0.152     4.01      3.15      3.13
69.9      1.90      19.8     0.304     3.92      2.95      4.15
70.0      2.82      17.8     0.623     3.85      2.93      5.33
70.0      3.70      15.3     0.641     3.45      2.74      4.08
69.9      4.59      13.0     0.431     2.72      2.29      2.78
69.9      5.47      11.6     0.498     2.12      2.02      1.84
69.9      6.35      10.5     0.407     1.61      1.42      0.775
69.9      7.23      9.73     0.349     1.14      1.15      0.328
69.9      8.11      9.47     0.252     0.567     0.627     0.234E-01
69.9      9.00      9.52     0.159     0.232     0.314     0.670E-02
70.0      9.88      9.49     0.155     0.158     0.275    -0.130E-02
```

```
C   FILENAME=   A15.JET
C
C  LDV SEED ADDED TO JET ONLY.
C  T999
C
C
C x/d      y/d        u         v          u'        v'        u'v'
15.2     -2.12      12.0     -2.15       4.25      3.43     -7.80
15.2     -1.68      23.3     -3.09       7.96      5.38     -19.9
15.2     -1.24      39.3     -3.08       10.0      7.06     -22.5
15.2    -0.800      57.4     -2.32       11.1      7.91     -27.2
15.2    -0.360      71.5    -0.579       8.04      7.45     -8.27
15.2     0.900E-01  73.5      1.08       7.41      7.22      2.93
15.2     0.530      61.8      2.97       10.1      8.13      19.4
15.2     0.970      43.9      3.94       11.3      8.49      37.8
15.2      1.40      28.5      3.89       9.59      7.19      32.0
15.2      1.91      14.0      2.21       5.44      4.29      12.0
15.2      2.36      8.58      1.10       2.10      2.23      1.33
```

```
C   FILENAME=  A30.JET
C
C   LDV SEED PARTICLES ADDED TO JET ONLY.
C   T980
C
C y/d      x/d        u        v          u'       v'       u'v'
30.2      -3.24      12.7     -2.33      4.01     3.40     -5.49
30.2      -2.88      16.8     -2.98      5.69     4.53     -12.0
30.2      -2.43      22.7     -3.60      7.12     5.54     -19.8
30.2      -1.99      28.9     -3.45      8.22     5.84     -21.0
30.2      -1.55      36.7     -3.71      8.14     6.15     -19.9
30.2      -1.15      43.1     -2.73      7.67     6.01     -13.8
30.2      -0.630     47.6     -2.01      7.63     6.14     -10.7
30.1      -0.190     50.9     -0.872     6.93     6.31     -3.88
30.2       0.210     50.8      0.126     6.83     6.40      3.83
30.1       0.620     47.3      1.47      7.34     6.38      10.9
30.2       1.16      42.2      2.69      7.98     6.59      18.7
30.2       1.60      36.1      3.08      8.54     6.76      24.4
30.1       2.00      28.3      3.25      8.39     6.47      26.7
30.2       2.48      21.4      2.98      7.05     5.60      19.1
30.2       2.92      15.8      2.37      5.51     4.57      13.3
30.2       3.36      12.2      1.75      3.90     3.58      6.50
30.2       3.81      9.92      1.42      2.69     2.92      2.91
```

```
C     FILENAME=   A50.JET
C
C    LDV SEED PARTICLES ADDED TO JET FLUID ONLY
C        T950
C
C x/d      y/d        u         v          u'         v'        u'v'
50.0     -4.34      14.4     -1.74       3.96       3.26      -6.49
50.0     -3.49      18.1     -2.09       4.56       3.93      -9.09
50.0     -2.54      22.7     -2.11       5.15       4.21      -9.18
50.0     -1.69      27.6     -1.70       5.49       4.23      -8.19
50.0    -0.770      31.6    -0.928       5.81       4.20      -5.38
50.0     0.700E-01  33.1    -0.301       5.70       4.31       1.00
50.0     0.150      33.4    -0.201       5.68       4.55       2.77
50.0     0.980      30.6     0.493       5.78       4.45       7.52
50.0      1.83      25.8      1.18       5.78       4.30       7.81
50.0      2.71      21.2      1.69       5.16       4.08       8.43
50.0      3.70      16.9      2.10       4.50       3.68       7.85
50.0      4.47      13.8      1.48       3.43       3.00       4.80
```

```
C     FILENAME=  A70.JET
C
C     LDV SEED PARTICLES ADDED TO JET ONLY
C         T950
C
```

C x/d	y/d	u	v	u'	v'	u'v'
70.0	-5.22	12.7	-1.12	2.70	2.45	-2.78
70.0	-4.34	14.7	-1.28	3.11	2.73	-4.00
70.0	-3.46	16.8	-1.36	3.60	3.03	-5.12
69.9	-2.54	19.4	-1.17	3.92	3.21	-4.03
69.9	-1.66	21.8	-0.960	4.16	3.10	-3.64
69.9	-0.770	23.3	-0.614	3.98	3.16	-1.86
70.0	0.150	23.8	-0.280	3.96	3.19	0.611
69.9	1.06	22.6	0.195	4.13	3.21	2.81
69.9	1.94	20.9	0.665	4.11	3.15	3.69
70.0	2.75	18.3	0.681	3.78	2.97	3.74
69.9	3.67	15.8	0.919	3.41	2.85	4.09
69.9	4.51	13.9	0.843	2.98	2.53	3.63
69.9	5.39	12.0	0.697	2.38	2.16	2.26

```
C  FILENAME=  A15.AIR
C
C   LDV SEED PARTICLES ADDED TO AIR ONLY
C
C   TIME 900
C
C x/d      y/d        u         v           u'        v'         u'v'
15.4     -4.32      9.17     -0.463      0.177     0.250      0.115E-01
15.5     -3.90      9.03     -0.477      0.214     0.266      0.157E-01
15.5     -3.48      8.96     -0.473      0.253     0.266      0.173E-01
15.4     -3.05      8.92     -0.510      0.414     0.358      0.322E-01
15.4     -2.60      8.73     -0.543      0.692     0.669     -0.597E-01
15.5     -2.15      9.31     -0.481       1.52      1.14     -0.695
15.5     -1.69      14.7     -0.477       5.65      3.12     -7.75
15.5     -1.28      32.2      -1.11       10.5      6.81     -35.4
15.4    -0.800      48.6     -0.660       11.2      8.28     -45.5
15.5    -0.330      64.2     -0.400E-03   9.34      8.11     -21.6
15.5     0.120      70.2      0.200       8.06      7.77      7.48
15.4     0.550      59.2      0.278       10.5      8.26      36.6
15.5      1.00      41.7      0.109E-01   11.7      8.36      54.3
15.5      1.44      24.6      0.554       9.61      5.91      31.0
15.5      1.87      11.4      0.143       3.83      2.14      4.21
15.5      2.33      8.86      0.299      0.950     0.876      0.281
15.5      2.77      8.89      0.288      0.418     0.426     -0.247E-01
15.5      3.20      9.03      0.320      0.285     0.290     -0.198E-01
15.5      3.64      9.10      0.276      0.185     0.234     -0.870E-02
15.5      4.53      9.14      0.276      0.119     0.205     -0.370E-02
```

```
C   FILENAME=  A30.AIR
C
C   LDV SEED PARTICLES ADDED TO BOTH JET AND AIR.
C   T920
C
C x/d     y/d       u       v          u'      v'       u'v'
30.5     -6.02     9.23   -0.504      0.172   0.263    0.260E-02
30.5     -5.54     9.22   -0.529      0.209   0.275    0.980E-02
30.5     -5.09     9.20   -0.546      0.275   0.348    0.169E-01
30.5     -4.64     9.22   -0.550      0.330   0.412   -0.200E-02
30.5     -4.21     9.24   -0.549      0.683   0.726   -0.116
30.5     -3.77     9.59   -0.541      1.27    1.24    -0.612
30.5     -3.33     10.6   -0.473      2.15    1.80    -2.04
30.5     -2.89     13.3   -0.897      4.34    3.06    -7.12
30.5     -2.39     17.5   -0.900      5.70    3.80    -11.1
30.5     -1.99     23.2   -1.32       6.96    5.18    -17.2
30.5     -1.51     31.0   -1.36       8.90    5.95    -24.2
30.5     -1.05     39.0   -1.27       8.76    6.39    -24.4
30.5    -0.610     45.1   -0.929      7.31    6.22    -12.0
30.5    -0.160     47.7   -0.532      6.57    6.21    -5.15
30.5     0.240     46.9   -0.884E-01  6.75    6.60     7.61
30.5     0.360     46.4   -0.197      6.78    6.41     10.5
30.5     0.800     42.9    0.705      7.52    6.47     18.3
30.5      1.27     35.7    0.720      8.91    6.22     26.6
30.5      1.72     26.6    0.340      8.89    5.41     23.1
30.5      2.15     21.1    1.10       7.18    4.82     17.0
30.5      2.55     14.7    0.223      4.96    3.31     8.38
30.5      3.04     11.5    0.184      2.78    2.05     2.82
30.5      3.50     10.0    0.268      1.75    1.37     0.804
30.5      3.93     9.33    0.384      0.721   0.909    0.174
30.5      4.34     9.21    0.363      0.366   0.483    0.103E-01
30.5      4.75     9.25    0.362      0.255   0.333    0.100E-03
```

```
C     FILENAME=  A50.AIR
C
C   LDV SEED PARTICLES ADDED TO AIR ONLY.
C                T1101
C
```

C x/d	y/d	u	v	u'	v'	u'v'
50.0	-5.92	9.73	-1.15	1.74	1.95	-1.00
50.0	-5.18	11.0	-1.02	2.17	2.12	-1.79
50.0	-4.15	13.2	-1.27	3.21	2.81	-5.21
50.0	-3.27	16.8	-1.45	4.60	3.58	-8.85
50.0	-2.39	21.9	-1.69	5.70	4.21	-11.1
50.0	-1.51	26.8	-1.11	5.96	4.46	-10.2
50.0	-0.620	31.0	-0.773	5.72	4.54	-4.06
50.0	0.330	32.0	-0.580	5.80	4.43	3.52
50.0	1.21	28.0	0.727E-01	6.21	4.49	9.32
50.0	2.09	22.6	0.366	5.85	3.99	9.77
50.0	2.90	17.7	0.415	4.71	3.42	6.96
50.0	3.85	13.6	0.354	3.20	2.54	3.84
50.0	4.66	11.2	0.431	2.22	1.86	1.53
50.0	5.54	9.86	0.381	1.26	1.20	0.509
50.0	6.43	9.24	0.754	1.01	1.61	0.267

C FILENAME= A70.AIR
C
C LDV SEED PARTICLES ADDED TO AIR ONLY
C T950
C

C x/d	y/d	u	v	u'	v'	u'v'
70.2	-8.54	9.54	-0.314	0.271	0.377	-0.128E-01
70.2	-7.76	9.61	-0.258	0.423	0.607	-0.280E-02
70.2	-6.88	9.85	-0.212	0.796	0.740	-0.195
70.2	-6.01	10.7	-0.239	1.46	1.19	-0.695
70.2	-5.08	11.7	-0.144	2.00	1.50	-1.37
70.2	-4.20	13.2	-0.232	2.73	2.08	-2.69
70.2	-3.25	15.3	-0.415	3.41	2.55	-4.24
70.2	-2.36	17.4	-0.321	3.67	2.71	-4.03
70.2	-1.47	19.6	-0.203	3.70	3.03	-3.79
70.2	-0.590	21.5	-0.234	3.69	3.17	-2.34
70.2	0.280	21.8	-0.177	3.45	3.19	1.09
70.2	1.17	20.4	-0.176	3.73	3.10	3.18
70.2	2.06	18.6	0.277E-01	3.78	2.86	4.18
70.2	2.99	15.8	-0.240	3.30	2.56	3.65
70.2	3.84	13.5	-0.180	2.72	2.19	2.68
70.2	4.76	11.9	0.654E-01	2.07	1.68	1.72
70.2	4.77	11.8	-0.131	2.18	1.60	1.58
70.2	5.64	10.8	-0.153E-01	1.49	1.20	0.820
70.2	5.65	10.9	0.817E-01	1.57	1.40	1.01
70.2	6.54	10.0	0.658E-01	0.984	0.886	0.334
70.2	7.41	9.59	0.164	0.577	0.680	0.153
70.2	8.30	9.51	0.154	0.276	0.435	-0.100E-02
70.2	9.19	9.50	0.170	0.205	0.318	-0.250E-02

```
C     AAX.DEN
C
C x/d        RHO        RHO'      %TURB
   5.00     0.337    2.192E-02  6.51
   7.00     0.291    2.857E-02  9.81
   9.00     0.281    3.885E-02  13.8
   11.0     0.251    2.942E-02  11.7
   13.0     0.226    3.463E-02  15.4
   15.0     0.190    3.555E-02  18.9
   17.0     0.177    2.011E-02  11.4
   19.0     0.155    2.485E-02  16.0
   20.0     0.150    2.537E-02  17.0
   20.0     0.150    2.034E-02  13.6
   25.0     0.129    1.001E-02  7.75
   30.0     0.123    1.189E-02  9.64
   35.0     0.116    7.074E-03  6.11
   40.0     0.114    7.365E-03  5.12
   45.0     0.118    7.423E-03  6.30
   50.0     0.121    7.133E-03  5.91
   60.0     0.133    2.267E-02  17.0
   70.0     0.153    2.302E-02  17.1
   85.      0.20     0.          0.
  104.      0.25     0.          0.
  150.      0.40     0.          0.
```

C FILENAME: A15.DEN
C DENSITY IS NORMALIZED BY DENSITY OF INLET AIR
C

C x/d	y/d	RHO	RHO'	%TURB	SKEW	FLAT	INT
15.6	-3.40	1.00	2.033E-02	2.02	-0.603	7.23	5.680E-03
15.6	-3.14	1.00	4.336E-02	4.32	-9.89	145.	1.910E-02
15.6	-2.84	0.967	0.126	13.1	-4.03	20.8	0.139
15.6	-2.57	0.813	0.261	32.0	-1.31	3.39	0.481
15.6	-2.27	0.512	0.305	59.5	0.234	1.56	0.891
15.6	-1.95	0.242	0.194	80.1	1.88	5.94	0.997
15.6	-1.65	0.123	6.074E-02	49.3	5.62	46.6	1.00
15.5	-1.32	0.110	1.844E-02	16.8	6.58	145.	1.00
15.6	-1.06	0.120	2.385E-02	19.9	8.89	264.	1.00
15.5	-0.714	0.143	2.713E-02	19.0	2.78	55.4	1.00
15.5	-0.407	0.170	3.303E-02	19.4	4.96	91.9	1.00
15.5	-7.670E-02	0.188	3.221E-02	17.2	4.41	81.0	1.00
15.5	0.244	0.181	3.434E-02	18.9	6.86	149.	1.00
15.5	0.556	0.157	3.098E-02	19.7	4.73	98.3	1.00
15.5	0.858	0.131	2.451E-02	18.6	1.79	20.7	1.00
15.5	1.17	0.115	1.910E-02	16.7	3.25	63.4	1.00
15.5	1.49	0.110	2.959E-02	26.9	9.59	190.	1.00
15.5	1.82	0.159	0.111	70.3	3.30	15.8	1.00
15.5	2.17	0.374	0.268	71.8	0.891	2.47	0.973
15.4	2.44	0.722	0.298	41.4	-0.714	2.02	0.628
15.5	2.80	0.943	0.166	17.5	-3.06	12.2	0.190
15.4	3.44	1.00	2.352E-02	2.31	-6.60	173.	2.570E-03
15.4	4.00	1.00	1.639E-02	2.30	-6.60	17.3	0.000E+00

C FILENAME: A30.DEN
C

C x/d	y/d	RHO	RHO'	%TURB	SKEW	FLAT	INT
30.6	-4.66	1.00	0.139	13.8	-4.48	23.2	6.770E-02
30.6	-4.13	0.852	0.279	32.6	-1.43	3.47	0.326
30.6	-3.55	0.503	0.312	62.1	0.415	1.64	0.840
30.6	-2.95	0.289	0.209	72.5	1.64	4.97	0.987
30.6	-2.31	0.156	7.975E-02	51.2	3.87	22.7	1.00
30.5	-1.69	0.130	2.467E-02	19.1	9.23	210.	1.00
30.5	-1.07	0.131	1.852E-02	14.1	20.3	817.	1.00
30.5	-0.450	0.139	1.254E-02	9.01	1.93	36.8	1.00
30.5	0.192	0.141	1.459E-02	10.3	13.8	677.	1.00
30.5	0.824	0.141	1.762E-02	12.5	21.3	1.040E+03	1.00
30.4	2.10	0.157	4.951E-02	31.5	5.25	42.4	1.00
30.4	2.76	0.230	0.149	65.2	2.61	10.4	0.996
30.4	3.38	0.457	0.302	66.1	0.757	2.11	0.867
30.4	4.04	0.756	0.337	44.5	-0.597	1.67	0.495
30.4	4.66	1.00	0.198	19.7	-3.01	11.0	0.119
30.4	6.00	1.00	2.295E-02	0.230	-6.60	17.3	0.000E+00

C FILENAME: A50.DEN
C

C x/d	y/d	RHO	RHO'	%TURB	SKEW	FLAT	INT
50.7	-7.67	1.00	4.385E-02	4.37	-10.5	148.	8.980E-03
50.8	-7.16	0.984	0.107	11.0	-5.27	31.5	4.880E-02
50.7	-6.59	0.926	0.187	20.1	-2.75	9.32	0.153
50.7	-6.02	0.789	0.275	34.9	-1.01	2.40	0.444
50.7	-5.39	0.619	0.305	49.3	-5.280E-02	1.36	0.734
50.7	-4.78	0.476	0.270	56.7	0.637	2.03	0.917
50.7	-4.15	0.344	0.207	60.2	1.39	4.21	0.986
50.7	-3.52	0.268	0.152	57.0	2.05	7.64	0.997
50.7	-2.92	0.209	0.102	49.2	2.63	12.2	1.00
50.7	-2.30	0.179	7.730E-02	43.2	3.35	19.1	1.00
50.7	-1.64	0.148	4.049E-02	27.4	4.73	38.7	1.00
50.6	-1.05	0.136	2.467E-02	18.1	5.01	42.4	1.00
50.6	-0.393	0.132	1.615E-02	12.2	4.96	56.3	1.00
50.6	0.230	0.131	1.516E-02	11.6	4.79	52.6	1.00
50.6	0.853	0.132	2.156E-02	16.3	6.96	105.	1.00
50.6	1.48	0.139	3.820E-02	27.4	4.96	40.1	1.00
50.6	2.11	0.154	5.664E-02	36.8	4.06	29.1	1.00
50.6	2.77	0.194	0.104	53.4	2.94	14.4	0.999
50.6	3.39	0.243	0.146	60.3	2.26	9.02	0.996
50.5	4.03	0.332	0.220	66.3	1.56	4.69	0.966
50.5	4.68	0.425	0.268	63.1	1.01	2.80	0.908
50.5	5.30	0.610	0.324	53.1	0.183	1.44	0.712
50.5	5.97	0.775	0.327	42.2	-0.564	1.63	0.475
50.5	6.60	0.943	0.257	27.4	-1.79	4.61	0.217
50.5	7.29	1.00	0.145	13.8	-4.13	19.6	6.270E-02
50.5	7.92	1.00	7.721E-02	7.23	-7.77	69.7	1.720E-02
50.5	8.59	1.00	2.041E-02	1.89	-0.780	14.3	4.280E-04

```
CC   FILENAME ALITAX.DAT
CC
CC     x/d      y/d       MEAN     SIG
      1.000    0.485     0.185     0.018
      4.730    0.485     0.209     0.029
      9.390    0.485     0.211     0.040
     14.150    0.485     0.211     0.044
     18.845    0.485     0.220     0.049
     18.840    0.485     0.221     0.049
     23.595    0.485     0.227     0.057
     28.295    0.485     0.231     0.059
     34.810    0.485     0.240     0.073
     39.400    0.480     0.236     0.074
     44.030    0.485     0.238     0.073
     48.750    0.485     0.219     0.060
     50.580    0.485     0.217     0.065
     55.300    0.485     0.196     0.059
     59.880    0.485     0.156     0.049
     64.575    0.485     0.115     0.051
     69.290    0.485     0.072     0.033
     74.060    0.480     0.051     0.023
     74.060    0.485     0.050     0.022
     78.895    0.485     0.040     0.011
     83.670    0.485     0.032     0.005
     88.450    0.485     0.034     0.005
```

```
C  FILENAME ALIT15.DAT
C
C  x/d     y/d        MEAN       SIG
15.3      3.30     0.416E-01 0.558E-02
15.3      2.42     0.437E-01 0.617E-02
15.3      1.95     0.795E-01 0.422E-01
15.3      1.49     0.300     0.904E-01
15.3      1.03     0.304     0.980E-01
15.3     0.560     0.233     0.550E-01
15.3     0.100     0.225     0.496E-01
15.3    -0.395     0.224     0.476E-01
15.3    -0.800     0.248     0.656E-01
15.3     -1.27     0.343     0.103
15.3     -1.73     0.159     0.714E-01
15.3     -2.18     0.528E-01 0.209E-01
15.3     -2.63     0.434E-01 0.597E-02
```

```
C  FILENAME ALIT30.DAT
C
C  x/d      y/d        MEAN       SIG
30.1       4.73       0.390E-01  0.500E-02
30.0       4.33       0.390E-01  0.500E-02
30.1       4.33       0.390E-01  0.500E-02
30.1       3.87       0.410E-01  0.900E-02
30.0       3.41       0.500E-01  0.220E-01
30.0       2.95       0.640E-01  0.390E-01
30.0       2.47       0.157      0.730E-01
30.0       2.00       0.236      0.820E-01
30.0       2.01       0.239      0.800E-01
30.1       1.53       0.301      0.980E-01
30.0       1.07       0.270      0.900E-01
30.0      0.610       0.240      0.660E-01
30.0      0.140       0.229      0.640E-01
30.0     -0.305       0.225      0.610E-01
30.0      -1.22       0.265      0.880E-01
30.0      -2.13       0.218      0.840E-01
30.0      -2.13       0.220      0.770E-01
30.0      -2.65       0.129      0.720E-01
30.0      -3.05       0.670E-01  0.420E-01
30.0      -3.96       0.400E-01  0.600E-02
30.0      -4.86       0.380E-01  0.500E-02
```

```
C  FILENAME ALIT50.DAT
C
C  x/d      y/d        MEAN      SIG
50.0        5.79      0.370E-01 0.500E-02
50.0        4.93      0.380E-01 0.800E-02
50.0        4.93      0.380E-01 0.700E-02
50.0        4.00      0.510E-01 0.240E-01
50.0        4.00      0.440E-01 0.150E-01
50.0        3.08      0.760E-01 0.430E-01
50.0        2.13      0.147     0.610E-01
50.0        1.21      0.209     0.620E-01
50.0       0.280      0.211     0.630E-01
50.0      -0.240      0.214     0.600E-01
50.0       -1.09      0.210     0.640E-01
50.0       -2.01      0.167     0.640E-01
50.0       -2.98      0.101     0.560E-01
50.0       -2.99      0.980E-01 0.540E-01
50.0       -3.84      0.520E-01 0.270E-01
50.0       -4.74      0.380E-01 0.700E-02
50.0       -5.64      0.360E-01 0.500E-02
```

```
C  FILENAME ALIT70.DAT
C
C  x/d     y/d         MEAN       SIG
70.2       6.24     0.310E-01 0.400E-02
70.2       5.39     0.320E-01 0.400E-02
70.2       4.46     0.330E-01 0.600E-02
70.2       3.55     0.360E-01 0.800E-02
70.2       2.61     0.420E-01 0.160E-01
70.2       1.68     0.550E-01 0.260E-01
70.2      0.740     0.590E-01 0.270E-01
70.2     -0.260     0.770E-01 0.340E-01
70.2      -1.18     0.610E-01 0.320E-01
70.2      -2.10     0.500E-01 0.220E-01
70.2      -3.00     0.390E-01 0.120E-01
70.2      -3.92     0.350E-01 0.800E-02
70.2      -4.83     0.320E-01 0.400E-02
70.2      -5.73     0.310E-01 0.400E-02
70.2     -0.245     0.800E-01 0.380E-01
```

```
C   FILENAME=  BAX.JET
C
C   AXIAL VELOCITY PROFILE, y/d=0.0
C
C y/d   x/d        u          v          u'        v'        u'v'
   0   3.5000    175.9802    1.4726    7.9599    6.4424    -1.8589
   0   3.9000    174.0092    2.5951    8.6906    7.8267    -2.9472
   0   10.5000   160.9253    6.0506   13.7154   10.1891    -7.8100
   0   15.4000   140.8872    7.8320   17.1013   11.2232   -26.6482
   0   20.5000   122.0559    5.1390   16.7506   11.7364     7.1377
   0   25.4000   102.8880    6.6849   15.8766   12.3028    -6.6898
   0   30.4000   91.6033     5.4030   15.2432   11.5883    -1.7962
   0   35.3000   78.7612     3.4673   14.7656   10.6861    -3.7038
   0   40.3000   69.4795     2.1429   12.6976   10.3222    -2.0507
   0   45.3000   61.2562     2.6146   12.3323    9.3438    -1.9487
   0   51.3000   53.4220     1.4968   10.1649    8.5551     0.8143
   0   50.2000   54.3121     1.6477   11.3366    8.4849     3.1888
   0   60.2000   44.6086    -0.0760    8.4066    7.8194     5.5201
   0   70.0000   36.9306    -0.0414    7.4858    6.2968     1.0942
   0   80.0000   31.5126    -0.0904    6.3450    5.2665     1.0429
```

```
C   FILENAME=  B03.BOT
C
C   LDV SEED ADDED TO BOTH JET AND AIR STREAM
C   clock  1000
C x/d        y/d        u          v          u'        v'        u'v'
 3.700     -4.880     8.873     -.2567     0.1178    0.3109    0.2000E-02
 3.700     -4.010     8.844     -.2320     0.1131    0.3067    0.3000E-03
 3.700     -3.120     8.810     -.2309     0.1473    0.3174    0.5800E-02
 3.700     -2.230     8.670     -.2724     0.3569    0.3670    0.3290E-01
 3.700     -1.340     7.820     -.3723     0.8446    0.7837    0.1338
 3.700     -.4500     99.83      3.323      22.42      13.33    -172.7
 3.700     0.4500     138.6     -.6029      16.81      9.412     53.76
 3.700      1.340     7.976   0.4580E-01    1.310      1.221    0.1800
 3.700      3.130     8.768   0.4200E-01 0.1794      0.3219    -.1200E-01
 3.700      4.020     8.826   0.5930E-01 0.1381      0.3433    -.4900E-02
```

C FILENAME= B70.BOT
C
C LDV PARTICLES ADDED TO BOTH AIR STREAM AND JET FLUID.
C T1100
C

C x/d	y/d	u	v	u'	v'	u'v'
70.1	-10.0	9.24	-0.321	0.829	1.48	0.139
70.1	-9.18	9.37	-0.286	0.931	2.04	-0.277
70.1	-8.31	10.7	-1.06	2.11	2.20	-1.72
70.1	-7.41	11.9	-1.08	2.82	2.68	-3.10
70.1	-6.50	13.9	-1.12	3.48	3.07	-4.35
70.1	-5.62	15.9	-1.19	4.27	3.74	-6.52
70.1	-4.72	18.7	-1.28	5.25	4.54	-9.79
70.1	-4.73	20.9	-1.30	6.10	4.94	-12.2
70.1	-2.95	25.8	-1.38	7.12	5.66	-15.8
70.1	-2.02	29.4	-1.23	8.04	5.83	-16.5
70.1	-1.13	33.8	-0.952	8.01	6.17	-12.2
70.1	-0.240	36.8	-0.646	7.82	6.18	-4.79
70.1	0.650	36.1	-0.246	7.60	6.20	5.41
70.1	1.54	32.7	-0.121	8.14	6.37	15.7
70.1	2.46	28.9	0.317	7.97	5.85	16.2
70.1	3.31	24.0	0.514	6.62	5.70	14.5
70.1	4.24	20.8	0.444	5.83	4.68	10.7
70.1	5.05	17.4	0.577	4.73	4.35	9.33
70.1	5.97	14.8	0.557	4.08	3.43	5.52
70.1	6.87	12.5	0.338	2.94	2.64	3.13
70.1	7.75	11.2	0.593	2.61	2.20	2.48
70.1	8.64	9.93	0.223	1.51	1.34	0.608

```
C    FILENAME=  B30.JET
C
C      CLOCK=1.0
C x/d       y/d        u         v         u'        v'        u'v'
 30.50     -3.640     17.04     -3.363     6.218     6.369     -17.05
 30.50     -3.230     21.63     -3.920     7.041     7.256     -22.51
 30.50     -2.710     24.71     -3.276     7.297     8.685     -22.01
 30.50     -2.340     27.83     -.9356     6.987     9.620     -20.91
 30.50     -1.890     49.87     -4.252     16.08     11.38     -79.64
 30.50     -1.440     61.80     -4.148     15.98     11.57     -62.17
 30.50     -1.020     72.71     -1.990     16.23     11.62     -64.40
 30.50     -.5800     82.46     -.4267     15.37     12.16     -49.91
 30.50     -.1200     87.99     -.3188     15.75     12.47     -32.59
 30.50     0.3300     86.90     0.7475     16.14     12.71      41.22
 30.50     0.8200     78.44      2.291     16.20     12.86      60.85
 30.50      1.250     67.61      2.730     17.30     12.81      98.10
 30.50      1.690     56.31      3.706     16.51     13.04      86.04
 30.50      2.140     41.79      3.468     13.98     12.01      63.45
 30.50      2.580     33.44      4.423     13.23     10.56      64.49
 30.50      3.020     25.20      3.932     10.14     8.855      41.62
 30.50      3.460     18.93      3.243     7.155     6.798      23.68
 30.50      3.900     15.14      2.775     5.763     5.774      17.23
 30.50      3.900     15.22      2.959     5.668     5.681      15.03
 30.50      4.340     12.50      2.426     4.043     4.529      7.701
 30.50      4.780     10.19      1.885     3.139     3.447      4.170
 30.50      5.230     9.229      1.666     2.214     3.053      1.907
```

C FILENAME= B50.JET
C CLOCK=1100

C x/d	y/d	u	v	u'	v'	u'v'
50.30	-4.820	18.27	-2.973	5.653	5.892	-14.85
50.30	-3.940	22.68	-2.983	6.748	6.975	-20.61
50.30	-3.050	26.96	-2.213	6.686	7.469	-15.93
50.30	-2.170	40.59	-3.362	10.77	8.519	-34.09
50.30	-1.260	48.98	-2.825	10.70	9.038	-26.52
50.30	-.3300	55.25	-1.788	11.11	9.370	-11.85
50.30	0.5500	55.16	0.7289	11.63	9.289	7.976
50.30	1.430	47.77	1.356	10.88	8.846	27.09
50.30	2.310	38.68	2.010	11.79	8.392	36.88
50.30	3.230	29.98	2.922	9.823	8.003	34.09
50.30	4.070	22.64	2.386	7.117	6.546	17.65
50.30	4.960	17.48	2.174	5.460	5.223	11.89
50.30	5.840	13.97	1.821	4.228	4.065	7.918

C FILENAME= B70.JET
C
C CLOCK 1150

C x/d	y/d	u	v	u'	v'	u'v'
70.10	-7.380	12.76	-1.478	3.189	3.244	-4.334
70.10	-6.530	15.31	-2.049	3.994	3.975	-5.768
70.10	-5.680	17.31	-2.289	4.628	4.623	-8.957
70.10	-4.790	19.59	-2.320	5.099	5.135	-10.97
70.10	-3.880	23.73	-2.350	6.444	5.736	-14.55
70.10	-3.020	26.86	-2.108	7.426	5.958	-16.25
70.10	-2.080	31.93	-2.247	7.930	6.410	-17.21
70.10	-1.190	35.97	-1.530	8.339	6.748	-11.35
70.10	-.2900	37.83	-1.332	7.529	6.219	-4.396
70.10	0.6000	37.68	0.1935	7.848	6.367	3.357
70.10	1.490	34.44	0.2664	8.238	6.184	12.46
70.10	2.380	29.28	0.6348	8.129	6.027	19.54
70.10	3.280	25.49	1.102	7.023	5.781	17.06
70.10	4.170	21.83	1.260	5.960	5.256	12.83
70.10	4.990	18.83	1.173	5.384	4.686	10.45
70.10	5.920	15.99	1.364	4.464	3.931	7.821
70.10	6.820	13.59	1.280	3.692	3.586	4.550
70.10	7.680	11.77	1.096	2.638	2.628	2.316
70.10	8.580	10.74	1.109	2.266	2.342	1.522
70.10	9.470	9.698	0.9465	1.657	2.332	0.7441

C FILENAME B30.AIR
C RADIAL VELOCITY PROFILES AT x/d=30, LDV PARTICLES ADDED TO AIR ONLY
C clock=1.0

C x/d	y/d	u	v	u'	v'	u'v'
30.50	-5.880	9.172	-.4865	0.2592	0.4372	0.5400E-02
30.50	-5.810	9.344	-.6129	0.7818	1.188	-.9300E-01
30.50	-5.450	9.189	-.5150	0.4102	0.5934	0.2170E-01
30.50	-5.070	9.285	-.6207	0.7305	1.194	-.2373
30.50	-4.630	9.724	-.5211	1.424	1.512	-.7383
30.50	-4.170	11.16	-.8154	2.953	2.658	-3.528
30.50	-3.730	13.83	-.8689	4.468	3.809	-7.948
30.50	-3.230	18.19	-1.667	6.842	5.870	-19.69
30.50	-2.790	23.02	-1.785	9.048	7.413	-32.39
30.50	-2.340	31.21	-1.809	11.95	9.205	-50.43
30.50	-1.900	41.40	-1.998	15.27	10.74	-76.39
30.50	-1.460	56.95	-1.795	17.12	11.90	-82.43
30.50	-1.020	66.25	-.7552	16.21	12.70	-78.29
30.50	-.5700	78.30	1.024	16.44	12.93	-61.26
30.50	-.1100	85.64	0.4951	15.57	12.86	-33.60
30.50	0.3100	84.04	0.8008	16.20	12.66	29.22
30.50	0.8200	75.41	0.7754	16.07	13.79	75.13
30.50	1.190	63.74	0.8758	17.00	13.30	97.99
30.50	1.650	50.39	1.375	17.38	12.43	107.3
30.50	2.130	37.38	1.320	14.56	10.76	70.44
30.50	2.580	27.38	1.189	11.54	8.525	47.50
30.50	3.020	20.57	1.243	8.761	7.274	33.09
30.50	3.460	15.41	0.9374	5.485	4.853	13.07
30.50	3.860	12.14	0.7515	3.766	3.423	5.943
30.50	4.340	10.34	0.4147	2.124	1.996	1.441
30.50	4.780	9.512	0.4680	1.017	1.298	0.4293
30.50	5.220	9.246	0.3782	0.5322	0.7121	-.7700E-02
30.50	6.110	9.214	0.4123	0.2351	0.4177	-.5600E-02

C FILENAME= B50.AIR
C
C CLOCK=1000

C x/d	y/d	u	v	u'	v'	u'v'
50.20	-7.710	9.321	-.5102	0.6040	0.8076	0.5660E-01
50.20	-7.350	9.399	-.5204	0.2448	0.4532	0.1400E-01
50.20	-7.350	9.623	-.6378	1.201	1.362	-.5530
50.20	-6.910	10.01	-.5947	1.523	1.523	-.8142
50.20	-6.020	11.94	-.9341	2.866	2.944	-3.809
50.20	-5.580	13.19	-.8103	3.355	3.184	-4.135
50.20	-5.580	15.09	-1.201	4.265	3.866	-6.306
50.20	-4.690	17.02	-1.202	5.397	4.555	-11.40
50.20	-4.230	19.55	-1.029	6.195	5.243	-14.60
50.20	-3.770	23.26	-1.810	7.905	6.113	-20.99
50.20	-3.330	25.77	-1.053	9.103	6.512	-28.40
50.20	-2.860	29.85	-1.497	10.26	7.324	-33.49
50.30	-2.350	33.97	-1.351	10.86	8.441	-37.92
50.30	-2.040	38.31	-.9754	11.85	8.363	-40.54
50.30	-1.540	44.22	-1.704	10.58	8.840	-30.69
50.30	-1.090	48.39	-.9741	10.82	9.110	-27.93
50.30	-.6500	51.65	-.7754	10.81	9.333	-20.18
50.30	-.2000	53.69	-.1906	10.79	9.270	-12.41
50.30	0.2400	53.74	-.1834	10.62	9.200	1.752
50.30	0.6800	51.97	0.5200	10.80	9.302	17.86
50.30	1.120	48.07	0.7178	10.55	9.135	27.92
50.30	1.550	44.25	0.7841	10.83	9.354	33.30
50.30	1.770	43.99	1.124	10.65	8.785	34.77
50.30	2.040	40.44	2.014	10.92	8.707	38.92
50.30	2.500	33.38	1.023	10.96	8.500	42.93
50.30	2.940	29.13	1.157	9.975	7.845	33.12
50.30	3.360	24.73	0.7608	9.182	6.768	28.40
50.20	3.800	20.61	0.6422	6.364	5.787	13.69
50.20	4.270	17.89	0.9634	5.648	5.113	11.29
50.20	4.680	13.93	0.5320	4.038	3.753	7.193
50.20	5.590	12.55	0.6919	3.503	2.921	4.911
50.20	6.040	11.17	0.4040	2.354	2.301	2.285
50.20	6.480	10.39	0.3547	1.723	1.859	1.387
50.20	6.910	9.773	0.3677	1.372	1.387	0.6606
50.20	7.340	9.571	0.3018	0.9118	1.069	0.2419
50.20	7.800	9.447	0.3416	0.4892	0.7814	0.2590E-01
50.20	8.240	9.419	0.2796	0.3471	0.5800	-.4040E-01
50.20	8.680	9.397	0.2905	0.2885	0.4775	-.2430E-01

C FILENAME= B70.AIR
C
C LDV PARTICLES ADDED AIR ONLY
C T1100
C

C x/d	y/d	u	v	u'	v'	u'v'
70.1	-10.9	9.21	-0.300	0.386	1.08	-0.650E-02
70.1	-10.1	9.17	-0.382	0.807	1.16	0.421E-01
70.1	-9.19	9.69	-0.633	1.48	1.83	-1.17
70.1	-7.53	12.0	-0.909	3.06	2.87	-3.45
70.1	-6.60	13.6	-0.997	3.44	3.22	-4.41
70.1	-5.71	16.1	-1.11	4.32	3.77	-6.95
70.1	-4.82	19.0	-1.45	4.99	4.49	-8.07
70.1	-3.95	21.7	-1.17	6.11	5.10	-13.6
70.1	-3.01	25.7	-1.14	7.12	5.84	-18.3
70.1	-2.14	31.0	-1.49	7.96	6.28	-17.9
70.1	-1.22	33.9	-0.376	8.01	6.12	-14.8
70.1	-0.330	36.3	-0.425	7.77	6.30	-6.43
70.1	0.550	37.0	-0.150	7.76	6.40	1.58
70.1	1.42	33.5	0.169	7.97	6.46	15.0
70.1	2.32	29.1	0.191	7.82	6.40	19.2
70.1	3.19	24.3	0.235	7.00	5.70	15.6
70.1	4.13	20.6	0.418	5.79	5.01	13.0
70.1	5.84	14.7	0.563	3.95	3.42	5.89
70.1	5.03	17.1	0.636	5.01	4.27	9.41
70.1	6.79	12.7	0.531	3.13	2.84	3.99
70.1	7.67	11.0	0.412	2.34	2.13	1.87
70.1	8.55	9.84	0.189	1.34	1.42	0.624
70.1	9.43	9.37	0.294	0.910	1.12	0.130
70.1	10.3	9.21	0.283	0.483	1.02	-0.340E-02
70.1	11.3	9.27	0.241	0.268	0.560	-0.100E-03

```
C  BAX.DEN
C
C  AT x/d GREATER THAN 70, RHO' IS NOT AVAILABLE,
C     THE 'NO DATA' ENTRY IS SIGNIFIED BY 0.
C
C x/d      RHO        RHO'      %TURB
5.00     0.327     2.058E-02  6.30
6.00     0.316     2.530E-02  8.00
7.00     0.311     2.426E-02  7.80
8.00     0.301     2.260E-02  7.50
9.00     0.279     2.166E-02  7.77
9.00     0.277     2.773E-02  10.0
9.00     0.277     1.828E-02  6.60
9.00     0.280     3.029E-02  10.8
9.00     0.277     2.684E-02  9.69
10.0     0.272     2.288E-02  8.42
11.0     0.247     2.795E-02  11.3
12.0     0.235     2.117E-02  9.00
13.0     0.211     2.635E-02  12.5
14.0     0.202     1.879E-02  9.30
15.0     0.188     1.637E-02  8.70
20.0     0.153     1.272E-02  8.30
25.0     0.150     9.739E-03  6.50
30.0     0.134     7.780E-03  5.80
35.0     0.129     6.833E-03  5.30
40.0     0.132     6.157E-03  4.65
45.0     0.120     6.972E-03  5.80
50.0     0.117     8.054E-03  6.90
60.0     0.124     1.472E-02  11.9
70.0     0.138     2.477E-02  18.0
85.0     0.201     0.          0.
104.     0.228     0.          0.
150.     0.375     0.          0.
```

C FILENAME= B15.DEN
C

C x/d	y/d	RHO	RHO'	%TURB	SKEW	FLAT	INT
15.5	-3.66	1.00	3.016E-02	3.00	-10.8	214.	6.230E-03
15.5	-3.12	0.918	0.190	20.7	-2.59	8.71	0.206
15.5	-2.83	0.779	0.275	35.3	-1.03	2.56	0.510
15.5	-2.56	0.530	0.296	55.7	0.194	1.56	0.896
15.5	-2.25	0.322	0.225	69.7	1.22	3.57	0.994
15.5	-1.93	0.189	0.128	67.8	2.40	9.72	1.00
15.5	-1.63	0.127	5.590E-02	44.0	4.51	33.3	1.00
15.5	-1.30	0.112	2.213E-02	19.7	11.0	260.	1.00
15.5	-1.03	0.120	1.803E-02	15.1	7.85	217.	1.00
15.4	-0.676	0.143	2.148E-02	15.1	4.77	183.	1.00
15.5	-0.383	0.173	2.508E-02	14.5	2.24	41.0	1.00
15.5	-6.710E-02	0.199	2.836E-02	14.2	7.85	199.	1.00
15.4	0.244	0.191	2.639E-02	13.8	4.09	75.5	1.00
15.4	0.580	0.161	2.672E-02	16.6	6.88	178.	1.00

```
C  FILENAME=  B30.DEN
C
C x/d     y/d      RHO      RHO'        %TURB   SKEW     FLAT        INT
30.6     -6.26    1.00     4.139E-02   4.13    -12.8    218.        6.350E-03
30.6     -5.33    0.934    0.178       19.1    -2.74    9.47        0.160
30.6     -4.49    0.630    0.298       47.2    -0.108   1.47        0.734
30.6     -3.89    0.399    0.244       61.2    0.968    2.85        0.966
30.5     -3.25    0.250    0.157       63.0    1.92     7.02        0.998
30.5     -2.64    0.163    8.066E-02   49.4    3.09     16.3        1.00
30.5     -2.00    0.129    3.516E-02   27.3    5.17     49.9        1.00
30.5     -0.115   0.131    1.352E-02   10.3    21.7     1.370E+03   1.00
30.4     3.07     0.225    0.130       58.0    2.29     9.40        0.999
30.3     4.66     0.684    0.300       43.9    -0.311   1.53        0.641
```

C FILENAME= B50.DEN
C

C x/d	y/d	RHO	RHO'	%TURB	SKEW	FLAT	INT
50.7	-10.5	1.00	2.008E-02	2.00	4.180E-03	2.97	3.480E-03
50.7	-8.45	0.959	0.113	11.8	-4.28	21.7	9.580E-02
50.7	-7.84	0.893	0.188	21.0	-2.17	6.40	0.282
50.7	-7.24	0.775	0.249	32.2	-0.877	2.24	0.589
50.6	-6.62	0.643	0.274	42.5	-0.178	1.50	0.848
50.7	-6.01	0.523	0.252	48.2	0.463	1.90	0.943
50.7	-5.41	0.401	0.212	52.9	1.03	3.20	0.993
50.6	-4.80	0.313	0.165	52.6	1.52	5.31	0.999
50.6	-4.16	0.253	0.126	49.9	1.87	7.53	1.00
50.6	-3.56	0.209	9.262E-02	44.2	2.26	10.3	1.00
50.6	-2.92	0.173	6.689E-02	38.7	2.74	15.3	1.00
50.6	-2.30	0.148	4.533E-02	30.6	3.26	21.7	1.00
50.6	-1.69	0.134	3.098E-02	23.2	3.14	18.4	1.00
50.6	-1.06	0.125	2.139E-02	17.0	4.02	32.7	1.00
50.6	-0.417	0.119	1.434E-02	12.0	3.73	40.9	1.00
50.6	0.187	0.116	1.246E-02	10.7	2.38	15.4	1.00
50.6	0.829	0.118	1.574E-02	13.3	4.51	45.7	1.00
50.5	2.74	0.146	5.074E-02	34.8	3.03	17.6	1.00
50.5	5.30	0.361	0.199	55.0	1.23	3.93	0.994

C FILENAME: CAX.DEN
C

C x/d	RHO	RHO'	%TURB
5.00	0.318	1.590E-02	5.00
6.00	0.310	1.822E-02	5.88
7.00	0.307	1.852E-02	6.04
8.00	0.298	1.572E-02	5.27
9.00	0.280	1.671E-02	5.96
10.0	0.270	1.853E-02	6.85
11.0	0.248	1.748E-02	7.06
12.0	0.226	1.762E-02	7.79
14.0	0.198	1.746E-02	8.80
15.0	0.187	1.508E-02	8.07
16.0	0.182	1.492E-02	8.20
17.0	0.170	1.620E-02	9.50
18.0	0.164	1.475E-02	9.00
19.0	0.158	1.180E-02	7.46
20.0	0.148	1.136E-02	7.70
25.0	0.139	8.918E-03	6.40
30.0	0.128	6.969E-03	5.45
35.0	0.120	5.984E-03	5.00
40.0	0.121	5.823E-03	4.80
45.0	0.116	7.042E-03	6.05
50.0	0.118	1.098E-02	9.30
60.0	0.126	1.881E-02	14.9
70.0	0.148	2.803E-02	19.0
80.0	0.213	3.054E-02	14.3

C FILENAME: C15.DEN
C

C x/d	y/d	RHO	RHO'	%TURB	SKEW	FLAT	INT
15.5	-3.91	1.00	2.721E-02	2.71	-8.92	179.	5.440E-03
15.5	-3.47	0.951	0.147	15.4	-3.39	14.1	0.126
15.5	-2.87	0.628	0.289	45.9	-0.156	1.55	0.785
15.5	-2.57	0.426	0.252	59.3	0.722	2.37	0.964
15.5	-2.25	0.261	0.170	65.0	1.64	5.56	0.999
15.5	-1.93	0.161	8.934E-02	55.4	2.89	14.3	1.00
15.5	-1.60	0.122	4.008E-02	32.8	4.46	34.5	1.00
15.5	-1.29	0.112	1.967E-02	17.5	14.5	492.	1.00
15.5	-0.695	0.147	2.336E-02	15.9	13.3	519.	1.00
15.5	-6.710E-02	0.206	2.844E-02	13.8	8.37	225.	1.00
15.5	0.585	0.171	2.295E-02	13.4	4.59	109.	1.00

C FILENAME: C30.DEN
C

C x/d	y/d	RHO	RHO'	%TURB	SKEW	FLAT	INT
30.6	-7.06	1.00	2.049E-02	2.04	-1.58	32.5	2.750E-03
30.6	-6.00	0.959	0.151	15.7	-3.35	13.6	0.111
30.6	-5.08	0.702	0.289	41.0	-0.388	1.61	0.624
30.6	-4.18	0.397	0.234	59.0	0.995	3.06	0.965
30.5	-3.56	0.250	0.148	59.0	1.98	7.56	0.998
30.5	-2.94	0.171	8.279E-02	48.3	2.78	13.8	1.00
30.5	-2.31	0.134	3.541E-02	26.5	4.16	30.7	1.00
30.5	-1.68	0.125	1.697E-02	13.5	18.9	1.080E+03	1.00
30.5	-0.441	0.134	1.303E-02	9.69	16.9	867.	1.00
30.5	0.824	0.136	1.877E-02	13.8	29.0	1.380E+03	1.00
30.4	4.02	0.319	0.190	59.6	1.49	4.90	0.989

C FILENAME: C50.DEN
C

C x/d	y/d	RHO	RHO'	%TURB	SKEW	FLAT	INT
50.8	-10.7	1.00	2.803E-02	2.79	-9.78	194.	4.580E-03
50.7	-9.61	0.984	8.607E-02	8.77	-6.02	42.3	4.200E-02
50.7	-8.42	0.852	0.223	26.2	-1.40	3.50	0.355
50.7	-7.82	0.738	0.265	35.9	-0.573	1.80	0.599
50.7	-7.23	0.602	0.266	44.3	0.143	1.60	0.821
50.7	-6.61	0.499	0.245	49.1	0.633	2.23	0.921
50.7	-6.00	0.389	0.201	51.7	1.16	3.71	0.985
50.7	-5.39	0.306	0.153	50.2	1.64	6.10	0.997
50.7	-4.78	0.253	0.120	47.5	1.94	8.19	0.999
50.7	-4.16	0.215	8.689E-02	40.4	2.02	8.88	1.00
50.6	-3.55	0.189	6.746E-02	35.6	2.56	13.4	1.00
50.6	-2.92	0.166	5.090E-02	30.7	2.97	18.8	1.00
50.6	-2.30	0.150	3.574E-02	23.8	3.24	20.9	1.00
50.6	-1.64	0.141	2.762E-02	19.6	3.57	24.6	1.00
50.6	-1.04	0.135	2.082E-02	15.4	3.19	19.6	1.00
50.6	-0.417	0.132	1.787E-02	13.5	3.62	27.3	1.00
50.6	0.216	0.129	1.566E-02	12.2	3.39	25.9	1.00
50.6	0.843	0.128	1.582E-02	12.4	3.40	28.4	1.00
50.6	1.50	0.130	1.918E-02	14.8	3.33	24.0	1.00
50.5	3.38	0.161	5.713E-02	35.4	3.21	20.4	1.00
50.5	6.58	0.421	0.217	51.6	1.01	3.23	0.965

APPENDIX B-2

SUMMARY OF G. E. DATA

The following tables provide Raman, saturated fluorescence and laser velocimetry data for the horizontal turbulent hydrogen/air jet diffusion flame, $Re_j = 8500$, studied by Drake and coworkers, c.f., Table 2 for sources.

The Raman data consist of radial profiles at x/d = 10, 25, 50, 100, 150 and 200. The radial distance, Y, listed in the tables, has not been corrected for a small centerline shift which was experimentally determined by matching Favre-averaged mixture fraction profiles above and below the geometric centerline. Tabulated values are conventional averages except for Favre-averaged mixture fraction (FMF) and Favre intermittency (FINT). The tabulated values are presented as processed and include more significant figures than warranted.

The saturated fluorescence data consist of radial profiles at x/d = 10, 25, 50, 150 and 200. In this case the tabulated values of Y have been corrected for the small measured displacement of the flame centerline; however, the value of the shift is given. The mean and rms values are conventionally averaged.

The velocity data consist of an axial scan and radial profiles at x/d = 50,100 and 200.

A final set of Raman data is also included. This provides mean and rms values of mixture fraction, similar to the first part of the tabulation. However, values of skewness, flatness and the first three normalized zero moments are also provided. These data are useful for comparing detailed shapes of mixture fraction PDF's.

**FILENAME= AMA01A:FH:CB CREATED 9:48 AM THU., 12 JAN., 1984
**AVG.TOTAL DATA
**MIXTURE FRACTION,DENSITY,INTERMITTENCY
**HYDROGEN JET FLAME RE=8500. X/D= 10. CUT-OFF MF= .0004
**
**YCL(MM)=-0.50 FAVRE MIXTURE FRAC HALF RAD=3.05

** Y **(MM)	TEMP (K)	DENS (E-4)	MF (E-3)	FMF (E-3)	INT	FINT	RMS TEMP	***RMS DENS	(E-4)****** MF	FMF	FILE NAME
7.0	345.8	10.86	.377	.173	.148	.095	155.2	1.886	15.2	7.6	M8P1F
6.5	491.1	9.19	1.750	.624	.430	.300	375.0	3.109	43.0	20.5	M8P1G
6.0	931.2	5.40	6.552	2.933	.845	.684	533.4	3.432	86.5	55.6	M8P1E
5.5	1510.6	2.59	19.67	12.46	.990	.957	489.6	1.922	198.8	162.8	M8P1H
5.0	1825.2	1.40	47.55	43.52	1.00	1.00	307.9	.289	328.1	312.3	M8P1D
4.5	1673.6	1.21	82.44	78.64	1.00	1.00	380.2	.154	495.3	477.9	M8P1I
4.0	1451.7	1.11	120.0	117.0	1.00	1.00	400.3	.153	638.6	628.5	M8P1C
3.0	1108.8	1.03	200.4	193.0	1.00	1.00	267.3	.213	870.4	843.3	M8P1J
2.0	764.4	1.02	313.3	310.6	1.00	1.00	242.1	.128	1108.	1132.	M8P1B
0.0	522.9	.99	462.9	461.1	1.00	1.00	103.5	.057	855.6	852.9	M8P1A
-4.0	1101.5	1.01	204.0	196.5	1.00	1.00	274.7	.162	807.4	786.9	M8P1K

**FILENAME= AXA01A:FH:CB CREATED 9:48 AM THU., 12 JAN., 1984
**AVG.TOTAL DATA
**TEMPERATURE,MOLE FRACTION,RMS
**HYDROGEN JET FLAME RE=8500. X/D= 10. CUT-OFF MF= .0004
**

** Y **(MM)	TEMP. (K)	***MOLE FRACTION (E-2) *** N2	H2O	H2	O2 ***	***RMS MOLE FRACTION (E-4)* N2	H2O	H2	O2 *	FILE NAME
7.0	345.8	76.39	2.39	.02	20.28	101.9	198.6	6.5	143.6	M8P1F
6.5	491.1	75.79	4.03	.15	19.11	237.0	488.6	66.8	333.2	M8P1G
6.0	931.2	73.27	9.16	.93	15.76	449.0	735.7	348.0	552.3	M8P1E
5.5	1510.6	67.25	18.40	4.85	8.70	965.5	881.8	1022.	675.5	M8P1H
5.0	1825.2	53.91	24.67	18.80	1.97	1350.	513.2	1727.	341.7	M8P1D
4.5	1673.6	40.94	23.59	34.80	.18	1399.	641.5	2011.	90.1	M8P1I
4.0	1451.7	31.73	17.48	50.30	.11	1165.	697.5	1793.	45.6	M8P1C
3.0	1108.8	19.50	12.84	67.40	.03	854.5	469.9	1322.	11.5	M8P1J
2.0	764.4	12.00	7.27	80.54	.04	634.0	361.5	993.0	10.8	M8P1B
0.0	522.9	5.98	3.86	90.05	.04	224.1	134.7	357.9	11.1	M8P1A
-4.0	1101.5	18.87	12.49	68.40	.03	798.9	502.7	1294.	12.3	M8P1K

**FILENAME= AMA02A:FH:CB CREATED 3:38 PM TUE., 10 JAN., 1984
**AVG.TOTAL DATA
**MIXTURE FRACTION,DENSITY,INTERMITTENCY
**HYDROGEN JET FLAME RE=8500. X/D= 25. CUT-OFF MF= .0004
**YCL(MM)=-0.40 FAVRE MIXTURE FRAC HALF RAD=6.40
**
**

** Y **(MM)	TEMP (K)	DENS (E-4)	MF (E-3)	FMF (E-3)	INT	FINT	RMS TEMP	***RMS DENS	(E-4)****** MF	FMF	FILE NAME
16.0	308.2	11.36	.086	.086	.020	.020	5.1	.190	1.4	1.4	M841G
14.0	321.3	11.27	.225	.108	.045	.032	124.0	1.058	13.7	6.1	M841F
13.0	394.1	10.69	1.072	.392	.231	.142	282.7	2.766	30.8	14.7	M841I
12.0	701.0	7.67	4.334	1.458	.539	.322	538.4	3.949	70.2	38.0	M841E
11.0	1073.9	5.49	10.53	3.685	.779	.535	692.6	4.120	130.8	80.4	M841J
10.0	1540.9	2.63	24.75	14.24	.974	.891	553.9	2.238	217.3	186.1	M841D
9.0	1841.9	1.56	42.95	35.46	1.00	1.00	380.4	1.046	253.8	263.3	M841K
8.0	1755.5	1.27	64.06	60.47	1.00	1.00	325.1	.271	323.2	326.5	M841C
7.0	1657.2	1.18	83.20	81.41	1.00	1.00	354.8	.137	371.9	364.5	M841L
6.0	1488.4	1.15	104.1	102.3	1.00	1.00	338.7	.121	418.2	411.9	M841M
4.0	1166.7	1.12	149.2	147.7	1.00	1.00	234.2	.098	432.7	427.8	M841B
2.0	1069.1	1.09	176.4	174.9	1.00	1.00	172.1	.140	383.8	384.7	M841O
0.0	954.2	1.08	202.5	200.9	1.00	1.00	128.8	.105	386.6	385.1	M841A
-8.0	1681.6	1.20	78.69	77.24	1.00	1.00	357.5	.123	355.6	348.5	M841P
-12.0	1069.3	4.86	9.263	4.159	.875	.713	606.5	3.472	101.7	69.0	M841N

**FILENAME= AXA02A:FH:CB CREATED 3:38 PM TUE., 10 JAN., 1984
**AVG.TOTAL DATA
**TEMPERATURE,MOLE FRACTION,RMS
**HYDROGEN JET FLAME RE=8500. X/D= 25. CUT-OFF MF= .0004
**

** Y **(MM)	TEMP. (K)	***MOLE FRACTION (E-2) *** N2	H2O	H2	O2 ***	***RMS MOLE FRACTION (E-4)* N2	H2O	H2	O2 *	FILE NAME
16.0	308.2	77.24	1.55	.11	20.17	72.9	15.1	13.7	70.8	M841G
14.0	321.3	77.15	1.75	.10	20.08	106.4	171.6	18.0	117.7	M841F
13.0	394.1	76.22	2.83	.15	19.88	174.1	366.1	44.8	243.2	M841I
12.0	701.0	74.64	6.55	.53	17.37	378.7	724.5	177.9	482.4	M841E
11.0	1073.9	71.35	12.03	1.99	13.78	689.5	1005.	551.3	697.4	M841J
10.0	1540.9	64.41	18.89	8.31	7.62	1111.	884.9	1175.	710.7	M841D
9.0	1841.9	54.85	25.02	16.69	2.79	1184.	624.3	1462.	485.1	M841K
8.0	1755.5	45.85	22.70	29.60	1.30	1210.	485.3	1658.	273.5	M841C
7.0	1657.2	38.85	22.26	38.01	.42	1080.	530.3	1584.	87.2	M841L
6.0	1488.4	33.26	19.19	46.86	.29	1006.	499.4	1488.	58.5	M841M
4.0	1166.7	24.27	13.63	61.46	.35	663.5	332.5	1003.	43.3	M841B
2.0	1069.1	20.03	12.45	67.03	.25	480.3	256.7	720.7	42.5	M841O
0.0	954.2	17.65	10.09	71.82	.23	396.9	211.2	603.6	28.6	M841A
-8.0	1681.6	40.35	22.97	35.84	.36	1099.	531.7	1616.	71.7	M841P
-12.0	1069.3	71.99	11.68	1.34	14.13	568.3	900.4	359.2	583.5	M841N

**FILENAME= AMA05A:FH:CB CREATED 5:19 PM WED., 21 DEC., 1983
**AVG.TOTAL DATA
**MIXTURE FRACTION,DENSITY,INTERMITTENCY
**HYDROGEN JET FLAME RE=8500. X/D= 50. CUT-OFF MF= .0004
**YCL(MM)=-0.80 FAVRE MIXTURE FRAC HALF RAD=10.70
**
**

** Y **(MM)	TEMP (K)	DENS (E-4)	MF (E-3)	FMF (E-3)	INT	FINT	RMS TEMP	***RMS DENS	(E-4)****** MF	FMF	FILE NAME
10.0	1993.8	1.19	56.84	54.37	1.00	1.00	310.1	.257	231.3	238.5	M9Q1B
12.0	1978.0	1.49	40.25	33.37	.997	.981	399.4	.956	211.7	226.6	M9T1B
14.0	1812.6	2.32	25.78	15.30	.971	.859	633.8	2.231	175.1	167.4	M9T1E
16.0	1349.2	4.12	14.65	5.996	.858	.629	755.0	3.461	140.7	100.6	M9T1G
18.0	820.8	7.36	6.402	1.808	.549	.294	673.8	4.316	96.6	50.4	M9U1B
20.0	474.7	9.97	2.029	.516	.230	.110	422.1	3.220	55.6	24.3	M9V1B
8.0	1898.5	1.09	73.09	71.57	1.00	1.00	304.9	.140	241.0	240.9	M9V1F
-15.0	1912.6	1.99	29.84	19.81	.990	.944	569.7	1.855	189.9	188.1	M9V1H
0.0	1533.7	1.04	109.8	108.5	1.00	1.00	192.8	.136	198.1	194.5	M9V1I

**FILENAME= AXA05A:FH:CB CREATED 5:19 PM WED., 21 DEC., 1983
**AVG.TOTAL DATA
**TEMPERATURE,MOLE FRACTION,RMS
**HYDROGEN JET FLAME RE=8500. X/D= 50. CUT-OFF MF= .0004
**

** Y **(MM)	TEMP. (K)	***MOLE FRACTION (E-2) *** N2	H2O	H2	O2	***RMS MOLE FRACTION (E-4)* *** N2	H2O	H2	O2	FILE * NAME
10.0	1993.8	48.10	26.93	23.89	.51	1069.	488.9	1440.	203.4	M9Q1B
12.0	1978.0	56.60	26.43	14.21	2.08	1131.	681.3	1316.	452.7	M9T1B
14.0	1812.6	63.85	24.19	5.37	5.83	977.3	1080.	865.2	709.3	M9T1E
16.0	1349.2	69.95	16.50	1.83	10.89	795.9	1239.	496.8	765.0	M9T1G
18.0	820.8	74.19	8.07	.61	16.24	531.4	999.4	237.9	638.9	M9U1B
20.0	474.7	76.80	3.02	.23	19.03	318.4	604.9	127.0	391.2	M9V1B
8.0	1898.5	41.06	24.70	33.44	.30	902.7	467.4	1302.	90.1	M9V1F
-15.0	1912.6	59.97	25.70	7.13	6.48	1042.	995.8	993.7	636.2	M9V1H
0.0	1533.7	29.67	19.31	50.41	.24	464.6	275.2	670.9	53.1	M9V1I

```
**FILENAME= AMA10A:FH:CB    CREATED  2:24 PM  WED., 11  JAN., 1984
**AVG.TOTAL DATA
**MIXTURE FRACTION,DENSITY,INTERMITTENCY
**HYDROGEN JET FLAME   RE=8500.   X/D=100.   CUT-OFF MF= .0004
**YCL(MM)=-0.20   FAVRE MIXTURE FRAC HALF RAD=12.90
**
**
```

** Y	TEMP	DENS	MF	FMF	INT	FINT	RMS	***RMS	(E-4)******		FILE
**(MM)	(K)	(E-4)	(E-3)	(E-3)			TEMP	DENS	MF	FMF	NAME
32.0	439.8	10.31	1.435	.356	.195	.081	360.9	3.155	39.6	18.9	M7V1G
30.0	546.2	9.62	2.627	.591	.260	.102	513.6	3.716	57.7	27.0	M7V1H
28.0	707.4	8.14	4.509	1.355	.491	.257	597.4	4.305	69.3	37.4	M7V1F
26.0	837.5	6.80	6.045	2.092	.630	.375	633.4	4.098	79.8	46.2	M7V1I
24.0	1155.0	4.82	10.21	4.279	.810	.552	684.6	3.725	98.0	69.8	M7V1J
22.0	1326.5	4.11	12.60	5.616	.845	.579	715.0	3.510	104.8	82.5	M7V1K
20.0	1481.1	3.38	15.58	7.812	.930	.774	706.5	2.928	120.3	100.6	M7V1L
18.0	1772.2	2.33	21.99	13.89	.990	.952	616.9	2.000	136.9	133.8	M7V1N
16.0	1919.8	1.98	25.07	17.48	.980	.897	556.0	1.685	134.5	145.2	M7V1O
12.0	2052.6	1.49	33.83	28.73	1.00	1.00	383.2	.802	148.8	165.9	M7V1P
8.0	2133.0	1.21	43.94	42.82	1.00	1.00	209.3	.173	122.8	128.8	M7V1Q
4.0	2091.1	1.16	50.63	50.11	1.00	1.00	190.8	.096	111.5	112.3	M7V1R
0.0	2050.8	1.14	53.95	53.59	1.00	1.00	180.4	.090	95.9	96.1	M7V1S
-22.0	1360.0	3.59	13.27	7.046	.945	.837	667.0	2.829	103.1	84.8	M7V1T
-26.0	883.2	6.73	6.515	2.141	.588	.316	662.9	4.205	80.0	48.4	M7V1U

```
**FILENAME= AXA10A:FH:CB    CREATED  2:24 PM  WED., 11  JAN., 1984
**AVG.TOTAL DATA
**TEMPERATURE,MOLE FRACTION,RMS
**HYDROGEN JET FLAME    RE=8500.    X/D=100.   CUT-OFF MF= .0004
**
```

** Y	TEMP.	***MOLE FRACTION (E-2)				***RMS MOLE FRACTION (E-4)*				FILE
**(MM)	(K)	*** N2	H2O	H2	O2 ***	N2	H2O	H2	O2 *	NAME
32.0	439.8	76.31	3.40	.04	19.34	198.3	497.9	19.1	332.9	M7V1G
30.0	546.2	75.80	4.88	.06	18.35	277.3	721.8	20.4	477.0	M7V1H
28.0	707.4	74.69	7.21	.17	17.04	307.4	850.5	85.5	581.8	M7V1F
26.0	837.5	74.19	9.10	.21	15.62	391.6	931.8	100.6	610.4	M7V1I
24.0	1155.0	72.19	13.79	.58	12.57	477.7	1043.	218.2	706.4	M7V1J
22.0	1326.5	71.13	16.48	.74	10.80	515.6	1116.	234.0	738.6	M7V1K
20.0	1481.1	69.40	18.93	1.50	9.34	624.2	1129.	372.2	749.4	M7V1L
18.0	1772.2	65.80	23.37	3.66	6.38	756.5	998.1	584.5	695.9	M7V1N
16.0	1919.8	64.75	25.67	4.53	4.28	766.4	917.4	659.6	631.0	M7V1O
12.0	2052.6	59.63	27.98	9.60	2.08	877.0	642.7	940.6	456.3	M7V1P
8.0	2133.0	53.60	29.40	16.04	.31	748.1	353.6	925.5	153.5	M7V1Q
4.0	2091.1	49.74	28.62	20.98	.06	608.8	318.1	825.5	74.5	M7V1R
0.0	2050.8	47.76	28.31	23.31	.04	504.3	291.6	666.2	21.8	M7V1S
-22.0	1360.0	70.21	17.11	.95	10.88	540.7	1059.	240.6	674.1	M7V1T
-26.0	883.2	74.08	9.71	.20	15.11	411.4	958.1	88.3	604.6	M7V1U

**FILENAME= AMA15A:FH:CB CREATED 2:34 PM THU., 12 JAN., 1984
**AVG.TOTAL DATA
**MIXTURE FRACTION,DENSITY,INTERMITTENCY
**HYDROGEN JET FLAME RE=8500. X/D=150. CUT-OFF MF= .0004
**YCL(MM)=1.50 FAVRE MIXTURE FRAC HALF RAD=14.60
**
**

** Y **(MM)	TEMP (K)	DENS (E-4)	MF (E-3)	FMF (E-3)	INT	FINT	***RMS TEMP	(E-4)****** DENS	MF	FMF	FILE NAME
34.0	623.2	8.49	3.805	1.191	.429	.219	525.8	3.979	66.2	34.1	M911N
30.0	885.5	6.34	7.025	2.739	.700	.453	613.6	4.084	77.0	50.7	M911M
28.0	905.5	6.20	7.519	2.927	.730	.491	635.5	4.067	85.8	53.9	M911L
26.0	1082.6	5.19	9.836	4.132	.779	.506	668.8	3.926	91.7	65.9	M911K
24.0	1339.9	4.01	13.52	6.383	.880	.653	722.9	3.447	105.8	84.8	M911J
22.0	1435.7	3.35	15.25	8.355	.960	.862	684.5	2.778	113.3	93.9	M911I
20.0	1521.2	2.92	16.11	10.05	.984	.937	641.3	2.291	101.4	93.4	M911H
16.0	1773.7	2.34	20.49	13.61	.970	.865	619.3	1.987	110.1	114.7	M911G
12.0	1947.2	1.70	23.90	20.67	1.00	1.00	445.8	.649	98.5	101.5	M911F
8.0	2086.8	1.54	26.93	23.69	1.00	1.00	415.0	.647	96.2	107.2	M911E
6.0	2141.2	1.42	29.68	27.39	1.00	1.00	323.0	.443	94.4	103.6	M911D
4.0	2078.6	1.46	30.13	27.00	1.00	1.00	353.7	.481	116.8	122.4	M911C
2.0	2141.7	1.39	31.47	29.02	1.00	1.00	317.7	.418	101.3	111.5	M911B
0.0	2112.5	1.42	29.92	27.65	1.00	1.00	309.0	.417	97.1	105.2	M911A
-20.0	1367.1	3.53	13.90	7.760	.950	.837	661.0	2.818	99.5	84.6	M911O
-28.0	860.4	6.42	6.793	2.721	.740	.533	594.9	4.016	76.3	49.3	M911P

**FILENAME= AXA15A:FH:CB CREATED 2:34 PM THU., 12 JAN., 1984
**AVG.TOTAL DATA
**TEMPERATURE,MOLE FRACTION,RMS
**HYDROGEN JET FLAME RE=8500. X/D=150. CUT-OFF MF= .0004
**

** Y **(MM)	TEMP. (K)	***MOLE FRACTION (E-2) *** N2	H2O	H2	O2 ***	***RMS MOLE FRACTION (E-4)* N2	H2O	H2	O2 *	FILE NAME
34.0	623.2	74.50	6.78	.13	17.70	389.3	797.7	45.8	463.4	M911N
30.0	885.5	72.57	10.91	.15	15.50	449.2	946.1	40.1	543.9	M911M
28.0	905.5	72.29	11.37	.23	15.24	484.3	1015.	64.1	593.6	M911L
26.0	1082.6	70.89	14.10	.37	13.80	493.8	1063.	84.4	648.7	M911K
24.0	1339.9	69.23	18.11	.68	11.15	578.4	1152.	152.0	686.9	M911J
22.0	1435.7	67.88	19.65	1.04	10.61	619.9	1128.	283.3	682.0	M911I
20.0	1521.2	67.42	20.83	1.06	9.88	549.2	1035.	193.6	627.8	M911H
16.0	1773.7	65.83	25.10	1.56	6.72	592.7	1050.	292.5	649.4	M911G
12.0	1947.2	64.81	27.91	2.44	4.07	572.6	788.2	367.1	501.5	M911F
8.0	2086.8	63.16	29.65	3.67	2.77	585.1	717.4	416.8	459.5	M911E
6.0	2141.2	61.72	30.66	5.13	1.74	599.9	559.2	547.1	351.1	M911D
4.0	2078.6	61.10	29.50	6.22	2.44	715.4	627.4	627.2	410.0	M911C
2.0	2141.7	60.36	30.39	6.76	1.77	620.5	546.9	585.3	366.1	M911B
0.0	2112.5	61.59	30.10	5.77	1.81	614.0	536.8	550.3	344.1	M911A
-20.0	1367.1	68.36	18.62	.72	11.48	530.9	1064.	162.8	659.0	M911O
-28.0	860.4	72.21	10.53	.23	16.15	447.1	912.8	62.4	536.5	M911P

**FILENAME= AMA20A:FH:CB CREATED 3:48 PM THU., 12 JAN., 1984
**AVG.TOTAL DATA
**MIXTURE FRACTION,DENSITY,INTERMITTENCY
**HYDROGEN JET FLAME RE=8500. X/D=200. CUT-OFF MF= .0004
**YCL(MM)=4.0 FAVRE MIXTURE FRAC HALF RAD=18.8
**
**

** Y **(MM)	TEMP (K)	DENS (E-4)	MF (E-3)	FMF (E-3)	INT	FINT	RMS TEMP	***RMS DENS	(E-4)****** MF	FMF	FILE NAME
38.0	642.1	8.01	3.909	1.389	.480	.270	487.0	3.815	59.2	34.5	M9M1I
32.0	820.3	6.03	5.564	2.655	.730	.505	497.8	3.520	60.7	42.2	M9M1H
26.0	1104.9	4.21	9.162	5.385	.905	.751	525.3	2.903	67.4	58.5	M9M1G
20.0	1279.6	3.53	11.42	7.143	.940	.815	570.4	2.535	74.4	68.0	M9M1F
14.0	1514.5	2.73	14.76	10.36	.990	.959	575.7	1.851	81.2	80.0	M9M1E
8.0	1568.8	2.66	15.62	10.74	.980	.920	580.4	1.965	85.2	85.9	M9M1D
4.0	1678.7	2.38	17.25	12.58	.970	.858	548.4	1.847	82.7	89.3	M9M1C
0.0	1581.9	2.39	15.64	12.34	1.00	1.00	512.4	1.257	75.2	74.7	M9M1B
-8.0	1562.2	2.58	15.39	11.24	.985	.939	552.4	1.708	79.2	80.4	M9M1K

**FILENAME= AXA20A:FH:CB CREATED 3:48 PM THU., 12 JAN., 1984
**AVG.TOTAL DATA
**TEMPERATURE,MOLE FRACTION,RMS
**HYDROGEN JET FLAME RE=8500. X/D=200. CUT-OFF MF= .0004
**

** Y **(MM)	TEMP. (K)	***MOLE FRACTION (E-2) *** N2	H2O	H2	O2 ***	***RMS MOLE FRACTION (E-4)* N2	H2O	H2	O2 *	FILE NAME
38.0	642.1	74.23	5.96	.29	18.63	356.2	724.4	56.2	425.0	M9M1I
32.0	820.3	73.73	8.40	.07	16.90	335.8	763.7	26.2	466.0	M9M1H
26.0	1104.9	72.02	12.94	.17	14.02	364.1	831.3	45.4	518.7	M9M1G
20.0	1279.6	71.01	15.67	.21	12.26	368.7	896.4	52.5	583.5	M9M1F
14.0	1514.5	69.40	19.62	.26	9.89	405.8	943.3	56.3	609.3	M9M1E
8.0	1568.8	69.07	20.49	.36	9.26	427.5	962.2	111.0	619.0	M9M1D
4.0	1678.7	68.57	22.28	.49	7.84	413.5	915.5	108.3	597.2	M9M1C
0.0	1581.9	69.17	20.63	.35	9.02	360.9	850.6	93.1	557.2	M9M1B
-8.0	1562.2	68.86	20.43	.24	9.64	406.7	917.8	70.7	584.4	M9M1K

```
**FILENAME= FB32SA:FH:FD        5:28 PM   MON.,  5  NOV., 1984
**
** AVERAGE FILE 6:43 PM  THU., 24 MAR., 1983
**
**RE=8500 H2 X/D=10
**
**FLOW MODEL= JET                    TUNNEL SPEED(%)= 40.0
**GAS= H2                            NOZZLE TYPE= A100A
**REYNOLDS NU= 8500.                 NOZZLE PRESS(PSIG)= 60.8
**ATM PRESS(MM HG AT OC)= 760.       NOZZLE TEMP(C)= 21.0
**ROOM TEMP(C)= 21.0
**
**
**UNCORRECTED Y CL.POSITION= 1.2500
**FLUORESCENCE INTENS. ZERO SHIFT (V)=  0.0000
**OH CALIB.START (PP  INTENS. (V) )  =   .0876
**OH CALIB.END   (PP  INTENS. (V) )  =   .0876
**NUMBER OF RUNS =   20.
**
** X/D     Y      OH CONC.      RMS       NO.    RUN
**POS.    POS.    10**16     OH CONC.    PTS.    NO.
**        (mm)   MOLEC/CM3
  10.0   -1.25      .0131     .02595    2048      1
  10.0     .75      .0105     .02549    2048      2
  10.0    2.75      .0144     .03427    2048      3
  10.0    3.75      .0622     .13164    2048      4
  10.0    4.75      .5196     .80294    2048      5
  10.0    5.75     2.6511    1.44037    2048      6
  10.0    6.75     1.2483    1.31896    2048      7
  10.0    7.75      .0341     .18288    2048      8
  10.0    8.25      .0072     .03971    2048      9
  10.0    7.25      .2732     .65617    2048     10
  10.0    6.25     2.4356    1.38520    2048     11
  10.0    5.25     1.4789    1.43631    2048     12
  10.0    4.25      .1632     .34184    2048     13
  10.0   -3.25      .0256     .04770    2048     14
  10.0   -5.25     1.4887    1.37275    2048     15
  10.0   -6.25     2.3976    1.37832    2048     16
  10.0   -7.25      .3302     .71311    2048     17
  10.0   -5.75     2.5306    1.43887    2048     18
  10.0   -6.75     1.2732    1.33717    2048     19
  10.0    5.75     2.6675    1.40066    2048     20
```

**FILENAME= FB32PB:FH:FD 4:51 PM MON., 5 NOV., 1984
**
**AVERAGE FILE 11:29 AM THU., 24 MAR., 1983
**
**RADIAL SCAN X/D=25
**
**FLOW MODEL= H2 JET TUNNEL SPEED(%)= 40.0
**GAS= H2 NOZZLE TYPE= A100A
**REYNOLDS NU= 8500. NOZZLE PRESS(PSIG)= 50.0
**ATM PRESS(MM HG AT OC)= 760. NOZZLE TEMP(C)= 22.0
**ROOM TEMP(C)= 22.0
**
**
**UNCORRECTED Y CL.POSITION= 1.2500
**FLUORESCENCE INTENS. ZERO SHIFT (V)= 0.0000
**OH CALIB.START (PP INTENS. (V)) = .0926
**OH CALIB.END (PP INTENS. (V)) = .0926
**NUMBER OF RUNS = 16.
**

** X/D POS.	Y POS. (mm)	OH CONC. 10**16 MOLEC/CM3	RMS OH CONC.	NO. PTS.	RUN NO.
25.0	-1.25	.0217	.02510	2048	1
25.0	2.75	.0285	.03341	2048	2
25.0	6.75	.2678	.57834	2048	3
25.0	8.75	1.6067	1.63323	2048	4
25.0	10.75	2.0381	1.76539	2048	5
25.0	12.75	.3490	.92602	2048	6
25.0	14.75	.0198	.10408	2048	7
25.0	16.75	.0087	.01822	2048	8
25.0	11.75	1.0612	1.47883	2048	9
25.0	9.75	2.1559	1.65040	2048	10
25.0	7.75	.7178	1.10318	2048	11
25.0	5.75	.1041	.27628	2048	12
25.0	-11.25	1.8472	1.53120	2048	14
25.0	-12.25	1.1282	1.42676	2048	15
25.0	-10.25	1.9867	1.52011	2048	16
25.0	9.75	2.0821	1.57143	2048	17

**FILENAME= FB32QA:FH:FD 5:26 PM MON., 5 NOV., 1984
**
**AVERAGE FILE 1:36 PM THU., 24 MAR., 1983
**
**X/D=50 RADIAL SCANS
**
**FLOW MODEL= JET
**GAS= H2
**REYNOLDS NU= 8500.
**ATM PRESS(MM HG AT OC)= 760.
**ROOM TEMP(C)= 21.0

TUNNEL SPEED(%)= 40.0
NOZZLE TYPE= A100A
NOZZLE PRESS(PSIG)= 60.8
NOZZLE TEMP(C)= 21.0
**
**
**UNCORRECTED Y CL.POSITION= 1.2500
**FLUORESCENCE INTENS. ZERO SHIFT (V)= 0.0000
**OH CALIB.START (PP INTENS. (V)) = .0926
**OH CALIB.END (PP INTENS. (V)) = .0926
**NUMBER OF RUNS = 15.
**

** X/D **POS. **	Y POS. (mm)	OH CONC. 10**16 MOLEC/CM3	RMS OH CONC.	NO. PTS.	RUN NO.
50.0	9.75	.5653	.93687	2048	1
50.0	11.75	1.1120	1.23534	2048	2
50.0	13.75	1.4065	1.31871	2048	3
50.0	15.75	1.2689	1.29206	2048	4
50.0	17.75	.7556	1.12209	2048	5
50.0	19.75	.3533	.82387	2048	6
50.0	21.75	.1054	.43360	2048	7
50.0	23.75	.0304	.22260	2048	8
50.0	14.75	1.3922	1.27879	2048	9
50.0	14.75	1.4121	1.29162	2048	10
50.0	12.75	1.2329	1.24272	2048	11
50.0	10.75	.7965	1.08372	2048	12
50.0	7.75	.2275	.51883	2048	13
50.0	5.75	.0942	.28254	2048	14
50.0	-1.25	.0260	.04104	2048	15

**FILENAME= FB32RA:FH:FD   5:28 PM MON., 5 NOV., 1984
**
**AVERAGE FILE 3:47 PM THU., 24 MAR., 1983
**
**H2 JET RE=8500, X/D=150
**
**FLOW MODEL= JET   TUNNEL SPEED(%)= 40.0
**GAS= H2   NOZZLE TYPE= A100A
**REYNOLDS NU= 8500.   NOZZLE PRESS(PSIG)= 60.8
**ATM PRESS(MM HG AT OC)= 760.   NOZZLE TEMP(C)= 21.0
**ROOM TEMP(C)= 21.0
**
**
**UNCORRECTED Y CL.POSITION= 1.2500
**FLUORESCENCE INTENS. ZERO SHIFT (V)= 0.0000
**OH CALIB.START (PP INTENS. (V)) =   .0876
**OH CALIB.END   (PP INTENS. (V)) =   .0876
**NUMBER OF RUNS =   18.
**

** X/D **POS. **	Y POS. (mm)	OH CONC. 10**16 MOLEC/CM3	RMS OH CONC.	NO. PTS.	RUN NO.
150.0	-1.25	1.1899	.88701	2048	1
150.0	2.75	1.1002	.83787	2048	2
150.0	4.75	1.1264	.82981	2048	3
150.0	6.75	1.1336	.81055	2048	4
150.0	8.75	1.1061	.81041	2048	5
150.0	10.75	1.0360	.80478	2048	6
150.0	16.75	.9252	.84462	2048	3
150.0	20.75	.7332	.80104	2048	4
150.0	24.75	.5019	.69483	2048	5
150.0	5.75	1.0825	.80891	2048	6
150.0	28.75	.3224	.57439	2048	7
150.0	32.75	.1946	.41785	2048	8
150.0	3.75	1.0169	.75891	2048	9
150.0	3.75	1.0451	.75989	2048	10
150.0	2.75	1.0235	.76029	2048	11
150.0	1.75	1.0235	.76625	2048	12
150.0	-1.25	1.0038	.74823	2048	13
150.0	12.75	1.0346	.81775	2048	7

```
**FILENAME= FB32ZA:FH:FD        5:29 PM  MON.,  5  NOV., 1984
**
**AVERAGE FILE  3:32 PM  TUE., 29  MAR., 1983
**
**FLOW MODEL= JET                       TUNNEL SPEED(%)= 40.0
**GAS= H2                               NOZZLE TYPE= A100A
**REYNOLDS NU= 8500.                    NOZZLE PRESS(PSIG)= 50.0
**ATM PRESS(MM HG AT OC)= 760.          NOZZLE TEMP(C)= 21.0
**ROOM TEMP(C)= 21.0
**
**
**UNCORRECTED Y CL.POSITION= 4.0000
**FLUORESCENCE INTENS. ZERO SHIFT (V)=  0.0000
**OH CALIB.START (PP  INTENS. (V) )  =   .0670
**OH CALIB.END   (PP  INTENS. (V) )  =   .0670
**NUMBER OF RUNS =   18.
**
```

** X/D **POS. **	Y POS. (mm)	OH CONC. 10**16 MOLEC/CM3	RMS OH CONC.	NO. PTS.	RUN NO.
200.0	6.00	.7582	.85021	2048	1
200.0	10.00	.6040	.75708	2048	2
200.0	14.00	.5020	.71364	2048	3
200.0	18.00	.3778	.62866	2048	4
200.0	22.00	.2296	.48739	2048	5
200.0	26.00	.1559	.38561	2048	6
200.0	30.00	.1148	.31519	2048	7
200.0	2.00	.7333	.78878	2048	8
200.0	-2.00	.7933	.81517	2048	9
200.0	-6.00	.7385	.79349	2048	10
200.0	-10.00	.6751	.78544	2048	11
200.0	-14.00	.5372	.71604	2048	12
200.0	-18.00	.4249	.64048	2048	13
200.0	-22.00	.3298	.56415	2048	14
200.0	-26.00	.2896	.58085	2048	15
200.0	-30.00	.1773	.43581	2048	16
200.0	-34.00	.0994	.29839	2048	17
200.0	-38.00	.0591	.24742	2048	18

**FILENAME= ZMN01A:FH:CD   CREATED 2:28 PM MON., 13 MAY , 1985
**NON-TURBULENT FLUID
**CONVENTIONAL AVERAGED
**MIXTURE FRACTION
**HYDROGEN JET FLAME   RE=8500.   X/D= 10.   CUT-OFF MF= .0004
** Y CENTER LINE POS.= -.50mm   CONV. MIX. FRACT. HALF RADIUS= 3.10mm
**

** Y ** mm	R/ R half	AVG (E-3)	RMS (E-4)	SKEW	FLAT	Z2	Z3	Z4	FILE NAME
7.0	2.419	.036	1.427	.3189	2.9433	16.985	69.336	930.51	M8P1F
6.5	2.258	.042	1.479	.2506	2.3878	13.694	50.419	507.31	M8P1G
6.0	2.097	.116	1.585	-.2059	2.1244	2.8559	6.0472	17.370	M8P1E
5.5	1.935	.065	.650	0.0000	1.0000	2.0000	4.0000	8.0000	M8P1H

**FILENAME= ZMT01A:FH:CD   CREATED 2:28 PM MON., 13 MAY , 1985
**TURBULENT FLUID
**CONVENTIONAL AVERAGED
**MIXTURE FRACTION
**HYDROGEN JET FLAME   RE=8500.   X/D= 10.   CUT-OFF MF= .0004
** Y CENTER LINE POS.= -.50mm   CONV. MIX. FRACT. HALF RADIUS= 3.10mm
**

** Y ** mm	R/ R half	AVG (E-3)	RMS (E-4)	SKEW	FLAT	Z2	Z3	Z4	FILE NAME
7.0	2.419	2.440	33.507	3.2236	13.348	2.8864	15.011	93.230	M8P1F
6.5	2.258	4.012	58.258	2.4245	8.9743	3.1086	14.749	83.248	M8P1G
6.0	2.097	7.729	89.172	2.4319	10.529	2.3311	8.7277	42.579	M8P1E
5.5	1.935	19.878	198.808	2.4774	10.461	2.0002	6.4790	27.381	M8P1H
5.0	1.774	47.557	328.145	1.5900	5.6391	1.4761	2.9506	7.2241	M8P1D
4.5	1.613	82.447	495.349	1.3473	5.0471	1.3610	2.3751	4.9922	M8P1I
4.0	1.452	120.041	638.612	1.2588	4.5661	1.2830	2.0386	3.8219	M8P1C
3.0	1.129	200.415	870.421	.7583	3.0701	1.1886	1.6280	2.4894	M8P1J
2.0	.806	313.330	1108.43	.1422	2.4642	1.1251	1.3817	1.8146	M8P1B
0.0	.161	462.971	855.628	-.3236	2.6904	1.0342	1.1004	1.1999	M8P1A
-4.0	1.129	203.998	807.445	.5802	3.2654	1.1567	1.5060	2.1640	M8P1K

**FILENAME= ZMA01A:FH:CD   CREATED 2:28 PM MON., 13 MAY , 1985
**AVERAGE TOTAL FLUID
**CONVENTIONAL AVERAGED
**MIXTURE FRACTION
**HYDROGEN JET FLAME   RE=8500.   X/D= 10.   CUT-OFF MF= .0004
** Y CENTER LINE POS.= -.50mm   CONV. MIX. FRACT. HALF RADIUS= 3.10mm
**

** Y ** mm	R/ R half	AVG (E-3)	RMS (E-4)	SKEW	FLAT	Z2	Z3	Z4	FILE NAME
7.0	2.419	.377	15.220	8.0234	79.091	17.284	577.12	23182.	M8P1F
6.5	2.258	1.749	42.982	3.8707	19.857	7.0378	76.539	990.81	M8P1G
6.0	2.097	6.552	86.487	2.5586	11.433	2.7425	12.112	69.709	M8P1E
5.5	1.935	19.678	198.791	2.4732	10.468	2.0205	6.6112	28.224	M8P1H
5.0	1.774	47.557	328.145	1.5900	5.6391	1.4761	2.9506	7.2241	M8P1D
4.5	1.613	82.447	495.349	1.3473	5.0471	1.3610	2.3751	4.9922	M8P1I
4.0	1.452	120.041	638.612	1.2588	4.5661	1.2830	2.0386	3.8219	M8P1C
3.0	1.129	200.415	870.421	.7583	3.0701	1.1886	1.6280	2.4894	M8P1J
2.0	.806	313.330	1108.43	.1422	2.4642	1.1251	1.3817	1.8146	M8P1B
0.0	.161	462.971	855.628	-.3236	2.6904	1.0342	1.1004	1.1999	M8P1A
-4.0	1.129	203.998	807.445	.5802	3.2654	1.1567	1.5060	2.1640	M8P1K

```
TEMPA  T=00004 IS ON CR LP   USING 00024 BLKS R=0000

0001  ** SORTED DATA FILE
0002  ** LVR INPUT FILE=L31PA
0003  **VELOCITY AVERAGE FILE= L31PA:BP
0004  ** 3:17 PM  MON., 24 JAN., 1983
0005  **
0006  **H2 AIR FLAME   RE=8500
0007  **AXIAL SCAN     Y=Z=0
0008  **
0009  **FLOW MODEL= JET                         TUNNEL SPEED(%)= 40.0
0010  **GAS= H2                                 NOZZLE TYPE= A100A
0011  **REYNOLDS NU= 8500.                      NOZZLE PRESS(PSIG)= 50.0
0012  **ATM PRESS(MM HG AT OC)= 746.            NOZZLE TEMP(C)= 21.5
0013  **ROOM TEMP(C)= 21.5
0014  **
0015  **LV PARAMETERS:MAXIMUM A/D VOLTAGE= 9.670
0016  **                  ACCURACY= 2
0017  **
0018  **X/D     Y      Z       U      URMS
0019  **       (MM)   (MM)   (M/S)   (M/S)
0020    40.0   0.0    0.0    52.76   8.320
0021    40.0   0.0    0.0    53.00   9.071
0022    40.0   0.0    0.0    53.38   8.686
0023    40.0   0.0    0.0    54.03   9.293
0024    50.0   0.0    0.0    47.76   6.929
0025    50.0   0.0    0.0    47.58   6.818
0026    50.0   0.0    0.0    47.65   6.935
0027    50.0   0.0    0.0    47.27   7.002
0028    60.0   0.0    0.0    43.45   5.872
0029    60.0   0.0    0.0    43.33   5.585
0030    60.0   0.0    0.0    43.52   5.768
0031    80.0   0.0    0.0    37.67   4.465
0032    80.0   0.0    0.0    37.77   4.579
0033    80.0   0.0    0.0    37.56   4.633
0034   100.0   0.0    0.0    35.14   4.136
0035   100.0   0.0    0.0    34.40   4.306
0036   100.0   0.0    0.0    34.14   4.565
0037   100.0   0.0    0.0    34.15   4.241
0038   100.0   0.0    0.0    34.09   4.005
0039   100.0   0.0    0.0    34.73   4.115
0040   120.0   0.0    0.0    31.89   4.136
0041   120.0   0.0    0.0    31.82   4.172
0042   120.0   0.0    0.0    31.88   3.950
0043   120.0   0.0    0.0    34.63   4.370
0044   120.0   0.0    0.0    33.58   4.718
0045   120.0   0.0    0.0    33.94   4.750
0046   120.0   0.0    0.0    33.79   4.697
0047   140.0   0.0    0.0    28.94   4.911
0048   140.0   0.0    0.0    30.29   4.544
0049   140.0   0.0    0.0    30.02   4.611
0050   140.0   0.0    0.0    30.48   4.731
0051   140.0   0.0    0.0    29.04   4.911
0052   140.0   0.0    0.0    28.79   4.843
0053   160.0   0.0    0.0    25.99   4.289
0054   160.0   0.0    0.0    25.97   4.143
0055   160.0   0.0    0.0    25.89   4.170
0056   180.0   0.0    0.0    23.47   3.388
0057   180.0   0.0    0.0    24.10   3.739
0058   180.0   0.0    0.0    23.79   3.566
0059   200.0   0.0    0.0    22.60   3.135
0060   200.0   0.0    0.0    22.79   2.925
0061   200.0   0.0    0.0    21.85   2.909
0063   225.0   0.0    0.0    21.43   2.493
0064   250.0   0.0    0.0    20.20   2.156
0065   250.0   0.0    0.0    20.54   2.257
```

EMP4 T=00004 IS ON CR LV USING 00024 BLKS R=0000

** SORTED, AVERAGED, CENTERED, FNC(R) DATA
** LVR INPUT FILE=L31JB
**VELOCITY AVERAGE FILE= L31JB:BP
** 4:22 PM TUE., 18 JAN., 1983
**
**RADIAL PROFILE X/D=50
**
**FLOW MODEL= JET   TUNNEL SPEED(%)= 40.0
**GAS= H2   NOZZLE TYPE= A100A
**REYNOLDS NU= 8500.   NOZZLE PRESS(PSIG)= 50.0
**ATM PRESS(MM HG AT OC)= 749.   NOZZLE TEMP(C)= 21.0
**ROOM TEMP(C)= 21.0
**
**LV PARAMETERS:MAXIMUM A/D VOLTAGE= 9.670
**   ACCURACY= 2
**   COMPARATOR(5/8=0,10/16=1)=1
**
**Y0(MM)= -1.20   Z0(MM)= 0.00
**

**X/D	ABS (Y-Y0) (MM)	ABS (Z-Z0) (MM)	U (M/S)	URMS (M/S)	# PTS
50.0	33.8	0.0	13.155	.7500	2
50.0	28.8	0.0	13.205	.7380	2
50.0	23.8	0.0	13.260	.9015	2
50.0	18.8	0.0	13.655	1.5405	2
50.0	16.8	0.0	15.440	3.1070	2
50.0	14.8	0.0	21.253	5.7565	4
50.0	12.8	0.0	26.370	6.5060	2
50.0	10.8	0.0	30.335	6.2770	2
50.0	8.8	0.0	34.485	6.7935	2
50.0	6.8	0.0	38.990	6.9970	2
50.0	4.8	0.0	42.785	7.2310	2
50.0	2.8	0.0	46.170	6.8770	2
50.0	.8	0.0	47.420	6.7858	5
50.0	1.2	0.0	46.207	6.5763	3
50.0	3.2	0.0	44.860	6.9145	2
50.0	5.2	0.0	41.935	7.0085	2
50.0	7.2	0.0	37.880	6.8295	2
50.0	9.2	0.0	33.735	6.7225	2
50.0	11.2	0.0	29.470	6.6685	2
50.0	13.2	0.0	26.070	6.2315	2
50.0	15.2	0.0	22.210	5.8945	2
50.0	16.2	0.0	16.200	3.3135	2
50.0	21.2	0.0	13.345	.5805	2
50.0	26.2	0.0	13.140	.2885	2
50.0	31.2	0.0	13.415	.2500	2

```
TEMP4  T=00004 IS ON CR LV   USING 00024 BLKS R=0000

0001  ** SORTED, AVERAGED, CENTERED, FNC(R) DATA
0002  ** LVR INPUT FILE=L339AC
0003  **MERGE L339A AND L339B,DELETE RANGE .NE. 5
0004  **
0005  **VELOCITY AVERAGE FILE= L339A:BP
0006  **11:14 AM  WED.,  9  MAR., 1983
0007  **
0008  **HYDROGEN/AIR FLAME
0009  **RE=8500
0010  **X/D=100
0011  **Z=0
0012  **
0013  **FLOW MODEL= JET                     TUNNEL SPEED(%)= 40.0
0014  **GAS= H2                             NOZZLE TYPE= A100A
0015  **REYNOLDS NU= 8500.                  NOZZLE PRESS(PSIG)= 50.0
0016  **ATM PRESS(MM HG AT OC)= 747.        NOZZLE TEMP(C)=  0.0
0017  **
0018  **Y0(MM)=    .80                      Z0(MM)=   0.00
0019  **
0020  **        ABS    ABS
0021  **X/D   (Y-Y0)(Z-Z0)   U     URMS   # PTS
0022  **        (MM)   (MM)  (M/S)   (M/S)
0023   100.0   50.8   0.0 12.387  .1937  3
0024   100.0   45.8   0.0 12.903  .2113  3
0025   100.0   40.3   0.0 12.337  .2560  3
0026   100.0   35.3   0.0 12.877  .4927  3
0027   100.0   32.8   0.0 12.985  .6220  2
0028   100.0   29.8   0.0 13.590 1.3905  2
0029   100.0   26.8   0.0 14.575 2.4445  2
0030   100.0   24.8   0.0 15.060 2.6407  3
0031   100.0   22.8   0.0 18.420 4.9697  3
0032   100.0   20.8   0.0 19.367 5.0017  3
0033   100.0   18.8   0.0 21.013 5.2750  3
0034   100.0   16.8   0.0 22.956 5.6024  5
0035   100.0   14.8   0.0 25.314 5.8966  5
0036   100.0   12.8   0.0 27.232 6.0790  6
0037   100.0   10.8   0.0 28.780 6.0212  5
0038   100.0    8.8   0.0 30.836 5.8444  5
0039   100.0    6.8   0.0 32.465 5.6442  6
0040   100.0    4.8   0.0 34.047 5.3918  6
0041   100.0    2.8   0.0 35.070 4.9408  6
0042   100.0     .8   0.0 35.935 4.7122 11
0043   100.0    1.2   0.0 35.515 4.5525  2
0044   100.0    3.2   0.0 34.795 4.9305  2
0045   100.0    5.2   0.0 33.405 5.4190  2
0046   100.0    7.2   0.0 32.230 5.6545  2
0047   100.0    9.2   0.0 30.890 5.9150  2
0048   100.0   11.2   0.0 28.565 5.9945  2
0049   100.0   13.2   0.0 27.495 6.2205  2
0050   100.0   15.2   0.0 25.045 6.0305  2
0051   100.0   17.2   0.0 23.020 5.8460  3
0052   100.0   19.2   0.0 21.870 6.0390  2
0053   100.0   21.2   0.0 20.830 6.1575  2
0054   100.0   23.2   0.0 15.970 2.9995  2
0055   100.0   25.2   0.0 15.190 2.7125  2
0056   100.0   27.2   0.0 14.540 2.4025  2
0057   100.0   29.2   0.0 13.925 2.1160  2
0058   100.0   31.2   0.0 13.635 1.9400  2
0059   100.0   33.2   0.0 13.695 2.0840  2
0060   100.0   35.2   0.0 13.645 2.1625  2
0061   100.0   37.2   0.0 13.635 2.2915  2
```

```
TEMP4  T=00004 IS ON CR LP   USING 00024 BLKS R=0000

** SORTED, AVERAGED, CENTERED, FNC(R) DATA
** LVR INPUT FILE=L31QBC
**VELOCITY AVERAGE FILE= L31QBC:BP
** 2:18 PM  TUE., 25  JAN., 1983
**
**H2 /AIR FLAME
**RE=8500
**X/D=200
**
**FLOW MODEL= JET                          TUNNEL SPEED(%)= 40.0
**GAS= H2                                  NOZZLE TYPE= A100A
**REYNOLDS NU= 8500.                       NOZZLE PRESS(PSIG)= 50.0
**ATM PRESS(MM HG AT OC)= 747.             NOZZLE TEMP(C)= 21.0
**ROOM TEMP(C)= 21.0
**
**LV PARAMETERS:MAXIMUM A/D VOLTAGE= 9.670
**
**Y0(MM)=    0.00                          Z0(MM)=    0.00
**
```

**X/D	ABS (Y-Y0) (MM)	ABS (Z-Z0) (MM)	U (M/S)	URMS (M/S)	# PTS
200.0	55.0	0.0	13.680	.6390	1
200.0	50.0	0.0	13.607	.4450	3
200.0	45.0	0.0	14.025	.6510	2
200.0	40.0	0.0	14.560	1.3035	2
200.0	35.0	0.0	15.155	1.6985	2
200.0	30.0	0.0	16.070	1.8445	2
200.0	25.0	0.0	16.775	2.1695	2
200.0	20.0	0.0	18.165	2.4530	2
200.0	15.0	0.0	19.350	2.7115	2
200.0	10.0	0.0	20.490	2.7075	2
200.0	5.0	0.0	21.515	2.8360	2
200.0	0.0	0.0	21.455	2.8540	2
200.0	5.0	0.0	21.145	2.7290	2
200.0	10.0	0.0	20.500	2.7865	2
200.0	15.0	0.0	19.350	2.6010	2
200.0	20.0	0.0	18.225	2.2220	2
200.0	25.0	0.0	17.290	2.2090	2
200.0	30.0	0.0	16.490	1.8110	2

**FILENAME= ZMN02A:FH:CD   CREATED 2:31 PM MON., 13 MAY , 1985
**NON-TURBULENT FLUID
**CONVENTIONAL AVERAGED
**MIXTURE FRACTION
**HYDROGEN JET FLAME   RE=8500.   X/D= 25.   CUT-OFF MF= .0004
** Y CENTER LINE POS.= -.40mm   CONV. MIX. FRACT. HALF RADIUS= 6.40mm
**

** Y ** mm	R/ R half	AVG (E-3)	RMS (E-4)	SKEW	FLAT	Z2	Z3	Z4	FILE NAME
16.0	2.563	.077	1.252	.1047	2.6539	3.6260	9.3232	36.837	M841G
14.0	2.250	.062	1.315	.0229	3.1900	5.5583	14.897	95.523	M841F
13.0	2.094	.086	1.282	.1695	2.7284	3.2368	8.2773	30.339	M841I
12.0	1.938	.102	1.250	.1704	2.6958	2.4918	5.7861	17.193	M841E
11.0	1.781	.122	1.588	-.1786	2.2251	2.6929	5.6853	15.960	M841J
10.0	1.625	.186	.520	-.3264	2.3204	1.0782	1.2273	1.4546	M841D
-12.0	1.813	.131	1.622	-.5500	1.9318	2.5427	4.5741	10.637	M841N

**FILENAME= ZMT02A:FH:CD   CREATED 2:31 PM MON., 13 MAY , 1985
**TURBULENT FLUID
**CONVENTIONAL AVERAGED
**MIXTURE FRACTION
**HYDROGEN JET FLAME   RE=8500.   X/D= 25.   CUT-OFF MF= .0004
** Y CENTER LINE POS.= -.40mm   CONV. MIX. FRACT. HALF RADIUS= 6.40mm
**

** Y ** mm	R/ R half	AVG (E-3)	RMS (E-4)	SKEW	FLAT	Z2	Z3	Z4	FILE NAME
16.0	2.563	.503	.634	.5021	1.5000	1.0159	1.0486	1.0997	M841G
14.0	2.250	3.687	53.315	1.5840	3.9797	3.0913	12.064	50.116	M841F
13.0	2.094	4.448	52.006	2.0011	7.8013	2.3673	8.3012	36.585	M841I
12.0	1.938	7.949	79.359	1.6649	6.3042	1.9967	5.6466	19.868	M841E
11.0	1.781	13.496	134.210	1.9135	8.4113	1.9890	5.8489	22.688	M841J
10.0	1.625	25.423	216.359	1.3431	5.0385	1.7243	4.0007	11.300	M841D
9.0	1.469	42.949	253.813	.9737	4.0149	1.3492	2.2487	4.3889	M841K
8.0	1.313	64.064	323.189	.8856	4.1102	1.2545	1.8772	3.2480	M841C
7.0	1.156	83.206	371.880	1.0253	4.0000	1.1998	1.6908	2.7243	M841L
6.0	1.000	104.184	418.179	.5740	2.5503	1.1611	1.5204	2.1813	M841M
4.0	.688	149.232	432.686	.2692	2.5307	1.0841	1.2588	1.5485	M841B
2.0	.375	176.458	383.774	-.0601	2.6595	1.0473	1.1413	1.2873	M841O
0.0	.063	202.567	386.595	-.2358	2.8429	1.0364	1.1076	1.2158	M841A
-8.0	1.188	78.697	355.579	1.0834	4.5677	1.2042	1.7124	2.8150	M841P
-12.0	1.813	10.568	102.274	1.7505	6.9962	1.9366	5.3963	19.102	M841N

**FILENAME= ZMA02A:FH:CD   CREATED 2:31 PM MON., 13 MAY , 1985
**AVERAGE TOTAL FLUID
**CONVENTIONAL AVERAGED
**MIXTURE FRACTION
**HYDROGEN JET FLAME   RE=8500.   X/D= 25.   CUT-OFF MF= .0004
** Y CENTER LINE POS.= -.40mm   CONV. MIX. FRACT. HALF RADIUS= 6.40mm
**

** Y ** mm	R/ R half	AVG (E-3)	RMS (E-4)	SKEW	FLAT	Z2	Z3	Z4	FILE NAME
16.0	2.563	.086	1.379	.5217	3.6987	3.5819	10.910	49.805	M841G
14.0	2.250	.226	13.673	10.198	112.91	37.755	2383.7	161848	M841F
13.0	2.094	1.072	30.754	4.5895	29.043	9.2293	134.03	2450.6	M841I
12.0	1.938	4.334	70.194	2.3350	9.4239	3.6227	18.786	121.23	M841E
11.0	1.781	10.539	130.807	2.0631	9.0584	2.5406	9.5670	47.524	M841J
10.0	1.625	24.759	217.282	1.3416	5.0295	1.7702	4.2174	12.231	M841D
9.0	1.469	42.949	253.813	.9737	4.0149	1.3492	2.2487	4.3889	M841K
8.0	1.313	64.064	323.189	.8856	4.1102	1.2545	1.8772	3.2480	M841C
7.0	1.156	83.206	371.880	1.0253	4.0000	1.1998	1.6908	2.7243	M841L
6.0	1.000	104.184	418.179	.5740	2.5503	1.1611	1.5204	2.1813	M841M
4.0	.688	149.232	432.686	.2692	2.5307	1.0841	1.2588	1.5485	M841B
2.0	.375	176.458	383.774	-.0601	2.6595	1.0473	1.1413	1.2873	M841O
-8.0	1.188	78.697	355.579	1.0834	4.5677	1.2042	1.7124	2.8150	M841P
-12.0	1.813	9.263	101.707	1.8092	7.2274	2.2055	7.0110	28.314	M841N

**FILENAME= ZMN05A:FH:CD CREATED 2:36 PM MON., 13 MAY , 1985
**NON-TURBULENT FLUID
**CONVENTIONAL AVERAGED
**MIXTURE FRACTION
**HYDROGEN JET FLAME RE=8500. X/D= 50. CUT-OFF MF= .0004
** Y CENTER LINE POS.= -.80mm CONV. MIX. FRACT. HALF RADIUS= 10.90mm
**

** Y ** mm	R/ R half	AVG (E-3)	RMS (E-4)	SKEW	FLAT	Z2	Z3	Z4	FILE NAME
12.0	1.174	.128	.487	.0282	1.7925	1.1450	1.4366	1.9140	M9T1B
14.0	1.358	.115	1.351	-.3234	2.5195	2.3778	4.6104	11.957	M9T1E
16.0	1.541	.115	1.338	-.0155	2.5485	2.3647	5.0693	13.835	M9T1G
18.0	1.725	.033	1.336	.4753	3.2144	17.772	83.967	1136.5	M9U1B
20.0	1.908	.029	1.301	.3784	3.0011	20.955	94.599	1450.8	M9V1B
-15.0	1.303	.275	.350	-.0000	1.0000	1.0162	1.0486	1.0975	M9V1H

**FILENAME= ZMT05A:FH:CD CREATED 2:36 PM MON., 13 MAY , 1985
**TURBULENT FLUID
**CONVENTIONAL AVERAGED
**MIXTURE FRACTION
**HYDROGEN JET FLAME RE=8500. X/D= 50. CUT-OFF MF= .0004
** Y CENTER LINE POS.= -.80mm CONV. MIX. FRACT. HALF RADIUS= 10.90mm
**

** Y ** mm	R/ R half	AVG (E-3)	RMS (E-4)	SKEW	FLAT	Z2	Z3	Z4	FILE NAME
10.0	.991	56.846	231.302	.4324	3.0124	1.1656	1.5258	2.1925	M9Q1B
12.0	1.174	40.352	211.053	.6036	3.3347	1.2736	1.9070	3.2364	M9T1B
14.0	1.358	26.570	171.844	.7218	3.5443	1.4183	2.4501	4.9109	M9T1E
16.0	1.541	17.074	137.819	.9867	3.8302	1.6516	3.4737	8.6114	M9T1G
18.0	1.725	11.673	104.483	1.2099	4.3823	1.8012	4.2715	12.091	M9U1B
20.0	1.908	8.750	87.228	1.6017	6.1487	1.9938	5.5684	19.383	M9V1B
8.0	.807	73.098	240.987	.3922	2.9872	1.1087	1.3401	1.7436	M9V1F
-15.0	1.303	30.139	188.482	.8560	3.9045	1.3911	2.3827	4.7812	M9V1H
0.0	.073	109.864	198.075	.2680	3.2005	1.0325	1.0991	1.2047	M9V1I

**FILENAME= ZMA05A:FH:CD CREATED 2:36 PM MON., 13 MAY , 1985
**AVERAGE TOTAL FLUID
**CONVENTIONAL AVERAGED
**MIXTURE FRACTION
**HYDROGEN JET FLAME RE=8500. X/D= 50. CUT-OFF MF= .0004
** Y CENTER LINE POS.= -.80mm CONV. MIX. FRACT. HALF RADIUS= 10.90mm
**

** Y ** mm	R/ R half	AVG (E-3)	RMS (E-4)	SKEW	FLAT	Z2	Z3	Z4	FILE NAME
10.0	.991	56.846	231.302	.4324	3.0124	1.1656	1.5258	2.1925	M9Q1B
12.0	1.174	40.251	211.744	.5933	3.3268	1.2767	1.9166	3.2607	M9T1B
14.0	1.358	25.788	175.115	.6941	3.4557	1.4611	2.6006	5.3706	M9T1E
16.0	1.541	14.657	140.720	1.0657	3.8768	1.9218	4.7084	13.596	M9T1G
18.0	1.725	6.402	96.599	1.8445	6.3882	3.2768	14.167	73.125	M9U1B
20.0	1.908	2.029	55.587	3.8362	20.867	8.5072	102.42	1537.7	M9V1B
8.0	.807	73.098	240.987	.3922	2.9872	1.1087	1.3401	1.7436	M9V1F
-15.0	1.303	29.840	189.877	.8371	3.8655	1.4049	2.4304	4.9258	M9V1H
0.0	.073	109.864	198.075	.2680	3.2005	1.0325	1.0991	1.2047	M9V1I

**FILENAME= ZMN10A:FH:CD   CREATED 2:46 PM MON., 13 MAY , 1985
**NON-TURBULENT FLUID
**CONVENTIONAL AVERAGED
**MIXTURE FRACTION
**HYDROGEN JET FLAME   RE=8500.   X/D=100.   CUT-OFF MF= .0004
** Y CENTER LINE POS.= -.20mm   CONV. MIX. FRACT. HALF RADIUS= 15.40mm
**

** Y ** mm	R/ R half	AVG (E-3)	RMS (E-4)	SKEW	FLAT	Z2	Z3	Z4	FILE NAME
32.0	2.091	-.044	.939	.3691	3.4964	5.6069	11.170	88.245	M7V1G
30.0	1.961	-.028	.927	.3560	3.7762	11.980	20.986	470.33	M7V1H
28.0	1.831	-.028	.902	.1914	2.9950	11.084	25.122	341.56	M7V1F
26.0	1.701	.018	1.160	.5455	3.4132	41.411	262.36	6378.0	M7V1I
24.0	1.571	.038	1.259	.8836	3.0331	11.737	64.298	539.45	M7V1J
22.0	1.442	.072	1.256	.1811	2.8161	4.0196	11.009	48.595	M7V1K
20.0	1.312	.089	1.385	.4928	2.1949	3.4454	10.220	36.336	M7V1L
18.0	1.182	.035	.550	-.0000	1.0000	3.4694	8.4082	21.914	M7V1N
16.0	1.052	.210	1.221	-1.108	2.2980	1.3379	1.7959	2.4188	M7V1O
-22.0	1.416	.130	1.573	.0476	1.5332	2.4642	5.4771	13.410	M7V1T
-26.0	1.675	.083	1.206	.0613	3.5258	3.1100	7.5178	30.108	M7V1U

**FILENAME= ZMT10A:FH:CD   CREATED 2:46 PM MON., 13 MAY , 1985
**TURBULENT FLUID
**CONVENTIONAL AVERAGED
**MIXTURE FRACTION
**HYDROGEN JET FLAME   RE=8500.   X/D=100.   CUT-OFF MF= .0004
** Y CENTER LINE POS.= -.20mm   CONV. MIX. FRACT. HALF RADIUS= 15.40mm
**

** Y ** mm	R/ R half	AVG (E-3)	RMS (E-4)	SKEW	FLAT	Z2	Z3	Z4	FILE NAME
32.0	2.091	7.539	58.569	1.1716	4.5265	1.6036	3.3602	8.4683	M7V1G
30.0	1.961	10.181	71.278	.3526	1.9753	1.4901	2.5914	4.8994	M7V1H
28.0	1.831	9.208	73.682	.8432	2.8943	1.6403	3.3529	7.7563	M7V1F
26.0	1.701	9.585	81.975	1.0765	3.4818	1.7314	3.8677	9.9449	M7V1I
24.0	1.571	12.602	94.084	.8873	3.5080	1.5574	3.0415	6.9115	M7V1J
22.0	1.442	14.905	97.949	.4597	2.3857	1.4319	2.4260	4.5579	M7V1K
20.0	1.312	16.748	116.697	.5793	2.7837	1.4855	2.6525	5.3531	M7V1L
18.0	1.182	22.213	135.816	.3446	2.2960	1.3738	2.2003	3.8791	M7V1N
16.0	1.052	25.577	131.064	.2509	2.8544	1.2626	1.8215	2.9073	M7V1O
12.0	.792	33.836	148.796	.0695	2.7507	1.1934	1.5861	2.2869	M7V1P
8.0	.532	43.940	122.851	-.3242	2.6087	1.0782	1.2274	1.4566	M7V1Q
4.0	.273	50.639	111.506	-.1097	2.7163	1.0485	1.1443	1.2926	M7V1R
0.0	.013	53.959	95.929	-.0442	2.5415	1.0316	1.0946	1.1912	M7V1S
-22.0	1.416	14.042	100.878	.6467	2.7802	1.5161	2.7882	5.7965	M7V1T
-26.0	1.675	11.028	77.113	.5656	2.8167	1.4889	2.6502	5.3805	M7V1U

**FILENAME= ZMA10A:FH:CD   CREATED 2:46 PM MON., 13 MAY , 1985
**AVERAGE TOTAL FLUID
**CONVENTIONAL AVERAGED
**MIXTURE FRACTION
**HYDROGEN JET FLAME   RE=8500.   X/D=100.   CUT-OFF MF= .0004
** Y CENTER LINE POS.= -.20mm   CONV. MIX. FRACT. HALF RADIUS= 15.40mm
**

** Y ** mm	R/ R half	AVG (E-3)	RMS (E-4)	SKEW	FLAT	Z2	Z3	Z4	FILE NAME
32.0	2.091	1.435	39.650	3.3705	15.897	8.6362	95.031	1258.3	M7V1G
30.0	1.961	2.626	57.679	2.2450	6.9898	5.8230	39.248	287.64	M7V1H
28.0	1.831	4.509	69.279	1.6393	4.9031	3.3608	14.028	66.276	M7V1F
26.0	1.701	6.045	79.796	1.5155	4.6778	2.7423	9.7122	39.594	M7V1I
24.0	1.571	10.215	97.977	.9811	3.5266	1.9200	4.6258	12.968	M7V1J
22.0	1.442	12.606	104.827	.5462	2.3465	1.6915	3.3886	7.5275	M7V1K
20.0	1.312	15.582	120.299	.5976	2.7252	1.5961	3.0632	6.6445	M7V1L
18.0	1.182	21.991	136.926	.3390	2.2895	1.3877	2.2449	3.9975	M7V1N
12.0	.792	33.836	148.796	.0695	2.7507	1.1934	1.5861	2.2869	M7V1P
8.0	.532	43.940	122.851	-.3242	2.6087	1.0782	1.2274	1.4566	M7V1Q
4.0	.273	50.639	111.506	-.1097	2.7163	1.0485	1.1443	1.2926	M7V1R
0.0	.013	53.959	95.929	-.0442	2.5415	1.0316	1.0946	1.1912	M7V1S
-22.0	1.416	13.277	103.066	.6608	2.7569	1.6026	3.1171	6.8538	M7V1T
-26.0	1.675	6.515	79.986	1.1134	3.3779	2.5075	7.5831	25.963	M7V1U

**FILENAME= ZMN15A:FH:CD CREATED 2:50 PM MON., 13 MAY , 1985
**NON-TURBULENT FLUID
**CONVENTIONAL AVERAGED
**MIXTURE FRACTION
**HYDROGEN JET FLAME RE=8500. X/D=150. CUT-OFF MF= .0004
** Y CENTER LINE POS.= 1.50mm CONV. MIX. FRACT. HALF RADIUS= 19.50mm
**

** Y ** mm	R/ R half	AVG (E-3)	RMS (E-4)	SKEW	FLAT	Z2	Z3	Z4	FILE NAME
34.0	1.667	.037	1.653	-.0793	2.9398	21.247	54.516	1298.7	M911N
30.0	1.462	.064	1.621	-.2422	3.3578	7.3452	16.164	158.77	M911M
28.0	1.359	.042	1.463	.0954	2.1408	13.321	42.090	416.44	M911L
26.0	1.256	.082	1.313	.1771	2.9962	3.5757	9.4592	39.259	M911K
24.0	1.154	.107	1.435	.0518	2.5916	2.7947	6.5086	20.613	M911J
22.0	1.051	.188	1.531	-.0564	1.2415	1.6668	2.9698	5.4303	M911I
20.0	.949	-.007	.899	-.1108	1.5000	183.00	818.99	51866.	M911H
16.0	.744	.260	1.197	-.0816	1.1734	1.2120	1.6281	2.2931	M911G
-20.0	1.103	.174	1.650	-.3246	1.7506	1.8992	3.4208	6.7036	M911O
-28.0	1.513	.121	1.635	-.3372	2.3352	2.8202	5.6325	16.345	M911P

**FILENAME= ZMT15A:FH:CD CREATED 2:50 PM MON., 13 MAY , 1985
**TURBULENT FLUID
**CONVENTIONAL AVERAGED
**MIXTURE FRACTION
**HYDROGEN JET FLAME RE=8500. X/D=150. CUT-OFF MF= .0004
** Y CENTER LINE POS.= 1.50mm CONV. MIX. FRACT. HALF RADIUS= 19.50mm
**

** Y ** mm	R/ R half	AVG (E-3)	RMS (E-4)	SKEW	FLAT	Z2	Z3	Z4	FILE NAME
34.0	1.667	8.816	76.192	1.2556	3.8693	1.7469	4.0511	10.881	M911N
30.0	1.462	10.009	74.157	.6062	2.4581	1.5490	2.8934	6.0208	M911M
28.0	1.359	10.284	85.149	1.1128	3.8920	1.6855	3.6880	9.4680	M911L
26.0	1.256	12.606	85.591	.5629	2.3794	1.4610	2.5593	4.9767	M911K
24.0	1.154	15.358	99.629	.4995	2.4797	1.4208	2.3988	4.5094	M911J
22.0	1.051	15.884	111.286	.7667	3.1092	1.4909	2.7363	5.7492	M911I
20.0	.949	16.373	100.133	.3984	2.3437	1.3740	2.2132	3.9367	M911H
16.0	.744	21.122	105.817	.0719	2.2060	1.2510	1.7620	2.6811	M911G
12.0	.538	23.901	98.459	.0457	2.1147	1.1697	1.5123	2.0919	M911F
8.0	.333	26.930	96.160	-.3134	2.5162	1.1275	1.3682	1.7488	M911E
6.0	.231	29.683	94.434	-.1488	2.8808	1.1012	1.2989	1.6176	M911D
4.0	.128	30.138	116.770	.0258	2.3950	1.1501	1.4518	1.9607	M911C
2.0	.026	31.474	101.332	-.3101	2.8000	1.1037	1.3006	1.6106	M911B
0.0	.077	29.927	97.134	-.1947	2.5320	1.1053	1.3094	1.6336	M911A
-20.0	1.103	14.632	96.923	.6303	2.8698	1.4388	2.4996	4.9181	M911O
-28.0	1.513	9.137	75.817	.8997	3.4084	1.6885	3.5793	8.8021	M911P

**FILENAME= ZMA15A:FH:CD CREATED 2:50 PM MON., 13 MAY , 1985
**AVERAGE TOTAL FLUID
**CONVENTIONAL AVERAGED
**MIXTURE FRACTION
**HYDROGEN JET FLAME RE=8500. X/D=150. CUT-OFF MF= .0004
** Y CENTER LINE POS.= 1.50mm CONV. MIX. FRACT. HALF RADIUS= 19.50mm
**

** Y ** mm	R/ R half	AVG (E-3)	RMS (E-4)	SKEW	FLAT	Z2	Z3	Z4	FILE NAME
34.0	1.667	3.806	66.198	2.1934	7.5597	4.0256	21.620	134.53	M911N
30.0	1.462	7.025	76.987	.9529	2.8712	2.2009	5.8565	17.361	M911M
28.0	1.359	7.519	85.798	1.3349	4.3923	2.3021	6.8896	24.192	M911L
26.0	1.256	9.837	91.693	.7266	2.4992	1.8689	4.1953	10.454	M911K
24.0	1.154	13.528	105.790	.5317	2.4227	1.6115	3.0888	6.5920	M911J
22.0	1.051	15.256	113.293	.7576	3.0758	1.5515	2.9647	6.4855	M911I
20.0	.949	16.117	101.403	.3875	2.3353	1.3959	2.2841	4.1272	M911H
16.0	.744	20.496	110.127	.0286	2.1976	1.2887	1.8705	2.9331	M911G
8.0	.333	26.930	96.160	-.3134	2.5162	1.1275	1.3682	1.7488	M911E
6.0	.231	29.683	94.434	-.1488	2.8808	1.1012	1.2989	1.6176	M911D
4.0	.128	30.138	116.770	.0258	2.3950	1.1501	1.4518	1.9607	M911C
2.0	.026	31.474	101.332	-.3101	2.8000	1.1037	1.3006	1.6106	M911B
0.0	.077	29.927	97.134	-.1947	2.5320	1.1053	1.3094	1.6336	M911A
-20.0	1.103	13.905	99.598	.6171	2.8158	1.5130	2.7659	5.7264	M911O
-28.0	1.513	6.793	76.279	1.1750	3.8390	2.2608	6.4459	21.321	M911P

```
**FILENAME= ZMN20A:FH:CD    CREATED  2:53 PM  MON., 13  MAY , 1985
**NON-TURBULENT FLUID
**CONVENTIONAL AVERAGED
**MIXTURE FRACTION
**HYDROGEN JET FLAME    RE=8500.   X/D=200.   CUT-OFF MF= .0004
** Y CENTER LINE POS.=   4.00mm    CONV. MIX. FRACT. HALF RADIUS= 22.80mm
**
```

** Y mm	R/ R half	AVG (E-3)	RMS (E-4)	SKEW	FLAT	Z2	Z3	Z4	FILE NAME
38.0	1.491	.057	1.452	-.0713	2.5605	7.5510	19.457	145.40	M9M1I
32.0	1.228	-.020	1.640	.7765	3.1011	70.811	-242.4	13721.	M9M1H
26.0	.965	.048	1.339	.5087	2.1036	8.8128	35.547	220.71	M9M1G
20.0	.702	.102	1.782	-.8740	2.8259	4.0715	5.5096	27.268	M9M1F
14.0	.439	.145	1.550	.0000	1.0000	2.1427	4.4281	9.1619	M9M1E
8.0	.175	.065	2.214	-.0365	1.0505	12.603	34.368	206.29	M9M1D
4.0	0.000	.092	1.575	.5565	1.8879	3.9531	12.683	46.477	M9M1C
-8.0	.526	.130	1.910	-.7057	1.5000	3.1578	5.2367	11.984	M9M1K

```
**FILENAME= ZMT20A:FH:CD    CREATED  2:53 PM  MON., 13  MAY , 1985
**TURBULENT FLUID
**CONVENTIONAL AVERAGED
**MIXTURE FRACTION
**HYDROGEN JET FLAME    RE=8500.   X/D=200.   CUT-OFF MF= .0004
** Y CENTER LINE POS.=   4.00mm    CONV. MIX. FRACT. HALF RADIUS= 22.80mm
**
```

** Y mm	R/ R half	AVG (E-3)	RMS (E-4)	SKEW	FLAT	Z2	Z3	Z4	FILE NAME
38.0	1.491	8.082	62.774	.7190	2.6970	1.6033	3.1469	6.9493	M9M1I
32.0	1.228	7.629	58.856	1.2820	4.2520	1.5952	3.3742	8.4321	M9M1H
26.0	.965	10.118	63.740	.6444	2.9770	1.3968	2.3516	4.4941	M9M1G
20.0	.702	12.144	70.845	.4365	2.4328	1.3403	2.1077	3.6705	M9M1F
14.0	.439	14.908	80.213	.2080	2.3070	1.2895	1.9008	3.0598	M9M1E
8.0	.175	15.940	83.051	.2442	2.5273	1.2715	1.8489	2.9532	M9M1D
4.0	0.000	17.784	78.188	.1254	2.2331	1.1933	1.5906	2.2859	M9M1C
0.0	.175	15.645	75.190	.2546	2.5676	1.2310	1.7212	2.6360	M9M1B
-8.0	.526	15.631	77.472	.1806	2.3097	1.2457	1.7590	2.7013	M9M1K

```
**FILENAME= ZMA20A:FH:CD    CREATED  2:53 PM  MON., 13  MAY , 1985
**AVERAGE TOTAL FLUID
**CONVENTIONAL AVERAGED
**MIXTURE FRACTION
**HYDROGEN JET FLAME    RE=8500.   X/D=200.   CUT-OFF MF= .0004
** Y CENTER LINE POS.=   4.00mm    CONV. MIX. FRACT. HALF RADIUS= 22.80mm
**
```

** Y mm	R/ R half	AVG (E-3)	RMS (E-4)	SKEW	FLAT	Z2	Z3	Z4	FILE NAME
38.0	1.491	3.909	59.161	1.5802	4.6306	3.2908	13.351	60.961	M9M1I
32.0	1.228	5.564	60.683	1.3728	4.5903	2.1896	6.3499	21.758	M9M1H
26.0	.965	9.162	67.445	.6042	2.8435	1.5419	2.8669	6.0511	M9M1G
20.0	.702	11.421	74.404	.3919	2.3875	1.4244	2.3815	4.4098	M9M1F
14.0	.439	14.761	81.152	.1932	2.3018	1.3023	1.9389	3.1522	M9M1E
8.0	.175	15.623	85.168	.2042	2.5034	1.2972	1.9247	3.1367	M9M1D
4.0	0.000	17.253	82.710	.0019	2.3340	1.2298	1.6897	2.5030	M9M1C
0.0	.175	15.645	75.190	.2546	2.5676	1.2310	1.7212	2.6360	M9M1B
-8.0	.526	15.398	79.164	.1422	2.3190	1.2643	1.8123	2.8252	M9M1K

**FILENAME= ZMN01F:FH:CD CREATED 12:19 PM THU., 2 MAY , 1985
**NON-TURBULENT FLUID
**FAVRE AVERAGED
**MIXTURE FRACTION
**HYDROGEN JET FLAME RE=8500. X/D= 10. CUT-OFF MF= .0004
** Y CENTER LINE POS.= -.50mm FAVRE MIX. FRACT. HALF RADIUS= 3.05mm
**

** Y ** mm	R/ R half	AVG (E-3)	RMS (E-4)	SKEW	FLAT	Z2	Z3	Z4	FILE NAME
7.0	2.459	.036	1.458	.2592	2.7712	17.246	66.874	904.02	M8P1F
6.5	2.295	.047	1.627	.0749	1.9081	12.766	39.637	359.24	M8P1G
6.0	2.131	.224	2.786	-1.009	1.2678	1.5082	1.6190	2.4291	M8P1E
5.5	1.967	.270	4.475	-.5443	.3099	.4815	.2318	.1116	M8P1H

**FILENAME= ZMT01F:FH:CD CREATED 12:19 PM THU., 2 MAY , 1985
**TURBULENT FLUID
**FAVRE AVERAGED
**MIXTURE FRACTION
**HYDROGEN JET FLAME RE=8500. X/D= 10. CUT-OFF MF= .0004
** Y CENTER LINE POS.= -.50mm FAVRE MIX. FRACT. HALF RADIUS= 3.05mm
**

** Y ** mm	R/ R half	AVG (E-3)	RMS (E-4)	SKEW	FLAT	Z2	Z3	Z4	FILE NAME
7.0	2.459	.998	16.617	6.8759	58.362	4.1487	41.793	593.94	M8P1F
6.5	2.295	1.387	28.459	5.8141	42.399	5.5119	64.441	979.21	M8P1G
6.0	2.131	3.428	57.247	4.3860	28.100	3.9794	30.176	318.59	M8P1E
5.5	1.967	12.591	161.488	3.1534	16.304	2.6782	12.653	81.694	M8P1H
5.0	1.803	43.524	312.292	1.6688	6.1466	1.5148	3.1609	8.1838	M8P1D
4.5	1.639	78.641	477.942	1.4128	5.3527	1.3694	2.4252	5.2150	M8P1I
4.0	1.475	117.025	628.536	1.3201	4.8286	1.2885	2.0700	3.9508	M8P1C
3.0	1.148	193.084	843.254	.7971	3.1301	1.1907	1.6386	2.5238	M8P1J
2.0	.820	310.679	1132.44	.1507	2.4074	1.1329	1.4059	1.8689	M8P1B
0.0	.164	461.106	852.896	-.2871	2.6208	1.0342	1.1008	1.2011	M8P1A
-4.0	1.148	196.590	786.928	.6459	3.3818	1.1602	1.5221	2.2139	M8P1K

**FILENAME= ZMA01F:FH:CD CREATED 12:19 PM THU., 2 MAY , 1985
**AVERAGE TOTAL FLUID
**FAVRE AVERAGED
**MIXTURE FRACTION
**HYDROGEN JET FLAME RE=8500. X/D= 10. CUT-OFF MF= .0004
** Y CENTER LINE POS.= -.50mm FAVRE MIX. FRACT. HALF RADIUS= 3.05mm
**

** Y ** mm	R/ R half	AVG (E-3)	RMS (E-4)	SKEW	FLAT	Z2	Z3	Z4	FILE NAME
7.0	2.459	.173	7.593	12.796	239.96	20.318	1145.5	94018.	M8P1F
6.5	2.295	.623	20.467	7.6866	78.928	11.779	305.36	10324.	M8P1G
6.0	2.131	2.932	55.626	4.2420	28.152	4.5982	40.748	502.89	M8P1E
5.5	1.967	12.467	162.757	3.0524	15.750	2.7044	12.904	84.147	M8P1H
5.0	1.803	43.524	312.292	1.6688	6.1466	1.5148	3.1609	8.1838	M8P1D
4.5	1.639	78.641	477.942	1.4128	5.3527	1.3694	2.4252	5.2150	M8P1I
4.0	1.475	117.025	628.536	1.3201	4.8286	1.2885	2.0700	3.9508	M8P1C
3.0	1.148	193.084	843.254	.7971	3.1301	1.1907	1.6386	2.5238	M8P1J
2.0	.820	310.679	1132.44	.1507	2.4074	1.1329	1.4059	1.8689	M8P1B
0.0	.164	461.106	852.896	-.2871	2.6208	1.0342	1.1008	1.2011	M8P1A
-4.0	1.148	196.590	786.928	.6459	3.3818	1.1602	1.5221	2.2139	M8P1K

**FILENAME= ZMN02F:FH:CD CREATED 2:44 PM THU., 2 MAY , 1985
**NON-TURBULENT FLUID
**FAVRE AVERAGED
**MIXTURE FRACTION
**HYDROGEN JET FLAME RE=8500. X/D= 25. CUT-OFF MF= .0004
** Y CENTER LINE POS.= -.40mm FAVRE MIX. FRACT. HALF RADIUS= 6.40mm
**

** Y ** mm	R/ R half	AVG (E-3)	RMS (E-4)	SKEW	FLAT	Z2	Z3	Z4	FILE NAME
16.0	2.563	.077	1.252	.1069	2.6529	3.6298	9.3452	36.948	M841G
14.0	2.250	.062	1.322	.0015	3.1535	5.5779	14.761	95.044	M841F
13.0	2.094	.095	1.351	-.0623	2.4053	2.9242	6.7061	22.167	M841I
12.0	1.938	.148	1.616	-.6856	1.7389	1.7250	2.7492	5.6646	M841E
11.0	1.781	.251	2.984	-1.012	1.2282	1.3162	1.3410	1.8349	M841J
10.0	1.625	.768	11.857	-.4985	.2505	.2617	.0723	.0208	M841D
-12.0	1.813	.292	3.518	-1.051	1.1856	1.1536	.9242	.9646	M841N

**FILENAME= ZMT02F:FH:CD CREATED 2:44 PM THU., 2 MAY , 1985
**TURBULENT FLUID
**FAVRE AVERAGED
**MIXTURE FRACTION
**HYDROGEN JET FLAME RE=8500. X/D= 25. CUT-OFF MF= .0004
** Y CENTER LINE POS.= -.40mm FAVRE MIX. FRACT. HALF RADIUS= 6.40mm
**

** Y ** mm	R/ R half	AVG (E-3)	RMS (E-4)	SKEW	FLAT	Z2	Z3	Z4	FILE NAME
16.0	2.563	.505	.636	.4129	1.4408	1.0118	1.0403	1.0866	M841G
14.0	2.250	1.104	25.526	4.9271	27.085	6.6350	78.574	1052.7	M841F
13.0	2.094	1.411	27.134	4.9285	32.844	5.0943	47.970	614.41	M841I
12.0	1.938	2.577	46.237	4.2221	24.133	4.6215	35.843	369.08	M841E
11.0	1.781	4.660	84.770	4.1115	24.745	4.6214	36.295	391.65	M841J
10.0	1.625	14.611	182.408	2.2363	8.5769	2.6429	10.195	48.842	M841D
9.0	1.469	35.465	263.313	.9169	3.8335	1.5513	3.0290	6.9736	M841K
8.0	1.313	60.470	326.453	.8075	3.9362	1.2915	2.0014	3.5913	M841C
7.0	1.156	81.419	364.504	1.0068	4.0086	1.2004	1.6916	2.7249	M841L
6.0	1.000	102.390	411.889	.6056	2.6425	1.1618	1.5249	2.1978	M841M
4.0	.688	147.752	427.813	.2811	2.5424	1.0838	1.2583	1.5482	M841B
2.0	.375	174.965	384.672	-.0369	2.6674	1.0483	1.1446	1.2947	M841O
0.0	.063	200.933	385.058	-.2385	2.8433	1.0367	1.1085	1.2175	M841A
-8.0	1.188	77.242	348.517	1.0693	4.5763	1.2036	1.7090	2.8041	M841P
-12.0	1.813	4.711	69.203	3.4454	18.070	3.3428	18.766	142.34	M841N

**FILENAME= ZMA02F:FH:CD CREATED 2:44 PM THU., 2 MAY , 1985
**AVERAGE TOTAL FLUID
**FAVRE AVERAGED
**MIXTURE FRACTION
**HYDROGEN JET FLAME RE=8500. X/D= 25. CUT-OFF MF= .0004
** Y CENTER LINE POS.= -.40mm FAVRE MIX. FRACT. HALF RADIUS= 6.40mm
**

** Y ** mm	R/ R half	AVG (E-3)	RMS (E-4)	SKEW	FLAT	Z2	Z3	Z4	FILE NAME
16.0	2.563	.086	1.379	.5237	3.6976	3.5845	10.929	49.910	M841G
14.0	2.250	.109	6.115	20.365	490.48	32.569	3708.2	503484	M841F
13.0	2.094	.392	14.692	8.7814	108.24	15.033	504.76	23249.	M841I
12.0	1.938	1.458	38.008	4.8192	33.778	7.7957	106.76	1943.2	M841E
11.0	1.781	3.685	80.384	4.0373	25.755	5.7576	57.169	780.10	M841J
10.0	1.625	14.247	186.122	2.0579	7.9022	2.7067	10.708	52.611	M841D
9.0	1.469	35.465	263.313	.9169	3.8335	1.5513	3.0290	6.9736	M841K
8.0	1.313	60.470	326.453	.8075	3.9362	1.2915	2.0014	3.5913	M841C
7.0	1.156	81.419	364.504	1.0068	4.0086	1.2004	1.6916	2.7249	M841L
6.0	1.000	102.390	411.889	.6056	2.6425	1.1618	1.5249	2.1978	M841M
4.0	.688	147.752	427.813	.2811	2.5424	1.0838	1.2583	1.5482	M841B
2.0	.375	174.965	384.672	-.0369	2.6674	1.0483	1.1446	1.2947	M841O
0.0	.063	200.933	385.058	-.2385	2.8433	1.0367	1.1085	1.2175	M841A
-12.0	1.813	4.159	69.014	3.1959	17.026	3.7542	23.870	205.10	M841N

**FILENAME= ZMN05F:FH:CD   CREATED 1:03 PM THU., 2 MAY , 1985
**NON-TURBULENT FLUID
**FAVRE AVERAGED
**MIXTURE FRACTION
**HYDROGEN JET FLAME   RE=8500.   X/D= 50.   CUT-OFF MF= .0004
** Y CENTER LINE POS.= -.80mm   FAVRE MIX. FRACT. HALF RADIUS= 10.70mm
**

** Y ** mm	R/ R half	AVG (E-3)	RMS (E-4)	SKEW	FLAT	Z2	Z3	Z4	FILE NAME
12.0	1.196	.952	22.480	-.3690	.1366	.1542	.0261	.0047	M9T1B
14.0	1.383	.546	9.991	-.5143	.2820	.5017	.2020	.1101	M9T1E
16.0	1.570	.293	3.635	-.8506	.8097	.9242	.7656	.8144	M9T1G
18.0	1.757	.047	1.671	.0673	1.9122	13.026	40.650	390.09	M9U1B
20.0	1.944	.033	1.394	.2552	2.5580	18.360	71.943	965.28	M9V1B
-15.0	1.327	1.524	29.486	-.4245	.1804	.1827	.0339	.0064	M9V1H

**FILENAME= ZMT05F:FH:CD   CREATED 1:03 PM THU., 2 MAY , 1985
**TURBULENT FLUID
**FAVRE AVERAGED
**MIXTURE FRACTION
**HYDROGEN JET FLAME   RE=8500.   X/D= 50.   CUT-OFF MF= .0004
** Y CENTER LINE POS.= -.80mm   FAVRE MIX. FRACT. HALF RADIUS= 10.70mm
**

** Y ** mm	R/ R half	AVG (E-3)	RMS (E-4)	SKEW	FLAT	Z2	Z3	Z4	FILE NAME
10.0	1.009	54.376	238.472	.3543	2.9617	1.1923	1.6069	2.3831	M9Q1B
12.0	1.196	33.456	222.285	.6779	3.1752	1.4575	2.5553	5.1109	M9T1B
14.0	1.383	15.752	159.005	1.6064	5.2855	2.1360	5.9433	19.562	M9T1E
16.0	1.570	6.944	99.383	2.7752	10.929	3.3159	15.814	92.479	M9T1G
18.0	1.757	3.266	60.527	3.8643	19.240	4.9033	36.845	348.46	M9U1B
20.0	1.944	2.140	44.506	4.6458	28.989	5.8476	56.797	737.72	M9V1B
8.0	.822	71.575	240.860	.3478	3.0446	1.1132	1.3530	1.7715	M9V1F
-15.0	1.327	20.002	183.151	1.3417	4.7949	1.8845	4.6376	13.660	M9V1H
0.0	.075	108.535	194.458	.2730	3.2786	1.0321	1.0979	1.2023	M9V1I

**FILENAME= ZMA05F:FH:CD   CREATED 1:03 PM THU., 2 MAY , 1985
**AVERAGE TOTAL FLUID
**FAVRE AVERAGED
**MIXTURE FRACTION
**HYDROGEN JET FLAME   RE=8500.   X/D= 50.   CUT-OFF MF= .0004
** Y CENTER LINE POS.= -.80mm   FAVRE MIX. FRACT. HALF RADIUS= 10.70mm
**

** Y ** mm	R/ R half	AVG (E-3)	RMS (E-4)	SKEW	FLAT	Z2	Z3	Z4	FILE NAME
10.0	1.009	54.376	238.472	.3543	2.9617	1.1923	1.6069	2.3831	M9Q1B
12.0	1.196	33.375	226.602	.5900	3.0280	1.4610	2.5676	5.1480	M9T1B
14.0	1.383	15.302	167.382	1.3002	4.4215	2.1965	6.2909	21.314	M9T1E
16.0	1.570	5.997	100.583	2.4623	9.8863	3.8135	21.060	142.62	M9T1G
18.0	1.757	1.808	50.356	4.3755	26.653	8.7549	118.75	2028.3	M9U1B
20.0	1.944	.516	24.271	8.2819	94.952	23.088	927.04	49901.	M9V1B
8.0	.822	71.575	240.860	.3478	3.0446	1.1132	1.3530	1.7715	M9V1F
-15.0	1.327	19.817	188.069	1.1920	4.3832	1.9007	4.7209	14.035	M9V1H
0.0	.075	108.535	194.458	.2730	3.2786	1.0321	1.0979	1.2023	M9V1I

**FILENAME= ZMN10F:FH:CD CREATED 2:48 PM THU., 2 MAY , 1985
**NON-TURBULENT FLUID
**FAVRE AVERAGED
**MIXTURE FRACTION
**HYDROGEN JET FLAME RE=8500. X/D=100. CUT-OFF MF= .0004
** Y CENTER LINE POS.= -.20mm FAVRE MIX. FRACT. HALF RADIUS= 12.90mm
**

** Y ** mm	R/ R half	AVG (E-3)	RMS (E-4)	SKEW	FLAT	Z2	Z3	Z4	FILE NAME
32.0	2.496	-.050	.998	.5080	3.0931	4.7819	8.5386	55.950	M7V1G
30.0	2.341	-.035	1.015	.4724	3.1536	9.2656	14.346	231.30	M7V1H
28.0	2.186	-.042	1.099	.5095	2.1248	7.2957	11.401	101.33	M7V1F
26.0	2.031	.026	1.488	.1903	1.9317	31.928	128.30	2254.9	M7V1I
24.0	1.876	.083	2.038	-.1570	.8544	5.7223	14.170	55.559	M7V1J
22.0	1.721	.190	2.847	-.8161	.8483	1.5308	1.5612	2.6219	M7V1K
20.0	1.566	.268	4.124	-.7024	.5311	1.1328	1.0792	1.2500	M7V1L
18.0	1.411	.176	3.270	-.5420	.3098	.6749	.3264	.1690	M7V1N
16.0	1.256	1.066	19.654	-.4558	.2127	.2639	.0699	.0186	M7V1O
-22.0	1.690	.364	4.950	-.7647	.6137	.8808	.6886	.5980	M7V1T
-26.0	2.000	.136	1.697	-.8150	1.9575	1.9008	2.7735	6.7962	M7V1U

**FILENAME= ZMT10F:FH:CD CREATED 2:48 PM THU., 2 MAY , 1985
**TURBULENT FLUID
**FAVRE AVERAGED
**MIXTURE FRACTION
**HYDROGEN JET FLAME RE=8500. X/D=100. CUT-OFF MF= .0004
** Y CENTER LINE POS.= -.20mm FAVRE MIX. FRACT. HALF RADIUS= 12.90mm
**

** Y ** mm	R/ R half	AVG (E-3)	RMS (E-4)	SKEW	FLAT	Z2	Z3	Z4	FILE NAME
32.0	2.496	2.030	35.114	3.7196	17.589	4.5799	30.412	255.31	M7V1G
30.0	2.341	2.369	45.095	3.2854	12.257	5.2310	35.746	276.14	M7V1H
28.0	2.186	2.803	45.359	3.2991	13.538	4.0942	23.785	166.86	M7V1F
26.0	2.031	3.305	50.490	3.4340	14.860	3.7381	21.055	146.14	M7V1I
24.0	1.876	5.263	68.054	2.7250	10.211	2.9899	12.541	64.087	M7V1J
22.0	1.721	6.611	77.759	2.2856	7.0159	2.6979	9.4984	38.548	M7V1K
20.0	1.566	8.380	96.108	1.9412	6.1840	2.4829	8.2095	31.806	M7V1L
18.0	1.411	14.031	130.935	1.0991	3.3267	1.9090	4.5821	12.435	M7V1N
16.0	1.256	17.824	135.170	.9419	3.1942	1.6596	3.3051	7.4040	M7V1O
12.0	.946	28.736	165.867	.1764	2.3104	1.3332	2.0334	3.3912	M7V1P
8.0	.636	42.820	128.757	-.3716	2.6218	1.0904	1.2611	1.5235	M7V1Q
4.0	.326	50.110	112.351	-.1252	2.7797	1.0503	1.1494	1.3030	M7V1R
0.0	.016	53.593	96.084	-.0225	2.5616	1.0321	1.0963	1.1950	M7V1S
-22.0	1.690	7.435	81.902	1.8475	5.9727	2.3280	7.3391	27.298	M7V1T
-26.0	2.000	3.548	54.097	2.8139	10.059	3.7878	18.875	110.60	M7V1U

**FILENAME= ZMA10F:FH:CD CREATED 2:48 PM THU., 2 MAY , 1985
**AVERAGE TOTAL FLUID
**FAVRE AVERAGED
**MIXTURE FRACTION
**HYDROGEN JET FLAME RE=8500. X/D=100. CUT-OFF MF= .0004
** Y CENTER LINE POS.= -.20mm FAVRE MIX. FRACT. HALF RADIUS= 12.90mm
**

** Y ** mm	R/ R half	AVG (E-3)	RMS (E-4)	SKEW	FLAT	Z2	Z3	Z4	FILE NAME
32.0	2.496	.355	18.875	6.8024	61.232	29.235	1106.3	53070.	M7V1G
30.0	2.341	.590	27.006	5.6080	37.326	21.941	601.23	18645.	M7V1H
28.0	2.186	1.355	37.380	3.7917	19.616	8.6050	103.33	1499.2	M7V1F
26.0	2.031	2.092	46.210	3.4014	16.556	5.8799	52.307	573.60	M7V1I
24.0	1.876	4.279	69.848	2.2790	8.7597	3.6646	18.906	118.83	M7V1J
22.0	1.721	5.616	82.529	1.7693	5.6047	3.1597	13.094	62.561	M7V1K
20.0	1.566	7.812	100.564	1.6184	5.2487	2.6571	9.4235	39.163	M7V1L
18.0	1.411	13.892	133.813	.9958	3.1169	1.9278	4.6734	12.809	M7V1N
16.0	1.256	17.488	145.199	.6305	2.6287	1.6893	3.4288	7.8284	M7V1O
8.0	.636	42.820	128.757	-.3716	2.6218	1.0904	1.2611	1.5235	M7V1Q
4.0	.326	50.110	112.351	-.1252	2.7797	1.0503	1.1494	1.3030	M7V1R
0.0	.016	53.593	96.084	-.0225	2.5616	1.0321	1.0963	1.1950	M7V1S
-22.0	1.690	7.046	84.835	1.6040	5.2752	2.4496	8.1484	31.981	M7V1T
-26.0	2.000	2.141	48.424	2.9497	12.302	6.1161	50.482	490.23	M7V1U

**FILENAME= ZMN15F:FH:CD CREATED 2:52 PM THU., 2 MAY , 1985
**NON-TURBULENT FLUID
**FAVRE AVERAGED
**MIXTURE FRACTION
**HYDROGEN JET FLAME RE=8500. X/D=150. CUT-OFF MF= .0004
** Y CENTER LINE POS.= 1.50mm FAVRE MIX. FRACT. HALF RADIUS= 14.60mm
**

** Y ** mm	R/ R half	AVG (E-3)	RMS (E-4)	SKEW	FLAT	Z2	Z3	Z4	FILE NAME
34.0	2.226	.048	1.932	-.2671	2.1716	16.843	31.465	598.27	M911N
30.0	1.952	.112	2.288	-.7802	1.9534	4.3485	5.2217	30.958	M911M
28.0	1.815	.077	2.065	-.4322	1.1360	7.3826	12.565	68.075	M911L
26.0	1.678	.176	2.425	-.8513	1.1335	1.6663	2.0014	3.8734	M911K
24.0	1.541	.302	4.134	-.7970	.7107	.9889	.8041	.9015	M911J
22.0	1.404	.639	8.863	-.6162	.3999	.4876	.2541	.1360	M911I
20.0	1.267	-.026	1.837	.2545	.3856	48.181	55.025	902.73	M911H
16.0	.993	1.167	19.477	-.4826	.2365	.2692	.0804	.0252	M911G
-20.0	1.473	.557	7.538	-.6792	.4967	.5930	.3330	.2037	M911O
-28.0	2.021	.213	2.528	-1.086	1.6179	1.6078	1.8133	2.9946	M911P

**FILENAME= ZMT15F:FH:CD CREATED 2:52 PM THU., 2 MAY , 1985
**TURBULENT FLUID
**FAVRE AVERAGED
**MIXTURE FRACTION
**HYDROGEN JET FLAME RE=8500. X/D=150. CUT-OFF MF= .0004
** Y CENTER LINE POS.= 1.50mm FAVRE MIX. FRACT. HALF RADIUS= 14.60mm
**

** Y ** mm	R/ R half	AVG (E-3)	RMS (E-4)	SKEW	FLAT	Z2	Z3	Z4	FILE NAME
34.0	2.226	2.710	43.982	3.8087	18.126	4.1245	26.160	209.10	M911N
30.0	1.952	3.865	52.210	2.6286	8.9461	3.1778	13.662	68.741	M911M
28.0	1.815	3.982	55.167	3.0425	12.611	3.2468	15.504	92.337	M911L
26.0	1.678	5.256	63.542	2.5208	8.1058	2.8125	10.541	45.956	M911K
24.0	1.541	7.213	79.101	2.1388	6.6023	2.4604	7.9448	29.825	M911J
22.0	1.404	8.676	90.374	1.8280	6.1905	2.1866	6.5240	23.365	M911I
20.0	1.267	10.212	90.504	1.2269	3.7900	1.8333	4.3060	11.609	M911H
16.0	.993	14.004	104.570	1.0143	3.0291	1.6663	3.3126	7.3027	M911G
12.0	.719	20.672	101.502	.3811	2.1292	1.2411	1.7684	2.7507	M911F
8.0	.445	23.695	107.249	-.0844	2.0939	1.2049	1.6068	2.2858	M911E
6.0	.308	27.398	103.638	-.1199	2.5316	1.1431	1.4228	1.8844	M911D
4.0	.171	27.007	122.373	.2149	2.1997	1.2053	1.6359	2.4045	M911C
2.0	.034	29.029	111.542	-.2005	2.3414	1.1476	1.4316	1.8914	M911B
0.0	.103	27.654	105.225	-.0733	2.2407	1.1448	1.4303	1.8995	M911A
-20.0	1.473	8.141	80.334	1.7038	5.5343	2.0923	5.7955	18.994	M911O
-28.0	2.021	3.602	51.155	2.7019	10.309	3.2957	15.344	86.799	M911P

**FILENAME= ZMA15F:FH:CD CREATED 2:52 PM THU., 2 MAY , 1985
**AVERAGE TOTAL FLUID
**FAVRE AVERAGED
**MIXTURE FRACTION
**HYDROGEN JET FLAME RE=8500. X/D=150. CUT-OFF MF= .0004
** Y CENTER LINE POS.= 1.50mm FAVRE MIX. FRACT. HALF RADIUS= 14.60mm
**

** Y ** mm	R/ R half	AVG (E-3)	RMS (E-4)	SKEW	FLAT	Z2	Z3	Z4	FILE NAME
34.0	2.226	1.191	34.072	4.5606	28.810	9.1863	132.38	2408.1	M911N
30.0	1.952	2.739	50.731	2.4508	9.0772	4.4311	26.869	190.75	M911M
28.0	1.815	2.927	53.870	2.7800	12.217	4.3864	28.483	230.72	M911L
26.0	1.678	4.133	65.914	2.0352	6.8538	3.5439	16.889	93.646	M911K
24.0	1.541	6.383	84.794	1.6177	5.1468	2.7646	10.085	42.781	M911J
22.0	1.404	8.355	93.926	1.5643	5.3927	2.2639	7.0142	26.087	M911I
20.0	1.267	10.052	93.363	1.0692	3.4562	1.8626	4.4444	12.173	M911H
16.0	.993	13.619	114.682	.6133	2.3864	1.7091	3.4935	7.9195	M911G
12.0	.719	20.672	101.502	.3811	2.1292	1.2411	1.7684	2.7507	M911F
6.0	.308	27.398	103.638	-.1199	2.5316	1.1431	1.4228	1.8844	M911D
4.0	.171	27.007	122.373	.2149	2.1997	1.2053	1.6359	2.4045	M911C
2.0	.034	29.029	111.542	-.2005	2.3414	1.1476	1.4316	1.8914	M911B
0.0	.103	27.654	105.225	-.0733	2.2407	1.1448	1.4303	1.8995	M911A
-20.0	1.473	7.760	84.556	1.3865	4.6492	2.1873	6.3558	21.853	M911O
-28.0	2.021	2.721	49.258	2.6157	10.670	4.2764	26.341	197.25	M911P

**FILENAME= ZMN20F:FH:CD CREATED 2:56 PM THU., 2 MAY , 1985
**NON-TURBULENT FLUID
**FAVRE AVERAGED
**MIXTURE FRACTION
**HYDROGEN JET FLAME RE=8500. X/D=200. CUT-OFF MF= .0004
** Y CENTER LINE POS.= 4.00mm FAVRE MIX. FRACT. HALF RADIUS= 18.80mm
**

** Y ** mm	R/ R half	AVG (E-3)	RMS (E-4)	SKEW	FLAT	Z2	Z3	Z4	FILE NAME
38.0	1.809	.079	1.740	-.4347	1.8670	5.4906	10.168	55.046	M9M1I
32.0	1.489	-.047	2.186	.8818	2.0300	21.715	-24.22	717.60	M9M1H
26.0	1.170	.113	2.419	-.5082	.6394	3.9814	6.5445	17.231	M9M1G
20.0	.851	.301	4.747	-.9352	.9818	1.3929	.6097	1.0439	M9M1F
14.0	.532	.570	9.214	-.5728	.3441	.5458	.2867	.1508	M9M1E
8.0	.213	.218	5.489	-.6700	.4711	4.3740	3.3766	6.2842	M9M1D
4.0	0.000	.401	7.659	-.5495	.3123	.9199	.6645	.5544	M9M1C
-8.0	.638	.485	8.345	-.6614	.4723	.8984	.3898	.2426	M9M1K

**FILENAME= ZMT20F:FH:CD CREATED 2:56 PM THU., 2 MAY , 1985
**TURBULENT FLUID
**FAVRE AVERAGED
**MIXTURE FRACTION
**HYDROGEN JET FLAME RE=8500. X/D=200. CUT-OFF MF= .0004
** Y CENTER LINE POS.= 4.00mm FAVRE MIX. FRACT. HALF RADIUS= 18.80mm
**

** Y ** mm	R/ R half	AVG (E-3)	RMS (E-4)	SKEW	FLAT	Z2	Z3	Z4	FILE NAME
38.0	1.809	2.809	41.706	2.9510	10.753	3.6421	18.151	106.47	M9M1I
32.0	1.489	3.654	40.731	2.9463	11.927	2.5503	9.4220	44.098	M9M1H
26.0	1.170	5.939	53.472	1.7104	5.4749	1.9813	5.0217	14.968	M9M1G
20.0	.851	7.580	61.968	1.4713	4.3990	1.8018	4.0759	10.591	M9M1F
14.0	.532	10.468	77.628	.7936	2.8792	1.5808	3.0351	6.5572	M9M1E
8.0	.213	10.964	81.036	.8816	3.1446	1.6070	3.1162	6.8219	M9M1D
4.0	0.000	12.965	76.191	1.0811	3.1829	1.4604	2.4855	4.6744	M9M1C
0.0	.213	12.346	74.740	.5629	2.7294	1.3665	2.2243	4.0650	M9M1B
-8.0	.638	11.408	76.020	.7656	2.8610	1.4907	2.6520	5.2748	M9M1K

**FILENAME= ZMA20F:FH:CD CREATED 2:56 PM THU., 2 MAY , 1985
**AVERAGE TOTAL FLUID
**FAVRE AVERAGED
**MIXTURE FRACTION
**HYDROGEN JET FLAME RE=8500. X/D=200. CUT-OFF MF= .0004
** Y CENTER LINE POS.= 4.00mm FAVRE MIX. FRACT. HALF RADIUS= 18.80mm
**

** Y ** mm	R/ R half	AVG (E-3)	RMS (E-4)	SKEW	FLAT	Z2	Z3	Z4	FILE NAME
38.0	1.809	1.389	34.466	3.4405	15.991	7.1564	72.023	854.23	M9M1I
32.0	1.489	2.655	42.223	2.3246	9.6903	3.5290	17.935	115.54	M9M1H
26.0	1.170	5.385	58.517	1.2102	4.1164	2.1807	6.0948	20.033	M9M1G
20.0	.851	7.143	68.038	.9908	3.3473	1.9073	4.5779	12.623	M9M1F
14.0	.532	10.369	79.990	.6677	2.6736	1.5951	3.0917	6.7430	M9M1E
8.0	.213	10.749	85.894	.6375	2.7090	1.6385	3.2407	7.2364	M9M1D
4.0	0.000	12.588	89.250	.3535	2.3034	1.5027	2.6340	5.1021	M9M1C
0.0	.213	12.346	74.740	.5629	2.7294	1.3665	2.2243	4.0650	M9M1B
-8.0	.638	11.244	80.411	.5297	2.5288	1.5115	2.7281	5.5052	M9M1K

APPENDIX B-3

RECOMMENDED FORMAT FOR DATA BASE DOCUMENTATION

1. Experimental Facility
   - general description of facility
2. Experimental Configurations
   - detailed description of experimental configurations; figures
3. Test Conditions
   - identification of test conditions including table listing conditions
4. Inlet and Boundary Conditions
   - identification and explanation of inlet and boundary conditions including axial pressure gradient
5. Quantities Measured
   - delineation of quantities measured, quantities tabulated, and quantities archived on tape and or disk
   - identification of diagnostic(s) used for each measurement
6. Diagnostics
   - description of diagnostics used; figures of configuration
7. Unusual Measurement Methods
   - description of methodology used in the acquisition of data with attention to techniques unique to the present experiment
8. Experimental Protocol
   - a description of the protocol adopted in the acquisition of the data; the order in which the data were collected; the elapsed period of time
9. Quality Control
   - a delineation of steps taken to assure accuracy of the data; mass balances; repeatability tests; reproducibility tests; diagnostic(s) performance including seeding uniformity and consistency in the case of laser anemometry; steps taken to assure identical test conditions throughout the duration of the study; tests of sensitivity of experiment to boundary conditions (e.g., exhaust suction)

10. Error Analysis

- an estimate of the uncertainty (in percent) associated with each of the measurement due to uncertainty in the measurement method, flow conditions, and so forth

11. Availability of Data

- explanation of the availability of the data (report number, source, ordering information) and the media (magnetic tape, floppies) on which the data are available

12. References

- citations of (1) reports and publications referred to in item 11, and (2) references referred to in text

13. Data

- still photographs of flame for the purposes of (1) identifying the physical nature of the experiment, and (2) the time-averaged structure of the flame
- presentation of successive frames from a high speed photographic sequence for the purposes of (1) describing the dynamic behavior of the flame, and (2) providing an indication of the scales of turbulent mixing
- description of the format in which the data are presented
- tables of data

APPENDIX C

TABULATED DATA FOR CHAPTER 4

SYNGAS/AIR FLAME

AXIAL PROFILES

Velocity Centerline Y = 0 mm			Free Stream Y = -50 mm		
x/d	$\overline{u}$ (m/s)	$(u')^{1/2}$ (m/s)	x/d	$\overline{u}$ (m/s)	$(u')^{1/2}$ (m/s)
1.0	65.9	5.0	0.0	2.41	0.03
2.0	64.7	5.0	10.0	2.42	0.03
5.0	62.4	4.5	20.0	2.43	0.03
8.0	61.0	5.6	30.0	2.43	0.03
11.0	57.9	6.3	40.0	2.42	0.03
14.0	55.1	7.4	50.0	2.44	0.04
17.0	50.7	7.2	60.0	2.46	0.04
20.0	46.9	6.9	70.0	2.49	0.04
25.0	40.8	6.3	80.0	2.47	0.05
30.0	36.2	6.0	90.0	2.50	0.05
35.0	33.4	6.5	100.0	2.53	0.06
40.0	28.7	6.0			
50.0	20.8	4.7			
60.0	15.1	3.6			
70.0	12.0	2.7			
80.0	8.9	2.0			
90.0	7.7	1.6			
100.0	7.0	1.5			

Radial Profiles

Velocity

x/d = 0.3			x/d = 25			x/d = 100		
|Z|	$\overline{u}$	$\overline{(u'^2)}^{1/2}$	|Y|	$\overline{u}$	$\overline{(u'^2)}^{1/2}$	|Y|	$\overline{u}$	$\overline{(u'^2)}^{1/2}$
(mm)	(m/s)	(m/s)	(mm)	(m/s)	m/s	(mm)	(m/s)	(m/s)
0.0	66.0	5.1	39.5	2.5	.03	65.5	2.49	.04
0.2	66.8	4.7	34.5	2.5	.03	60.5	2.46	.05
0.4	67.1	4.8	29.5	2.5	.04	55.5	2.49	.07
0.6	66.2	4.6	24.5	2.5	.04	50.5	2.47	.10
0.8	64.6	4.6	19.5	2.5	.08	45.5	2.53	.22
1.0	62.5	4.9	14.5	2.6	.30	40.5	2.68	.35
1.2	60.0	5.0	11.5	4.1	1.79	35.5	3.04	.72
1.4	56.8	5.9	9.5	10.1	4.73	30.5	3.55	.89
1.6	51.3	8.2	7.5	15.2	5.42	25.5	3.99	1.02
1.8	42.0	9.1	5.5	25.6	7.79	20.5	4.92	1.22
2.0	30.0	8.0	3.5	33.8	7.04	15.5	5.71	1.36
2.2	7.0	2.5	1.5	39.7	6.26	10.5	6.46	1.46
2.4	2.6	0.52	.5	41.1	6.22	7.5	6.80	1.54
3.0	1.1	0.11	.5	40.3	6.23	5.5	7.00	1.53
3.5	1.3	0.16	1.5	38.2	6.54	3.5	7.03	1.53
4.0	1.6	0.17	2.5	37.2	7.65	1.5	7.29	1.55
5.0	2.0	0.20	3.5	33.4	7.58	.5	7.11	1.5
6.0	2.2	0.13	4.5	29.0	7.48	2.5	7.17	1.51
7.0	2.3	0.07	5.5	25.0	7.33	4.5	7.01	1.49
			6.5	20.9	6.98	6.5	6.88	1.50
			7.5	14.4	5.81	8.5	6.68	1.41
			8.5	11.4	4.80	11.5	6.29	1.45
			9.5	9.9	4.90	14.5	5.85	1.36
			10.5	5.1	2.41	17.0	5.37	1.27
			11.5	4.2	1.83	19.5	5.17	1.31
			12.5	3.4	1.32	22.5	4.56	1.15
			13.5	2.7	0.53	26.5	4.04	1.01
			14.5	2.6	0.3[illegible]	30.5	3.51	.95
			15.5	2.5	0.23			
			16.5	2.5	0.15			
			18.5	2.5	0.10			
			20.5	2.5	0.07			
			25.5	2.5	0.05			

Radial profiles

Temperature in °K

Density in kg/m^3

Composition in mole fractions: X_i

Mixture fraction: $\bar{f}$ conventional average
$\tilde{f}$ Favre average

$x/d = 10$

$\|2y/d\|$	$\tilde{f}$	$\bar{f}$	$\bar{\rho}$	$\bar{T}$	$\bar{X}_{CO_2}$	$\bar{X}_{O_2}$	$\bar{X}_{CO}$	$\bar{X}_{N_2}$	$\bar{X}_{H_2O}$	$\bar{X}_{H_2}$
0.0	0.77	0.77	0.49	521	.01	.00	.36	.37	.03	.23
0.0	0.76	0.76	0.46	548	.01	.00	.36	.37	.03	.23
0.6	0.73	0.72	0.39	718	.02	.00	.34	.39	.05	.20
0.6	0.74	0.73	0.43	634	.01	.00	.35	.38	.04	.21
1.3	0.62	0.61	0.27	1189	.04	.00	.28	.45	.09	.14
1.9	0.45	0.44	0.19	1731	.09	.01	.17	.55	.13	.05
2.5	0.27	0.28	0.22	1646	.12	.06	.05	.63	.12	.01
3.1	0.09	0.12	0.45	901	.07	.15	.01	.70	.06	.00
3.1	0.13	0.15	0.37	1066	.09	.14	.01	.68	.07	.00
3.8	0.00	0.00	0.94	337	.02	.21	.00	.76	.01	.00

$x/d = 10$

$\|2y/d\|$	f''	f'	ρ'	T'	X'_{CO_2}	X'_{O_2}	X'_{CO}	X'_{N_2}	X'_{H_2O}	X'_{H_2}
0.0	.19	.05	.10	194	.02	.00	.04	.02	.02	.03
0.0	.19	.06	.10	189	.02	.00	.03	.02	.02	.03
0.6	.23	.06	.10	266	.03	.00	.05	.03	.03	.04
0.6	.22	.06	.11	243	.03	.00	.04	.03	.03	.03
1.3	.24	.08	.07	360	.04	.00	.07	.05	.03	.05
1.9	.15	.09	.03	342	.05	.01	.08	.06	.02	.04
2.5	.05	.07	.04	275	.04	.04	.06	.04	.02	.01
3.1	.03	.07	.19	414	.03	.04	.01	.04	.03	.00
3.1	.03	.07	.15	381	.03	.04	.02	.03	.03	.00
3.8	.02	.02	.14	88	.01	.01	.00	.02	.01	.00

$x/d = 25$

$\lvert 2y/d \rvert$	$\tilde{f}$	$\overline{f}$	$\overline{\rho}$	$\overline{T}$	$\overline{X}_{CO_2}$	$\overline{X}_{O_2}$	$\overline{X}_{CO}$	$\overline{X}_{N_2}$	$\overline{X}_{H_2O}$	$\overline{X}_{H_2}$
0.0	.51	.50	.21	1457	.05	.00	.23	.51	.12	.08
1.3	.50	.49	.21	1496	.04	.01	.23	.52	.11	.08
2.5	.43	.43	.19	1633	.06	.01	.19	.57	.12	.05
2.5	.30	.31	.20	1639	.09	.04	.10	.63	.12	.02
3.8	.32	.33	.19	1683	.08	.03	.12	.62	.12	.03
5.0	.19	.22	.25	1471	.10	.08	.04	.67	.09	.01
6.3	.09	.13	.40	1042	.08	.14	.01	.70	.06	.00
7.6	.03	.06	.60	712	.05	.17	.00	.73	.04	.00
8.8	.01	.02	.80	467	.03	.19	.00	.75	.02	.00
10.1	.00	.00	1.01	320	.01	.21	.00	.76	.01	.00
11.3	.00	.00	1.06	292	.01	.21	.00	.77	.00	.00

x/d = 25

|2y/d|	f''	f'	ρ'	T'	X'_{CO_2}	X'_{O_2}	X'_{CO}	X'_{N_2}	X'_{H_2O}	X'_{H_2}
0.0	.15	.08	.03	348	.05	.01	.07	.05	.02	.04
1.3	.14	.08	.03	330	.04	.01	.07	.05	.02	.03
2.5	.14	.09	.02	320	.05	.02	.08	.06	.01	.03
2.5	.10	.11	.05	417	.05	.05	.08	.06	.02	.03
3.8	.11	.11	.04	380	.05	.04	.09	.06	.02	.03
5.0	.06	.10	.11	469	.04	.05	.06	.04	.03	.01
6.3	.04	.08	.21	482	.04	.05	.03	.04	.03	.01
7.6	.04	.07	.29	403	.04	.04	.01	.03	.03	.00
8.8	.03	.05	.28	267	.03	.03	.00	.03	.02	.00
10.1	.01	.02	.16	123	.01	.01	.00	.01	.01	.00
11.3	.01	.01	.08	59	.01	.01	.00	.01	.01	.00

x/d = 50

$\lvert 2y/d \rvert$	$\tilde{f}$	$\bar{f}$	$\bar{\rho}$	$\bar{T}$	$\bar{X}_{CO_2}$	$\bar{X}_{O_2}$	$\bar{X}_{CO}$	$\bar{X}_{N_2}$	$\bar{X}_{H_2O}$	$\bar{X}_{H_2}$
0.0	.21	.21	.20	1775	.12	.06	.02	.69	.10	.00
1.3	.20	.21	.20	1690	.11	.07	.03	.68	.10	.00
1.3	.21	.22	.19	1800	.10	.07	.04	.68	.10	.01
2.5	.19	.20	.22	1653	.11	.08	.02	.68	.10	.00
2.5	.19	.20	.21	1652	.12	.07	.01	.69	.10	.00
3.8	.18	.19	.23	1555	.11	.09	.02	.69	.09	.00
5.0	.16	.18	.25	1463	.10	.10	.02	.69	.09	.00
6.3	.14	.16	.28	1357	.10	.11	.01	.69	.08	.00
7.6	.13	.15	.31	1200	.09	.12	.01	.70	.07	.00
8.8	.10	.12	.38	1016	.07	.14	.01	.71	.06	.00
10.1	.07	.09	.46	846	.06	.16	.01	.72	.05	.00
11.3	.06	.08	.51	739	.06	.16	.01	.72	.04	.00
12.6	.05	.07	.56	693	.05	.17	.00	.73	.04	.00
13.8	.03	.05	.67	570	.04	.18	.00	.74	.03	.00
15.1	.02	.03	.77	484	.03	.19	.00	.74	.02	.00
16.4	.01	.02	.88	400	.03	.19	.00	.75	.02	.00
17.6	.00	.01	.99	330	.02	.20	.00	.76	.01	.00

x/d = 50

|2y/d|	f''	f'	ρ'	T'	X'_{CO_2}	X'_{O_2}	X'_{CO}	X'_{N_2}	X'_{H_2O}	X'_{H_2}
0.0	.04	.05	.06	382	.03	.04	.03	.04	.02	.01
1.3	.03	.05	.05	344	.02	.04	.02	.02	.02	.00
1.3	.06	.07	.05	393	.04	.04	.05	.05	.02	.01
2.5	.03	.05	.06	351	.02	.04	.02	.03	.02	.00
2.5	.04	.05	.05	364	.03	.04	.02	.04	.02	.01
3.8	.03	.05	.07	374	.03	.04	.02	.02	.02	.00
5.0	.03	.05	.09	407	.03	.04	.02	.02	.02	.00
6.3	.03	.05	.11	409	.03	.04	.01	.03	.02	.00
7.6	.03	.06	.12	415	.03	.04	.01	.02	.02	.00
8.8	.02	.06	.16	415	.03	.04	.01	.03	.02	.00
10.1	.03	.06	.20	374	.03	.03	.01	.03	.02	.00
11.3	.03	.05	.20	315	.03	.03	.01	.03	.02	.00
12.6	.03	.06	.23	332	.03	.03	.01	.03	.02	.00
13.8	.03	.05	.26	289	.02	.03	.01	.03	.02	.00
15.1	.02	.05	.28	241	.02	.03	.00	.02	.02	.00
16.4	.04	.04	.27	187	.02	.02	.00	.02	.02	.01
17.6	.01	.02	.19	127	.01	.01	.00	.02	.01	.00

Concentration in 10^{16} molecules/cc

x/d = 10			x/d = 25			x/d = 50		
2y/d	$\overline{C_{OH}}$	C'_{OH}	|2y/d|	$\overline{C_{OH}}$	C_{OH}'	|2y/d|	$\overline{C_{OH}}$	C_{OH}'
.4	.01	.02	.1	.19	.47	0.3	1.68	0.77
.7	.01	.03	.3	.18	.44	0.3	1.67	0.75
1.0	.03	.10	.4	.20	.47	0.3	1.61	0.73
1.7	.51	.74	.9	.23	.53	0.9	1.68	0.78
2.0	1.32	1.27	1.5	.43	.77	1.5	1.57	0.80
2.0	1.48	1.27	1.6	.54	.84	2.1	1.53	0.81
2.3	2.45	1.16	2.1	.75	1.00	2.8	1.47	0.83
2.3	2.62	1.41	2.7	1.27	1.15	3.4	1.39	0.84
2.6	2.43	1.00	2.8	1.33	1.10	4.0	1.31	0.92
2.6	2.86	1.11	3.4	1.66	1.15	4.7	1.07	0.83
2.9	1.21	0.96	3.5	1.62	1.08	5.3	1.06	0.90
2.9	1.34	1.05	4.0	1.65	1.07	6.0	0.89	0.83
2.9	1.62	1.24	4.1	1.55	1.05	6.6	0.76	0.84
2.9	1.95	1.30	4.6	1.46	1.10	7.2	0.62	0.72
3.3	0.40	0.65	4.8	1.25	1.09	8.5	0.38	0.55
3.3	0.62	0.85	5.2	1.01	1.05	11.0	0.15	0.28
3.5	0.07	0.25	5.4	.88	1.03			
3.9	0.01	0.11	5.9	.59	.86			
4.2	0.00	0.02	6.5	.34	.65			
4.9	0.00	0.02	7.1	.17	.39			
			7.7	.09	.25			
			8.4	.06	.13			
			9.0	.04	.07			
			9.7	.04	.04			
			10.9	.04	.02			

x/D = 100 continued: *0.8% (vol.) Ammonia added to fuel

y/D	$\overline{T}$ [°C]	$\overline{C}_{NO}$ [ppm]	$\overline{C}_{NO}$* [ppm]
0.0	483	3.6	114
1.26	465	3.5	105
2.83	430	3.1	93
4.25	382	2.5	78
6.0	320	1.9	60
7.55	245	1.3	44
9.12	175	1.0	29
10.7	112	0.6	16.5
12.25	55	0.17	7.3
13.84	33	0.08	4.0
15.4	25	0.0	2.0

EXPERIMENTAL DATA FOR METHANE JET

Initial Condition x/d = 1

r/x	$\bar{u}/\bar{u}_o$	u'/u'_c	v'/u'_c	w'/u'_c	k/k_c
Re = 11700, $\bar{u}_o$ = 49.8 m/s, $k_c^{1/2}/\bar{u}_o$ = 0.0160:					
0.4	0.999	0.952	0.810	0.813	1.069
0.2	0.995	0.857	0.719	0.759	0.879
0.0	1.015	1.000	0.714	0.754	1.000
0.2	0.985	0.905	0.762	0.848	1.019
0.4	0.996	1.095	0.905	0.953	1.408

Axial Variation of Quantities

Centerline Mean Velocity and Velocity Fluctuation

Re	11700	
x/d	$\bar{u}_c/\bar{u}_o$	u'/u_c
1.00	1.000	0.013
1.71	1.000	0.013
2.22	1.001	0.012
4.76	0.998	0.012
7.30	0.998	0.021
9.84	0.993	0.033
12.38	0.973	0.030
14.92	0.962	0.050
52.2	0.226	0.136
101.6	0.170	0.183
150.0	0.117	0.206
198.0	0.083	0.215
303.0	0.072	0.245
418.0	0.058	0.267

Centerline Mean Temperature

Re	11700
x/d	T(K)
22.0	758
29.9	1003
52.2	1335
79.0	1543
101.6	1742
150.0	1550
198.0	951
303.0	555
418.0	424

Centerline Mean Species Concentrations

x/d	Mass Fraction						
	CH_4	O_2	N_2	CO_2	H_2O	CO	H_2
13	0.558	0.011	0.352	0.008	0.048	0.010	0.013
24	0.252	0.026	0.594	0.029	0.067	0.024	0.008
36	0.176	0.010	0.644	0.042	0.086	0.035	0.007
52	0.111	0.004	0.662	0.070	0.110	0.047	0.006
80	0.032	0.001	0.682	0.080	0.100	0.050	0.005
100	0.002	0.039	0.743	0.092	0.076	0.044	0.003
150	0.000	0.097	0.755	0.069	0.075	0.004	0.000
200	0.000	0.167	0.752	0.041	0.040	0.000	0.000
300	0.000	0.203	0.760	0.009	0.028	0.000	0.000
400	0.000	0.210	0.761	0.007	0.020	0.000	0.000

Radial Variation of Quantities

Mean Velocity

Re	11700
r/x	$\bar{u}/\bar{u}_c$
x/d = 52.2:	
0.000	1.000
0.014	0.963
0.024	0.921
0.043	0.858
0.063	0.675
0.083	0.462
0.102	0.301
0.123	0.197
0.142	0.142
0.162	0.085
0.182	0.053
0.201	0.035
x/d = 102:	
0.000	1.000
0.010	0.975
0.030	0.923
0.049	0.788
0.069	0.537
0.089	0.356
0.108	0.261
0.128	0.177
0.148	0.125
0.167	0.100
0.187	0.076

r/x	$\bar{u}/\bar{u}_c$
x/d = 150:	
0.000	1.000
0.005	0.981
0.024	0.917
0.039	0.802
0.052	0.649
0.069	0.070
0.083	0.392
0.100	0.298
0.115	0.229
0.131	0.208
0.145	0.117
0.160	0.076
0.175	0.039
x/d = 198:	
0.000	1.000
0.008	0.961
0.023	0.903
0.038	0.805
0.053	0.677
0.068	0.517
0.083	0.389
0.098	0.329
0.113	0.259
0.128	0.215
0.144	0.149
0.159	0.105
0.174	0.055

r/x	$\bar{u}/\bar{u}_c$
x/d = 303:	
0.000	1.000
0.013	0.971
0.027	0.899
0.040	0.818
0.053	0.709
0.067	0.626
0.080	0.495
0.093	0.448
0.107	0.357
0.127	0.261
0.147	0.171
0.167	0.120
0.187	0.070
x/d = 418.0:	
0.000	1.000
0.015	0.976
0.031	0.905
0.046	0.853
0.061	0.732
0.077	0.590
0.092	0.471
0.107	0.378
0.122	0.292
0.138	0.207
0.153	0.138
0.168	0.076

Radial Variation of Quantities

Mean Temperature

Re	11700
r/x	T(K)
x/d = 52.5:	
0.000	1335
0.008	1341
0.019	1363
0.031	1412
0.042	1458
0.054	1534
0.065	1609
0.077	1663
0.088	1658
0.100	1626
0.111	1513
0.123	1327
0.133	1116
0.146	926
0.157	750
0.169	602
0.180	500
0.192	411
0.203	361
x/d = 102:	
0.000	1742
0.011	1735
0.021	1745
0.030	1732
0.040	1710
0.050	1665
0.060	1580
0.070	1482
0.080	1382
0.090	1259
0.099	1041
0.109	1009
0.119	834
0.129	780
0.139	685
0.149	633
0.158	521
0.168	479
0.178	442
0.188	411

r/x	T(K)
x/d = 150:	
0.000	1550
0.005	1552
0.019	1462
0.032	1339
0.045	1214
0.059	1034
0.072	390
0.085	732
0.099	634
0.112	572
0.125	498
0.139	438
0.152	399
0.165	364
0.179	337
0.192	323
x/d = 198.0:	
0.000	951
0.003	943
0.013	923
0.023	902
0.033	850
0.043	807
0.053	758
0.063	696
0.073	633
0.083	581
0.094	534
0.104	492
0.114	458
0.124	425
0.134	—
0.144	379
0.154	—
0.164	344
0.174	—

r/x	T(K)
x/d = 303:	
0.000	555
0.007	548
0.020	525
0.033	498
0.046	470
0.059	440
0.073	409
0.086	385
0.099	372
0.112	352
0.125	340
0.139	328
0.152	320
0.165	314
0.178	311
0.191	308
0.205	305
x/d = 418:	
0.000	424
0.005	423
0.015	415
0.024	410
0.034	390
0.044	382
0.053	380
0.063	373
0.072	363
0.082	354
0.091	344
0.101	338
0.111	332
0.121	325
0.130	320
0.139	317
0.149	312
0.158	309
0.168	308

Radial Variation of Quantities

Mass Fraction

r/x	CH_4	O_2	N_2	CO_2	H_2O	CO	H_2
Re = 11700 x/d = 52.5							
0.000	0.108	0.004	0.656	0.075	0.109	0.043	0.005
0.015	0.076	0.003	0.673	0.076	0.126	0.041	0.005
0.031	0.052	0.019	0.671	0.102	0.118	0.030	0.008
0.046	0.028	0.058	0.644	0.129	0.111	0.024	0.006
0.061	0.013	0.065	0.666	0.130	0.105	0.018	0.003
0.076	0.006	0.079	0.722	0.092	0.085	0.014	0.002
0.092	0.001	0.123	0.727	0.070	0.075	0.003	0.001
0.107	0.000	0.138	0.744	0.051	0.067	0.000	0.000
0.122	0.000	0.152	0.787	0.025	0.036	0.000	0.000
0.138	0.000	0.187	0.764	0.018	0.031	0.000	0.000
0.150	0.000	0.190	0.771	0.015	0.024	0.000	0.000
0.161	0.000	0.192	0.780	0.009	0.019	0.000	0.000
0.172	0.000	0.195	0.786	0.005	0.014	0.000	0.000
0.188	0.000	0.203	0.782	0.002	0.013	0.000	0.000
Re = 11700 x/d = 100							
0.000	0.002	0.041	0.745	0.079	0.082	0.041	0.010
0.015	0.002	0.042	0.716	0.074	0.117	0.042	0.007
0.030	0.001	0.045	0.721	0.077	0.115	0.034	0.007
0.045	0.000	0.063	0.731	0.083	0.089	0.029	0.005
0.060	0.000	0.066	0.732	0.088	0.086	0.025	0.003
0.075	0.000	0.083	0.746	0.076	0.081	0.014	0.001
0.090	0.000	0.107	0.752	0.063	0.069	0.009	0.000
0.105	0.000	0.140	0.746	0.049	0.060	0.005	0.000
0.120	0.000	0.173	0.738	0.047	0.041	0.001	0.000
0.135	0.000	0.191	0.734	0.038	0.037	0.000	0.000
0.150	0.000	0.208	0.744	0.023	0.025	0.000	0.000
0.165	0.000	0.213	0.750	0.014	0.023	0.000	0.000
Re = 11700 x/d = 200							
0.000	0.000	0.161	0.764	0.033	0.042	0.000	0.000
0.015	0.000	0.165	0.767	0.027	0.041	0.000	0.000
0.030	0.000	0.172	0.761	0.025	0.042	0.000	0.000
0.045	0.000	0.179	0.758	0.026	0.037	0.000	0.000
0.060	0.000	0.187	0.759	0.020	0.034	0.000	0.000
0.075	0.000	0.192	0.762	0.018	0.028	0.000	0.000
0.090	0.000	0.199	0.761	0.015	0.025	0.000	0.000
0.105	0.000	0.208	0.762	0.010	0.020	0.000	0.000
0.120	0.000	0.215	0.763	0.007	0.015	0.000	0.000
0.135	0.000	0.217	0.767	0.005	0.011	0.000	0.000
0.155	0.000	0.218	0.774	0.002	0.006	0.000	0.000

Radial Variation of Quantities

Re = 11700   x/d = 52.5

r/x	$u'/\bar{u}_c$	$v'/\bar{u}_c$	$w'/\bar{u}_c$	$\overline{u'v'}/\bar{u}_c^2$	$k/\bar{u}_c^2$
0.000	0.130	0.103	0.094	0.0004	0.0181
0.019	0.135	0.098	0.090	0.0018	0.0180
0.038	0.145	0.107	0.096	0.0066	0.0208
0.058	0.145	0.112	0.095	0.0107	0.0213
0.077	0.128	0.110	0.096	0.0083	0.0188
0.096	0.115	0.098	0.085	0.0056	0.0150
0.115	0.084	0.089	0.098	0.0092	0.0123
0.134	0.065	0.070	0.085	0.0011	0.0082
0.153	0.033	0.040	0.062	0.0007	0.0063
0.173	0.028	0.030	0.050	0.0003	0.0021

Re = 11700   x/d - 101

0.000	0.219	0.139	0.139	0.0010	0.0433
0.012	0.220	0.140	0.144	0.0019	0.0443
0.030	0.236	0.142	0.143	0.0097	0.0482
0.050	0.243	0.142	0.153	0.0136	0.0513
0.070	0.244	0.135	0.148	0.0139	0.0498
0.090	0.231	0.132	0.134	0.0127	0.0443
0.111	0.184	0.122	0.102	0.0089	0.0295
0.132	0.135	0.108	0.088	0.0076	0.0188
0.146	0.117	0.091	0.084	0.0064	0.0145
0.172	0.090	0.076	0.075	0.0039	0.0097
0.189	0.067	0.065	0.065	0.0013	0.0064

Re = 11700   x/d = 52.5

0.000	0.294	0.195	0.195	-0.0006	0.0812
0.020	0.287	0.197	0.191	0.0087	0.0788
0.040	0.290	0.197	0.184	0.0191	0.0783
0.060	0.273	0.190	0.176	0.0219	0.0708
0.080	0.254	0.186	0.160	0.0187	0.0623
0.100	0.228	0.179	0.141	0.0136	0.0519
0.120	0.205	0.154	0.117	0.0078	0.0397
0.140	0.173	0.143	0.100	0.0031	0.0302
0.160	0.144	0.113	0.090	0.0011	0.0208
0.180	0.121	0.104	—	0.0006	0.0181

Re = 11700   x/d = 400

0.000	0.258	0.212	—	0.0007	0.0782
0.020	0.261	0.215	—	0.0056	0.0800
0.040	0.260	0.215	—	0.0109	0.0800
0.060	0.251	0.205	—	0.0141	0.0735
0.080	0.247	0.195	—	0.0166	0.0685
0.100	0.215	0.183	—	0.0150	0.0566
0.120	0.183	0.157	—	0.0122	0.0413
0.140	0.165	0.139	—	0.0096	0.0329
0.160	0.135	0.129	—	0.0052	0.0231
0.180	0.107	0.099	—	0.0014	0.0155
0.200	0.087	0.082	—	0.0001	0.0105

EXPERIMENTAL DATA FOR PROPANE DIFFUSION FLAME

Propane diffusion flame

Re = 42700

$\overline{u}_j$ = 31.34 m/s, $\overline{u}_e$ = 0.0, D = 6 mm

Composition in mole fractions X_i

x/D = 20:

y/D	$\overline{X}_{CO_2}$	y/D	$\overline{X}_{CO}$	y/D	$\overline{X}_{UHC}$	y/D	$\overline{X}_{O_2}$
0.0	0.011	0.0	0.016	0.0	0.067	1.4	0.004
0.4	0.015	0.4	0.02	0.3	0.0675	1.5	0.011
0.8	0.035	0.8	0.029	0.6	0.061	1.5	0.016
1.2	0.039	1.4	0.047	0.8	0.051	2.4	0.056
1.6	0.056	1.6	0.055	1.1	0.048	2.75	0.071
2.4	0.044	2.0	0.051	1.3	0.0325	2.85	0.074
2.8	0.019	2.3	0.021	1.7	0.027	3.7	0.083
3.2	0.011	2.9	0.005	2.1	0.014	4.0	0.0855
3.8	0.003	3.1	0.004	2.4	0.0012		
4.0	0.0015	3.8	0.001	2.9	0.0005		

x/D = 40:

y/D	$\bar{X}_{CO_2}$	y/D	$\bar{X}_{CO}$	y/D	$\bar{X}_{UHC}$	y/D	$\bar{X}_{O_2}$
0.0	0.037	0.0	0.0428	0.0	0.0314	2.0	0.004
0.4	0.0365	0.8	0.0446	0.8	0.0308	2.6	0.009
0.6	0.0376	0.9	0.0458	1.8	0.0225	3.3	0.026
1.0	0.039	1.9	0.051	2.9	0.0113	3.6	0.043
1.5	0.0428	2.4	0.0558	3.9	0.0026	4.3	0.088
2.3	0.0469	2.9	0.0573	4.9	0.001	4.7	0.119
2.6	0.0534	3.9	0.0406			5.3	0.16
3.1	0.0572	4.1	0.0217			5.6	0.174
4.0	0.058	4.6	0.0112			6.5	0.184
4.2	0.0423	5.3	0.0028				
4.6	0.037	5.9	0.0006				
5.2	0.0113						
6.1	0.0026						

x/D = 60:

y/D	$\bar{x}_{CO_2}$	y/D	$\bar{x}_{CO}$	y/D	$\bar{x}_{UHC}$	y/D	$\bar{x}_{O_2}$
0.0	0.0442	0.0	0.0537	0.0	0.0846	1.9	0.005
0.8	0.0439	0.9	0.0541	0.9	0.0821	2.8	0.008
1.5	0.0462	1.2	0.0557	2.0	0.0758	3.2	0.012
2.4	0.0494	1.8	0.0578	2.8	0.061	3.7	0.015
3.4	0.0557	1.9	0.059	3.1	0.0573	4.2	0.024
4.5	0.0612	3.1	0.0602	3.7	0.0397	4.9	0.045
5.6	0.072	3.7	0.058	4.1	0.035	5.4	0.07
6.4	0.054	4.1	0.0578	4.8	0.0202	5.5	0.082
7.0	0.0364	4.8	0.0498	5.8	0.0103	6.2	0.106
8.0	0.0222	5.1	0.0441	6.2	0.006	6.4	0.112
8.8	0.0141	5.7	0.0358	6.8	0.0026	7.1	0.133
9.1	0.012	6.2	0.0248	7.3	0.0015	7.8	0.152
10.8	0.004	6.8	0.0137			8.8	0.165
		7.1	0.0102			9.1	0.176
		7.9	0.004			11.1	0.198
		8.9	0.0016			12.9	0.208
		9.3	0.0015				

x/D = 100:

y/D	$\bar{X}_{CO_2}$	y/D	$\bar{X}_{CO}$	y/D	$\bar{X}_{UHC}$	y/D	$\bar{X}_{O_2}$
0.0	0.0551	0.0	0.0641	0.0	0.067	0.0	0.01
0.5	0.0556	1.3	0.0622	0.3	0.0674	0.2	0.012
1.0	0.0569	3.8	0.0572	1.3	0.0635	1.6	0.013
1.9	0.057	4.8	0.0523	2.8	0.055	2.2	0.015
3.0	0.0614	6.0	0.0395	3.1	0.0534	3.5	0.018
4.6	0.0622	6.9	0.0314	4.2	0.0375	4.3	0.024
5.4	0.0628	8.8	0.0178	4.3	0.0362	4.8	0.03
6.7	0.06	10.9	0.0072	5.6	0.025	6.2	0.052
7.0	0.0595	13.0	0.002	6.2	0.018	7.6	0.08
8.7	0.0518	15.0	0.0005	7.5	0.011	8.3	0.091
9.1	0.0489	16.0	0.0	8.2	0.008	9.6	0.12
10.7	0.038			9.4	0.0038	10.3	0.134
11.1	0.035			10.3	0.0018	11.5	0.149
12.8	0.02			11.5	0.0008	12.2	0.157
14.8	0.013			12.1	0.0005	13.4	0.169
15.9	0.012					14.3	0.181
18.0	0.0057					16.5	0.194
20.9	0.002					17.2	0.197
						20.2	0.212

x/D = 80:

y/D	$\bar{x}_{CO_2}$	y/D	$\bar{x}_{CO}$	y/D	$\bar{x}_{UHC}$	y/D	$\bar{x}_{O_2}$
0.0	0.048	0.0	0.059	0.0	0.059	0.15	0.003
0.8	0.0488	1.1	0.0593	1.1	0.0557	2.0	0.005
1.3	0.0491	2.1	0.592	2.1	0.05	3.2	0.013
1.9	0.0513	3.0	0.058	3.0	0.039	4.0	0.019
2.9	0.0512	4.0	0.057	4.0	0.0296	5.0	0.031
3.8	0.0568	5.0	0.052	5.0	0.0192	6.0	0.047
4.9	0.0603	6.0	0.0436	6.0	0.0112	7.0	0.076
5.8	0.0591	7.0	0.031	8.0	0.0028	9.0	0.135
6.6	0.0552	9.0	0.09	10.0	0.0005	11.0	0.169
7.3	0.0488	11.0	0.0015			14.0	0.196
7.6	0.044					17.0	0.21
8.4	0.0369						
9.5	0.0288						
10.5	0.0202						
11.3	0.011						
13.7	0.0052						
14.4	0.002						

x/D = 150:

y/D	$\bar{X}_{CO_2}$	y/D	$\bar{X}_{CO}$	y/D	$\bar{X}_{UHC}$	y/D	$\bar{X}_{O_2}$
0.0	0.0738	0.0	0.0463	0.0	0.0175	0.0	0.032
1.9	0.0725	2.0	0.044	1.9	0.016	0.8	0.034
4.0	0.069	3.6	0.038	4.0	0.0103	3.0	0.038
7.0	0.0608	5.0	0.031	6.0	0.006	5.7	0.061
9.0	0.0545	7.0	0.021	8.0	0.004	7.0	0.088
11.0	0.044	9.0	0.014	10.0	0.002	8.0	0.098
13.0	0.033	11.0	0.008	12.0	0.001	9.0	0.109
14.0	0.0308	13.0	0.0038	13.0	0.0004	9.1	0.104
16.0	0.0207	14.0	0.0027			11.0	0.13
17.0	0.017	17.0	0.001			13.0	0.15
19.0	0.012	20.0	0.0004			16.0	0.172
23.0	0.005					17.0	0.176
27.0	0.0016					19.0	0.185
						23.0	0.197
						27.0	0.21

x/D = 120:

y/D	$\bar{X}_{CO_2}$	y/D	$\bar{X}_{CO}$	y/D	$\bar{X}_{UHC}$	y/D	$\bar{X}_{O_2}$
0.0	0.062	0.0	0.06	0.0	0.0421	1.9	0.024
0.6	0.0618	0.8	0.0588	1.8	0.0375	3.8	0.036
1.2	0.0618	2.8	0.0562	3.9	0.0264	5.9	0.054
2.4	0.0638	4.9	0.047	5.9	0.017	7.9	0.075
3.2	0.065	6.9	0.0325	7.8	0.0073	9.9	0.108
4.4	0.0663	8.7	0.0218	9.8	0.004	11.9	0.148
5.2	0.0659	9.0	0.018	11.9	0.0015	14.9	0.178
7.0	0.062	10.9	0.0102	12.9	0.001	18.0	0.193
8.5	0.0566	12.5	0.005			21.0	0.198
9.0	0.0518	15.5	0.001				
10.6	0.0441						
11.0	0.041						
12.5	0.0322						
14.0	0.023						
15.7	0.017						
17.1	0.0122						
18.8	0.0068						
21.6	0.0018						

x/D = 200:

y/D	$\bar{X}_{CO_2}$	y/D	$\bar{X}_{CO}$	y/D	$\bar{X}_{UHC}$	y/D	$\bar{X}_{O_2}$
0 0	0.06	0.0	0.006			0.0	0.078
2.0	0.0594	2.0	0.005			2.0	0.08
4.0	0.0573	4.0	0.0048			4.0	0.084
6.0	0.0522	6.0	0.003			6.0	0.095
8.0	0.0491	8.0	0.0028			8.0	0.104
10.0	0.0421	10.0	0.0012			10.0	0.125
12.0	0.0346	12.0	0.0005			12.0	0.139
15.0	0.023	15.0	0.0			14.0	0.163
18.0	0.015					15.0	0.165
20.8	0.0121					18.0	0.187
25.0	0.0037					21.0	0.2
						25.0	0.204

APPENDIX D

Yoshida, A. (1981) Experimental study of wrinkled laminar flame. 18th Symposium (International) on Combustion, 931.

Yoshida A. and Gunther, R. (1980) Experimental investigation of thermal structures of turbulent premixed flames. Comb. and Flame 38, 249.

Yoshida, A. and Gunther, R. (1981) An experimental study of structure and reaction rate in premixed flames. Comb. Sci. and Tech. 26, 43.

FLOW ARRANGEMENT AND MEASUREMENTS

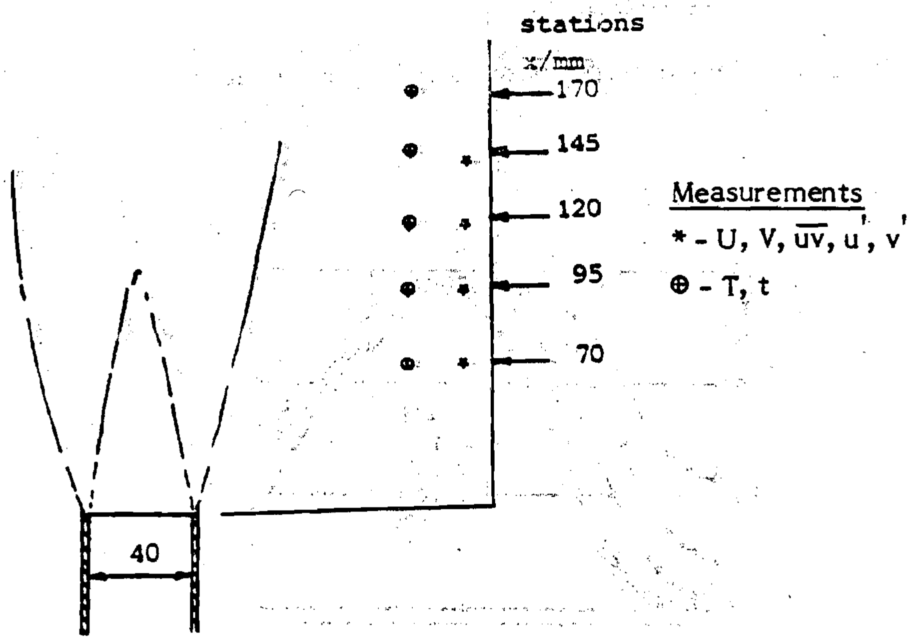

Premixed methane + air flame

$\phi = 0.8$

U_o = 5.44 m/s, Re = 14500

u'_o/U_o = 0.06

Velocity profile at pipe exit is not specified in detail but stated as uniform except close to the edge.

The mean temperatures are all presented as values in excess of the ambient temperature.

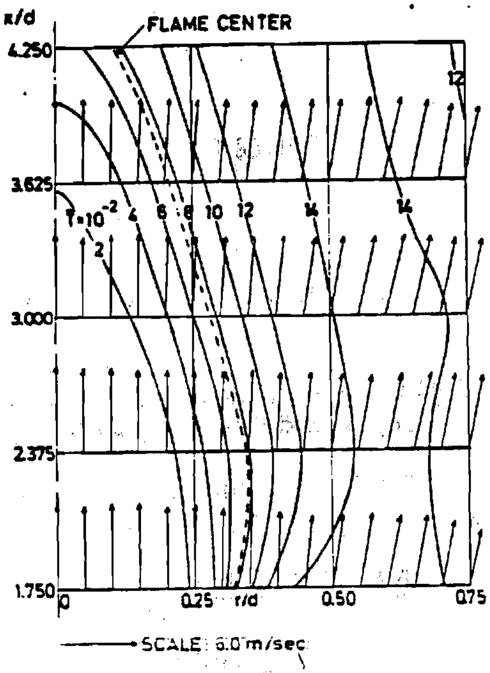

Fig. D.1. Temperature contours and velocity vectors

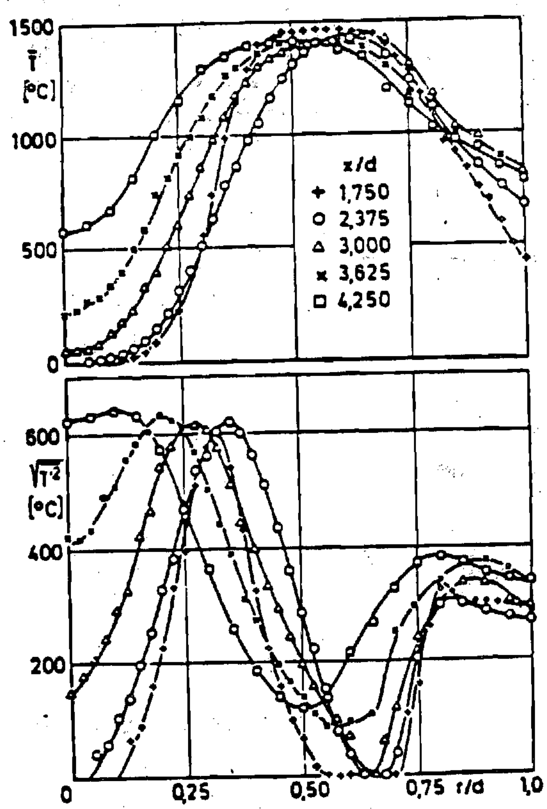

Fig. D.2. Mean and fluctuating temperature distributions for $\phi = 0.80$, $u = 5.44$ m/sec, and $T_u = 6\%$.

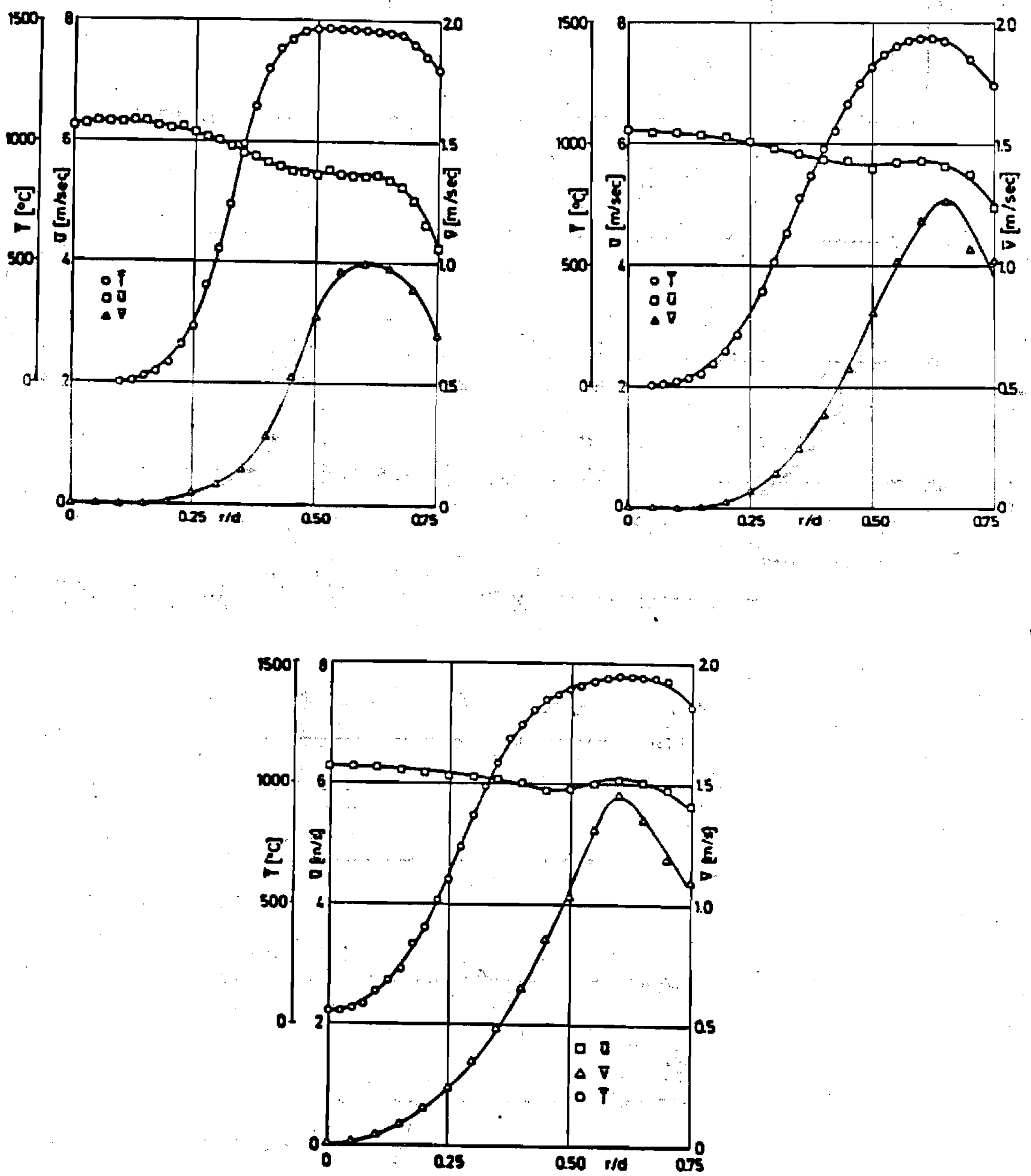

Fig. D.3 Radial distributions of axial and radial components of mean velocity and mean temperature

(a) x/d = 1.750
(b) x/d = 2.375
(c) x/d = 3.000

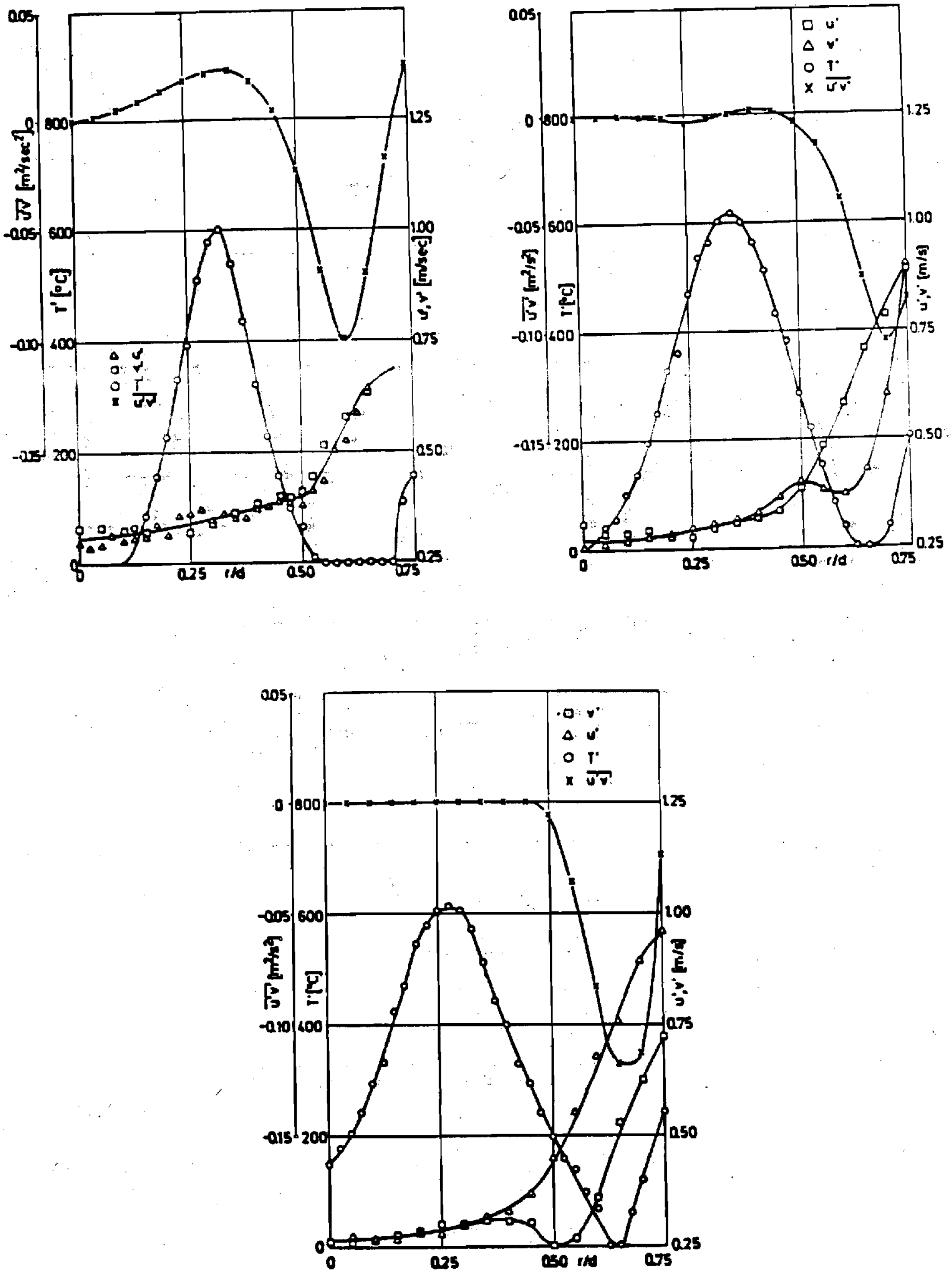

Fig. D.4. Radial distributions of axial and radial components of fluctuating velocity, Reynolds shear stress and fluctuating temperature

(a) x/d = 1.750
(b) x/d = 2.375
(c) x/d = 3.000

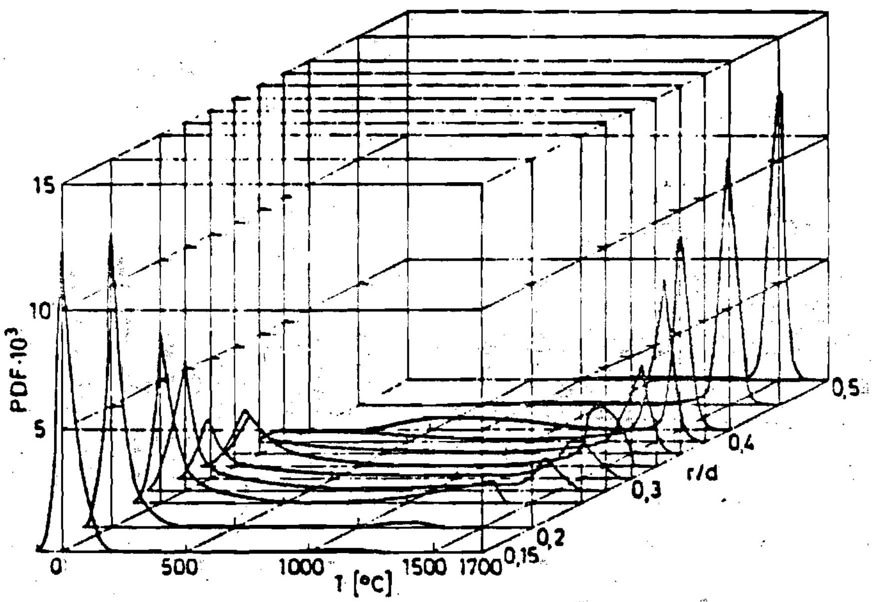

Fig. D.5. Radial variations of PDF of fluctuating temperature for $\phi = 0.80$, $T_u = 6\%$, $\bar{u} = 5.44$ m/sec and $x/d = 1.75$

Keller, J.O. and Daily, J.W. (1983) The effect of large heat release on a two-dimensional mixing layer. AIAA paper 83-0472.

Shepherd, I.G. and Daily, J.W. (1984) Rayleigh scattering measurements in a two-stream free mixing layer. University of California, Berkeley College of Engineering, Mech. Eng. Paper 84-45.

Daily, J. W. and Lundquist, W.J. (1984) Three-dimensional structure in a tubulent combusting mixing layer. Submitted for publication.

<u>FLOW ARRANGEMENT AND MEASUREMENTS</u>

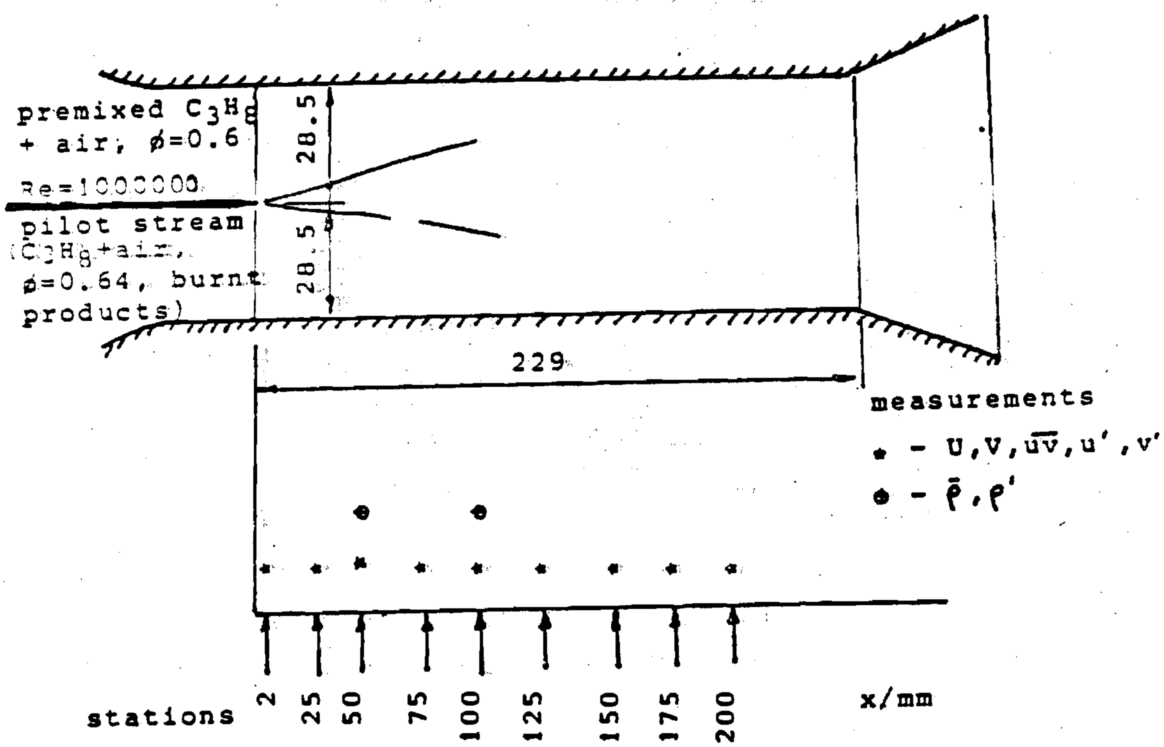

Premixed propane-air flame

Premixed stream: propane-air mixture of equivalence ratio 0.6 at 293 K U_o = 15 m/s

Pilot stream: products of combustion of propane-air mixture of equivalence ratio 0.68 at 1170 K U_o = 5 m/s

Streamwise mean and fluctuating velocities specified 2 mm downstream of splitter plate.

All velocities, except in Fig. 2.2 are normalized with respect to a volume averaged inlet velocity, V_c = 10 m/s.

Boundary layer profiles on splitter plate are normalized with respect to the relevant freestream mean velocity. (Fig. 2.2).

Density profiles and pdfs are normalized against the density of unburnt air-fuel mixture.

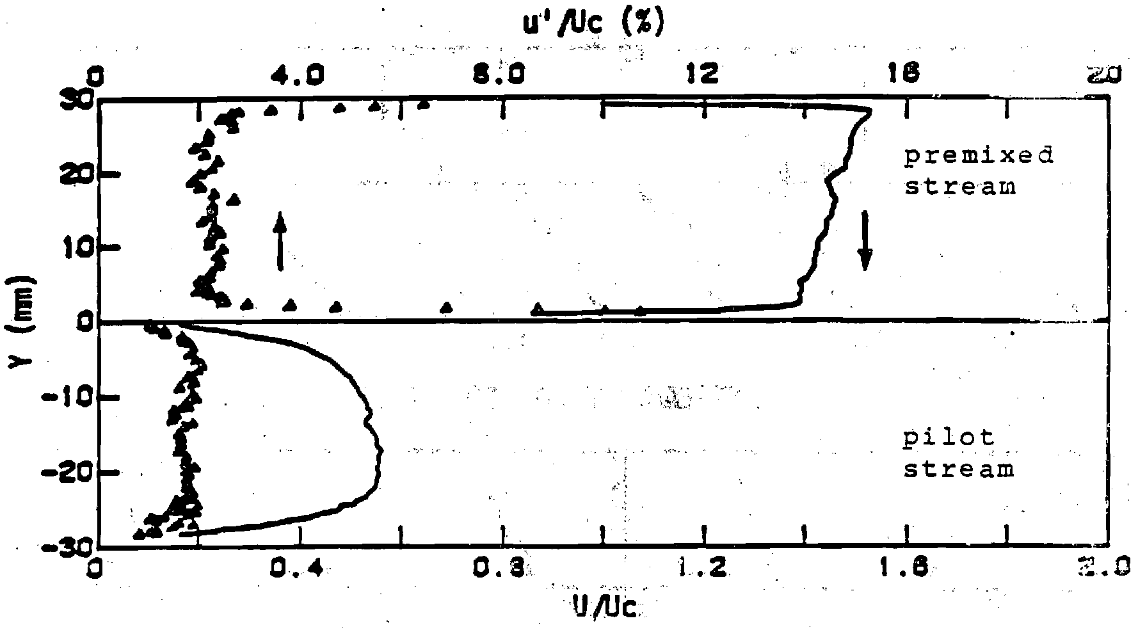

Fig. D.6 Mean and fluctuating streamwise velocity at x = 2mm

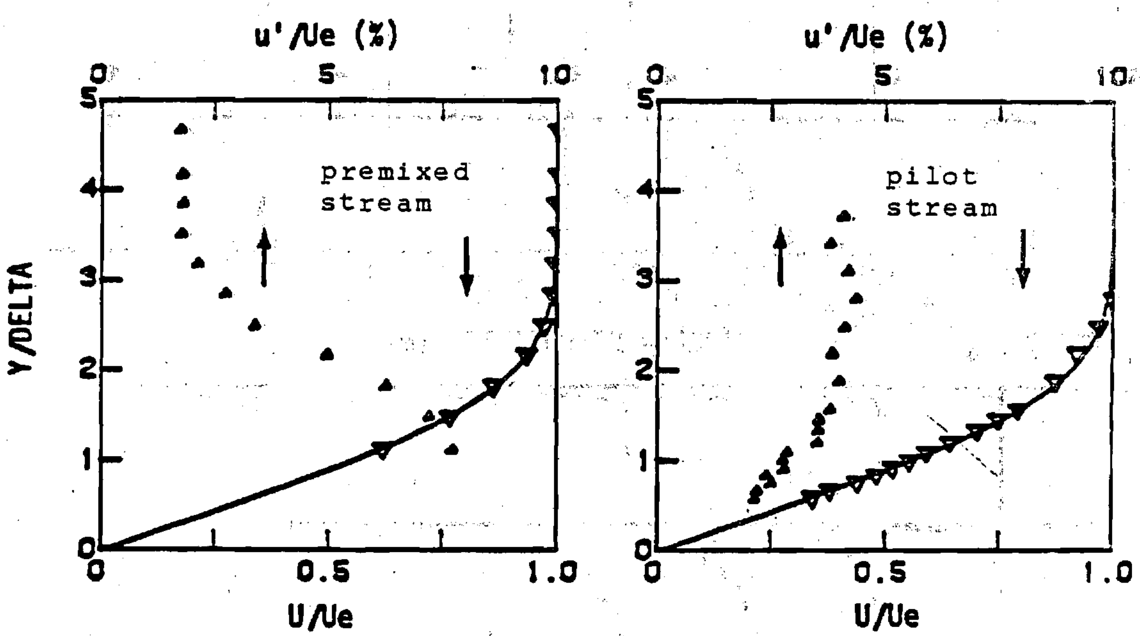

Fig. D.7. Boundary layer on splitter plate measured at x = 2mm

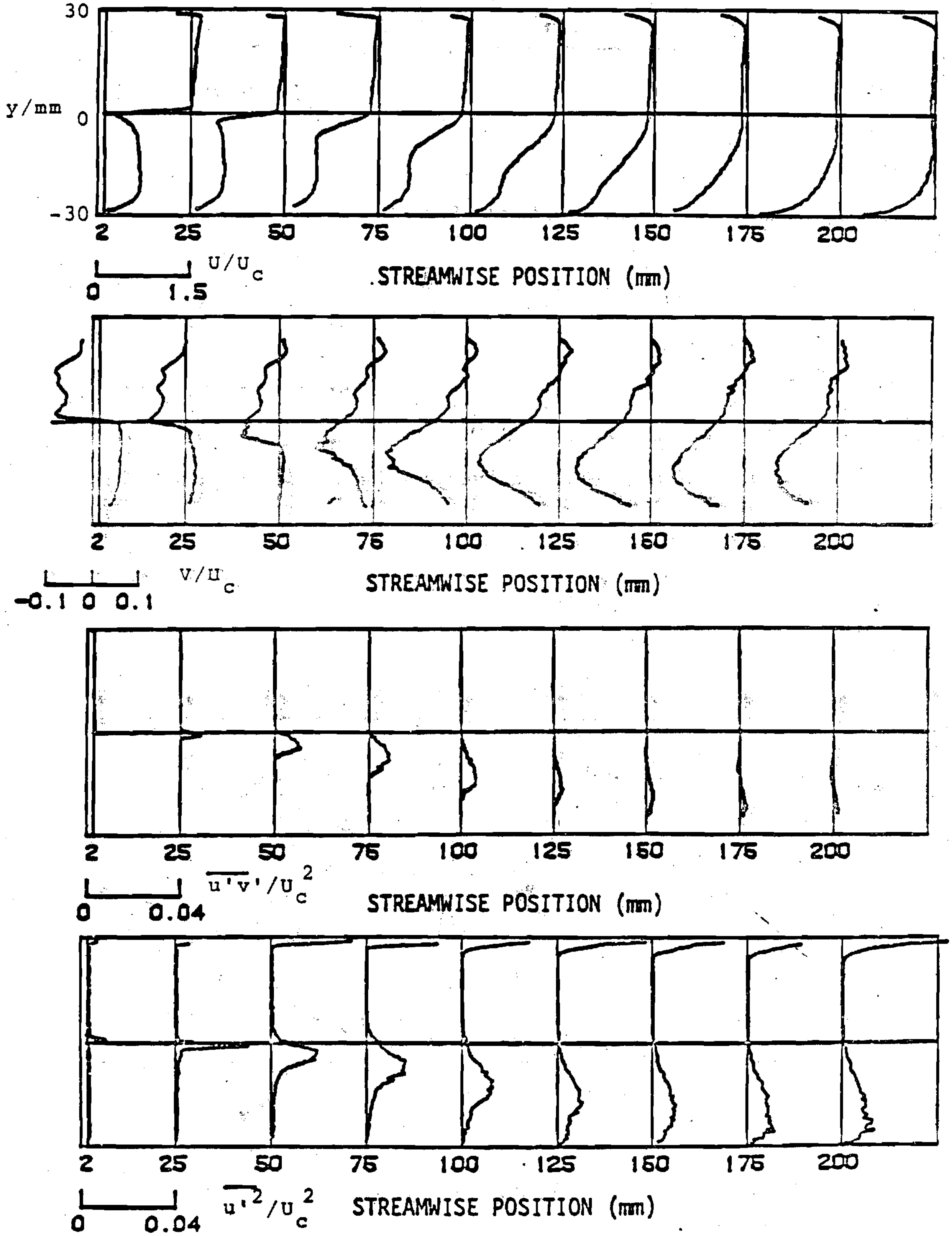

Fig. D.8. Mean and fluctuating velocity profiles

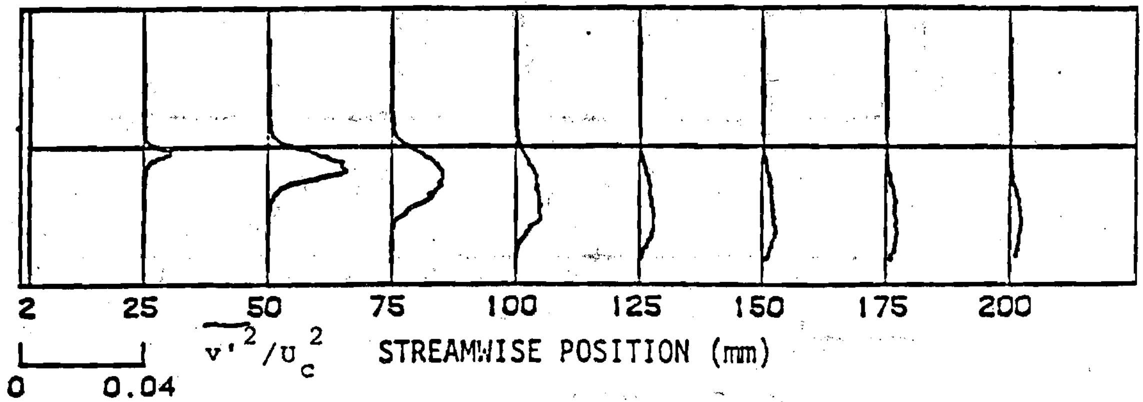

Fig. D.8. Mean and fluctuating velocity profiles (Cont'd.)

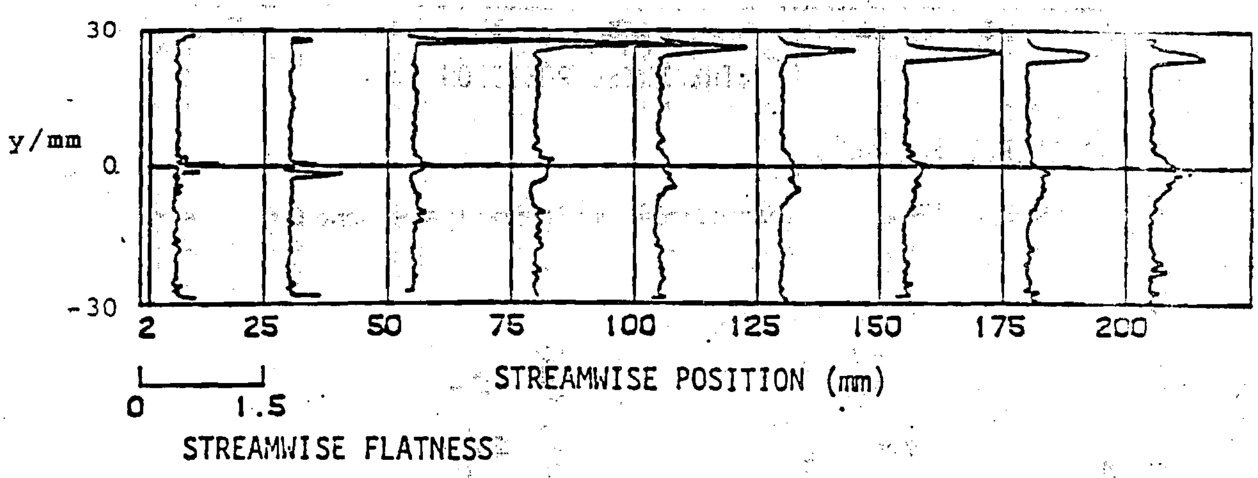

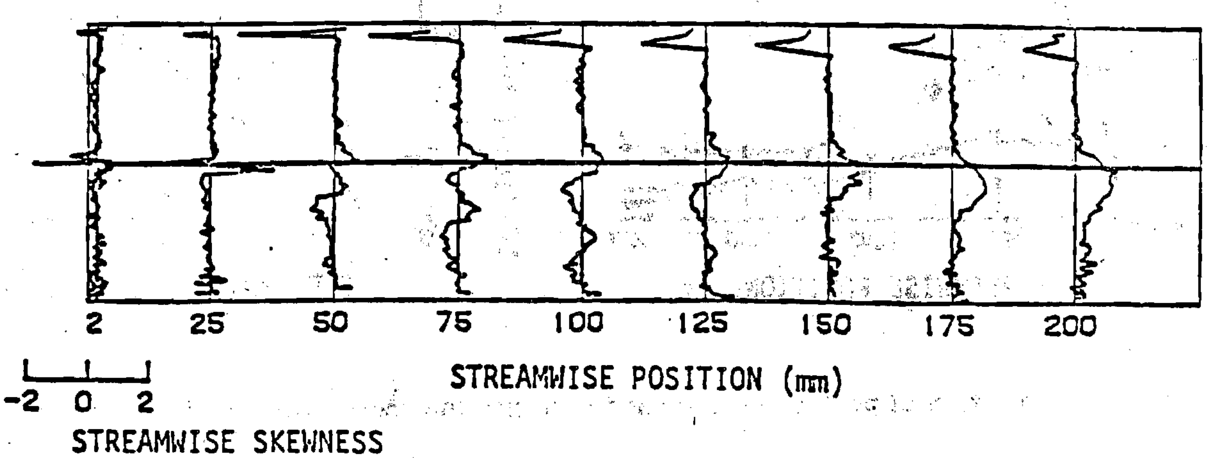

Fig. D.9 Characteristics of velocity components

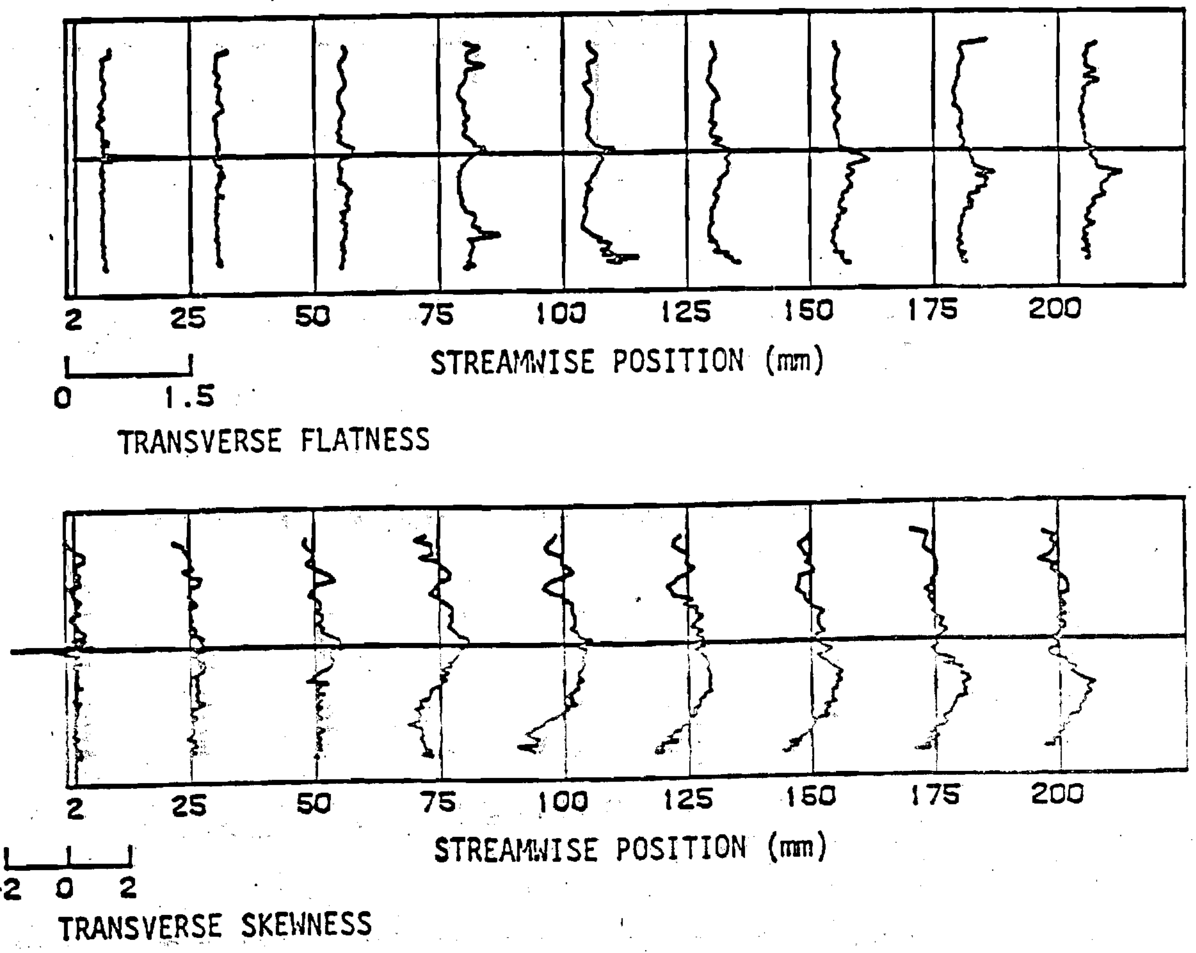

Fig. D.9 Characteristics of velocity components. (Cont'd.)

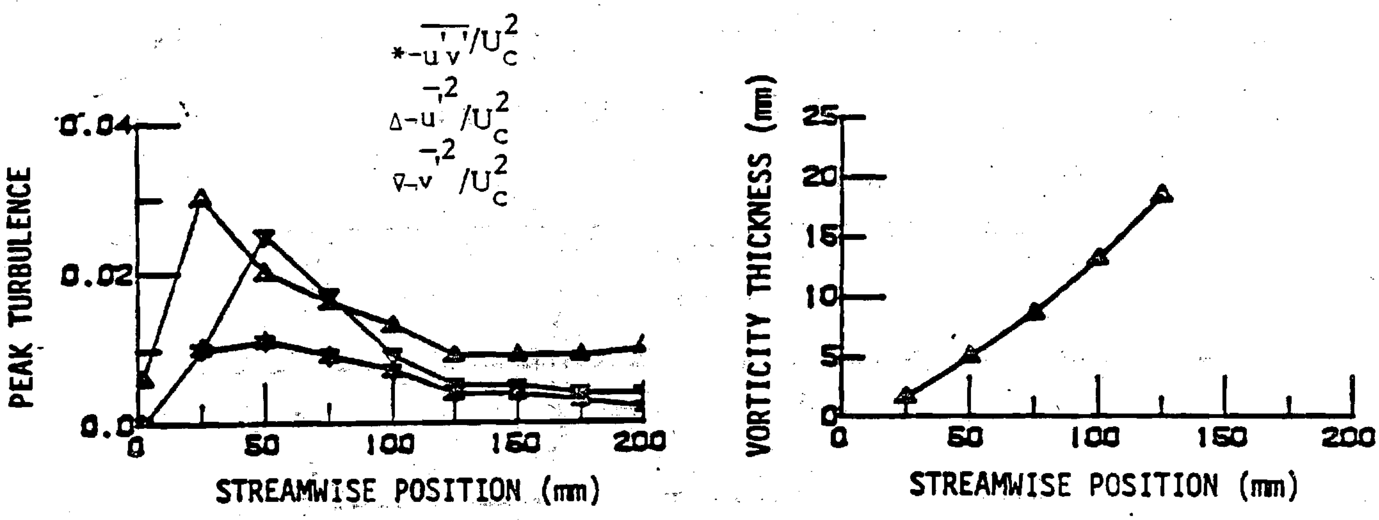

Fig. D.10. Variation of peak turbulence and vorticity thickness with streamwise distance

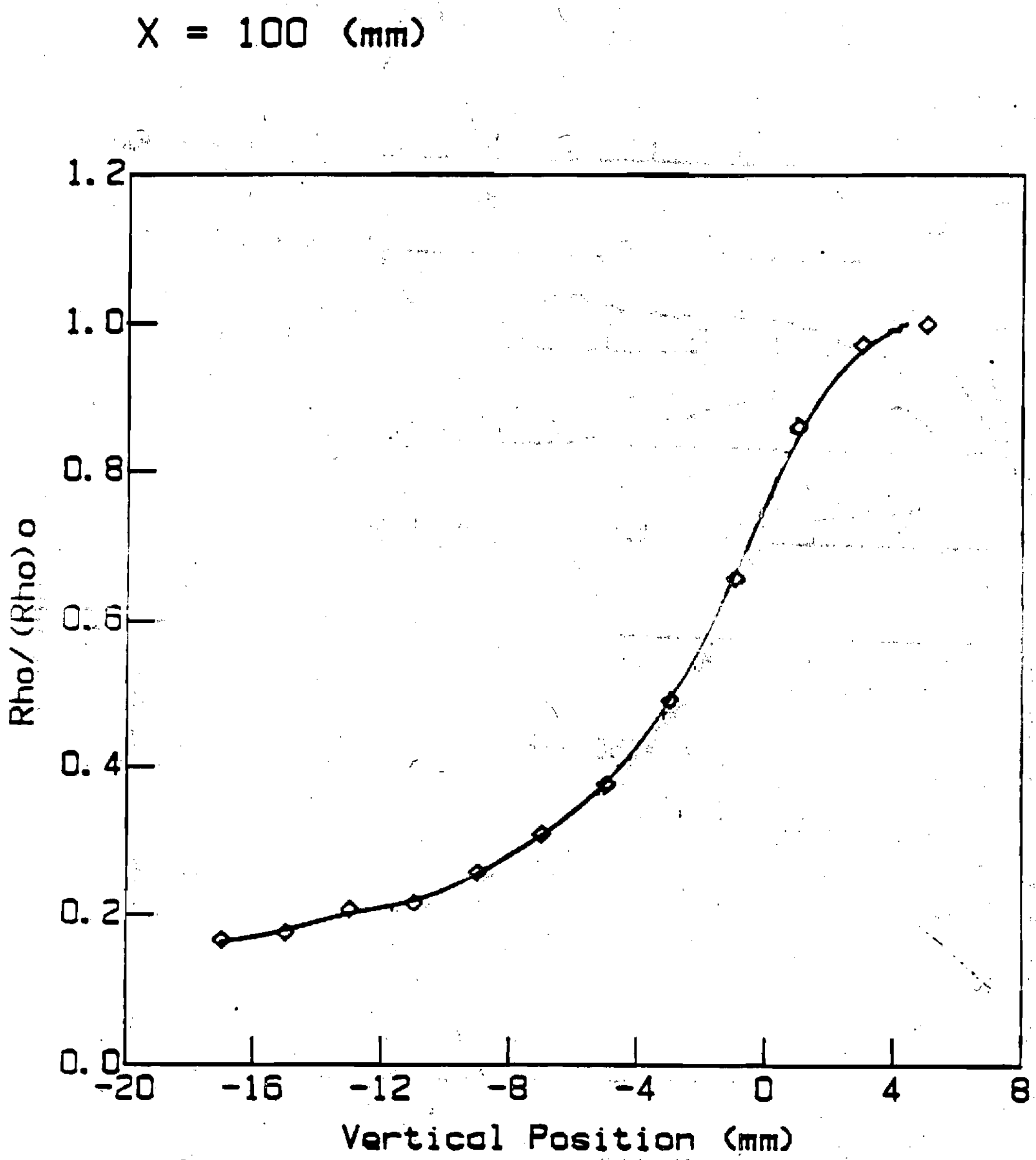

Fig. D.11. Mean density profile at x = 100 mm

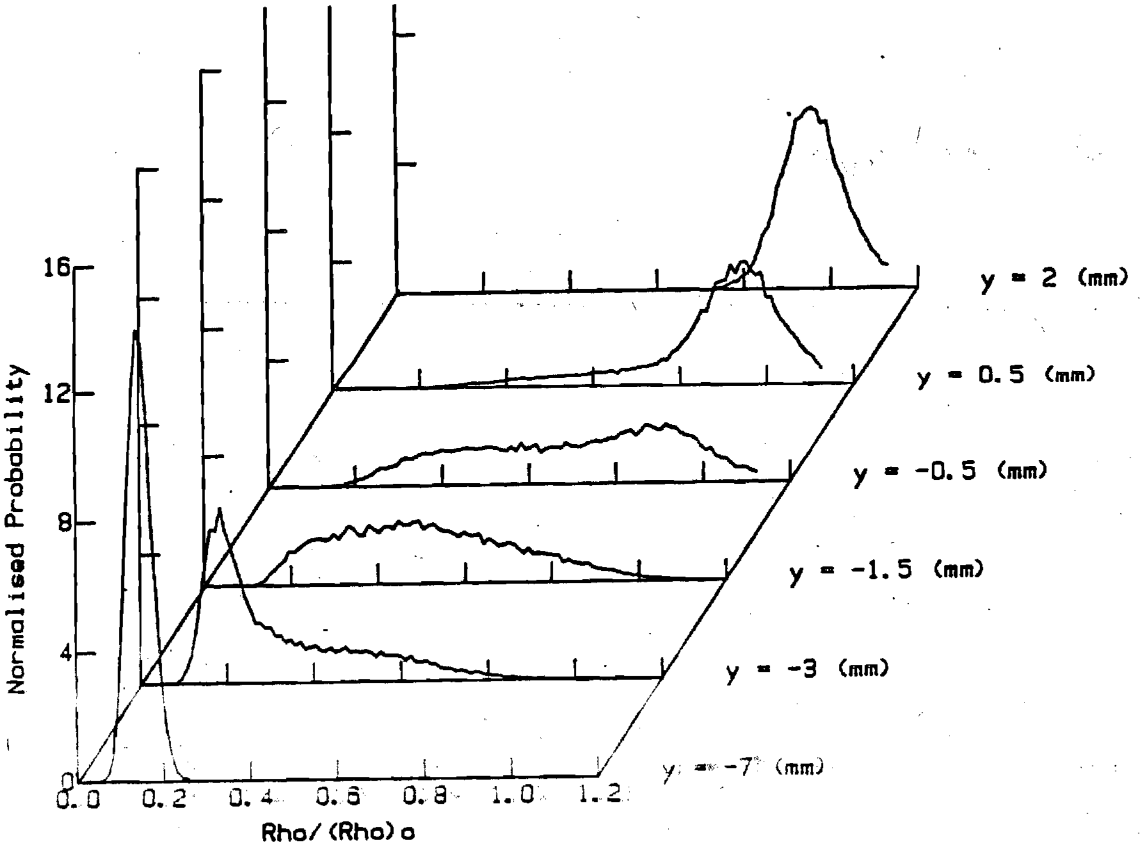

X = 50 (mm)

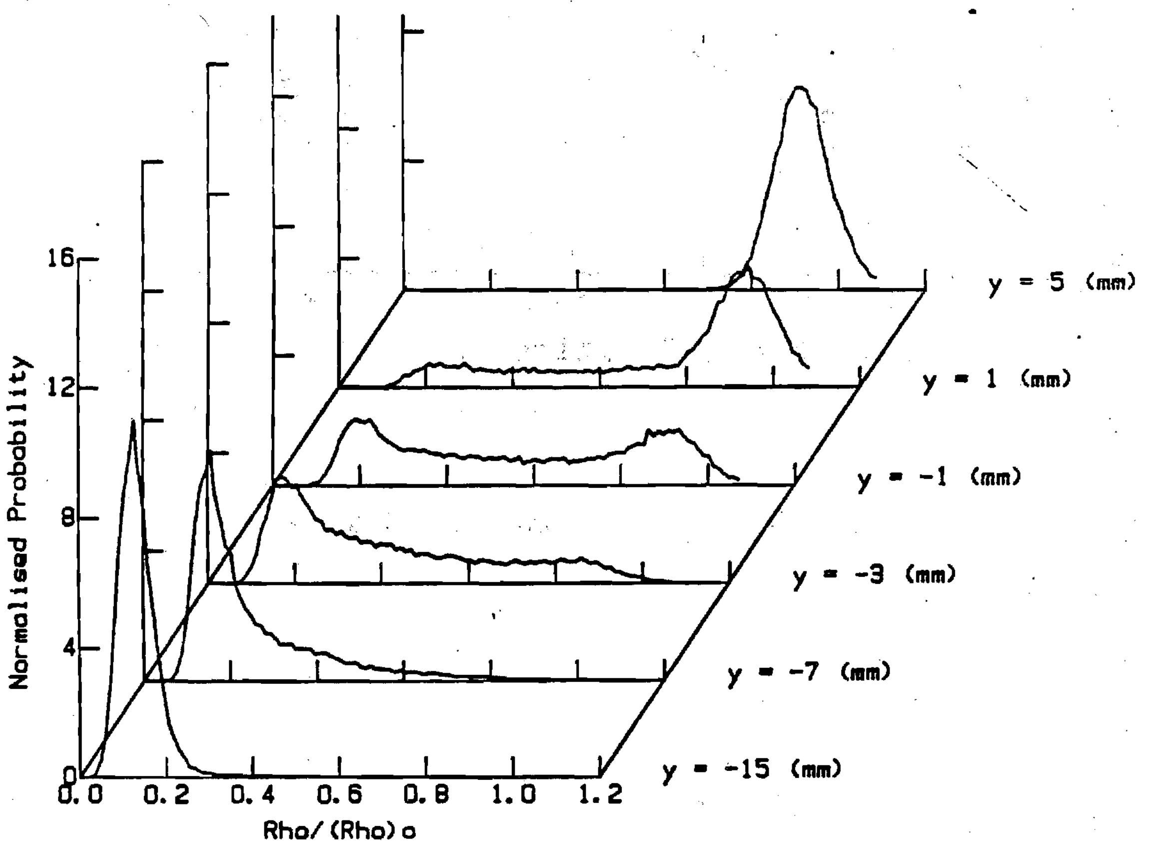

X = 100 (mm)

Fig. D.12. Pdfs of density

SECURITY CLASSIFICATION OF THIS PAGE (When Data Entered)

REPORT DOCUMENTATION PAGE		READ INSTRUCTIONS BEFORE COMPLETING FORM
1. REPORT NUMBER	2. GOVT ACCESSION NO.	3. RECIPIENT'S CATALOG NUMBER
4. TITLE (and Subtitle) Heterogeneous Diffusion Flame Stabilization		5. TYPE OF REPORT & PERIOD COVERED Interim Scientific 10/1/85 - 9/30/86
		6. PERFORMING ORG. REPORT NUMBER
7. AUTHOR(s) J. I. Jagoda, Warren C. Strahle, Ronald E. Walterick, W. A. de Groot		8. CONTRACT OR GRANT NUMBER(s) AFOSR-83-0356 H
9. PERFORMING ORGANIZATION NAME AND ADDRESS Georgia Institute of Technology School of Aerospace Engineering Atlanta, GA 30332		10. PROGRAM ELEMENT, PROJECT, TASK AREA & WORK UNIT NUMBERS
11. CONTROLLING OFFICE NAME AND ADDRESS Air Force Office of Scientific Research/NA Bldg. 410 Bolling AFB DC 20332		12. REPORT DATE Sept. 30, 1986
		13. NUMBER OF PAGES
14. MONITORING AGENCY NAME & ADDRESS (if different from Controlling Office)		15. SECURITY CLASS. (of this report)
		15a. DECLASSIFICATION/DOWNGRADING SCHEDULE

16. DISTRIBUTION STATEMENT (of this Report)

17. DISTRIBUTION STATEMENT (of the abstract entered in Block 20, if different from Report)

Approved for public release; distribution unlimited

18. SUPPLEMENTARY NOTES

19. KEY WORDS (Continue on reverse side if necessary and identify by block number)

Turbulence, Flameholding, Combustion, Ramjets

20. ABSTRACT (Continue on reverse side if necessary and identify by block number)

See reverse side

DD FORM 1 JAN 73 1473 EDITION OF 1 NOV 65 IS OBSOLETE

UNCLASSIFIED

SECURITY CLASSIFICATION OF THIS PAGE (When Data Entered)

Progress is reported concerning a two-dimensional wind tunnel experiment and associated analysis, with emphasis upon flameholding iN a solid fueled ramjet configuration. The dominant experimental results for the past year have concerned mass fraction and velocity-mass fraction covariance measurements by LDV and Rayleigh molecular scattering techniques. These measurements have been made with CO_2 injection behind the backward facing step in the wind tunnel, simulating mass addition in a SFRJ. Analysis has proceeded to the case of injection of a combustible with infinitely fast chemical kinetics, using a two equation turbulence model. Wind tunnel construction/modification has progressed to the point where the combustion experiments may now proceed. Development of the Raman spectroscopy system continues.

Interim Scientific Report

AFOSR-83-0356 H

HETEROGENEOUS DIFFUSION FLAME STABILIZATION

Prepared by:

J. I. Jagoda

W. C. Strahle

Submitted to:

Air Force Office of Scientific Research

Bolling Air Force Base

DC 20332

September 30, 1986

Georgia Institute of Technology

School of Aerospace Engineering

Atlanta, Georgia 30332

Heterogeneous Diffusion Flame Stabilization

J. I. Jagoda Warren C. Strahle
Ronald E. Walterick Wilhelmus A. de Groot

A. Research Objectives

The overall objective is to understand and be able to predict recirculatory turbulent reactive flows, flame stabilization limits and fuel regression rates in a flame stabilization region as occurs in a solid fueled ramjet. The specific goals for the past year were to a) develop the data reduction procedure for and complete measurements on mass fraction and velocity-mass fraction covariance with mass injection behind a backward facing step, b) develop a two-equation turbulence model and calculation procedure for calculating turbulent reacting flow behind a backward facing step, c) continue development of a Raman spectroscopy system for temperature measurement in the wind tunnel facility and d) complete development of the hot section of the wind tunnel for combustion measurements.

B. Status of Research

The work on this project, both analytical and experimental, has been divided into three consecutive parts: 1) cold flow tests without bleed flow, 2) cold flow test with bleed flow and 3) tests with bleed flow and combustion. In part 1 the velocity flow field was measured using Laser Doppler Velocimetry (LDV). In part 2 the velocities and concentrations of bleed gas in the flow field were determined using LDV and molecular Rayleigh scattering, both separately and simultaneously. In the case with combustion (part 3), velocities will be determined using LDV while bleed gas concentrations and local temperatures will be measured using spontaneous Raman scattering. In addition, all three flows are being modelled using a modified k-ε code and their predictions compared with the measurements. The results from part 1 were reported in the September 1984 Annual Report while those from the velocity measurement in the cold flow with blowing were given in the renewal proposal dated May, 1985. Also reported were the results from the modeling efforts of the cold flows without and with bleed. All this work was published in the Journal of Propulsion and Power. This report will, therefore, concentrate on the results obtained from the concentration and combined velocity-concentration measurements obtained in cold flow and on the preparations completed for the reacting flow work.

The wind tunnel configuration is a two dimensional subsonic tunnel with a backward facing step, with provision for gas injection behind the step. As mentioned above, bleed gas concentrations were measured using Rayleigh scattering. CO_2 was used for the bleed because of its large scattering cross-section compared with the N_2 and O_2 in the air which constituted the main flow. Pure Rayleigh and combined LDV-Rayleigh data were acquired and reduced using software written inhouse and described in the last Annual Report. This permitted concentration data to be acquired either continuously or in bursts of 20 data points at 8μsec intervals just before and just after each validated velocity measurement. Signals above a threshold voltage, selected to discard Mie scattering from particles in the flow while still accepting those from CO_2 molecules, were rejected. 32,000 data points were collected at each station for the continuous data acquisition and processed into pdf's from which the means and variances of the concentrations were determined. Since successful Rayleigh measurements require very low seeding levels, natural seeding in the form of dust particles in the air was used to carry out the combined LDV-Rayleigh determinations. Because of the resulting low data rate only 1000 LDV triggered concentration bursts were measured for each position. Comparison of continuous and LDV triggered concentration measurements permitted a check for a possible concentration bias towards higher air levels when the Rayleigh signal was only accepted as seed particles passed through the test volume. Such a bias towards higher apparent air levels would have been possible since only the air could be seeded.

The Rayleigh measurements in this flow configuration differed significantly from those made by other investigators which were mostly carried out under ideal conditions. Because of the geometry of the tunnel the LDV measurements had to be made in backscatter while the optical axis of the Rayleigh detection system had to be placed at an angle of 27.5 degrees to the incident laser beam and not at right angles which would have resulted in minimum Mie scattering noise from the particles in the flow. In addition, the F number of the Rayleigh collection optics was limited to 10 because of the short height and large width of the tunnel required to assure 2-D flow. Furthermore, the scattering volume was often located in the immediate vicinity of the porous plate and surrounded by scattering surfaces which significantly increased the background scatter. Finally, and most significantly, the air drawn into the tunnel from the laboratory contained a large number of dust particles of various sizes which caused a widening and skewing of the pdf's. All this noticeably reduced the signal to noise ratio. As a result, the fluctuating scattering signals caused by the turbulent fluctuating CO_2 concentrations were seriously contaminated by glare caused by the windows and the walls of the tunnel, by light scattered from the particles (before it reached the present threshold mentioned above) and by Shot noise in the photomultiplier and Johnson noise in the electronics.

As a first cut the data were reduced by assuming that the electronic noise, the background glare and the noise generated by the particles made equal mean contributions to the measured signal at each location whether the tunnel was operated only with pure air or with CO_2 injection. The local CO_2 concentrations were then determined at each point from the differences in scattering intensities between the CO_2 injection and the no injection cases. Details of this part of the work were submitted as a Technical Note to the AIAA Journal.

Local bleed gas concentrations were measured for an axial inlet velocity of 70 m/s and a bleed gas velocity of .5 m/s which corresponds to a typical gasification rate of the fuel in a SFRJ. None of the pdf's obtained were bimodal, indicating that the residence times in the recirculation zone were long enough for molecular mixing to prevent any pockets of pure bleed gas to be observed above .1 step heights above the bleed plate.

Figure 1 shows the mean concentration of bleed gas vs. height above the bleed plate at 2.9, 4.4, 5.9, 7.3 and 8.8 step heights downstream from the step. The first three stations lie within the recirculation zone with reattachment at 6.7 step heights for this flow. The circles and squares correspond to two separate runs using continuous Rayleigh measurements while the triangles represent data collected by triggering off the seed particles via the LDV. The solid line was obtained from the modified k-ε model. Good agreement was observed between the measured and calculated bleed gas concentrations except that the concentration gradient was somewhat underpredicted in the forward part of the recirculation zone and slightly overpredicted near reattachment. This suggests that near the reattachment point the main and bleed gases are slightly better mixed than predicted while close to the step the mixing process seems more diffusion controlled. This observation is in close agreement with the expectations from the velocity measurements.

In addition, the data obtained in all these runs agree to within experimental accuracy. This agreement between the mean concentration obtained from the continuous and velocity triggered Rayleigh measurements is of particular importance for the simultaneous velocity-concentration measurements. Clearly, no significant bias in these mean concentration values is introduced by measuring the bleed gas levels only in the vicinity of seed particles.

However, when the covariances of the velocity and concentration were calculated from the experimental data, it became apparent that because of the small covariance of these quantities the assumptions outlined above introduced an unacceptable error. A more sophisticated data reduction technique was, therefore, developed in which the variation in the contribution of the particle noise to the measured pdf's between the cases without and with blowing at each point were accounted for. In addition, the actual pdf's of the electronic and particle generated noise rather than only their mean contributions were subtracted out. The details of this novel deconvolution technique are described in an article submitted to <u>Combustion and Flame</u>. Briefly, as shown in Fig. 2 the measured pdf's consist of a Gaussian due to electronic noise, a delta function due to glare and a contribution by the particles which was found to be double peaked plus a delta function at zero intensity due to instants when no particles were in the test volume. The schematic also includes delta functions due to pure air and pure CO_2 which are replaced by a single broad band pdf in the case of mixed air and CO_2. As the content of CO_2 increases, the pdf experiences a leftward shift due to a decrease in particle contamination and a rightward shift due to the measured level of CO_2. Similarly, the width of the pdf changes due to the effect of the CO_2 fluctuations and a change in the particle contributions.

In order to separate these effects, an analytical method involving Fourier transforms was developed which permitted the deconvolution of the joint pdf's of velocity and concentration. This technique resulted in a much improved joint covariance of the velocity and CO_2 fluctuations examples of which obtained at various vertical locations at reattachment are shown in Fig. 3. Also shown are the predicted covariances. Although the data do not appear as consistent as those for the mean concentrations the quality of the data is remarkable considering the extremely low signal to noise ratio. The variances of the CO_2 concentrations are still being calculated from the measured data.

As part of Task 3, the tunnel has been readied for the combustion experiments. The wooden settling chamber has been replaced by a steel version, seals have been improved, the duct work has been extensively leak-checked and H_2 detecters and a variety of safety devices have been installed and tested. Also added were a retractable ignition spark plug and a pilot burner near reattachment. The facility is now ready for trials and should be lit for the first time in October, 1986. As soon as a satisfactory flame is stabilized it will be visualized using high speed Schlieren followed by LDV and Raman measurements.

On the modeling effort, the flow fields for the cold case with and without blowing as well as the means and variances of the bleed gas concentrations and their joint covariances with the velocities were calculated and previously reported. These were also published in the Journal of Propulsion and Power. In these calculations the law of the wall was used as the boundary condition at the floor of the tunnel. This resulted in good results for the mean flow pattern but presented some problems in satisfying continuity for the bleed gas because of the coarse grid spacing near the wall where steep bleed gas concentration gradients exist. This was particularly evident once reacting flow calculations were started.

The cold flow calculations with blowing were, therefore, repeated using a different well treatment as suggested by Gorski. In this technique different formulations for k and ε were used inside and outside the laminar sublayer which were then matched at its boundary. This resulted in a virtually unchanged mean flow pattern but an increase of approximately 20% in the bleed gas concentrations near the wall and much improved continuity for the bleed flow. The joint covariance of velocity and bleed concentration was also somewhat increased.

In the model of the reacting flow field the density weighted (Favre-averaged) equations along with the improved wall boundary condition are being used. As a first step, equilibrium calculations (assuming fast chemistry) have been carried out in which the turbulent fluctuations of composition were neglected. The equilibrium compositions for various thermodynamic conditions were calculated using the Thermochemical Code. This part of the work is now complete. The equilibrium model is currently being refined by allowing for turbulent fluctuations of the mixture fractions. Upon completion of this task, the effect of finite rate chemistry will be incorporated in the model. A perturbation approach by Bilger will be adopted for the finite rate chemistry case. This will allow calculations of blowoff limits.

C. Publications in Past Year

Richardson, J., de Groot, W. A., Jagoda, J. I., Walterick, R. E., Hubbartt, J. E. and Strahle, W. C., "Solid Fueled Ramjet Simulator Results: Experiments and Analysis in Cold Flow," Journal of Propulsion and Power, 1, 488-493 (1985).

de Groot, W. A., Latham, R., Jagoda, J. I., and Strahle, W. C., "Rayleigh Measurements of Species Concentration in a Complex Turbulent Flow," submitted to AIAA Journal.

Strahle, W. C. and de Groot, W. A., "Deconvolution of Complex PDF Data," submitted to Combustion and Flame.

D. Personnel

Principal Investigators

Jechiel I. Jagoda

Warren C. Strahle

Research Engineers

Ronald E. Walterick

Wilhelmus A. de Groot

Ralph Latham

Graduate Research Assistant

Brian Mysiak

E. Special Professional Activities

W. C. Strahle, Seminar on program at Aberdeen Proving Ground, November, 1985.

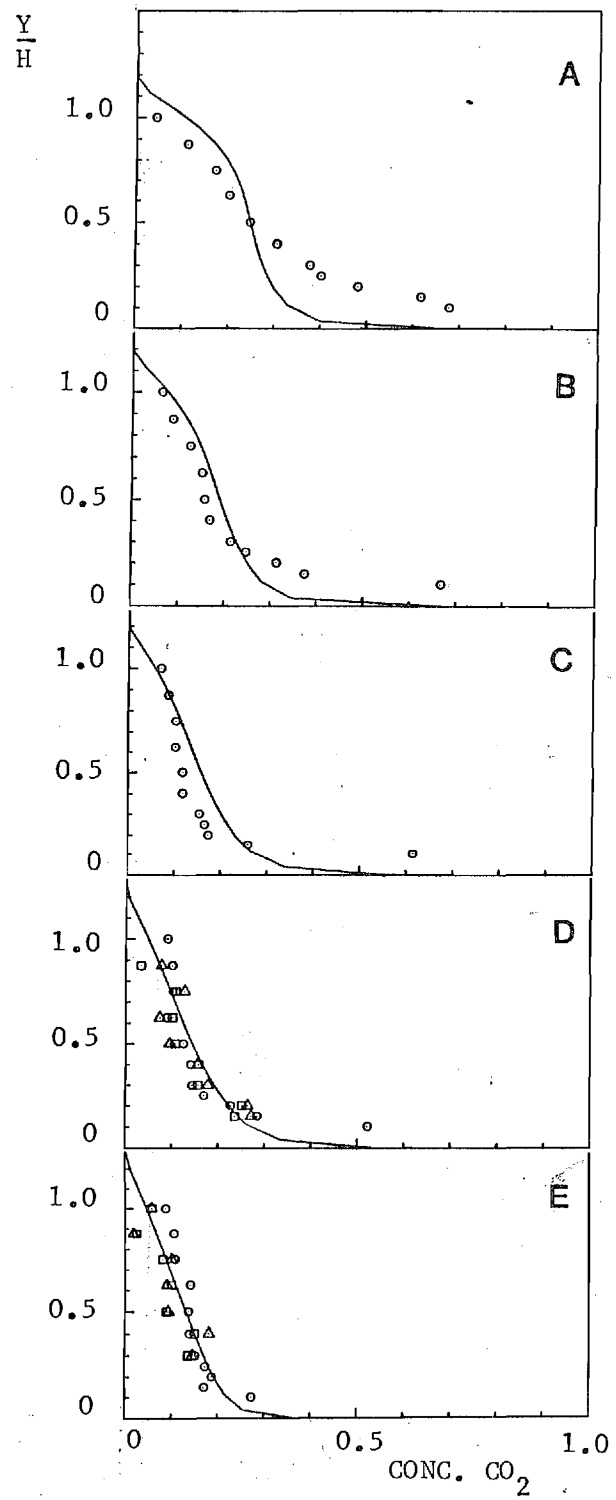

Figure 1. Concentration of bleed gas vs height above the tunnel floor for CO_2-air mixture as injectant at different axial locations: A-2.9 stepheights. B-4.4 stepheights, C-5.9 stepheights, D-7.3 stepheights and E-8.8 stepheights. O and □ continuous data acquisition, △ seed particle triggered data acquisition, predicted using k-ε.

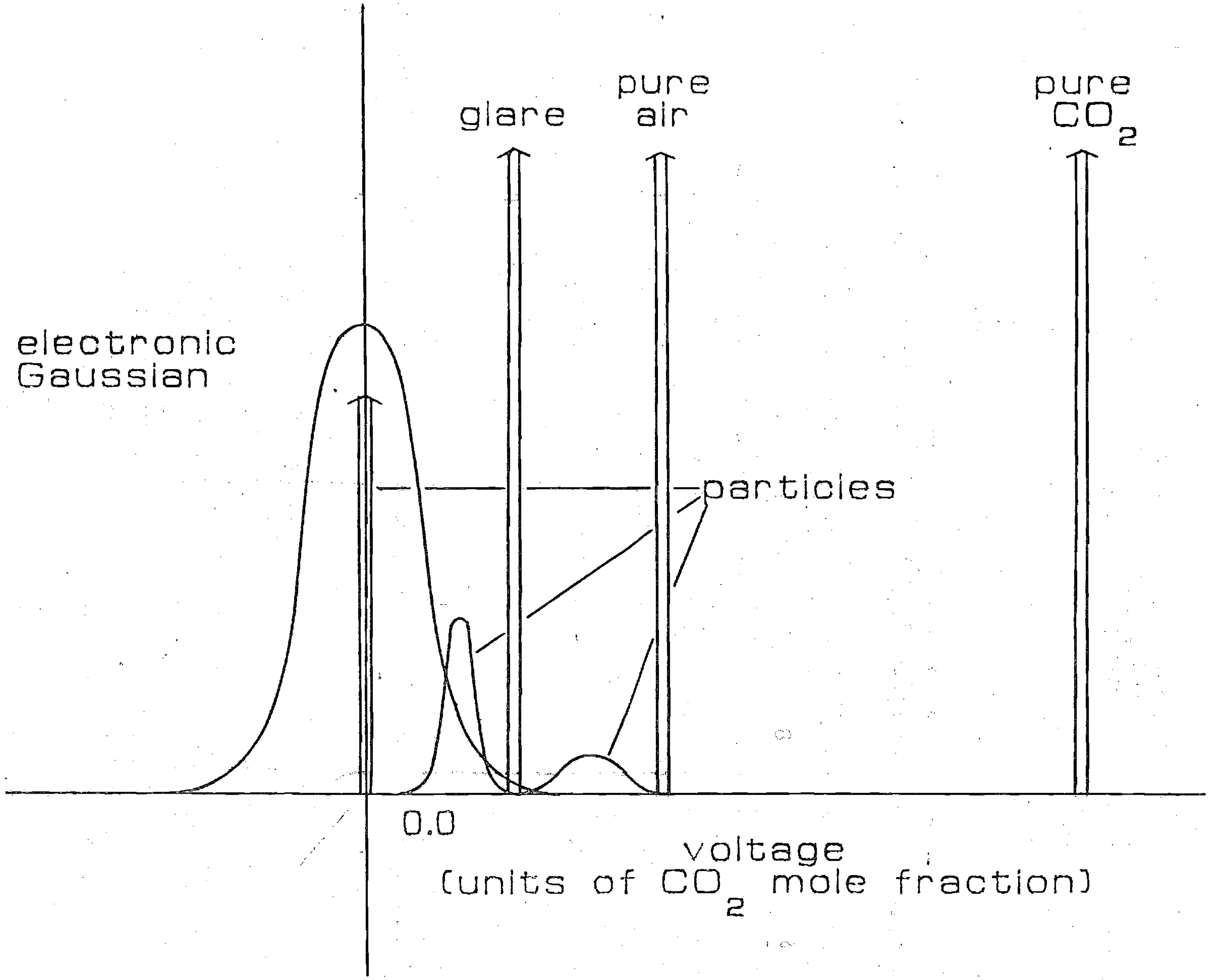

Figure 2. Individual component pdfs of the Rayleigh molecular scattering signal.

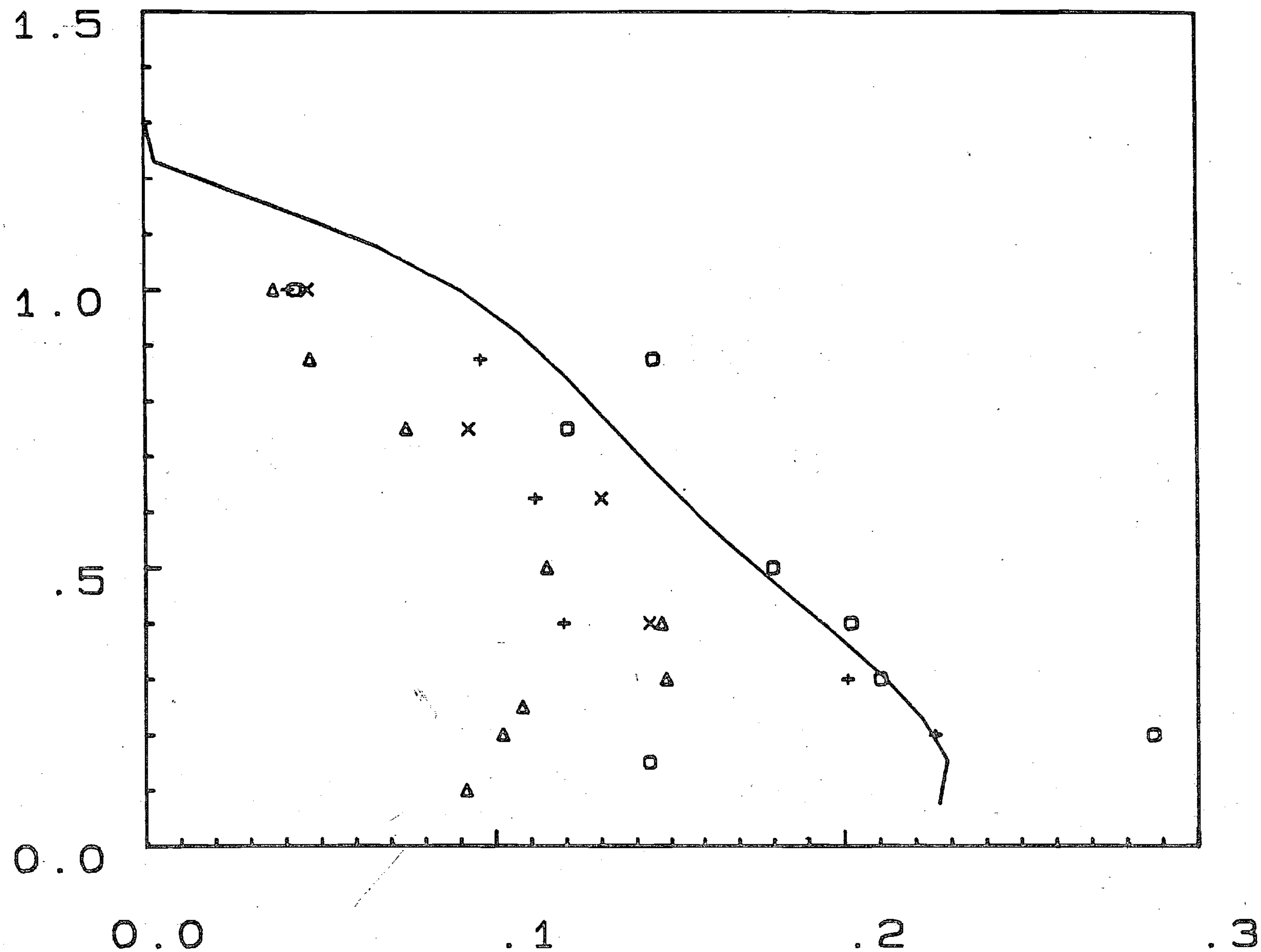

Figure 3. Covariance of velocity and mole concentration fluctuations at various vertical locations at reattachment. Different symbols denote different runs; solid line model predictions.

Unclassified

SECURITY CLASSIFICATION OF THIS PAGE

REPORT DOCUMENTATION PAGE

Form Approved OMB No. 0704-0188

1a. REPORT SECURITY CLASSIFICATION: Unclassified	1b. RESTRICTIVE MARKINGS: None
2a. SECURITY CLASSIFICATION AUTHORITY	3. DISTRIBUTION/AVAILABILITY OF REPORT: Unlimited
2b. DECLASSIFICATION/DOWNGRADING SCHEDULE	
4. PERFORMING ORGANIZATION REPORT NUMBER(S)	5. MONITORING ORGANIZATION REPORT NUMBER(S)
6a. NAME OF PERFORMING ORGANIZATION: Georgia Institute of Technology; 6b. OFFICE SYMBOL (If applicable)	7a. NAME OF MONITORING ORGANIZATION: AFOSR
6c. ADDRESS (City, State, and ZIP Code): School of Aerospace Engineering, Georgia Institute of Technology, Atlanga, GA 30332	7b. ADDRESS (City, State, and ZIP Code): Bldg. 410, Bolling, AFB, DC 20332
8a. NAME OF FUNDING/SPONSORING ORGANIZATION: AFOSR; 8b. OFFICE SYMBOL (If applicable): NA	9. PROCUREMENT INSTRUMENT IDENTIFICATION NUMBER: AFOSR - 83 - 0356
8c. ADDRESS (City, State, and ZIP Code): Bldg. 410, Bolling AFB, DC 20332	10. SOURCE OF FUNDING NUMBERS: PROGRAM ELEMENT NO. / PROJECT NO. / TASK NO. / WORK UNIT ACCESSION NO.

11. TITLE (Include Security Classification)
Heterogeneous Diffusion Flame Stabilization

12. PERSONAL AUTHOR(S)
W. C. Strahle and J. I. Jagoda

13a. TYPE OF REPORT	13b. TIME COVERED	14. DATE OF REPORT (Year, Month, Day)	15. PAGE COUNT
Final	FROM 10/83 TO 9/87	87/11/29	

16. SUPPLEMENTARY NOTATION

17. COSATI CODES			18. SUBJECT TERMS (Continue on reverse if necessary and identify by block number)
FIELD	GROUP	SUB-GROUP	

19. ABSTRACT (Continue on reverse if necessary and identify by block number)

Analytical modelling and several experimental diagnostics were applied to an experimental flow in a two-dimensional subsonic windtunnel with a backward facing step and provision for injection of inerts and combustibles through the porous floor behind the step. The analytical techniques were based on a two equation model of turbulence with several variants of near wall models and numerical approaches. Conventional experimental techniques, where applicable in the cold flow, included hot film and pitot anemometry. Laser - based diagnostics in the cold and hot flows for velocity and species concentration measurements (both mean and instantaneous) included laser velocimetry in two components and Rayleigh molecular scattering.

20. DISTRIBUTION/AVAILABILITY OF ABSTRACT: ☒ UNCLASSIFIED/UNLIMITED ☒ SAME AS RPT. ☐ DTIC USERS	21. ABSTRACT SECURITY CLASSIFICATION: Unclassified
22a. NAME OF RESPONSIBLE INDIVIDUAL: W.C. Strahle	22b. TELEPHONE (Include Area Code): (404) 894-3032; 22c. OFFICE SYMBOL

DD Form 1473, JUN 86 — Previous editions are obsolete.

SECURITY CLASSIFICATION OF THIS PAGE

Unclassified

Major findings in this complex turbulent flow with chemical reactions were a) there was general agreement between analysis and experiment in cold flow both with and without wall injection, b) this agreement occurred at the the most detailed level of turbulent shear stress and mass transport, c) in hot flow there was acceptable agreement as to the gross features of the mean flow field , but some theoretical details, such as reattachment length, went counter to experimental results. Further detailed probing of velocity, concentration and temperature along with a more sophisticated turbulence model are required for full documentation and predictability of this hot flow.

AFOSR FINAL REPORT

HETEROGENEOUS DIFFUSION FLAME STABILIZATION

Co-Principal Investigators
Warren C. Strahle
Jechiel I. Jagoda

Prepared for

AIR FORCE OFFICE OF SCIENTIFIC RESEARCH
AEROSPACE SCIENCES DIRECTORATE
BOLLING AIR FORCE BASE, DC

Under Contract No. AFOSR-83-0356

November, 1987

GEORGIA INSTITUTE OF TECHNOLOGY
School of Aerospace Engineering
Atlanta, Georgia 30332

SUMMARY

Analytical modelling and several experimental diagnostics were applied to an experimental flow in a two-dimensional subsonic windtunnel with a backward facing step and provision for injection of inerts and combustibles through the porous floor behind the step. The analytical techniques were based on a two equation model of turbulence with several variants of near wall models and numerical approaches. Conventional experimental techniques, where applicable in the cold flow, included hot film and pitot anemometry. Laser - based diagnostics in the cold and hot flows for velocity and species concentration measurements (both mean and instantaneous) included laser velocimetry in two components and Rayleigh molecular scattering.

Major findings in this complex turbulent flow with chemical reactions were a) there was general agreement between analysis and experiment in cold flow both with and without wall injection, b) this agreement occurred at the the most detailed level of turbulent shear stress and mass transport, c) in hot flow there was acceptable agreement as to the gross features of the mean flow field , but some theoretical details, such as reattachment length, went counter to experimental results. Further detailed probing of velocity, concentration and temperature along with a more sophisticated turbulence model are required for full documentation and predictability of this hot flow.

RESEARCH OBJECTIVES

The primary objective was to determine the limits of scientific understanding and predictability of a particular complex turbulent reacting flow. Secondary objectives included the development of several laser diagnostic methods operating under particularly severe conditions of signal to noise ratio and the necessary developments to modify two-equation turbulence models to treat the complex flow field studied. A tertiary objective was to provide technical information on the reattachment combustion dynamics of a flow field simulating that of a solid fueled ramjet, which was the flow field that the experimental and theoretical studies simulated.

ACCOMPLISHMENTS

Facility

The facility, which underwent continual development during the course of this program, is fully described in Ref. A, in the REFERENCES AND PUBLICATIONS section of this report. The combustion windtunnel developed was a two dimensional, backward facing step facility with provision for injection of inerts and combustibles through a porous floor behind the step. Injectants actually used were air, CO_2, CH_4 and H_2. The facility simulated the flame reattachment region of a solid-fueled ramjet. For scientific purposes, however, it was of use as a highly complex, turbulent, recirculatory reacting flow with mass addition.

Experimental Effort

As discussed above, the flame holding region of the solid fueled ramjet was simulated in this study in a facility in which air from the laboratory was drawn over a backward facing step. The evaporating solid fuel was simulated by blowing bleed gases through a porous floor behind the step. The tunnel was fitted with quartz side walls to permit access for optional diagnostics and fully instrumented with pressure and thermocouple probes. A detailed description of the facility along with its associated safety features is given in Ref. A.

The investigation of the flow in this facility was divided into three consecutive tasks: a) recirculatory flow without blowing, b) non-reacting recirculatory flow with injection of air or carbon dioxide through the porous floor, and c) reacting recirculatory flow using hydrogen or methane as fuel. The quantities measured include local velocities, turbulence intensities and shear stresses for the non-bleed flow. Mean velocities, turbulence intensities, shear stresses, bleed gas concentrations and velocity - concentration correlations were determined for the non-reacting flow with bleed. Finally, mean velocities, turbulence intensities, shear stresses, fuel concentrations and temperatures as well as the correlations of concentrations, temperatures and velocities are required for the reacting flow. All but the concentration and temperature measurements in the reacting flow have been completed.

Initially, mean velocities and turbulence intensities were measured at selected locations in the flow field without blowing using a pitot probe (mean velocities only), a hot wire and a laser Doppler velocimeter (LDV). Very good agreement between the values obtained by the three techniques were obtained. Good agreement was also observed with data reported by other workers for similar flows. These results were reported in Ref. B.

As a next step, the entire flow field without bleed was mapped out using LDV. The results obtained were in good agreement with those predicted using the modified k-ε model described in the following section. The comparisons carried out included velocity profiles at various axial locations, positions of zero axial velocities, location of the reattachment point and the axial positions of the maximum shear stresses, as reported in Refs. B and C.

The non-reacting velocity flow field with bleed was mapped for bleed flow rates corresponding to injection velocities of .5 and .25 m/s using both air and carbon dioxide as an injectant. Local bleed gas concentration distributions were determined using Rayleigh scattering for injectant velocities of .5 m/s. At selected locations the velocity and concentration measurements were carried out simultaneously in order to gain insight into the turbulent mass transport.

The results from the velocity measurements were reported in Ref. D. Blowing has very little effect upon the location of the zero axial velocity line. A shortening of the main recirculation zone at its downstream end, which had been predicted by the model, was, thus, not observed. As predicted, however, a small, secondary recirculation zone next to the step appeared upon blowing. The vertical locations of the measured maximum shear stresses at various axial locations were in good agreement with those predicted although the measured values were generally a little higher.

The local bleed gas concentrations for the cold flow were reported in Ref. E. Dust drawn with the air from the laboratory into the tunnel was used as seed particles for the LDV in the combined velocity - concentration measurements. The Mie scattering from the particles is many orders of magnitude stronger than the Rayleigh scattering from the molecules. Therefore, a data acquisition and reduction technique had to be developed which permitted the removal of the contributions by the particles and by the glare from the windows from the signal. A relatively simple data reduction scheme based upon mean noise levels was reported in Ref. E. Good agreement was obtained between the measured and calculated bleed gas concentrations except immediately behind the step where the vertical concentration gradient seemed somewhat overpredicted. Acceptable velocity concentration correlations could not, however, be obtained with the results from this simplistic data reduction technique.

A more sophisticated, Fourier transformation based date reduction technique was, therefore, developed. The details of this technique in which the actual noise pdf's generated by the particles, the glare and the electronic noise rather than only their mean contributions were removed from the signal were given in Ref. F. The results obtained with this novel reduction technique were reported in Ref. G and H. The agreement between the measured mean concentrations and those calculated using the modified k-ε model was notably improved over those reported in Ref. E. In addition, velocity - concentration data could be obtained from the improved data despite the low signal to noise ratio. It was found that the model correctly calculated the covariance profiles but tended to somewhat overpredict their magnitudes.

Reacting flow experiments were carried out using methane and hydrogen as fuels. The methane flame generally was found to be shorter and formed three axial prongs near reattachment. The hydrogen fuel resulted in a longer, smoother flame which was overall more two-dimensional in nature. Hydrogen was chosen as the fuel for all the diagnostic work not only because it resulted in a better, more stable flame but also because hydrogen flames produce a cleaner spectrum and are, therefore, more amenable to Raman measurements.

The vertical distributions of axial velocity are shown for three axial locations in Figure 1. Two of these locations are inside the recirculation zone while the third is at reattachment. These results do not agree with the model predictions, as explained below. While the model calculates a shortening of the recirculation zone for the reacting case as opposed to the cold flow, a lengthening of the recirculation zone upon heat addition is, in fact, observed. The experimental observations have, as yet, not been published, but the analysis will appear as Ref. H.

Analytical Effort

The analysis has evolved over several years roughly in accord with the experimental schedule, but the analysis has usually led the experiments in time. The analysis began through use of a numerical code generated by Imperial College, called TEACH. It is based upon a two equation (k-ε) model of turbulence for two-dimensional flows and uses what are known as law of the wall approximations to match the turbulent flow through a laminar sublayer to the wall boundary conditions. The original code and analysis was based upon incompressible flow.

The analysis and numerical code went through the following evolution process:

a) Modification of the law of the wall to incorporate wall blowing

b) Conversion of the equations to Favre averaged equations to incorporate variable density

c) Incorporation of an approximation for pressure - velocity correlations

d) Certain changes suggested in the literature to speed convergence rate

e) Change from the law of the wall model to a new type of model suggested in the literature to remove some shortcomings of the old model in combustion calculations

f) Incorporation of a calculation of transport of the variance of a conserved scalar

g) Incorporation of equilibrium combustion properties for both methane and hydrogen

h) Calculation using several assumed forms of probability density functions for the fuel element mass fraction

i) Change to finite rate chemical kinetics for hydrogen - air, as opposed to chemical equilibrium calculations

Results of calculations on item a) - c) above are contained in Refs. B - D. These calculations were made in cold flow, but incorporated wall blowing. Partial calculations in cold flow incorporating d) - f) are located in Refs. E - G. The general conclusions in cold flow, with and without blowing, are that there is quite good agreement between theory and experiment and the improvements incorporated for cold flow modelling speed both convergence rate and agreement between theory and experiment.

Results of the hot flow calculations, testing both methods of treatment of the chemistry and comparison with experiment, have been mixed in success. On the positive side, a) there is little difference in analytical results if fluctuations in species concentration are allowed or neglected (except in the region of the flow where the maximum temperature occurs) and b) the form of the assumed mixture fraction probability density function makes little analytical difference. However, in regions of the flow where the maximum temperature occurs, species fluctuation substantially depress average temperature and this turbulence effect must be included in calculation procedures. On the negative side, the calculation says that heat addition by combustion should somewhat shorten the reattachment length behind the step, whereas experimentally this length becomes somewhat larger. On the other hand, many of the gross features of the flow are preserved in a qualitative sense. It must remain as a future program to determine analytical remedies for the details of the prediction. The hot flow calculations are presented in Ref. H.

The finite rate chemistry calculations were not completed by the end of this contract and are therefore not included in this report. A future publication will contain these results and the Air Force will be properly acknowledged.

REFERENCES AND PUBLICATIONS
(INCLUDING PRESENTATIONS)

A. "Combustion Test Facility and Optical Instrumentation for Complex Turbulent Reacting Flow," Walterick, R. E., De Groot, W. A., Jagoda, J. I. and Strahle, W. C., printed as AIAA Paper #88-0052, to be presented at the 26th Aerospace Sciences Meeting, Reno, Nevada, January 1988.

B. "Experiments and Analysis on Two-Dimensional Turbulent Flow over a Backward Facing Step," Walterick, R. E., Jagoda, J. I., Richardson, J. R. J., De Groot, W. A., Strahle W. C. and Hubbartt, J. E., printed as AIAA Paper #84-0013, presented at the 22nd Aerospace Science Meeting, Reno, Nevada, 1984.

C. "SFRJ Simulator Results: Experiment and Analysis in Cold Flow," Richardson, J. R. J., De Groot, W. A., Jagoda, J. I., Walterick, R. E., Hubbartt, J. E. and Strahle, W. C., printed as AIAA Paper #85-0329, presented at the 23rd Aerospace Science Meeting, Reno, Nevada, January 1985.

D. "SFRJ Simulator Results: Experiment and Analysis in Cold Flow, " Richardson, J. R. J., De Groot, W. A., Jagoda, J. I., Walterick, R. E., Hubbartt, J. E. and Strahle, W. C., Journal of Propulsion and Power, Vol. 1, Nov.-Dec. 1985, pp 488-493.

E. "Rayleigh Measurements of Species Concentration in a Complex Turbulent Flow," De Groot, W. A., Latham, R., Jagoda, J. I. and Strahle, W. C., AIAA Journal Vol. 25, No. 8, Aug. 1987, pp 1142-1144.

F. "Extraction of Useful Data from Noise-Contaminated PDFs," Strahle, W. C. and De Groot, W. A., accepted by Combustion and Flame, 1988 and

presented at the Eastern States Section of the Combustion Institute Fall Technical Meeting, San Juan, Puerto Rico, December, 1986.

G. "Combined LDV and Rayleigh Measurements in a Complex Turbulent Mixing Flow," De Groot, W. A., Walterick, R. E. and Jagoda, J. I., printed as AIAA Paper #87-1328 and presented at the 19th Fluid Dynamics, Plasma Dynamics and Lasers Conference, Honolulu, Hawaii, June 1987; also accepted for publication in revised form for the AIAA Journal, 1988.

H. "Flow Field behind a Backward Facing Step," Tsau, F. H. and Strahle, W. C., printed as AIAA Paper No. 88-0340 and presented at the 26th Aerospace Science Meeting, Reno, Nevada, January, 1988; submitted to AIAA Journal, 1987.

Other interactions include all AFOSR Contractors' Meetings between October, 1983 and September, 1987.

PARTICIPANTS

Co-Principal Investigators

Dr. Warren C. Strahle, Regents' Professor
Dr. Jechiel I. Jagoda, Associate Professor

Research Engineers

Mr. Ronald E. Walterick
Dr. Wilhelmus A. de Groot

Students Graduated

Mr. F. H. Tsau, M.S., 1985
Mr. W. H. Mc Nicol, M.S., 1983
Mr. B. K. Mosoal, M.S., 1985
Dr. J. R. J. Richardson, Ph.D., 1984, dissertation entitled "Analysis of Sudden Expansion Flow in a Two-Dimensional Duct with and without

Side Wall Injection using the $k-\varepsilon$ Turbulence Model"

Dr. W. A. de Groot, Ph.D., 1985, dissertation entitled "Laser Doppler Diagnostics of the Flow behind a Backward Facing Step"

AWARDS

Warren C. Strahle

AIAA Pendray Aerospace Literature Award, 1985

Fellow AIAA, 1987

Member of Combustion Institute International Board of Directors, 1986

Jechiel I. Jagoda

Member, AIAA Technical Committee on Propellants and Combustion, 1983-85

Sigma Xi Junior Faculty Research Award, 1985

AFOSR PROGRAM MANAGER INFORMATION

The facility developed under this program is extremely versatile and well-equipped from a diagnostic viewpoint. It should be viewed as a National facility for compilation of turbulent reacting flow data and one in which AFOSR has had a great financial stake. Consideration should be given towards using this facility for data base creation in the spirit of the Introduction and History section of "Evaluation of Data on Simple Turbulent Reacting Flows", AFOSR TR-85-0880. Sept. 1985.

Fig. 1: **HYDROGEN COMBUSTION VELOCITY PROFILES**